Ali Mohammad · Inamuddin *Editors*

Green Solvents I

Properties and Applications in Chemistry

Springer

Green Solvents I

Ali Mohammad · Inamuddin
Editors

Green Solvents I

Properties and Applications in Chemistry

Springer

Editors
Ali Mohammad
Department of Applied Chemistry
Faculty of Engineering and Technology
Aligarh Muslim University
Aligarh, India

Inamuddin
Department of Applied Chemistry
Faculty of Engineering and Technology
Aligarh Muslim University
Aligarh, India

ISBN 978-94-007-1711-4 e-ISBN 978-94-007-1712-1
DOI 10.1007/978-94-007-1712-1
Springer Dordrecht Heidelberg New York London

Library of Congress Control Number: 2012933835

Printed on acid-free paper

Springer is part of Springer Science+Business Media (www.springer.com)

Preface

The fast-growing process of urbanization, industrialization, and unethical agriculture that has been implemented until recently has neither taken in consideration nor foreseen its effect on the environment, flora and fauna, and peoples' health and safety. Thus, over the last decade, green chemistry research has been focusing on finding and using safer and more environmentally friendly solvents.

Indeed, every process in chemistry, physics, biology, biotechnology, and other interdisciplinary fields of science and technology makes use of *solvents, reagents, and energy* that not only are highly toxic but also produce a great amount of undesirable waste, damaging irreparably our environment.

However, according to one of the green chemistry principles, the use of solvents should either be avoided or limited as much as possible, and although sometimes this is not possible, we ought to try to use greener alternatives to toxic solvents.

Green Solvents Volume I and II has been compiled to broadly explore the developments in the field of Green Solvents.

Written by 87 leading experts from various disciplines, these remarkable volumes cover the most comprehensive, in-depth, and state-of-the-art research and reviews about green solvents in the fields of science, biomedicine, biotechnology, biochemistry, chemical engineering, applied chemistry, metallurgical engineering, environmental engineering, petrochemicals engineering, etc.

With more than 3,000 references, 325 figures, 95 tables, and 25 equations, *Green Solvents Volume I and II* will prove to be a highly useful source for any scientists working in the fields of organic synthesis, extraction and purification of bioactive compounds and metals, industrial applications of green solvents, bio-catalysis, acylation, alkylation and glycosylation reactions, oxidation of alcohols, carbon nanotube functionalization, hydrogen sulfide removal, pharmaceutical industry, green polymers, nanofluids coolants, high-performance liquid chromatography, and thin layer chromatography. Based on thematic topics, the book edition contains the following 14 chapters:

Chapter 1 provides an overview of the use of green solvent systems such as water, superficial fluids, ionic liquids, room temperature ionic liquids, and fluorinated solvents

for a wide range of chemical applications including synthetic chemistry, extraction and material science.

Chapter 2 reviews green solvent extraction and purification of few marker compounds from propolis and rice bran using supercritical carbon dioxide (SC-CO_2). The central composite response surface methodology (RSM) was applied to predict the optimal operating conditions and to examine the significance of experimental parameters by a statistic analysis.

Chapter 3 focuses on coupling the attractive properties of green solvents with the advantages of using enzymes for developing biocatalytic processes.

Chapter 4 reviews the use of ionic liquids in the pharmaceutical industry and the production of fine chemicals.

Chapter 5 presents a complete picture of current knowledge on a useful and green bio-solvent "*d*-limonene" obtained from citrus peels through a steam distillation procedure followed by a deterpenation process.

Chapter 6 investigates selected examples of potential uses of glycerol in organic reactions as well as the advantages and disadvantages of such a green methodology.

Chapter 7 deals with the use of water as medium in synthetic processes based on the epoxide ring opening. Water has been presented as effective reaction medium to realize green epoxide–based processes.

Chapter 8 reviews the various aspects of ionanofluids together with their thermophysical properties for their potential applications as heat transfer fluids and novel media for green energy technologies.

Chapter 9 offers an overview of the polymerization of methyl methacrylate (MMA) to poly methyl methacrylate (PMMA) using ionic liquids, surfactants, and fluorous media as green solvents.

Chapter 10 analyzes the recent trends in converting fatty acids into green polymers and green composite materials in addition to providing insights to future trends.

Chapter 11 examines the work performed on the use of green solvents in the analysis of organic and inorganic substances by thin layer chromatography (TLC) during 2005–2010. The chapter discusses the usefulness of water, ethylene glycol, ethyl acetate, surfactants, etc., as green solvents in TLC analyses.

Chapter 12 explores the most important uses of dimethyl carbonate as solvent in supercapacitors, lithium batteries, and other emerging devices for energy storage and a dual behaviour as methylating and carbamoylating reagent.

Chapter 13 discusses supercritical carbon dioxide (SC-CO_2) extraction of triglycerides from powdered *Jatropha curcas* kernels and seeds, followed by CO_2 subcritical hydrolysis and supercritical methylation of the extracted (SC-CO_2) oil to obtain a 98.5% purity level of biodiesel.

Chapter 14 reviews experimental investigations on two major cooling features: convective and boiling heat transfer of nanofluids together with critical review of recent research progress in important areas of nanofluids. Nanofluids development along with their potential benefits and applications are also briefly discussed.

Aligarh, India

Ali Mohammad Inamuddin

Editors' bios

Ali Mohammad is Professor of Chemistry in the Department of Applied Chemistry, Faculty of Engineering and Technology, Aligarh Muslim University, Aligarh, India. His scientific interests include physico-analytical aspects of solid-state reactions, micellar thin layer chromatography, surfactants analysis, and green chromatography. He is the author or coauthor of 230 scientific publications including research articles, reviews, and book chapters. He has also served as editor of *Journal, Chemical and Environmental Research* being published from India since 1992 and as the Associate Editor for Analytical Chemistry section of the *Journal of Indian Chemical Society*. He has been the member of editorial boards of Acta Chromatographica, Acta Universitatis Cibiniensis Seria F. Chemia, Air Pollution, and Annals of Agrarian Science. He has attended as well as chaired sessions in various international and nation conferences. Dr. Mohammad obtained his M.Phil. (1975), Ph.D. (1978), and D.Sc. (1996) degrees from Aligarh Muslim University, Aligarh, India. He has supervised 51 students for Ph.D./M.Phil. and M.Tech. degrees.

Inamuddin is currently working as Assistant Professor in the Department of Applied Chemistry, Aligarh Muslim University (AMU), India. He received his Master of Science degree in Organic Chemistry from Chaudhary Charan Singh (CCS) University, Meerut, India, in 2002. He received his Master of Philosophy and Doctor of Philosophy degrees in Applied Chemistry from AMU in 2004 and 2007, respectively. He has extensive research experience in multidisciplinary fields of Analytical Chemistry, Material Chemistry, and Electrochemistry and, more specifically, Renewable Energy and Environment. He has worked on different projects funded by University Grant Commission (UGC), Government of India, and Council of Scientific and Industrial Research (CSIR), Government of India. He has received Fast Track Young Scientist Award of Department of Science and Technology, India, to work in the area of bending actuators and artificial muscles. He has published 28 research articles and four book chapters of international repute. He is editing one more book entitled *Ion-Exchange Technology: Theory, Materials and Applications* to be published by Springer, United Kingdom. Recently, he edited a book entitled *Advanced Organic-Inorganic Composites: Materials, Devices*

and Allied Applications published by Nova Science Publishers, Inc. He is presently working as editor in chief of *The Journal of Chemical and Environmental Research* published from The Muslim Association for the Advancement of Science, which is published in India. He has worked as a Postdoctoral Fellow leading a research team at Creative Research Initiative Center for Bio-Artificial Muscle, Hanyang University, South Korea, in the field of renewable energy, especially biofuel cells. He has also worked as Postdoctoral Fellow at Center of Research Excellence in Renewable Energy, King Fahd University of Petroleum and Minerals, Saudi Arabia, in the field of polymer electrolyte membrane fuel cells and computer fluid dynamics of polymer electrolyte membrane fuel cells. He is a life member of the *Journal of the Indian Chemical Society*.

Acknowledgments

We are most indebted to the grace of the Almighty "One Universal Being," who inspires the entire Humanity to knowledge and who has given us the required favor to complete this work.

These books are the outcome of the remarkable contribution of experts from various interdisciplinary fields of science and cover the most comprehensive, in-depth, and up-to-date research and reviews. We are thankful to all the contributing authors and their coauthors for their esteemed work. We would also like to thank all publishers, authors, and others who granted us permission to use their figures, tables, and schemes.

We would like to express our deep gratitude to Prof. T. Urushadze (Georgia State Agriculture University, Georgia), Prof. K. Aoki (Toyohashi University of Technology, Japan), Prof. Rajeev Jain (Jiwaji University, India), Prof. S. Shtykov (Saratov State University, Russia), Prof. M. M. Srivastava (Dayal Bagh University, India), Prof. M. C. Chattopadhyaya (Allahabad University, India), Prof. U. S. Roy (Visva-Bharti Santiniketan, India), Dr. Ajay Taneja (Dr. B. R. Ambedkar University, Agra, India), Prof. A. P. Gupta (Delhi Technological University, India), Prof. Anca Sipos (Lucian Blaga University of Sibiu, Romania), Prof. J. K. Rozylo (Maria Curie-Skloclowska, Poland), Prof. P. K. Sharma (JNV University, Jodhpur), Prof. Ravi Bhusan (I.I.T. Roorkee, India), Prof. Ibraheem (Jamia Millia Islamia, India), Prof. El-Sayed Ali Abdel-Aal (CMRDI, Cairo, Egypt), Dr. Ajay Taneja (Dr. B. R. Ambedkar University, India), Dr. Reeta Mehra (MDS University, Ajmer), Prof. M. Kidwai (University of Delhi, India), Prof. M. S. Chauhan (Himachal Pradesh University, India), Prof. A. S. Aswar (SGB Amaravati University, India), Dr. Anees Ahmad and Prof. Syed Ashfaq Nabi (Department of Chemistry, Aligarh Muslim University (A.M.U.), India), Prof. J. Sherma (USA) and Prof. M. Mascini (University of Firenze, Italy), Prof. Ishtiaq Ahmad and Prof. Rakesh Kumar Mahajan (Department of Chemistry, Guru Nanak Dev University, Amritsar, India), Dr. B. D. Malhotra (Scientist-F, NPL, New Delhi, India), Dr. Raju Khan (Scientist-C, NEIST, Assam, India), Prof. Seon Jeon Kim (Hanyang University, South Korea), Prof. Kenneth I. Ozoemena (University of Pretoria, South Africa), Prof. Saleem-ur-Rahman and Prof. S. M. J. Zaidi (King Fahd University of Petroleum and Minerals, Saudi Arabia), Prof. Gaber Eldesoky

and Prof. Zeid-AL-Othman (King Saud University, Saudi Arabia), Prof. Sheikh Raisuddin (Jamia Hamdard University, New Delhi, India), Byong-Hun Jeon (Yonsei University, South Korea), and Prof. A. I. Yahya (Nizwa University, Oman) for their valuable suggestions, guidance, and constant inspiration.

It is with immense gratitude that we thank our departmental colleagues Prof. M. Mobin, Prof. Asif Ali Khan, Prof. R. A. K. Rao, Prof. Faiz Mohammad, Dr. M. Z. A. Rafiqui, Dr. Abu Nasar, Dr. Rais Ahmad, and Dr. Yasser Azim, without whose continuous encouragement these books would have not been completed. Dr. Inamuddin cannot thank enough his friends and colleagues Dr. M. M. Alam (USA), Dr. Amir-Al-Ahmad (KFUPM, Saudi Arabia), Dr. Zafar Alam, Dr. Mu. Naushad, Dr. Mohammad Luqman, Dr. Salabh Jain, Dr. Hemendra Kumar Tiwari, Dr. Adesh Bhadana, Dr. Shakeel Ahmad Khan, Satish Singh, and others, for their timely help, good wishes, encouragement, and affections. The help received from our research group (Arshi Amin, Asma Siddiq, Nida Khan, and Sardar Hussain) is appreciatively acknowledged.

Finally, we feel short of words and full of emotions in thanking our family members for their constant inspiration and gracious support.

Ali Mohammad and Inamuddin

Contents

1 **Green Solvents Fundamental and Industrial Applications** 1
Shadpour Mallakpour and Zahra Rafiee

2 **Green Fluids Extraction and Purification of Bioactive Compounds from Natural Materials** 67
Chao-Rui Chen, Ying-Nong Lee, Chun-Ting Shen, Ling-Ya Wang, Chih-Hung Wang, Miau-Rong Lee, Jia-Jiuan Wu, Hsin-Ling Yang, Shih-Lan Hsu, Shih-Ming Lai, and Chieh-Ming J. Chang

3 **Green Solvents for Biocatalysis** 121
Marco P.C. Marques, Nuno M.T. Lourenço, Pedro Fernandes, and Carla C.C.R. de Carvalho

4 **Green Solvents for Pharmaceutical Industry** 147
Rosa María Martín-Aranda and J. López-Sanz

5 **Limonene as Green Solvent for Extraction of Natural Products** 175
Smain Chemat, Valérie Tomao, and Farid Chemat

6 **Glycerol as an Alternative Solvent for Organic Reactions** 187
V. Calvino-Casilda

7 **Water as Reaction Medium in the Synthetic Processes Involving Epoxides** 209
Daniela Lanari, Oriana Piermatti, Ferdinando Pizzo, and Luigi Vaccaro

8 **Ionanofluids: New Heat Transfer Fluids for Green Processes Development** 233
Carlos A. Nieto de Castro, S.M. Sohel Murshed, Maria J.V. Lourenço, Fernando J.V. Santos, Manuel L.M. Lopes, and João M.P. França

9 **Green Solvents for Polymerization of Methyl Methacrylate to Poly(Methyl Methacrylate)** 251
S. Krishna Mohan

10 Use of Fatty Acids to Develop Green Polymers and Composites 299
Dipa Ray and Ershad Mistri

11 Green Solvents in Thin-Layer Chromatography 331
Ali Mohammad, Inamuddin, Asma Siddiq, Mu. Naushad, and Gaber E. El-Desoky

12 Application of Dimethyl Carbonate as Solvent and Reagent 363
Belen Ferrer, Mercedes Alvaro, and Hermenegildo Garcia

13 Application of Supercritical Fluids for Biodiesel Production 375
Ikumei Setsu, Ching-Hung Chen, Chao-Rui Chen, Wei-Heng Chen, Chien-Hsiun Tu, Shih-Ming Lai, and Chieh-Ming J. Chang

14 Nanofluids as Advanced Coolants 397
S.M. Sohel Murshed and Carlos A. Nieto de Castro

Index 417

Contributors

Mercedes Alvaro Departamento de Química, Instituto Universitario de Tecnología Química, Universidad Politécnica de Valencia, Valencia, Spain

V. Calvino-Casilda Instituto de Catálisis y Petroleoquímica, CSIC, Catalytic Spectroscopic Laboratory, Madrid, Spain

Carla C.C.R. de Carvalho Department of Bioengineering, Instituto Superior Técnico (IST), Universidade Técnica de Lisboa, Lisbon, Portugal

Institute for Biotechnology and Bioengineering, Centre for Biological and Chemical Engineering, IST, Lisbon, Portugal

Carlos A. Nieto de Castro Centre for Molecular Sciences and Materials, Department of Chemistry and Biochemistry, Faculty of Sciences, University of Lisbon, Lisbon, Portugal

Chieh-Ming J. Chang Department of Chemical Engineering, National Chung Hsing University, Taichung, Taiwan, ROC

Farid Chemat Université d'Avignon et des Pays de Vaucluse, INRA, Avignon, France

Smain Chemat Centre de Recherche Scientifique et Technique en Analyses Physico-chimiques (CRAPC), Algiers, Algeria

Chao-Rui Chen Department of Chemical Engineering, National Chung Hsing University, Taichung, Taiwan, ROC

Chemical Engineering Division, Institute of Nuclear Energy Research, Lungtan, Taoyuan, Taiwan, ROC

Ching-Hung Chen Department of Chemical Engineering, National Chung Hsing University, Taichung, Taiwan, ROC

Wei-Heng Chen Department of Chemical Engineering, National Chung Hsing University, Taichung, Taiwan, ROC

Gaber E. El-Desoky Department of Chemistry, College of Science, King Saud University, Riyadh, Saudi Arabia

Pedro Fernandes Department of Bioengineering, Instituto Superior Técnico (IST), Universidade Técnica de Lisboa, Lisbon, Portugal

Institute for Biotechnology and Bioengineering, Centre for Biological and Chemical Engineering, IST, Lisbon, Portugal

Belen Ferrer Departamento de Química, Instituto Universitario de Tecnología Química CSIC-UPV, Universidad Politécnica de Valencia, Valencia, Spain

João M.P. França Centre for Molecular Sciences and Materials, Department of Chemistry and Biochemistry, Faculty of Sciences, University of Lisbon, Lisbon, Portugal

Hermenegildo Garcia Departamento de Química, Instituto Universitario de Tecnología Química CSIC-UPV, Universidad Politécnica de Valencia, Valencia, Spain

Instituto Universitario de Tecnología Química, Universidad Politécnica de Valencia, Valencia, Spain

Shih-Lan Hsu Education and Research Department, Taichung Veterans General Hospital, Taichung, Taiwan, ROC

Inamuddin Department of Applied Chemistry, Faculty of Engineering and Technology, Aligarh Muslim University, Aligarh, India

Shih-Ming Lai Department of Chemical and Materials Engineering, National Yunlin University of Science and Technology, Touliu, Yunlin, Taiwan, ROC

Daniela Lanari Laboratory of Green Synthetic Organic Chemistry, CEMIN–Dipartimento di Chimica, Università di Perugia, Perugia, Italy

Miau-Rong Lee Department of Biochemistry, China Medical University, Taichung, Taiwan, ROC

Ying-Nong Lee Department of Chemical Engineering, National Chung Hsing University, Taichung, Taiwan, ROC

Manuel L.M. Lopes Centre for Molecular Sciences and Materials, Department of Chemistry and Biochemistry, Faculty of Sciences, University of Lisbon, Lisbon, Portugal

J. López-Sanz Departamento de Química Inorgánica y Química Técnica, Universidad Nacional de Educación a Distancia, UNED, Madrid, Spain

Maria J.V. Lourenço Centre for Molecular Sciences and Materials, Department of Chemistry and Biochemistry, Faculty of Sciences, University of Lisbon, Lisbon, Portugal

Nuno M.T. Lourenço Department of Bioengineering, Instituto Superior Técnico (IST), Universidade Técnica de Lisboa, Lisbon, Portugal

Institute for Biotechnology and Bioengineering, Centre for Biological and Chemical Engineering, IST, Lisbon, Portugal

Shadpour Mallakpour Organic Polymer Chemistry Research Laboratory, Department of Chemistry, Isfahan University of Technology, Isfahan, I. R. Iran

Nanotechnology and Advanced Materials Institute, Isfahan University of Technology, Isfahan, I. R. Iran

Marco P.C. Marques Department of Bioengineering, Instituto Superior Técnico (IST), Universidade Técnica de Lisboa, Lisbon, Portugal

Institute for Biotechnology and Bioengineering, Centre for Biological and Chemical Engineering, IST, Lisbon, Portugal

Rosa María Martín-Aranda Departamento de Química Inorgánica y Química Técnica, Universidad Nacional de Educación a Distancia, UNED, Madrid, Spain

Ershad Mistri School of Materials Science and Engineering, Bengal Engineering and Science University, Shibpur, Howrah, West Bengal, India

Ali Mohammad Department of Applied Chemistry, Faculty of Engineering and Technology, Aligarh Muslim University, Aligarh, India

S. Krishna Mohan Material Development Division (MDD), Directorate of Engineering (DOE), Defence Research & Development Laboratory (DRDL), Hyderabad, India

S.M. Sohel Murshed Centre for Molecular Sciences and Materials, Department of Chemistry and Biochemistry, Faculty of Sciences, University of Lisbo, Lisbon, Portugal

Mu. Naushad Department of Chemistry, College of Science, King Saud University, Riyadh, Saudi Arabia

Oriana Piermatti Laboratory of Green Synthetic Organic Chemistry, CEMIN–Dipartimento di Chimica, Università di Perugia, Perugia, Italy

Ferdinando Pizzo Laboratory of Green Synthetic Organic Chemistry, CEMIN–Dipartimento di Chimica, Università di Perugia, Perugia, Italy

Zahra Rafiee Department of Chemistry, Yasouj University, Yasouj, I. R. Iran

Dipa Ray Department of Polymer Science & Technology, University of Calcutta, Kolkata, West Bengal, India

Fernando J.V. Santos Centre for Molecular Sciences and Materials, Department of Chemistry and Biochemistry, Faculty of Sciences, University of Lisbon, Lisbon, Portugal

Ikumei Setsu Department of Chemical Engineering, National Chung Hsing University, Taichung, Taiwan, ROC

Chun-Ting Shen Department of Chemical Engineering, National Chung Hsing University, Taichung, Taiwan, ROC

Asma Siddiq Department of Applied Chemistry, Faculty of Engineering and Technology, Aligarh Muslim University, Aligarh, India

Valérie Tomao Université d'Avignon et des Pays de Vaucluse, INRA, Avignon, France

Chien-Hsiun Tu Department of Applied Chemistry, Providence University, Taichung, Taiwan, ROC

Luigi Vaccaro Laboratory of Green Synthetic Organic Chemistry, CEMIN–Dipartimento di Chimica, Università di Perugia, Perugia, Italy

Chih-Hung Wang Department of Chemical Engineering, National Chung Hsing University, Taichung, Taiwan, ROC

Ling-Ya Wang Department of Chemical Engineering, National Chung Hsing University, Taichung, Taiwan, ROC

Jia-Jiuan Wu Department of Chemical Engineering, National Chung Hsing University, Taichung, Taiwan, ROC

Department of Nutrition, China Medical University, Taichung, Taiwan, ROC

Hsin-Ling Yang Department of Nutrition, China Medical University, Taichung, Taiwan, ROC

Chapter 1
Green Solvents Fundamental and Industrial Applications

Shadpour Mallakpour and Zahra Rafiee

Abstract The toxicity and volatile nature of many organic solvents, widely utilized in huge amounts for organic reactions, have posed a serious threat to the environment. Thus, the principles of green chemistry direct to use safer and environmentally friendly solvents. The alternative solvent systems such as water, supercritical fluids, ionic liquids, and fluorinated solvents are employed for a wide range of chemical applications including synthetic, extractions, and materials chemistry. This chapter provides an overview about the use of these alternative solvents in various academic and industrial fields.

1.1 Introduction

Most chemical reactions of organic substances conducted in the laboratory as well as in industry need conventional organic solvents as reaction media. The use of these organic solvents such as benzene, toluene, xylene, methanol, and ethanol in many industrial chemical processes is an issue of great environmental concern. These solvents are characterized by high volatility and limited liquidus ranges (at atmospheric pressure, ~85–200°C). As a result, about 20 million tons per year of volatile organic compounds (VOCs) are discharged into the atmosphere owing to

S. Mallakpour (✉)
Organic Polymer Chemistry Research Laboratory, Department of Chemistry, Isfahan University of Technology, Isfahan 84156-83111, I. R. Iran

Nanotechnology and Advanced Materials Institute, Isfahan University of Technology, Isfahan 84156-83111, I. R. Iran
e-mail: mallakpour84@alumni.ufl.edu; mallak@cc.iut.ac.ir; mallak777@yahoo.com

Z. Rafiee
Department of Chemistry, Yasouj University, Yasouj 75914-353, I. R. Iran

A. Mohammad and Inamuddin (eds.), *Green Solvents I: Properties and Applications in Chemistry*, DOI 10.1007/978-94-007-1712-1_1,

industrial processes [1], contributing to global climatic changes, air pollution, and human health-related issues [2]. Therefore, the concept of green chemistry is becoming one of the main goals of designing process and reaction [3, 4]. Green chemistry is the utilization of a set of principles that will help to reduce the use and generation of hazardous substances during the manufacture and application of chemical products. Use of safer solvents and auxiliaries is one of the important principles of green chemistry. However, there is no perfect green solvent that can apply to all circumstance. Over the past several years, a number of alternative solvents such as water, supercritical fluids (SCFs), fluorous solvents, and ionic liquids (ILs) have been reported [5–8]. The utilization of these alternative solvents has inherent benefits such as enhanced rates of reaction, more readily isolated side products and main product recovery.

1.2 Solvent-Free Reactions

Obviously, the solvents are the ideal medium to transport heat to and from endo- and exothermic chemical reactions. On dissolution of solutes, solvents break the crystal lattice of solid reactants, dissolve liquid or gaseous reactants, and exert a significant influence on reaction rates and on the positions of chemical equilibrium. Additionally, the reactants can interact efficiently when they are in a homogeneous solution, which facilitates stirring, shaking, or other forms of agitation, whereby the reactant molecules come together rapidly and continuously [9–11].

Furthermore, uniform heating or cooling of the mixture in solution can be carried out easily. The role of a solvent in respect of organic reactions is complex. A solvent has the power to increase or decrease the speed of a reaction, sometimes extremely. Changing the solvent can influence the rate of reaction, and it can even alter the course of reaction. This may manifest in altered yields and ratios of products. Therefore, a solvent can be deeply and inseparably associated with the process of an organic reaction through the solvation of the reactants, products, transition state, or other intervening species.

Environmental concerns about solvent-based chemistry have stimulated a renewed interest in the study of chemical reactions under solvent-free conditions. Solvent-free organic syntheses are gaining increasing attention from the viewpoints of green chemistry [12–15]. One noticeable route to reduce waste involves generation of chemicals from reagents in the absence of solvents. However, by far the best green alternative is, of course, to avoid the use of any solvent. Moreover, the exclusion of solvents can offer access to new products and materials that are not readily accessible by conventional solution methods. In many solvent-free reactions, one of the reagents is a liquid and is sometimes present in excess. This liquid is often acting as the solvent and making a homogeneous reaction solution. In other solvent-free reactions, there may be a liquid, for example, water, formed during the course of the reaction, and this liquid assists the reaction at the interface between the reagents and acts like a solvent.

In comparison to reactions in organic solvents, benefits of solvent-free reactions include (1) there is no reaction medium to collect, purify, and recycle; (2) the compounds formed are often sufficiently pure to avoid extensive purification by chromatography, and in some cases, there is not even the require for recrystallization; (3) sequential solvent-free reactions are possible; (4) the reactions are often quick, sometimes reaching completion in several minutes as compared to hours with organic solvents; (5) energy usage may be considerably lower; (6) functional group protection-deprotection can be avoided; (7) there may be lower capital outlay for equipment when setting up industrial processes; and (8) significant batch-size reduction and processing cost savings, production of solvent-free protocols is not only more environmentally benign but also more economically feasible [9, 16].

There are some disadvantages to solvent-free reactions, which can be minimized by developments in engineering reactor technology [17]. Objections to the use of solvent-less reaction conditions include the formation of hot spots and the possibility of runaway reactions. Instead of operating in the old paradigm, notably the employment of a reaction medium or solvent as a heat sink or heat transfer agent, consideration could be given to applying developments in reactor design either for continuous flow or for batch systems. If highly exothermic reactions are identified, which are otherwise suited to solvent-less conditions, the problem could be addressed through advanced reactor design. Another objection can be difficulties in handling solid or highly viscous material. Again this can be overcome by advances in engineering and innovative reactor design. Solvent-less reactions may be more suitable for small volume commodity chemicals rather than high throughput, although it is possible to envisage extrusion type continuous reactors [16].

Traditionally, solvent-free reactions have been performed using a mortar and pestle, but recently high speed ball milling (HSBM) has shown to be a more attractive alternative. In the HSBM method, a ball bearing is placed inside a vessel that is shaken at high speeds. The high speed achieved by the ball bearing has enough force to create an atmosphere which can facilitate a chemical reaction. The use of commercial ball mills has allowed these reactions to be scaled up to industrial levels. The use of this methodology can significantly reduce solvent waste [18].

1.2.1 Organic Synthesis

The development of solvent-free green processes has gained significant attention in organic synthesis owing to certain advantages such as high efficiency and selectivity, easy separation and purification, mild reaction conditions, reduction in waste, and benefits to the industry as well as the environment [11]. Solvent-free organic reactions based on grinding two macroscopic particles together mostly involve the formation of a liquid phase prior to the reaction, that is, formation of a eutectic melt of uniform distribution where the reacting components being in proximity are capable to react in a controlled way [19].

1.2.1.1 Protection/Deprotection Reactions

The protection/deprotection reaction sequences form an integral part of organic manipulations such as the preparation of monomer building blocks, fine chemicals, and precursors for pharmaceuticals, and these reactions often involve the utilization of acidic, basic, or hazardous and corrosive reagents and toxic metal salts.

Aldehydes and diols have been transformed into 1,3-dioxolane in excellent yields using oxorhenium(V) oxazoline as a catalyst under solvent-free conditions at mild temperatures (Scheme 1.1) [20]. The reaction is applicable to biomass-derived furfural and glycerol. The obtained cyclic acetals may find use as value-added chemicals and/or oxygenate fuel additives.

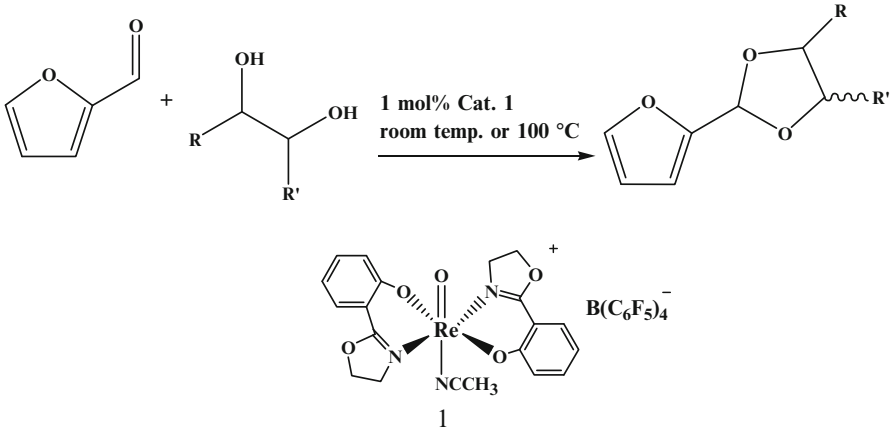

Scheme 1.1 1,3-Dioxolane formation from furfural and diols catalyzed by oxorhenium(V) 1 (Reprinted from Ref. [20]. With kind permission of The American Chemical Society)

In the presence of mesoporous strong acidic cation-exchange resin as the catalyst, solvent-free reaction between methacrolein and acetic anhydride led to the formation of 2-methylallylidene diacetate [21].

The solvent-free selective demethylation and debenzylation of aryl methyl/benzyl ethers have been reported using magnesium iodide to synthesize natural flavone and biphenyl glycosides [22].

1.2.1.2 Tishchenko Reaction

The conversion of aldehydes to their dimeric esters, better known as the Tishchenko reaction, has been known for more than a 100 years. This reaction is heavily used in industry, and it is inherently environmentally benign since it utilizes catalytic conditions and is 100% atom economic.

Using solvent-free ball-milling conditions, the Tishchenko reaction for aryl aldehydes has been developed in the presence of sodium hydride as the catalyst in high yields in 0.5 h [18].

1.2.1.3 Condensation Reactions

The formation of kinetic and thermodynamic enolates has been reported under solvent-free HSBM conditions. The thermodynamic or kinetic enolate in high selectivity was obtained using 2-methylcyclohexanone as the substrate and sodium hydroxide or lithium hexamethyldisilazide as the base [23].

The application of methanesulfonic acid/morpholine catalyst to Knoevenagel condensation of ketones with malononitrile has been described under solvent-free conditions [24]. Ylidenemalononitriles were obtained with good yields in short reaction time.

The mechanochemical reaction of malononitrile with various aldehydes was investigated to achieve quantitative stoichiometric conversion in absence of any solvents and catalysts in vibration and planetary ball mills as well as in a melt under microwave irradiation [25]. A successful quantitative conversion appeared to be substrate dependent.

The synthesis of jasminaldehyde has been reported by the condensation of 1-heptanal with benzaldehyde using chitosan as a solid base catalyst under solvent-free conditions (Scheme 1.2) [26]. Jasminaldehyde was obtained with maximum conversion of >99% and 88% selectivity at 160°C.

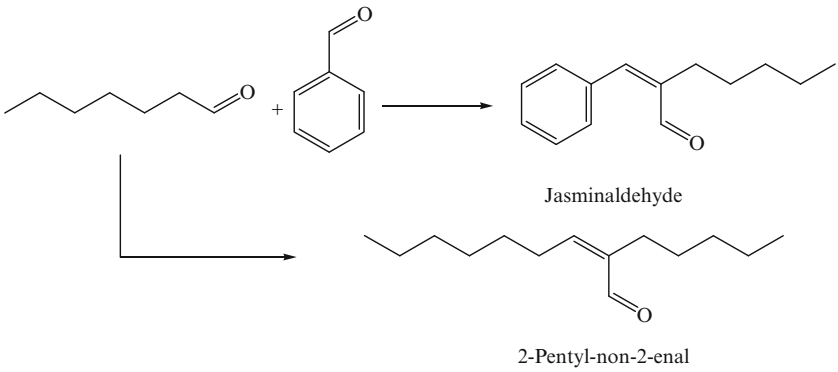

Scheme 1.2 Synthesis of jasminaldehyde (Reprinted from Ref. [26]. With kind permission of Elsevier)

The aryl-*14H*-dibenzo [*a.j*] xanthenes have been synthesized via the condensation of β-naphthol with aromatic aldehydes using cellulose sulfuric acid as a catalyst under solvent-free conditions in excellent yields and short reaction times [27].

1.2.1.4 Aldol Reaction

The direct aldol reaction has been extensively used in industry either in bulk or in fine chemical manufacture and pharmaceutical target production to prepare poly-oxygenated architectures from two carbonyl compounds.

The utilization of polystyrene-supported binam-prolinamide as catalyst has been studied in the aldol reaction between several ketones and aldehydes in the presence of benzoic acid under solvent-free or aqueous conditions [28]. Under these conditions, the corresponding aldol product was obtained in high yields, regio-, diastereo-, and enantioselectivity.

1.2.1.5 Sonogashira Reaction

The Sonogashira coupling of aryl halides with aryl and alkyl-substituted acetylenes has been studied without the use of copper or additional ligands and in the presence of $Pd(OAc)_2$ or $Pd(PPh_3)_4$ in combination with 1,4-diazabicyclo[2.2.2]octane as catalysts and base, respectively, in a planetary ball mill [29]. All coupling reactions exhibited high selectivity according to the desired Sonogashira products.

The solvent-free Sonogashira coupling of a variety of *para*-substituted aryl halides with trimethylsilylacetylene or phenylacetylene has been reported using HSBM [30]. Iodo- and bromo-substituted aromatics successfully undergo Sonogashira coupling, while chloro- and fluoro-substituted aryl compounds were unreactive.

1.2.1.6 Metathesis Reactions

The cross-metathesis of allyl benzene with *cis*-1,4-diacetoxy-2-butene and the ring-closing metathesis of diethyl diallylmalonate have been investigated under solvent-free media (Scheme 1.3) [31]. It was found that only the bulk conditions permitted a simple 25-fold reduction of the amount of metathesis catalyst for both studied metathesis reactions.

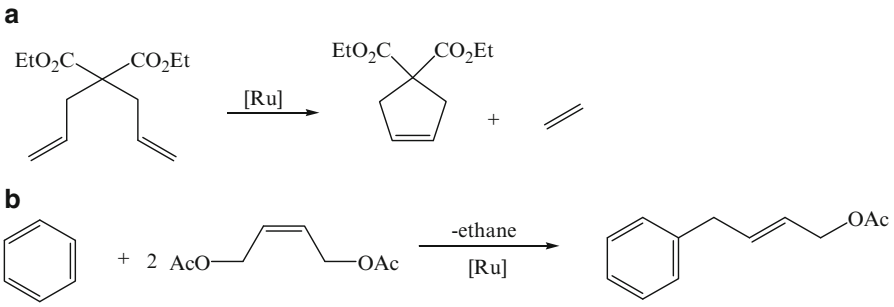

Scheme 1.3 (**a**) Ring-closing metathesis of diethyl diallylmalonate, (**b**) cross-metathesis of allyl benzene with *cis*-1,4-diacetoxy-2-butene (Reprinted from Ref. [31]. With kind permission of The Royal Society of Chemistry)

1.2.1.7 Diels-Alder Reactions

Diels-Alder reactions have been reported via heating a mixture of dicyclopentadiene and a dienophile under solvent-free conditions [32]. Cyclopentadiene, generated in situ, reacted with the dienophile in a thermodynamically controlled reaction.

The aza-Diels-Alder reaction between a variety of benzaldimines and Danishefsky's diene has been described in solvent-free conditions using porous zirconium hydrogen phosphate in the presence of sodium dodecyl sulfate at 30°C with excellent yields (Scheme 1.4) [33].

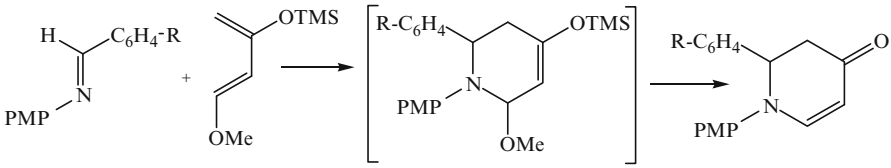

PMP = pOMe-C_6H_4
R = H, *p*Cl, *m*Cl, *o*Cl, *p*Br, *p*F, *p*NO_2, *p*SMe, *p*OMe, *p*Me, *p*CN

Scheme 1.4 Aza-Diels-Alder reaction of benzaldimines with Danishefsky's diene (Reprinted from Ref. [33]. With kind permission of Elsevier)

1.2.1.8 Heck Reaction

The use of Pd catalyst supported on 1,1,3,3-tetramethylguanidinium-modified molecular sieve SBA-15 has been introduced for Heck arylation of olefins with aryl halides in solvent-free conditions [34].

1.2.1.9 Mannich Reaction

The Mannich-type reactions provide one of the most classical and useful methods for the preparation of β-amino ketones and aldehydes, which constitute various pharmaceuticals, natural products, and versatile synthetic intermediates.

The one-pot three-component Mannich reaction of aromatic aldehydes, aromatic ketones, and aromatic amines has been investigated in the presence of an acidic catalyst, pyridinium trifluoroacetate under solvent-free conditions at room temperature [35]. The resulting β-amino carbonyl compounds were obtained in reasonably good yields.

1.2.1.10 Hydrogenation

The hydrogenation of quinolines has been reported using phosphine-free chiral cationic catalyst under solvent-free or highly concentrated conditions with high levels of enantioselectivities (>97%) and excellent yields only at 0.02–0.10 mol% catalyst loading [36].

The solvent-free hydrogenation of solid alkenes and nitro-aromatic compounds has been developed in the presence of Pd nanoparticles entrapped in aluminum oxyhydroxide to obtain corresponding alkanes and aromatic amines in nearly quantitative yields [37].

1.2.1.11 Esterification

The solvent-free direct esterification of various carboxylic acids with alcohols has been described in the presence of 5 mol% surfactant-catalyst, *para*-dodecylbenzene sulfonic acid, or copper para-dodecylbenzene sulfonate at room temperature with moderate to excellent yield [38].

1.2.1.12 Meyers' Lactamization

Meyers' lactamization is a typical bielectrophile-binucleophile reaction that produces quaternary centers, most of the time in a stereoselective manner. It is a well-known tool for the synthesis of natural products, especially alkaloids. This stereoselective reaction is the first step to access erythrina and amaryllidaceae alkaloids.

The solvent-free microwave-assisted synthesis of Meyers' bicyclic lactams has been introduced to obtain chiral lactams in good yield with high diastereoselectivity in short times [39].

1.2.1.13 Synthesis of 1,3,5-Triarylbenzene

1,3,5-Triarylbenzenes are very useful compounds used as electroluminescent materials, electrode devices, or conducting polymers. These compounds can also serve as versatile intermediates for the synthesis of buckminsterfullerenes, pharmaceuticals, and conjugated star polyaromatics.

The synthesis of 1,3,5-triarylbenzenes from acetophenones in the presence of *p*-toluenesulfonic acid as a catalyst under solvent-free conditions has been described as a chemoselective method without using any metal catalyst or solvent [40].

1.2.1.14 Hydroaminovinylation of Olefins

Olefin hydroaminovinylation is a valuable atom-economical domino reaction combining terminal alkene hydroformylation with in situ formation of enamine/imine, the firstly generated aldehyde reacting in a second step with an amine. When carrying out the reaction with secondary amines, hydroaminovinylation is often followed by another reaction, namely, the formation of amines through catalytic hydrogenation. A current industrial challenge is to stop the reaction at stage of the formation of the enamine. It is worth mentioning here that the linear selectivity in enamine mainly depends upon the regioselectivity of the hydroformylation step.

The solvent-free hydroaminovinylation of α-olefins using rhodium complexes containing hemispherical diphosphites based on a calix[4]arene skeleton as a catalyst allows access to high proportions of linear enamines/amines or imines [41]. A comparison of standard solvent vs. solvent-free reactions was undertaken. Under solvent-free conditions with an Rh/olefin ratio of 1:5,000, the reaction turned out to be about 15 times faster than when operating in toluene at the same Rh/olefin ratio and at an olefin concentration of 6.6 mol L^{-1}.

1.2.1.15 Synthesis of Diynes

The acid-treated K10 montmorillonite has been used as a catalyst in the solvent-free nucleophilic substitution of propargylic alcohols with alkynylsilanes to afford 1,4-diynes [42].

Using catalytic amounts of $CuCl_2$ and triethylamine, an environmentally friendly, efficient method has been reported for transforming terminal acetylenes into 1,3-diynes that are very important materials in the fields of biology and materials science [43].

1.2.1.16 Synthesis of Lactic Acid

The microwave-assisted conversion of sugar source into lactic acid has been reported under solvent-free conditions using alumina-supported potassium hydroxide (KOH) [44]. The reaction proceeded in yielding 75C% of lactic acid starting from D-glucose using 1.5 equiv of KOH at 180°C.

1.2.1.17 Synthesis of Thioglycosides

The synthesis of thioglycosides from a range of readily available glycosyl halides has been described in the ball mill in excellent yields [45].

1.2.1.18 Synthesis of Lipidyl-Cyclodextrins

The lipase-catalyzed amidation reaction between fatty acyl donors and mono-6-amino-permethylated β-cyclodextrin has been studied under solvent-free conditions [46].

1.2.1.19 Synthesis of Unsaturated Ketones

Under solvent-free conditions, unsaturated ketones have been synthesized with high conversion and good selectivity via Saucy-Marbet reactions of unsaturated alcohols with unsaturated ethers catalyzed by simple ammonium ILs [47].

1.2.1.20 Synthesis of Nitrotoluene

Solvent-free nitration of toluene has been carried out in the presence of sulfated titania as the catalyst at ambient temperature and atmospheric pressure to yield nitrotoluenes with good selectivity [48].

1.2.1.21 Synthesis of Quinazoline-2,4(1*H*,3*H*)-Diones

An efficient approach for the synthesis of quinazoline-2,4(1*H*,3*H*)-diones has been described via chemical fixation of carbon dioxide to 2-aminobenzonitriles catalyzed by low amounts of organic guanidines without the need of any additional solvent [49].

1.2.1.22 Synthesis of Monomethine Indocyanine Dyes

The solvent-free condensation of indole quaternary salts with 2-methylthio quinoline quaternary salt has been developed in the presence of triethylamine under microwave irradiation to obtain asymmetric monomethine indocyanine dyes (Scheme 1.5) [50].

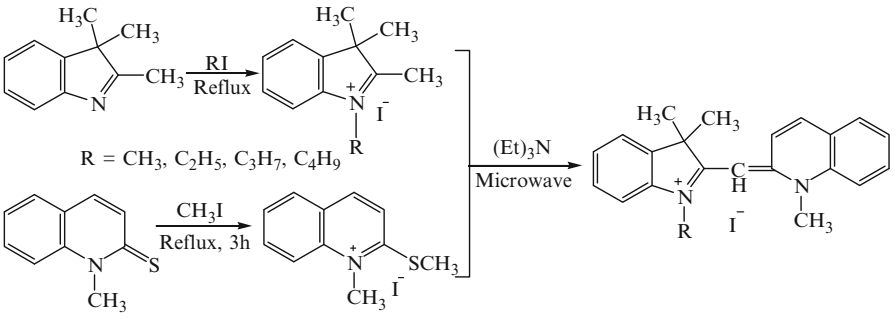

Scheme 1.5 Synthesis of monomethine indocyanine dyes (Reprinted from Ref. [50]. With kind permission of Elsevier)

1.2.1.23 Synthesis of Acetyl Salicylic Acid

The solvent-free synthesis of acetyl salicylic acid has been reported by acetylation of salicylic acid with acetic anhydride using solid acid catalysts such as sulfated metal oxides, zeolites, and K-10 clay [51]. Among the catalysts applied, nanocrystalline-sulfated zirconia exhibited highest catalytic activity and was found to be efficient in minimal amount to obtain acetyl salicylic acid crystals with excellent yield.

1.2.1.24 Oxidation

The asymmetric oxidation of sulfides has been investigated using aluminum (salalen) complex as a catalyst under solvent-free or highly concentrated conditions [52]. Under these conditions, optically active sulfoxides were resulted in high yields with excellent enantioselectivity in the presence of only 0.002–0.01 mol% catalyst.

Microwave-assisted oxidation of secondary alcohols using *tert*-butylhydroperoxide as the oxidant in the presence of copper(II) 2,4-alkoxy-1,3,5-triazapentadienato complexes under solvent-free conditions, providing ketones with >100% yields, >890 turnover numbers (TON)s, and >1,780 h^{-1} turnover frequencies (TOF)s, has been reported [53].

A facile method for the aerobic oxidation of benzyl alcohol to benzaldehyde has been developed using Pd/organoclay catalysts [54]. Under base- and solvent-free conditions and in the presence of 0.2 wt% Pd/organoclay, a remarkably high TOF (up to 6,813 h^{-1}) was obtained.

The supported gold nanoparticles as a green and reusable catalyst have been employed for the oxidation of various alcohols to the corresponding carbonyl compounds in the presence of aqueous hydrogen peroxide as an environmentally benign oxidant [55]. The reaction proceeded with good yields for nonactivated alcohols under base-free conditions.

The use of iodine-pyridine-*tert*-butylhydroperoxide as a catalytic system has been described for the solvent-free oxidation of benzylic methylenes and primary amines under quite mild conditions [56]. The oxidation of benzylic methylenes led to formation of the corresponding ketones in excellent yields with complete chemoselectivity, while the oxidation of primary amines was complete in several minutes, affording various nitriles in moderate to good yields.

The solvent-free oxidation of benzyl alcohol has been studied using supported gold palladium bimetallic nanoparticles and comparing their activity and performance with monometallic catalysts [57]. It found that the Au-Pd catalysts are all more active than the corresponding monometallic supported Au or Pd catalysts.

Ni^{2+}-containing IL, 1-methyl-3-[(triethoxysilyl)propyl] imidazolium chloride immobilized on silica has been developed as catalyst for the oxidation of styrene to benzaldehyde in the presence of H_2O_2 as the oxidant under solvent-free conditions as well as in the presence of acetonitrile [58]. Under solvent-free conditions, the conversion of styrene could reach 18.5% and the selectivity to benzaldehyde could be as high as 95.9%.

The solvent-free aerobic oxidation of α-isophorone to ketoisophorone has been reported using *N*-hydroxy phthalimide (NHPI) as the catalyst without a cocatalyst at 60°C for 10 h (Scheme 1.6) [59]. Under these conditions, the isomerization process of α-isophorone to β-isophorone was eliminated.

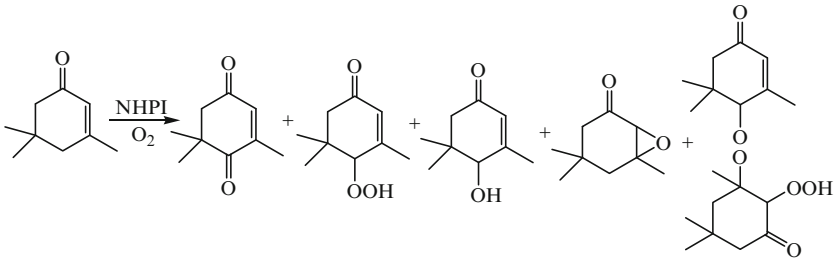

Scheme 1.6 The oxidation of α-isophorone catalyzed by NHPI with dioxygen (Reprinted from Ref. [59]. With kind permission of Elsevier)

The use of nanosize gold particles deposited on MgO with excellent reusability for the solvent-free selective oxidation of benzyl alcohol to benzaldehyde, providing very high catalytic activity with nearly 100% conversion in a short reaction period (0.5 h), has been reported [60].

Layered Sn(IV) phosphonate materials have been designed as catalysts for the Baeyer-Villiger oxidation of aromatic aldehydes using 30% aqueous H_2O_2 solution as the oxidant under solvent-free conditions [61].

The solvent-free oxidative dehydrogenation of **γ**-terpinene in the presence of alumina as a grinding auxiliary, with $KMnO_4$ as the oxidant in a planetary ball mill, led to formation of *p*-cymene in quantitative yields after 5 min [62].

1.2.1.25 Reduction

The catalytic use of IL-supported organotin reagent (down to 0.1 mol%) has been reported for the direct solvent-free reductive amination of aldehydes and ketones mediated by phenylsilane [63]. This method facilitated purification of the products, thus minimizing the contamination by tin.

1.2.1.26 Synthesis of Heterocyclic Compounds

A solvent-free process has been developed for the synthesis of a series of NH-pyrazoles involving the reaction of β-dimethylaminovinylketones and hydrazine sulfate in solid state on grinding, using *p*-toluenesulfonic acid as a catalyst [64]. The short reaction time coupled with the simplicity of the reaction procedure made this method one of the most efficient methods for the synthesis of this class of compounds.

1,4-Dihydropyridine derivatives have been synthesized from various aldehydes, β-dicarbonyl compounds, and amines using supported heteropoly acids as catalysts under solvent-free conditions [65].

1.2.2 Inorganic and Materials Synthesis

A facile chemical method has been developed for the fabrication of nonionic nanofluid hybrid material of multiwall carbon nanotubes (MWNT)s decorated with silica nanoparticles under solvent-free conditions [66]. Colloidal silica was dispersed in a 3-(trimethoxysilyl)-1-propanethiol aqueous solution to enhance silica nanoparticle dispersion and then the solvent-free nonionic nanofluid hybrid material consisting of MWNTs and silica nanoparticles were fabricated by carboxylic MWNTs and poly(ethylene oxide)-*block*-poly(propylene oxide)-*block*-poly(ethylene oxide).

The synthesis of magnetite octahedral microcrystals of Fe_3O_4 has been investigated from the thermolysis of single $Fe_3(CH_3COO)_6(OH)_2CH_3COO$ precursor in a closed reactor at 700°C without using catalyst under solvent-free conditions [67].

The one-pot, solvent-less synthesis process for the fabrication of lanthanum hydroxycarbonate superstructures decorated with carbon spheres has been reported which involved the thermal dissociation of the lanthanum acetate hydrate single precursor using autogenic pressure at elevated temperature [68].

The solvent-free sublimation has been used for the preparation of fibrillar nanostructures from low molecular weight organogelators with one-dimensional morphologies [69]. This methodology seems to be highly convenient in order to avoid uncontrollable solvent effects.

The solvent-free production of nanoscale zero-valent iron (nZVI) has been reported using a precision milling system with major physicochemical properties consistent with, in some cases superior to, those of the chemically synthesized [70]. The proposed milling method is completely scalable for large quantity production of nZVI, delivers nearly 100% yield of iron, uses no hazardous materials, and produces no waste in the production process. A series of reactive hydrogen-bonded crystalline supermolecules has been formed via solvent-free and liquid-assisted grinding [71].

High-density Co_3O_4 nanowire arrays have been produced via a simple, solvent-free synthesis method using narrow pores of the anodic alumina oxide template [72]. An amorphous coordination polymeric networked Pd(II) catalyst based on 3,5-bis(diphenylphosphino)benzoic acid has been synthesized through a mechanochemistry approach [73].

1.2.3 Polymerization

The living and highly stereoselective ring-opening polymerization of rac-lactide under solvent-free conditions using zirconium- and hafnium-based initiators supported by amine tris(phenolate) ligands, providing an unprecedented combination of high stereocontrol and high activity in <30 min, has been reported [74]. The solvent-free polymerization of cyclic ester monomers and lactides has been studied using bis(imino)phenoxide complexes of zirconium as initiators [75]. *N*-Heterocyclic carbine [1,3-bis-(diisopropyl)imidazol-2-ylidene] has been employed for the metal- and solvent-free ring-opening polymerization of propylene oxide at 50°C to afford well-defined α,ω-heterodifunctionalized poly(propylene oxide) oligomers [76].

The solvent-free lipase-catalyzed synthesis of long-chain starch esters with a high degree of substitution has been reported using microwave heating [77].

1.3 Water

Water is a green solvent with much to contribute to this steadily growing field. Organic synthesis in water is a rapidly growing area of research since it holds great promise for the future in terms of the cheap and environmentally friendly production of chemicals [78–82]. The use of water has numerous benefits in terms of reactivity and selectivity that are not achieved in organic solvents. In addition, in water, phase separation is facile because most of the organic compounds are not soluble in water, therefore, can easily be separated from aqueous phase. Water, due to its small size, high polarity, and the three-dimensional hydrogen-bonded network system of bulk water, offers some unique properties, which include large cohesive energy density, a high surface tension, and hydrophobic effect. Another important aspect is the development of chemical reactions in water that can achieve the desired chemical transformations without the need for the protection-deprotection of reactive functional groups or for generation of anhydrous conditions. This fact is particularly important in industrial scale-up processes to replace the use of hazardous and flammable organic solvents. Water is, obviously, the cleanest and safest available solvent, but it is not commonly used, as most organic compounds are poorly soluble in water. This issue can be overcome by using superheated water (>100°C) under microwave irradiation. Water is a good absorber for microwave energy and has been successfully employed as a solvent for various microwave-promoted organic syntheses.

1.3.1 Organic Synthesis

1.3.1.1 Suzuki-Miyaura Reactions

The ligand-free Suzuki-Miyaura reactions using stilbene-4,4′-bis[(1-azo)-3,4-dihydroxybenzene]-2,2′-disulfonic acid diammonium salt as a promoter in water have been reported. The desired carbon-carbon bond formation proceeded under mild conditions with high efficiency and good functional group tolerance [83].

The one-pot chemoenzymatic enantioselective synthesis of chiral biaryl alcohols has been reported via Suzuki-Miyaura cross-coupling catalyzed by protein-stabilized palladium nanoparticles under aerobic conditions in water [84]. The highly efficient heterogeneous palladium catalyst has been prepared for the Suzuki-Miyaura cross-coupling reaction in water via a simple procedure [85]. The polystyrene-supported palladium catalyst can be recycled up to ten times without significant loss of activity. The Suzuki-Miyaura C-C cross-coupling reactions of several *para*-substituted bromobenzenes with excellent yields have been reported using $[Pd(HQS)_2]$ (HQS = 8-hydroxyquinoline-5-sulfonic acid) as a catalyst in neat water under relatively mild conditions in the absence of phosphine or other additive [86].

The palladium-catalyzed Suzuki-Miyaura reactions of potassium aryltrifluoroborates with 5-iodo-1,3-dioxin-4-ones using n-Bu_4NOH as base in water have been utilized to get 5-aryl-1,3-dioxin-4-ones in good yields [87]. The obtained products were transformed into corresponding α-aryl-β-ketoesters by reaction with an alcohol in the absence of solvent.

1.3.1.2 Michael Reactions

The highly enantioselective Michael addition reactions of aldehydes with nitroolefins have been developed in the presence of water-soluble catalyst di(methylimidazole) prolinol silyl ether using water as solvent in high yields (Scheme 1.7) [88].

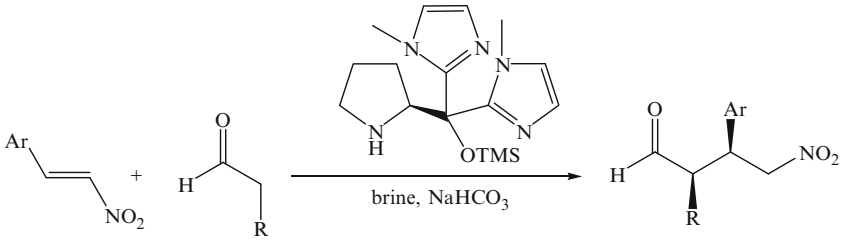

Scheme 1.7 Organocatalytic asymmetric Michael reaction using aldehydes and nitroolefins (Reprinted from Ref. [88]. With kind permission of The American Chemical Society)

Microwave-assisted Mannich reaction for highly stereoselective synthesis of β-aminoketones has been studied by controlling the steric hindrance of the substituents using potassium carbonate as a catalyst and water as the reaction medium (Scheme 1.8) [89].

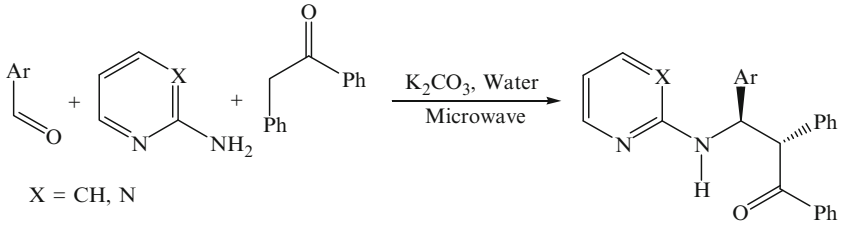

Scheme 1.8 The synthesis of β-aminoketones (Reprinted from Ref. [89]. With kind permission of The Royal Society of Chemistry)

The Michael addition reactions of β-ketoesters have been reported using 4-(dimethylamino)pyridine-related organocatalysts such as 4-(didecylamino)pyridine in water in the absence of cosolvents to afford Michael adducts in good to high yields [90]. The nitro-Michael addition of indoles and pyrroles has been developed using a combination of water and microwave irradiation without any catalyst [91].

1.3.1.3 Knoevenagel Reactions

4-Aza-1-azoniabicyclo[2.2.2]-octane-base ILs have been employed as recyclable catalysts for the Knoevenagel condensation reactions of a wide range of aldehydes (aromatic/aliphatic/heterocyclic/α,β-unsaturated) and aliphatic ketones using water as solvent [92]. The tetraketones have been synthesized via a simple, environmentally friendly, tandem Knoevenagel condensation and Michael addition of cyclic-13-diketones and a variety of aldehydes in water [93]. In this method, water as solvent itself catalyzes the reaction by hydrogen bonding, hence avoiding the utilization of any other catalysts.

1.3.1.4 Aldol Reactions

The direct asymmetric aldol reaction of various cyclic ketones with aryl aldehydes has been developed using primary-tertiary diamine-Brønsted acid as a catalyst in the presence of water [94]. The direct asymmetric aldol reactions between cyclic ketones and aromatic aldehydes have been reported using natural tryptophan as a catalyst in the presence of water [95]. Solvent studies demonstrated that water is the best reaction medium for the described direct asymmetric aldol reactions, and the desired products can be obtained with excellent *anti*selectivity and good enantioselectivity.

The direct aldol reactions of cyclic ketones with several aromatic aldehydes have been described in the presence of 4-*tert*-butyldimethylsiloxy-substituted organocatalysts. The resulting products were obtained with excellent diastereoselectivity and enantioselectivity using low-catalyst loadings (only 3 mol%), without using any additional additives [96].

1.3.1.5 Telomerisation Reactions

Two-phase telomerisation reactions with methanol, diethylamine, ethylene glycol, and glycerol and recycling of the homogeneous palladium catalysts have been studied using water as a solvent [97].

1.3.1.6 Amination Reactions

The palladium-catalyzed allylic aminations of allylic alcohols have been described in the presence of nanomicelle-forming amphiphile polyoxyethanyl α-tocopheryl sebacate in pure water [98].

1.3.1.7 Alkylation

The direct alkylation of amines with alcohols has been described using $[Cp^*IrI_2]_2$ (Cp* = pentamethylcyclopentadienyl) as a catalyst in water in the absence of base or other additives [99].

The direct mono-*N*-alkylation of aromatic amines has been described by alkyl halides in water under microwave irradiation without any catalyst [100].

1.3.1.8 Cycloaddition Reactions

The 1,3-dipolar cycloaddition reactions of several hydrophobic nitrones have been investigated in both homogenous organic solutions and aqueous suspensions [101]. Reactions in water suspensions exhibited great rate accelerations over homogenous solutions. Small changes were also observed to the stereoselectivity of the reactions. Hydrophobic interactions are invoked for the observed behavior.

1.3.1.9 Hydroxylation

Copper-catalyzed direct hydroxylation of aryl halides has been investigated in the presence of lithium pipecolinate as a ligand in water with yields up to 92% [102].

1.3.1.10 Alkynylation

Alkynylation of terminal alkynes with aryl halides has been demonstrated in the presence of perfluoro-tagged palladium nanoparticles immobilized on silica gel under aerobic, copper-, and phosphine-free conditions in water with high yields [103].

1.3.1.11 Condensation Reactions

A one-pot three-component condensation of an amine, carbon disulfide, and an aryl iodide or styrenyl bromide has been reported using copper nanoparticles as a catalyst in water under ligand- and base-free conditions. The (*E*)- and (*Z*)-styrenyl bromides produced the corresponding (*E*)- and (*Z*)-styrenyl dithiocarbamates in high diastereoselectivities [104].

1.3.1.12 Diels-Alder Reactions

Extended triptycenes have been prepared with high efficiencies via Diels-Alder reactions of anthracene and endoxides in water under microwave radiation (Scheme 1.9) [105].

C_2-symmetric 3,3′-dialkoxy-2,2′-bipyrrolidines catalysts have been employed for asymmetric Diels-Alder reactions of α,β-unsaturated aldehydes [106]. Lower chemical yields and enantioselectivity were attained in organic solvents, while, using water as solvent, the reaction rate was remarkably accelerated. The reaction completed within 2 h and afforded the Diels-Alder adduct in 95% yield with good enantioselectivity and moderate exoselectivity.

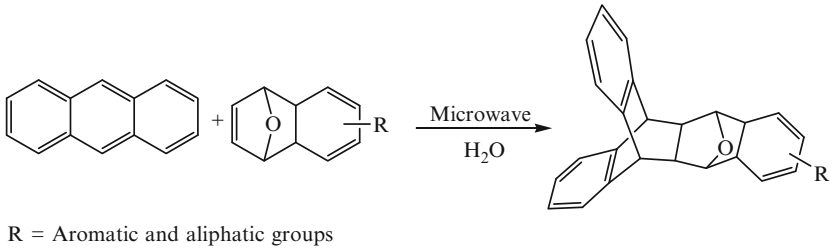

Scheme 1.9 Diels-Alder reactions between anthracene and various endoxides under microwave radiation in water (Reprinted from Ref. [105]. With kind permission of Elsevier)

The synthesis of β-aminophosphoryl compounds has been reported via the aza-Michael reaction in water without using catalyst or cosolvent in excellent yields over short reaction times [107].

1.3.1.13 Mannich Reactions

The diastereoselective synthesis of β-amino ketones has been investigated via three-component Mannich-type reaction of benzaldehyde, aniline, and cyclohexanone using $Cs_{2.5}H_{0.5}PW_{12}O_{40}$ as a catalyst in water [108].

The one-pot three-component Mannich reaction involving aldehydes, aromatic amines, and cycloalkanones has been studied using boric acid and glycerol in water to obtain major syn diastereoselectivity [109]. These reactions, which proceed very slowly in organic solvents, become quite faster in water.

1.3.1.14 Condensation Reactions

The synthesis of benzo[*c*]xanthene derivatives has been investigated via a one-pot condensation of α-naphthol, aldehydes, and cyclic 1,3-dicarbonyl compounds in the presence of proline triflate as a catalyst in water with good yields [110].

The three-component condensation reactions of primary amines with alkyl propiolates have been reported in the presence of alloxan derivatives in water for the high-yielding preparation of alkyl 2-(5-hydroxy-2,4,6-trioxohexahydro-5-pyrimidinyl)-3-(alkyl or arylamino)-2-propenoates [111].

1.3.1.15 Sonogashira-Hagihara Reaction

The palladium-catalyzed Sonogashira-Hagihara of aryl halides coupling has been reported using 2-aminophenyl diphenylphosphinite ligand in water under copper-free condition [112].

The Sonogashira coupling of various aryl halides with terminal acetylenes has been developed in the presence of an amphiphilic polystyrene-poly-(ethylene glycol) resin-supported palladium-phosphine complex in water under copper-free conditions to offer the corresponding biarylacetylene derivatives in high yields [113].

1.3.1.16 Hydrolysis

The oxidative hydrolysis of cyclic acetals by (diacetoxy)iodobenzene ($PhI(OAc)_2$) in the presence of lithium bromide (LiBr) in water, providing the corresponding hydroxyalkyl carboxylic esters in good to excellent yields at a short reaction time under mild reaction conditions, has been reported (Scheme 1.10) [114].

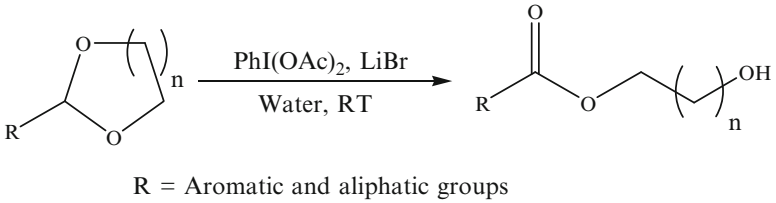

Scheme 1.10 Oxidation of acetals with $PhI(OAc)_2$/LiBr in water (Reprinted from Ref. [114]. With kind permission of Elsevier)

1.3.1.17 Aza-Friedel-Crafts Reaction

The synthesis of 1-naphthoyl tetrahydroisoquinolines has been reported via an aza-Friedel-Crafts reaction under solvent-free conditions or in/on water with 100% atom economy in the absence of any additional catalyst (Scheme 1.11) [115]. Yields were increased using water as a solvent.

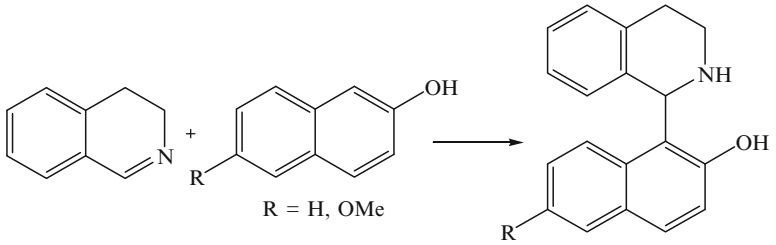

Scheme 1.11 The reaction between 3,4-dihydroisoquinoline and 2-naphthol or 6-methoxy-2-naphthol (Reprinted from Ref. [115]. With kind permission of Elsevier)

1.3.1.18 Cyanation of Aryl Iodides

The cyanation of aryl iodides has been investigated using copper iodide as the catalyst, $K_4[Fe(CN)_6]$ as the cyanide source, and small quantities of water and tetraethylene glycol as the solvent within 30 min under microwave heating at 175°C [116].

1.3.1.19 Suzuki Reaction

The Suzuki cross-coupling reaction in water in the presence of a chitosan-g-(methoxy triethylene glycol)- or (methoxy polyethylene glycol)-supported palladium (0) catalyst has been described without additional phase transfer reagents [117].

1.3.1.20 Cycloaddition Reactions

The 1,3-dipolar cycloadditions of a galacto-configured cyclic nitrone with arabino- or galacto-furanosides containing a C-vinyl or O-allyl substituent have been found to produce galactofuranose-disaccharide analogues having a 1,4-dideoxy-1,4-imino-D-galactitol moiety [118]. The cycloadditions could be performed efficiently and stereoselectively in water using unprotected nitrone and sugar-derived dipolarophile as reaction partners.

1.3.1.21 Aminohalogenation Reaction

The aminohalogenation reaction of olefins has been reported with $TsNH_2$ and *N*-bromosuccinimide as nitrogen and bromine sources, respectively, in pure water in the presence of $PhI(OAc)_2$ as a catalyst [119]. This aqueous reaction permitted the aminobromination of olefins to proceed smoothly and efficiently, giving the useful vicinal bromoamines with high yields and selectivity.

1.3.1.22 Photooxygenation of Furans

The dye-sensitized photooxygenation of furans has been investigated in aqueous solution in the presence of ILs [120]. The reaction was generally selective, and the final products derive from rearrangement of the intermediate endoperoxides, depending mainly on the polarity and/or nucleophilic nature of the solvent.

1.3.1.23 Electrooxidation

The *N*-oxyl-mediated electrooxidation of nanoemulsion-forming alcohols has been reported in the oil-in-water nanoemulsion system to form the corresponding carboxylic acids [121].

1.3.1.24 Synthesis of 1,8-Dioxo-9,10-Diaryldecahydroacridines

The Brønsted acidic imidazolium salts containing perfluoroalkyl tails have been employed as a highly effective catalyst for three-component one-pot synthesis of 1,8-dioxo-9,10-diaryldecahydroacridines in water in good to excellent yields [122].

1.3.1.25 Oxidation

The production of Acid Blue 9 has been reported via catalytic oxidation using hydrogen peroxide as an oxidant and iron phthalocyanine sulfonamide as a catalyst in aqueous media at room temperature within 3 h in high yield (Scheme 1.12) [123]. The reaction was successfully scaled up in a 3,000-L reactor, and the product was free from toxic metal impurities.

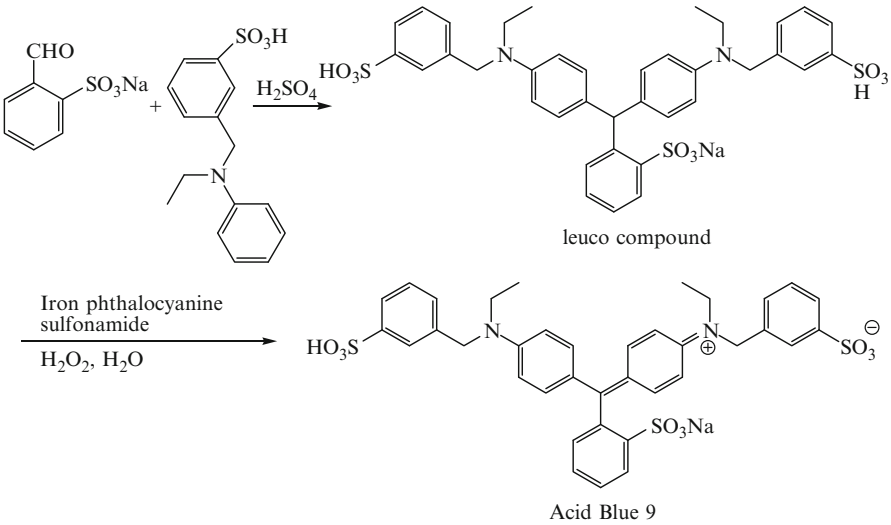

Scheme 1.12 The production process for Acid Blue 9 (Reprinted from Ref. [123]. With kind permission of The American Chemical Society)

Selective aerobic oxidation of styrene to benzaldehyde has been investigated using a green and water-soluble palladium(II) complex as a catalyst under neutral, chloride-, and base-free conditions in aqueous phase [124].

The metal-free aqueous oxidation of alcohols using the combination of the trivalent iodine reagents and tetraethylammonium bromide in water, offering ketones without racemization in good yields, has been reported [125].

The mild and selective aerobic oxidation of benzyl alcohols to benzaldehydes has been developed in water catalyzed by aqua-soluble multicopper(II) triethanolaminate compounds using air (or O_2) as oxidant at 50°C [126]. Molar yields of benzaldehydes up to 99% with high selectivity were reported. Hydroxyapatite-supported gold nanoparticles have been employed for the oxidation of a wide range of silanes into the corresponding silanols using water [127].

1.3.1.26 Reduction

A comparison between the microorganism- and ruthenium-based catalysts has been undertaken at the enantioselective reduction of ketoesters in water [128].

1.3.1.27 Synthesis of Heterocyclic Compounds

A series of 2-imidazolines with ability to inhibit the activity of the A and B isoforms of monoamine oxidase has been synthesized by condensation of aldehydes and ethylenediamine in the presence of *N*-bromosuccinimide in water as solvent under ultrasonic irradiation in high yields within short reaction times [129].

Microwave-assisted synthesis of indole and azaindole derivatives has been described via cycloisomerization of 2-alkynylanilines and alkynylpyridinamines in the presence of amines or catalytic amounts of neutral or basic salts in water (Scheme 1.13) [130].

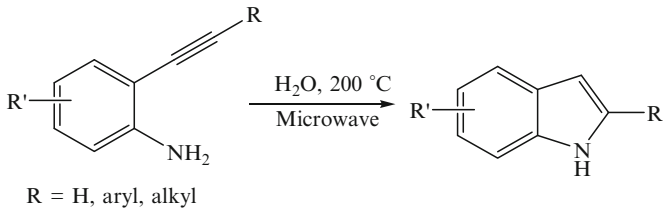

Scheme 1.13 Synthesis of indole derivatives (Reprinted from Ref. [130]. With kind permission of Elsevier)

Microwave-promoted synthesis of C6-cyclo secondary amine-substituted purine analogues in neat water, providing a rapid, efficient, and convenient method for the preparation of acyclic nucleosides, has been recommended (Scheme 1.14) [131].

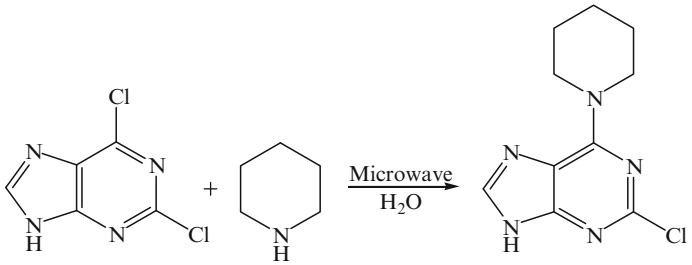

Scheme 1.14 Microwave promoting nucleophilic substitution reaction of 2,6-dichloropurine with piperidine (Reprinted from Ref. [131] with kind permission of The Royal Society of Chemistry)

Microwave-assisted three-component reaction between an aromatic aldehyde, aniline, and mercaptoacetic acid has been reported for the synthesis of benzo[*e*][1, 4]thiazepin-2(1*H*,3*H*,5*H*)-ones in aqueous media (Scheme 1.15) [132].

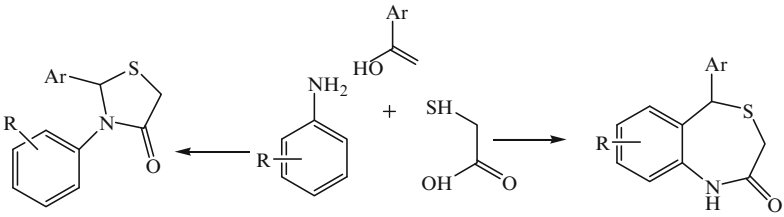

Scheme 1.15 The synthetic route to the benzothiazepinones and thiazolidinones (Reprinted from Ref. [132]. With kind permission of The Royal Society of Chemistry)

The one-pot synthesis of a series of polycyclic-fused isoxazolo[5,4-*b*]pyridines has been studied under microwave irradiation in water and organic solvents, without use of additional reagent or catalyst (Scheme 1.16) [133]. Water showed a superior advantage not only in promoting the reaction but also in isolation procedure, and the best yield was achieved.

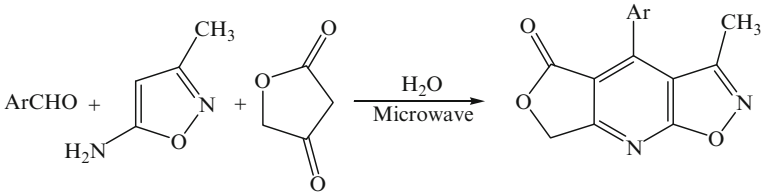

Scheme 1.16 The synthesis of novel polycyclic-fused isoxazolo[5,4-*b*]pyridines under microwave irradiation in water (Reprinted from Ref. [133]. With kind permission of The American Chemical Society)

1.3.2 Synthesis of Metal Nanoparticles

The synthesis of silver nanoparticles as well as other noble metals has been described using glutathione as both a reducing and capping agent under microwave irradiation in aqueous medium within 30–60 s at a power level as low as 50 W [134].

1.4 Supercritical Fluids

Supercritical fluid (SCF) technology has rapidly grown as an alternative to some of the conventional methods of extraction, separation, reaction, fractionation, materials processing, particle formation processes, and analysis [135–148]. SCFs may be defined as the state of a compound, mixture, or element above its critical pressure (P_c) and critical temperature (T_c), but below the pressure required to condense it into a solid. In this region, the SCF exists in an intermediate phase between liquid and

gas phases. The macroscopic appearance of the SCF is a homogeneous and opalescent system without phase separation (single phase) because of identical values of the densities of the gas and liquid. Nevertheless, a SCF does not show a specific aggregation state. These fluids have liquid-like density with gas-like transport properties and moderate solvent power, which moreover can be adjusted with changes in pressure and temperature.

Carbon dioxide (CO_2), water, ethane, ethene, propane, xenon, ammonia, nitrous oxide, and fluoroform are some of the significant compounds useful as SCFs. CO_2 is the most common candidate for use as a SCF due to its low toxicity, flammability, and cost, ready availability, stability, and environmental acceptability. In addition, the critical point conditions of 304 K (31°C) and 74 bar are readily attainable. As such, supercritical CO_2 (SC-CO_2) has been employed in a diverse range of applications, including polymer synthesis, drug delivery, powder production (e.g., proteins and ceramics), and powder coating. Water has good environmental and other advantages, although need more extreme conditions of T_c 647 K (374°C) and P_c 221 bar. SCF water is being used, at a research level, as a medium for the oxidative destruction of toxic waste. There is a particular attention in both supercritical and near-critical water owing to the behavior of its polarity.

The properties of SCFs (e.g., solubility, diffusivity, viscosity, and heat capacity) are different from those of ordinary liquids and gases and are tunable simply by changing the pressure and temperature. In particular, the density and viscosity change drastically at conditions close to the critical point.

The expected advantages of the reactions in SCFs are the increased reaction rates and selectivity resulting from the high solubility of the reactant gases, rapid diffusion of solvents, weakening of the solvation around the reacting species, and the local clustering of reactants or solvents. It is also fascinating to note, in a practical sense, that these fluids are easily recycled and allow the separation of dissolved compounds by a gradual release of pressure.

1.4.1 Extraction

The SCF extraction (SCFE) of lycopene from tomato juice has been studied without the need to dry the raw material [149]. The extraction of microbial phospholipid fatty acids (PLFA)s from activated sludge has been described using SC-CO_2 extraction [150]. It was found that the application of SC-CO_2 extraction to microbial PLFA analysis has the potential to drastically reduce the amount of solvent used and extraction time needed and could simplify the procedure.

The mesoporous TiO_2 crystals have been synthesized via the combination of a sol–gel process and surfactant-assisted templating method [151]. Either conventional calcinations or SC-CO_2 extraction was applied to remove surfactant from the as-synthesized material. The results showed that the SCFE approach provided materials with good crystallinity, considerably higher mesoporosity, and environmentally friendly.

The extraction of phenolic and phosphorus antioxidants from low-density and high-density polyethylene has been described using SCFE, conventional reflux, and automatic Soxhlet system [152]. SCFEs of polymer were successfully carried out, and these were associated with better recoveries (>94.9%), simplicity, and speed of the extraction process. The extraction of trivalent lanthanides with oxa-diamides has been described in SC-CO_2 [153].

1.4.2 Organic Synthesis

The SCFs have been employed as reaction media in the ethylbenzene disproportionation on ZSM-5 [154]. The oxidation of oleic acid with ozone and potassium permanganate has been studied in SC-CO_2 [155]. The Schiff base macrocycles have been synthesized using SC-CO_2 as both solvent and acid catalyst [156]. The designed SC route is not only a greener and safer method than the classical procedure but also a one-stage process that would lead to high yield, thus allowing a sustainable use of resources. The synthesized Schiff bases had an empty core, not filled with solvent molecules, since the SC-CO_2 was eliminated as a gas during depressurization.

The production of linear alkane has been described with >99% selectivity via hydrogenative ring opening of a furfural-derived compound in SC-CO_2 using Pd/Al-MCM-41 catalyst [157]. The self-stabilized dispersion nitroxide-mediated polymerization of methyl methacrylate has been investigated in SC-CO_2 in the presence of a CO_2-philic perfluorinated stabilizer generated in situ [158]. The hydrosilylation of alkenes has been reported using $Rh(PPh_3)_3Cl$ as a catalyst in a SC-CO_2/IL system [159]. No hydrogenation by-product (alkane) was detected in the SC-CO_2/IL system. During hydrosilylation in the SC-CO_2/IL system, the reactants were possibly transferred into the IL phase by SC-CO_2, in which the catalyst was dissolved. The products can be flushed with SC-CO_2 after the reaction and the catalyst/IL system reused.

The oxidation reactions using photochemically generated singlet oxygen have been performed in the presence of fluorous surfactants and a cosolvent to solubilize more polar photosensitizers and reactants in SC-CO_2 [160].

1.4.3 Materials Synthesis and Modifications

Cross-linking of starch blends has been described by phosphorylation using reactive SCF extrusion [161]. SC-CO_2-based expansion offered light weight and nonporous skin starch foams with excellent water resistance which would be desirable properties for their utilization as a biodegradable material. The synthesis of silver nanostructures has been reported using SC-CO_2 in the presence of polyvinylpyrrolidone and ethylene glycol [162].

The micronization of sodium cellulose sulfate polymer has been reported with a controlled size, suitable for drug delivery system using the SCF-assisted atomization introduced by hydrodynamic cavitation mixer with water as the solvent [163]. The synthesis of polymeric materials with chiral recognition capability has been studied by molecular imprinting in SC-CO_2 [164]. This technology showed to be a promising "greener" alternative to conventional techniques in the preparation of chromatographic columns for enantioseparation.

The SC-CO_2 has been employed to prepare hollow silica and titanium dioxide microspheres using the cross-linked polystyrene (PS) microspheres as template [165]. Compared with other methods, this work has some advantages as the following: (a) the uniform cross-linked PS microspheres with different size as template can be easily obtained by emulsion or emulsifier-free emulsion copolymerization methods; (b) the solid microspheres are more robust than the hollow or soft templates, which will facilitate the formation of hollow microspheres of uniform particle size; (c) the SC-CO_2 treatment is more simple and efficient than the general methods such as layer-by-layer deposition or sulfonated techniques; (d) this method is more environment benign.

The SC phase-inversion technique has been used to prepare inorganic particles loaded starch-based porous composite matrixes in a one-step process for bone tissue engineering purposes [166]. The use of SCF methods for the screening, design, and development of cocrystals in a single step, providing advantages over classical pharmaceutical techniques, such as extended control of the particle morphology and the size distribution, has been reported [167].

The preparation of chitosan scaffolds loaded with dexamethasone has been reported for tissue engineering applications using SCF technology [168]. The SC-CO_2 has been applied as a solvent to obtain ceramides from wool fibers [169]. A SCF-assisted technique has been employed for the formation of 3D scaffolds, which consists of three subprocesses: the formation of a polymeric gel loaded with a solid porogen, the drying of the gel using SC-CO_2, and the washing with water to eliminate the porogen [170].

Polyethylene/poly(vinyl acetate) tubing has been prepared by the polymerization of vinyl acetate using the SC-CO_2 method [171]. The organic conducting aerogel has been prepared from SC-CO_2 drying of a poly(styrenesulfonate)-doped poly(3,4-ethylenedioxythiophene) hydrogel [172]. The resulting aerogels show light weight, large Brunauer-Emmett-Teller (BET) surface area and hierarchically porous structure with wide-pore size distribution.

The large-scale synthesis of ceria nanowires has been reported in SC-CO_2-ethanol solution using cerium nitrate as precursor [173]. This approach makes use of the intermediate to direct the anisotropic growth of ceria, which avoids additional templates and thereby simplifies the synthesis process.

Poly(styrene-co-acrylonitrile)/clay nanocomposites have been prepared with a high degree of clay exfoliation via melt-blending the polymer with highly filled poly(3-caprolactone)/clay masterbatches in SC-CO_2 [174].

1.4.4 Solubility in Supercritical Carbon Dioxide (SC-CO_2)

The solubility of lycopene from tomato-processing residue materials has been studied in SC-CO_2 [175]. Under supercritical conditions, increasing solubility of lycopene was stimulated by an increase in temperature and pressure. The highest solubility obtained was 1.9×10^{-6} mol fraction at a pressure of 250 bar and at a temperature of 80°C.

1.5 Room Temperature Ionic Liquids (RTIL)s

Since the introduction of air and water stable salts that are liquid at room temperature in 1992, there has been an explosion of interest in the use of these liquids as solvents for chemical process and allied industries [176–187]. Much of this attention has been centered on their possible use as greener alternatives to traditional molecular solvents, although this remains highly controversial. These compounds, which typically consist of nitrogen- or phosphorus-containing organic cations; corresponding anions are halides, tetrafluoroborate, hexafluorophosphates, etc. The cations are characterized by sufficient unsymmetry to inhibit their crystallization and thus reduce their melting temperature. There has been a report that the utilization of RTILs in industrial production of alkoxyphenylphosphine leads to an increase in productivity by a factor of 80,000 compared with the conventional process [188]. Perhaps the greatest potential of these ILs is that they might offer process advantages over molecular solvents or even novel behaviors that cannot be achieved from molecular solvents. Negligibly small vapor pressure, fire resistance, excellent chemical and thermal stability, wide liquid temperature ranges, and wide electrochemical windows are examples of the useful properties typical of ILs. They have the great versatility in cation-anion combination. The right choice of the cation-anion pair permits the modulation of physicochemical properties, such as density and viscosity. Furthermore, the structural properties of these solvent media are controlled both by cation-anion and cation-cation interactions. The hydrophilicity/lipophilicity of an IL can be readily adjusted by an appropriate selection of anion; for example, 1-butyl-3-methylimidazolium tetrafluoroborate ([BMIM]BF_4) is completely miscible with water, while the PF_6 salt is largely immiscible with water. The lipophilicity of dialkylimidazolium salts, or other ILs, can also be enhanced by increasing the chain length of the alkyl groups. Their properties, preparation, applications, and advantages compared to conventional solvents have been outlined in many excellent books and reviews [176–187].

RTILs show promises for a variety of applications in chemical industry including chemical synthesis, catalysis, separation, and preparation of materials. Therefore, RTILs have attracted considerable attentions from both the academic and industrial communities in recent years.

Despite potential benefits of using ILs to improve reactions or processes for many applications, industrial applications of ILs are still in its infancy.

1.5.1 Organic Synthesis

1.5.1.1 Enzymatic Reactions

The enzymatic reactions in ILs have been reviewed by (Moniruzzaman et al. 2010) [189]. Compared to conventional organic solvents, the use of enzymes in ILs has exhibited many advantages such as high conversion rates, high enantioselectivity, better enzyme stability, as well as better recoverability and recyclability.

The enhanced catalytic activity of α-chymotrypsin has been reported in the enzymatic peptide synthesis in ILs, as compared to organic solvents [190]. The one-pot chemoenzymatic synthesis of optically active *O*-acetyl cyanohydrins has been studied as both reaction media and promoter [191].

The lipase-catalyzed glycerolysis of triglycerides in a series of ILs, providing an efficient reaction protocol for diglyceride formation with good selectivity and high conversion, has been reported [192].

1.5.1.2 Transesterification

The transesterification reaction of methyl caffeate with various alcohols has been reported to produce caffeic acid phenethyl ester analogues with a lipase using an IL, 1-butyl-3-methylimidazolium bis(trifluoromethylsulfonyl)imide ([BMIM]Tf_2N), as the reaction medium [193]. Several basic binuclear functional ILs with an imidazolium structure have been synthesized and used as the catalyst in the preparation of biodiesel through transesterification from cottonseed oil [194].

The synthesis of organic esters, which are commonly used in the perfumery, flavor, and pharmaceutical industries, has been reported in the presence of free Candida antarctica lipase B as a catalyst via transesterification from vinyl esters and alcohols in two water-immiscible ILs, [BMIM]PF_6 and 1-octyl-3-methylimidazolium hexafluorophosphate [195]. The lipase *Pseudomonas cepacia*–catalyzed esterification of 3-(furan-2-yl) propanoic acid and transesterification of ethyl 3-(furan-2-yl) propanoate with a variety of alcohols have been reported in three ILs: [BMIM]BF_4, 1-butyl-3-methylimidazolium hexafluorophosphate ([BMIM]PF_6) and [BMIM]Tf_2N and hexane [196]. [BMIM]Tf_2N markedly enhanced the yields of the products after esterification (98–67%), while in [BMIM]PF_6 and in hexane, the yields (60–17%) were comparable. The lipase *Pseudomonas cepacia*–hydrophobic IL mixture was found to be operationally stable up to 10 months and can be recycled five times.

The reaction of lipase-catalyzed transesterification has been investigated in an IL, 2-methoxyethyl(tri-*n*-butyl)phosphonium Tf_2N solvent system to proceed faster than in a conventional organic solvent such as diisopropyl ether [197].

1.5.1.3 Hydroesterificaton

The promoting effect of several Brønsted acidic ILs at different acidities has been investigated for the hydroesterificaton of olefins catalyzed by a triphenylphosphine-palladium complex [198]. The ester product was obtained with excellent selectivity in moderate to high conversions, depending on the acidity of IL used.

1.5.1.4 Diels-Alder Reactions

The effects of ILs on the Diels-Alder reactions have been reviewed by Chiappe et al. [199]. The Diels-Alder reactions between different dienes and dienophiles have been investigated using erbium triflate as a catalyst in ILs [200]. The increased product yields, better selectivities, and shorter reaction times were observed compared with the analogous cycloadditions performed in conventional solvents. The ILs containing the catalyst can be readily separated from the reaction products and recovered in very high purity for direct reuse, up to six cycles.

The direct asymmetric aza-Diels-Alder reaction has been performed in the presence of chiral 2-pyrrolidinecarboxylic acid IL to formation of cyclic α,β-unsaturated ketones in modest to good yields with excellent enantioselectivities and diastereomeric ratios [201]. The catalytic system can be recycled and reused for six times without any significant loss of catalytic activity. A series of chiral ammonium and imidazolium-based ILs has been synthesized and used as a chiral reaction medium and catalyst for an asymmetric aza-Diels-Alder reaction [202]. The imidazolium family chiral ILs derived from isosorbide have been synthesized and employed as chiral reaction medium and catalyst for an asymmetric aza-Diels-Alder reaction (Scheme 1.17) [203].

1.5.1.5 Michael Reaction

The use of chiral ammonium ILs as organocatalysts has been reported for asymmetric Michael addition of aldehydes to nitroolefins with excellent yields, high enantioselectivity, and modest to high diastereoselectivity [204]. Acidic IL, *N*-methyl-2-pyrrolidonium dihydrogen phosphate has been synthesized and employed as catalyst and reaction medium for preparation of β-alkoxyketones with high yields via the oxa-Michael addition reactions [205]. The used IL was stable and could be reused at least five times with a slight loss of activity. The Michael

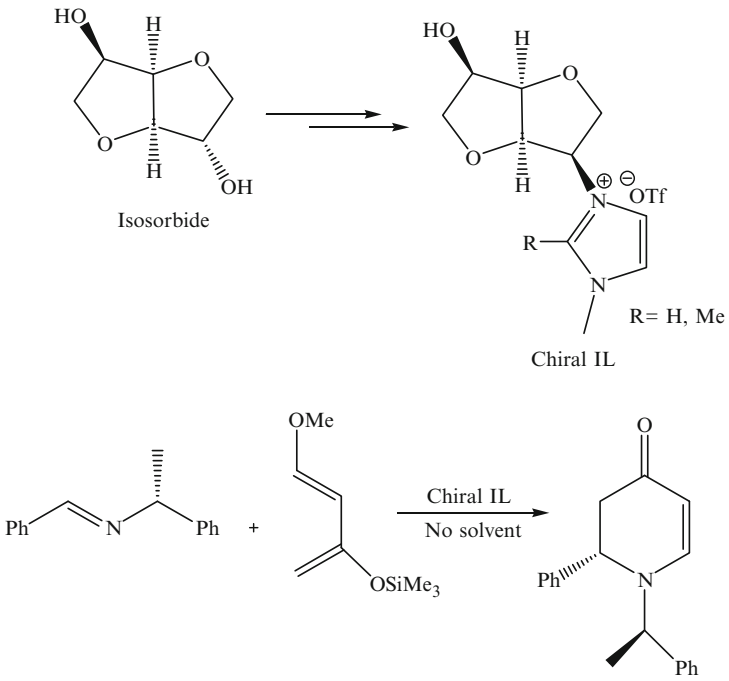

Scheme 1.17 Structure of chiral IL and asymmetric aza-Diels-Alder reaction of Danishefsky's diene with imine (Reprinted from Ref. [203]. With kind permission of Elsevier)

addition of aliphatic aldehydes to β-nitrostyrene has been studied in the presence of proline-derived organocatalysts as catalyst with high yields, excellent diastereoselectivity, and moderate enantioselectivity in several ILs [206]. The recyclable pyrrolidine-based functionalized chiral ILs have been employed for the asymmetric Michael addition reactions of aldehydes with nitrostyrenes [207]. These catalysts led to high yields, good enantioselectivities, and high diastereoselectivities.

1.5.1.6 Friedel-Crafts Reactions

The use of Lewis acidic ILs as both catalyst and solvent has been reported in the Friedel-Crafts acylation of salicylamide with acetyl chloride to 5-acetylsalicylamide [208]. A series of pyrrolidinium-based salts with new fluorine-containing anions has been synthesized and used as a solvent and catalyst for Friedel-Crafts alkylations of indoles with nitroalkenes (Scheme 1.18) [209].

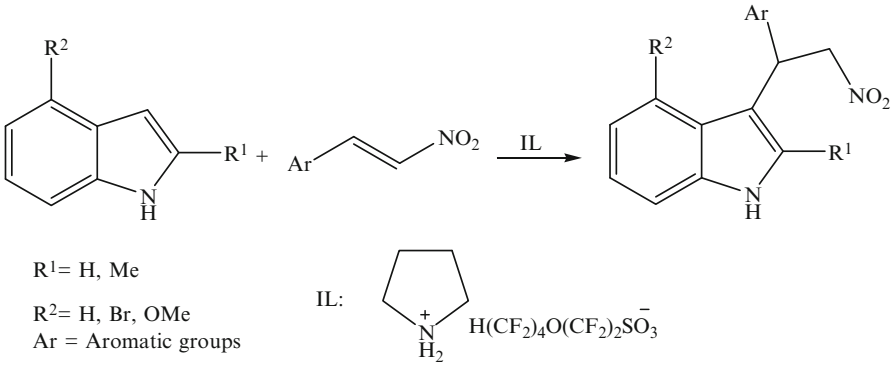

Scheme 1.18 Friedel-Crafts alkylation of indoles with nitroalkenes in IL (Reprinted from Ref. [209]. With kind permission of Elsevier)

1.5.1.7 Condensation Reactions

The several imidazolium- and pyridinium-based ILs have been synthesized and employed as precatalysts for the benzoin condensation using solvent-free and microwave activation methods [210]. IL, 1-methyl-3-pentylimidazolium tetrafluoroborate, has been employed for the synthesis of 2-aryl benzimidazoles via condensation of *o*-phenylenediamine and aromatic aldehydes under mild reaction conditions, low energy consumption, high yields, and reusability of IL [211].

1.5.1.8 Cyclocondensation Reactions

The use of ILs has been described as an efficient media for the cyclocondensation reactions of β-enamino ketones and different 1,2- and 1,3-dinucleophiles [212]. The synthesized heterocycles were obtained in high regioselectivity, good yields, and short reaction times. The effects of several ILs have been studied in regioselective pyrazole synthesis by the cyclocondensation reaction of β-dimethylaminovinyl ketones with *tert*-butylhydrazine hydrochloride (Scheme 1.19) [213].

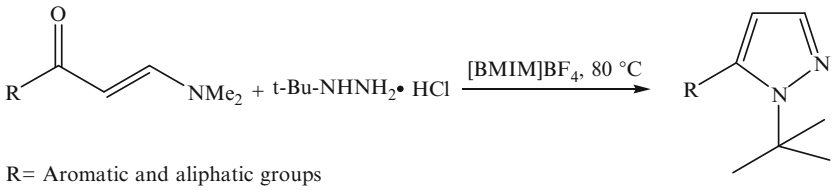

Scheme 1.19 Reaction of β-dimethylaminovinyl ketones with *tert*-butylhydrazine hydrochloride (Reprinted from Ref. [213]. With kind permission of Elsevier)

1.5.1.9 Mannich Reaction

The Brønsted acid–surfactant-combined IL, 3-(*N,N*-dimethyldodecylammonium)-propanesulfonic acid hydrogen sulfate, has been prepared and used as the recyclable catalyst for the three-component Mannich-type reaction in water at room temperature [214]. The catalyst could be reused at least six times without a noticeably decrease in the catalytic activity.

The highly chemoselective synthesis of 2,2-dimethyl-6-substituted 4-piperidones has been reported via multicomponent tandem Mannich reaction of ammonia, aldehydes, and acetone using the [BMIM]PF_6 as the solvent [215]. The IL significantly enhanced the chemoselectivity.

1.5.1.10 Hydrolysis

The acid-promoted hydrolysis of chitosan has been reported in imidazolium-based ILs under mild conditions with good yield of total reducing sugars [216]. The one-pot hydrolysis and dehydration of di/polysaccharides containing fructose units in 1-ethyl-3-methylimidazolium hydrogen sulfate, providing fairly high yields of furfural or 5-hydroxymethyl-2-furaldehyde at 100°C, have been studied [217]. The solid acid-promoted hydrolysis of cellulose has been investigated in ILs under microwave irradiation [218].

1.5.1.11 Dehydration

The acid-catalyzed dehydration of fructose to 5-hydroxymethylfurfural has been reported in dialkylimidazolium halide ILs in high isolated yields at 80°C (Scheme 1.20) [219].

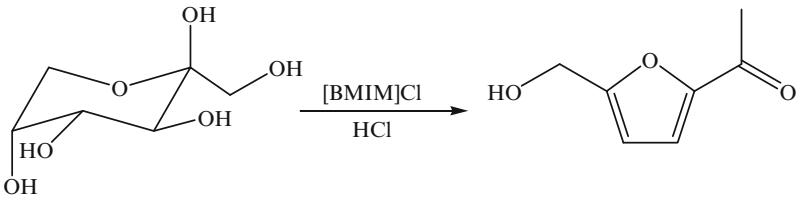

Scheme 1.20 The dehydration of fructose to 5-hydroxymethylfurfural in IL (Reprinted from Ref. [219]. With kind permission of Elsevier)

The $CuCl_2$-catalyzed heterocyclodehydration of 1-(2-aminoaryl)-2-yn-1-ols has been reported in IL, [BMIM]BF_4, at 100°C for 15–24 h [220]. The solvent-catalyst system could be recycled up to six times without significant loss of activity.

The dehydration of fructose into 5-hydroxymethylfurfural in IL has been described using [BMIM]Cl as solvent in the presence of a strong acidic ion exchange resin as catalyst [221]. The yield was 85.9% at 80°C within 10 min. The IL and catalyst could be recycled, and the catalyst showed constant activity over 7 cycles of evaluation.

1.5.1.12 Epoxidation

The enantioselective epoxidation of 6-cyano-2,2-dimethylchromene, a biologically important alkene, has been studied using Jacobsen as a catalyst in the presence of sodium hypochlorite (NaOCl) as oxygen source in a series of 1,3-dialkylimidazolium- and tetra-alkyl-dimethylguanidium-based ILs (Scheme 1.21) [222].

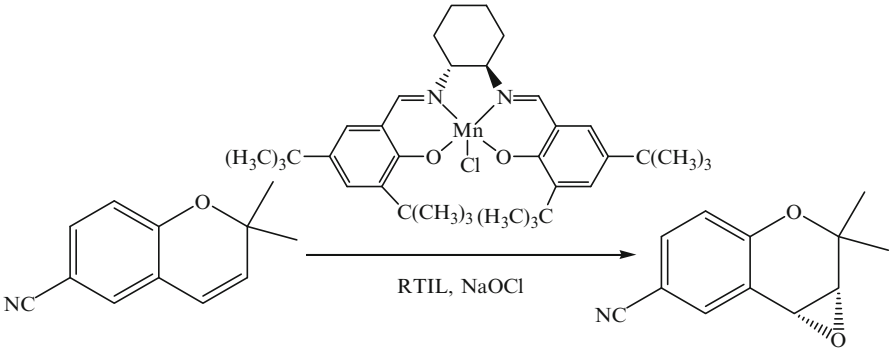

Scheme 1.21 Epoxidation reaction of 6-cyano-2,2-dimethylchromene catalyzed by the Jacobsen complex (Reprinted from Ref. [222]. With kind permission of Elsevier)

Chiral epichlorohydrin with high yields and enantioselectivity has been prepared via chloroperoxidase (CPO)-catalyzed epoxidation of 3-chloropropene in the presence of an IL as cosolvent [223]. Compared with conventional organic solvents, CPO in ILs showed enhanced activity, stability, and selectivity. Furthermore, the presence of ILs improved substrate solubility in the reaction medium. The cyclooctene epoxidation has been investigated using t-butyl-hydroperoxide as oxidant in the presence of ionic Schiff base dioxomolybdenum(VI) complexes as catalysts in IL media [224]. The selective epoxidation of cyclooctene and other olefin substrates to their corresponding epoxides catalyzed by oxodiperoxomolybdenum species has been demonstrated in IL, [BMIM]PF_6 [225].

1.5.1.13 Synthesis of Imidazoles

The one-pot, three-component preparation of trisubstituted imidazoles has been developed with high yields at room temperature under ultrasonication using IL, 1-ethyl-3-methylimidazole acetate as catalyst [226].

1.5.1.14 Synthesis of Diacetals and Diketals

Pentaerythritol diacetals and diketals have been synthesized with good to excellent yields using SO_3H-functionalized ILs as catalysts [227]. This catalytic system was stable, easily separable, and reusable.

1.5.1.15 Bonds Cleavage Reactions

The use of IL, 1-butyl-3-methylimidazolium bromide ([BMIM]Br) has been studied as an alternative medium for the catalytic cleavage of aromatic C-F and C-Cl bonds [228].

1.5.1.16 Oligomerization

The selective synthesis of the oligoalkylnaphthenic oils has been reported by oligomerization of 1-hexene in the presence of chloroaluminate type IL catalysts [229].

1.5.1.17 Synthesis of 5-Hydroxymethylfurfural and Furfural

The microwave-assisted, direct conversion of lignocellulosic biomass into 5-hydroxymethylfurfural and furfural has been reported in the presence of $CrCl_3$ in ILs within a few minutes [230].

1.5.1.18 Preparation of Biodiesel Fuel

The production of biodiesel fuel from the methanolysis of soybean oil catalyzed by fungus whole-cell biocatalysts has been reported in ILs [231].

1.5.1.19 Synthesis of Tributyl Citrate

Tributyl citrate has been synthesized with conversion 97% using acid functionalized IL as catalyst. The IL could be reused 13 times without any disposal, and the conversion of citric acid was not less than 93% [232].

1.5.1.20 Synthesis of Dimethyl Carbonate

The highly selective synthesis of dimethyl carbonate (DMC) from urea and methanol catalyzed by IL has been reported [233]. The DMC selectivity was almost 100% with the yield of 26% in a batch reactor.

1.5.1.21 Nitration of Aromatic Compounds

The regioselective mononitration of aromatic compounds has been reported in the presence of Brønsted acidic ILs as recoverable catalysts [234].

1.5.1.22 Alkylation and Acylation

The alkylation of isobutane with 2-butene has been developed using various triethylamine hydrochloride-aluminum chloride catalysts [235]. Compared to sulfuric acid under identical reaction conditions, the composite IL showed higher trimethylpentane selectivity. The application of ILs has been reported in the *N*-alkylation reaction of trifluoromethylpyrazoles. The shorter reaction times and better yields were achieved compared with the reaction performed in molecular solvents [236].

The alkylation of the secondary amine 3-azabicyclo[3.2.2]nonane has been studied using ILs, [BMIM][PF_6], and 1-butyl-1-methylpyrrolidinum Tf_2N in conjunction with KOH under mild conditions [237]. The alkylation of phenols with alkenes in the presence of chloroindate(III) ILs yields high conversion to alkylated phenols with high selectivities [238]. The catalytic performance of 1-n-octyl-3-methylimidazolium bromide aluminum chloride–based ILs has been investigated for the alkylation of isobutene and 2-butene [239]. The preparation of 1,2-aceanthrylenedione has been reported via acylation of anthracene with oxalyl chloride in the presence of [BMIM]-based IL [240]. The acetylation of starch with vinyl acetate in imidazolium ILs provides starches with different acetylation patterns [241].

1.5.1.23 Synthesis of Fatty Acid Esters of Steroids

The one-pot synthesis of long-chain fatty acid esters of steroids has been reported in a microwave reactor using neutral IL in high yield within 1 min [242].

1.5.1.24 Aldol Reaction

The direct asymmetric aldol reaction of cyclic ketones with aromatic aldehydes has been demonstrated using protonated forms of basic α-amino acids in ILs and dimethyl sulfoxide (DMSO) [243]. Higher yields were obtained in *N*-butyl *N*-methyl pyrrolidinium triflate compared to DMSO.

1.5.1.25 Synthesis of 1,4-Dibromo-Naphthalene

The synthesis of 1,4-dibromo-naphthalene (1,4-DBN) has been described by the reaction of naphthalene and molecular bromine in the aqueous solution of ILs in a short reaction time with 100% yield and 100% selectivity (Scheme 1.22) [244]. This method is readily applicable to large-scale preparation of 1,4-DBN.

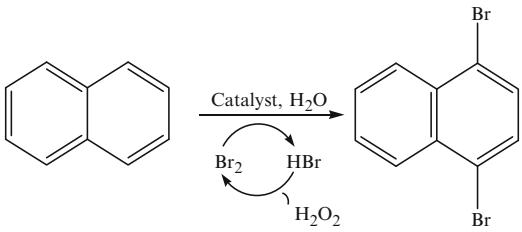

Scheme 1.22 The strategy for synthesis of 1,4-DBN (Reprinted from Ref. [244]. With kind permission of Elsevier)

1.5.1.26 Heck and the Knoevenagel Reactions

A series of ILs has been prepared with a tethered base functionality and tunable basicity and used as effective catalysts for the Heck and the Knoevenagel reactions [245].

1.5.1.27 Synthesis of Aromatic Chloroamines

The selective synthesis of aromatic chloroamines from aromatic chloronitro compounds has been developed using IL-like copolymer-stabilized platinum nanocatalysts in ILs [246]. Compared to reactions in organic solvents, the ILs provide superior selectivity with functionalized ILs containing an alcohol group demonstrating the best recyclability and ultimately achieving a turnover number of 2,025 which is 750-fold higher than Raney nickel catalyst.

1.5.1.28 Esterification

The several lactam-based Brønsted acidic ILs with different acidities have been synthesized and used as catalysts for esterification of carboxylic acids with alcohols under mild reaction conditions without addition of any organic solvents or cocatalysts [247]. ILs could be reused several times without substantial loss of activity.

1.5.1.29 Hydrosilylation of Alkenes

The hydrosilylation of alkenes has been studied using a rhodium complex as a catalyst in a SC-CO_2/IL system [159].

1.5.1.30 Coupling Reactions

The coupling of acyl chlorides with diphenyl diselenide in the presence of a nanocrystalline CuO in IL provides selenoesters with excellent yields [248].

1.5.1.31 Synthesis of Cellulose Propionate

The alkoxycarbonylation of ethylene with carbon monoxide and cellulose in 1-*n*-butyl-3-methylimidazolium methanesulfonate yields cellulose propionate with a degree of substitution of 1–2 [249].

1.5.1.32 Synthesis of Hydroxy Ester

The ozonation of cyclic acetals in IL, 1-butyl-1-methylpyrrolidinium dicyanamide leads to the formation of selective hydroxy ester without use of acetylating reagents [250].

1.5.1.33 Sonogashira Reactions

The copper- and phosphine-free Sonogashira coupling reactions have been investigated in biodegradable ILs derived from nicotinic acid [251].

1.5.1.34 Metathesis Reaction

The use of ILs as (co)solvents for the olefin metathesis reaction has been reviewed by Sledz et al. [180].

1.5.1.35 Aziridination Reaction

The aziridination of olefins with equimolar amounts of iminoiodinane using a catalytic system based on iron(II) triflate, quinaldic acid, and an IL provides products in good to moderate yields [252].

1.5.1.36 Synthesis of [60] Fullerene

The quantitative cycloreversion of fulleropyrrolidines to [60] fullerene has been achieved in ILs within minutes under microwave irradiation [253].

1.5.1.37 Methanolysis

The methanolysis of polycarbonate (PC) to its starting monomer bisphenol A (BPA) and dimethyl carbonate (DMC) has been demonstrated under moderate conditions in presence of IL [BMIM]Cl without use of any acid or base catalyst [254]. The methanolysis conversion of PC was almost 100%, and the yields of both BPA and

DMC were over 95%. The IL could be reused eight times without obvious decrease in the conversion of PC and yields of BPA and DMC.

1.5.1.38 Dimerization

The nickel-catalyzed dimerization of propene has been investigated in acidic chloroaluminate ILs [255].

1.5.1.39 Synthesis of Drugs

The synthesis of nucleoside-based antiviral drugs has been reported using imidazolium-based ILs as reaction medium [256]. It was found that ILs were better solvents for all the nucleoside in terms of solubility and reaction medium than conventional molecular solvents.

1.5.1.40 Oxidation

The synthesis of lactones and esters from the corresponding ketones has been reported using Oxone® as the oxidant in the presence of ILs in short time [257]. The used ILs were efficiently recycled in the Baeyer-Villiger reaction without significant loss of activity.

The selective oxidation of organic halides to aldehydes or ketones has been carried out in good to high yields using H_5IO_6 in IL 1-dodecyl-3-methylimidazolium iron chloride under mild conditions [258]. The catalytic system can be recycled and reused without any significant loss of catalytic activity. The application of an oxygen/benzaldehyde system as the oxidant and ILs as solvents has been reported for the synthesis of lactones following Baeyer-Villiger oxidation of ketones [259]. The synthesis of 1,2-allenic ketones has been developed by $RuCl_3$-catalyzed oxidation of homopropargyl alcohols in IL using *tert*-butylhydroperoxide (TBHP) as the oxidant (Scheme 1.23) [260].

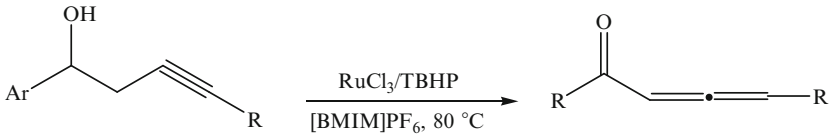

Scheme 1.23 The oxidation of homopropargyl alcohols in IL (Reprinted from Ref. [260]. With kind permission of Elsevier)

The oxidation of Alcell lignin, soda lignin, and lignin model compounds has been reported in ILs using several transition metal catalysts and molecular oxygen under mild conditions [261].

1.5.1.41 Synthesis of Heterocyclic Compounds

The synthesis of pyrazolone derivatives has been developed in the presence of catalytic amount of IL, 1-methylimidazolium hydrogen sulfate, under ultrasonic irradiation at room temperature in short reaction time [262]. The Prins cyclization of homoallylic alcohols, thiols, and amines with various aldehydes has been investigated in an IL hydrogen fluoride salt, providing the corresponding 4-fluorinated heterocycles in excellent yields [263].

1.5.2 Materials Synthesis and Modifications

1.5.2.1 Synthesis of Nanoparticles

IL, 1-butyl-3-methylimidazolium lauryl sulfate, has been employed for the synthesis of gold nanocrystals with particle size ranging from 20 to 50 nm by seeding growth method stable up to 168 h storage at ambient temperature [264]. The stabilizing efficiency of the IL was due to the formation of a double-layer micellar structure via electrostatic interaction between the nanoparticle and the imidazole ring of the cation, and the Van der Waals interaction of the alkyl chains of the IL. Utilizing this type of IL offered great advantage because it is an environmentally benign solvent useful to clean industrial technology.

The gold nanoparticles have been synthesized in ILs by irradiation using accelerated electron beams and γ-rays [265]. The step-by-step, ligand-free nucleation and nanocrystal growth of gold nanoparticles have been reported by the reduction of $KAuCl_4$ with $SnCl_2$ in ILs [266]. The effects of a set of ILs based on the 1-ethyl-3-methylimidazolium cation and different anions have been studied on the formation of gold nanoparticles [267]. It was found that the anion has a strong influence on the particle size, particle shape, and particle aggregation. The one-step synthesis of gold-silver alloy nanoparticles has been described in ILs via a sputter deposition technique [268]. The synthesis of uniform silver nanoparticles and silver/polystyrene core-shell nanoparticles has been developed via chemical reduction and deposition polymerization in $[BMIM]BF_4$ [269]. IL plays a protective role to prevent the nanoparticles from aggregation during the preparation process. The pure, oxygen free, small-size, polycrystalline GdF_3: Eu^{3+} nanoparticles have been synthesized via microwave synthesis using $[BMIM]BF_4$ as the synthesis medium as well as the fluoride source [270].

The preparation of monodisperse magnetite nanoparticles has been reported using a small amount of ILs as microwave absorber and assistant stabilizer within 10 min. IL can be recovered and reused in successive reactions for many times [271]. The ultra long-time stable, luminescent europium(II) fluoride (EuF_2) nanoparticles have been synthesized with a size below 10 nm via evaporation of molecular EuF_2 into ILs [272]. The aluminum oxide nanoparticles have been synthesized by the hydrolysis of $AlCl_3$ dissolved in the ILs, 1-butyl-1-methylpyrrolidinium Tf_2N and 1-ethyl-3-methylimidazolium

Tf_2N [273]. PtRu nanoparticles supported on multiwalled carbon nanotubes have been prepared by a simple and rapid microwave-assisted IL method [274]. The synthesis of flower-like and leaf-like cupric oxide single-crystal nanostructures has been described using IL, 1-octyl-3-methylimidazolium trifluoroacetate, under microwave-heating method [275]. The SnO_2 nanoparticles have been prepared in aqueous solution of 1-ethyl-3-methylimidazolium ethyl sulfate via ultrasonic irradiation [276].

The synthesis of MoS_2 nanostructures of different morphologies has been described via an IL-assisted hydrothermal route [277]. The synthesis of poly(3-methylthiophene) nanospheres has been reported with size ranging around 50–60 nm in a magnetic IL, 1-butyl-3-methylimidazolium tetrachloroferrate, without the additional dopant or oxidant [278]. The yield and conductivity of obtained nanospheres in IL were better than those synthesized in conventional solution polymerizations.

The direct synthesis of ZnO nanorods from $Zn(CH_3COO)_{22}H_2O$ and NaOH has been investigated in the neat RTIL, [BMIM]Tf_2N without further use of organic solvents, water, surfactants, or templates under ultrasound irradiation [279].

The iron oxide nanorods and nanocubes have been synthesized in the presence of [BMIM]Tf_2N [280]. The findings showed that imidazolium-based ILs could be used as solvent for achieving very high level control over the size and shape of nanostructures. The Co, Rh, and Ir nanoparticles have been prepared from metal carbonyls in ILs and employed as biphasic liquid-liquid hydrogenation nanocatalysts for cyclohexene [281].

The poly(3,4-ethylenedioxythiophene) nanospheres of about 60 nm in size have been synthesized in a magnetic IL, 1-butyl-3-methylimidazolium tetrachloroferrate [282].

The synthesis of nanostructure rutile TiO_2 has been reported in a carboxyl-containing IL, 1-methylimidazolium-3-acetate chlorine, using $TiOCl_2$ solution as a precursor at low temperature [283].

The leaf-like, chrysanthemum-like, and rod cupric oxide nanostructures have been synthesized by microwave-assisted method using an IL [BMIM]BF_4 [284]. The preparation of silica/polystyrene core-shell composite nanospheres has been reported via in situ radical dispersion polymerization in an IL, *N,N*-diethyl-*N*-methyl-*N*-(2-methoxyethyl)ammonium Tf_2N [285]. The polycrystalline CdS nanometer-sized hollow spheres have been synthesized by simple one-step hydrothermal method in the presence of water-immiscible IL, [BMIM]PF_6 [286]. The nest-like Bi_2WO_6 hierarchical structures consisting of nanosheets have been successfully obtained using IL, [BMIM]BF_4, as capping reagents under the IL-assisted hydrothermal conditions [287].

The synthesis of photocatalytically active crystalline anatase nanoparticles from titanium tetraisopropoxide has been reported via sonochemistry in the IL, 1-(3-hydroxypropyl)-3-methylimidazolium Tf_2N [288].

The spindle-like ZnO nanostructures with high surface area and narrow mesoporous pore distribution have been obtained by a polyoxometalate-assisted electrodeposition route in IL at room temperature [289]. The synthesis of uniform peachstone-like CuO 3D architectures consisting of single-crystal nanosheets has

been reported using IL, 1-octyl-3-methylimidazolium trifluoroacetate, as capping reagents under the IL-assisted hydrothermal condition [290]. The preparation of transition metal oxalates submicrometer cubes, nanorods, and nanoparticles has been reported by IL-assisted one-step solid-state reaction at room temperature within short reaction time [291]. Many nanostructured materials have been successfully synthesized by employing ILs as precursors [292–295].

1.5.2.2 Synthesis of Silicas

The acidic ILs 1-alkyl-3-methylimidazolium hydrogen sulfate (alkyl = octyl, decyl, dodecyl, hexadecyl) have been applied as both templates and acid source for the synthesis of ordered, high-surface-area mesoporous silicas [296].

The synthesis of hollow and porous silica particles as drug delivery system has been reported by a simple acid gelation route in IL, [BMIM]BF_4, using the sodium silicate as the reactant [297].

1.5.2.3 Synthesis of Zeolites

The ionothermal synthesis of siliceous zeolites has been reported using IL, 1-butyl-3-methylimidazolium hydroxide, as the solvent and structure-directing agent/template [298].

1.5.2.4 Bioreactors

Quijano et al. 2010 has reviewed the applications of ILs in bioreactor technologies [299].

1.5.2.5 Synthesis of Tin Oxide Microspheres

The one-step controlled synthesis of rutile structure tin oxide microspheres has been reported with an average 2.5 μm in diameters via hydrothermal reaction of $SnCl_4 \cdot 5H_2O$ with sodium hydroxide by microwave in the presence of [BMIM] BF_4 [300].

1.5.2.6 Synthesis of ZnO Mesocrystals

The one-dimensional Mn-doped room temperature ferromagnetic ZnO mesocrystals have been prepared in a hydrated IL precursor tetrabutylammonium hydroxide at low temperature [301].

1.5.2.7 Functionalization of Multiwalled Carbon Nanotubes (MWNTs)

The functionalization of MWNTs have been performed by free radical addition of 4,4′-azobis(4-cyanopentanol) in aqueous media to generate the terminal-hydroxyl-modified MWNTs, followed by surface-initiated in situ ring-opening polymerization of ε-caprolactone in [BMIM]BF_4 to obtain poly(ε-caprolactone)-grafted MWNTs [302].

1.5.2.8 Desulfurization of Diesel

The Brønsted acidic ILs 1-butyl-3-methylimidazolium hydrogen sulfate ([BMIM][HSO_4]) and *N*-butylpyridinium hydrogen sulfate have been employed as extractants and catalysts for the desulfurization of diesel [303]. [BMIM][HSO_4] can be recycled up to six times without a significant decrease in the desulfurization performance.

1.5.2.9 Removal of Sulfur Dioxide

The removal of sulfur dioxide from the flue gas has been studied using a series of hydroxyl ammonium ILs synthesized with water-bath microwave [304].

1.5.2.10 Decomposition

Decomposition of halophenols has been reported in RTILs by γ-ray and pulsed electron radiolyses [305]. The degradation of polylactic acid has been examined in the presence of ILs having phosphonium cation and decanoate or tetrafluoroborate anions [306].

1.5.2.11 Carbonization

Ionothermal carbonization of sugars in a protic IL at low temperature under ambient pressure results in the formation of mesoporous carbon [307]. The success of this ionothermal approach was based on the suppressed solvent volatility and latent acidity of a protic IL.

1.5.2.12 Synthesis of Hydrogels and Composite Hydrogels

Preparation of hydrogels and composite hydrogels has been described from pineapple peel cellulose using 1-allyl-3-methylimidazolium chloride [308].

1.5.2.13 Absorption

An enhanced absorption of CO_2 along with its increased absorption rate has been realized in *N*-methyldiethanolamine aqueous solutions in amino acid–based ILs [309].

1.5.2.14 Corrosion Protection

The corrosion protection has been reported by ILs containing imidazolium and pyridinium cations with efficiency 82–88% at 100 ppm for mild steel in contact with 1.0 M aqueous solution of sulfuric acid [310]. It appears that by a chemical adsorption, process is operative in this case.

The effect of three imidazolium-based ILs on the corrosion inhibition of aluminum in 1.0 M HCl solution has been investigated [311]. The inhibiting influence of IL, [BMIM]Br, has been studied on mild-steel corrosion in 1.0 M hydrochloric acid solution [312].

1.5.2.15 Electrodeposition

The electrochemical codeposition of aluminum-cerium metallic protective coating with active inhibiting effect has been investigated using [BMIM]Cl as an electrolyte [313]. Cerium was successfully codeposited with aluminum on surface of platinum and AA2024 aluminum alloy forming uniform films with globular microstructure and thickness up to 75 μm.

1.5.2.16 Depolymerization

The depolymerization of cellulose and wood has been studied in ILs using a solid catalyst [314]. Upon the depolymerization, three types of substances including total reducing sugar, glucose, and ethanol are produced.

The depolymerization of poly(ethylene terephthalate) (PET) has been examined in ethylene glycol using imidazolium-based Fe-containing IL, 1-butyl-3-methylimidazolium tetrachloroferrate, as a catalyst [315]. This magnetic IL showed higher catalytic activity for the glycolysis of PET, compared with $FeCl_3$ or [BMIM]Cl.

1.5.2.17 Inhibitor

The application of dialkylimidazolium-based ILs with halide anions has been investigated as dual function inhibitors for methane hydrate [316].

1.5.2.18 Synthesis of Inorganic Materials

The synthesis of inorganic materials has been reported from IL precursors with the assistance of microwave heating [317]. The preparation of biocompatible and blood compatible heparin-cellulose-charcoal composites has been reported using RTILs [318].

1.5.3 Polymerization

The advantages and limitations of application of ILs as solvents for polymerization processes have been reviewed [185, 319]. ILs have been employed as solvents in free radical polymerizations to replace conventional organic solvents [320]. It has been shown that polymer synthesis in solution using ILs as solvents is associated with advantages of achieving higher polymerization rates and higher molecular weights products.

The well-controlled atom transfer radical polymerization of acrylonitrile has been described using ethyl 2-bromoisobutyrate as the initiator and $FeBr_2$ as the catalyst in the absence of any ligand in imidazolium-based ILs [321]. All the ILs could be easily recycled and reused after simple purification. Atom transfer radical polymerization process using activators generated by electron transfer of acrylonitrile in imidazolium-based ILs and $FeBr_3$ as the catalyst for preparing polyacrylonitrile with high molecular weight and narrow polydispersity has been developed [234]. The preparation of cellulose graft poly(methyl methacrylate) copolymers by atom transfer radical polymerization in an IL, 1-allyl-3-methylimidazolium chloride, has been reported [277]. The reverse atom transfer radical polymerization of ethyl acrylate catalyzed by azobisisobutyronitrile/$CuBr_2$/*N*,*N*,*N*′,*N*″,*N*″-pentamethyldiethylenetriamine has been studied in ILs based on imidazolium [322]. The synthesis of amphiphilic ABA triblock copolymers has been reported by ring-opening metathesis polymerization and atom transfer radical polymerization in IL, [BMIM]BF_4 [323]. The reversible addition fragmentation chain transfer (RAFT) controlled polymerization of methyl methacrylate in imidazole-based ILs with broadly similar cations, but different anions have been described [324]. It has been shown that the anion plays an extremely important role in the success of RAFT control in ILs.

The high molar mass polyesters of poly(12-hydroxydodecanoic acid) have been prepared via polyesterification of 12-hydroxydodecanoic acid in sulfonic acid group-containing ILs at low to moderate temperature in short reaction time and at atmospheric pressure in the absence of catalyst [325].

The direct anodic oxidation electropolymerization of fluorine has been demonstrated in IL, [BMIM]PF_6, without any additional supporting electrolyte [326]. Electroactive polyfluorene films with good redox activity, structural stability, and compact surfaces were found efficient to act as blue light-emitting materials. They exhibited stable electrocatalytic activity for formic acid oxidation.

The polymerization of phenols in the presence of soybean peroxidase as a catalyst in ILs results in the formation of phenolic polymers with number average molecular weights ranging from 1,200 to 4,100 Da, depending on the composition of the reaction medium and the nature of the phenol [327]. The synthesis of thermally stable aromatic optically active polyamides has been investigated using microwave irradiation in conjunction with an IL, 1,3-diisopropylimidazolium bromide or 1,3-dipropylimidazolium bromide, in the presence of triphenyl phosphite [328, 329]. The photo-induced polymerization of poly(ethylene glycol) dimethacrylate and poly(ethylene glycol) monomethacrylate has been reported in four imidazolium-based ILs [330]. The polymerization conducted in ILs was considerably faster than in a reference solvent.

The ILs, *N*-butyl-*N*-methyl-pyrrolidinium trifluoromethanesulfonate and *N*-methyl-*N*-propyl-pyrrolidinium Tf_2N, have been employed as electropolymerization media for poly(3-methylthiophene) (pMeT) in view of their use in carbon/IL/pMeT hybrid supercapacitors [331].

The electrochemical polymerization of selenophene in an IL, $[BMIM][PF_6]$, results in the production of free-standing and highly conducting polyselenophene (PSe) films with electrical conductivity as high as 2.3 S/cm, higher than PSe electrodeposited in conventional media [332].

The anionic polymerization of styrene has been reported at ambient temperatures in an IL trihexyl(tetradecyl) phosphonium Tf_2N under milder reaction conditions than classical methods [333]. Ionothermal syntheses of two coordination polymers constructed from 5-sulfoisophthalic acid ligands have been reported with $[BMIM]BF_4$ as solvent [334].

1.5.4 Extraction

The use of ILs as a solvent to enhance the capabilities and applications of solvent extraction methods has been reviewed by Poole and Poole [335]. 1-Ethylpyridinium ethylsulfate IL has been employed in liquid extraction processes for the separation of benzene from alkanes [336]. ILs have been used as solvents in liquid-liquid extractions for separating 1-butanol from water, with selectivities ranging from 30 to 300 and high distribution coefficients [337]. The use of 1-ethyl-3-methylpyridinium ethylsulfate IL as solvent has been reported for the liquid extraction of xylenes from hexane [338]. The solubility of the employed IL in the binary systems {hexane + aromatic compounds} was zero or very low, which made the recycle of IL much easier.

The use of ILs for extraction of sulfur and nitrogen compounds from fuel oils has been described [339]. The extraction of lanthanide ions from aqueous solutions has been investigated using bis(2-ethylhexyl)phosphoric acid with RTILs [340]. The IL system exhibited about three times greater extractability for lanthanide compared to that of hexane. The use of functional amino acid IL has been reported as solvent and selector to separate racemic amino acids in chiral liquid-liquid extraction with

distinct enantioselectivity [341]. The quaternary phosphonium IL, trihexyl(tetradecyl) phosphonium chloride, has been employed for the separation of Fe(III) and Ni(II) from 6 M hydrochloride solution via liquid-liquid extraction [342]. The selective extraction of cycloolefins from their mixtures in the presence of cyclohexane has been achieved via chemical complexation with silver ions in IL solutions [343].

1.5.5 Solubility

The solubility and diffusion coefficient of H_2S and CO_2 have been determined in 1-ethyl-3-methylimidazolium ethylsulfate at temperatures ranging from 303.15 to 353.15 K [344]. Comparison showed that H_2S is more soluble than CO_2 and its diffusion coefficient is about two orders of magnitude as that of CO_2. IL (1-ethyl-3-methylimidazolium acetate) has been used for the dissolution or extraction of crustacean shells to produce high molecular weight purified chitin and direct production of chitin films and fibers [345].

The dissolution, regeneration, and derivatization of cellulose in RTILs have been discussed, and their applications in cellulose industry have been reviewed [184, 346]. The dissolution of nonmetallic solid elements (sulfur, selenium, tellurium, and phosphorus) has been studied in ILs [347]. The high solubilities of ammonia have been reported [348] in four imidazolium-based ILs at temperatures from 293.15 to 333.15 K, and the pressure ranges from 0 to 1 MPa. Pinkert et al. and Mikkola et al. have been reviewed the use of ILs in dissolution of lignocellulosic materials and their constituents [349, 350]. High CO_2 solubilities have been reported in trihexyltetradecylphosphonium-based ILs [351]. The solubility, ionic conductivity, and viscosity of lithium salts used in batteries have been investigated in several ILs with broadly similar cations, but with different anions [352]. They found that the nature of the anion played a significant role in the solubilization of lithium salts in ILs.

1.6 Perfluorinated Solvents

The fluorous media such as perfluorocarbons or perfluorinated solvents have been receiving increasing attention in organic synthesis and related unit operations due to their unique properties [353–362]. They exhibit low toxicity and chemical reactivity as well as miscibility with many organic solvents. In addition, these solvents are inflammable and show a relatively low volatility. Perfluorinated solvents possess a high density (1.7–1.9 g cm^{-3}) and a very low solubility both in water and most organic solvents. Fluorocarbons exhibit very weak Vander-Waals interactions due to the low polarizability of the electrons of a C–F bond and low availability of the lone pair of fluorine. This implies that, in contrast to most organic solvents, the replacement of a molecule of perfluoroalkane by another molecule, which has little interaction

with his neighbors, needs little energy. Therefore, it is expected that gases should have an exceptionally high solubility in perfluorinated compounds. This is in fact the case, and especially, molecular oxygen has an excellent solubility in most perfluorinated solvents (up to 57 mL of gaseous oxygen in 100 mL of C_7F_{14}) leading to numerous synthetic applications in reactions which involve oxygen. Their chemical inertness, low toxicity, and easy recovery after the reaction make these compounds an interesting class of solvents with potential uses for both industrial and academic chemists. Various perfluorinated solvents are commercially available and could be obtained in a range of boiling points.

When solid products are formed, the perfluorocarbons could be separated on completion of the reaction simply by filtration or decantation, owing to their high density and low miscibility in water and common organic solvents. In addition to the benefits in work-up of reactions, perfluorocarbons display other fascinating solvent properties. They are extremely nonpolar (much less than their analogous alkanes) and inert and are available in a wide range of boiling points (from 56°C for C_6F_{14} to 220°C for $(C_5F_{11})_3N$), and hence are useful for carrying out reactions under vigorous conditions.

The common advantage of the use of fluorous media is the easiness of the separation or purification in the work-up of the reaction. In addition to the unique property, fluorous solvents exhibit low toxicity and high solubility of gases such as oxygen, which can make it possible to mammals (mice and cats) to breathe and survive in the liquid.

1.6.1 Extraction

The use of fluorous media in extraction has been reviewed by Weber et al. [363]. The use of fluorous solvents as a novel extraction/cleanup procedure has been reported for perfluorinated compounds in fat-containing samples [364].

1.6.2 Organic Synthesis

The homogeneous and heterogeneous catalytic reactions in the nonconventional solvents have been reviewed by Liu and Xiao [365]. The synthesis of polyhydroquinoline derivatives via unsymmetrical Hantzsch reaction has been reported in the presence of Hafnium (IV) bis(perfluorooctanesulfonyl)imide complex in fluorous medium at 60°C in high yields and short reaction time [366].

The polymer-supported ytterbium perfluorooctanesulfonate has been used as a catalyst for esterification, nitration, Fridel-Crafts acylation, and aldol condensation. The catalyst is easily separated and can be reused several times without a noticeable change in activity under fluorous solvent-free conditions [367]. The trisubstituted imidazoles have been synthesized using ytterbium perfluorooctanesulfonates as

catalysts in fluorous solvents. The fluorous phase containing only catalyst can be reused several times [368]. The droplet reactors with catalytically active walls have been generated using microfluidic techniques and a fluorous-tagged palladium catalyst and employed for Suzuki-Miyaura coupling reactions [369].

The use of fluorous biphasic system and SC-CO_2 as solvents has been described for a transesterification catalyzed by α-chymotrypsin [370].

The 14-substituted-14*H*-dibenzo[*a*,*j*]xanthenes have been synthesized via one-pot condensation of β-naphthol with aryl or alkyl aldehydes in the presence of scandium bis(perfluorooctanesulfonyl)imide complex as catalyst and perfluorodecalin as sole solvent [371]. The syntheses of fluorous quaternary ammonium salts and their application as phase transfer catalysts for halide substitution reactions have been investigated in extremely nonpolar fluorous solvents [372]. The synthesis of 2-substituted-N_1-carbethoxy-2,3-dihydro-4(1*H*)-quinazolinones has been studied via condensation of substituted *N*-carbethoxyanthranilamide with aldehydes and refluxing in 2,2,2-trifluoroethanol or hexafluoroisopropanol media using *p*-toluenesulfonic acid as catalyst [373].

The hydrolysis of *p*-nitrophenyl esters has been reported in mixtures of water and a fluorous solvent [374]. The Corey-Bakshi-Shibata (CBS) reduction of acetophenone has been developed using a fluorous prolinol immobilized in a hydrofluoroether solvent in high yield and in high enantiomeric excess in the absence of any organic solvent [375]. The fluorous nanoparticles have been synthesized using fluorinated microemulsions as reaction media [376].

1.7 Conclusions

There has been a paradigm shift from the traditional concept of process efficiency to that allocates economic value to conserving energy and raw materials, eliminating waste, and avoiding the utilization of toxic and/or hazardous chemicals. The green alternative solvents and approaches have been developed and employed for a wide range of reactions. In the absence of the greenest solvent, in terms of reducing waste, solvent-free synthesis seems to be a highly useful technique, especially for industry. The solvent-less approach has diverse advantages including reduction or elimination of solvents, thereby preventing pollution in organic synthesis, enhancement of the reactions rate, and reduction in energy usage. Water is the most abundant and environmentally friendly solvent in nature. The different chemical reactions in laboratory and on industrial scales have been studied in water, and a significant number of these reactions are actually promoted by an aqueous reaction medium. Although water has unique properties, it has not traditionally been the solvent of choice for performing organic reactions. Because (a) most organic substances are insoluble in water, as a result, water does not function as a reaction medium and (b) many reactive substrates, reagents, and catalysts are decomposed or deactivated by water. There has been considerable attention in SCFs because of their unique properties and relatively low environmental impact. SCFs have been successfully

employed for particle production, as reaction media, and for the destruction of toxic waste. SC-CO_2 has been the most widely used SCF, mainly because it is cheap, relatively nontoxic, and has convenient critical values. SCFs have also been used on analytical and preparative scales for many biological and other applications. ILs are a new class of solvents which can be easily synthesized and their properties can be tailored. Although, some of these liquids may be more expensive than other alternatives, but the chance to make task-specific solvents for particular processes is very exciting. The challenge of sustainability and green chemistry is leading to fundamental, game-changing innovations in organic synthesis that will eventually cause economic, environmental, and societal advantages in the laboratory and industry chemical processes.

Acknowledgments We wish to express our gratitude to the Research Affairs Division Isfahan University of Technology (IUT) for financial support. Further financial supports from National Elite Foundation (NEF) and Center of Excellency in Sensors and Green Research (IUT) are also gratefully acknowledged.

References

1. Brennecke JF, Maginn EJ (2001) Ionic liquids: innovative fluids for chemical processing. AIChE J 47:2384
2. Sheldon R (2001) Catalytic reactions in ionic liquids. Chem. Comm. (Camb) 2399
3. Lancaster M (2002) Green chemistry: an introductory text. Royal Society of Chemistry, Cambridge
4. Anastas PT, Warner JC (1998) Green chemistry: theory and practice. Oxford University Press, New York
5. Kerton FM (2009) Alternative solvents for green chemistry. RSC publishing, Cambridge
6. Mikami K (2005) Green reaction media in organic synthesis. Wiley-Blackwell, Oxford
7. Adams DJ, Dyson PJ, Taverner SJ (2004) Chemistry in alternative reaction media. Wiley, Chichester
8. Nelson WM (2003) Green solvents for chemistry: perspective and practice. Oxford University Press, Oxford
9. Martins MAP, Frizzo CP, Moreira DN, Buriol L, Machado P (2009) Solvent-free heterocyclic synthesis. Chem Rev 109:4140–4182
10. Nagendrappa G (2002) Organic synthesis under solvent-free condition: an environmentally benign procedure – I. Resonance 7:59–68
11. Tanaka K (2003) Solvent-free organic synthesis. Wiley-VHC, Weinheim
12. Varma RS (1999) Solvent-free organic syntheses. Green Chem 1:43–55
13. Toda F, Tanaka K (2000) Solvent-free organic synthesis. Chem Rev 100:1025–1074
14. Garay AL, Pichon A, James SL (2007) Solvent-free synthesis of metal complexes. Chem Soc Rev 36:846–855
15. Walsh PJ, Li H, de Parrodi CA (2007) A green chemistry approach to asymmetric catalysis: solvent-free and highly concentrated reactions. Chem Rev 107:2503–2545
16. Cave GWV, Raston CL, Scott JL (2001) Recent advances in solventless organic reactions: towards benign synthesis with remarkable versatility. Chem Commun 21:2159–2169
17. Dunk B, Jachuck R (2000) A novel continuous reactor for UV irradiated reactions. Green Chem 2:G13–G14
18. Waddell DC, Mack J (2009) An environmentally benign solvent-free Tishchenko reaction. Green Chem 11:79–82

19. Rothenberg G, Downie AP, Raston CL, Scott JL (2001) Understanding solid/solid organic reactions. J Am Chem Soc 123:8701–8708
20. Wegenhart BL, Abu-Omar MM (2010) A solvent-free method for making dioxolane and dioxane from the biorenewables glycerol and furfural catalyzed by oxorhenium(V) oxazoline. Inorg Chem 49:4741–4743
21. Wang B, Zhang H, Jing X, Zhu J (2010) Solvent free catalytic synthesis of 2-methylallylidene diacetate using cation-exchange resin. Catal Commun 11:753–757
22. Bao K, Fan A, Dai Y, Zhang L, Zhang W, Cheng M, Yao X (2009) Selective demethylation and debenzylation of aryl ethers by magnesium iodide under solvent-free conditions and its application to the total synthesis of natural products. Org Biomol Chem 7:5084–5090
23. Waddell DC, Thiel I, Clark TD, Marcum ST, Mack J (2010) Making kinetic and thermodynamic enolates via solvent-free high speed ball milling. Green Chem 12:209–211
24. Gora M, Kozik B, Jamrozy K, Łuczynski MK, Brzuzan P, Wozny M (2009) Solvent-free condensations of ketones with malononitrile catalysed by methanesulfonic acid/morpholine system. Green Chem 11:863–867
25. Trotzki R, Hoffmann MM, Ondruschka B (2008) Studies on the solvent-free and waste-free Knoevenagel condensation. Green Chem 10:767–772
26. Sudheesh N, Sharma SK, Shukla RS (2010) Chitosan as an eco-friendly solid base catalyst for the solvent-free synthesis of jasminaldehyde. J Mol Catal A Chem 321:77–82
27. Madhav JV, Reddy YT, Reddy PN, Reddy MN, Kuarm S, Crooks PA, Rajitha B (2009) Cellulose sulfuric acid: an efficient biodegradable and recyclable solid acid catalyst for the one-pot synthesis of aryl-14H-dibenzo[*a.j*]xanthenes under solvent-free conditions. J Mol Catal A Chem 304:85–87
28. Banon-Caballero A, Guillena G, Najera C (2010) Solvent-free direct enantioselective aldol reaction using polystyrene-supported *N*-sulfonyl-(R_a)-binam-D-prolinamide as a catalyst. Green Chem 12:1599–1606
29. Thorwirth R, Stolle A, Ondruschka B (2010) Fast copper-, ligand- and solvent-free Sonogashira coupling in a ball mill. Green Chem 12:985–991
30. Fulmer DA, Shearouse WC, Medonza ST, Mack J (2009) Solvent-free Sonogashira coupling reaction via high speed ball milling. Green Chem 11:1821–1825
31. Kniese M, Meier MAR (2010) A simple approach to reduce the environmental impact of olefin metathesis reactions: a green and renewable solvent compared to solvent-free reactions. Green Chem 12:169–173
32. Huertas D, Florscher M, Dragojlovic V (2009) Solvent-free Diels-Alder reactions of in situ generated cyclopentadiene. Green Chem 11:91–95
33. Bellezza F, Cipiciani A, Costantino U, Fringuelli F, Orru M, Piermatti O, Pizzo F (2010) Aza-Diels-Alder reaction of Danishefsky's diene with immines catalyzed by porous α-zirconium hydrogen phosphate and SDS under solvent-free conditions. Catal Today 152:61–65
34. Ma X, Zhou Y, Zhang J, Zhu A, Jiang T, Han B (2008) Solvent-free Heck reaction catalyzed by a recyclable Pd catalyst supported on SBA-15 via an ionic liquid. Green Chem 10:59–66
35. Yue CB, Yi TF, Zhu CB, Liu G (2009) Mannich reaction catalyzed by a novel catalyst under solvent-free conditions. J Ind Eng Chem 15:653–656
36. Wang ZJ, Zhou HF, Wang TL, He YM, Fan QH (2009) Highly enantioselective hydrogenation of quinolines under solvent-free or highly concentrated conditions. Green Chem 11:767–769
37. Chang F, Kim H, Lee B, Park S, Park J (2010) Highly efficient solvent-free catalytic hydrogenation of solid alkenes and nitro-aromatics using Pd nanoparticles entrapped in aluminum oxy-hydroxide. Tetrahedron Lett 51:4250–4252
38. Gang L, Xinzong L, Eli W (2007) Solvent-free esterification catalyzed by surfactant-combined catalysts at room temperature. New J Chem 31:348–351
39. Jida M, Deprez-Poulain R, Malaquin S, Roussel P, Agbossou-Niedercorn F, Deprez B, Laconde G (2010) Solvent-free microwave-assisted Meyers' lactamization. Green Chem 12:961–964

40. Zhao Y, Li J, Li C, Yin K, Ye D, Jia X (2010) PTSA-catalyzed green synthesis of 1,3, 5-triarylbenzene under solvent-free conditions. Green Chem 12:1370–1372
41. Monnereau L, Semeril D, Matt D (2010) Calix[4]arene-diphosphite rhodium complexes in solvent-free hydroaminovinylation of olefins. Green Chem 12:1670–1673
42. Wang T, Ma R, Liu L, Zhan Z (2010) Solvent-free solid acid-catalyzed nucleophilic substitution of propargylic alcohols: a green approach for the synthesis of 1,4-diynes. Green Chem 12:1576–1579
43. Wang D, Li J, Li N, Gao T, Hou S, Chen B (2010) An efficient approach to homocoupling of terminal alkynes: solvent-free synthesis of 1,3-diynes using catalytic Cu(II) and base. Green Chem 12:45–48
44. Epane G, Laguerre JC, Wadouachi A, Marek D (2010) Microwave-assisted conversion of D-glucose into lactic acid under solvent-free conditions. Green Chem 12:502–506
45. Patil PR, Kartha KPR (2009) Solvent-free synthesis of thioglycosides by ball milling. Green Chem 11:953–956
46. Favrelle A, Bonnet V, Avondo C, Aubry F, Djedaïni-Pilard F, Sarazin C (2010) Lipase-catalyzed synthesis and characterization of novel lipidyl-cyclodextrins in solvent free medium. J Mol Catal B Enzym 66:224–227
47. Wang C, Zhao W, Li H, Guo L (2009) Solvent-free synthesis of unsaturated ketones by the Saucy-Marbet reaction using simple ammonium ionic liquid as a catalyst. Green Chem 11:843–847
48. Mao W, Ma H, Wang B (2009) A clean method for solvent-free nitration of toluene over sulfated titania promoted by ceria catalysts. J Hazard Mater 167:707–712
49. Gao J, He LN, Miao CX, Chanfreau S (2010) Chemical fixation of CO_2: efficient synthesis of quinazoline-2,4(1H, 3H)-diones catalyzed by guanidines under solvent-free conditions. Tetrahedron 66:4063–4067
50. Fu YL, Huang W, Li CL, Wang LY, Wei YS, Huang Y, Zhang XH, Wen ZY, Zhang ZX (2009) Monomethine cyanine dyes with an indole nucleus: microwave-assisted solvent-free synthesis, spectral properties and theoretical studies. Dyes Pigments 82:409–415
51. Tyagi B, Mishra MK, Jasra RV (2010) Solvent free synthesis of acetyl salicylic acid over nano-crystalline sulfated zirconia solid acid catalyst. J Mol Catal A Chem 317:41–45
52. Matsumoto K, Yamaguchi T, Katsuki T (2008) Asymmetric oxidation of sulfides under solvent-free or highly concentrated conditions. Chem Commun 1704–1706
53. Figiel PJ, Kopylovich MN, Lasri J, Guedes da Silva MFC, Frausto da Silva JJR, Pombeiro AJL (2010) Solvent-free microwave-assisted peroxidative oxidation of secondary alcohols to the corresponding ketones catalyzed by copper(II) 2,4-alkoxy-1,3,5-triazapentadienato complexes. Chem Commun 46:2766–2768
54. Wang H, Deng SX, Shen ZR, Wang JG, Ding DT, Chen TH (2009) Facile preparation of Pd/organoclay catalysts with high performance in solvent-free aerobic selective oxidation of benzyl alcohol. Green Chem 11:1499–1502
55. Ni J, Yu WJ, He L, Sun H, Cao Y, He HY, Fan KN (2009) A green and efficient oxidation of alcohols by supported gold catalysts using aqueous H_2O_2 under organic solvent-free conditions. Green Chem 11:756–759
56. Zhang J, Wang Z, Wang Y, Wan C, Zheng X, Wang Z (2009) A metal-free catalytic system for the oxidation of benzylic methylenes and primary amines under solvent-free conditions. Green Chem 11:1973–1978
57. Dimitratos N, Lopez-Sanchez JA, Morgan D, Carley AF, Tiruvalam R, Kiely CJ, Bethell D, Hutchings GJ (2009) Solvent-free oxidation of benzyl alcohol using Au-Pd catalysts prepared by sol immobilization. Phys Chem Phys 11:5142–5153
58. Liu G, Hou M, Song J, Zhang Z, Wu T, Han B (2010) Ni^{2+}-containing ionic liquid immobilized on silica: effective catalyst for styrene oxidation with H_2O_2 at solvent-free condition. J Mol Catal A Chem 316:90–94
59. Wang C, Wang G, Mao J, Yao Z, Li H (2010) Metal and solvent-free oxidation of α-isophorone to ketoisophorone by molecular oxygen. Catal Commun 11:758–762

60. Choudhary VR, Dumbre DK (2009) Magnesium oxide supported nano-gold: a highly active catalyst for solvent-free oxidation of benzyl alcohol to benzaldehyde by TBHP. Catal Commun 10:1738–1742
61. Kirumakki S, Samarajeewa S, Harwell R, Mukherjee A, Herber RH, Clearfield A (2008) Sn(IV) phosphonates as catalysts in solvent-free Baeyer-Villiger oxidations using H_2O_2. Chem Commun 5556–5558
62. Szuppa T, Stolle A, Ondruschka B, Hopfe W (2010) Solvent-free dehydrogenation of γ-terpinene in a ball mill: investigation of reaction parameters. Green Chem 12:1288–1294
63. Pham PD, Bertus P, Legoupy S (2009) Solvent-free direct reductive amination by catalytic use of an organotin reagent incorporated on an ionic liquid. Chem Commun 6207–6209
64. Longhi K, Moreira DN, Marzari MRB, Floss VM, Bonacorso HG, Zanatta N, Martins MAP (2010) An efficient solvent-free synthesis of NH-pyrazoles from β-dimethylaminovinylketones and hydrazine on grinding. Tetrahedron Lett 51:3193–3196
65. Rafiee E, Eavani S, Rashidzadeh S, Joshaghani M (2009) Silica supported 12-tungstophosphoric acid catalysts for synthesis of 1,4-dihydropyridines under solvent-free conditions. Inorg Chim Acta 362:3555–3562
66. Zhang J-X, Zheng Y-P, Lan L, Mo S, Yu P-Y, Shi W, Wang R-M (2009) Direct synthesis of solvent-free multiwall carbon nanotubes/silica nonionic nanofluid hybrid material. ACS Nano 3:2185–2190
67. Pol VG, Daemen LL, Vogel S, Chertkov G (2010) Solvent-free fabrication of ferromagnetic Fe_3O_4 octahedra. Ind Eng Chem Res 49:920–924
68. Pol VG, Thiyagarajan P, Calderon Moreno JM, Popa M (2009) Solvent-free fabrication of rare $LaCO_3OH$ luminescent superstructures. Inorg Chem 48:6417–6424
69. Tsekova DS, Saez JA, Escuder B, Miravet JF (2009) Solvent-free construction of self-assembled 1D nanostructures from low-molecular-weight organogelators: sublimation vs. gelation. Soft Matter 5:3727–3735
70. Li S, Yan W, Zhang W (2009) Solvent-free production of nanoscale zero-valent iron (nZVI) with precision milling. Green Chem 11:1618–1626
71. Atkinson MBJ, Bucar DK, Sokolov AN, Friscic T, Robinson CN, Bilal MY, Sinada NG, Chevannes A, MacGillivray LR (2008) General application of mechanochemistry to templated solid-state reactivity: rapid and solvent-free access to crystalline supermolecules. Chem Commun 5713–5715
72. Ji G, Gong Z, Zhu W, Zheng M, Liao S, Shen K, Liu J, Cao J (2009) Simply synthesis of Co_3O_4 nanowire arrays using a solvent-free method. J Alloys Comp 476:579–583
73. Wang X, He L, He Y, Zhang J, Su CY (2009) Solvent-free synthesis of a Pd(II) coordination networked complex as reusable catalyst based on 3,5-bis(diphenylphosphino)benzoic acid. Inorg Chim Acta 362:3513–3518
74. Chmura AJ, Davidson MG, Frankis CJ, Jones MD, Lunn MD (2008) Highly active and stereoselective zirconium and hafnium alkoxide initiators for solvent-free ring-opening polymerization of *rac*-lactide. Chem Commun 1293–1295
75. Kumar Saha T, Rajashekhar B, Gowda RR, Ramkumar V, Chakraborty D (2010) Bis(imino) phenoxide complexes of zirconium: synthesis, structural characterization and solvent-free ring-opening polymerization of cyclic esters and lactides. Dalton Trans 39:5091–5093
76. Raynaud J, Ottou WN, Gnanou Y, Taton D (2010) Metal-free and solvent-free access to α, ω-heterodifunctionalized poly(propylene oxide)s by N-heterocyclic carbene-induced ring opening polymerization. Chem Commun 46:3203–3205
77. Horchani H, Chaabouni M, Gargouri Y, Sayari A (2010) Solvent-free lipase-catalyzed synthesis of long-chain starch esters using microwave heating: optimization by response surface methodology. Carbohydr Polym 79:466–474
78. Lubineau A, Augé J (1999) Water as solvent in organic synthesis. Springer, Berlin
79. Li CJ (1999) Organic reactions in aqueous media-with a focus on carbon-carbon bond formation. Chem Rev 93:2023–2035
80. Li CJ, Chan TH (2007) Comprehensive organic reactions in aqueous media. Wiley-Interscience, Hoboken

81. Lindstrom UM (2007) Organic reactions in water, principles, strategies and applications. Blackwell Publishing, Oxford
82. Raj M, Singh VK (2009) Organocatalytic reactions in water. Chem Commun 6687–6703
83. Peng YY, Liu J, Lei X, Yin Z (2010) Room-temperature highly efficient Suzuki-Miyaura reactions in water in the presence of Stilbazo. Green Chem 12:1072–1075
84. Prastaro A, Ceci P, Chiancone E, Boffi A, Cirilli R, Colone M, Fabrizi G, Stringaro A, Cacchi S (2009) Suzuki-Miyaura cross-coupling catalyzed by protein-stabilized palladium nanoparticles under aerobic conditions in water: application to a one-pot chemoenzymatic enantioselective synthesis of chiral biaryl alcohols. Green Chem 11:1929–1932
85. Ohtaka A, Teratani T, Fujii R, Ikeshita K, Shimomura O, Nomura R (2009) Facile preparation of linear polystyrene-stabilized Pd nanoparticles in water. Chem Commun 7188–7190
86. Lipshutz BH, Ghorai S (2010) PQS-2: ring-closing- and cross-metathesis reactions on lipophilic substrates; in water only at room temperature, with in-flask catalyst recycling. Tetrahedron 66:1057–1063
87. Vieira AS, Cunha RLOR, Klitzke CF, Zukerman-Schpector J, Stefani HA (2010) Highly efficient palladium-catalyzed Suzuki-Miyaura reactions of potassium aryltrifluoroborates with 5-iodo-1,3-dioxin-4-ones in water: an approach to α-aryl-β-ketoesters. Tetrahedron 66: 773–779
88. Wu J, Ni B, Headley AD (2009) Di(methylimidazole)prolinol silyl ether catalyzed highly michael addition of aldehydes to nitroolefins in water. Org Lett 11:3354–3356
89. Hao WJ, Jiang B, Tu SJ, Cao XD, Wu SS, Yan S, Zhang XH, Han ZG, Shi F (2009) A new mild base-catalyzed Mannich reaction of hetero-arylamines in water: highly efficient stereoselective synthesis of β-aminoketones under microwave heating. Org Biomol Chem 7:1410–1414
90. Ko K, Nakano K, Watanabe S, Ichikawa Y, Kotsuki H (2009) Development of new DMAP-related organocatalysts for use in the Michael addition reaction of β-ketoesters in water. Tetrahedron Lett 50:4025–4029
91. De Rosa M, Soriente A (2010) A combination of water and microwave irradiation promotes the catalyst-free addition of pyrroles and indoles to nitroalkenes. Tetrahedron 66:2981–2986
92. Xu DZ, Liu Y, Shi S, Wang Y (2010) A simple, efficient and green procedure for Knoevenagel condensation catalyzed by $[C_4dabco][BF_4]$ ionic liquid in water. Green Chem 12:514–517
93. Yu JJ, Wang LM, Liu JQ, Guo FL, Liu Y, Jiao N (2010) Synthesis of tetraketones in water and under catalyst-free conditions. Green Chem 12:216–219
94. Lin JH, Zhang CP, Xiao JC (2009) Enantioselective aldol reaction of cyclic ketones with aryl aldehydes catalyzed by a cyclohexanediamine derived salt in the presence of water. Green Chem 11:1750–1753
95. Jiang Z, Yang H, Han X, Luo J, Wong MW, Lu Y (2010) Direct asymmetric aldol reactions between aldehydes and ketones catalyzed by L-tryptophan in the presence of water. Org Biomol Chem 8:1368–1377
96. Fu SD, Fu XK, Zhang SP, Zou XC, Wu XJ (2009) Highly diastereo- and enantioselective direct aldol reactions by 4-tert-butyldimethylsiloxy-substituted organocatalysts derived from N-prolylsulfonamides in water. Tetrahedron Asymmetry 20:2390–2396
97. Behr A, Leschinski J (2009) Application of the solvent water in two-phase telomerisation reactions and recycling of the homogeneous palladium catalysts. Green Chem 11:609–613
98. Nishikata T, Lipshutz BH (2009) Amination of allylic alcohols in water at room temperature. Org Lett 11:2377–2379
99. Saidi O, Blacker AJ, Farah MM, Marsden SP, Williams JMJ (2010) Iridium-catalysed amine alkylation with alcohols in water. Chem Commun 46:1541–1543
100. Marzaro G, Guiotto A, Chilin A (2009) Microwave-promoted mono-N-alkylation of aromatic amines in water: a new efficient and green method for an old and problematic reaction. Green Chem 11:774–776
101. Coutouli-Argyropoulou E, Sarridis P, Gkizis P (2009) Water as the medium of choice for the 1,3-dipolar cycloaddition reactions of hydrophobic nitrones. Green Chem 11:1906–1914

102. Jing L, Wei J, Zhou L, Huang Z, Lia Z, Zhou X (2010) Lithium pipecolinate as a facile and efficient ligand for copper-catalyzed hydroxylation of aryl halides in water. Chem Commun 46:4767–4769
103. Bernini R, Cacchi S, Fabrizi G, Forte G, Petrucci F, Prastaro A, Niembro S, Shafir A, Vallribera A (2009) Alkynylation of aryl halides with perfluoro-tagged palladium nanoparticles immobilized on silica gel under aerobic, copper- and phosphine-free conditions in water. Org Biomol Chem 7:2270–2273
104. Bhadra S, Saha A, Ranu BC (2008) One-pot copper nanoparticle-catalyzed synthesis of S-aryl- and S-vinyl dithiocarbamates in water: high diastereoselectivity achieved for vinyl dithiocarbamates. Green Chem 10:1224–1230
105. Pei BJ, Lee AWM (2010) Highly efficient synthesis of extended triptycenes via Diels-Alder cycloaddition in water under microwave radiation. Tetrahedron Lett 51:4519–4522
106. Ma Y, Jin S, Kan Y, Zhang YJ, Zhang W (2010) Highly active asymmetric Diels-Alder reactions catalyzed by C_2-symmetric bipyrrolidines: catalyst recycling in water medium and insight into the catalytic mode. Tetrahedron 66:3849–3854
107. Matveeva EV, Petrovskii PV, Klemenkova ZS, Bondarenko NA, Odinets IL (2010) A practical and efficient green synthesis of β-aminophosphoryl compounds via the aza-Michael reaction in water. C R Chimie 13:964–970
108. Rafiee E, Eavani S, Khajooei Nejad F, Joshaghani M (2010) $Cs_{2.5}H_{0.5}PW_{12}O_{40}$ catalyzed diastereoselective synthesis of β-amino ketones via three component Mannich-type reaction in water. Tetrahedron 66:6858–6863
109. Mukhopadhyay C, Datta A, Butcher RJ (2009) Highly efficient one-pot, three-component Mannich reaction catalysed by boric acid and glycerol in water with major 'syn' diastereoselectivity. Tetrahedron Lett 50:4246–4250
110. Li J, Lu L, Su W (2010) A new strategy for the synthesis of benzoxanthenes catalyzed by proline triflate in water. Tetrahedron Lett 51:2434–2437
111. Teimouri MB, Abbasi T, Mivehchi H (2008) Novel multicomponent reactions of primary amines and alkyl propiolates with alloxan derivatives in water. Tetrahedron 64:10425–10430
112. Firouzabadi H, Iranpoor N, Gholinejad M (2010) Recyclable palladium-catalyzed Sonogashira-Hagihara coupling of aryl halides using 2-aminophenyl diphenylphosphinite ligand in neat water under copper-free condition. J Mol Catal A Chem 321:110–116
113. Suzuka T, Okada Y, Ooshiro K, Uozumi Y (2010) Copper-free Sonogashira coupling in water with an amphiphilic resin-supported palladium complex. Tetrahedron 66:1064–1069
114. Panchan W, Chiampanichayakul S, Snyder DL, Yodbuntung S, Pohmakotr M, Reutrakul V, Jaipetch T, Kuhakarn C (2010) Facile oxidative hydrolysis of acetals to esters using hypervalent iodine(III)/LiBr combination in water. Tetrahedron 66:2732–2735
115. MacLeod PD, Li Z, Li CJ (2010) Self-catalytic, solvent-free or in/on water protocol: aza-Friedel-Crafts reactions between 3,4-dihydroisoquinoline and 1- or 2-naphthols. Tetrahedron 66:1045–1050
116. DeBlase C, Leadbeater NE (2010) Ligand-free CuI-catalyzed cyanation of aryl halides using $K_4[Fe(CN)_6]$ as cyanide source and water as solvent. Tetrahedron 66:1098–1101
117. Sin E, Yi SS, Lee YS (2010) Chitosan-g-mPEG-supported palladium (0) catalyst for Suzuki cross-coupling reaction in water. J Mol Catal A Chem 315:99–104
118. Liautard V, Desvergnes V, Martin OR (2008) Novel Galf-disaccharide mimics: synthesis by way of 1,3-dipolar cycloaddition reactions in water. Tetrahedron Asymmetry 19:1999–2002
119. Wu XL, Wang GW (2009) Hypervalent iodine-mediated aminobromination of olefins in water. Tetrahedron 65:8802–8807
120. Astarita A, Cermola F, DellaGreca M, Iesce MR, Previtera L, Rubino M (2009) Photooxygenation of furans in water and ionic liquid solutions. Green Chem 11:2030–2033
121. Kuroboshi M, Yoshida T, Oshitani J, Goto K, Tanaka H (2009) Electroorganic synthesis in oil-in-water (O/W) nanoemulsion: TEMPO-mediated electrooxidation of amphiphilic alcohols in water. Tetrahedron 65:7177–7185

122. Shen W, Wang LM, Tian H, Tang J, Yu JJ (2009) Brønsted acidic imidazolium salts containing perfluoroalkyl tails catalyzed one-pot synthesis of 1,8-dioxo-decahydroacridines in water. J Fluorine Chem 130:522–527
123. Wang J, Wang H (2009) Clean production of Acid Blue 9 via catalytic oxidation in water. Ind Eng Chem Res 48:5548–5550
124. Feng B, Hou Z, Wang X, Hu Y, Li H, Qiao Y (2009) Selective aerobic oxidation of styrene to benzaldehyde catalyzed by water-soluble palladium(II) complex in water. Green Chem 11:1446–1452
125. Takenaga N, Goto A, Yoshimura M, Fujioka H, Dohi T, Kita Y (2009) Hypervalent iodine(III)/$Et_4N^+Br^-$ combination in water for green and racemization-free aqueous oxidation of alcohols. Tetrahedron Lett 50:3227–3229
126. Figiel PJ, Kirillov AM, Karabach YY, Kopylovich MN, Pombeiro AJL (2009) Mild aerobic oxidation of benzyl alcohols to benzaldehydes in water catalyzed by aqua-soluble multicopper(II) triethanolaminate compounds. J Mol Catal A Chem 305:178–182
127. Mitsudome T, Noujima A, Mizugaki T, Jitsukawa K, Kaneda K (2009) Supported gold nanoparticle catalyst for the selective oxidation of silanes to silanols in water. Chem Commun 5302–5304
128. Zeror S, Collin J, Fiaud JC, Aribi Zouioueche L (2010) Enantioselective ketoester reductions in water: a comparison between microorganism- and ruthenium-catalyzed reactions. Tetrahedron Asymmetry 21:1211–1215
129. Sant' Anna Gds, Machado P, Sauzem PD, Rosa FA, Rubin MA, Ferreira J, Bonacorso HG, Zanattaa N, Martins MAP (2009) Ultrasound promoted synthesis of 2-imidazolines in water: a greener approach toward monoamine oxidase inhibitors. Bioorg Med Chem Lett 19:546–549
130. Carpita A, Ribecai A, Stabile P (2010) Microwave-assisted synthesis of indole- and azaindole-derivatives in water via cycloisomerization of 2-alkynylanilines and alkynylpyridinamines promoted by amines or catalytic amounts of neutral or basic salts. Tetrahedron 66:7169–7178
131. Qu GR, Zhao L, Wang DC, Wu J, Guo HM (2008) Microwave-promoted efficient synthesis of C6-cyclo secondary amine substituted purine analogues in neat water. Green Chem 10:287–289
132. Tu SJ, Cao XD, Hao WJ, Zhang XH, Yan S, Wu SS, Han ZG, Shi F (2009) An efficient and chemoselective synthesis of benzo[*e*][1,4]thiazepin-2-(1*H*,3*H*,5*H*)-ones via a microwave-assisted multi-component reaction in water. Org Biomol Chem 7:557–563
133. Tu SJ, Zhang XH, Han ZG, Cao XD, Wu SS, Yan S, Hao WJ, Zhang G, Ma N (2009) Synthesis of isoxazolo[5,4-b]pyridines by microwave-assisted multi-component reactions in water. J Comb Chem 11:428–432
134. Baruwati B, Polshettiwar V, Varma RS (2009) Glutathione promoted expeditious green synthesis of silver nanoparticles in water using microwaves. Green Chem 11:926–930
135. Jessop PG, Leitner W (1999) Chemical synthesis using supercritical fluids. Wiley-VCH, Weinheim
136. Williams JR, Clifford AA (2000) Supercritical fluid methods and protocols. Humana Press Totowa, Totowa
137. Hyde JR, Licence P, Carter D, Poliakoff M (2001) Continuous catalytic reactions in supercritical fluids. Appl Catal A Gen 222:119–131
138. Señoráns FJ, Ibañez E (2002) Analysis of fatty acids in foods by supercritical fluid chromatography. Anal Chim Acta 465:131–144
139. Sarrade S, Guizard C, Rios GM (2003) New applications of supercritical fluids and supercritical fluids processes in separation. Sep Purif Technol 32:57–63
140. Goodship V, Ogur EO (2004) Polymer processing with supercritical fluids, Rapra review reports. Rapra Technology Ltd, Shawbury
141. Prajapati D, Gohain M (2004) Recent advances in the application of supercritical fluids for carbon-carbon bond formation in organic synthesis. Tetrahedron 60:815–833

142. Yeo SD, Kiran E (2005) Formation of polymer particles with supercritical fluids: a review. J Supercrit Fluid 34:287–308
143. Aymonier C, Loppinet-Serani A, Reveron H, Garrabos Y, Cansell F (2006) Review of supercritical fluids in inorganic materials science. J Supercrit Fluid 38:242–251
144. Martínez JL (2008) Supercritical fluid extraction of nutraceuticals and bioactive compounds. CRC Press, Taylor & Francis Group, Boca Raton
145. Mishima K (2008) Biodegradable particle formation for drug and gene delivery using supercritical fluid and dense gas. Adv Drug Deliv Rev 60:411–432
146. Sunarso J, Ismadji S (2009) Decontamination of hazardous substances from solid matrices and liquids using supercritical fluids extraction: a review. J Hazard Mater 161:1–20
147. Ramsey E, Sun Q, Zhang Z, Zhang C, Gou W (2009) Mini-review: green sustainable processes using supercritical fluid carbon dioxide. J Environ Sci 21:720–726
148. Herrero M, Mendiola JA, Cifuentes A, Ibanez E (2010) Supercritical fluid extraction: recent advances and applications. J Chromatogr A 1217:2495–2511
149. Egydio JA, Moraes AM, Rosa PTV (2010) Supercritical fluid extraction of lycopene from tomato juice and characterization of its antioxidation activity. J Supercrit Fluid 54:159–164
150. Hanif M, Atsuta Y, Fujie K, Daimon H (2010) Supercritical fluid extraction of microbial phospholipid fatty acids from activated sludge. J Chromatogr A 1217:6704–6708
151. Nguyen-Phan TD, Pham HD, Kim S, Oh ES, Kim EJ, Shin EW (2010) Surfactant removal from mesoporous TiO_2 nanocrystals by supercritical CO_2 fluid extraction. J Ind Eng Chem 16:823–828
152. Arias M, Penichet I, Ysambertt F, Bauza R, Zougagh M, Ríos A (2009) Fast supercritical fluid extraction of low- and high-density polyethylene additives: comparison with conventional reflux and automatic Soxhlet extraction. J Supercrit Fluid 50:22–28
153. Tian G, Liao W, Wai CM, Rao L (2008) Extraction of trivalent lanthanides with oxa-diamides in supercritical fluid carbon dioxide. Ind Eng Chem Res 47:2803–2807
154. Sotelo JL, Rodrıguez A, Agueda VI, Gomez P (2010) Supercritical fluids as reaction media in the ethylbenzene disproportionation on ZSM-5. J Supercrit Fluid 55:241–245
155. Sparks DL, Estevez LA, Hernandez R (2009) Supercritical-fluid-assisted oxidation of oleic acid with ozone and potassium permanganate. Green Chem 11:986–993
156. Lopez-Periago AM, Garcıa-Gonzalez CA, Domingo C (2010) Towards the synthesis of Schiff base macrocycles under supercritical CO_2 conditions. Chem Commun 46:4315–4317
157. Chatterjee M, Matsushima K, Ikushima Y, Sato M, Yokoyama T, Kawanami H, Suzuki T (2010) Production of linear alkane via hydrogenative ring opening of a furfural-derived compound in supercritical carbon dioxide. Green Chem 12:779–782
158. Grignard B, Phan T, Bertin D, Gigmes D, Jerome C, Detrembleur C (2010) Dispersion nitroxide mediated polymerization of methyl methacrylate in supercritical carbon dioxide using in situ formed stabilizers. Polym Chem 1:837–840
159. Li J, Peng J, Zhang G, Bai Y, Lai G, Li X (2010) Hydrosilylation catalysed by a rhodium complex in a supercritical CO_2/ionic liquid system. New J Chem 34:1330–1334
160. Han X, Bourne RA, Poliakoff M, George MW (2009) Strategies for cleaner oxidations using photochemically generated singlet oxygen in supercritical carbon dioxide. Green Chem 11:1787–1792
161. Manoi K, Rizvi SSH (2010) Physicochemical characteristics of phosphorylated cross-linked starch produced by reactive supercritical fluid extrusion. Carbohyd Polym 81:687–694
162. Cheng WT, Chih YW (2010) Manipulation of silver nanostructures using supercritical fluids in the presence of polyvinylpyrrolidone and ethylene glycol. J Supercrit Fluid 54:272–280
163. Wang Q, Guan YX, Yao SJ, Zhu ZQ (2010) Microparticle formation of sodium cellulose sulfate using supercritical fluid assisted atomization introduced by hydrodynamic cavitation mixer. Chem Eng J 159:220–229
164. da Silva MS, Vão ER, Temtem M, Mafr L, Caldeira J, Aguiar-Ricardo A, Casimiro T (2010) Clean synthesis of molecular recognition polymeric materials with chiral sensing capability using supercritical fluid technology. Application as HPLC stationary phases. Biosens Bioelectron 25:1742–1747

165. Chen Z, Li S, Xue F, Sun G, Luo C, Chen J, Xu Q (2010) A simple and efficient route to prepare inorganic hollow microspheres using polymer particles as template in supercritical fluids. Colloids Surf A Physicochem Eng Aspects 355:45–52
166. Duarte ARC, Caridade SG, Mano JF, Reis RL (2009) Processing of novel bioactive polymeric matrixes for tissue engineering using supercritical fluid technology. Mater Sci Eng C 29:2110–2115
167. Padrela L, Rodrigues MA, Velaga SP, Matos HA, de Azevedo EG (2009) Formation of indomethacin-saccharin cocrystals using supercritical fluid technology. Eur J Pharm Sci 38:9–17
168. Duarte ARC, Mano JF, Reis RL (2009) Preparation of chitosan scaffolds loaded with dexamethasone for tissue engineering applications using supercritical fluid technology. Eur Polym J 45:141–148
169. Ramírez R, Garay I, Álvarez J, Martí M, Parra JL, Coderch L (2008) Supercritical fluid extraction to obtain ceramides from wool fibers. Sep Purif Technol 63:552–557
170. Reverchon E, Cardea S, Rapuano C (2008) A new supercritical fluid-based process to produce scaffolds for tissue replacement. J Supercrit Fluid 45:365–373
171. Hoshi T, Sawaguchi T, Matsuno R, Konno T, Takai M, Ishihara K (2010) Control of surface modification uniformity inside small-diameter polyethylene/poly(vinyl acetate) composite tubing prepared with supercritical carbon dioxide. J Mater Chem 20:4897–4904
172. Zhang X, Chang D, Liu J, Luo Y (2010) Conducting polymer aerogels from supercritical CO_2 drying PEDOT-PSS hydrogels. J Mater Chem 20:5080–5085
173. Sun Z, Zhang H, An G, Yang G, Liu Z (2010) Supercritical CO_2-facilitating large-scale synthesis of CeO_2 nanowires and their application for solvent-free selective hydrogenation of nitroarenes. J Mater Chem 20:1947–1952
174. Urbanczyk L, Calberg C, Benali S, Bourbigot S, Espuche E, Gouanve F, Dubois P, Germain A, Jerome C, Detrembleur C, Alexandre M (2008) Poly(caprolactone)/clay masterbatches prepared in supercritical CO_2 as efficient clay delamination promoters in poly(styrene-co-acrylonitrile). J Mater Chem 18:4623–4630
175. Shi J, Khatri M, Xue SJ, Mittal GS, Ma Y, Li D (2009) Solubility of lycopene in supercritical CO_2 fluid as affected by temperature and pressure. Sep Purif Technol 66:322–328
176. Welton T (1999) Room-temperature ionic liquids. Solvents for synthesis and catalysis. Chem Rev 99:2071–2083
177. Wasserscheid P, Welton T (2008) Ionic liquids in synthesis. Wiley-VCH Verlag GmbH & Co. KGaA, Weinheim
178. Keskin S, Kayrak-Talay D, Akman U, Hortacsu O (2007) A review of ionic liquids towards supercritical fluid applications. J Supercrit Fluid 43:150–180
179. Parvulescu VI, Hardacre C (2007) Catalysis in ionic liquids. Chem Rev 107:2615–2665
180. Sledz P, Mauduit M, Grela K (2008) Olefin metathesis in ionic liquids. Chem Soc Rev 37:2433–2442
181. Zhu S, Wu Y, Chen Q, Yu Z, Wang C, Jin S, Ding Y, Wu G (2006) Dissolution of cellulose with ionic liquids and its application: a mini-review. Green Chem 8:325–327
182. Antonietti M, Kuang D, Smarsly B, Zhou Y (2004) Ionic liquids for the convenient synthesis of functional nanoparticles and other inorganic nanostructures. Angew Chem Int Ed 43:4988–4992
183. Martins MAP, Frizzo CP, Moreira DN, Zanatta N, Bonacorso HG (2008) Ionic liquids in heterocyclic synthesis. Chem Rev 108:2015–2050
184. Cao Y, Wu J, Zhang J, Li H, Zhang Y, He J (2009) Room temperature ionic liquids (RTILs): a new and versatile platform for cellulose processing and derivatization. Chem Eng J 147:13–21
185. Kubisa P (2009) Ionic liquids as solvents for polymerization processes-progress and challenges. Prog Polym Sci 34:1333–1347
186. Plechkova NV, Seddon KR (2008) Applications of ionic liquids in the chemical industry. Chem Soc Rev 37:123–150
187. Rogers RD, Seddon KR (2002) Ionic liquids: industrial applications to green chemistry, vol 818, ACS symposium series. American Chemical Society, Washington, DC

188. Rogers RD, Seddon KR (2003) Ionic liquids–solvents of the future? Science 302:792–793
189. Moniruzzaman M, Nakashima K, Kamiya N, Goto M (2010) Recent advances of enzymatic reactions in ionic liquids. Biochem Eng J 48:295–314
190. Noritomi H, Suzuki K, Kikuta M, Kato S (2009) Catalytic activity of α-chymotrypsin in enzymatic peptide synthesis in ionic liquids. Biochem Eng J 47:27–30
191. Shen ZL, Zhou WJ, Liu YT, Ji SJ, Loh TP (2008) One-pot chemoenzymatic syntheses of enantiomerically-enriched *O*-acetyl cyanohydrins from aldehydes in ionic liquid. Green Chem 10:283–286
192. Kahveci D, Guo Z, Ozcelik B, Xu X (2009) Lipase-catalyzed glycerolysis in ionic liquids directed towards diglyceride synthesis. Process Biochem 44:1358–1365
193. Kurata A, Kitamura Y, Irie S, Takemoto S, Akai Y, Hirota Y, Fujita T, Iwai K, Furusawa M, Kishimoto N (2010) Enzymatic synthesis of caffeic acid phenethyl ester analogues in ionic liquid. J Biotechnol 148:133–138
194. Liang JH, Ren XQ, Wang JT, Jinag M, Li ZJ (2010) Preparation of biodiesel by transesterification from cottonseed oil using the basic dication ionic liquids as catalysts. J Fuel Chem Technol 38:275–280
195. de los AP Rıos, Hernandez-Fernandez FJ, Tomas-Alonso F, Gomez D, Vıllora G (2008) Synthesis of esters in ionic liquids. The effect of vinyl esters and alcohols. Process Biochem 43:892–895
196. Vidya P, Chadha A (2010) Pseudomonas cepacia lipase catalyzed esterification and transesterification of 3-(furan-2-yl) propanoic acid/ethyl ester: a comparison in ionic liquids vs hexane. J Mol Catal B Enzym 65:68–72
197. Abe Y, Kude K, Hayase S, Kawatsura M, Tsunashima K, Itoh T (2008) Design of phosphonium ionic liquids for lipase-catalyzed transesterification. J Mol Catal B Enzym 51:81–85
198. Yang J, Zhou H, Lu X, Yuan Y (2010) Brønsted acidic ionic liquid as an efficient and recyclable promoter for hydroesterification of olefins catalyzed by a triphenylphosphine-palladium complex. Catal Commun 11:1200–1204
199. Chiappe C, Malvaldi M, Pomelli CS (2010) The solvent effect on the Diels-Alder reaction in ionic liquids: multiparameter linear solvation energy relationships and theoretical analysis. Green Chem 12:1330–1339
200. Bortolini O, De Nino A, Garofalo A, Maiuolo L, Procopio A, Russo B (2010) Erbium triflate in ionic liquids: a recyclable system of improving selectivity in Diels-Alder reactions. Appl Catal A Gen 372:124–129
201. Zheng X, Qian Y, Wang Y (2010) Direct asymmetric aza Diels-Alder reaction catalyzed by chiral 2-pyrrolidinecarboxylic acid ionic liquid. Catal Commun 11:567–570
202. Van Buu ON, Aupoix A, Hong NDT, Vo-Thanh G (2009) Chiral ionic liquids derived from isosorbide: synthesis, properties and applications in asymmetric synthesis. New J Chem 33:2060–2072
203. Buu ONV, Aupoix A, Vo-Thanh G (2009) Synthesis of novel chiral imidazolium-based ionic liquids derived from isosorbide and their applications in asymmetric aza Diels-Alder reaction. Tetrahedron 65:2260–2265
204. Wang WH, Wang XB, Kodama K, Hirose T, Zhang GY (2010) Novel chiral ammonium ionic liquids as efficient organocatalysts for asymmetric Michael addition of aldehydes to nitroolefins. Tetrahedron 66:4970–4976
205. Guo H, Li X, Wang JL, Jin XH, Lin XF (2010) Acidic ionic liquid $[NMP]H_2PO_4$ as dual solvent-catalyst for synthesis of β-alkoxyketones by the oxa-Michael addition reactions. Tetrahedron 66:8300–8303
206. Meciarova M, Toma Š, Šebesta R (2009) Asymmetric organocatalyzed Michael addition of aldehydes to β-nitrostyrene in ionic liquids. Tetrahedron Asymmetry 20:2403–2406
207. Zhang Q, Ni B, Headley AD (2008) Asymmetric Michael addition reactions of aldehydes with nitrostyrenes catalyzed by functionalized chiral ionic liquids. Tetrahedron 64:5091–5097
208. Chen W, Yin H, Zhang Y, Lu Z, Wang A, Shen Y, Jiang T, Yu L (2010) Acylation of salicylamide to 5-acetylsalicylamide using ionic liquids as dual catalyst and solvent. J Ind Eng Chem 16:800–804

209. Lin JH, Zhang CP, Zhu ZQ, Chen QY, Xiao JC (2009) A novel pyrrolidinium ionic liquid with 1,1,2,2-tetrafluoro-2-(1,1,2,2-tetrafluoroethoxy)ethanesulfonate anion as a recyclable reaction medium and efficient catalyst for Friedel-Crafts alkylations of indoles with nitroalkenes. J Fluorine Chem 130:394–398
210. Aupoix A, Pegot B, Vo-Thanh G (2010) Synthesis of imidazolium and pyridinium-based ionic liquids and application of 1-alkyl-3-methylimidazolium salts as pre-catalysts for the benzoin condensation using solvent-free and microwave activation. Tetrahedron 66:1352–1356
211. Saha D, Saha A, Ranu BC (2009) Remarkable influence of substituent in ionic liquid in control of reaction: simple, efficient and hazardous organic solvent free procedure for the synthesis of 2-aryl benzimidazoles promoted by ionic liquid, [pmim]BF_4. Green Chem 11:733–737
212. Moreira DN, Longhi K, Frizzo CP, Bonacorso HG, Zanatta N, Martins MAP (2010) Ionic liquid promoted cyclocondensation reactions to the formation of isoxazoles, pyrazoles and pyrimidines. Catal Commun 11:476–479
213. Frizzo CP, Marzari MRB, Buriol L, Moreira DN, Rosa FA, Vargas PS, Zanatta N, Bonacorso HG, Martins MAP (2009) Ionic liquid effects on the reaction of β-enaminones and tert-butylhydrazine and applications for the synthesis of pyrazoles. Catal Commun 10:1967–1970
214. Dong F, Zhenghao F, Zuliang L (2009) Functionalized ionic liquid as the recyclable catalyst for Mannich-type reaction in aqueous media. Catal Commun 10:1267–1270
215. Feng LC, Sun YW, Tang WJ, Xu LJ, Lam KL, Zhou Z, Chan ASC (2010) Highly efficient chemoselective construction of 2,2-dimethyl-6-substituted 4-piperidones via multi-component tandem Mannich reaction in ionic liquids. Green Chem 12:949–952
216. Zhang Z, Li C, Wang Q, Zhao ZK (2009) Efficient hydrolysis of chitosan in ionic liquids. Carbohyd Polym 78:685–689
217. Lima S, Neves P, Antunes MM, Pillinger M, Ignatyev N, Valente AA (2009) Conversion of mono/di/polysaccharides into furan compounds using 1-alkyl-3-methylimidazolium ionic liquids. Appl Catal A Gen 363:93–99
218. Zhang Z, Zhao ZK (2009) Solid acid and microwave-assisted hydrolysis of cellulose in ionic liquid. Carbohyd Res 344:2069–2072
219. Li C, Zhao ZK, Wang A, Zheng M, Zhang T (2010) Production of 5-hydroxymethylfurfural in ionic liquids under high fructose concentration conditions. Carbohyd Res 345:1846–1850
220. Gabriele B, Mancuso R, Lupinacci E, Spina R, Salerno G, Veltri L, Dibenedetto A (2009) Recyclable catalytic synthesis of substituted quinolines: copper-catalyzed heterocyclization of 1-(2-aminoaryl)-2-yn-1-ols in ionic liquids. Tetrahedron 65:8507–8512
221. Qi X, Watanabe M, Aida TM, Smith RL Jr (2009) Efficient process for conversion of fructose to 5-hydroxymethylfurfural with ionic liquids. Green Chem 11:1327–1331
222. Teixeira J, Silva AR, Branco LC, Afonso CAM, Freire C (2010) Asymmetric alkene epoxidation by Mn(III)salen catalyst in ionic liquids. Inorg Chim Acta 363:3321–3329
223. Wu J, Liu C, Jiang Y, Hu M, Li S, Zhai Q (2010) Synthesis of chiral epichlorohydrin by chloroperoxidase-catalyzed epoxidation of 3-chloropropene in the presence of an ionic liquid as co-solvent. Catal Commun 11:727–731
224. Bibal C, Daran JC, Deroover S, Poli R (2010) Ionic Schiff base dioxidomolybdenum(VI) complexes as catalysts in ionic liquid media for cyclooctene epoxidation. Polyhedron 29:639–647
225. Herbert M, Montilla F, Moyano R, Pastor A, Álvarez E, Galindo A (2009) Olefin epoxidations in the ionic liquid [C_4mim][PF_6] catalysed by oxodiperoxomolybdenum species in situ generated from molybdenum trioxide and urea-hydrogen peroxide: the synthesis and molecular structure of [Mo(O)$(O_2)_2$(4-MepyO)$_2$].H_2O. Polyhedron 28:3929–3934
226. Zang H, Su Q, Mo Y, Cheng BW, Jun S (2010) Ionic liquid [EMIM]OAc under ultrasonic irradiation towards the first synthesis of trisubstituted imidazoles. Ultrason Sonochem 17:749–751
227. Wang Y, Gong X, Wang Z, Dai L (2010) SO_3H-functionalized ionic liquids as efficient and recyclable catalysts for the synthesis of pentaerythritol diacetals and diketals. J Mol Catal A Chem 322:7–16

228. Prikhod'ko SA, Adonin NY, Parmon VN (2010) The ionic liquid [bmim]Br as an alternative medium for the catalytic cleavage of aromatic C-F and C-Cl bonds. Tetrahedron Lett 51:2265–2268
229. Azizov AH, Aliyeva RV, Kalbaliyeva ES, Ibrahimova MJ (2010) Selective synthesis and the mechanism of formation of the oligoalkylnaphthenic oils by oligocyclization of 1-hexene in the presence of ionic-liquid catalysts. Appl Catal A Gen 375:70–77
230. Zhang Z, Zhao ZK (2010) Microwave-assisted conversion of lignocellulosic biomass into furans in ionic liquid. Bioresour Technol 101:1111–1114
231. Arai S, Nakashima K, Tanino T, Ogino C, Kondo A, Fukuda H (2010) Production of biodiesel fuel from soybean oil catalyzed by fungus whole-cell biocatalysts in ionic liquids. Enzyme Microb Technol 46:51–55
232. Junming XU, Jianchun J, Zhiyue Z, Jing L (2010) Synthesis of tributyl citrate using acid ionic liquid as catalyst. Process Saf Environ Protect 88:28–30
233. Wang H, Lu B, Wang X, Zhang J, Cai Q (2009) Highly selective synthesis of dimethyl carbonate from urea and methanol catalyzed by ionic liquids. Fuel Process Technol 90:1198–1201
234. Fang D, Shi QR, Cheng J, Gong K, Liu ZL (2008) Regioselective mononitration of aromatic compounds using Brnsted acidic ionic liquids as recoverable catalysts. Appl Catal A Gen 345:158–163
235. Liu Y, Hu R, Xu C, Su H (2008) Alkylation of isobutene with 2-butene using composite ionic liquid catalysts. Appl Catal A Gen 346:189–193
236. Frizzo CP, Moreira DN, Guarda EA, Fiss GF, Marzari MRB, Zanatta N, Bonacorso HG, Martins MAP (2009) Ionic liquid as catalyst in the synthesis of N-alkyl trifluoromethyl pyrazoles. Catal Commun 10:1153–1156
237. Ruther T, Ross T, Mensforth EJ, Hollenkamp AF (2009) N-alkylation of N-heterocyclic ionic liquid precursors in ionic liquids. Green Chem 11:804–809
238. Gunaratne HQN, Lotz TJ, Seddon KR (2010) Chloroindate(III) ionic liquids as catalysts for alkylation of phenols and catechol with alkenes. New J Chem 34:1821–1824
239. Bui TLT, Korth W, Aschauer S, Jess A (2009) Alkylation of isobutane with 2-butene using ionic liquids as catalyst. Green Chem 11:1961–1967
240. Xin-hua Y, Min C, Qi-xun D, Xiao-nong C (2009) Friedel-Crafts acylation of anthracene with oxalyl chloride catalyzed by ionic liquid of [bmim]Cl/$AlCl_3$. Chem Eng J 146:266–269
241. Shogren RL, Biswas A (2010) Acetylation of starch with vinyl acetate in imidazolium ionic liquids and characterization of acetate distribution. Carbohyd Polym 81:149–151
242. Deb S, Wähälä K (2010) Rapid synthesis of long chain fatty acid esters of steroids in ionic liquids with microwave irradiation: expedient one-pot procedure for estradiol monoesters. Steroids 75:740–744
243. Lombardo M, Easwar S, Pasi F, Trombini C, Dhavale DD (2008) Protonated arginine and lysine as catalysts for the direct asymmetric aldol reaction in ionic liquids. Tetrahedron 64:9203–9207
244. Zhao X, Gu Y, Li J, Ding H, Shan Y (2008) An environment-friendly method for synthesis of 1,4-dibromo-naphthalene in aqueous solution of ionic liquids. Catal Commun 9:2179–2182
245. Forsyth SA, Frohlich U, Goodrich P, Gunaratne HQN, Hardacre C, McKeown A, Seddon KR (2010) Functionalised ionic liquids: synthesis of ionic liquids with tethered basic groups and their use in Heck and Knoevenagel reactions. New J Chem 34:723–731
246. Yuan X, Yan N, Xiao C, Li C, Fei Z, Cai Z, Kou Y, Dyson PJ (2010) Highly selective hydrogenation of aromatic chloronitro compounds to aromatic chloroamines with ionic-liquid-like copolymer stabilized platinum nanocatalysts in ionic liquids. Green Chem 12:228–233
247. Zhou H, Yang J, Ye L, Lin H, Yuan Y (2010) Effects of acidity and immiscibility of lactam-based Brønsted-acidic ionic liquids on their catalytic performance for esterification. Green Chem 12:661–665
248. Singh D, Narayanaperumal S, Gul K, Godoi M, Rodrigues OED, Braga AL (2010) Efficient synthesis of selenoesters from acyl chlorides mediated by CuO nanopowder in ionic liquid. Green Chem 12:957–960

249. Osichow A, Mecking S (2010) Alkoxycarbonylation of ethylene with cellulose in ionic liquids. Chem Commun 46:4980–4981
250. Van Doorslaer C, Peeters A, Mertens P, Vinckier C, Binnemans K, De Vos D (2009) Oxidation of cyclic acetals by ozone in ionic liquid media. Chem Commun 6439–6441
251. Harjani JR, Abraham TJ, Gomez AT, Garcia MT, Singer RD, Scammells PJ (2010) Sonogashira coupling reactions in biodegradable ionic liquids derived from nicotinic acid. Green Chem 12:650–655
252. Mayer AC, Salit AF, Bolm C (2008) Iron-catalysed aziridination reactions promoted by an ionic liquid. Chem Commun 5975–5977
253. Guryanov I, Lopez AM, Carraro M, Da Ros T, Scorrano G, Maggini M, Prato M, Bonchio M (2009) Metal-free, retro-cycloaddition of fulleropyrrolidines in ionic liquids under microwave irradiation. Chem Commun 3940–3942
254. Liu F, Li Z, Yu S, Cui X, Ge X (2010) Environmentally benign methanolysis of polycarbonate to recover bisphenol A and dimethyl carbonate in ionic liquids. J Hazard Mater 174:872–875
255. Eichmann M, Keim W, Haumann M, Melcher BU, Wasserscheid P (2009) Nickel catalyzed dimerization of propene in chloroaluminate ionic liquids: detailed kinetic studies in a batch reactor. J Mol Catal A Chem 314:42–48
256. Kumar V, Malhotra SV (2008) Synthesis of nucleoside-based antiviral drugs in ionic liquids. Bioorg Med Chem Lett 18:5640–5642
257. Chrobok A (2010) The Baeyere-Villiger oxidation of ketones with Oxone® in the presence of ionic liquids as solvents. Tetrahedron 66:6212–6216
258. Hu YL, Liu QF, Lu TT, Lu M (2010) Highly efficient oxidation of organic halides to aldehydes and ketones with H_5IO_6 in ionic liquid $[C_{12}mim][FeCl_4]$. Catal Commun 11:923–927
259. Chrobok A (2010) Baeyer-Villiger oxidation of ketones in ionic liquids using molecular oxygen in the presence of benzaldehyde. Tetrahedron 66:2940–2943
260. Fan X, Qu Y, Wang Y, Zhang X, Wang J (2010) Ru(III)-catalyzed oxidation of homopropargyl alcohols in ionic liquid: an efficient and green route to 1,2-allenic ketones. Tetrahedron Lett 51:2123–2126
261. Zakzeski J, Jongerius AL, Weckhuysen BM (2010) Transition metal catalyzed oxidation of Alcell lignin, soda lignin, and lignin model compounds in ionic liquids. Green Chem 12:1225–1236
262. Zang H, Su Q, Mo Y, Cheng B (2010) Ionic liquid under ultrasonic irradiation towards a facile synthesis of pyrazolone derivatives. Ultrason Sonochem 18:68–72
263. Kishi Y, Nagura H, Inagi S, Fuchigami T (2008) Facile and highly efficient synthesis of fluorinated heterocycles via Prins cyclization in ionic liquid hydrogen fluoride salts. Chem Commun 3876–3878
264. Obliosca JM, Arellano IHJ, Huang MH, Arco SD (2010) Double layer micellar stabilization of gold nanocrystals by greener ionic liquid 1-butyl-3-methylimidazolium lauryl sulfate. Mater Lett 64:1109–1112
265. Tsuda T, Seino S, Kuwabata S (2009) Gold nanoparticles prepared with a room-temperature ionic liquid-radiation irradiation method. Chem Commun 6792–6794
266. Redel E, Walter M, Thomann R, Hussein L, Kruger M, Janiak C (2010) Stop-and-go, stepwise and "ligand-free" nucleation, nanocrystal growth and formation of Au-NPs in ionic liquids (ILs). Chem Commun 46:1159–1161
267. Khare V, Li Z, Mantion A, Ayi AA, Sonkaria S, Voelkl A, Thunemann AF, Taubert A (2010) Strong anion effects on gold nanoparticle formation in ionic liquids. J Mater Chem 20:1332–1339
268. Okazaki K, Kiyama T, Hirahara K, Tanaka N, Kuwabata S, Torimoto T (2008) Single-step synthesis of gold-silver alloy nanoparticles in ionic liquids by a sputter deposition technique. Chem Commun 691–693
269. An J, Wang D, Luo Q, Yuan X (2009) Antimicrobial active silver nanoparticles and silver/polystyrene core-shell nanoparticles prepared in room-temperature ionic liquid. Mater Sci Eng C 29:1984–1989

270. Lorbeer C, Cybinska J, Mudring AV (2010) Facile preparation of quantum cutting GdF_3: Eu^{3+} nanoparticles from ionic liquids. Chem Commun 46:571–573
271. Hu H, Yang H, Huang P, Cui D, Peng Y, Zhang J, Lu F, Liand J, Shi D (2010) Unique role of ionic liquid in microwave-assisted synthesis of monodisperse magnetite nanoparticles. Green Chem 12:957–960
272. von Prondzinski N, Cybinska J, Mudring AV (2010) Easy access to ultra long-time stable, luminescent europium(II) fluoride nanoparticles in ionic liquids. Chem Commun 46:4393–4395
273. Farag HK, Endres F (2008) Studies on the synthesis of nano-alumina in air and water stable ionic liquids. J Mater Chem 18:442–449
274. Guo DJ (2010) Novel synthesis of PtRu/multi-walled carbon nanotube catalyst via a microwave-assisted imidazolium ionic liquid method for methanol oxidation. J Power Sources 195:7234–7237
275. Xia J, Li H, Luo Z, Shi H, Wang K, Shu H, Yan Y (2009) Microwave-assisted synthesis of flower-like and leaf-like CuO nanostructures via room-temperature ionic liquids. J Phys Chem Solids 70:1461–1464
276. Taghvaei V, Habibi-Yangjeh A, Behboudnia M (2009) Preparation and characterization of SnO_2 nanoparticles in aqueous solution of [EMIM][$EtSO_4$] as a low cost ionic liquid using ultrasonic irradiation. Powder Technol 195:63–67
277. Ma L, Chen WX, Li H, Xu ZD (2009) Synthesis and characterization of MoS_2 nanostructures with different morphologies via an ionic liquid-assisted hydrothermal route. Mater Chem Phys 116:400–405
278. Shang S, Li L, Yang X, Zheng L (2009) Synthesis and characterization of poly(3-methyl thiophene) nanospheres in magnetic ionic liquid. J Colloid Interface Sci 333:415–418
279. Alammar T, Mudring AV (2009) Facile ultrasound-assisted synthesis of ZnO nanorods in an ionic liquid. Mater Lett 63:732–735
280. Wang Y, Yang H (2009) Synthesis of iron oxide nanorods and nanocubes in an imidazolium ionic liquid. Chem Eng J 147:71–78
281. Redel E, Krämer J, Thomann R, Janiak C (2009) Synthesis of Co, Rh and Ir nanoparticles from metal carbonyls in ionic liquids and their use as biphasic liquid-liquid hydrogenation nanocatalysts for cyclohexene. J Organomet Chem 694:1069–1075
282. Li L, Huang Y, Yan G, Liu F, Huang Z, Ma Z (2009) Poly(3,4-ethylenedioxythiophene) nanospheres synthesized in magnetic ionic liquid. Mater Lett 63:8–10
283. Zhai Y, Zhang Q, Liu F, Gao G (2008) Synthesis of nanostructure rutile TiO_2 in a carboxyl-containing ionic liquid. Mater Lett 62:4563–4565
284. Xu X, Zhang M, Feng J, Zhang M (2008) Shape-controlled synthesis of single-crystalline cupric oxide by microwave heating using an ionic liquid. Mater Lett 62:2787–2790
285. Haldorai Y, Lyoo WS, Noh SK, Shim JJ (2010) Ionic liquid mediated synthesis of silica/polystyrene core-shell composite nanospheres by radical dispersion polymerization. React Funct Polym 70:393–399
286. Li X, Gao Y, Yu L, Zheng L (2010) Template-free synthesis of CdS hollow nanospheres based on an ionic liquid assisted hydrothermal process and their application in photocatalysis. J Solid State Chem 183:1423–1432
287. Xia J, Li H, Luo Z, Xu H, Wang K, Yin S, Yana Y (2010) Self-assembly and enhanced optical absorption of Bi_2WO_6 nests via ionic liquid-assisted hydrothermal method. Mater Chem Phys 121:6–9
288. Alammar T, Birkner A, Shekhah O, Mudring AV (2010) Sonochemical preparation of TiO_2 nanoparticles in the ionic liquid 1-(3-hydroxypropyl)-3-methylimidazolium-bis (trifluoromethylsulfonyl)amide. Mater Chem Phys 120:109–113
289. Ju M, Li Q, Gu J, Xu R, Li Y, Wang X, Wang E (2010) Polyoxometalate-assisted electrochemical deposition of ZnO spindles in an ionic liquid. Mater Lett 64:643–645
290. Xia J, Li H, Luo Z, Wang K, Yin S, Yan Y (2010) Ionic liquid-assisted hydrothermal synthesis of three-dimensional hierarchical CuO peachstone-like architectures. Appl Surf Sci 256: 1871–1877

291. Luo H, Zou D, Zhou L, Ying T (2009) Ionic liquid-assisted synthesis of transition metal oxalates via one-step solid-state reaction. J Alloys Compd 481:L12–L14
292. Gautam UK, Bando Y, Zhan J, Costa PMFJ, Fang XS, Golberg D (2008) Ga-doped ZnS nanowires as precursors for ZnO/$ZnGa_2O_4$ nanotubes. Adv Mater 20:810–814
293. Li Z, Luan Y, Mu T, Chen G (2009) Unusual nanostructured ZnO particles from an ionic liquid precursor. Chem Commun 1258–1260
294. Sadeghzadeh H, Morsali A, Retailleau P (2010) Ultrasonic-assisted synthesis of two new nano-structured 3D lead(II) coordination polymers: precursors for preparation of PbO nanostructures. Polyhedron 29:925–933
295. Langi B, Shah C, Singh K, Chaskar A, Kumar M, Bajaj PN (2010) Ionic liquid-induced synthesis of selenium nanoparticles. Mater Res Bull 45:668–671
296. Pujari AA, Chadbourne JJ, Ward AJ, Costanzo L, Masters AF, Maschmeyer T (2009) The use of acidic task-specific ionic liquids in the formation of high surface area mesoporous silica. New J Chem 33:1997–2000
297. Pang J, Luan Y, Li F, Cai X, Li Z (2010) Ionic liquid-assisted synthesis of silica particles and their application in drug release. Mater Lett 64:2509–2512
298. Wheatley PS, Allan PK, Teat SJ, Ashbrook SE, Morris RE (2010) Task specific ionic liquids for the ionothermal synthesis of siliceous zeolites. Chem Sci 1:483–487
299. Quijano G, Couvert A, Amrane A (2010) Ionic liquids: applications and future trends in bioreactor technology. Bioresour Technol 101:8923–8930
300. Dong WS, Li MY, Liu C, Lin F, Liu Z (2008) Novel ionic liquid assisted synthesis of SnO_2 microspheres. J Colloid Interface Sci 319:115–122
301. Xiao W, Chen Q, Wu Y, Wu T, Dai L (2010) Ferromagnetism of $Zn_{0.95}Mn_{0.05}O$ controlled by concentration of zinc acetate in ionic liquid precursor. Mater Chem Phys 123:1–4
302. Yang Y, Qiu S, He C, He W, Yu L, Xie X (2010) Green chemical functionalization of multi-walled carbon nanotubes with poly(ε-caprolactone) in ionic liquids. Appl Surf Sci 257:1010–1014
303. Gao H, Guo C, Xing J, Zhao J, Liu H (2010) Extraction and oxidative desulfurization of diesel fuel catalyzed by a Brønsted acidic ionic liquid at room temperature. Green Chem 12:1220–1224
304. Zhai L, Zhong Q, He C, Wang J (2010) Hydroxyl ammonium ionic liquids synthesized by water-bath microwave: synthesis and desulfurization. J Hazard Mater 177:807–813
305. Kimura A, Taguchi M, Kondoh T, Yang J, Nagaishi R, Yoshida Y, Hirota K (2010) Decomposition of halophenols in room-temperature ionic liquids by ionizing radiation. Radiat Phys Chem 79:1159–1164
306. Park KI, Xanthos M (2009) A study on the degradation of polylactic acid in the presence of phosphonium ionic liquids. Polym Degrad Stab 94:834–844
307. Lee JS, Mayes RT, Luo H, Dai S (2010) Ionothermal carbonization of sugars in a protic ionic liquid under ambient conditions. Carbon 48:3364–3368
308. Hu X, Hu K, Zeng L, Zhao M, Huang H (2010) Hydrogels prepared from pineapple peel cellulose using ionic liquid and their characterization and primary sodium salicylate release study. Carbohyd Polym 82:62–68
309. Feng Z, Cheng-Gang F, You-Ting W, Yuan-Tao W, Ai-Min L, Zhi-Bing Z (2010) Absorption of CO_2 in the aqueous solutions of functionalized ionic liquids and MDEA. Chem Eng J 160:691–697
310. Likhanova NV, Domínguez-Aguilar MA, Olivares-Xometl O, Nava-Entzana N, Arce E, Dorantes H (2010) The effect of ionic liquids with imidazolium and pyridinium cations on the corrosion inhibition of mild steel in acidic environment. Corros Sci 52:2088–2097
311. Zhang QB, Hua YX (2010) Corrosion inhibition of aluminum in hydrochloric acid solution by alkylimidazolium ionic liquids. Mater Chem Phys 119:57–64
312. Ashassi-Sorkhabi H, Es'haghi M (2009) Corrosion inhibition of mild steel in acidic media by [BMIm]Br Ionic liquid. Mater Chem Phys 114:267–271
313. Lisenkov A, Zheludkevich ML, Ferreira MGS (2010) Active protective Al-Ce alloy coating electrodeposited from ionic liquid. Electrochem Commun 12:729–732

314. Watanabe H (2010) The study of factors influencing the depolymerisation of cellulose using a solid catalyst in ionic liquids. Carbohyd Polym 80:1168–1171
315. Wang H, Yan R, Li Z, Zhang X, Zhang S (2010) Fe-containing magnetic ionic liquid as an effective catalyst for the glycolysis of poly(ethylene terephthalate). Catal Commun 11:763–767
316. Xiao C, Wibisono N, Adidharma H (2010) Dialkylimidazolium halide ionic liquids as dual function inhibitors for methane hydrate. Chem Eng Sci 65:3080–3087
317. Pang J, Luan Y, Wang Q, Du J, Cai X, Li Z (2010) Microwave-assistant synthesis of inorganic particles from ionic liquid precursors. Colloids Surf A Physicochem Eng Aspects 360:6–12
318. Park TJ, Lee SH, Simmons TJ, Martin JG, Mousa SA, Snezhkova EA, Sarnatskaya VV, Nikolaev VG, Linhardt RJ (2008) Heparin-cellulose-charcoal composites for drug detoxification prepared using room temperature ionic liquids. Chem Commun 5022–5024
319. Lu J, Yan F, Texter J (2009) Advanced applications of ionic liquids in polymer science. Prog Polym Sci 34:431–448
320. Schmidt-Naake G, Schmalfuß A, Woecht I (2008) Free radical polymerization in ionic liquids-influence of the IL-concentration and temperature. Chem Eng Res Des 86:765–774
321. Hou C, Qu R, Sun C, Ji C, Wang C, Ying L, Jiang N, Xiu F, Chen L (2008) Novel ionic liquids as reaction medium for ATRP of acrylonitrile in the absence of any ligand. Polymer 49:3424–3427
322. Li Z, Luan Y, Wang Q, Zhuang G, Qi Y, Wang Y, Wang C (2009) ZnO nanostructure construction on zinc foil: the concept from an ionic liquid precursor aqueous solution. Chem Commun 6273–6275
323. Xie M, Kong Y, Han H, Shi J, Ding L, Song C, Zhang Y (2008) Amphiphilic ABA triblock copolymers via combination of ROMP and ATRP in ionic liquid: synthesis, characterization, and self-assembly. React Funct Polym 68:1601–1608
324. Puttick S, Irvine DJ, Licence P, Thurecht KJ (2009) RAFT-functional ionic liquids: towards understanding controlled free radical polymerisation in ionic liquids. J Mater Chem 19:2679–2682
325. Dukuzeyezu EM, Lefebvre H, Tessier M, Fradet A (2010) Synthesis of high molar mass poly(12-hydroxydodecanoic acid) in Brønsted acid ionic liquids. Polymer 51:1218–1221
326. Dong B, Song D, Zheng L, Xu J, Li N (2009) Electrosynthesis of polyfluorene in an ionic liquid and characterization of its stable electrocatalytic activity for formic acid oxidation. J Electroanal Chem 633:63–70
327. Eker B, Zagorevski D, Zhu G, Linhardt RJ, Dordick JS (2009) Enzymatic polymerization of phenols in room-temperature ionic liquids. J Mol Catal B Enzym 59:177–184
328. Mallakpour S, Rafiee Z (2008) Use of ionic liquid and microwave irradiation as a convenient, rapid and eco-friendly method for synthesis of novel optically active and thermally stable aromatic polyamides containing N-phthaloyl-L-alanine pendent group. Polym Degrad Stab 93:753–759
329. Mallakpour S, Rafiee Z (2008) Safe and fast polyamidation of 5-[4-(2-phthalimidiylpropanoylamino)-benzoylamino]isophthalic acid with aromatic diamines in ionic liquid under microwave irradiation. Polymer 49:3007–3013
330. Andrzejewska E, Podgorska-Golubska M, Stepniak I, Andrzejewski M (2009) Photoinitiated polymerization in ionic liquids: kinetics and viscosity effects. Polymer 50:2040–2047
331. Biso M, Mastragostino M, Montanino M, Passerini S, Soavi F (2008) Electropolymerization of poly(3-methylthiophene) in pyrrolidinium-based ionic liquids for hybrid supercapacitors. Electrochim Acta 53:7967–7971
332. Dong B, Xing Y, Xu J, Zheng L, Hou J, Zhao F (2008) Electrosyntheses of free-standing and highly conducting polyselenophene films in an ionic liquid. Electrochim Acta 53: 5745–5751
333. Vijayaraghavan R, Pringle JM, MacFarlane DR (2008) Anionic polymerization of styrene in ionic liquids. Eur Polym J 44:1758–1762
334. Zhang N, Liu QY, Wang YL, Shan ZM, Yang EL, Hu HC (2010) Ionothermal syntheses of two coordination polymers constructed from 5-sulfoisophthalic acid ligands with

1-n-butyl-3-methylimidazolium tetrafluoroborate ionic liquid as solvent. Inorg Chem Commun 13:706–710
335. Poole CF, Poole SK (2010) Extraction of organic compounds with room temperature ionic liquids. J Chromatogr A 1217:2268–2286
336. Gómez E, Domínguez I, Calvar N, Domínguez Á (2010) Separation of benzene from alkanes by solvent extraction with 1-ethylpyridinium ethylsulfate ionic liquid. J Chem Thermodyn 42:1234–1239
337. Simoni LD, Chapeaux A, Brennecke JF, Stadtherr MA (2010) Extraction of biofuels and biofeedstocks from aqueous solutions using ionic liquids. Comput Chem Eng 34:1406–1412
338. González EJ, González B, Calvar N, Domínguez A (2010) Application of [EMpy][ESO_4] ionic liquid as solvent for the liquid extraction of xylenes from hexane. Fluid Phase Equilibria 295:249–254
339. Francisco M, Arce A, Soto A (2010) Ionic liquids on desulfurization of fuel oils. Fluid Phase Equilibria 294:39–48
340. Yoon SJ, Lee JG, Tajima H, Yamasaki A, Kiyono F, Nakazato T, Tao H (2010) Extraction of lanthanide ions from aqueous solution by bis(2-ethylhexyl)phosphoric acid with room-temperature ionic liquids. J Ind Eng Chem 16:350–354
341. Tang F, Zhang Q, Ren D, Nie Z, Liu Q, Yao S (2010) Functional amino acid ionic liquids as solvent and selector in chiral extraction. J Chromatogr A 1217:4669–4674
342. Kogelnig D, Stojanovic A, Jirsa F, Körner W, Krachler R, Keppler BK (2010) Transport and separation of iron(III) from nickel(II) with the ionic liquid trihexyl(tetradecyl)phosphonium chloride. Sep Purif Technol 72:56–60
343. Gorri D, Ruiz A, Ortiz A, Ortiz I (2009) The use of ionic liquids as efficient extraction medium in the reactive separation of cycloolefins from cyclohexane. Chem Eng J 154:241–245
344. Jalili AH, Mehdizadeh A, Shokouhi M, Ahmadi AN, Hosseini-Jenab M, Fateminassab F (2010) Solubility and diffusion of CO_2 and H_2S in the ionic liquid 1-ethyl-3-methylimidazolium ethylsulfate. J Chem Thermodyn 42:1298–1303
345. Qin Y, Lu X, Sun N, Rogers RD (2010) Dissolution or extraction of crustacean shells using ionic liquids to obtain high molecular weight purified chitin and direct production of chitin films and fibers. Green Chem 12:968–971
346. Feng L, Chen Z (2008) Research progress on dissolution and functional modification of cellulose in ionic liquids. J Mol Liquids 142:1–5
347. Boros E, Earle MJ, Gılea MA, Metlen A, Mudring AV, Rieger F, Robertson AJ, Seddon KR, Tomaszowska AA, Trusov L, Vyle JS (2010) On the dissolution of non-metallic solid elements (sulfur, selenium, tellurium and phosphorus) in ionic liquids. Chem Commun 46:716–718
348. Li G, Zhou Q, Zhang X, Wang L, Zhang S, Li J (2010) Solubilities of ammonia in basic imidazolium ionic liquids. Fluid Phase Equilibria 297:34–39
349. Pinkert A, Marsh KN, Pang S, Staiger MP (2009) Ionic liquids and their interactions with cellulose. Chem Rev 108:6712–6728
350. Mäki-Arvela P, Anugwom I, Virtanen P, Sjöholma R, Mikkola JP (2010) Dissolution of lignocellulosic materials and its constituents using ionic liquids-a review. Ind Crops Prod 32:175–201
351. Carvalho PJ, Álvarez VH, Marrucho IM, Aznar M, Coutinho JAP (2010) High carbon dioxide solubilities in trihexyltetradecylphosphonium-based ionic liquids. J Supercrit Fluid 52:258–265
352. Rosol ZP, German NJ, Gross SM (2009) Solubility, ionic conductivity and viscosity of lithium salts in room temperature ionic liquids. Green Chem 11:1453–1457
353. Cornils B (1997) Fluorous biphase systems-the new phase-separation and immobilization technique. Angew Chem Int Ed 36:2057–2059
354. Curran DP (1998) Strategy-level separations in organic synthesis: from planning to practice. Angew Chem Int Ed 37:1174–1196

355. Barthel-Rosa LP, Gladysz JA (1999) Chemistry in fluorous media: a user's guide to practical considerations in the application of fluorous catalysts and reagents. Coord Chem Rev 192:587–605
356. Cavazzini M, Montanari F, Pozzi G, Quici S (1999) Perfluorocarbon-soluble catalysts and reagents and the application of FBS (fluorous biphase system) to organic synthesis. J Fluorine Chem 94:183–193
357. Kitazume T (2000) Green chemistry development in fluorine science. J Fluorine Chem 105:265–278
358. Curran D (2001) Fluorous techniques for the synthesis and separation of organic molecules. Green Chem 3(1):G3–G7
359. Gladysz JA, Curran DP, Horvath IT (2004) Handbook of fluorous chemistry. Wiley-VCH, Weinheim
360. Hobbs HR, Thomas NR (2007) Biocatalysis in supercritical fluids, in fluorous solvents, and under solvent-free conditions. Chem Rev 107:2786–2820
361. Zhang W, Cai C (2008) New chemical and biological applications of fluorous technologies. Chem Commun 5686–5694
362. Zhang W (2009) Green chemistry aspects of fluorous techniques-opportunities and challenges for small-scale organic synthesis. Green Chem 11:911–920
363. O'Neal KL, Zhang H, Yang Y, Hong L, Lu D, Weber SG (2009) Fluorous media for extraction and transport. J Chromatogr A 1217:2287–2295
364. Bailey VA, Clarke D, Routledge A (2010) Extraction of perfluorinated compounds from food matrices using fluorous solvent partitioning. J Fluorine Chem 131:691–697
365. Liu S, Xiao J (2007) Toward green catalytic synthesis-transition metal-catalyzed reactions in non-conventional media. J Mol Catal A Chem 270:1–43
366. Hong M, Cai C, Yi WB (2010) Hafnium (IV) bis(perfluorooctanesulfonyl)imide complex catalyzed synthesis of polyhydroquinoline derivatives via unsymmetrical Hantzsch reaction in fluorous medium. J Fluorine Chem 131:111–114
367. Yi WB, Cai C (2008) Polymer-supported ytterbium perfluorooctanesulfonate [Yb(OPf)$_3$]: a recyclable catalyst for organic reactions. J Fluorine Chem 129:524–528
368. Shen MG, Cai C, Yi WB (2008) Ytterbium perfluorooctanesulfonate as an efficient and recoverable catalyst for the synthesis of trisubstituted imidazoles. J Fluorine Chem 129:541–544
369. Theberge AB, Whyte G, Frenzel M, Fidalgo LM, Wootton RCR, Huck WTS (2009) Suzuki-Miyaura coupling reactions in aqueous microdroplets with catalytically active fluorous interfaces. Chem Commun 6225–6227
370. Benaissi K, Poliakoff M, Thomas NR (2010) Solubilisation of α-chymotrypsin by hydrophobic ion pairing in fluorous systems and supercritical carbon dioxide and demonstration of efficient enzyme recycling. Green Chem 12:54–59
371. Hong M, Cai C (2009) Sc[N(SO2C8F17)2]3 catalyzed condensation of β-naphthol and aldehydes in fluorous solvent: One-pot synthesis of 14-substituted-14H-dibenzo[a, j]xanthenes. J Fluorine Chem 130:989–992
372. Mandal D, Gladysz JA (2010) Syntheses of fluorous quaternary ammonium salts and their application as phase transfer catalysts for halide substitution reactions in extremely nonpolar fluorous solvents. Tetrahedron 66:1070–1077
373. Xu BL, Chen JP, Qiao RZ, Fu DC (2008) Facile and efficient synthesis of 2-substituted-N$_1$-carbethoxy-2,3-dihydro-4(1H)-quinazolinones in fluorous solvent. Chinese Chem Lett 19:537–540
374. Zhu Y, Ford WT (2009) Hydrolysis of p-nitrophenyl esters in mixtures of water and a fluorous solvent. Langmuir 25:3435–3439
375. Chu Q, Yu MS, Curran DP (2008) CBS reductions with a fluorous prolinol immobilized in a hydrofluoroether solvent. Org Lett 10:749–752
376. Hollamby MJ, Eastoe J, Mutch KJ, Rogers S, Heenan RK (2010) Fluorinated microemulsions as reaction media for fluorous nanoparticles. Soft Matter 6:971–976

Chapter 2
Green Fluids Extraction and Purification of Bioactive Compounds from Natural Materials

Chao-Rui Chen, Ying-Nong Lee, Chun-Ting Shen, Ling-Ya Wang, Chih-Hung Wang, Miau-Rong Lee, Jia-Jiuan Wu, Hsin-Ling Yang, Shih-Lan Hsu, Shih-Ming Lai, and Chieh-Ming J. Chang

Abstract This article introduces green solvent extraction and purification of few marker compounds from propolis and rice bran using supercritical carbon dioxide (SC-CO_2). The purity (41.2 wt%) of 3,5-diprenyl-4-hydroxycinnamic acid (DHCA) was recovered from propolis using SC-CO_2 at 207 bar and 323 K with ethyl acetate (6 wt%) addition. The addition of a normal-phase column adsorption approach was directly employed to obtain purified product containing 95 DHCA by weight. SC-CO_2 antisolvent micronization at 200 bar and 328 K generated the submicron particulates containing DHCA (35.2 wt%) from the solution of Brazilian propolis extracts, and the enhancement factor for DHCA concentration reached to 1.61. The DHCA effectively inhibited the growth of human leukemia, colon as well as breast cancer cells, and the human serum low-density lipid oxidation in bioassay. This work also elucidates SC-CO_2 extraction of rice bran oil at 300 bar and 313 K from 1.03-kg powdered rice bran. The total yield of oil was 15.7% with a free fatty acid (FFA) content of 3.75%, obtained from 20.5 kg of carbon dioxide. An oil retention efficiency of 82.2% and an FFA removal efficiency of 97.8% were achieved by

C.-R. Chen
Department of Chemical Engineering, National Chung Hsing University,
250 Kuo-Kuang Road, Taichung 402, Taiwan, ROC

Chemical Engineering Division, Institute of Nuclear Energy Research,
1000 Wen-Hua Road, Lungtan, Taoyuan 325, Taiwan, ROC
e-mail: g8965128@mail.nchu.edu.tw

Y.-N. Lee • C.-T. Shen • L.-Y. Wang • C.-H. Wang • C.-M.J. Chang (✉)
Department of Chemical Engineering, National Chung Hsing University,
250 Kuo-Kuang Road, Taichung 402, Taiwan, ROC
e-mail: odl1123@hotmail.com; shen811@yahoo.com.tw; coldcoldisme@hotmail.com;
afat520@hotmail.com; cmchang@dragon.nchu.edu.tw; Changcmchang@dragon.nchu.edu.tw

M.-R. Lee
Department of Biochemistry, China Medical University, 91 Hsueh-Shih Road,
Taichung 404, Taiwan, ROC
e-mail: mrlee@mail.cmu.edu.tw

A. Mohammad and Inamuddin (eds.), *Green Solvents I: Properties and Applications in Chemistry*, DOI 10.1007/978-94-007-1712-1_2,

using SC-CO_2 deacidification at 250 bar and 353 K with 2,700 g of carbon dioxide consumed. Besides, the two purest γ-oryzanols (>98 wt%) were isolated by preparative reverse-phase high-performance liquid chromatography (HPLC). Furthermore, the central composite response surface methodology (RSM) was applied to predict the optimal operating conditions and to examine the significance of experimental parameters by a statistic analysis.

2.1 Introduction

Propolis is a resinous product, collected from beehives and gathered by honeybees from various plant exudates. This product is composed of 45% resins, 30% waxes and fatty acids, 10% essential oils, 5% pollens, and 10% organic compounds and minerals [1]. Propolis has been utilized in folk medicine for several years, especially in Europe and Japan, because of its various therapeutic activities, including antimicrobial, antiviral, anti-inflammatory, antioxidant, immunomodulatory, free radical scavenging, hepatoprotective, and antiproliferative [2–7]. A few bioactive compounds in propolis are flavonoids and phenolic acids, as well as derivatives [8, 9], which include two major anticancer materials – caffeic acid phenethyl ester (CAPE) and 3,5-diprenyl-4-hydroxycinnamic acid (DHCA). Numerous recent studies have been reported on the biological properties of the DHCA compound, especially those associated with the inhibition of growth of cancer cells, such as human leukemia and colon cells [10–16]. DHCA exhibits an antioxidative activity toward normal cells and an excellent inhibitory effect on growth of gram-positive bacteria such as *Staphylococcus aureus* [17–20]. Bohlmann and Jakupovic [21] were the first to identify the DHCA compound, which exclusively exists in Brazilian propolis.

In recent year, various supergreen approaches based on supercritical fluid have been applied on propolis to yield high valuable products. Stahl et al. [22] first

J.-J. Wu
Department of Chemical Engineering, National Chung Hsing University,
250 Kuo-Kuang Road, Taichung 402, Taiwan, ROC

Department of Nutrition, China Medical University, 91 Hsueh-Shih Road,
Taichung 404, Taiwan, ROC
e-mail: jjwu@mail.cmu.edu.tw

H.-L. Yang
Department of Nutrition, China Medical University, 91 Hsueh-Shih Road,
Taichung 404, Taiwan, ROC
e-mail: hlyang@mail.cmu.edu.tw

S.-L. Hsu
Education and Research Department, Taichung Veterans General Hospital,
160 Chung-Kang Road, Taichung 407, Taiwan, ROC

S.-M. Lai
Department of Chemical and Materials Engineering, National Yunlin University of Science
and Technology, 123 University Road, Touliu, Yunlin 640, Taiwan, ROC

removed wax using supercritical carbon dioxide (SC-CO_2) extraction to enhance the concentration of flavonoids in the extract. You et al. [23] increased the amount of flavonoids in water-soluble propolis using SC-CO_2 extraction. Wang et al. [24] extracted the antioxidant components from propolis by SC-CO_2 fractionation. Catchpole et al. [25] concentrated flavonoids from propolis tincture using SC-CO_2 antisolvent. Lee et al. [17] extracted DHCA from Brazilian propolis using SC-CO_2 that was modified with cosolvent, followed by column chromatography to obtain highly pure DHCA. An SC-CO_2 extract containing DHCA (41.2 wt%) has been found to suppress growth of human colo-205 cancer cells. However, total yield of the SC-CO_2 extract was relatively low compared to with Soxhlet ethyl acetate extract [14].

Supercritical antisolvent precipitation of solutes from liquid-phase solution has been extensively applied in pigment dispersion, pharmaceutical recrystallization, and food production to generate fine particles with high yield [26–28]. This approach has also been utilized in the separation of bioactive compounds from natural materials, including flavonoids, DHCA, β-carotene, ginkgolides, lycopene, and astaxanthin [25, 29–35]. Additionally, experimental data on the phase equilibrium between SC-CO_2 and organic solvent are important for understanding the supercritical antisolvent (SAS) process [36]. Two dimensionless parameters, Reynolds number ($\rho vd/\mu$) and Weber number ($\rho v^2 d/\sigma$), have been recognized as major parameters that govern the mechanism of particle formation associated with SAS precipitation [37]. Supersaturation of solutes in a high-pressure solution is important in generating micronized particles in an SC-CO_2 antisolvent precipitation process. However, the transient supersaturation of the solutes in such a high-pressure system that is mixed with SC-CO_2 is difficult [38].

Rice bran, a by-product of the rice-refining process, consists of 11–15% proteins, 34–62% carbohydrates, 7–11% crude fibers, 7–10% ashes, and 15–20% lipids. Rice bran oil contains 95.6% saponifiable lipids, including glycolipid and phospholipids, and 4.2% unsaponifiable lipids, including tocopherols, tocotrienols, γ-oryzanols, sterols, and carotenoids [39]. The saponifiable lipids are mainly triglycerides. However, these triglycerides are easily hydrolyzed by lipase to form free fatty acids. The γ-oryzanol content in the rice bran oil is approximately 1.8–3%, according to the experimental data of Hu et al. [40]. Xu and Godber [41] adopted a low-pressure normal-phase silica column to obtain oryzanol-containing fractions, which were further partitioned using a preparative normal-phase HPLC column. They have reported that ten molecular structures of γ-oryzanols were identified using a reverse-phase HPLC column that is coupled with a GC-mass chromatograph. Cycloartenyl ferulate, 24-methylenecycloartanyl ferulate, and campesteryl ferulate are evidently major γ-oryzanols in rice bran. γ-Oryzanols have certain biological and physiological properties, such as antioxidation [42], anti–blood cholesterol [43], and anticarcinogenic [44–47]. The liquid chromatography/mass spectrometry (LC/MS) method has been frequently adopted in elucidating the structures of γ-oryzanols [48]. Stöggl et al. [49] have identified and quantified tocopherols, γ-oryzanols, and carotenoids in rice bran. Aguilar-Garcia et al. [50] performed a biological study regarding the correlation between the quantity of γ-oryzanols and antioxidant capacity.

The edible rice bran oil only allows a maximal acid value of 0.2, in general, equivalent to 0.1 by weight of free fatty acid. The Indian regulation for the refined rice bran

oil allows a maximal acid value of 0.5, which is equivalent to 0.25 free fatty acid by weight [51]. Triglycerides in the wasted rice bran oil had been processed into biodiesel by acid-catalyzed transesterification [52]. In recent years, supercritical fluid extractions of powdered rice bran have shown that the odor and the flavor of extracted oil are superior to that obtained by Soxhlet *n*-hexane extraction [53–55]. Deacidification of rice bran oil using supercritical carbon dioxide has been recognized as a very environmentally friendly process [56, 57]. Kim et al. [58] investigated the time-related mass transfer kinetics of oil components that migrated between solid (rice bran) and fluid (carbon dioxide) phases in supercritical carbon dioxide extraction. Chang et al. [59, 60] studied supercritical carbon dioxide extraction kinetics and high-pressure vapor–liquid-phase equilibrium measurements between oil compounds and carbon dioxide. Several multistage supercritical fluid deacidifications of rice bran oil have been conducted to remove free fatty acids or triglycerides from raffinate oil using a packed column at a middle-high pressure at 333–353 K to increase concentrations of γ-oryzanols and phytosterols in the oil [61–65].

This article introduced the green solvent extraction and purification of bioactive materials from propolis and rice bran using supercritical carbon dioxide. Firstly, SC-CO_2 extraction of DHCA from Brazilian propolis was investigated. The addition of ethyl acetate during the extraction of DHCA is examined, and SC-CO_2 extraction based on response surface methodology is discussed. Growth inhibition tests of human leukemia, colon, and breast cancer cells were performed to verify the anticancer ability of these SC-CO_2 extracts. The SC-CO_2 antisolvent precipitation of flavonoids and DHCA from the Brazilian propolis solution was also developed. The effect of the operation conditions on particle formation in this SC-CO_2 antisolvent process, based on two-factor center composite response surface methodology, was examined to determine the change of the mean particle size of the SC-CO_2 precipitates and the recovery of the marker compounds. Moreover, SC-CO_2 extraction of rice bran oil from powdered rice bran and a semipreparative HPLC method to obtain purest γ-oryzanol standard were demonstrated, followed by the concentration of γ-oryzanols in the extracted oil using a middle-pressure column partition fractionation. Finally, the SC-CO_2 extraction of rice bran oil from powdered rice bran, followed by SC-CO_2 deacidification using a response surface methodology (RSM) was also examined.

2.2 Isolation and Purification of 3,5-Diprenyl-4-Hydroxycinnamic Acid (DHCA) in Brazilian Propolis

2.2.1 Classical Solvent Extractions

For the Soxhlet extractions, 20 g of propolis powder was loaded in a 250-mL reflux-type Soxhlet system and extracted by 300-mL deionized water, ethanol, ethyl acetate, and *n*-hexane for 2–24 h. For the ultrasonic extractions, 10 g of propolis powder was

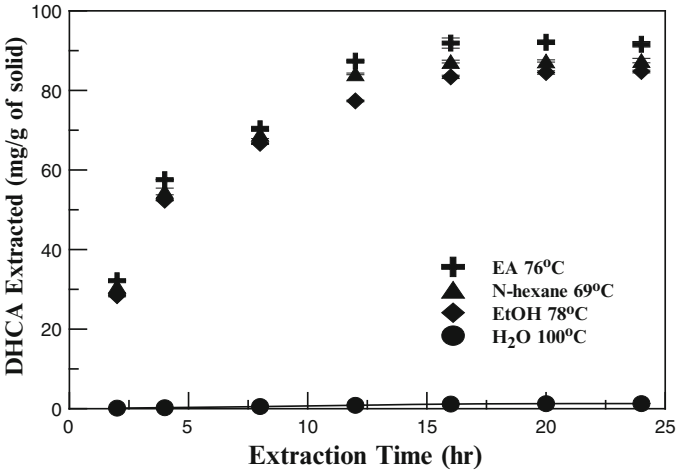

Fig. 2.1 Four Soxhlet solvent extractions of the DHCA from Brazilian propolis lump (Reprinted from Ref. [18]. With kind permission of © Elsevier)

ultrasonicated in the 1,200 g ethyl acetate for a period of 1.5, 2.5, and 3.5 h, operated at 308, 328, and 348 K, respectively. For the hot-pressurized extractions, 10 g of propolis powder dissolved in 1,200 g of ethyl acetate was loaded in an autoclave extractor, and the solution was purged by 4.5-bar nitrogen for 10 min to strip off the oxygen entrapped in the solution. The experiments were carried out and controlled at 4.5-bar and 300-rpm agitation speed with temperature ranging from 348 to 388 K. All the extracts were filtered through the Whatman no.1 filter paper and weighted to calculate the total yield as well as the recovery and the purity of DHCA in the extracts.

Figure 2.1 indicates the effect of extraction time on the amount of DHCA extracted by four Soxhlet extractions. After 16 h of extraction, the maximal DHCA in the propolis extract was 91.9 mg/g, obtained with 120 mL of ethyl acetate Soxhlet extraction of 1-g propolis lump. This was recognized as a 100% recovery of DHCA from this Brazilian propolis lump. For the hot-pressurized extraction, the recovery of DHCA attained 88.5%, but the extraction time was reduced from 16 down to 2.5 h. In addition, reduced standardized concentration factors (i.e., $\alpha = \beta/\beta_{Soxhlet} < 1.0$) revealed that the DHCA purity in propolis extracts was less than that of the Soxhlet ethyl acetate extraction (16.9 wt%). For the ultrasonic extraction, the recovery of DHCA was only 75%, and the DHCA purity was also less than that of the Soxhlet ethyl acetate extraction.

2.2.2 Purification and Identification of 3,5-Diprenyl-4-Hydroxycinnamic Acid (DHCA)

Two methods, namely, liquid-liquid solvent partition and normal-phase column chromatography were employed to purify DHCA from the propolis extracts. In the

first method, the waxes were removed by *n*-hexane washing firstly and the raffinate was then dried to redissolve in methanol. Contrarily, the second method was adopted to avoid *n*-hexane and methanol partitions. The final residue was then collected by removing the supernatant using a centrifuge at 8,000 rpm for 10 min. The residue was dissolved in a mixture of 7:3 (v/v) *n*-hexane and ethyl acetate (EA) to form a crude solution. The crude solution was manually loaded and fractionated on a silica gel 60 column (2.5-cm I.D.), eluted by a mixed mobile phase consisting of *n*-hexane and EA in different volume ratios. Every 10-mL eluent was collected at the flow rate of 2.5 mL/min. The sample containing 95-wt% DHCA was dissolved in $CDCl_3$ and analyzed by a 400-Hz ^{1}H-NMR spectrophotometer (Varian, Mercury, USA).

Experimental data (Table 2.1) resulted from these column purifications of the propolis extracts with solvent pretreatment (i.e., first method) indicated DHCA purities of the purified products as 95 wt%, except for the Soxhlet extract (91 wt%). The highest total recovery by this procedure was only 4.2% for the purified product. Major losses of DHCA were found in the *n*-hexane layer (20%) and methanol layer (60%). Table 2.2 lists experimental results of purified DHCA without solvent pretreatment (i.e., second method). Solely the purified products of those SC-CO_2 extracts contained 95 wt% DHCA, and the largest total recovery could reach 9.4%, which is 2.3 times to that of the hot-pressurized extract in the first method. These SC-CO_2 extracts containing 40 wt% DHCA are easy to be purified by column purification alone.

2.2.3 Quantification of 3,5-Diprenyl-4-Hydroxycinnamic Acid (DHCA)

A Waters HPLC system, which comprised a 600E multisolvent delivery pump, a 717 plus autosampler, a 486 UV/Vis detector, and Millennium 2010 system manager software, was employed to analyze the extracts. (10 μL) Samples were filtered through a 0.45-μm polyvinylidene fluoride (PVDF) membrane (Millipore, USA) and were injected into a C18 reversed-phase column (4.6×250 mm, 5U, Hichrom, UK) to quantify the DHCA of the extracts. The column temperature was controlled at 308 K, and the UV absorption was detected at a wavelength of 280 nm. A two-solvent gradient mobile phase comprising 55% methanol (A) and 80% methanol (B) in 0.5% acetic acid aqueous solution was used for this analysis. A calibration curve was established by linear regression between the area under the UV absorption curve and the concentration of the samples. A protocol sample containing 95 wt% DHCA was isolated from the 61 to 75 fractions collected and was used as the standard for this study. The purity of this standard was an averaged value verified by the HPLC method, and the concentration ranged from 20 to 620 μg/mL. The R^2 coefficients exceeded 0.99, and the limits of detection in these analyses were 3,220 ng/mL. Figure 2.2 represents HPLC spectra of samples including the 95 wt% DHCA spectrum and its chemical shift pattern of ^{1}H-NMR, which is exactly corresponding to that reported by Bohlmann et al. [21].

Table 2.1 Experimental data purifying DHCA from propolis extracts by the first method with solvent pretreatments (Reprinted from Ref. [18]. With kind permission of © Elsevier)

	Extracts			Purified Products					DHCA Loss		
							Recovery (%)				
Method	W_{DHCA} (mg/g)	$W_{propolis}$ (mg/g)	P_{DHCA} (wt%)	W_{PD} (mg/g)	W_{PT} (mg/g)	P_{PD} (wt%)	R_{PD}	R_T	L_{hexane} (mg/g) [LP_{hexane} (%)]	L_{MeOH} (mg/g) [LP_{MeOH} (%)]	L_{others} (mg/g) [LP_{others} (%)]
Soxhlet	91.9±0.90	543.4±3.76	16.9±0.20	3.82±0.12	4.20±0.14	91±0.3	4.16±0.09	4.16±0.09	18.75±2.03 [20.40±2.21]	56.79±1.24 [61.79±1.35]	12.54±2.49 [13.67±2.84]
HPE	83.2±0.35	506.9±5.00	16.4±0.23	3.72±0.11	3.92±0.13	95±0.4	4.47±0.11	4.05±0.12	16.26±1.22 [19.53±1.47]	50.76±1.08 [61.01±1.30]	12.41±2.06 [14.94±2.54]
Sonic	69.0±0.35	432.4±0.55	16.0±0.06	3.14±0.12	3.31±0.15	95±0.4	4.56±0.20	3.42±0.13	13.42±0.88 [19.44±1.28]	41.61±1.23 [60.31±1.78]	10.83±2.58 [15.69±3.66]
SCF1	12.6±0.12	30.7±0.34	41.2±0.04	0.72±0.05	0.76±0.07	95±0.5	5.71±0.34	0.78±0.05	2.86±0.42 [22.70±3.33]	7.12±0.81 [56.51±6.43]	1.90±0.74 [15.08±5.87]
SCF2	12.7±0.04	31.1±0.16	40.8±0.01	0.68±0.06	0.72±0.05	95±0.2	5.34±0.45	0.74±0.07	2.66±0.56 [20.94±4.41]	7.98±0.92 [62.83±7.24]	1.39±0.27 [10.94±2.13]
SCF	3.7±0.10	8.17±0.85	45.3±0.10	0.21±0.02	0.22±0.02	95±0.3	5.67±0.39	0.23±0.02	0.72±0.13 [19.46±3.51]	2.41±0.27 [65.14±7.29]	0.36±0.09 [9.73±2.43]

Soxhlet: 16-h EA; *HPE*: 2.5-h, 368-K hot-pressurized EA; *Sonic*: 2.5-h, 348-K ultrasonic-EA; *SCF1*: 323-K, 207-bar, 6-wt% EA + 475 L CO_2; *SCF2*: 333-K, 207-bar, 6-wt% EA + 475-L CO_2; *SCF*: 323-K, 207-bar, 475-L CO_2

W_{DHCA} the DHCA weight in the extracted propolis, $W_{propolis}$ the extracted weight of propolis, P_{DHCA} the DHCA purity of the extracted propolis = 100% × (W_{DHCA}/$W_{propolis}$), W_{PD} the purified weight of DHCA, W_{PT} total weight of the purified product, P_{PD} the DHCA purity of the purified product = 100% × (W_{PD}/W_{PT}), R_{PD} recovery of 95 wt% DHCA for the first purification process = 100% × (W_{PD}/W_{DHCA}), R_T total recovery of 95 wt% DHCA = 100% × (W_{PD}/$W_{DHCA,Soxhlet}$), L_{hexane} the weight loss of DHCA in *n*-hexane = (W_{DHCA}-W_{PD}-L_{MeOH}-L_{others}), L_{MeOH} the weight loss of DHCA in MeOH = (W_{DHCA}-W_{PD}-L_{hexane}-L_{others}), L_{others} the weight loss of DHCA in others = (W_{DHCA}-W_{PD}-L_{hexane}-L_{MeOH}), *LP* the percentage of DHCA lost in each step = 100% × (L/W_{DHCA})

Table 2.2 Experimental data purifying DHCA from propolis extracts by the second method without solvent pretreatments (Reprinted from Ref. [18]. With kind permission of © Elsevier)

	Extracts			Purified products			DHCA recovery		DHCA loss
									L_{DHCA} (mg/g)
Method	W_{DHCA} (mg/g)	$W_{propolis}$ (mg/g)	P_{DHCA} (wt%)	W_{PD} (mg/g)	W_{PT} (mg/g)	P_{PD} (wt%)	R_{PD} (%)	R_T (%)	[LP_{DHCA} (%)]
Soxhlet	91.9 ± 0.90	543.4 ± 3.76	16.9 ± 0.20	42.74 ± 2.10	60.20 ± 2.09	71 ± 1.2	46.49 ± 1.83	46.49 ± 1.83	49.16 ± 0.90 [53.49 ± 0.48]
HPE	83.2 ± 0.35	506.9 ± 5.00	16.4 ± 0.23	43.14 ± 2.13	56.03 ± 2.15	77 ± 0.6	51.87 ± 2.34	46.94 ± 2.32	40.06 ± 0.35 [48.14 ± 0.23]
Sonic	69.0 ± 0.35	432.4 ± 0.55	16.0 ± 0.06	32.14 ± 1.70	41.21 ± 1.71	78 ± 0.5	46.63 ± 2.70	34.97 ± 1.85	36.83 ± 0.35 [53.38 ± 0.25]
SCF1	12.6 ± 0.12	30.7 ± 0.34	41.2 ± 0.04	8.64 ± 0.32	9.09 ± 0.31	95 ± 0.5	68.55 ± 1.89	9.40 ± 0.35	3.96 ± 0.12 [31.43 ± 0.68]
SCF2	12.7 ± 0.04	31.1 ± 0.16	40.8 ± 0.01	8.65 ± 0.43	9.11 ± 0.41	95 ± 0.4	67.99 ± 3.17	9.41 ± 0.47	4.05 ± 0.04 [31.99 ± 0.22]
SCF	3.7 ± 0.10	8.17 ± 0.85	45.3 ± 0.10	2.56 ± 0.21	2.69 ± 0.22	95 ± 0.6	69.09 ± 3.81	2.79 ± 0.23	1.14 ± 0.10 [30.81 ± 2.02]

Soxhlet: 16-h EA; *HPE*: 2.5-h, 368-K hot-pressurized EA; *Sonic*: 2.5-h, 348-K ultrasonic EA; *SCF1*: 323-K, 207-bar, 6-wt% EA + 475-L CO_2; *SCF2*: 333-K, 207-bar, 6-wt% EA + 475-L CO_2; *SCF*: 323-K, 207-bar, 475-L CO_2

W_{DHCA} the DHCA weight in the extracted propolis, $W_{propolis}$ the extracted weight of propolis, P_{DHCA} the DHCA purity of the extracted propolis = 100% × (W_{DHCA}/$W_{propolis}$), W_{PD} the purified weight of DHCA, W_{PT} total weight of the purified product, P_{PD} the DHCA purity of the purified product = 100% × (W_{PD}/W_{PT}), R_{PD} recovery of 95 wt% DHCA for the first purification process = 100% × (W_{PD}/W_{DHCA}), R_T total recovery of 95 wt% DHCA = 100% × (W_{PD}/$W_{DHCA,Soxhlet}$), L_{DHCA} the weight loss of DHCA in experiments = (W_{DHCA}-W_{PD}), LP_{DHCA} the percentage of DHCA lost in experiments = 100% × (W_{DHCA}-W_{PD})/W_{DHCA}

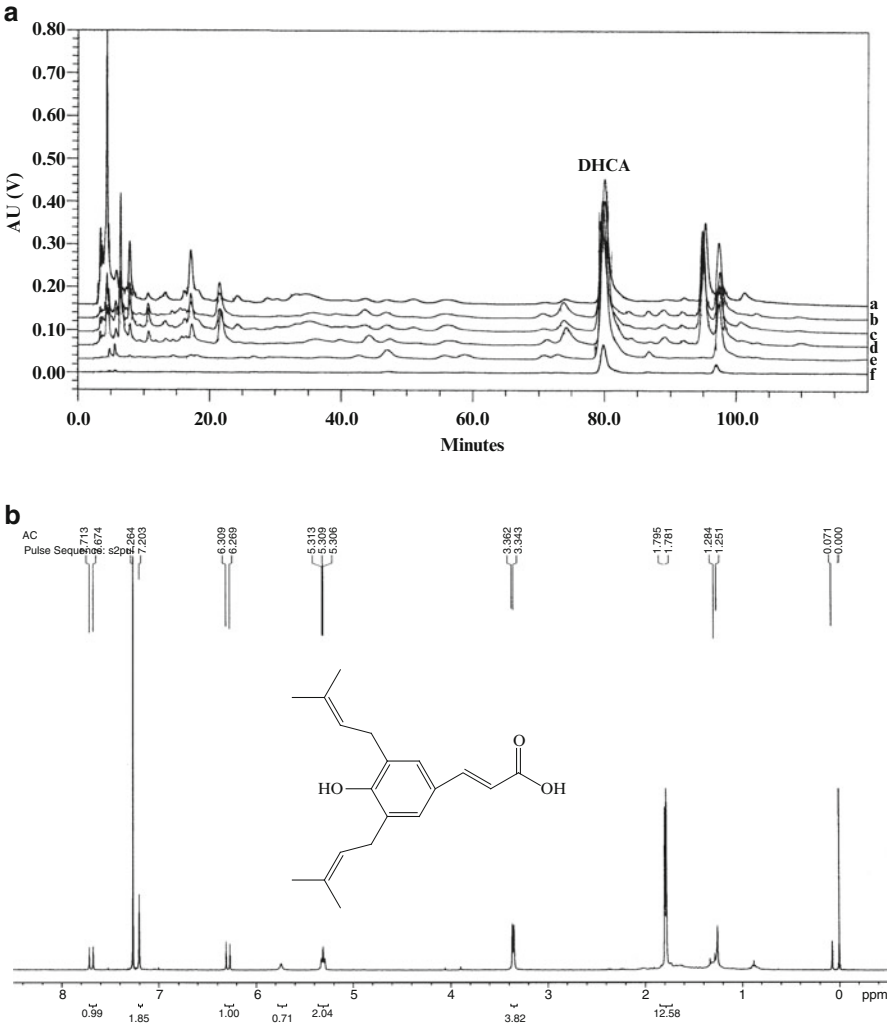

Fig. 2.2 (**a**) HPLC chromatograms of the extracts detected at 280 nm [a: Soxhlet-EA; b: SC-CO_2 + 2-wt% *n*-hexane; c: SC-CO_2 + 6-wt% EA; d: SC-CO_2; e: 80-wt% DHCA; f: purest 95-wt% DHCA]. (**b**) A 400-Hz ^{1}H NMR spectrum of the 95-wt% DHCA [δ: 7.69 (1H, d, J = 15.9 Hz), 7.20 (2H, s), 6.29 (1H, d, J = 15.9 Hz), 5.31 (2H, br, t), 3.35 (2H, d, J = 7.2 Hz), 1.79 (6H, s), and 1.78 (6H, s)] (Reprinted from Ref. [18]. With kind permission of © Elsevier)

2.3 Green Fluid Extraction of 3,5-Diprenyl-4-Hydroxycinnamic Acid (DHCA) from Brazilian Propolis

2.3.1 Sensitivity Test of Supercritical Carbon Dioxide (SC-CO_2) Extractions

Propolis lumps were ground into 2-mm particles using a blade-type grinder and then collected by sieving through a 10-mesh international-type stainless steel screen before use. The maximum recovery of DHCA in Brazilian propolis was obtained by Soxhlet ethyl acetate extraction during a period of 16 h. Figure 2.3 presents the SC-CO_2 extraction that was used by You et al. [23]. Before the extraction, 10 g of ground propolis powder and 30 g of steel beads were uniformly loaded into an extractor (75 mL, L/D = 30) (8); a 5-cm thickness of glass wool was placed on both the top and the bottom of the extractor to prevent the entrainment of propolis particles, and 200 mL of 95% ethanol was loaded into the absorber (750 mL, L/D = 10) (11), which acted as a absorbent. Then, liquid CO_2 was pumped using a high-pressure pump (CM-3200, Thermo Separation Products, USA) and flowed into the extractor at a constant flow rate of 10 mL/min after preheating. The extraction pressure varied from 138 to 276 bar and was regulated using a back-pressure regulator (26–1721, Tescom, USA) (9–1), and the extraction temperature ranged from 308 to 333 K, controlled by a PI-type controller. The pressure of the absorber was set to 50 bar, and another back-pressure regulator (9–2) was used to separate CO_2 from the extracts that were collected at ambient temperature. The consumed CO_2 volume was measured using a wet gas meter (TG3, Ritter, Germany) (13). Furthermore, the amount of ethyl acetate, from 0 to 6 wt%, was weighed and preloaded in the extractor as a cosolvent.

The 91.9 mg/$g_{propolis}$ of DHCA was yielded via Soxhlet ethyl acetate extraction from Brazilian propolis lumps. Table 2.3 presents the results of Soxhlet and SC-CO_2 extractions of DHCA. It states that only few DHCA could be extracted by adding *n*-hexane as cosolvent and both recovery and purity of DHCA were lower than that by adding ethyl acetate. Furthermore, the standardized concentration factors of DHCA of modified SC-CO_2 extracts obtained by addition of ethyl acetate and *n*-hexane were 2.59 and 2.14, respectively. Figure 2.4 shows the addition of EA on the recovery and purity of DHCA obtained from SC-CO_2 extractions. The recovery of DHCA increased with the consumption of CO_2 up to 475 L, and the addition of up to 6 wt% EA significantly enhanced the DHCA recovery. Other compounds in propolis were also easily extracted under this condition, and the purity of DHCA decreased as more ethyl acetate was added. Experimental data revealed that the amount of DHCA increased with temperature at pressures from 207 to 276 bar.

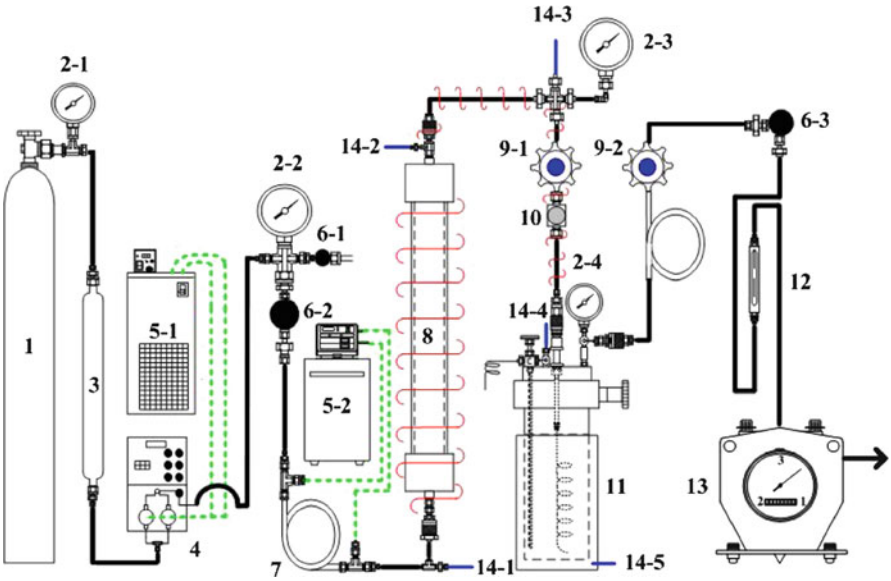

1. CO_2 Cylinder	8. Extractor
2-1~2-4. Pressure gaugea	9-1~9-2. Back pressure regulator
3. Gas dryer	10. Micro-metering valve
4. High-pressure pump	11. Absorber
5-1~5-2. Circulator	12. Float flow meter
6-1~6-3. Metering valve	13. Wet gas meter
7. Heat exchanger	14-1~14-5. Thermocouple

Fig. 2.3 Schematic diagram of SC-CO_2 extraction of propolis (Reprinted from Ref. [14]. With kind permission of © Elsevier)

2.3.2 Response Surface Methodology (RSM): Designed Supercritical Carbon Dioxide (SC-CO_2) Extractions

Following study of the effects of temperature and cosolvent addition on a few preliminary SC-CO_2 extractions, two-factor central composite response surface methodology (RSM) software (Stat-Ease, USA) was adopted to study the effect of the operating conditions of SC-CO_2 extractions on the purity of the DHCA in the extracts as well as to search for the optimum conditions in this procedure. The extraction temperature and the addition of the cosolvent were selected as two

Table 2.3 The purity of DHCA and concentration factor of Soxhlet and SC-CO_2 modified cosolvent extract (Reprinted from Ref. [14]. With kind permission of © Elsevier)

Solvent	W_{DHCA} (mg/g_{solid})	TY (%)	R (%)	P_E (wt%)	β	α
Soxhlet-EA[a]	91.9	55.6	100	16.9	1.80	1.00
SC-CO_2[b]	2.6	0.6	2.9	45.3	4.83	2.68
SC-CO_2+2% EA[b]	7.7	1.8	8.4	43.3	4.67	2.59
SC-CO_2+2% *n*-hexane[b]	4.6	1.3	5.0	35.5	3.85	2.14

W_{DHCA} weight of DHCA, *TY* total yield = ($W^*_{extract}/W_{propolis}$) × 100%, *R* recovery of DHCA = ($W_{DHCA}/W_{DHCA,Soxhlet}$) × 100%, P_E DHCA purity of extract = ($W_{DHCA}/W_{extract}$) × 100%, β concentration factor of DHCA = R/TY, α standardized concentration factor of DHCA = $\beta/\beta_{Soxhlet}$

[a]Soxhlet ethyl acetate extraction for 16 h

[b]SC-CO_2 extraction at 207 bar and 323 K

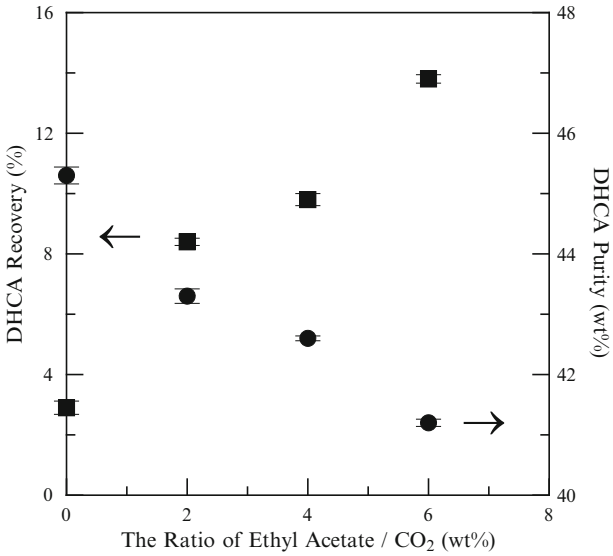

Fig. 2.4 Effect of the ratio of ethyl acetate to CO_2 on the recovery and purity of DHCA using 475 L SC-CO_2 extraction at 207 bar and 323 K (■, DHCA recovery; ●, DHCA purity) (Reprinted from Ref. [14]. With kind permission of © Elsevier)

factors that influence the recovery and purity of DHCA. The addition ratio ranged from 2 to 6 wt%, and extraction temperatures from 313 to 333 K were examined for these central composite RSM-designed SC-CO_2 extractions. The recovery and purity of DHCA were calculated by Eqs. 2.1 and 2.2, respectively:

$$R_{\mathrm{DHCA}} = \frac{\text{Weight of DHCA in the extracts}}{\text{Weight of DHCA in Soxhlet extract}} \times 100(\%), \text{ recovery.} \tag{2.1}$$

$$P_{\mathrm{DHCA}} = \frac{\text{Weight of DHCA}}{\text{Weight of extracts}} \times 100(\%), \text{ purity.} \tag{2.2}$$

Table 2.4 Two factorial central composite RSM-designed SC-CO_2 extractions of DHCA from propolis at 207 bar (Reprinted from Ref. [14]. With kind permission of © Elsevier)

RSM #	EA (wt%)	T (K)	W_{DHCA} (mg/g_{solid})	R (%)	$W_{extract}$ (mg/g_{solid})	P_E (wt%)
1(F)	2	313	6.6±0.4	7.1±0.4	15.3±0.8	42.9±0.1
2(A)	2	323	7.7±0.1	8.4±0.1	17.7±0.3	43.3±0.1
3(F)	2	333	7.7±0.2	8.4±0.2	18.0±0.5	42.7±0.1
4(A)	4	313	8.3±0.1	9.0±0.1	19.4±0.3	42.8±0.1
5(C)	4	323	9.0±0.2	9.8±0.2	21.0±0.4	42.6±0.1
6(A)	4	333	9.1±0.1	9.9±0.1	21.5±0.2	42.2±0.1
7(F)	6	313	11.2±0.2	12.2±0.2	26.8±0.3	41.8±0.1
8(A)	6	323	12.6±0.1	13.8±0.1	30.7±0.3	41.2±0.1
9(F)	6	333	12.7±0.1	13.8±0.1	31.1±0.2	40.8±0.1

EA addition ratio = W_{EA} / W_{CO_2} (475 L, 860 g), *T* temperature, W_{DHCA} weight of DHCA, $W_{extract}$ weight of extract, *R* recovery of DHCA = $(W_{DHCA}/W_{DHCA,Soxhlet}) \times 100\%$, P_E DHCA purity of extract = $(W_{DHCA}/W_{extract}) \times 100\%$, *F-testing* $R_{(R)}^2 = 0.9910$, $S.D._{(R)} = 0.23$, $R_{(PE)}^2 = 0.9738$, $S.D._{(PE)} = 0.14$

Based on the sensitivity of independent factors, tested in Sect. 2.3.1, the consumption of 475-L CO_2, 1-h soaking time of the cosolvent and a pressure of 207 bar were set for RSM-designed SC-CO_2 extractions. Table 2.4 presents these RSM results. The addition ratio was more effective than temperature in enhancing the recovery and purity of DHCA. Figure 2.5a shows that three-dimensional responses of DHCA recovery achieves 13.8% with the addition of 6 wt% EA. Figure 2.5b shows that responded DHCA purity attains 43.3 wt% at 323 K with 2 wt% EA addition ratio. Although DHCA purities in SC-CO_2 extracts decreased as the addition ratio is increasing, those were still above 40 wt% and were more than two times to that in the Soxhlet extract (16.9 wt%). In summary, 13.8% recovery and 41.2 wt% purity were obtained at CO_2 consumption of 475 L, 207 bar, and 323 K with extraction by the addition of 6-wt% ethyl acetate according to a quadratic polynomial model. The use of these operative conditions was effective in yielding high-purity DHCA in the SC-CO_2 extract.

2.4 Precipitation of Submicron Particles in Brazilian Propolis via Supercritical Carbon Dioxide (SC-CO_2) Antisolvent

2.4.1 Supercritical Carbon Dioxide (SC-CO_2) Micronization Process

Figure 2.6 schematically depicts SC-CO_2 antisolvent device/equipment. At the start of an experiment, liquid CO_2 was charged from a CO_2 cylinder (1), passed through a gas dryer (3), and compressed by a high-pressure double-piston pump (*Spe-ed* SFE, Applied Separations, USA) (4) into a 75-mL high-pressure surge tank (8) and

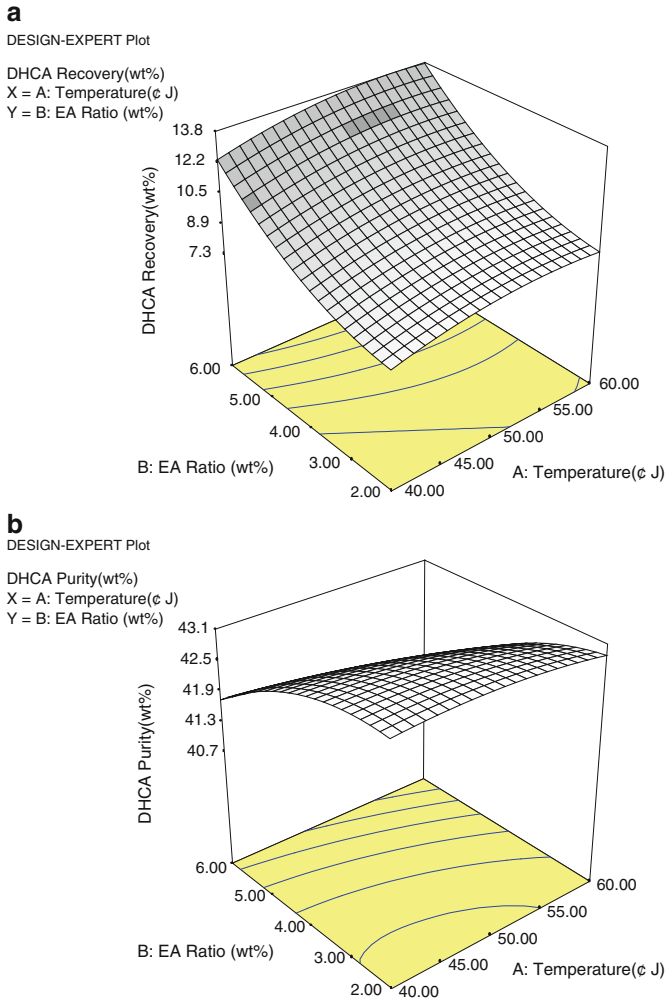

Fig. 2.5 The RSM responding plots showing (**a**) the DHCA recovery and (**b**) the DHCA purity in the SC-CO_2 extracts (F-testing: $R_{(a)}{}^2 = 0.9810$, S.D.$_{(a)} = 0.23$; $R_{(b)}{}^2 = 0.9638$, S.D.$_{(b)} = 0.14$) (Reprinted from Ref. [18]. With kind permission of © Elsevier)

a 750-mL middle-pressure surge tank (11) at constant flow rate after it had been preheated using a double-pipe heat exchanger (7). The temperatures in pump and heat exchanger were controlled using two circulators (5–1, 5–2). Then, CO_2 was expanded through two back-pressure regulators (9–1, 9–2) and a metering valve (6–3) and flowed into a 200-mL visible precipitator that was equipped with two pieces of safety glass (TST, Taiwan) (12).

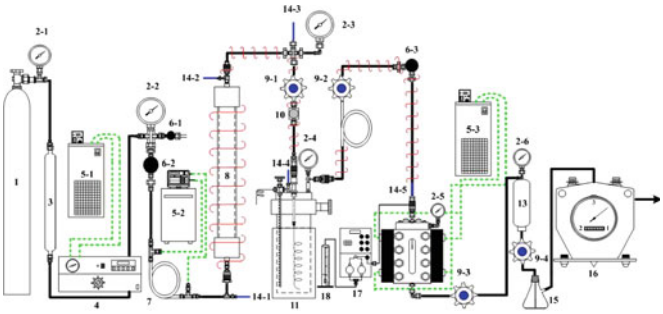

1. CO_2 cylinder	7. Heat exchanger	13. Separator
2-1~2-6. Pressure gauge	8. 1 Surge tank	14-1~14-5. Thermocouple
3. Gas dryer	9-1~9-4. Back-pressure regulator	15. Flask separator
4. High-pressure pump	10. Metering valve	16. Wet gas meter
5-1~5-3. Temperature circulator	11. 2 Surge tank	17. HPLC pump
6-1~6-3. Needle valve	12. Precipitator	18. Feeding

Fig. 2.6 Schematic flow diagram of SC-CO_2 antisolvent micronization of DHCA and flavonoids from propolis (Reprinted from Ref. [34]. With kind permission of © Elsevier)

For each SC-CO_2 antisolvent experiment, after the CO_2 entered into the precipitator under a selected supercritical condition, a solution of the propolis extract in ethyl acetate (or ethanol) was delivered from a feeding burette (18) into the precipitator through a coaxial nozzle at a constant flow rate of 1 mL/min using a HPLC pump (CM-3200, Thermo Separation Products, USA) (17). Meanwhile, the supercritical CO_2 was continuously charged into the precipitator. A stainless sintered frit filter (37 μm) and an online filter (0.5 μm) were tightly packed in that order at the bottom of the precipitator to prevent an entrainment of particles. Pressure was varied from 100 to 200 bar manually using a back-pressure regulator (9–3), and temperature was varied from 308 to 328 K using a water bath circulator (5–3). Following the antisolvent process, a vapor–liquid stainless steel separator (13) that was installed behind the precipitator was maintained at 50 bar using a back-pressure regulator (9–4) to stabilize the expanded mixture. A 250-mL flask separator was placed therein to collect the mixture of CO_2 and the solvent under ambient conditions. The consumption of CO_2 was measured using a wet gas meter (TG3, Ritter, Germany) (16). Temperatures in the system were monitored using several K-type thermocouples (14–1 ~ 14–5), and pressures in the system were monitored by several Bourdon-type pressure gauges (2–1 ~ 2–6).

2.4.2 Analysis of Micronized Precipitates

2.4.2.1 Determination of Particles Size, Distribution, and Morphology

After each antisolvent precipitation and drying process using CO_2 to remove solvent residue, the precipitator was open, the precipitate was collected, and the particulate was suspended in a deionized water to form a sample. The mean particle size and particle size distribution were determined using a light scattering particle size analyzer (Beckman Coulter, Counter F5, USA). To determine the particle morphology, the dried particulate was preliminarily coated with a platinum film by vacuum sputter and then analyzed under a field emission scanning electron microscope (FE-SEM) (JSM-7401 F, JEOL, Japan).

2.4.2.2 Quantification of DHCA and Flavonoids

A Waters HPLC system (USA), which comprises a 600E multisolvent delivery pump, a 717 plus autosampler, a 486 UV/Vis detector, and a Millennium 2010 system manager software, was adopted to analyze the SC-CO_2 precipitates. The samples were filtered through a 0.45-μm PVDF membrane (Millipore, USA) before the analysis, and then, a 20-μL sample was injected into a C8 column (4.6×250 mm, 5U, Macherey-Nagel, Germany) and a C18 column (4.6×250 mm, 5U, Hichrom, UK) reversed-phase column at a flow rate of 1 mL/min to partition the flavonoids and DHCA, respectively. The mobile phase that was used to analyze flavonoids consisted of 0.1% phosphoric acid (A) and methanol (B). The gradient was initially set to 65% A, reduced linearly to 50% A within 15 min, held at 50% A for 20 min, and finally reduced to 35% A within 15 min. The correlation coefficient (R^2) exceeded 0.996 for each linear calibration curve from 10 to 400 μg/g for flavonoids, and the limit of detection was in the range of 90–150 ng/g. The HPLC analysis of seven flavonoids was reported by Chen et al. [66]. The gradient of mobile phase utilized to analyze DHCA was described in Sect. 2.2.3. The R^2 of another linear calibration curve exceeded 0.99 from 50 to 800 μg/g for DHCA, and the limit of detection was 4,300 ng/g. The temperature of the column was controlled at 308 K, and the detection wavelength was set to 280 nm for both analyses.

The weight of the precipitates was calculated as a difference between the weight of fed and the solid content of the liquid eluent that was collected in the flask separator. The total yield (*TY*), recovery of *i* component (R_i), and enhancement factor of i component (β_i^*) were then calculated by Eqs. 2.3, 2.4, and 2.5:

$$TY = \frac{\text{Weight of precipitate}}{\text{Weight of feed material}} \times 100(\%), \text{ total yield.} \tag{2.3}$$

$$R_i = \frac{\text{Weight of } i \text{ in precipitate}}{\text{Weight of } i \text{ in Soxhlet extract}} \times 100(\%), \text{ recovery.} \tag{2.4}$$

$$\beta_i^* = \frac{\text{Concentration of } i \text{ in precipitate}}{\text{Concentration of } i \text{ in Soxhlet extract}}, \text{ enhancement factor.} \quad (2.5)$$

2.4.3 Experimental Results of Supercritical Carbon Dioxide ($SC\text{-}CO_2$) Antisolvent Micronization

2.4.3.1 Preliminary Experiment of Supercritical Carbon Dioxide ($SC\text{-}CO_2$) Precipitation

Two feeding solutions were obtained using two Soxhlet solvent extractions of Brazilian propolis. Table 2.5 presents experimental data that compare salting-out quantities from the Soxhlet ethyl acetate solution with those from the Soxhlet ethanol solution. The solid content of ethanol extract exceeded that of ethyl acetate extract, suggesting that the wax in the propolis was easily extracted by ethanol, leading to a high total yield. The DHCA concentration of ethanol extract was lower than that of ethyl acetate extract which contained 20.4% of DHCA. However, both extracts contained almost equal amounts of flavonoids. Accordingly, the Soxhlet ethyl acetate extracts were selected as the feeding solutions in the following $SC\text{-}CO_2$ antisolvent precipitations.

The effects of pressure and temperature of the $SC\text{-}CO_2$ antisolvent precipitations on total yield, recovery, and enhancement factor of the particulates were preliminary examined. Table 2.6 presents experimental results concerning the batch and continuous $SC\text{-}CO_2$ precipitation of the DHCA and flavonoids from 4 mL ethyl acetate solutions of propolis extracts at concentration of 200 mg/mL. In batch $SC\text{-}CO_2$ runs, the highest DHCA concentration was 30.4%, which obtained in an antisolvent experiment at 150 bar and 318 K (datum #3 in Table 2.6). This antisolvent pressure and temperature is suitable to obtain the purest DHCA precipitates. The DHCA concentration in the precipitates is substantially affected by the solubility of the desired compounds in the solution that is expanded with $SC\text{-}CO_2$ because of the associated change in the amount of carbon dioxide. Nevertheless, the low enhancement factor of the DHCA compound in the continuous $SC\text{-}CO_2$

Table 2.5 Experimental data concerning 250 mL of ethyl acetate or ethanol Soxhlet extractions of 15 g of Brazilian propolis lumps (Reprinted from Ref. [34]. With kind permission of © Elsevier)

Exp. #	$W_{ext.}$ (g)	TY_{ext} (%)	W_{DHCA} (mg/g)	β_{DHCA}	$W_{fla.}$ (mg/g)	β_{fla}
Sox-EA	9.3	61.8	204	1.62	22	1.62
Sox-EtOH	12.9	85.9	182	1.16	24	1.16

Sox-EA: ethyl acetate at 349 K; *Sox-EtOH*: ethanol at 351 K

$W_{ext.}$ weight of the extract, TY_{ext} total yield of the extract $= (W_{ext.}/W_{feed}) \times 100\%$, W_{DHCA} concentration of DHCA in extract, $W_{fla.}$ concentration of flavonoids in extract, β_{DHCA} concentration factor of DHCA $= R_{DHCA}/TY$, $\beta_{fla.}$ concentration factor of flavonoids $= R_{fla.}/TY$

Table 2.6 Experimental data on SC-CO_2 precipitation of 4 mL solutions of propolis extracts at concentration of 200 mg/mL (Reprinted from Ref. [34]. With kind permission of © Elsevier)

Exp. #	P (MPa)	T (K)	W_{DHCA} (%)	β^*_{DHCA}
Batch SC-CO_2				
1	10	308	20.6	1.01
2	15	308	21.6	1.06
3	15	318	30.4	1.49
Continuous SC-CO_2				
4	20	328	30.6	1.50
5[a]	20	328	20.5	1.13
6[a]	15	318	19.2	1.05

P pressure, *T* temperature, W_{DHCA} concentration of DHCA in precipitates, β^*_{DHCA} enhancement factor of DHCA = $W_{DHCA}/W_{DHCA,\ Soxhlet}$, $W_{DHCA,\ Soxhlet\text{-}EA}$ 20.4%, $W_{DHCA,\ Soxhlet\text{-}EtOH}$ 18.2%
[a]Propolis in EtOH, others are propolis in EA

precipitation at 200 bar and 328 K (datum #5 in Table 2.6) disfavors the use of the ethanol feeding solution, suggesting that the type of solvent is an another important factor in the SC-CO_2 precipitation.

2.4.3.2 Response Surface Methodology (RSM): Designed Supercritical Carbon Dioxide (SC-CO_2) Precipitation

Based on the effectiveness of varied operation conditions in obtaining the results of SC-CO_2 precipitation, discussed in the Sect. 2.4.3.1, a pressure of 200 bar and a temperature of 328 K were set in the experimental SC-CO_2 precipitation. A center-factor and factor-composite scheme, based on the expansion volume of carbon dioxide (EV_{CO_2}) and the mass flow rate of carbon dioxide (F_{CO_2}) in an RSM, was designed herein to study the continuous SC-CO_2 antisolvent micronization process. Table 2.7 presents experimental data on this RSM-based continuous SC-CO_2 antisolvent process at EV_{CO_2} from 50 to 150 L and F_{CO_2} from 10.8 to 32.6 g/min. The effects of these two factors on the RSM response parameters, including total yield, concentration, and recovery, of DHCA and flavonoids as well as mean particle size were analyzed using an ANOVA table in the Design-Expert software package with a quadratic regression model. The variation in the 3D plots of RSM response surfaces with independent factors is investigated below. Figure 2.7a demonstrates that the total yield at CO_2 flow rate of 10.8 g/min markedly exceeded that at 32.6 g/min because the expansion process provided a sufficient contact time between the CO_2 and the solution for precipitation. Experimental data also show that the CO_2 expansion volume slightly influenced the total yield when the volume exceeded 50 L. On the other side, both factors substantially affected the concentration of DHCA, as presented in Fig. 2.7b, suggesting that the concentration of DHCA decreased as the amount and flow rate of CO_2 increased. Figure 2.8a plots the obvious effect of these two factors on the recovery of DHCA. The fact that the 3D shape of the DHCA

Table 2.7 RSM-designed SC-CO_2 antisolvent precipitation at 200 bar and 328 K with two factors of expansion volume and flow rate of CO_2 (Reprinted from Ref. [34]. With kind permission of © Elsevier)

RSM #	EV_{CO_2} (L)	F_{CO_2} (g/min)	TY (%)	W_{DHCA} (%)	R_{DHCA} (%)	β^*_{DHCA}	$W_{fla.}$ (%)	$R_{fla.}$ (%)	$\beta^*_{fla.}$	χ_{PSD} (μm)
1(A)	50	10.8	58.6	32.1	92.2	1.57	2.73	71.4	1.22	8.80
2(F)	50	21.7	55.2	26.8	72.5	1.31	2.67	65.8	1.19	7.64
3(A)	50	32.6	51.4	27.7	69.8	1.36	3.07	70.4	1.37	6.54
4(F)	100	10.8	61.4	29.5	88.8	1.45	2.74	75.1	1.22	7.92
5(C)	100	21.7	58.1	23.1	65.8	1.13	3.12	80.9	1.39	6.03
6(F)	100	32.6	51.4	25.4	64.0	1.25	3.14	72.1	1.40	4.02
7(A)	150	10.8	57.1	25.6	71.7	1.25	2.80	71.4	1.25	6.34
8(F)	150	21.7	59.5	19.5	56.9	0.96	2.89	76.8	1.29	4.65
9(A)	150	32.6	58.1	18.6	53.0	0.91	2.96	76.8	1.32	3.95

Feed 200 mg/mL, $V_{solution}$ 4 mL, EV_{CO_2} expansion volume of CO_2, F_{CO_2} flow rate of CO_2, *TY* total yield of crystallization powders = $(W_{crystallization}/W_{feed}) \times 100\%$, W_{DHCA} concentration of DHCA in precipitate, R_{DHCA} recovery of DHCA = $(4 \times 200 \times TY \times W_{DHCA})/(4 \times 200 \times 20.4\%)$, $W_{fla.}$ concentration of flavonoids in precipitate, $R_{fla.}$ recovery of flavonoids = $(4 \times 200 \times TY \times W_{fla.})/(4 \times 200 \times 2.24\%)$, β^*_{DHCA} enhancement factor of DHCA = $W_{DHCA}/W_{DHCA,Soxhlet}$, $\beta^*_{fla.}$ enhancement factor of flavonoids = $W_{fla.}/W_{fla.,\ Soxhlet}$, $W_{DHCA,\ Soxhlet\text{-}EA}$ 20.4%, $W_{fla.,\ Soxhlet\text{-}EtOH}$ 2.24%

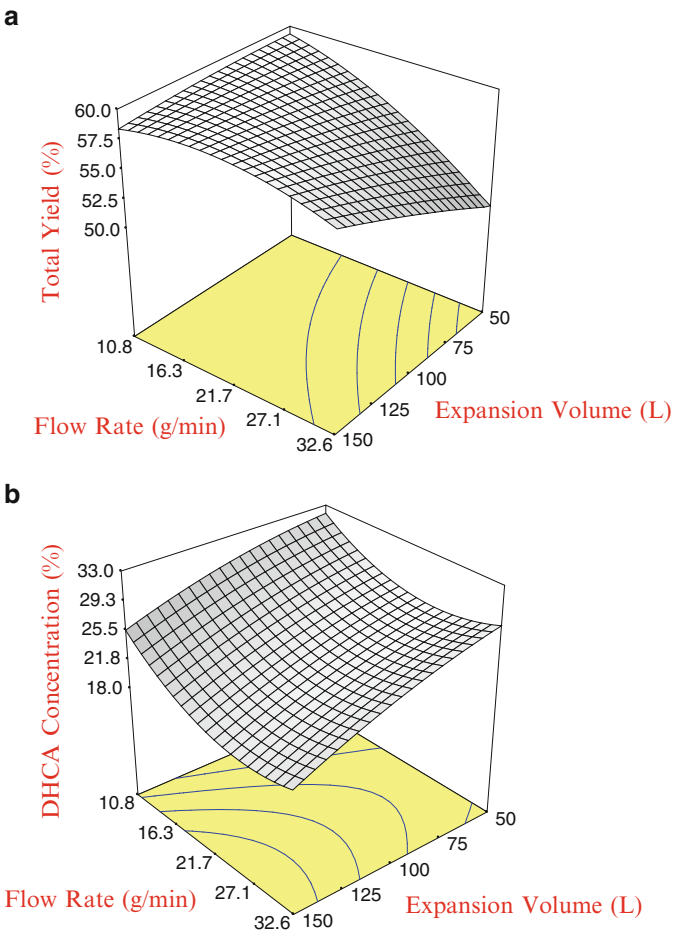

Fig. 2.7 Effects of expansion volume and flow rate on SC-CO_2 precipitation of DHCA (**a**) total yield and (**b**) DHCA concentration (*F*-testing: $R_{(a)}{}^2=0.8310$, $S.D._{(a)}=2.29$; $R_{(b)}{}^2=0.9875$, $S.D._{(b)}=0.80$) (Reprinted from Ref. [34]. With kind permission of © Elsevier)

recovery surface was similar to that of the DHCA concentration surface indicates that the DHCA precipitation increased with the total amount of precipitate. In contrast, Fig. 2.8b displays the drop in the mean particle size of the precipitate as the F_{CO_2} and the EV_{CO_2} are increased. This phenomenon reveals that a high flow rate is associated with rapid expansion of the feed solution and high supersaturation for the nucleation of small particles. Figure 2.9 plots the particle size distribution (PSD) of particles that were generated by continuous SC-CO_2 precipitations at 200 bar, 328 K with a CO_2 volume of 100 L. A narrower PSD pattern corresponds to a higher CO_2 flow rate, and the smallest mean particle size of the precipitate was 4.02 μm (datum # 6 in Table 2.7).

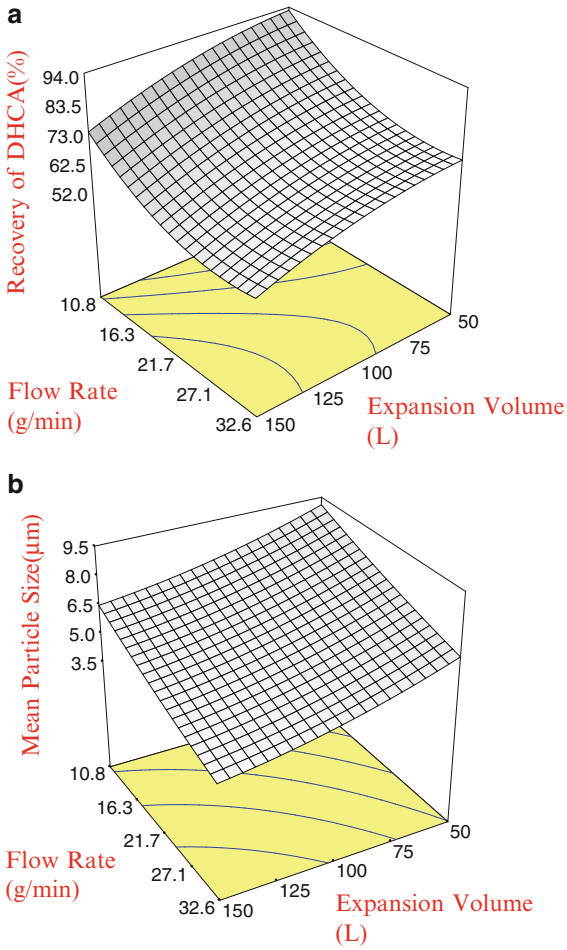

Fig. 2.8 Effects of expansion volume and flow rate on SC-CO_2 precipitation of DHCA (**a**) recovery of DHCA and (**b**) mean particle size (*F*-testing: $R_{(a)}{}^2=0.9891$, $S.D._{(a)}=2.23$; $R_{(b)}{}^2=0.9609$, $S.D._{(b)}=0.56$) (Reprinted from Ref. [34]. With kind permission of © Elsevier)

A center composite approach that involves solution concentration and flow rate of CO_2 as two factors was also designed for the SC-CO_2 antisolvent micronization of DHCA-containing propolis solution at 200 bar and 328 K. Table 2.8 presents experimental data concerning this RSM-designed at feeding concentrations from 9 to 27 mg/mL and flow rate of CO_2 from 10 to 20 L/min. The effects of these two factors on the total yield, concentration, and recovery of DHCA, as well as on the mean particle size, were demonstrated. Experimental data indicate that the SAS process operated at the same pressure, temperature, and CO_2 flow rate and both particle size and supersaturation mildly increase with the feed concentration, represented earlier by Bristow et al. [67]; however, supersaturation dramatically increases

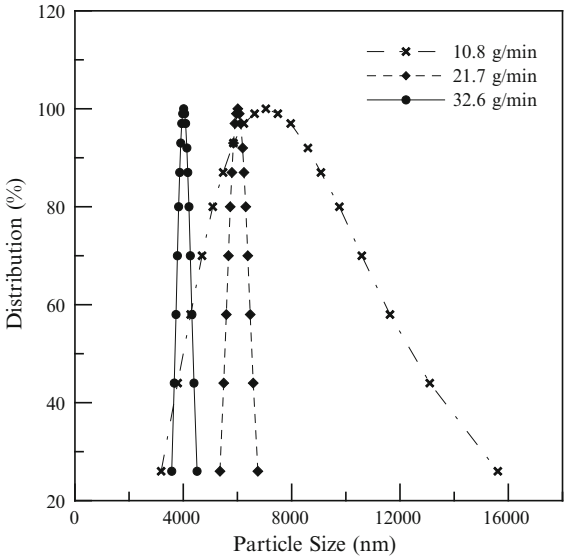

Fig. 2.9 Particle size distribution of precipitates produced in SC-CO_2 antisolvent process at 200 bar and 328 K with 100 L of CO_2 (Reprinted from Ref. [34]. With kind permission of © Elsevier)

Table 2.8 RSM-designed SC-CO_2 antisolvent micronization at 200 bar and 328 K with two factors of feed concentration and flow rate of CO_2 (Reprinted from Ref. [35]. With kind permission of © Elsevier)

RSM #	C_F (mg/mL)	Q_{CO_2} (L/min)	TY (%)	W_{DHCA} (%)	R_{DHCA} (%)	β^*_{DHCA}	χ_{PSD} (μm)
1(A)	9	10	57.6	35.2	92.6	1.61	4.74
2(F)	9	15	55.4	29.2	73.9	1.33	3.69
3(A)	9	20	46.6	22.1	47.2	1.01	1.95
4(F)	18	10	60.4	35.0	96.5	1.60	6.95
5(C)	18	15	58.6	32.9	88.0	1.50	5.27
6(F)	18	20	54.4	29.7	73.8	1.36	4.40
7(A)	27	10	71.0	29.9	96.9	1.37	9.00
8(F)	27	15	68.8	25.8	81.1	1.18	7.25
9(A)	27	20	62.2	21.6	61.3	0.99	6.19

Q_F 1-mL/min flow rate of feed, V_F 4-mL volume of feed, C_F concentration of feed, Q_{CO_2} flow rate of CO_2, *TY* total yield of precipitates $= (W_{crystallization}/W_{feed.}) \times 100\%$, W_{DHCA} purity of DHCA in precipitates, R_{DHCA} recovery of DHCA $= (4 \times 200 \times TY \times W_{DHCA})/(4 \times 200 \times 21.9\%)$, β^*_{DHCA} enhancement factor of DHCA concentration $= W_{DHCA}/W_{DHCA,Soxhlet.}$, χ_{PSD} mean particle size, $W_{DHCA,Soxhlet\text{-}EA}$ 21.9%

with the CO_2 flow rate and results in the smallest particle size. This demonstrates that the CO_2 flow rate significantly affected the particle size. Figure 2.10a indicates that the total yield at a CO_2 flow rate of 20 L/min was lower than that at 10 L/min because the precipitates were easily entrained by CO_2 at the higher flow rate. Figure 2.10b reveals that the DHCA concentration decreased as the flow rate of CO_2 and the feeding concentration increased. Figure 2.10c indicates that the recovery of

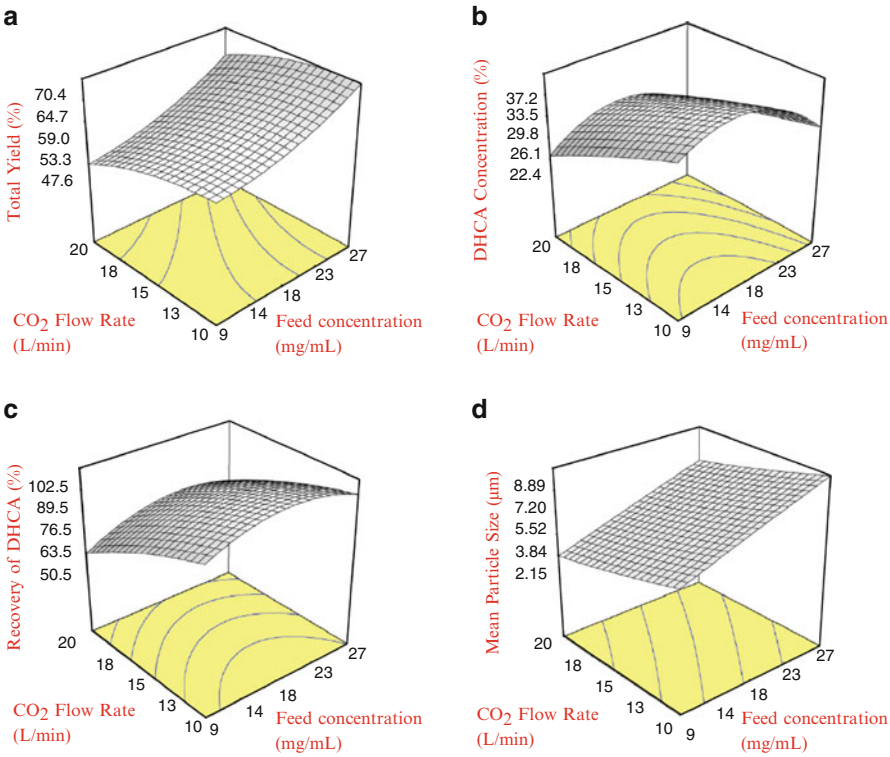

Fig. 2.10 Response surface curve effect of CO_2 flow rate and feeding concentration on SC-CO_2 antisolvent micronization of DHCA (**a**) total yield, (**b**) DHCA concentration, (**c**) recovery of DHCA, and (**d**) mean particle size (*F*-testing: $R_{(a)}{}^2=0.9851$, $S.D._{(a)}=1.48$; $R_{(b)}{}^2=0.9517$, $S.D._{(b)}=1.81$; $R_{(c)}{}^2=0.9530$, $S.D._{(c)}=5.97$; $R_{(d)}{}^2=0.9929$, $S.D._{(d)}=0.29$) (Reprinted from Ref. [35]. With kind permission of © Elsevier)

DHCA decreased as the flow rate of CO_2 increased and increased as the feeding concentration increased. These results show that increasing the flow rate of CO_2 caused DHCA to be removed in the CO_2 gas from the propolis solution. Figure 2.10d indicates that a higher flow rate of CO_2 and a lower feeding concentration yielded a narrower range of mean particle sizes of precipitates. Large particles were formed at feeding concentrations from 18 to 27 mg/mL. Figure 2.11 presents triplicate analyses of particle size distributions of precipitates obtained at 200 bar and 328 K. A narrow PSD was obtained at high CO_2 flow rate, 20 L/min, and a low feeding concentration, 9 mg/mL. The reason may be that a high CO_2 flow rate is associated with rapid expansion of the feed solution and high supersaturation for the nucleation of small particles. For a given degree of expansion, reducing the feeding concentration promotes the supersaturation of the solute and thus promotes the easy formation of a narrow particles size distribution. In contrast, increasing the feeding

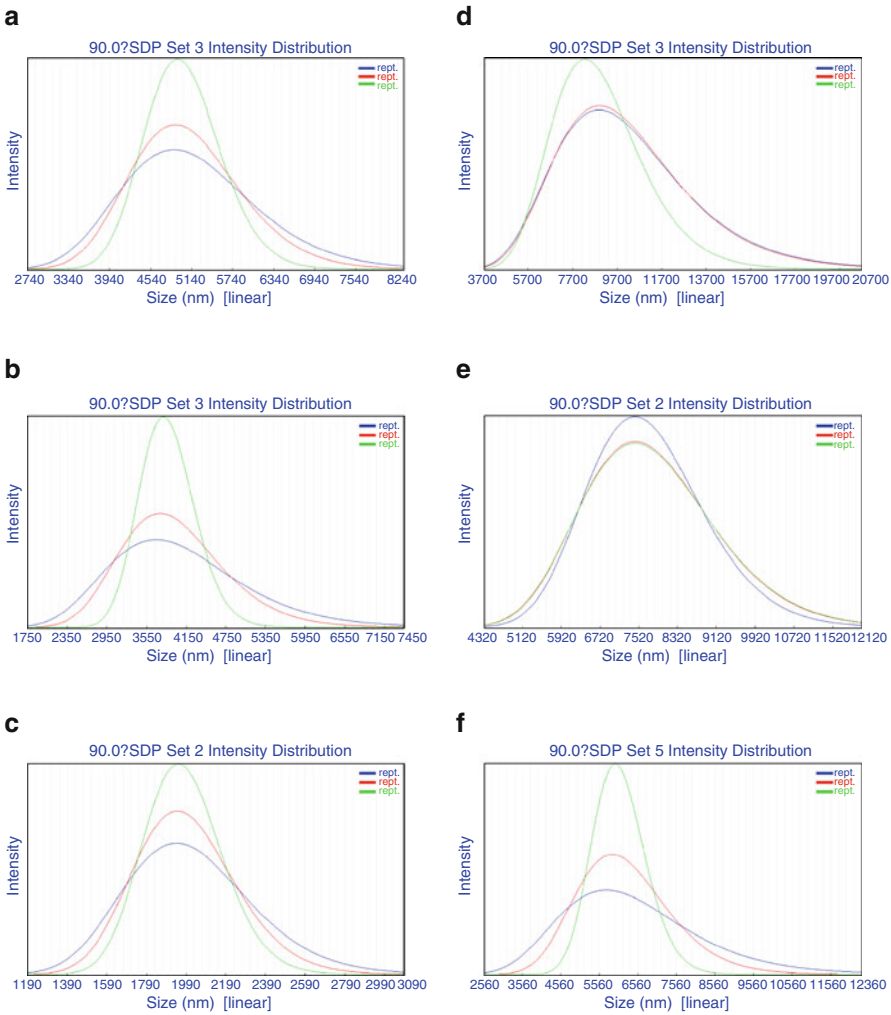

Fig. 2.11 Particle size distribution of precipitates in SC-CO_2 antisolvent micronization at 200 bar and 328 K. (**a**) Q_{CO_2} : 10 L/min; C_F: 9 mg/mL, (**b**) Q_{CO_2} : 15 L/min; C_F: 9 mg/mL, (**c**) Q_{CO_2} : 20 L/min; C_F: 9 mg/mL, (**d**) Q_{CO_2} : 10 L/min; C_F: 27 mg/mL, (**e**) Q_{CO_2} : 15 L/min; C_F: 27 mg/mL, (**f**) Q_{CO_2} : 20 L/min; C_F: 27 mg/mL (Reprinted from Ref. [35]. With kind permission of © Elsevier)

concentration causes the agglomeration of precipitates such that the particles become large. Figure 2.12 displays a few microphotographs of propolis precipitates, obtained using an FE-SEM. Particles with a mean diameter of less than 2 μm were formed at a CO_2 flow rate of 20 L/min and a feeding concentration of 9 mg/mL, as presented in Fig. 2.10c.

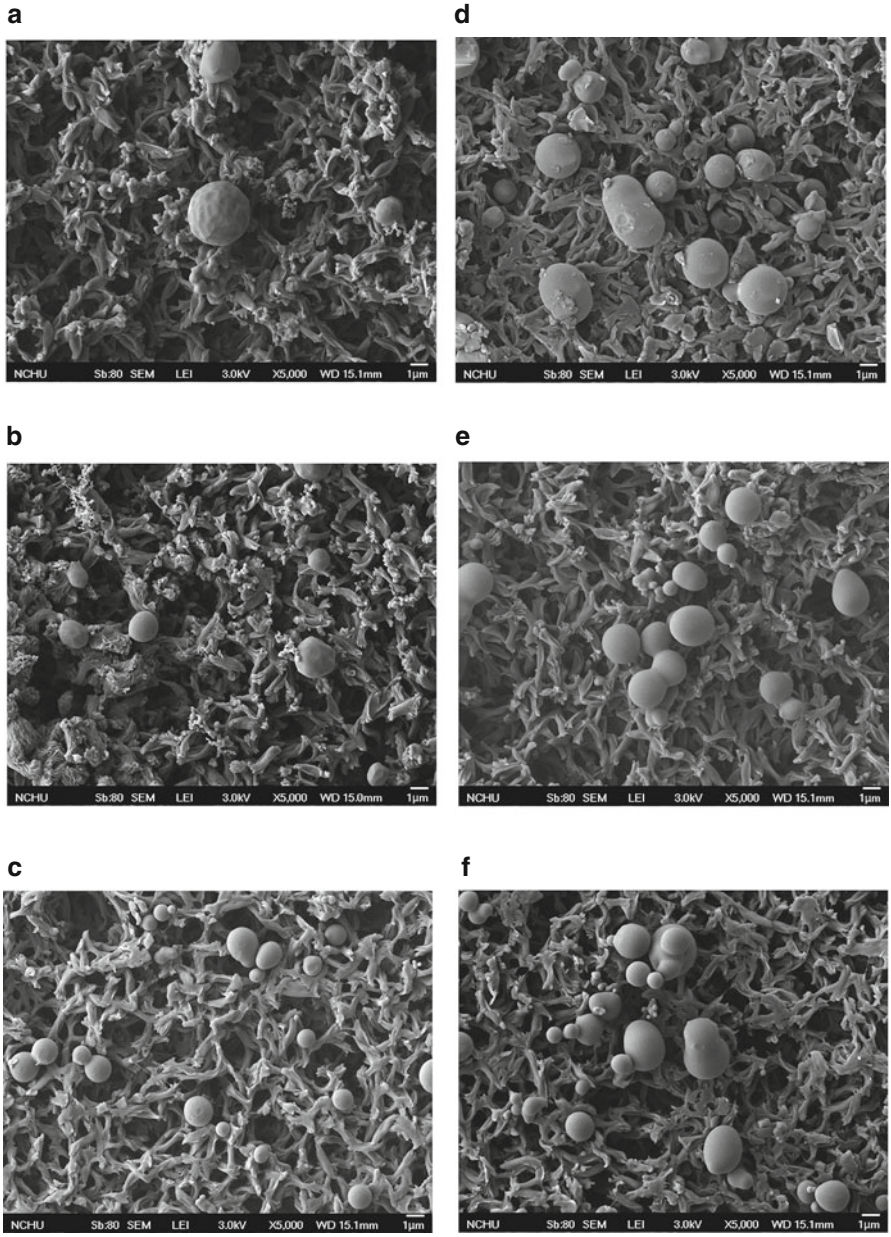

Fig. 2.12 FE-SEM images of particles in SC-CO_2 antisolvent micronization at 200 bar and 328 K. (**a**) Q_{CO_2} : 10 L/min; C_F: 9 mg/mL, (**b**) Q_{CO_2} : 15 L/min; C_F: 9 mg/mL, (**c**) Q_{CO_2} : 20 L/min; C_F: 9 mg/mL, (**d**) Q_{CO_2} : 10 L/min; C_F: 27 mg/mL, (**e**) Q_{CO_2} : 15 L/min; C_F: 27 mg/mL, (**f**) Q_{CO_2} : 20 L/min; C_F: 27 mg/mL (Reprinted from Ref. [35]. With kind permission of © Elsevier)

2.5 Biological Activity of Propolis Samples Produced by Supercritical Fluid Procedure

2.5.1 Cytotoxic Assay of Human Cells

2.5.1.1 Supercritical Carbon Dioxide (SC-CO_2) Extracts

Human leukemia cells (HL-60, CCL-240) were cultivated in an RPMI-1640 culture medium (Gibco BRL, USA) to which was added 5% fetal calf serum (FCS). Human colon cancer cells (colo-205, CCL-222) and skin normal cells (WS1, CRL-1502) were also cultivated in the RPMI-1640 medium to which was added 10% FCS. Human hepatoma cells (Huh7) and mouse liver normal cells (BNL, TIB-73) were cultivated in the Dulbecco's modified eagle medium (DMEM) to which 10% FCS was added. Moreover, the cultured media were supplemented with 100 units/mL penicillin, 100 μg/mL streptomycin, and 2 mM L-glutamine (Gibco BRL, USA), and all of the cells were incubated in a humidified incubator with 5% CO_2 at 310 K. Before treatment, cells were collected, resuspended, and stained with an equal volume of 0.4% trypan blue solution (Sigma, USA). The cells were counted using a hemocytometer (0.0025 mm^2, Marienfeld, Germany) under a phase-contrast-inverted microscope (Axiovert 25, Zeiss, Germany).

5×10^3 cells were individually seeded in each well of a 96-well dish and dosed with the SC-CO_2 extracts and purified DHCA, while 95% ethanol was dosed and used as a negative control. Following 48 h of incubation, 20 μL of yellow 3-(4,5-dimethylthiazol-2-yl)-2,5-diphenyltetrazolium bromide (MTT) reagent (Sigma, USA) was added into each well to react with the mitochondrial dehydrogenase enzyme of living cells for 3 h at 310 K. A solution of sodium dodecyl sulfate in 0.01-M HCl was then added to dissolve the insoluble purple formazan crystals, and the color of each well was measured at 570 nm using an enzyme-linked immunosorbent assay (ELISA) reader (Anthos 2001, Austria). The cell viability was quantified by the ratio of optical density at a wavelength of 570 nm (OD_{570}) of the dosed sample to that of the control sample. The half maximal effective concentration (EC_{50}) values of cytotoxic assay for each treated sample were regressed by a linear calibration curve ($R^2 = 0.99$). All data are presented as means obtained from triplicate experiments.

Table 2.9 presents the cell viability and EC_{50} values of the suppression of the proliferation of three cancer cells treated with the 95% EtOH control and seven samples of 95 wt% DHCA, 80 wt% DHCA, three SC-CO_2 extracts, one Soxhlet ethyl acetate extract, and one beeswax (white powder). After 48 h of treatment, the inhibition of the growth of cancer cells depends on the concentration of these samples. Both EC_{50} values of SC-CO_2 and SC-CO_2 + EA samples were inferior to those of 80 wt% and 95 wt% DHCA samples, suggesting that the purity of DHCA is very important in suppressing the growth of Huh7, colo-205, and HL-60 cancer cells. Furthermore, three statistical correlation coefficients between the DHCA purity and the EC_{50} values of colo-205 cells were almost close to unity (Table 2.9). The inhibition of the growth of leukemia and colon cancer cells was superior to that of liver

Table 2.9 EC_{50} values of growth inhibition of human cancer cells treated with DHCA at seven levels of purity for 48 h (Reprinted from Ref. [14]. With kind permission of © Elsevier)

Samples	P_{DHCA} (wt%)	HL-60	Colo-205(μg/mL)	Huh7
Beeswax	0	1,565	1,672	2,717
Soxhlet-EA	16.9	708	922	1,189
SC-CO_2 + 2% *n*-hexane	35.5	376	567	525
SC-CO_2 + 6% EA	41.2	382	763	568
SC-CO_2	45.3	731	557	532
80 wt% DHCA	80.3	136	176	411
95 wt% DHCA	95.4	56	79	274
		P = 0.8337	P = 0.9138	P = 0.7591
		S = 0.7500	S = 0.9643	S = 0.8929
		K = 0.6190	K = 0.9048	K = 0.8095

Dose concentration of 95% EtOH control = 7,800 μg/mL
P_{DHCA} purity of DHCA, *HL-60* leukemia cells, *Colo-205* colon cancer cells, *Huh7* hepatoma cells, *P* Pearson coefficient, *S* Spearman coefficient, *K* Kendall's tau-b coefficient

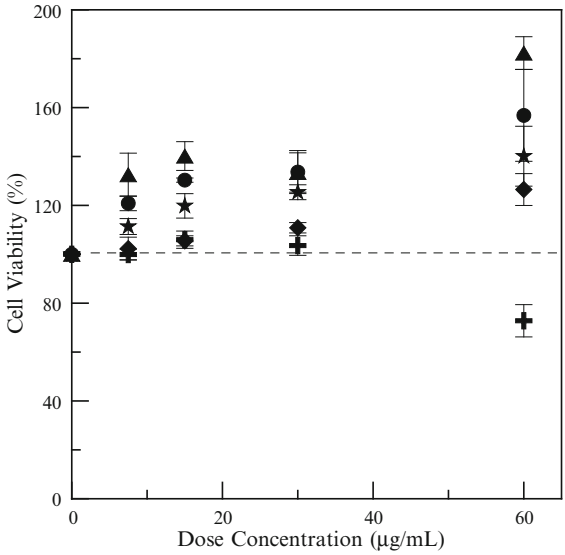

Fig. 2.13 Viability of normal BNL cells treated with five samples containing various DHCA purities for 48 h (+, 95-wt% DHCA; ●, SC-CO_2 extract; ▲, SC-CO_2 + 6-wt% EA extract; ★, SC-CO_2 + 2-wt% *n*-hexane extract; ◆, Beeswax) (Reprinted from Ref. [14]. With kind permission of © Elsevier)

cancer cells, and the apoptosis mechanism was possible. The EC_{50} values of HL-60 and colo-205 cancer cells upon treatment with the purest 95 wt% DHCA were 56 and 79 μg/mL, respectively. Two normal cells were also treated with pure DHCA. Figures 2.13 and 2.14 show the viability of BNL cells and WS1 cells, respectively. They indicate that the cell viabilities were higher than 100%. Restated, DHCA did not suppress the growth of these two normal cells, although it did suppress the growth of BNL when at high concentration. Consequently, DHCA was harmless to normal cells herein.

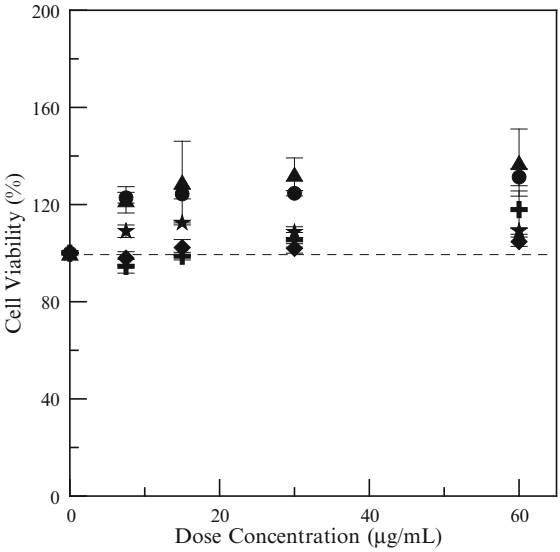

Fig. 2.14 Viability of normal WS1 cells treated with five samples containing various DHCA purities for 48 h (+, 95-wt% DHCA; ●, SC-CO_2 extract; ▲, SC-CO_2 + 6-wt% EA extract; ★, SC-CO_2 + 2-wt% *n*-hexane extract; ◆, Beeswax) (Reprinted from Ref. [14]. With kind permission of © Elsevier)

2.5.1.2 Supercritical Carbon Dioxide (SC-CO_2) Precipitates

Cell viability was evaluated using the method of Mossman and Churg with minor modifications [68]. Five thousand cells per well of human colon (colo-205) and breast (MDA-MB-231) cancer cell lines and normal keratinocytes (HaCaT) were grown in 0.1 mL RPMI 1640 and DMEM medium, respectively, in the wells of 96-well dish that contained 10% fetal bovine serum (FBS) by heat deactivation (329 K for 30 min) and 1% glutamine, followed by incubation at 310 K in 5% CO_2 for 24 h. Cells were then treated with 25- to 250-μg/mL samples for 24 h. After the medium had been drawn out and the cells are washed with phosphate-buffered saline, then the 3-(4,5-dimethylthiazol-2-yl)-2,5-diphenyltetrazolium bromide (MTT) reagent (1 mg/mL, 100 μL) was added to them. They were then incubated at 310 K with 5% CO_2 for 2.5 h. Finally, the dimethyl sulfoxide (DMSO) solvent was added to the cells, and their viability was determined at 550-nm absorption in a test with control using an ELISA reader. The EC_{50} values of the cytotoxic assay for each treated sample were regressed to obtain a linear calibration curve ($R^2 = 0.99$). All data are presented as averages from triplicate experiments.

Table 2.10 presents the EC_{50} values of colo-205, MDA-MB-231 cancer cells for 24, 48, and 72 h of treatment with Soxhlet ethyl acetate extracts and SC-CO_2 precipitates. The table indicates that Soxhlet ethyl acetate extracts and SC-CO_2 precipitates inhibited the growth of both cancer cells. The EC_{50} values of cancer cells that were treated with SC-CO_2 precipitates were lower than those of Soxhlet extracts at 24, 48, and 72 h of incubation. These data indicate that the inhibitive effect of SC-CO_2 precipitates on colon and breast cancer cells exceeded that of Soxhlet extracts. A lower DHCA concentration results in a lower EC_{50}, suggesting that the

Table 2.10 EC_{50} values for inhibition of growth of cancer cells by treatment with Soxhlet extracts and SC-CO_2 precipitate for 24–72 h (Reprinted from Ref. [35]. With kind permission of © Elsevier)

		Colo-205 (μg/mL)			MDA-MB-231 (μg/mL)		
Sample	W_{DHCA} (%)	24 h	48 h	72 h	24 h	48 h	72 h
RSM #1	35.2	268	284	281	494	301	259
RSM #2	29.2	300	293	318	630	330	294
RSM #3	22.1	372	317	342	689	348	394
Soxhlet	21.9	388	327	362	799	350	418

W_{DHCA} purity of DHCA in precipitate, *Colo-205* human colon cancer cell lines, *MDA-MB-231* human breast cancer cell lines

concentration of DHCA may be important to affect the inhibition of growth of cancer cells. Figure 2.15 presents a cytotoxic test of normal keratocytes (HaCaT) that were treated with Soxhlet ethyl acetate extracts and SC-CO_2 precipitates. The figure indicates that treatment with samples with a concentration less than 200 μg/mL did not inhibit the growth of normal keratocytes. This finding indicates that a high dose of these propolis precipitates is cytotoxic to normal keratocytes. Ozkul et al. [69] also demonstrated the anticarcinogenic effect of propolis on a culture of human lymphocytes, while a high concentration of propolis was carcinogenic.

2.5.2 Antioxidative Ability Tests

2.5.2.1 2,2-Diphenyl-1-Picrylhydrazyl (DPPH) Free Radical

7.9 mg of DPPH powder was dissolved in the 100-mL methanol to form a 200-μM purple-blue stock solution, 2 mL of the stock solution mixed with 2 mL of the propolis extract in a quartz tube reacted for 30 min, and the absorption of this solution measured at 517 nm by a UV–vis spectrum (Hitachi, UV-3000, Japan) to obtain the DPPH concentration. The DPPH scavenging ratio (SR) for five concentrations of the propolis extract was calculated to determine an effective concentration of the extract (i.e., EC_{50} value), which 50% of DPPH free radicals in the solution were being suppressed, that is, 50% of the SR value. The SR value is defined by $[(AB\text{-}ABs)/AB] \times 100\%$, where AB is the absorption without the propolis extract and ABs is the absorption with the extract.

In screening antioxidative ability of the propolis extracts, solutions of 125-, 62.5-, 31.3-, 15.6-, and 7.8-mg/L concentrations of seven propolis extracts in methanol, ferulic acid, cinnamic acid, caffeic acid, and *p*-coumaric acid were individually prepared and used in scavenging DPPH free radicals. Table 2.11 lists the EC_{50} value of these propolis extracts in scavenging 50% DPPH free radicals. Although the propolis extracts containing DHCA are not so effective in scavenging DPPH radicals compared with those references, propolis might still be one of antioxidative candidates.

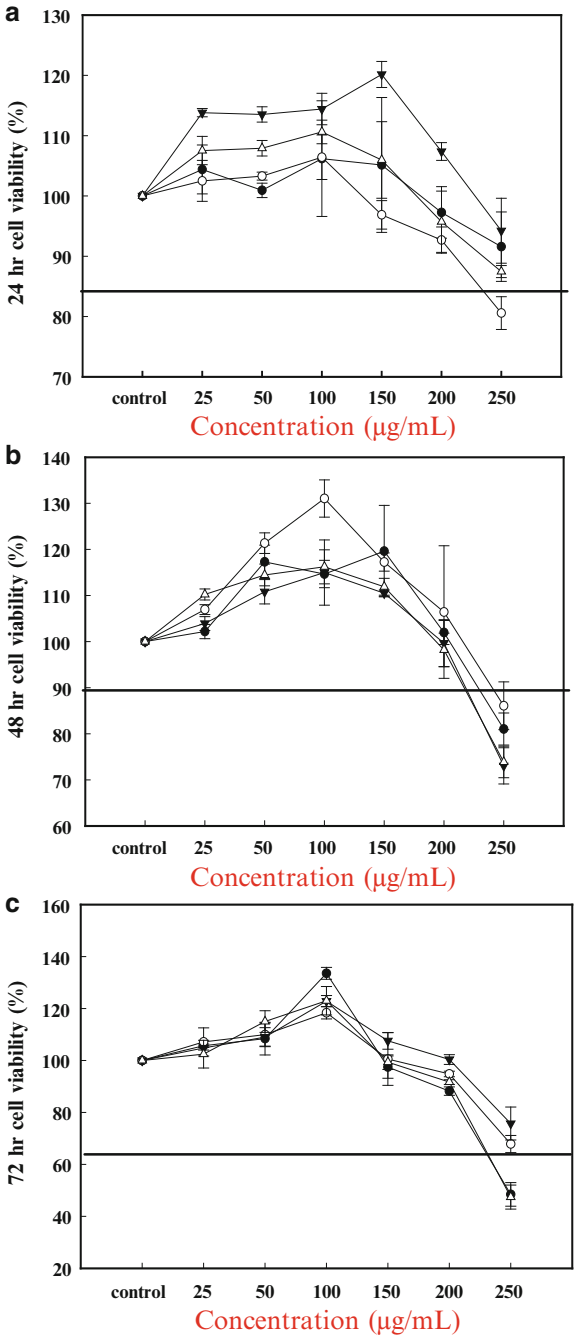

Fig. 2.15 Cell viability of keratocytes HaCaT cells treated with SC-CO_2 precipitates for 24–72 h (R^2>0.99) (Δ, RSM # 1; ▼, RSM # 2; ○, RSM # 3; ●, Soxhlet) (Reprinted from Ref. [35]. With kind permission of © Elsevier)

Table 2.11 Scavenging DPPH free radicals by the propolis extracts and phenolic acids (Reprinted from Ref. [18]. With kind permission of © Elsevier)

Sample	DPPH-absorption equation	R^2	EC_{50} [a] (mg/L)
DHCA	$Y=0.2886x+35.796$	0.9957	49.2
Soxhlet	$Y=0.6544x+24.434$	0.9904	39.1
HPE	$Y=0.7714x+22.899$	0.9989	35.1
Sonic	$Y=0.6010x+25.139$	0.9973	41.4
SCF1	$Y=0.1818x+39.765$	0.9972	56.3
SCF2	$Y=0.2119x+38.611$	0.9989	53.5
SCF	$Y=0.1101x+43.127$	0.9965	62.4
Ferulic acid	$Y=3.5588x+31.616$	0.9910	5.2
Cinnamic acid	$Y=0.0018x+0.5515$	0.9913	>2,000
Caffeic acid	$Y=24.131x+7.1941$	0.9906	1.8
p-Coumaric acid	$Y=0.0104x+7.6095$	0.9963	>2,000

DHCA, 95-wt% DHCA; *Soxhlet*, 16-h Soxhlet-EA; *HPE*, 2.5-h, 368-K hot-pressurized EA; *Sonic*, 2.5-h, 348-K ultrasonic EA; *SCF1*, 323-K, 207-bar, 6-wt% EA + 475-L CO_2; *SCF2*, 333-K, 207-bar, 6-wt% EA + 475-L CO_2; *SCF*, 323-K, 207-bar, 475-L CO_2

[a] EC_{50}: concentration suppressing 50% DPPH free radicals

2.5.2.2 Low-Density Lipid Protein

The human serum containing sodium chloride was obtained by centrifuge at 283 K for 10 min. Samples containing human low-density lipid (LDL) serum dissolved in desalt buffer solutions comprising the propolis extracts were prepared. Each sample mixed with Cu^{2+} aqueous solution was reacted for 24 h at 310 K and cooled for 1 h to stop the oxidation. The cold sample was mixed with the tris-acetate-EDTA buffer solution containing 1 wt% agarose gel. After electrophoresis by charging a 100 V, the treated sample was dried and dyed by the Sudan Black B. Figure 2.16a showed that the purified DHCA at 350 mg/L was effective to inhibit one half of the LDL oxidation. Figure 2.16b elucidated that the ability of anti-LDL oxidation is correspondent to the DHCA purity in the SC-CO_2 extracts.

2.6 Column Partition Fractionation of γ-Oryzanols

2.6.1 Isolation and Identification of Two γ-Oryzanols

A semipreparative HPLC system with C18 column (YMC, 250- × 10-mm I.D.) connected to a UV detector (785A, Perkin-Elmer) via a high-pressure pump (410, Perkin-Elmer) was used. The 1.5-mL (500 ppm) 95% mixed standard of γ-oryzanols (Wako, Japan) dissolved in methanol was injected into a 5-mL loop, and this sample was partitioned using a mixed solvent of acetonitrile, dichloromethane, and acetic acid (90:6:4) at a flow rate of 5 mL/min as mobile phase. The eluates were detected

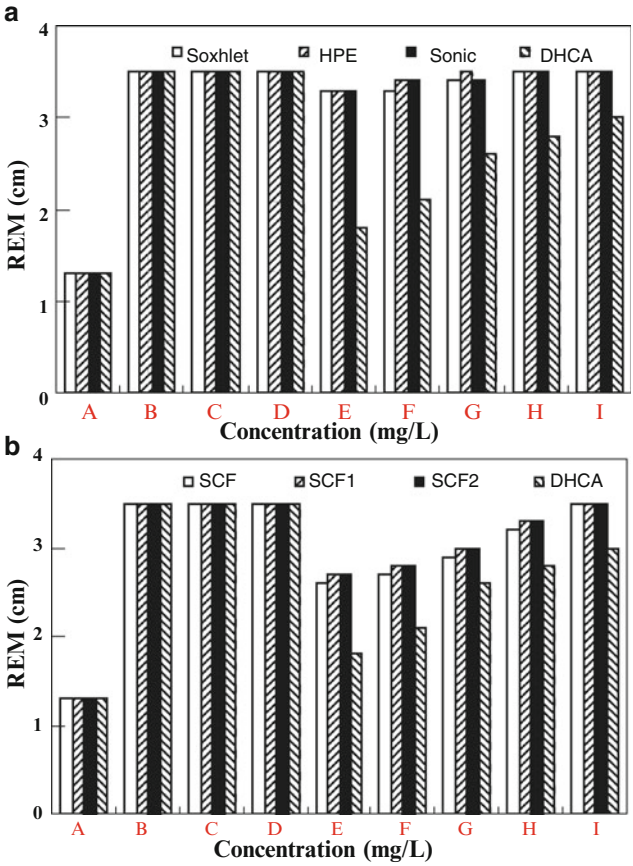

Fig. 2.16 Anti-LDL oxidation ability (**a**) solvent extracts and (**b**) SC-CO_2 extracts (*DHCA*: 95 wt% DHCA; *Soxhlet*: 16.9-wt% DHCA; *HPE*: 16.4-wt% DHCA; *Sonic*: 16.0-wt% DHCA; *SCF1*: 41.2-wt% DHCA; *SCF2*: 40.8-wt% DHCA; *SCF*: 45.3-wt% DHCA; *REM*: relative electron mobile length; *A*: Control; *B*: Cu^{2+}; *C*: 25% EtOH; *D*: 95% EtOH; *E*: 500 mg/L; *F*: 400 mg/L; *G*: 300 mg/L; *H*: 200 mg/L; *I*: 100 mg/L) (Reprinted from Ref. [18]. With kind permission of © Elsevier)

at a wavelength of 330 nm, and four isolated compounds were collected based on their retention time. Figure 2.17 presents the HPLC spectra of four isolated γ-oryzanols. The isolated 24-methylenecycloartanyl ferulate and campesteryl ferulate were obtained at the 10-mg level. Their chemical structures were identified using a 400-Hz ^{1}H NMR spectrophotometer.

The 98.5% pure second-largest 24-methylenecycloartanyl ferulate and the 98% pure third-largest campesteryl ferulate were obtained using semipreparative HPLC. Figure 2.18b, c present the ^{1}H NMR chemical shifts of 24-methylenecycloartanyl ferulate and campesteryl ferulate, respectively. The chemical shift patterns are identified with those described by Yasukawa et al. [44].

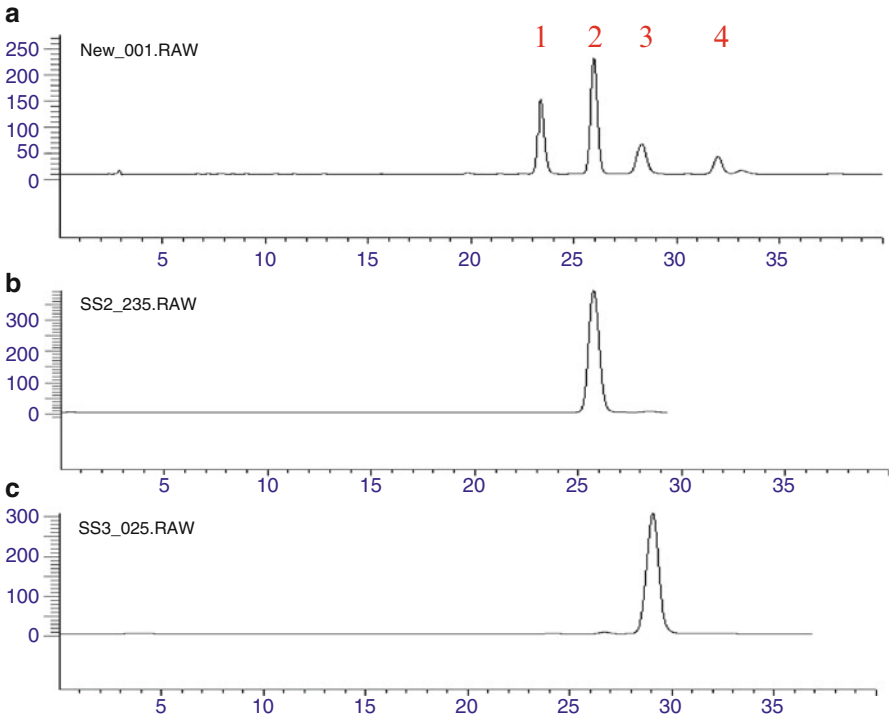

Fig. 2.17 HPLC spectra of isolated oryzanols (**a**, mixed γ-oryzanols; *1*, cycloartenyl ferulate; *2*, 24-methylenecycloartanyl ferulate; *3*, campesteryl ferulate; *4*, sitosteryl ferulate; **b**, the purest 98.5% 24-methylenecycloartanyl ferulate; **c**, the purest 98% campesteryl ferulate)

2.6.2 Quantification of γ-Oryzanols, Free Fatty Acids, and Triglycerides

HPLC quantifications of four γ-oryzanols (cycloartenyl ferulate, 24-methylenecycloartanyl ferulate, campesteryl ferulate, and sitosteryl ferulate) and three free fatty acids (oleic acid, linoleic acid, and linolenic acid) were performed using a reverse-phase analytical column (5 μm, 250-×4.6-mm I.D., YMC RP-18, Japan). The column temperature was maintained at 313 K, and the UV absorption was detected at the wavelength of 330 nm and 210 nm for γ-oryzanols and FFAs, respectively. One mobile phase of the mixed solvent of 90% acetonitrile, 6% dichloromethane, and 4% acetic acid was utilized for the γ-oryzanol analysis. The other mobile phase of the mixed solvent of 85% acetonitrile, 5% methanol, and 10% deionized water with 1% acetic acid was used to analyze the FFAs. Gas chromatography (GC) quantification of seven fatty acid methyl ester (FAMEs) representing total triglycerides (TGs) was performed using a nonpolar capillary column (DB-5, J&W, USA). The column temperature was set to 443 K initially and programmed to 503 K within 20 min. The injection volume was 1 μL with 3.4:1 of split ratio, and the temperature of flame ionization detector was set to 553 K.

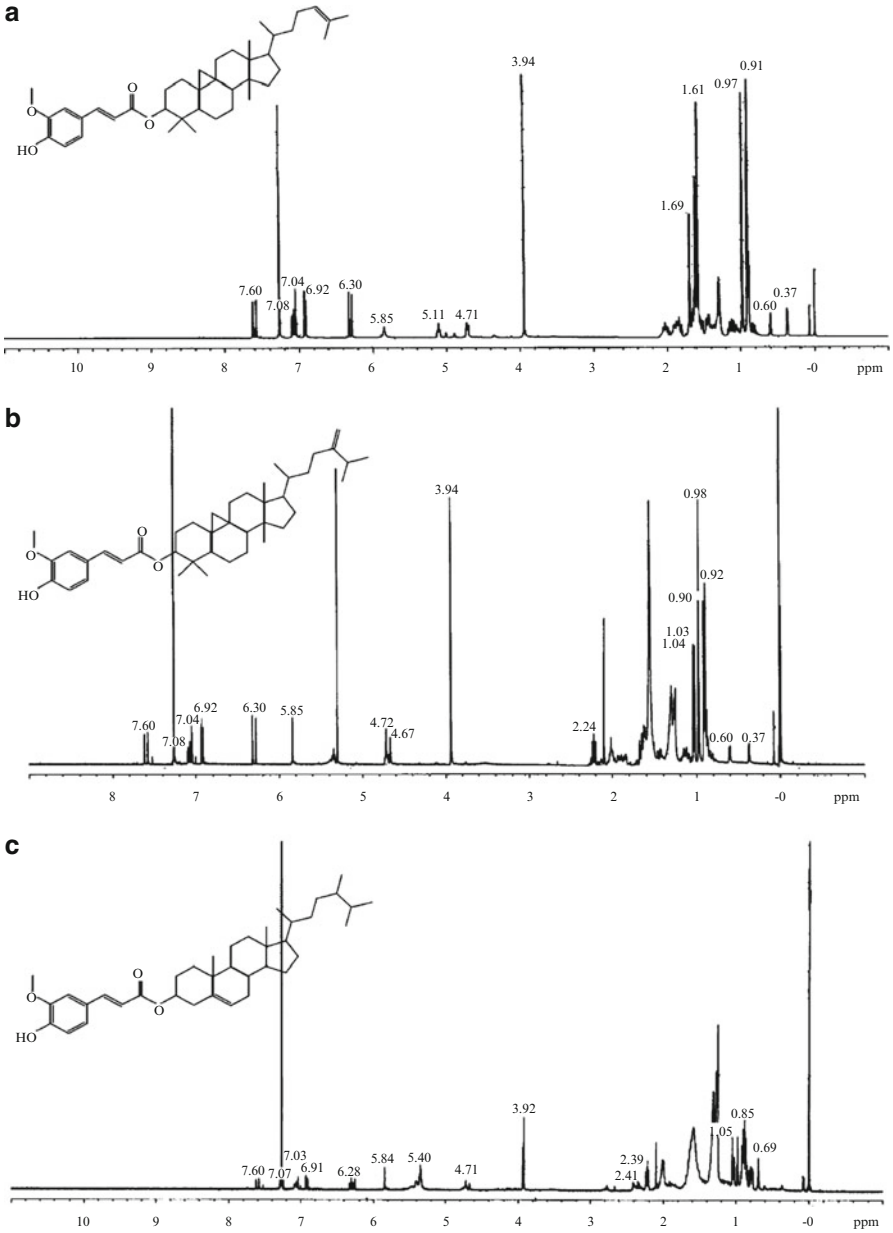

Fig. 2.18 Four-hundred-megahertz ^{1}H NMR spectra of (**a**) purest 99% cycloartenyl ferulate, (**b**) purest 98.5% 24-methylenecycloartanyl ferulate, and (**c**) purest 98% campesteryl ferulate (Reprinted from Ref. [57]. With kind permission of © Elsevier)

2.6.3 Soxhlet Solvent Extractions

In Soxhlet extractions, 15-g sample of rice bran powder was individually loaded into a 250-mL reflux Soxhlet extractor and extracted using 300-mL solvent for 4 h. All of the extracts were collected and weighed. The total amount of extract, the extraction efficiencies, and the concentration factors of γ-oryzanols, free fatty acids, and triglycerides were then calculated by Eqs. 2.6, 2.7, and 2.8:

$$TY = \frac{\text{Weight of the extracted oil}}{\text{Weight of feeding material}} \times 100(\%), \text{ total yield.} \tag{2.6}$$

$$R_i = \frac{\text{Weight of } i \text{ component in the extracted oil}}{\text{Weight of } i \text{ component in Soxhlet extracted oil}} \times 100(\%),$$
$$i = \begin{Bmatrix} \text{Oryzanols} \\ \text{FFAs} \\ \text{TGs} \end{Bmatrix}, \text{extraction efficiency.} \tag{2.7}$$

$$\beta_i = \frac{\text{Extraction efficiency of } i \text{ component}}{\text{Total yield}},$$
$$i = \begin{Bmatrix} \text{Oryzanols} \\ \text{FFAs} \\ \text{TGs} \end{Bmatrix}, \text{concentration factor.} \tag{2.8}$$

Table 2.12 presents the total yield (*TY*) of the extract, the extracted amounts (W_{ory}, W_{FFA}, and W_{TG}), the extraction efficiencies (R_{ory}, R_{FFA}, and R_{TG}), and the concentration factors (β_{ory}, β_{FFA}, and β_{TG}) of γ-oryzanols, free fatty acid, and triglycerides obtained by Soxhlet solvent extractions. The maximal concentrations of γ-oryzanols, free fatty acids, and triglycerides in the Soxhlet *n*-hexane extracted oil were 15.2, 95.0, and 800 mg/g of rice bran oil, respectively. Amounts of γ-oryzanols, free fatty acids, and triglycerides in rice bran reached to 3.03, 19.0, and 160 mg/g of rice bran, respectively, after 4 h of 300-mL *n*-hexane extraction of 15-g rice bran powder. These data were regarded as representing 100% recovery of γ-oryzanols, free fatty acids, and triglycerides.

2.6.4 Purification of Rice Bran Oil Using Column Partition

In this study, a total 15 g of SC-CO_2-extracted oil was obtained and diluted with *n*-hexane in a batch. The diluted solution was then loaded into a medium-pressure column (440-mm L × 37-mm I.D.) that was packed with silica gel 60 resin

Table 2.12 Experimental data on Soxhlet extractions of rice bran oil from 15 g rice bran powder (Reprinted from Ref. [54]. With kind permission of © Elsevier)

Exp #	Solvent	W_{oil} (g)	TY (%)	W_{Ory} (mg/g_{oil})	W^*_{Ory} (mg/g_{RB})	R_{Ory} (%)	β_{Ory}	W_{FFA} (mg/g_{oil})	W^*_{FFA} (mg/g_{RB})	R_{FFA} (%)	β_{FFA}	W_{TG} (mg/g_{oil})	W^*_{TG} (mg/g_{RB})	R_{TG} (%)	β_{TG}	Others (mg/g_{oil})
1	HA	3.00	20.0	15.2	3.03	100	5.00	95.0	19.0	100	5.00	800	160	100	5.00	89.8
2	IPA	3.97	26.4	9.07	2.40	79.1	2.99	68.1	18.0	94.8	3.59	555	147	91.7	3.47	368
3	MeOH	3.49	23.3	12.3	2.87	94.5	4.06	70.0	16.3	85.7	3.68	574	134	83.5	3.59	344
4	EA	3.30	22.0	12.3	2.70	89.2	4.05	82.1	18.1	95.0	4.32	666	147	91.6	4.16	240
5	EE	3.84	25.6	8.94	2.29	75.5	2.95	74.2	19.0	99.9	3.90	625	160	99.9	3.90	292
6	IPA + HA	2.93	19.5	14.0	2.72	89.8	4.60	90.2	17.6	92.6	4.75	789	154	96.2	4.93	107

HA *n*-hexane, *IPA* isopropanol, *MeOH* methanol, *EA* ethyl acetate, *EE* ethyl ether, W_{oil} weight of the extracted, *TY* total oil yield = $(W_{oil}/W_{RB}) \times 100\%$, W_{RB} weight of rice bran, W_{Ory} weight of oryzanols, W^*_{Ory} yield of oryzanols, W_{FFA} weight of free fatty acids, W^*_{FFA} yield of free fatty acids, W_{TG} weight of triglycerides, W^*_{TG} yield of triglycerides, R_{Ory} oryzanol extraction efficiency = $(W^*_{Ory}/W^*_{Ory,\,HA}) \times 100\%$, R_{FFA} free fatty acids extraction efficiency = $(W^*_{FFA}/W^*_{FFA,\,HA}) \times 100\%$, R_{TG} triglycerides extraction efficiency = $(W^*_{TG}/W^*_{TG,\,HA}) \times 100\%$, β_{Ory} concentration factor of oryzanols = R_{Ory}/TY, β_{FFA} concentration factor of free fatty acids = R_{FFA}/TY, β_{TG} concentration factor of triglycerides = R_{TG}/TY, *Others* weight of waxes, glycolipids, and phospholipids

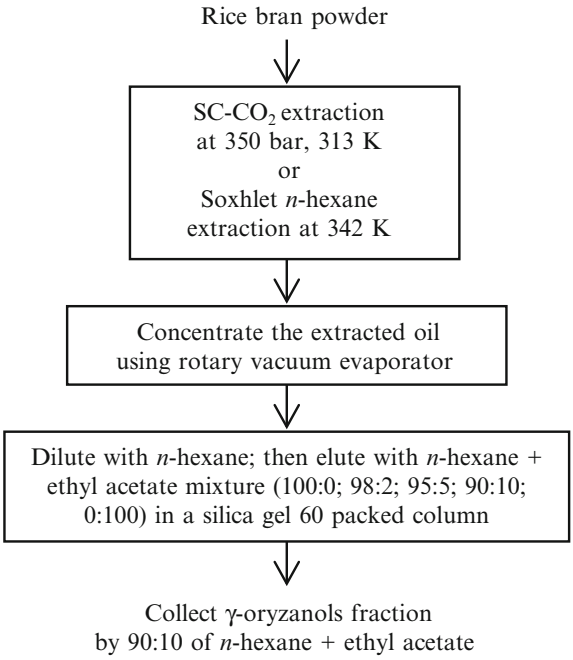

Fig. 2.19 Block diagram of solid–liquid column partition fractionation of rice bran oil (Reprinted from Ref. [54]. With kind permission of © Elsevier)

(LiChroprep-Si-60, 40–63 μm, Merck, Germany). The diluted solution of SC-CO_2-extracted oil was pumped into the medium-pressure column through an intelligent pump (PU-1580, Jasco, Japan). Based on the difference between polarities, solutes were retained and partitioned in the normal-phase resin. One-step elution chromatography was employed to fractionate the γ-oryzanols with an affinity for fat from other species in the oil. The eluting solvent consists of *n*-hexane (H) and ethyl acetate (EA). It was used to partition continuously the compounds and slowly elute them out, finally yielding the fraction collectors (Fig. 2.19). In these stepwise elution processes, most triglycerides and free fatty acids were initially washed out by the eluent, but the γ-oryzanols were retained and eluted finally. The flow rate of feeding, elution, and washing was held constant at 2 mL/min. Five eluting solvent mixtures of *n*-hexane with ethyl acetate in volume ratios of 100:0, 98:2, 95:5, 90:10, and 0:100 were used in this fractionation study. After the solvent had been dried out, each fraction was concentrated and analyzed.

A medium-pressure normal-phase column partition fractionation was adopted herein to purify γ-oryzanols from the Soxhlet and SC-CO_2-extracted oil. Table 2.13 presents the amount of γ-oryzanols, triglycerides, free fatty acids, and total fatty acids in each fraction. After the sixth fraction of *n*-hexane, extracted oil (datum # F6 in Table 2.13) was eluted using the 90:10 solution of *n*-hexane and ethyl acetate; 37.0 wt% of γ-oryzanols was obtained. The fifth fraction that contained 18.9 wt% of γ-oryzanols of the SC-CO_2-extracted oil was obtained using the same mobile phase. The concentration of free fatty acids in the *n*-hexane-extracted oil from rice bran

Table 2.13 Experimental data on column partition fractionation of rice bran oil (Reprinted from Ref. [54]. With kind permission of © Elsevier)

Sample	Eluent	W_{oil} (g)	Ory (%)	TG (%)	FFA (%)	FA (%)	Others (%)
Soxhlet n-hexane-extracted oil							
Feed F		20.2	2.1	53.9	40.0	93.9	4.0
F1	100:0	0.91	0	42.9	0	42.9	57.1
F2	200:1	6.61	0	61.5	30.5	92.0	8.0
F3	98:2	2.94	0	43.6	52.3	95.9	4.1
F4	95:5	2.19	0.6	30.8	64.3	95.1	4.3
F5	90:10	0.72	4.4	28.9	65.0	93.9	1.7
F6	90:10	0.92	37.0	22.5	32.5	55.0	8.0
F7	0:100	1.90	0.2	63.0	25.1	88.1	11.7
SC-CO_2-extracted oil							
Feed J		14.7	1.3	83.6	12.0	95.6	3.1
J1	100:0	8.99	0	96.9	0	96.9	3.1
J2	98:2	0.30	0	93.4	0	93.4	6.6
J3	95:5	1.63	0.3	71.2	23.2	94.4	5.3
J4	90:10	0.55	0.6	45.6	51.4	97.0	2.4
J5	90:10	0.84	18.9	48.1	23.6	71.7	9.4
J6	0:100	1.41	0.6	81.4	11.6	93.0	6.4

Eluent n-hexane + ethyl acetate, *Ory* percentage of oryzanols = $(W_{Ory}/W_{oil}) \times 100\%$, *TG* percentage of triglycerides = $(W_{TG}/W_{oil}) \times 100\%$, *FFA* percentage of free fatty acids = $(W_{FFA}/W_{oil}) \times 100\%$, *FA* percentage of fatty acids = $(W_{FA}/W_{oil}) \times 100\%$, *Others* percentage of waxes, glycolipids, and phospholipids = $(W_{oil} - W_{Ory} - W_{FA})/W_{oil} \times 100\%$, W_{oil} weight of the extracted, W_{Ory} weight of oryzanols, W_{TG} weight of triglycerides, W_{FFA} weight of free fatty acids, W_{FA} weight of fatty acids = $W_{TG} + W_{FFA}$

powder with 40% FFA was higher than that in the SC-CO_2-extracted oil from the powder with 10% FFA, so the purity of γ-oryzanols was lower. In these column partition fractionations, most triglycerides and free fatty acids had been removed by the preceding solvent elutions of large fractions of *n*-hexane. However, the remaining elutions retained a few free fatty acids in the purified γ-oryzanol fraction, as revealed by data # F6 and # J5 in Table 2.13.

2.7 Supercritical Carbon Dioxide (SC-CO_2) Extraction and Deacidification of Rice Bran Oil

2.7.1 Experimentally Designed Supercritical Carbon Dioxide (SC-CO_2) Extraction

Figure 2.20 displays a schematic flow diagram of SC-CO_2 extraction. 35-g powdered rice bran was packed inside a 250-mL stainless steel tubular extractor with an internal diameter of 2.5 cm and a height of 54 cm. A specified amount of glass wool

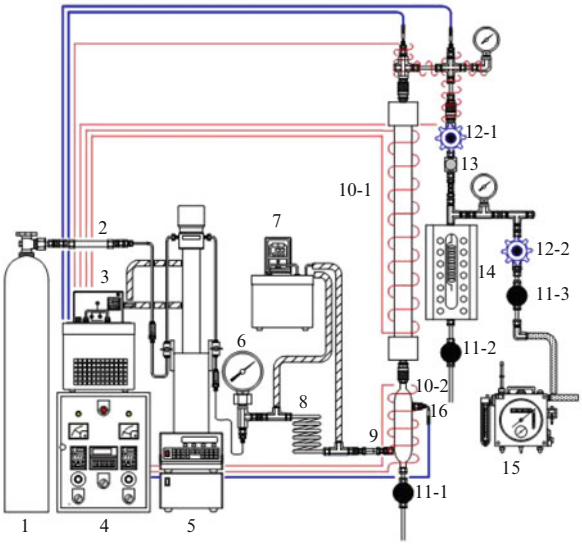

1. CO_2 cylinder
2. CO_2 cleanup column
3. Cold liquid circulator
4. Temperature controller
5. High pressure pump
6. Pressure gauge
7. Hot liquid circulator
8. Preheater
9. Check valve

10-1. Extraction vessel
10-2. Reboiler
11-1~11-3. Metering valve
12-1~12-2. Back pressure regulator
13. Needle valve
14. Separator
15. Wet gas meter
16. Thermocouple

Fig. 2.20 Schematic flow diagram of SC-CO_2 extraction of rice bran oil (Reprinted from Ref. [55]. With kind permission of Wiley-VCH Verlag GmbH & Co)

was packed into the two ends of the extractor to prevent the rice bran powder escaping from the extractor. Liquid CO_2 from a cylinder (1) into which was inserted a siphon tube passed through a cooling bath (3) at 277 K was compressed to the desired working pressure using a syringe pump (100DX, ISCO, USA) (5) and was heated to supercritical conditions using a double-pipe heat exchanger (8) and a reboiler (10–2). This carbon dioxide, maintained at a flow rate of 5 L/min (STP), flowed into the extractor (10–1), came into contact with the rice bran powder, and was used to extract the oil. A heating element equipped with a PID temperature

controller (4) was thermostatically maintained at a constant temperature; two back-pressure regulators (12–1, 12–2) located at the outlet were manually adjusted to maintain constant extraction pressure. Following the extraction, the oil-laden CO_2 was driven into a 130-mL separator (14) by a drop in pressure and expanded through a spiral-type nozzle at 50 bar and 303 K. The amount of low-pressure CO_2 was measured using a wet gas meter (W-NK-Da-1B, Shinagawa, Japan) (15) and thus returned to the ambient conditions. At the end of each experiment, the extracted solution was collected, and the solvent was evaporated using a vacuum rotary evaporator. The residue was weighed and stored in 273 K before use. The total yield, the extraction efficiency, and the concentration factor of γ-oryzanols, free fatty acids, and triglycerides in the extracts were then calculated.

Table 2.14 presents experimental data on the RSM-designed SC-CO_2 extractions of rice bran oil at temperatures from 313 to 333 K and pressures from 250 to 350 bar. The effects of these two factors on the extraction efficiencies and the concentration factors seem to be of the same order of magnitude. Figure 2.21a–c show that the total oil yield, extraction efficiency of γ-oryzanols (R_{ory}), and triglycerides (R_{TG}) reached to maxim value as 19.6%, 94.4%, and 94.5%, respectively, at 350 bar and 333 K (datum#9 in Table 2.14) and increased dramatically with pressure. However, the effect of temperature was not significant. Figure 2.21d shows that the extraction efficiency of free fatty acids is reduced as the pressure increased. The low concentration of free fatty acids at high-pressure extraction may be explained by the high yield of other components in the extracted oil. Figure 2.22 plots the concentration factors of γ-oryzanols and triglycerides (β_{ory} and β_{TG}) from where it is evident that concentration factors (β_{ory} and β_{TG}) are increased with the increasing pressure (Fig. 2.22a, b), but the concentration factor of free fatty acids (β_{FFA}) decreased as shown in Fig. 2.22c.

2.7.2 Pilot-Scale Supercritical Carbon Dioxide (SC-CO_2) Extraction

Figure 2.23 displays a schematic flow diagram of pilot-scale SC-CO_2 extraction of rice bran oil from powdered rice bran. A mass of rice bran powder varying from 0.6 to 1 kg was individually packed inside a 5-L stainless steel tubular extractor. Liquid CO_2 from a cylinder (1) was passed through a chiller (3) at 277 K and was compressed to the desired working pressure using a high-pressure pump (2) and heated to supercritical conditions using a preheater (6–1). This carbon dioxide flowed into the extractor (7), came into contact with the rice bran powder, and was used to extract the oil. A heating circulator (9–1) was maintained at a constant temperature; a metering valve (12–5) located at the outlet was manually adjusted to maintain constant extraction pressure. A drop in the pressure drove the oil-laden CO_2 into a 1-L separator (8) at 50 bar and 308 K following the extraction. The amount of low-pressure CO_2 was measured using a wet gas meter (10) and thus returned to the

Table 2.14 SC-CO_2 extractions of rice bran oil designed using response surface methodology (Reprinted from Ref. [55]. With kind permission of Wiley-VCH Verlag GmbH & Co)

RSM #	P (bar)	T (K)	W_{oil} (g)	TY (%)	W_{Ory} (mg/g_{oil})	W^*_{Ory} (mg/g_{RB})	R_{Ory} (%)	β_{Ory}	W_{FFA} (mg/g_{oil})	W^*_{FFA} (mg/g_{RB})	R_{FFA} (%)	β_{FFA}	W_{TG} (mg/g_{oil})	W^*_{TG} (mg/g_{RB})	R_{TG} (%)	β_{TG}	Others (mg/g_{oil})
1(A)	250	313	5.618	16.1	4.29	0.69	22.7	1.42	118	19.0	99.8	6.22	825	132	82.8	5.16	56
	250	313	5.582	15.9	4.49	0.72	23.6	1.48	118	18.8	99.1	6.21	826	132	82.3	5.16	56
2(F)	250	323	5.568	15.9	4.17	0.66	21.9	1.38	118	18.7	98.4	6.19	834	133	82.9	5.21	48
	250	323	5.626	16.1	4.27	0.69	22.7	1.41	117	18.9	99.3	6.18	834	134	83.8	5.21	48
3(A)	250	333	5.350	15.3	4.01	0.61	20.2	1.32	120	18.3	96.5	6.31	835	128	79.8	5.22	44
	250	333	5.378	15.4	4.17	0.64	21.1	1.38	120	18.4	96.8	6.30	835	128	80.2	5.22	44
4(F)	300	313	6.138	17.5	15.2	2.66	87.9	5.01	106	18.6	97.6	5.56	831	146	91.1	5.19	61
	300	313	6.162	17.6	15.3	2.70	89.0	5.06	105	18.5	97.5	5.54	830	146	91.4	5.19	62
5(C)	300	323	6.312	18.0	14.9	2.68	88.4	4.90	104	18.7	98.4	5.46	819	148	92.3	5.12	75
	300	323	6.358	18.2	15.0	2.72	89.7	4.94	103	18.8	98.8	5.44	819	149	93.0	5.12	75
6(F)	300	333	6.557	18.7	14.4	2.70	89.0	4.75	101	19.0	99.7	5.32	811	152	95.0	5.07	85
	300	333	6.603	18.9	14.6	2.75	90.8	4.81	101	19.0	100	5.30	812	153	95.7	5.07	85
7(A)	350	313	6.437	18.4	13.6	2.50	82.5	4.49	97.0	17.8	93.8	5.10	777	143	89.3	4.85	124
	350	313	6.373	18.2	13.7	2.50	82.4	4.52	96.5	17.6	92.4	5.07	776	141	88.3	4.85	125
8(F)	350	323	6.602	18.9	14.0	2.65	87.4	4.63	99.7	18.8	98.9	5.24	766	145	90.4	4.79	131
	350	323	6.594	18.8	14.2	2.68	88.5	4.70	99.4	18.7	98.6	5.23	767	144	90.3	4.79	131
9(A)	350	333	6.844	19.6	14.7	2.87	94.7	4.84	97.0	19.0	99.8	5.10	771	151	94.3	4.82	129
	350	333	6.876	19.6	14.5	2.85	94.1	4.79	96.8	19.0	100	5.09	771	151	94.6	4.82	130

W_{oil} weight of the extracted, *TY* total oil yield = $(W_{oil}/W_{RB}) \times 100\%$, W_{RB} weight of rice bran, W_{Ory} weight of oryzanols, W^*_{Ory} yield of oryzanols, W_{FFA} weight of free fatty acids, W^*_{FFA} yield of free fatty acids, W_{TG} weight of triglycerides, W^*_{TG} yield of triglycerides, R_{Ory} oryzanol extraction efficiency = $(W^*_{Ory}/W^*_{Ory,Soxhlet}) \times 100\%$, R_{FFA} free fatty acids extraction efficiency = $(W^*_{FFA}/W^*_{FFA,Soxhlet}) \times 100\%$, R_{TG} triglycerides extraction efficiency = $(W^*_{TG}/W^*_{TG,Soxhlet}) \times 100\%$, β_{Ory} concentration factor of oryzanols = R_{Ory}/TY, β_{FFA} concentration factor of free fatty acids = R_{FFA}/TY, β_{TG} concentration factor of triglycerides = R_{TG}/TY, *Others* weight of waxes, glycolipids, and phospholipids.

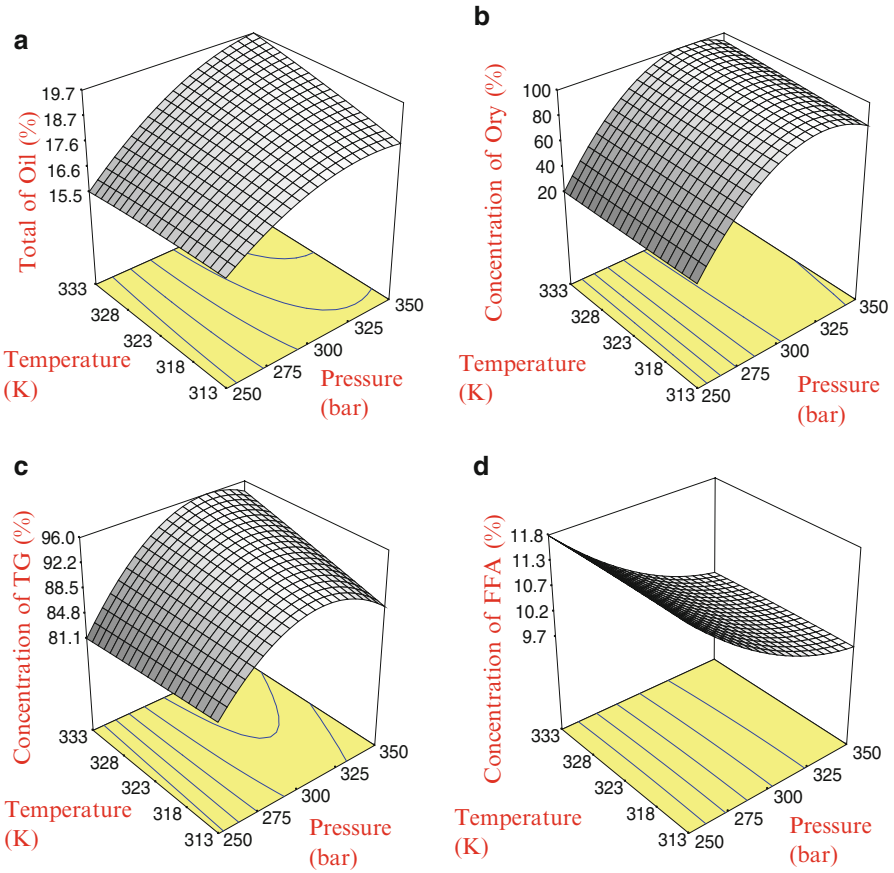

Fig. 2.21 Effects of pressure and temperature on SC-CO_2 extractions of rice bran oil (**a**) total oil yield, (**b**) extraction efficiency of oryzanols, (**c**) extraction efficiency of triglycerides, and (**d**) extraction efficiency of free fatty acids (*F*-testing: $R_{(a)}{}^2=0.9808$, S.D.$_{(a)}=0.34$; $R_{(b)}{}^2=0.9996$, S.D.$_{(b)}=1.12$; $R_{(c)}{}^2=0.9731$, S.D.$_{(c)}=1.48$; $R_{(d)}{}^2=0.9163$, S.D.$_{(d)}=0.98$) (Reprinted from Ref. [55]. With kind permission of Wiley-VCH Verlag GmbH & Co)

ambient conditions. At the end of each experiment, the extracted oil was collected through a metering valve (13–3).

Table 2.15 presents experimental data on the SC-CO_2 extraction of rice bran oil from 0.6 to 1.03 kg of powder. The total oil yield exceeded 15% upon extraction at 300 bar and 313 K using a constant solvent-to-feed ratio of 20. The concentrations of γ-oryzanols, free fatty acids, and triglycerides remain unchanged. The oil extracted in Exp. #4 was used for following SC-CO_2 deacidifications.

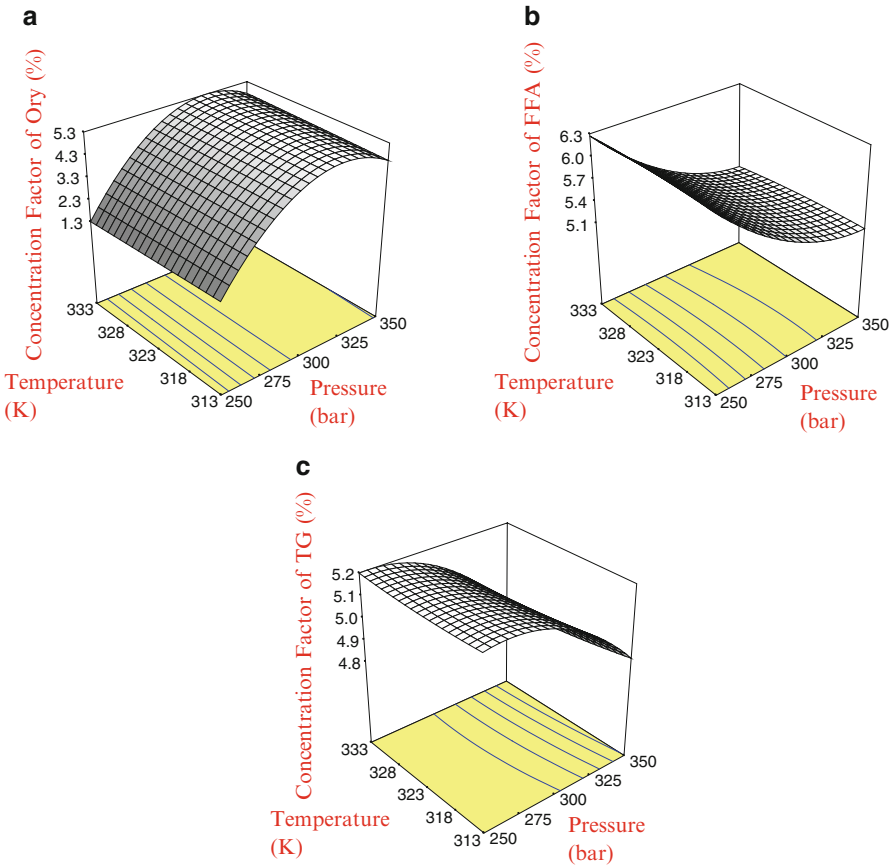

Fig. 2.22 Effects of concentration factors on SC-CO_2 extractions of rice bran oil (**a**) concentration factor of oryzanols, (**b**) concentration factor of free fatty acids, and (**c**) concentration factor of triglycerides (*F*-testing: $R_{(a)}^2=0.9981$, $S.D._{(a)}=0.12$; $R_{(b)}^2=0.9751$, $S.D._{(b)}=0.13$; $R_{(c)}^2=0.9703$, $S.D._{(c)}=0.05$) (Reprinted from Ref. [55]. With kind permission of Wiley-VCH Verlag GmbH & Co)

2.7.3 Experimentally Designed Supercritical Carbon Dioxide (SC-CO_2) Deacidification

Figure 2.24 presents a schematic flow diagram of the SC-CO_2 deacidification of rice bran oil. Thirteen grams of the SC-CO_2 oil obtained by extraction at 300 bar and 313 K and the θ type of packed materials were vertically loaded into the bottom of the deacidified column (8) in succession. Liquid CO_2 from a cylinder (1) was passed through a cooling bath (3) at 277 K, preheated by a hot plate (6) through an oil bath (7), and was compressed using a syringe pump (4). This carbon dioxide, maintained at a flow rate of 10 g/min, flowed into the deacidification column whose pressure

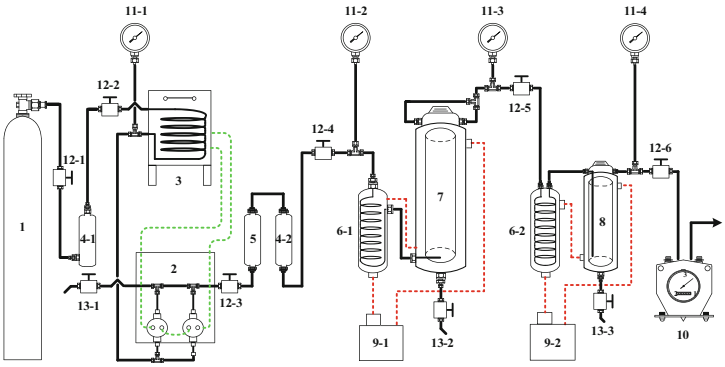

1. CO_2 cylinder 2. Pump 3. Chiller 4-1~2. CO_2 cleaner
5. Mixer 6-1~2. Pre-heater 7. Extractor 8. Separator
9-1~2. Circulator 10. Wet gas meter 11-1~4. Gauge 12-1~6. Metering valve
13-1~3. Vent valve

Fig. 2.23 Schematic flow diagram of pilot-scale SC-CO_2 extraction of rice bran oil (Reprinted from Ref. [57]. With kind permission of © Elsevier)

was maintained by a back-pressure regulator (9–1). A heating element, equipped with a PID temperature controller (16), was thermostatically maintained at a constant temperature. Following SC-CO_2 deacidification, a drop in pressure drove the acid-laden CO_2 into a separator (12), and the gas was then expanded through a spiral-type nozzle at 50 bar. The amount of low-pressure CO_2 was measured using a wet gas meter (14) before the gas was returned to the ambient conditions. Following this process, the deacidified oil was collected in a flask (13) by opening the metering valve (11–3) after depressurization and was then ready for analysis and calculation. In addition, the free fatty acid–enriched extracted oil was also gathered by opening the metering valve (11–2).

Table 2.16 displays experimental data on the RSM-designed SC-CO_2 deacidification. In these experiments, the amount of remaining triglycerides and the removal efficiencies of free fatty acids are two major variables of interest. The free fatty acid content, 0.13%, in the deacidified oil was obtained at 250 bar, 353 K, and 2,700 g of CO_2 extraction. This experiment demonstrated that the retention efficiency of oil and the removal efficiency of free fatty acids were 82.2 and 97.8%, respectively. The product of these two responses reached 80.4, which is the highest value among all 15 RSM experiments. Further examination of these data revealed that the concentration factors of γ-oryzanols and triglycerides increased, but the concentration factors of free fatty acids decreased to zero (datum # 9), implying that active compounds in the deacidified oil were concentrated and the free fatty acid content in the

Table 2.15 Experimental data on SC-CO_2 extractions of rice bran oil from 0.6- to 1.03-kg powder at 300 bar and 313 K (Reprinted from Ref. [57]. With kind permission of © Elsevier)

Exp #	W_{RB} (kg)	W_{CO_2} (kg)	W_{oil} (g)	TY (%)	W_{Ory} (mg/g_{oil})	R_{Ory} (%)	β_{Ory}	W_{FFA} (mg/g_{oil})	R_{FFA} (%)	β_{FFA}	W_{TG} (mg/g_{oil})	R_{TG} (%)	β_{TG}	W_{others} (mg/g_{oil})
3	0.60	12.1	90.7	15.1	6.0	52.0	3.44	35.4	82.3	5.45	864	89.0	5.89	94.6
4	1.03 ± 0.01	20.5 ± 0.2	157 ± 5	15.7 ± 0.5	6.3 ± 0.1	56.3 ± 2.4	3.58 ± 0.04	37.5 ± 0.8	90.7 ± 4.5	5.76 ± 0.13	866 ± 7	93.4 ± 3.7	5.93 ± 0.05	89.9 ± 7.2

W_{RB} weight of rice bran, W_{CO_2} weight of carbon dioxide, W_{oil} weight of extracted oil, TY total oil yield = $(W_{oil}/W_{RB}) \times 100\%$, W_{Ory} concentration of oryzanols, W_{FFA} concentration of free fatty acids, W_{TG} concentration of triglycerides, W_{others} concentration of waxes, glycolipids, and phospholipids, R_{Ory} oryzanol extraction efficiency = $[(W_{Ory} \times TY)/(W_{Ory,Soxhlet} \times TY_{Soxhlet})] \times 100\%$, R_{FFA} free fatty acids extraction efficiency = $[(W_{FFA} \times TY)/(W_{FFA,Soxhlet} \times TY_{Soxhlet})] \times 100\%$, R_{TG} triglycerides extraction efficiency = $[(W_{TG} \times TY)/(W_{TG,Soxhlet} \times TY_{Soxhlet})] \times 100\%$, β_{Ory} oryzanol concentration factor = R_{Ory}/TY, β_{FFA} free fatty acids concentration factor = R_{FFA}/TY, β_{TG} triglycerides concentration factor = R_{TG}/TY

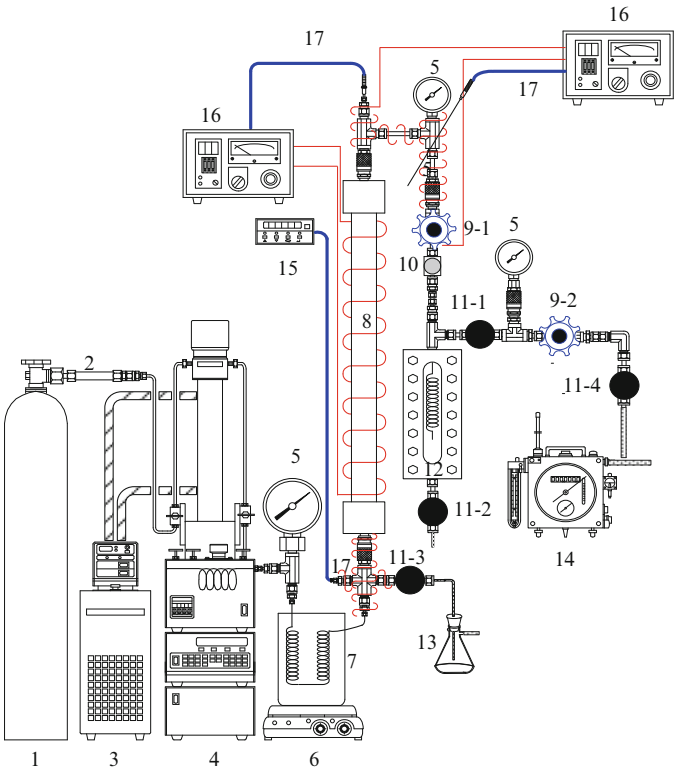

1. CO_2 cylinder
2. CO_2 cleanup column
3. Constant temperature circulator
4. High-pressure pump
5. Pressure gauge
6. Hot plate
7. Oil bath
8. Extraction vessel
9-1~2. Back-pressure regulator
10. Micro-metering valve
11-1~4. Metering valve
12. Separator
13. Collection flask
14. Wet gas meter
15. Temperature display
16. Temperature controller
17. Thermocouple

Fig. 2.24 Schematic flow diagram of SC-CO_2 deacidification of rice bran oil (Reprinted from Ref. [57]. With kind permission of © Elsevier)

Table 2.16 Experimentally designed SC-CO_2 deacidifications of rice bran oil obtained by SC-CO_2 extraction at 300 bar and 313 K (Reprinted from Ref. [57]. With kind permission of © Elsevier)

RSM #	W_{CO_2} (g)	P (bar)	T (K)	W_{oil} (g)	R_{oil} (%)	Ory (%)	FFA (%)	TG (%)	R_{Ory} (%)	R_{FFA} (%)	R_{TG} (%)	β_{Ory}	β_{FFA}	β_{TG}	RR_{FFA} (%)	$R_{oil} \times RR_{FFA}$
Oil contained 0.63% Ory, 3.75% FFA, 86.6% TG before deacidification																
1(F)	900	200	343	11.4	87.6	0.64	1.96	95.2	89.7	45.9	96.4	1.02	0.52	1.10	63.8	55.9
2(F)	2,700	200	343	10.9	83.9	0.64	0.35	95.8	85.7	7.8	92.7	1.02	0.09	1.11	93.7	78.6
3(A)	1,800	200	353	11.2	85.8	0.63	0.80	94.4	86.7	18.4	93.9	1.00	0.21	1.09	85.3	73.2
4(F)	900	200	363	11.5	88.1	0.59	2.50	93.9	83.5	59.1	96.0	0.94	0.67	1.09	55.4	48.8
5(F)	2,700	200	363	11.2	85.8	0.58	0.89	94.2	79.7	20.4	93.6	0.92	0.24	1.09	83.9	72.0
6(A)	1,800	250	343	10.2	78.1	0.67	0.30	95.2	84.0	6.3	86.2	1.06	0.08	1.10	95.5	74.6
7(A)	900	250	353	11.3	86.9	0.62	1.62	95.8	86.3	37.7	96.4	0.98	0.43	1.11	70.5	61.3
8(C)	1,800	250	353	11.1	84.9	0.62	0.38	93.5	84.5	8.6	92.1	0.98	0.10	1.08	93.4	79.3
9(A)	2,700	250	353	10.7	82.2	0.65	0.13	94.9	85.5	2.9	90.2	1.03	0.03	1.10	97.8	80.4
10(A)	1,800	250	363	10.8	83.1	0.61	0.42	94.6	81.0	9.3	90.8	0.97	0.11	1.09	92.7	77.0
11(F)	900	300	343	9.2	70.8	0.66	0.82	93.3	74.6	15.5	76.2	1.05	0.22	1.08	90.2	63.9
12(F)	2,700	300	343	6.5	49.7	0.88	0.01	94.9	70.1	0.1	54.6	1.40	0.003	1.10	99.9	49.7
13(A)	1,800	300	353	9.2	70.9	0.75	0.21	93.9	84.6	4.0	76.6	1.19	0.06	1.09	97.2	68.9
14(F)	900	300	363	10.5	80.9	0.66	0.73	94.6	85.1	15.7	88.2	1.05	0.20	1.09	88.5	71.6
15(F)	2,700	300	363	9.1	70.1	0.81	0.05	94.2	90.6	0.9	76.1	1.29	0.01	1.09	99.3	69.6

W_{CO_2} weight of carbon dioxide, W_{oil} weight of extracted oil, R_{oil} oil retention $= W_{oil}/W_{oil,feed} \times 100\%$, *Ory* oryzanol concentration $= (W_{Ory}/W_{oil}) \times 100\%$, *FFA* free fatty acids concentration $= (W_{FFA}/W_{oil}) \times 100\%$, *TG* triglycerides concentration $= (W_{TG}/W_{oil}) \times 100\%$, R_{Ory} oryzanol recovery $= (W_{Ory}/W_{Ory,feed}) \times 100\%$, R_{FFA} free fatty acids recovery $= (W_{FFA}/W_{FFA,feed}) \times 100\%$, R_{TG} triglycerides recovery $= (W_{TG}/W_{TG,feed}) \times 100\%$, β_{Ory} oryzanol concentration factor $= Ory/Ory_{feed}$, β_{FFA} free fatty acids concentration factor $= FFA/FFA_{feed}$, β_{TG} triglycerides concentration factor $= TG/TG_{feed}$, RR_{FFA} free fatty acids removal $= (W_{FFA,feed} - W_{FFA})/W_{FFA,feed} \times 100\%$

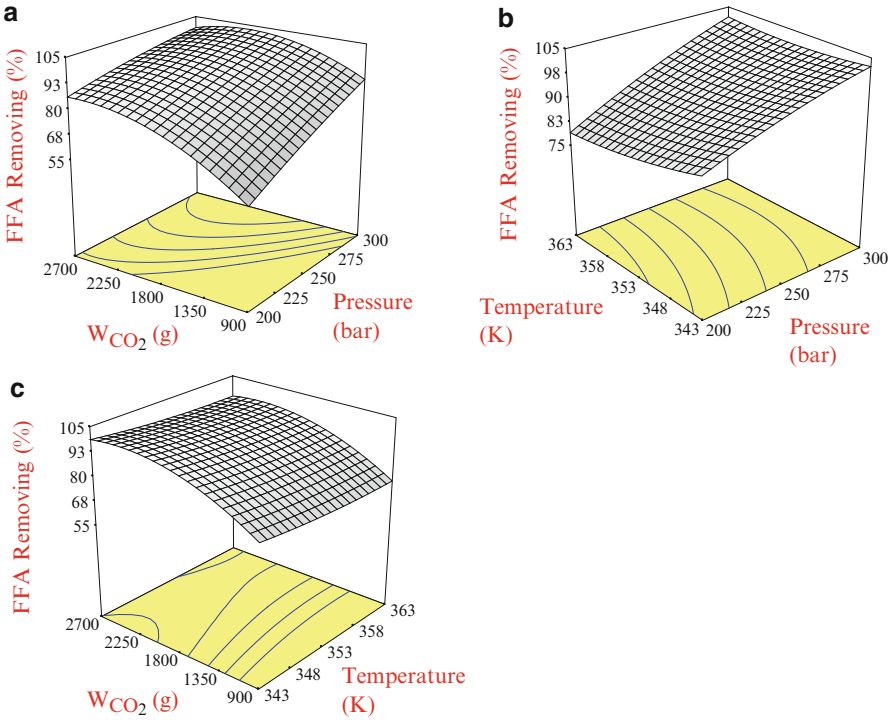

Fig. 2.25 Three-dimensional responded experimental data on removal efficiency of free fatty acids using SC-CO_2 deacidification (**a**) temperature: 363 K, (**b**) W_{CO_2} : 1,800 g, and (**c**) pressure: 250 bar, datum #10 in Table 2.16 (*F*-testing: R^2=0.9788, S.D. = 3.30) (Reprinted from Ref. [57]. With kind permission of © Elsevier)

oil was substantially decreased. Figure 2.25 shows that effects of pressure and the amount of consumed CO_2 are important to the removal efficiency of free fatty acids. Figure 2.26 reveals that the effect of pressure is more significant than that of CO_2 consumption. The effect of temperature is insignificant because the operative region is close to the crossover pressure and the solubility of triglycerides in supercritical carbon dioxide increases as the fluid density increases with pressure. Figure 2.27 plots the effects of the pressure and CO_2 consumption associated with a multiple response of the retention of oil and the removal efficiency of free fatty acids. The value of this response is optimal at 260 bar, 363 K, and with 2,160 g of CO_2 consumed.

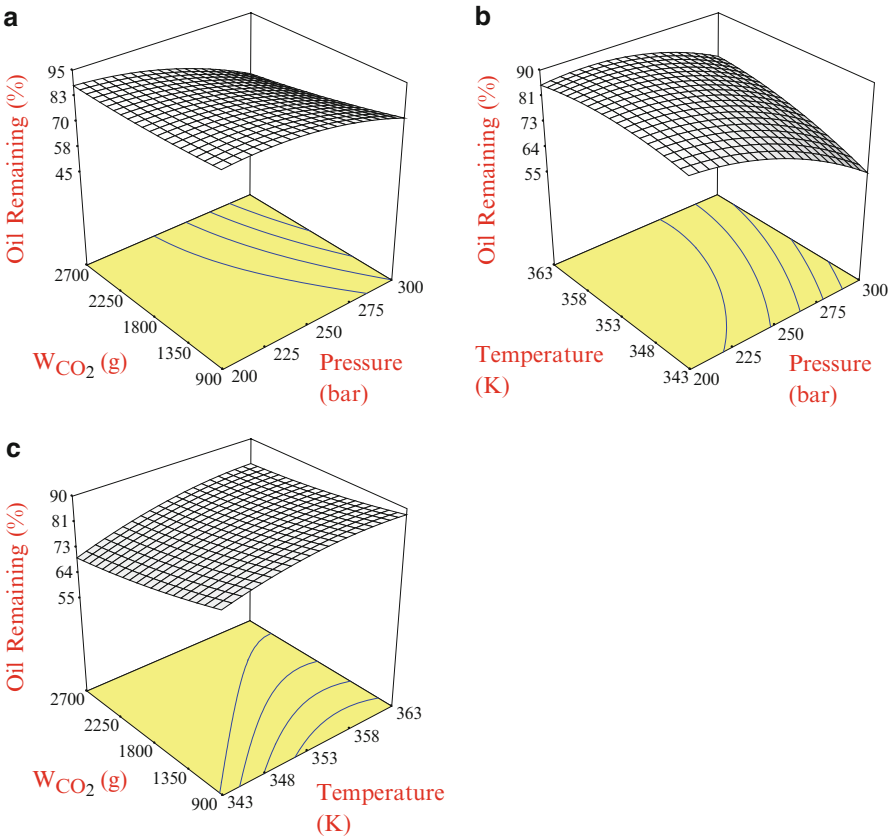

Fig. 2.26 Three-dimensional responded experimental data on retention efficiency of oil using SC-CO_2 deacidification (**a**) temperature: 353 K, (**b**) W_{CO_2} : 1,800 g, (**c**) pressure: 250 bar, datum # 8 in Table 2.16 (*F*-testing: $R^2 = 0.9798$, S.D. = 2.44) (Reprinted from Ref. [57]. With kind permission of © Elsevier)

2.8 Conclusions

For SC-CO_2 extraction of the DHCA from Brazilian propolis, the addition of ethyl acetate significantly affects the recovery and purity of DHCA. The purity of DHCA extracted by SC-CO_2 extraction is superior to that obtained by Soxhlet ethyl acetate extraction. Furthermore, SC-CO_2 extraction has been recognized as an environmentally benign method to produce natural healthy materials. The purest DHCA could be obtained by further purification of the SC-CO_2 extracts using a normal-phase column adsorption chromatography without solvent pretreatment. Therefore, the SC-CO_2 is a green solvent to avoid several organic solvent partitions in obtaining the purest DHCA in the product. For SC-CO_2 antisolvent precipitation of Brazilian

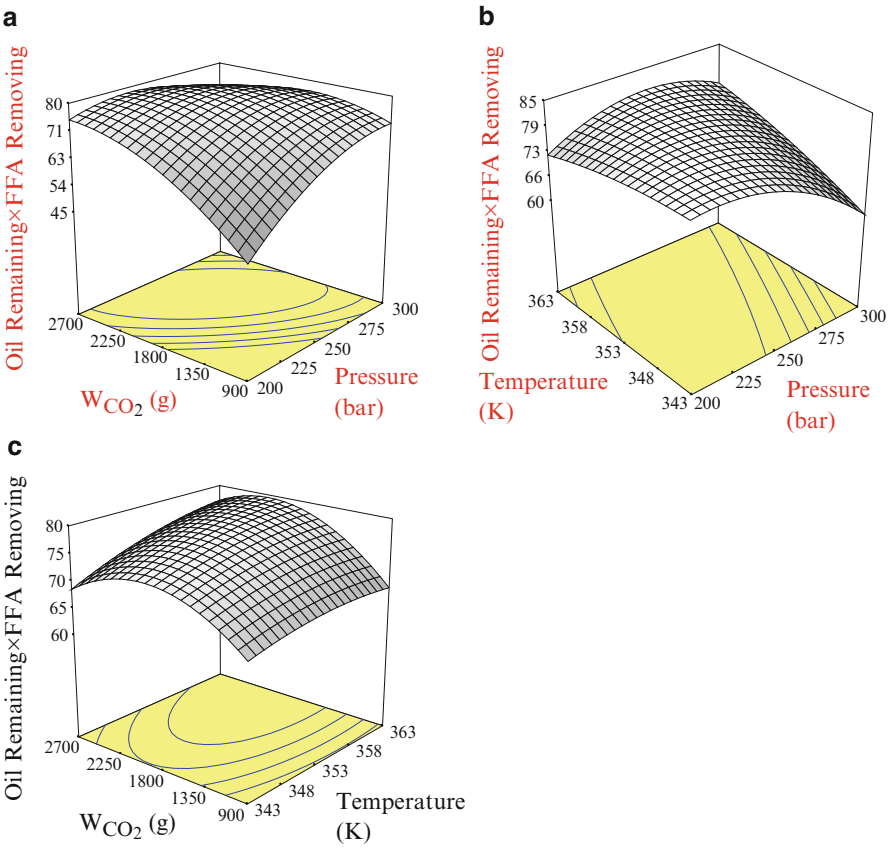

Fig. 2.27 Response surface methodology optimization of the multiple value of oil retention and free fatty acids removal efficiency responses (**a**) temperature: 363 K, (**b**) W_{CO_2} : 2,160 g, (**c**) pressure: 260 bar (F-testing: $R^2 = 0.9451$, S.D. = 4.04) (Reprinted from Ref. [57]. With kind permission of © Elsevier)

propolis, solution was successfully performed herein to generate submicron particles that contain a large amount of DHCA. This supergreen SC-CO_2 antisolvent process demonstrated that the micronization of bioactive compounds from natural materials is feasible, with great potential for the food and pharmaceutical industries. Furthermore, the bioassay experiments established that the SC-CO_2 extracts and precipitates effectively inhibit the growth of human leukemia, colon, and breast cancer cells. The purity of DHCA was found to play an important role in anticancer activities and anti-LDL oxidations.

The purest 24-methylenecycloartanyl ferulate and campesteryl ferulate were successfully isolated from a mixture of γ-oryzanols using preparative C18 high-pressure liquid chromatography. The light-yellowish color, odor, and simple

postremoving of paraffins from the SC-CO_2-extracted oil are superior to that obtained by Soxhlet *n*-hexane extraction. In addition, the three-factor center composite-designed SC-CO_2 deacidifications of rice bran oil demonstrate that the consumption of carbon dioxide and operative pressure significantly influence the removal efficiency of free fatty acids and the retention efficiency of triglycerides. SC-CO_2 extraction followed by deacidification has also been recognized as an environmentally friendly method to produce edible oil. In summary, SC-CO_2 extraction, SC-CO_2 antisolvent precipitation, and SC-CO_2 deacidification are alternative methods applied for producing bioactive products from natural materials.

Acknowledgments The authors gratefully acknowledge funding from the National Science Council of the Republic of China, Taiwan (contract no. NSC96-2628-E005-085-MY2; NSC98-2221-E005-053-MY3; NSC99-2622-B005-CC2), and Taichung Veterans General Hospital and National Chung Hsing University, Taiwan (contract no. TCVGH-NCHU 977603) as well as partial support from the Ministry of Education of the Republic of China, Taiwan, under the ATU plan.

References

1. Ghisalberti EL, Jefferies PR, Lanteri R, Matisons J (1978) Constituents of propolis. Experientia 15:157–158
2. Marcucci MC (1995) Propolis: chemical composition, biological properties and therapeutic activity. Apidologie 26:83–99
3. Kujumgiev A, Tsvetkova I, Serkedjieva Y, Bankova V, Christov R, Popov S (1999) Antibacterial, antifungal and antiviral activity of propolis of different geographic origin. J Ethnopharmacol 64:235–240
4. Kumazawa S, Hamasaka T, Nakayama T (2004) Antioxidant activity of propolis of various geographic origins. Food Chem 84:329–339
5. Oršolić N, Knezević AH, Šver L, Terzić S, Bašić I (2004) Immunomodulatory and antimetastatic action of propolis and related polyphenolic compounds. J Ethnopharmacol 94:307–315
6. Banskota AH, Tezuka Y, Adnyana IK, Midorikawa K, Matsushige K, Message D, Huertas AAG, Kadota S (2000) Cytotoxic, hepatoprotective and free radical scavenging effects of propolis from Brazil, Peru, the Netherlands and China. J Ethnopharmacol 72:239–246
7. Russo A, Cardile V, Sanchez F, Troncoso N, Vanella A, Garbarino JA (2004) Chilean propolis: antioxidant activity and antiproliferative action in human tumor cell lines. Life Sci 76:545–558
8. Park YK, Paredes-Guzman JF, Aguiar CL, Alencar SM, Fujiwara FY (2004) Chemical constituents in *Baccharis dracunculifolia* as the main botanical origin of southeastern Brazilian propolis. J Agric Food Chem 52:1100–1103
9. Silva JFM, Souza MC, Matta SR, Andrade MR, Vidal FVN (2006) Correlation analysis between phenolic levels of Brazilian propolis extracts and their antimicrobial and antioxidant activities. Food Chem 99:431–435
10. Matsuno T, Jung SK, Matsumoto Y, Saito M, Morikawa J (1997) Preferential cytotoxicity to tumor cells of 3,5-diprenyl-4-hydroxycinnamic acid (artepillin C) isolated from propolis. Anticancer Res 17:3565–3568
11. Kimoto T, Arai S, Kohguchi M, Aga M, Nomura Y, Micallef MJ, Kurimoto M, Mito K (1998) Apoptosis and suppression of tumor growth by artepillin C extracted from Brazilian propolis. Cancer Detect Prev 22:506–515

12. Kimoto T, Aga M, Hino K, Miyata SK, Yamamoto Y, Micallef MJ, Hanaya T, Arai S, Ikeda M, Kurimoto M (2001) Apoptosis of human leukemia cells induced by artepillin C, an active ingredient of Brazilian propolis. Anticancer Res 21:221–228
13. Akao Y, Maruyama H, Matsumoto K, Ohguchi K, Nishizawa K, Sakamoto T, Araki Y, Mishima S, Nozawa Y (2003) Cell growth inhibitory effect of cinnamic acid derivatives from propolis on human tumor cell lines. Biol Pharm Bull 26:1057–1059
14. Chen CR, Lee YN, Lee MR, Chang CJ (2009) Supercritical fluids extraction of cinnamic acid derivatives from Brazilian propolis and the effect on growth inhibition of colon cancer cells. J Taiwan Inst Chem Eng 40:130–135
15. Shimizu K, Das SK, Hashimoto T, Sowa Y, Yoshida T, Sakai T, Matsuura Y, Kanazawa K (2005) Artepillin C in Brazilian propolis induces G0/G1 arrest via stimulation of cip1/p21 expression in human colon cancer cells. Mol Carcinog 44:293–299
16. Messerli SM, Ahn M, Kunimasa K, Yanagihara M, Tatefuji T, Hashimoto K, Mautner V, Uto Y, Hori H, Kumazawa S, Kaji K, Ohta T, Maruta H (2009) Artepillin C (ARC) in Brazilian green propolis selectively blocks oncogenic PAK1 signaling and suppresses the growth of NF tumors in mice. Phytother Res 23:423–427
17. Lee YN, Chen CR, Yang HL, Lin CC, Chang CJ (2007) Isolation and purification of 3,5-diprenyl-4-hydroxycinnamic acid (artepillin C) in Brazilian propolis by supercritical fluid extractions. Sep Purif Technol 54:130–138
18. Nakanishi I, Uto Y, Ohkubo K, Miyazaki K, Yakumaru H, Urano S, Okuda H, Ueda JI, Ozawa T, Fukuhara K, Fukuzumi S, Nagasawa H, Hori H, Ikota N (2003) Efficient radical scavenging ability of artepillin C, a major component of Brazilian propolis, and the mechanism. Org Biomol Chem 1:1452–1454
19. Shimizu K, Ashida H, Matsuura Y, Kanazawa K (2004) Antioxidative bioavailability of artepillin C in Brazilian propolis. Arch Biochem Biophys 424:181–188
20. Aga H, Shibuya T, Sugimoto T, Kurimoto M, Nakajima S (1994) Isolation and identification of antimicrobial compounds in Brazilian propolis. Biosci Biotechnol Biochem 58:945–946
21. Bohlmann F, Jakupovic J (1979) Neue sesquiterpene, triterpene, flavanone und andere aromatische verbindungen aus flourensia heterolepis. Phytochemistry 18:1189–1194
22. Stahl E, Quirin KW, Gerard D (1988) Dense gases for extraction and refining. Springer, Berlin
23. You GS, Lin SC, Chen CR, Tsai WC, Chang CJ, Huang WW (2002) Supercritical carbon dioxide extraction enhances flavonoids in water-soluble propolis. J Chin Inst Chem Eng 33:233–241
24. Wang BJ, Lien YH, Yu ZR (2004) Supercritical fluid extractive fractionation-study of the antioxidant activities of propolis. Food Chem 86:237–243
25. Catchpole OJ, Grey JB, Mitchell KA, Lan JS (2004) Supercritical antisolvent fractionation of propolis tincture. J Supercrit Fluids 29:97–106
26. Wu HT, Lee MJ, Lin HM (2005) Nano-particles formation for pigment red 177 via a continuous supercritical anti-solvent process. J Supercrit Fluids 33:173–182
27. Fages J, Lochard H, Letourneau JJ, Sauceau M, Rodier E (2004) Particle generation for pharmaceutical applications using supercritical fluid technology. Powder Technol 141:219–226
28. Weidner E (2009) High pressure micronization for food applications. J Supercrit Fluids 47:556–565
29. Cocero MJ, Ferrero S (2002) Crystallization of β-carotene by a GAS process in batch effect of operating conditions. J Supercrit Fluids 22:237–245
30. Chen KX, Zhang XY, Pan J, Zhang WC, Yin WH (2005) Gas antisolvent precipitation of *Ginkgo ginkgolides* with supercritical CO_2. Powder Technol 152:127–132
31. Miguel F, Martín A, Gamse T, Cocero MJ (2006) Supercritical anti solvent precipitation of lycopene effect of the operating parameters. J Supercrit Fluids 36:225–235
32. Hong HL, Suo QL, Han LM, Li CP (2009) Study on precipitation of astaxanthin in supercritical fluid. Powder Technol 191:294–298
33. Mattea F, Martin A, Cocero MJ (2009) Carotenoid processing with supercritical fluids. J Food Eng 93:255–265

34. Chen CR, Shen CT, Wu JJ, Yang HL, Hsu SL, Chang CJ (2009) Precipitation of sub-micron particles of 3,5-diprenyl-4-hydroxycinnamic acid in Brazilian propolis from supercritical carbon dioxide anti-solvent solutions. J Supercrit Fluids 50:176–182
35. Wu JJ, Shen CT, Jong TT, Young CC, Yang HL, Hsu SL, Chang CJ, Shieh CJ (2009) Supercritical carbon dioxide anti-solvent process for purification of micronized propolis particulates and associated anti-cancer activity. Sep Purif Technol 70:190–198
36. Chang CJ, Randolph AD (1989) Precipitation of microsize organic particles from supercritical fluids. AIChE J 35:1876–1882
37. Rantakylä M, Jäntti M, Aaltonen O, Hurme M (2002) The effect of initial drop size on particle size in the supercritical antisolvent precipitation (SAS) technique. J Supercrit Fluids 24:251–263
38. Chang CJ, Randolph AD, Craft NE (1991) Separation of β-carotene mixtures precipitated from liquid solvents with high pressure CO_2. Biotechnol Prog 7:275–278
39. Juliano BO, Hicks PA (1996) Rice functional properties and rice food products. Food Rev Int 12:71–103
40. Hu W, Wells JH, Shin TS, Godber JS (1996) Comparison of isopropanol and hexane for extraction of vitamin E and oryzanols from stabilized rice bran. J Am Oil Chem Soc 73:1653–1656
41. Xu Z, Godber JS (1999) Purification and identification of components of γ-oryzanols in rice bran oil. J Agric Food Chem 47:2724–2728
42. Duve JK, White PJ (1991) Extraction and identification of antioxidants in oats. J Am Oil Chem Soc 68:365–370
43. Seetharamaiah GS, Chandrasekhara N (1989) Studies on hypocholesterolemic activity of rice bran oil. Atherosclerosis 78:219–223
44. Yasukawa K, Akihisa T, Kimura Y, Tamura T, Takido M (1998) Inhibitory effect of cycloartenol ferulate, a component of rice bran, on tumor promotion in two-stage carcinogenesis in mouse skin. Biol Pharm Bull 21:1072–1076
45. Nam SH, Choi SP, Kang MY, Kozukue N, Friedman M (2005) Antioxidative, antimutagenic, and anticarcinogenic activities of rice bran extracts in chemical and cell assays. J Agric Food Chem 53:816–822
46. Akihisa T, Yasukawa K, Yamaura M, Ukiya M, Kimura Y, Shimizu N, Arai K (2000) Triterpene alcohol and sterol ferulates from rice bran and their anti-inflammatory effects. J Agric Food Chem 48:2313–2319
47. Luo HF, Li Q, Yu S, Badger TM, Fang N (2005) Cytotoxic hydroxylated triterpene alcohol ferulates from rice bran. J Nat Prod 68:94–97
48. Fang N, Yu S, Badger TM (2003) Characterization of triterpene alcohol and sterol ferulates in rice bran using LC-MS/MS. J Agric Food Chem 51:3260–3267
49. Stöggl W, Huck C, Wongyai S, Scherz H, Bonn G (2005) Simultaneous determination of carotenoids, tocopherols, and γ-oryzanols in crude rice bran oil by liquid chromatography coupled to diode array and mass spectrometric detection employing silica C30 stationary phases. J Sep Sci 28:1712–1718
50. Aguilar-Garcia C, Gavino G, Baragaño-Mosqueda M, Hevia P, Gavino VC (2007) Correlation of tocopherol, tocotrienol, γ-oryzanols and total polyphenol content in rice bran with different antioxidant capacity assays. Food Chem 102:1228–1232
51. Krishna AGG, Hemakumar KH, Khatoon S (2006) Study on the composition of rice bran oil and its higher free fatty acids value. J Am Oil Chem Soc 83:117–120
52. Zullaikah S, Lai CC, Vali SR, Ju YH (2005) A two-step acid-catalyzed process for the production of biodiesel from rice bran oil. Bioresour Technol 96:1889–1896
53. Shen Z, Palmer MV, Ting SST, Fairclough RJ (1996) Pilot scale extraction of rice bran oil with dense carbon dioxide. J Agric Food Chem 44:3033–3039
54. Chen CR, Wang LY, Wang CH, Ho WJ, Chang CJ (2008) Supercritical carbon dioxide extraction of rice bran oil and column partition fractionation of γ-oryzanols. Sep Purif Technol 61:358–365

55. Wang CH, Chen CR, Wu JJ, Wang LY, Chang CJ, Ho WJ (2008) Designing supercritical carbon dioxide extraction of rice bran oil that contain oryzanols using response surface methodology. J Sep Sci 31:1399–1407
56. Bhosle BM, Subramanian R (2005) New approaches in deacidification of edible oils–a review. J Food Eng 69:481–494
57. Chen CR, Wang CH, Wang LY, Hong ZH, Chen SH, Ho WJ, Chang CJ (2008) Supercritical carbon dioxide extraction and deacidification of rice bran oil. J Supercrit Fluids 45:322–331
58. Kim HJ, Lee SB, Park KA, Hong IK (1999) Characterization of extraction and separation of rice bran oil rich in EFA using SFE process. Sep Purif Technol 15:1–8
59. Chang CJ, Chen CC (1999) High-pressure densities and P-T–x-y diagrams for carbon dioxide + linalool and carbon dioxide + limonene. Fluid Phase Equilib 163:119–126
60. Chang CJ, Lee MS, Li BC, Chen PY (2005) Vapor–liquid equilibria of CO_2 with four unsaturated fatty acid esters at elevated pressure. Fluid Phase Equilib 233:56–65
61. Shen Z, Palmer MV, Ting SST, Fairclough RJ (1997) Pilot scale extraction and fractionation of rice bran oil using supercritical carbon dioxide. J Agric Food Chem 45:4540–4544
62. Dunford NT, King JW (2000) Phytosterol enrichment of rice bran oil by a supercritical carbon dioxide fractionation technique. J Food Sci 65:1395–1399
63. Dunford NT, King JW (2001) Thermal gradient deacidification of crude rice bran oil utilizing supercritical carbon dioxide. J Am Oil Chem Soc 78:121–125
64. Dunford NT, Teel JA, King JW (2003) A continuous countercurrent supercritical fluid deacidification process for phytosterol ester fortification in rice bran oil. Food Res Int 36:175–181
65. Danielski L, Zetzl C, Hense H, Brunner G (2005) A process line for the production of raffinated rice oil from rice bran. J Supercrit Fluids 34:133–141
66. Chen CR, Lee YN, Chang CJ, Lee MR, Wei IC (2007) Hot-pressurized fluid extraction of flavonoids and phenolic acids from Brazilian propolis and their cytotoxic assay in vitro. J Chin Inst Chem Eng 38:191–196
67. Bristow S, Shekunov T, Shekunov BY, York P (2001) Analysis of the supersaturation and precipitation process with supercritical CO_2. J Supercrit Fluids 21:257–271
68. Mossman BT, Churg A (1998) Mechanisms in the pathogenesis of asbestosis and silicosis. Am J Respir Crit Care Med 157:1666–1680
69. Ozkul Y, Silici S, Ero lu E (2005) Anticarcinogenic effect of propolis in human lymphocytes culture. Phytomedicine 12:742–747

Chapter 3
Green Solvents for Biocatalysis

Marco P.C. Marques, Nuno M.T. Lourenço, Pedro Fernandes, and Carla C.C. R. de Carvalho

Abstract In order to comply with environmental regulations, the agrochemical, the pharmaceutical, and other biotech-based industries are impelled to implement sustainable industrial technologies. To achieve this, the use of biocatalysts (enzymes or cells), leading to high chemo-, regio-, and stereoselectivities under mild conditions, as well as green nonaqueous solvents required to solubilize substrates that are poorly soluble in water, appear as good solutions. In this chapter we will focus on different attempts to combine the properties of green solvents with the advantages of using enzymes for developing biocatalytic processes.

3.1 Introduction

In recent years, and in order to comply with the increasingly restrictive environmental regulations, the transformation industries are gradually modifying their production processes. Industries anchored in biological matrices are among the leading partners committed to this endeavor. This effort is also based on the higher demands on process economics, product specification, alongside with the reduction of the time span of process development. In order to achieve sustainable processes and products, there is a continuously growing interest in introducing environmental, health, and safety considerations into the early stages of process development and design [1–5].

M.P.C. Marques (✉) • N.M.T. Lourenço • P. Fernandes • C.C.C.R. de Carvalho
Department of Bioengineering, Instituto Superior Técnico (IST),
Universidade Técnica de Lisboa, Av. Rovisco Pais, Lisbon 1049-001, Portugal

Institute for Biotechnology and Bioengineering, Centre for Biological and Chemical Engineering, IST, Lisbon, Portugal
e-mail: mpc.marques@ist.utl.pt

A. Mohammad and Inamuddin (eds.), *Green Solvents I: Properties and Applications in Chemistry*, DOI 10.1007/978-94-007-1712-1_3,

The industry could reduce up to 50% or more in project cost if they adopt the strategy "Design for the Environment" [6]. This concept aims at the production of compounds based on the green chemistry principles proposed by Anastas and Horváth [7, 8]. Accordingly, the production relies on using less synthetic steps (atom economization), occurs under mild temperature, using nonhazardous reagents and intermediates (preferably derived from waste and/or renewable feed stocks), in the absence of traditional organic solvents or in solvents that are 100% recoverable and with no adverse safety issues. All of this needs to be accomplished while minimizing energy consumption that is to be produced from renewable energy sources.

An important aspect to take into account is the atom economization. This is a measure of the amount of atoms of the reagent that are incorporated into the product. Since atom economy does not account for solvents, a complementary metric was proposed by Sheldon [9, 10], called the E-factor. The E-factor refers to the amount of unit of waste produced per unit of product, and ideally would be equal to zero [11, 12]. Typically, this factor falls in the range 5–50 for the fine chemicals, 25–100 for the pharmaceuticals sector and well over 100 for the biotechnology sector [11, 13].

Furthermore, Anastas and Zimmerman [14] combined the former principles with process engineering in order to achieve process sustainability [4]. Aspects like pollutants and toxic wastes, transport of hazardous materials, restrictive regulations, and greenhouse gas emission taxes, among others, must also be taken into account in the overall process [2, 15]. Companies that have waste reduction policies are likely to be more successful economically. Most of the successes in the implementation of these principles over the last 20 years are related to waste minimization [11].

Industry guidelines as well as appropriate computer-based algorithms are currently available and include all these aspects and/or data into process design and development [16]. The evaluation of case scenarios is performed by a series of quantitative and qualitative indicators including mass intensity, energy intensity, and safety issues, among others. The alternatives are ranked in four major categories: environment, energy, safety, and efficiency [17, 18].

The agrochemical and pharmaceutical industries have employed different strategies to obtain enantiomerically pure and specifically functionalized compounds. These strategies can rely on the use of a simply chemical route, by the combination of chemical and biocatalytic steps or by the use of purely biocatalytic steps. The latter reactions are anchored on enzymes and whole cells and present advantages over chemical reactions, namely, their (1) high chemo-, regio-, and enantioselectivity; (2) occurrence under mild reaction conditions (e.g., reasonable pH and temperature); and (3) limited (or no) requirements for the use of protection groups, while maintaining the possibility of carrying out reactions in nonconventional media.

From the perspective of green chemistry, the use of isolated enzymes or resting cells is generally favored, due to the fact that less biomass is produced, improving, as a result, the production yield and product recovery. Ultimately, the E-factors for processes that use whole cells are in general high [19].

Table 3.1 Major advantages and disadvantages of using enzymes in organic solvent systems [22, 23]

Advantages	Disadvantages
Enhanced solubility of lipophilic substrates, concomitantly favoring volumetric productivity	Increased complexity of the bioconversion system, mainly due to mass transfer effects
Synthesis is favored over hydrolysis	Careful control of water activity in nearly anhydrous systems
Controlled enzyme selectivity	Risk of enzyme inactivation
In situ product recovery is favored, hence downstream processing simplified	To counter this, enzyme immobilization can be considered, again increasing complexity and cost of the systems
Enhanced thermostability	
Reduced risk of microbial contamination	

The use of solvents as reaction media for biocatalytic reactions has proven to be an extremely useful approach to expand the applications and efficiency of biocatalysis [20, 21]. The use of solvents as substrate and/or product pool, in order to improve the efficiency of bioconversion and biotransformation systems, is the most widely chosen approach to overcome the toxicity and/or low solubility of substrates and products [22]. Using aqueous organic two-phase systems or even single organic systems for enzymatic reactions rather than aqueous systems has many advantages, but there are some inherent problems, including enzyme deactivation, along with the explosive and environmentally hazardous nature of the solvents [22]. The significant advantages and disadvantages of using enzymes in organic systems are listed in Table 3.1.

Significant progress has been made toward identifying solvents with a reduced ecological footprint compared to traditional organic solvents, the so-called first generation of green solvents. Advanced fluids or second-generation green solvents can hold considerable additional benefits as they can lead to further improvements and innovating solutions both in reaction and processing technologies, which go far beyond the replacement of conventional solvents in the already implemented processes [24]. Example of advantages on the use of these second-generation green solvents is the solubilization of hydrophobic compounds at high concentration [25]. Traditionally, green solvents can be classified in five main categories, nonetheless, in this chapter we are mainly focused on four categories, which are: (1) water, (2) ionic liquids, (3) fluorous solvents, and (4) super critical fluids. There is still controversy concerning the classification of some of these categories as green. In this sense, it is interesting to compare these alternative solvents against key criteria for determining their effectiveness as a useful solvent to be used in the process (Table 3.2). The proper solvent selection should be based on the combination of both engineering and chemistry criteria's with health and safety concerns [26].

Table 3.2 Major advantages and drawbacks of green solvents [26]

Solvent	Main advantages	Main drawbacks
Water	Fully safe and easy to handle, nonhazardous, nontoxic and nonflammable, cheap, well-established properties and behavior, easily separates from organics. Favorable life cycle assessment	Poor solvent for lipophilic molecules. Downstream processing from aqueous media can be energy demanding
Supercritical CO_2	Easy to recover, efficient, selective and nontoxic solvent. End-of-life concerns are negligible, if any	The range of molecules solubilized is relatively scarce, a feature that can be countered by using cosolvents or surfactants. The gas is cheap but the costs related to its application are high, due to energy and high pressure reactor requirements
Ionic liquids	Can be custom made to tackle specific situations. Volatile products can be easily removed. Moderate cost	There is still limited data regarding health, safety, and environmental hazards. Synthesis of ionic liquids may be energy demanding and waste management may be complex
Fluorous solvents	Lead to two-phase systems and can be easily distilled and reused	Application limited to the solubilization of markedly hydrophobic molecules. Expensive. Can lead to a buildup of greenhouse gases. Synthesis of these solvents is resource demanding and they tend to persist in the environment

3.2 Water

Water has been considered the ultimate green solvent since it is widely available, nontoxic, nonflammable, and cheap [27, 28]. The polar nature of the water molecule and its ability to establish large, three dimensional networks of hydrogen bonds, are key aspects in the definition of the properties of water as a solvent [29]. As an outcome, water is an outstanding solvent for salts, acids, bases, and compounds that have H, O, and N atoms enabling the formation of hydrogen bonds. Furthermore, it has a relatively low volatility, it is transparent above 200 nm, which eases quantitative measurements, has a high dielectric constant, about 78 at 25°C, minimizing kinetic complexities due to ion-pair formation. Besides, several significant mechanistic parameters, viz. pKa values, substituent constants, are well known for water as solvent [28, 29]. Water (with all its features) has been acknowledged as a fundamental element in life processes [29]. In particular, water has been shown to be required to maintain the active conformation of enzymes, even if in minute amounts, which may vary according to the enzyme, but fully dehydrated proteins are inactive [30, 31]. It is therefore easily understandable how critical is the presence of water

when biocatalysts are involved, even when operating in nonconventional environments [32, 33]. Actually, when enzyme activity in organic solvents is considered, it has been shown to be related to the amount of water bound to the enzyme, rather than on the total water concentration [34]. Bound water strongly depends on the thermodynamic activity of water, which has been acknowledged as the most adequate parameter to quantify water in low water environments [34–36]. Chymotrypsin and subtilisin, when used as biocatalysts in organic environment, require about 50 molecules of water per protein molecule to display activity, which is less than the amount needed to form a monolayer on the surface, roughly 850, in the case of subtilisin [37–39]. Lipases are less demanding, displaying noticeable biocatalytic activity for water activity values as low as 0.0001 [34]. Also, when bioconversion with whole cells is performed, some level of hydration has been shown to be required for cells to display the required catalytic activity [40, 41].

The low water solubility and/or toxicity toward the biocatalyst of several relevant molecules for drug production, or the need for low water environments when synthetic reactions are targeted, usually (but not exclusively) involving amidations or (trans)esterifications (viz. production of semisynthetic antibiotics, aroma ester compounds, biodiesel production) has led to the use of nonconventional media in biocatalysis and biotransformations [42, 43]. The use of such media results in reduced risk of microbial contamination, radical changes in the enantioselectivity of the reaction, reversing the thermodynamic equilibrium of hydrolysis reactions, and prevents water-dependent side reactions [44]. Nevertheless, aqueous environments are still largely the most common when processes implemented in industrial scale are considered [30, 45].

Food processing is naturally one of the areas where application of enzymes in aqueous environment is most common. These include some large-scale applications, viz. starch processing. Some examples are given in Table 3.3.

Aqueous environments are also used in bioconversion systems targeted for organic synthesis. These are of particular interest since they allow for the production of added-value molecules or intermediates for said molecules, often in chemoenzymatic processes. Among such reactions are: the reductions of ketones, C–C double bonds, hydroperoxides, and sulfoxides; oxidation of alcohols; Baeyer–Villiger oxidations for lactone production; oxidative polymerization; or ester hydrolysis, which ultimately allow the production of optically active compounds [67]. Some of these reactions require the regeneration of expensive cofactors. The economic feasibility of such processes requires the in situ regeneration of said cofactors, which relies on second redox enzymatic reaction, and the use of whole cells may be favored in these cases [68, 69]. Further examples of industrially implemented bioconversion processes anchored in the use of enzyme formulations in aqueous environment can be found elsewhere [66–69].

A broader application of aqueous-based biocatalysis is partly hindered due to the low water solubility of plenty of organic substrates. This feature considerably limits volumetric productivity, hence the competitiveness of the process. Different approaches have been developed for substrate supply, mostly involving organic solvents or a more environmentally friendly approach involving a solid (resin) phase,

Table 3.3 Some examples of representative bioconversion processes in aqueous environment

Application	Reference
Starch hydrolysis with α-amylase or β-amylases, in a buffered environment (4.5–6.5), to produce maltodextrins or maltose and maltose oligosaccharides	[46–49]
Hydrolysis of α-galactosides (viz. raffinose and stachyose) and of lactose—sugars related to flatulence and gastrointestinal disturbance—catalyzed by α-galactosidase and β-galactosidase, respectively. Processes were performed in buffered environment (pH 4.0–7.0) and in skimmed and whole milk	[50–52]
Production of galactooligosaccharides (prebiotics) in buffered environments (pH of roughly 4.5–7.5) with β-galactosidase as catalyst. Processes are mostly anchored in lactose as substrate, delivered under high initial concentrations (viz. 200 kg m^{-3})	[53, 54]
Production of fructooligosaccharides (prebiotics and nonnutritive sweeteners [55]) in buffered environments (pH of roughly 4.0–6.0) catalyzed by fructosyltransferases. Processes are carried out with sucrose as substrate, delivered under high initial concentrations (about or in excess of 450 kg m^{-3})	[56–58]
Production of glucooligosaccharides (prebiotics) in buffered environments (pH of roughly 5.0–5.5) catalyzed by dextransucrases (glucosyltransferases). Unlike fructo- and galactooligogosaccharides, α-1,2-glucooligosaccharides promote the growth of the cellulolytic intestinal flora [59]. Processes are carried out with sucrose and maltose, or sucrose and glucose as substrate	[60–62]
Production of monossacharides through isomerization of the substrate to produce sweeteners with enhanced properties. Processes are performed with glucose and galactose as substrates, and L-arabinose or xylose (glucose) isomerases as catalysts, in buffered media, typically in the neutral to slightly alkaline range [46]	[46, 63, 64]
Production of cyclodextrins form liquefied starch with cyclodextrin glycosyltransferases in a buffered environment (pH around 6.0). Cyclodextrins are cyclic α-1,4-glucans consisting of six to more than 100 glucose units, arranged in such a manner to produce molecules shaped as a hollow truncated cone. This structure presents a hydrophilic external surface (water soluble) and a hydrophobic inner cavity, allowing cyclodextrins to form inclusion compounds with hydrophobic compounds. Given this characteristic, cyclodextrins are widely used in several industries, viz. agrochemical, cosmetics, food and pharma [65]	[66]

such as Amberlite [2]. Other approaches for the solubilization of sparingly water-soluble compounds, while allowing operation in a roughly bulk aqueous environment include the use of liposomes, vesicles composed of phospholipids that provide a biomimetic environment [70, 71], or the use of miniemulsions for the enzymatic production of alkyl esters as aroma compounds [72].

3.3 Supercritical fluids

A supercritical fluid (SCF) is defined as the state of a compound at a temperature and pressure above its critical point. SCFs have a density comparable to that of a liquid, and viscosity is comparable to that of a gas, i.e., they exhibit properties

between those of gases and liquids [73]. One of the major advantages is that close to the critical point, the density of the SCF may be adjusted to a wide range of values by promoting small variations in temperature and pressure. The solvent properties dependent on density (dielectric constant, solubility, and partition coefficient) may thus be rationally influenced by small changes in pressure or temperature. Adjustments in the applied pressure in supercritical fluoroform, ethane, sulfur hexafluoride and propane changed the dielectric constant and the Hildebrand solubility parameter, with repercussions on the activity of lipase in the transesterification of methylmethacrylate with 2-ethyl-1-hexanol [74], showing that both selectivity and activity of an enzyme could be predicted by changing pressure.

In biocatalytic systems, SCFs present properties similar to organic solvents, including the ability to solubilize hydrophobic substrates and the possibility of carrying out reactions thermodynamically unfavorable by the presence of water such as the synthesis of esters and amides [75, 76]. However, SCFs present unique properties (a) by allowing high mass transfer due to improved solubility, high diffusivity, low viscosity, and low surface tension that contribute to reduce substrate-diffusion limitations and (b) due to the facility in product recovering by post-reactional depressurization. The solubility of a compound in an SCF is helped by a high vapor pressure, low polarity, and low molecular weight [77]. At the end of the reaction, both product(s) and unreacted substrate(s) may be easily recovered as solvent-free which reduces costs and facilitates downstream processing.

The use of supercritical fluids in biocatalysis using enzymes was first reported in the mid-1980s by Randolph et al. [78], Hammond et al. [79], and Nakamura et al. [80]. The first work demonstrated that alkaline phosphatase could produce *p*-nitrophenol from disodium *p*-nitrophenyl phosphate in supercritical carbon dioxide. Hammond et al. showed that the enzyme polyphenol oxidase could oxidize phenols in supercritical carbon dioxide and fluoroform. The work reported by Nakamura et al. showed the possibility of using a lipase in SCF to carry out hydrolysis and interesterifications. In 1988, Chi and coworkers demonstrated that lipase could conduct hydrolysis and interesterification in $SCCO_2$ faster than in *n*-hexane depending on the water content [81]. For a water content of 20%, the initial velocity in $SCCO_2$ was four times faster than in *n*-hexane. In another work, Randolph et al. [82] demonstrated that solution pressure and the addition of cosolvents affected cholesterol aggregation and thus the activity of cholesterol oxidase. In recent years, several reviews were published on the application of SCFs in biocatalysis processes using enzymes and whole cells [19, 75, 83–88], which demonstrate the interest in this subject. Several types of enzymatic reactions have been reported to occur using supercritical fluids as solvents (Table 3.4). Nevertheless, SCFs are mainly used both in laboratorial and industrial levels in extraction processes such as the extraction of caffeine from coffee and tea, removal of undesirable compounds from crude vegetable oils, essential oils from plants, and extraction of omega-3 enriched fatty acids from fish oils [89].

The most extensively used SCF is supercritical carbon dioxide ($SCCO_2$) since it presents a critical temperature close to ambient temperature (31.1°C, Fig. 3.1) and a relatively low critical pressure (7.38 MPa), is nontoxic and noninflammable, and

Table 3.4 Examples of enzymatic reactions that may be carried out using SCFs as solvent

Reaction	Enzyme	Reference
Esterification	Lipase, cutinase	[80, 90–95]
Transesterification	Subtilisin	
Interesterification	Carlsberg	
Transglycosylation	Xylanase	[96]
Transgalactosylation	β-D-Galactosidase	[97]
Peptidic synthesis	α-Chymotrypsin	[98]

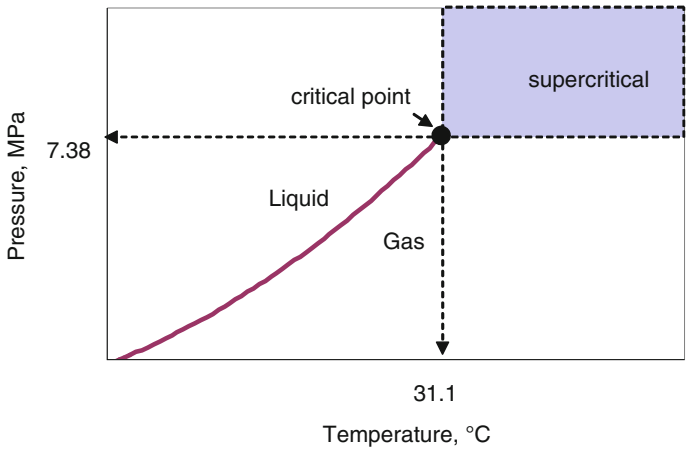

Fig. 3.1 Phase diagram of carbon dioxide

is cheap in comparison to other SCFs. Since it is easily removed by post-reactional depressurisation, it offers a good solution in terms of product purity at reduced costs.

Several examples of successful application of $SCCO_2$ in biocatalysis using enzymes or whole cells have been reported [87, 88]. The kinetic resolution of racemic 3-hydroxy esters may be efficiently achieved through lipase catalysis [99]. Cells of *Bacillus megaterium* PYR 2910 could be used for the conversion of pyrrole to pyrrole-2-carboxylate in $SCCO_2$, which allowed the fixation of CO_2 at higher yields than that observed at atmospheric pressure [100]. Lipases from *Candida antartica* and *M. miehei*, encapsulated in lecithin water-in-oil microemulsion-based organogels were able to carry out the esterification of lauric acid and 1-propanol, the initial reaction rates obtained being better in $SCCO_2$ than in the reference solvent isooctane [101]. In fact, immobilized enzymes present several benefits over free catalysts, including reusability which reduces costs by efficient recycling of the biocatalyst [102]. The behavior of enzymes in SCF is greatly influenced by the water content available to maintain the level of enzyme hydration as water plays an

important role in the noncovalent interactions that allow the enzyme to maintain its native conformation [83, 84]. This should be particularly addressed when immobilization supports are used.

Dumont et al. performed the esterification of myristic acid by an immobilized lipase from *Mucor miehei* both in *n*-hexane and in $SCCO_2$ [90]. It was demonstrated that the enzyme was stable at 15 MPa and 323 K, but it was influenced by the water concentration and by the reaction medium composition. A lipase from *Rhizomucor miehei* immobilized in polypropylene based hydrophobic granules, was not affected by pressure but temperature affected positively the activity and negatively the stability while no diffusion limitations occurred [103]. An enzymatic membrane reactor containing immobilized lipase on a ceramic support acting as a membrane was used in the interesterification reaction between castor oil triglycerides and methyl oleate, with $SCCO_2$ being injected to decrease the viscosity of the substrates solution [104]. As mentioned by the authors, this system could be used for the biotransformation of highly viscous biological compounds.

Although carbon dioxide is very popular as solvent in biocatalysis, the possibility of $SCCO_2$ causing adverse effects on the catalytic activity by decreasing the pH of the microenvironment of the enzyme has been reported [105]. Furthermore, evidence that CO_2 could change the free amino groups at the surface of enzymes causing the formation of carbamates has been reported [106]. Several other gases have been tested as supercritical solvents. In one of the first studies reporting the use of SCFs in biocatalysis, Hammon et al. used both $SCCO_2$ and SC-fluoroform for the oxidation of *p*-cresol by polyphenol oxidase [79]. Karmee et al. discussed the technical aspects of conducting biocatalysis in non-CO_2 supercritical fluids [107]. The authors concluded that the technology established for CO_2 could be used for other SCFs with minor modifications and that the latter should be included in future industrial applications since they provide better enzyme stability and activity than $SCCO_2$. Celia et al. compared the ability of supercritical sulfur hexafluoride with $SCCO_2$ to catalyze the transesterification reaction of 1-phenylethanol and vinyl acetate [93]. The enzyme was stable in this SCF and reaction rates increased in comparison to the case when $SCCO_2$ was used. Kamat et al. used supercritical fluoroform, ethane, sulfur hexafluoride, and propane to study the effect of adjusting pressure in the activity of lipase in the transesterification of methylmethacrylate with 2-ethyl-1-hexanol [74].

Recently, some groups have studied new green systems using both an ionic liquid and a supercritical fluid. De los Rios and coworkers studied the synthesis of butyl propionate in a recirculating bioreactor in ionic liquid/$SCCO_2$ biphasic systems at 50°C and 80 bar [108]. The enhanced selectivity in this system was observed compared with $SCCO_2$ alone. The efficiency of the system was found to depend on both the interactions between the ionic liquid and the enzyme and the mass transfer between the ionic liquid and the $SCCO_2$ immiscible phases. When the transesterification activity of immobilized cutinase was studied in SCF, it was found that the cutinase activity was lower in $SCCO_2$ than in SC-ethane and increased with the water activity [91]. On the other hand, the same work showed that both the initial rates of transesterification and of hydrolysis of immobilized *C. antarctica* lipase B

(Novozym 453) decreased with an increase in water activity and no deleterious effect of $SCCO_2$ was observed, reaching the same level as in SC-ethane. A similar result was achieved with enzymes immobilized on silica supports modified with specific side chains and coated with ionic liquids: their activity increased up to six times in $SCCO_2$ when compared to *n*-hexane media at 95°C [109].

The wide application of SFCs in industry has been hampered by intrinsic limitations such as the limited solubilities of certain substrates, the lack of sufficient data regarding the exposure of workers to SCFs and economical issues [88]. It has been estimated that the relative cost of a process with SCFs roughly increases with the square root of the capacity [110] and so smaller, more efficient reactors should be developed.

3.4 Fluorous Solvents

3.4.1 Properties and Applications

The "fluorous" term was first introduced by Horváth and Rábai for highly fluorinated (or perfluorinated) solvents, in an analogous way to "aqueous" for water-based systems [111]. Perfluorinated compounds (PFCs) have been studied since 1948 [112] and have been used for many chemical industrial applications. The widespread use is due to PFC's unique physical–chemical properties, and in particular to a better effectiveness and a higher chemical and thermal stability than non-fluorinated chemicals, correlated to the strength, the chemical inertness and the low polarizability of C–F bonds. A variety of fluorous solvents are commercially available (Table 3.5).

Associated to these properties, fluorous solvents are distinguished by their temperature-dependent miscibility with conventional organic solvents. At low temperatures, fluorous solvents form two different layers with most of organic solvents becoming completely miscible at certain temperatures (Table 3.6) [113].

This immiscibility was crucial to the early success of fluorous solvents in clean technology applications, namely in case of fluorous–organic biphasic system catalysis (FOBS). These systems involve catalysis in two immiscible phases, a fluorous and a nonfluorous phase. The catalyst is totally soluble in the fluorous phase while the substrates and products prefer the nonfluorous phase. After reaction, the product

Table 3.5 Commercial fluorous solvents and their applications

PFC	Formula	Principal/probable uses
Perfluorooctanoic acid (PFOA)	$CF_3(CF_2)_6COOH$	Fluorosurfactant
Perfluorooctanesulfonic acid (PFOS)	$CF_3(CF_2)_7SO_3H$	Fluorosurfactant
Perfluorohexane FC-72	$CF_3(CF_2)_4CF_3$	Heat transfer media
Perfluoropentane FC-87	$CF_3(CF_2)_3CF_3$	Heat transfer media
Perfluorooctane FC-77	$CF_3(CF_2)_6CF_3$	Heat transfer media

Table 3.6 Temperature-dependent miscibility of perfluoro-methyl-cyclohexane with different organic solvents

	One phase formation temperature (°C)
Carbon Tetrachloride	>26.8
Chloroform	>50.3
Benzene	>85.3
Toluene	>88.8
Clorobenzene	>126.8

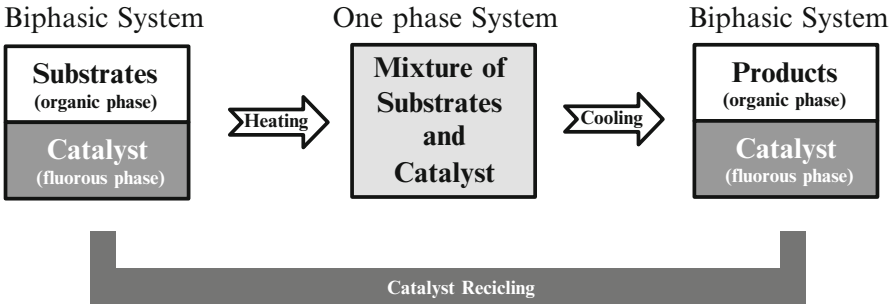

Fig. 3.2 Fluorous–organic biphasic systems catalysis strategy

is recovered from the nonfluorous phase and the catalyst from the fluorous phase, which can then be recycled. FOBS allow easy product separation and recycle of catalysts (Fig. 3.2).

Other promising technologies using fluorous solvents comprise fluorous separations, fluorous synthesis, and fluorous mixture synthesis [114]. In these applications, the solubility of the catalyst, reagent, or substrate in a fluorous phase is achieved by attaching a fluorinated "ponytail" to the compound.

Although man-made PFCs have been widely used for several decades, their potential impacts on human health and the global environment did not draw much attention until the turn of the century when facts of their widespread presence in various environmental media, nature, and human tissue became clear [115, 116].

Some of the negative aspects that prevent fluorochemicals to be considered as totally environmental friendly are the following:

– Their persistence in the environment is very high because of C–F bond strength, and consequent stability, which is especially appreciated when perfluorinated compounds are used as solvents, but that assumes a negative role in terms of degradation.
– PFCs are highly resistant to the oxidative chemical processes in the lower atmosphere that break down most atmospheric pollutants, and the removal mechanism by UV radiation in the mesosphere is extremely slow. As a result PFCs accumulate in the atmosphere and remain there for several thousand years.

– Their synthesis involves large quantities of fluorine and hydrogen fluoride, which are very corrosive and harsh.
– They resist to biodegradation and present high potential to accumulate in organisms and to be amplified. All of the known biologically produced fluorinated molecules contain only one fluorine atom, in contrasts to several man-made PFCs which are fully fluorinated. Natural fluorous compounds, such as monofluoroacetate and fluororganic acids (e.g., fluorooleic and fluoropalmitic acids), produced by different plant species, can rarely undergo to the direct breaking of the carbon–fluorine bond and, more often, the functional groups or bonds attached to the fluorinated moiety are involved in the biodegradation. Analogously PFCs can undergo in the environment to the same abiotic and biotic transformations, becoming precursors of more persistent perfluorinated compounds, such as perfluorooctane sulfonate (PFOS) and perfluorooctanoate (PFOA), which do not breakdown further. In addition, both PFOS and PFOA are very bioaccumulative and toxic, and that is why they are classified persistent organic pollutants by the Stockholm Convention [117, 118].
– The high costs of fluorous solvents limit their industrial interest.

One possible solution for the replacement of perfluorinated compounds are hydrofluoroethers (HFEs), which have been introduced as a cost-effective and environmentally safe alternative to fluorous phase of a biphasic system with different miscibility properties [119]. Some of the commercially available HFEs, such as HFE-7100 and HFE-7500 (Table 3.7), show a higher polarity than PFC because of the introduction of one oxygen atom between a fluoroalkyl group and alkyl group.

Additionally, HFEs are nonflammable, have low toxicity and possess peculiar physical–chemical properties to replace PFCs and HFCs in a large number of applications.

3.4.2 Applications of Fluorous Biphasic Systems in Biocatalysis (FBS)

Biocatalysis in FBSs is a modern area of research that has been receiving increasing interest from different research laboratories over the last decade. As previously illustrated, the uniqueness of fluorous solvents (e.g., perfluorohexane, FC-72) is the

Table 3.7 Commercial HFEs and their applications

HFEs	Formula	Principal/probable uses
HFE-125	CF_3OCF_2H	Heat transfer media
HFE-134	CHF_2OCHF_2	Heat transfer media
HFE-143a	CF_2OCH_3	Heat transfer media
HFE-7000	n-$C_3F_7OCH_3$	Heat transfer media, clean solvent
HFE-7100	$C_4F_9OCH_3$	Clean solvent
HFE-7200	$C_4F_9OCH_2CH_3$	Clean solvent
HFE-7500	$C_7F_{15}OCH_2CH_3$	Clean solvent

property of being either miscible or immiscible with organic solvents (e.g., hexane) depending on the temperature. This miscibility–immiscibility property was crucial to the early success of fluorous chemistry and its resulting applications, namely in biocatalysis: on the basis of "like dissolves like," it led to quick and simple separation of fluorous-soluble compounds from organic ones [19]. In a pioneering example, Theil and coworkers described the efficient enzymatic resolution of sec-alcohols using fluorous acylating agents in the presence of *Candida antarctica* Lipase B [120, 121]. In order to isolate the products from the reaction medium, four steps were needed: (1) the enzyme was filtered, (2) the organic solvent was distilled, (3) the residue dissolved in MeOH, and (4) the MeOH solution was extracted six times with n-C_6H_{14}. The product of the reaction, (R)-fluorous ester (98% ee), was isolated from fluorous phase, and the unreacted (S)-alcohol (99% ee) was isolated from the MeOH phase.

In 2002, the groups of Curran and Theil described another attractive kinetic resolution process involving fluorous triphasic reaction [122, 123]. A simple U-tube holding a lower fluorous phase (perfluorohexane) that serves a barrier to separate two organic phases was used on the enantiomers separation. The two organic phases were MeOH/CH_3Cl, as source phase, and MeOH/MeO, as a receiving phase. A mixture of (S)-fluorous ester (99% ee) and the unreacted (R)-alcohol (91% ee) obtained from enzymatic kinetic resolution without biocatalyst was added to the source side of the U-tube, and it was possible to separate each enantiomer of alcohol with only a slight loss in ee of about 2–4%. The long time, 2–3 days, required for separation plus an enzymatic reaction time of 7 days is however a big issue.

In the same year, the enantioselective esterification of rac-2-methylpentanoic acid with highly fluorinated decanol catalyzed by *Candida rugosa* lipase in a perflurohexane–hexane biphasic system was reported [124]. The acid substrate was dissolved in hexane, while the fluorinated alcohol was dissolved in the fluorous phase. The reaction was initiated by warming the reaction mixture, with consequent one-phase formation, followed by the enzyme addition. At the end of the reaction, the biocatalyst is removed by filtration, and the two phases recovered by cooling the reaction at 0°C. The fluorous phase results in the retention of the fluorinated product, while the unreacted (R)-2-methylpentanoic acid remains in the hexane phase. An important problem of this strategy is the need to use substrate(s) miscible in the fluorous phase, as well as the long reaction time required (95–145 h) to reach 49–53% conversion and 95% ee for the (S)-product.

In 2004, a homogeneous fluorous–organic solvent system was used on the alcoholysis between vinyl cinnamate and benzyl alcohol in the presence of a poly(ethylene glycol)-lipase PL complex. The alcoholysis reaction was performed in a mixture of fluorous solvent (FC-77 perfluorooctane) and organic solvent (isooctane) in order to dissolve nonfluorinated substrates. The enzymatic complex exhibited markedly higher alcoholysis activities in fluorous solvents than in conventional organic solvents such as isooctane and n-hexane. In this strategy, the results could be explained by the localization of substrates around lipase molecules, induced by adsorption of the substrates to the PEG layer of the PEG–lipase complex [125].

Table 3.8 Comparison between enzymatic resolution of 1-phenylethanol in fluorous and nonfluorous solvents (Partly reproduced from Ref. [126]. With kind permission of John Wiley and Sons, Inc.)

Solvent	T (h)	Conv (%)	ee Product (%)
R-32	5	50	>99
R-227ea	3.5	49	>99
R-134a	4	49	>99
Hexane	8	46	>99
MTBE	35	49	>99

In the same year, the Micklefield group tested three low boiling point fluorocarbon solvents for the kinetic resolution of racemic 1-phenylethanol in the presence of vinyl acetate using Novozym 435 as a catalyst. Compared to similar reactions carried out in hexane and methyl *tert*-butyl ether (MTBE), reactions in fluorinated solvents were faster and gave better yields (Table 3.8). However, concerning the products' separation, the use of low-boiling-point fluorocarbon solvents has no benefit since this strategy does not allow a partition of the products in two phases. The enhancement on the performance is attributed to the low viscosity of fluorinated solvents that increased the solute diffusivity [126].

3.5 Ionic Liquids

3.5.1 Properties and Applications

Ionic Liquids are liquid compounds that are entirely composed of ions: however, the definition differs from the classical molten salts' definition. Thus, the term ionic liquids (ILs) is mainly used for compounds that are fluid at or near room temperature with low viscosity, while the molten salt refers to compounds with high melting point, very viscous and highly corrosive [127]. The first description of an IL was probably carried out by Ray and Rakshit in 1911 [128]. These authors prepared different ethylamine nitrates, dimethylamine and triethylamine, which, however, spontaneously decomposed over time.

A few years later in 1914, the first stable IL, ammonium ethyl nitrate, was prepared by Walder [129]. One attribute of this IL was the content of small amounts of water (200–600 ppm) [130]. A few years later, in the mid-1950s Hurley and Wier [131] prepared and described, low melting point salts containing anions of chloroaluminates, as electrolytes for electrodeposition of aluminum. These ILs returned to awaken new interest, when in 1970, Osteryoung and Wilkes rediscovered them. Later on, these were developed and applied in electrochemistry [132].

The first application of ILs as solvents in organic chemistry was described in 1985–1986 by two different research groups, represented by Fry [133] and Boon

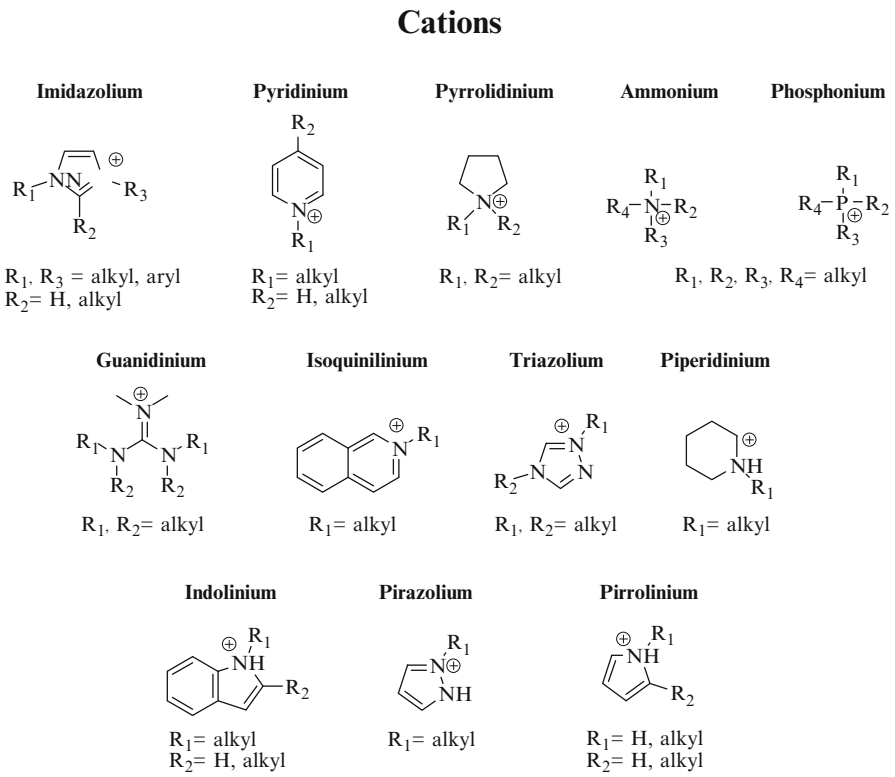

Fig. 3.3 The most representative structures of IL containing several cations and anions

[134]. Since then, new ILs with melting points below 100°C, containing more stable anions to air and water have been published extensively in the literature [135–137]. An excellent compilation of about 300 different ionic liquids was published by Poole [138]. The most representative structures of IL containing several cations and anions are described in Fig. 3.3.

The peculiar properties of these compounds, such as the almost nonexistent vapor pressure [139], the high thermal stability [140], their electrochemical nature [141] and high ionic conductivity have made them central molecules in numerous areas by replacing the use of flammable and highly volatile organic solvents [142].

Another characteristic that made them particularly useful refers to its ability to solubilize various organic, inorganic, and even metals [143, 144]. These compounds may also be immiscible in water and in a variety of organic solvents [145]. Areas as organic chemistry [146–149], chemical engineering [150], materials science [151], physical chemistry [152, 153], analytical chemistry [154, 155], and biotechnology [156], among others, have been able to take advantages of these properties.

3.5.2 Biocatalysis in Ionic Liquids

Biocatalysis as a greener process has provided a plausible alternative to classical organic chemistry due to the replacement of organometallic catalyst by biocatalyst, namely enzymes. Like other areas, biocatalysis is utilizing advantage of ionic liquids [19, 157]. Since the pioneer work of Erbeldinger et al. [158] in 2000 on the use of 1-butyl-3-methylimidazolium hexafluorophosphate [bmim][PF_6] together with thermolysin on the formation of *Z*-aspartame, the ILs have been use intensively over the last decade in several enzymatic transformations. The more illustrative enzymatic transformations are centered on esterification, transesterification, alcoholysis, aminolysis, hydrolysis, and polymerization [157].

The enzymatic kinetic resolution of racemic mixtures of secondary alcohols is a well-known established method, for the preparation of enantiomerically pure secondary alcohols [159]. One of the first reports concerning the lipase-catalyzed transesterifications in ionic liquids was described by Kim et al. [160] in 2001 with markedly enhanced enantioselectivity. The authors observed that lipases were up to 25 times more enantioselective in ionic liquids than in conventional organic solvents.

A comparative study on biocatalysis in nonconventional solvents, ionic liquids, supercritical fluids, and organic media was published by Barreiros and coworkers illustrating the main differences between solvents for a model transesterification reaction [91]. The catalytic activities of *Candida antarctica* lipase B (CAL B) immobilized on an acrylic resin (Novozym 435) and cutinase immobilized on zeolite (NaY) were measured in three imidazolium-cation-based ionic liquids, supercritical (SC) ethane, supercritical carbon dioxide (SC-CO_2) and *n*-hexane, at different water activities. Both initial rates of transesterification and of hydrolysis of Novozym decreased with an increase in the water activity. $SCCO_2$ did not have a detrimental effect on Novozym activity, which was as high as in SC-ethane and *n*-hexane. The transesterification activity of cutinase was highest and similar in 1-butyl-3-methylimidazolium hexafluorophosphate ([bmim][PF_6]), SC-ethane and *n*-hexane, more than one order of magnitude lower in $SCCO_2$, and increased with an increase in the water activity. Hydrolysis was not detected either in sc-fluids or *n*-hexane, but was observed in ILs at high water activity only. $SCCO_2$ did not negatively affect the catalytic activity of cutinase suspended in [bmim][PF_6], suggesting a protective effect of the IL. In the case of Novozym, a marked increase in the rate of transesterification was obtained in the [bmim][PF_6]/SC-CO_2 system, compared to the IL alone.

Table 3.9 Preparative enzymatic resolution of (±)-cis-benzyl N-(1-hydroxyindan-2-yl)carbamate using CALB in [aliq][N(CN)$_2$] at 25°C and 60 h reaction time (Reproduced from Ref. [161]. With kind permission of The Royal Society of Chemistry)

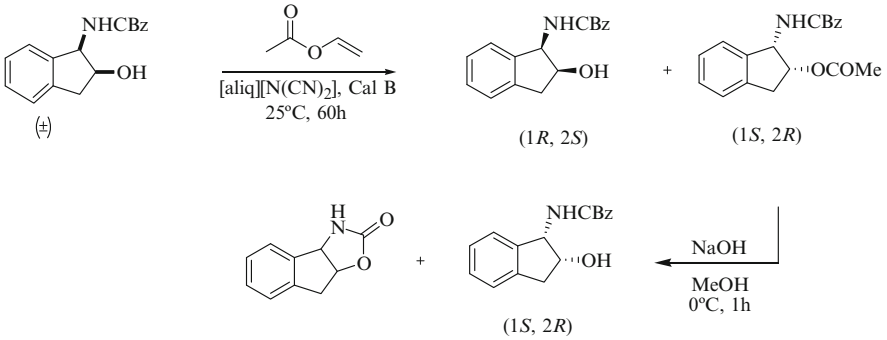

Entry	Time (h)	Isolation Method	Conv. (%)	Substrate yield (%)	Substrate ee (%)	Product yield (%)	Product ee (%)
1	24	Column	28	71	34	27	90
2	24	Column	31	67	40	28	97
3	60	Sublimation	48	47e	80	36	92
4 (reuse)	60	Column	44	55	65	40	88

From the authors' point of view this observation may reflect improved mass transfer of solutes to the pores of the immobilization matrix due to a high concentration of dissolved CO_2 and a reduction in viscosity of the IL.

Through the years the use of ionic liquids as a medium for enzymatic resolution left only to focus on the selectivity and enzymatic stability and moved toward the edge of taking advantage of chemical–physical properties, namely, negligible vapor pressure. An example described by Lourenço et al. [161] was an efficient enzymatic resolution of (±)-*cis*-benzyl *N*-(1-hydroxyindan-2-yl)carbamate in [aliq][N(CN)$_2$] by acylation using CAL B as a biocatalyst. The reaction proceeds to the formation of the corresponding acetate in moderate yield and high enantiomeric excess for the first and second cycles. Additionally, the biocatalyst could be recovered by filtration with the possibility of catalyst and medium reuse (Table 3.9). The reaction products could be easily removed from the ionic liquid by direct sublimation under high vacuum (Fig. 3.4).

One of the newest progresses on the development of new ionic liquids has been the design of task specific ionic liquids (TSILs). In this connection, the Afonso group [162] reported an efficient process for resolution and separation of racemic mixture of sec-alcohols without need of laborious chromatographic separation using different TSIL. Interestingly, one of these new TSIL shows to be liquid at room temperature. The innovation of this process was based on the simultaneous use of TSIL as acylating and anchoring agent allowing the separation of both free sec-alcohols enantiomers only by enzymatic resolution (Fig. 3.5).

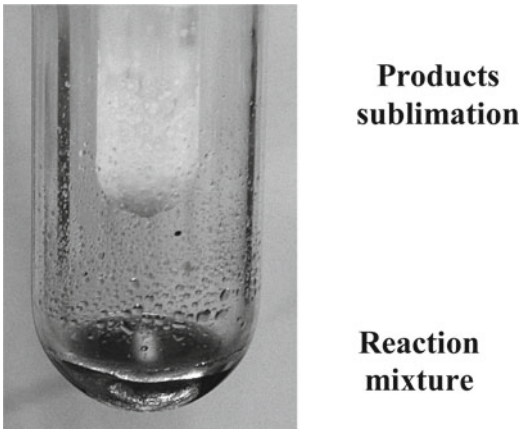

Fig. 3.4 Reaction products removal from the ionic liquid by direct sublimation under high vacuum (Reproduced from Ref. [161]. With kind permission of The Royal Society of Chemistry)

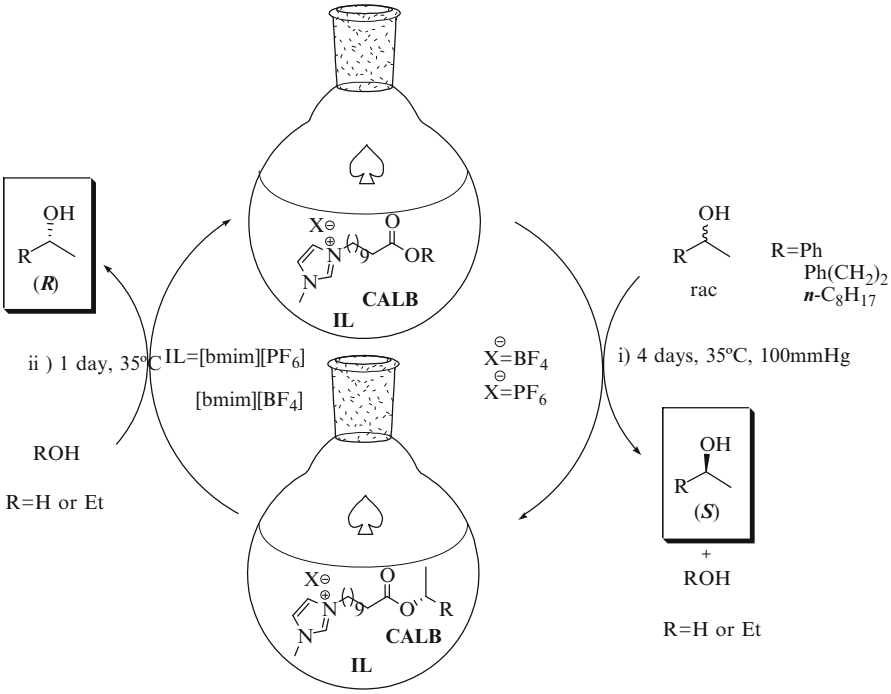

Fig. 3.5 Enzymatic resolution and separation of different sec-alcohols using TSILs as ionic acylating agents (Reproduced from Ref. [162]. With kind permission of John Wiley & Sons, Inc.)

Table 3.10 Enzymatic resolution and separation of racemic sec-alcohols using CAL B as a biocatalyst (Reproduced from Ref. [162]. With kind permission of John Wiley and Sons, Inc.)

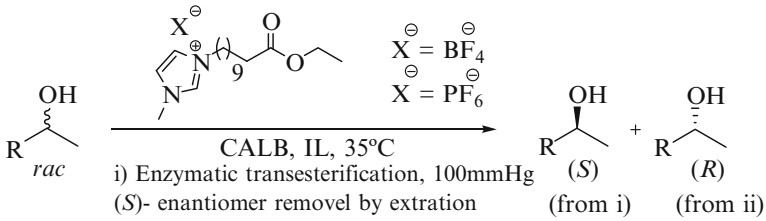

Racemic alcohol R	Acylating AgentX-	IL	Step 1 Time (h)	Step 1 Enantiomer (S) Yield (%)	Step 1 Enantiomer (S) ee (%)	Step 2 Time (h)	Step 2 Enantiomer (R) Yield (%)	Step 2 Enantiomer (R) ee (%)
Ph	BF_4	[bmim][PF_6]	48	67.0	54.5	24	25.9	88.9
			96	68.8	62.2	24	22.5	98.5
	PF_6	[bmim][PF_6]	48	62.1	61.8	24	29.7	94.0
			96	51.0	80.9	24	41.3	99.3
	BF_4	[bmim][BF_4]	96	74.3	56.2	24	19.2	98.9
	BF_4	–	48	64.5	39.4	24	19.4	99.0
$Ph(CH_2)_2$	BF_4	[bmim][PF_6]	96	50.5	62.4	24	33.2	96.4
	PF_6	[bmim][PF_6]	96	51.6	60.0	24	30.6	91.9
n-C_8H_{17}	BF_4	[bmim][PF_6]	96	51.5	38.5	24	25.0	96.5

The central topic in this strategy is the combination of the ionic acylating agent with an ionic liquid. The authors envisaged an acylating agent, containing two distinct sections: an ionic and ester or acid moiety recognized by enzyme that allowed the selective resolution and separation of ionic anchored ester from unreacted alcohol. The major advantage of this process compared with other procedures described before is the possibility to separate both free enantiomers of racemic mixture only by enzymatic resolution in one pot reaction in the presence of small excess of acylating agent (1 eq.). This approach took advantage of unique properties of ionic liquids (formed only by ions), which provides an ionic pool decisive for entrapping one of enantiomers as an ionic ester moiety. Additionally, due to IL being imimiscible in organic solvents, allowed the extraction of unreacted alcohol by repeated extraction with an apolar solvent.

The fact that IL being almost nonvolatile [139] allowed the evaporation of ethanol or H_2O formed during transterification or esterification, moving the equilibrium reaction to the formation of products. The anchored enantiomer could be removed in consecutive step by a second enzymatic transterification or hydrolysis (reversible reaction) using ethanol or H_2O.

This methodology was applied to different substrates, allowing the isolation of both enantiomers in good yields and ee, as demonstrated in Table 3.10.

3.6 Conclusions

Industry has struggled in the recent years to comply with the legislative initiatives to increase the "green qualification" of the production processes and products. The use of biocatalytic systems in nonconventional solvents (green solvents) is highly beneficial from an environmental perspective. By using enzymes, milder reaction conditions and higher selectivity's are achieved in comparison with conventional chemical processes. The use of solvents with low ecological footprint definitely provides a suitable alternative.

Nonetheless, and despite the intense research efforts in performing biocatalysis in nonconventional solvents, there are still several questions that need to be clarified, namely in terms of solvent biocompatibilities, catalytic yields and product recovery while maintaining low E-factors and process economical viability.

Acknowledgments The authors would like to thank the Fundação para a Ciência e a Tecnologia, Portugal, for financial support: postdoctoral grants SFRH/BPD/64160/2009 and SFRH/BPD/41175/2007 awarded to M.P.C. Marques and N.M.T. Lourenço, respectively; contracts under the program Ciência2007 awarded to P. Fernandes and C.C.C.R. de Carvalho.

References

1. Armor JN (1999) Striving for catalytically green processes in the 21st century. Appl Catal A 189:153–162
2. Curzons AD, Constable DJC, Mortimer DN et al (2001) So you think your process is green, how do you know? Using principles of sustainability to determine what is green—a corporate perspective. Green Chem 3:1–6
3. Diwekar U (2005) Green process design, industrial ecology, and sustainability: a systems analysis perspective. Resour Conserv Recycl 44:215–235
4. Segars JW, Bradfield SL, Wright JJ et al (2003) EcoWorx, green engineering principles in practice. Environ Sci Technol 37:5269–5277
5. Jiménez-González C, Constable DJC, Curzons AD et al (2002) Developing GSK's green technology guidance: methodology for case-scenario comparison of technologies. Clean Technol Environ Policy 4:22–53
6. Little AD (2001) Making EHS an integral part of process design. Wiley-AIChE, New York
7. Horváth IT, Anastas PT (2007) Introduction: green chemistry. Chem Rev 107:2167–2168
8. Horváth IT, Anastas PT (2007) Innovations and green chemistry. Chem Rev 107:2169–2173
9. Sheldon RA (2007) The E-factor: 15 years on. Green Chem 9:1273–1283
10. Sheldon RA (2008) E factors, green chemistry and catalysis: an odyssey. Chem Commun 7:3352–3365
11. Beach EV, Cui Z, Anastas PT (2009) Green chemistry: a design framework for sustainability. Energy Environ Sci 2:1038–1049
12. Tucker JL (2006) Green chemistry, a pharmaceutical perspective. Org Process Res Dev 10:315–319
13. Calvo-Flores FG (2009) Sustainable chemistry metrics. ChemSusChem 2:905–919
14. Anastas PT, Zimmerman JB (2003) Design through the 12 principles of green engineering. Environ Sci Technol 37:95–101
15. Manley JB, Anastas PT, Cue BW Jr (2008) Frontiers in green chemistry: meeting the grand challenges for sustainability in R&D and manufacturing. J Clean Prod 16:743–750

16. Andraos J (2009) Global green chemistry metrics analysis algorithm and spreadsheets: evaluation of the material efficiency performances of synthesis plans for Oseltamivir phosphate (Tamiflu) as a test case. Org Process Res Dev 13:161–185
17. Woodley JM (2008) New opportunities for biocatalysis: making pharmaceutical processes greener. Trends Biotechnol 26:321–327
18. Jiménez-González C, Curzons AD, Constable DJC et al (2005) Expanding GSK's solvent selection guide—application of life cycle assessment to enhance solvent selections. Clean Technol Environ Policy 7:42–50
19. Hernáiz M, Alcántara A, García J, Sinisterra J (2010) Applied biotransformations in green solvents. Chem Eur J 16:9422–9437
20. Lee MY, Dordick JS (2002) Enzyme activation for nonaqueous media. Curr Opin Biotechnol 13:376–384
21. Serdakowski AL, Dordick JS (2008) Enzyme activation for organic solvents made easy. Trends Biotechnol 26:48–54
22. Kim PY, Pollard DJ, Woodley JM (2007) Substrate supply for effective biocatalysis. Biotechnol Prog 23:74–82
23. Doukyu N, Ogino H (2010) Organic solvent-tolerant enzymes. Biochem Eng J 48:270–282
24. Leitner W (2009) Green solvents—progress in science and application. Green Chem 11:603–1603
25. Wang Z (2007) The potential of cloud point system as a novel two-phase partitioning system for biotransformation. Appl Microbiol Biotechnol 75:1–10
26. Clark JH, Tavener SJ (2007) Alternative solvents: shades of green. Org Process Res Dev 11:149–155
27. Sheldon RA (2005) Green solvents for sustainable organic synthesis: state of the art. Green Chem 7:267–278
28. Manahan SE (2006) Green chemistry and the ten commandments of sustainability, 2nd edn. ChemChar Research, Inc, Columbia
29. Engberts JBFN (2007) Structure and properties of water. In: Lindström UM (ed) Organic reactions in water: principles, strategies and applications. Blackwell Publishing, Oxford
30. Illanes A (2008) Introduction. In: Illanes A (ed) Enzyme biocatalysis—principles and applications. Springer, New York
31. Frauenfelder H, Chen G, Berendzen J et al (2009) A unified model of protein dynamics. Proc Natl Acad Sci USA 106:5129–5134
32. Clark DS (2004) Characteristics of nearly dry enzymes in organic solvents: implications for biocatalysis in the absence of water. Philos Trans R Soc Lond B 359:1299–1307
33. Lozano P (2010) Enzymes in neoteric solvents: from one-phase to multiphase systems. Green Chem 12:555–569
34. Adlercreutz P (2008) Fundamentals of biocatalysis in neat organic solvents. In: Carrea G, Riva S (eds) Organic synthesis with enzymes in non-aqueous media. Wiley-VCH Verlag GmbH & Co. KGaA, Weinheim
35. Adamczak M, Krishna SH (2004) Enzyme for efficient biocatalysis. Food Technol Biotechnol 42:251–264
36. Xia X, Wang C, Yang B et al (2009) Water activity dependence of lipases in non-aqueous biocatalysis. Appl Biochem Biotechnol 3:759–767
37. Zaks A, Klibanov AM (1988) Enzymatic catalysis in nonaqueous solvent. J Biol Chem 263:3194–3201
38. Bommarius AS, Riebel BR (2004) Biocatalysis: fundamentals and applications. Wiley-VCH, Weinheim
39. Yang L, Dordick JS, Garde S (2004) Hydration of enzyme in nonaqueous media is consistent with solvent dependence of its activity. Biophys J 87:812–821
40. Fernandes P, Cabral JMS, Pinheiro HM (1998) Influence of some operational parameters on the bioconversion of sitosterol with immobilized whole cells in organic medium. J Mol Catal B Enzym 5:307–310

41. Cruz A, Angelova B, Fernandes P et al (2004) Study of key operational parameters for the side-chain cleavage of sitosterol by free mycobacterial cells in bis-(2-ethylhexyl) phthalate. Biocat Biotrans 22:189–194
42. Hou CT (2005) Handbook of industrial biocatalysis. CRC Press, Boca Raton
43. Carrea G, Riva S (2008) Organic synthesis with enzymes in non-aqueous media. Wiley-VCH Verlag GmbH & Co. KGaA, Weinheim
44. Castro GR, Knubovets T (2003) Homogeneous biocatalysis in organic solvents and water-organic mixtures. Crit Rev Biotechnol 23:195–231
45. Straathof AJJ (2006) Quantitative analysis of industrial biotransformations. In: Liese A, Seelbach K, Wandrey C (eds) Industrial biotransformations, 2nd edn. Wiley-VCH, Weinheim
46. Fernandes P (2010) Enzymes in sugar industries. In: Panesar P, Marwaha SS, Chopra HK (eds) Enzymes in food processing: fundamentals and potential applications. IK International Publishing House Pvt Ltd, New Delhi
47. Olsen HS (2002) Enzymes in starch modification. In: Whitehurst RJ, Law BA (eds) Enzymes in food technology. Sheffield Academic Press Ltd, Sheffield
48. Norman BE, Anders V-N, Olsen HS, Pedersen S (2009) Processes for hydrolysis of starch. US Patent 20,090,142,817
49. Hobbs L (2009) Sweeteners from starch: production, properties and uses. In: Miller JB, Whistler R (eds) Starch: chemistry and technology, 3rd edn. Academic, Burlington
50. Girigowda K, Mulimani VH (2006) Hydrolysis of galacto-oligosaccharides in soymilk by k-carrageenan-entrapped α-galactosidase from *Aspergillus oryzae*. World J Microbiol Biotechnol 22:437–442
51. Grano V, Diano N, Rossi S et al (2004) Production of low-lactose milk by means of nonisothermal bioreactors. Biotechnol Prog 20:1393–1401
52. Grosová Z, Rosenberg M, Rebroš M et al (2008) Entrapment of β-galactosidase in polyvinylalcohol hydrogel. Biotechnol Lett 30:763–767
53. Nakkharat P, Haltrich D (2007) β-galactosidase from *Talaromyces thermophilus* immobilized on to Eupergit C for production of galacto-oligosaccharides during lactose hydrolysis in batch and packed-bed reactor. World J Microbiol Biotechnol 23:759–764
54. Park A-R, Oh D-K (2010) Galacto-oligosaccharide production using microbial β-galactosidase: current state and perspectives. Appl Microbiol Biotechnol 85:1279–1286
55. Mabel MJ, Sangeetha PT, Platel K, Srinivasan K et al (2008) Physicochemical characterization of fructooligosaccharides and evaluation of their suitability as a potential sweetener for diabetics. Carbohydr Res 343:56–66
56. Yun JW, Song SK (1996) Continuous production of fructooligosaccharides using fructosyltransferase immobilized on ion exchange resin. Biotechnol Bioprocess Eng 1:18–21
57. Santos AMP, Maugeri F (2007) Synthesis of fructooligosaccharides from sucrose using inulinase from *Kluyveromyces marxianus*. Food Technol Biotechnol 45:181–186
58. Henderson WE, King W, Shetty JK (2010) Situ fructooligosaccharide production and sucrose reduction. US Patent 20,100,040,728
59. Monsan P, Potocki de Montalk G, Sarçabal P et al (2000) Glucansucrases: efficient tools for the synthesis of oligosaccharides of nutritional interest. In: Bielecki S, Tramper J, Polak J (eds) Food biotechnology. Elsevier, Amsterdam
60. Buchholz K, Monsan PF (2003) Dextransucrase. In: Whitaker JR, Voragen AG, Wong DWS (eds) Handbook of food enzymology. Marcel Dekker, New York
61. Kubik C, Sikora B, Bielecki S (2004) Immobilization of dextransucrase and its use with soluble dextranase for glucooligosaccharides synthesis. Enzyme Microb Technol 34:555–560
62. Berensmieier S, Jördening H-J, Bucholz K (2006) Isomaltose formation by free and immobilized dextransucrase. Biocat Biotrans 24:280–290
63. Ryu S-A, Kim CS, Kim H-J et al (2003) Continuous D-tagatose production by immobilized thermostable L-arabinose isomerase in a packed-bed bioreactor. Biotechnol Prog 19:1643–1647
64. Dehkordi AM, Tehrany MS, Safari I (2009) Kinetics of glucose isomerization to fructose by immobilized glucose isomerase (Sweetzyme IT). Ind Eng Chem Res 48:3271–3278

65. Li Z, Wang M, Wang F et al (2007) γ-cyclodextrin: a review on enzymatic production and applications. Appl Microbiol Biotechnol 77:245–255
66. Liese A, Seelbach K, Buchholz A (2006) Processes. In: Liese A, Seelbach K, Wandrey C (eds) Industrial biotransformations, 2nd edn. Wiley-VCH, Weinheim
67. Nakamura K, Matsuda T (2007) Biocatalysis in water. In: Lindström UM (ed) Organic reactions in water: principles, strategies and applications. Blackwell Publishing, Oxford
68. Lopez-Gallego F, Schmidt-Dannert C (2010) Multi-enzymatic synthesis. Curr Opin Chem Biol 14:174–183
69. Ghisalba O, Meyer H-P, Wohlgemuth R (2010) Industrial biotransformation. In: Flickinger M (ed) Encyclopedia of industrila biotechnology – bioprocess, bioseparation, and cell technology. Wiley, New York
70. Goetschel R, Barenholz Y, Bar R (1992) Microbial conversions in a liposomal medium. Part 2: cholesterol oxidation by *Rhodococcus erythropolis*. Enzyme Microb Technol 14:390–395
71. Llanes N, Pendás J, Falero A et al (2002) Conversion of liposomal 4-androsten-3,17-dione by *A. simplex* immobilized cells in calcium pectate. J Steroid Biochem Mol Biol 80:131–133
72. de Barros DPC, Fonseca LP, Cabral JMS (2010) Miniemulsion as efficient system for enzymatic synthesis of acid alkyl esters. Biotechnol Bioeng 106:507–515
73. Perry RH, Green DW (1997) Perry's chemical engineers' handbook, 7th edn. McGraw-Hill, New York
74. Kamat SV, Iwaskewycz B, Beckman EJ et al (1993) Biocatalytic synthesis of acrylates in supercritical fluids: tuning enzyme activity by changing pressure. Proc Natl Acad Sci 90:2940–2944
75. Hobbs HR, Thomas NR (2007) Biocatalysis in supercritical fluids, in fluorous solvents, and under solvent-free conditions. Chem Rev 107:2786–2820
76. Condoret JS, Vankan S, Joulia X et al (1997) Prediction of water adsorption curves for heterogeneous biocatalysis in organic and supercritical solvents. Chem Eng Sci 52:213–220
77. Rezaei K, Temelli F, Jenab E (2007) Effects of pressure and temperature on enzymatic reactions in supercritical fluids. Biotechnol Adv 25:272–280
78. Randolph TW, Blanch HW, Prausnitz JM et al (1985) Enzymatic catalysis in a supercritical fluid. Biotechnol Lett 7:325–328
79. Hammond D, Karel M, Klibanov A et al (1985) Enzymatic reactions in supercritical gases. Appl Biochem Biotechnol 11:393–400
80. Nakamura K, Chi YM, Yamada Y et al (1986) Lipase activity and stability in supercritical carbon dioxide. Chem Eng Commun 45:207–212
81. Chi YM, Nakamura K, Yano T (1988) Enzymatic interesterification in supercritical carbon-dioxide. Agric Biol Chem 52:1541–1550
82. Randolph TW, Clark DS, Blanch HW et al (1988) Cholesterol aggregation and interaction with cholesterol oxidase in supercritical carbon dioxide. Proc Natl Acad Sci 85:2979–2983
83. Mesiano AJ, Beckman EJ, Russell AJ (1999) Supercritical biocatalysis. Chem Rev 99(2):623–634
84. Cantone S, Hanefeld U, Basso A (2007) Biocatalysis in non-conventional media-ionic liquids, supercritical fluids and the gas. Green Chem 9:954–971
85. Darani KK, Mozafari MR (2009) Supercritical fluids technology in bioprocess industries: a review. J Biochem Tech 2:144–152
86. Habulin M, Primozic M, Knez Z (2007) Supercritical fluids as solvents for enzymatic reactions. Acta Chim Slovenica 54:667–677
87. Matsuda T, Harada T, Nakamura K (2005) Biocatalysis in supercritical CO_2. Curr Org Chem 9:299–315
88. Munshi P, Bhaduri S (2009) Supercritical CO_2: a twenty-first century solvent for the chemical industry. Curr Sci 97:63–72
89. Herrero M, Mendiola JA, Cifuentes A et al (2010) Supercritical fluid extraction: recent advances and applications. J Chromatogr A 1217:2495–2511
90. Dumont T, Barth D, Corbier C et al (1992) Enzymatic reaction kinetic: comparison in an organic solvent and in supercritical carbon dioxide. Biotechnol Bioeng 40:329–333

91. Garcia S, Lourenco NMT, Lousa D et al (2004) A comparative study of biocatalysis in non-conventional solvents: ionic liquids, supercritical fluids and organic media. Green Chem 6:466–470
92. Pasta P, Mazzola G, Carrea G et al (1989) Subtilisin-catalyzed transesterification in supercritical carbon dioxide. Biotechnol Lett 11:643–648
93. Celia E, Cernia E, Palocci C et al (2005) Tuning *Pseudomonas cepacea* lipase (pcl) activity in supercritical fluids. J Supercrit Fluids 33:193–199
94. Goddard R, Bosley J, Al-Duri B (2000) Lipase-catalysed esterification of oleic acid and ethanol in a continuous packed bed reactor, using supercritical CO_2 as solvent: approximation of system kinetics. J Chem Technol Biotechnol 75:715–721
95. Olsen T, Kerton F, Marriott R et al (2006) Biocatalytic esterification of lavandulol in supercritical carbon dioxide using acetic acid as the acyl donor. Enzyme Microb Technol 39:621–625
96. Nakamura T, Toshima K, Matsumura S (2000) One-step synthesis of n-octyl-D-xylotrioside, xylobioside and xyloside from xylan and n-octanol using acetone powder of *Aureobasidium pullulans* in supercritical fluids. Biotechnol Lett 22:183–1189
97. Okahata Y, Fujimoto Y, Ijiro K (1995) A lipid-coated lipase as an enantioselective ester synthesis catalyst in homogeneous organic solvents. J Org Chem 60:2244–2250
98. Noritomi H, Miyata M, Kato S et al (1995) Enzymatic synthesis of peptide in acetonitrile/supercritical carbon dioxide. Biotechnol Lett 17:1323–1328
99. Bornscheuer U, Capewell A, Wendel V et al (1996) On-line determination of the conversion in a lipase-catalyzed kinetic resolution in supercritical carbon dioxide. J Biotechnol 46:139–143
100. Matsuda T, Ohashi Y, Harada T et al (2001) Conversion of pyrrole to pyrrole-2-carboxylate by cells of Bacillus megaterium in supercritical CO_2. Chem Commun 2194–2195
101. Blattner C, Zoumpanioti M, Kroner J et al (2006) Biocatalysis using lipase encapsulated in microemulsion-based organogels in supercritical carbon dioxide. J Supercrit Fluids 36:182–193
102. Cao L (2005) Immobilised enzymes: science or art? Curr Opin Chem Biol 9:217–226
103. Al-Duri B, Goddard R, Bosley J (2001) Characterisation of a novel support for biocatalysis in supercritical carbon dioxide. J Mol Catal B: Enzym 11:825–834
104. Pomier E, Delebecque N, Paolucci-Jeanjean D et al (2007) Effect of working conditions on vegetable oil transformation in an enzymatic reactor combining membrane and supercritical CO_2. J Supercrit Fluids 41:380–385
105. Nakamura K (1990) Biochemical reactions in supercritical fluids. Trends Biotechnol 8:288–292
106. Kamat S, Critchley G, Beckman EJ et al (1995) Biocatalytic synthesis of acrylates in organic solvents and supercritical fluids: III. Does carbon dioxide covalently modify enzymes? Biotechnol Bioeng 46:610–620
107. Karmee SK, Casiraghi L, Greiner L (2008) Technical aspects of biocatalysis in non-CO_2-based supercritical fluids. Biotechnol J 3:104–111
108. de los Ríos AP, Hernández-Fernández FJ, Gómez D et al (2007) Understanding the chemical reaction and mass-transfer phenomena in a recirculating enzymatic membrane reactor for green ester synthesis in ionic liquid/supercritical carbon dioxide biphasic systems. J Supercrit Fluids 43:303–309
109. Lozano P, De Diego T, Gmouh S et al (2007) Toward green processes for fine chemicals synthesis: biocatalysis in ionic liquid-supercritical carbon dioxide biphasic systems. In: Malhotra SV (ed) Ionic liquids in organic synthesis. American Chemical Society, Washington, DC, pp 209–223
110. Perrut M (2000) Supercritical fluid applications: industrial developments and economic issues. Ind Eng Chem Res 39:4531–4535
111. Horváth IT, Rábai J (1994) Facile catalyst separation without water: fluorous biphase hydroformylation of olefins. Science 266:72–75
112. Scott RL (1948) Liquid-liquid solubility of perfluorornethylcyclohexane with benzene, carbon tetrachloride, chlorobenzene, chloroform and toluene. J Am Chem Soc 70:4090
113. Hildebrand JH, Cochran DRF (1949) Liquid-liquid solubility of perfluoromethylcyclohexane with benzene, carbon tetrachloride, chlorobenzene, chloroform and toluene. J Am Chem Soc 71:22–25

114. Curran D, Lee Z (2001) Fluorous techniques for the synthesis and separation of organic molecules. Green Chem 3:G3–G7
115. Paul AG, Jones KC, Sweetman AJ (2009) A first global production, emission, and environmental inventory for perfluorooctane sulfonate. Environ Sci Technol 43:386–392
116. Prevedouros K, Cousins IT, Buck RC et al (2006) Sources, fate and transport of perfluorocarboxylates. Environ Sci Technol 40:32–44
117. European Union, Directive 2006/122/ECOF of the European Parliament and of the council of 12 December 2006. Off J Eur Union, L/372/32–34, 27 Dec 2006
118. Council Decision 2006/507/EC of 14 October 2004 concerning the conclusion obotEC, of the Stockholm convention on persistent organic pollutants (OJ L 209, 31 Jul 2006, p 1)
119. Kehren J (2001) HFEs offer a cost-effective, environmentally safe alternative to aqueous cleaning. Data storage, 98–0212–2543–2, PennWell Corporation
120. Hungerhoff B, Sonnenschein H, Theil F (2002) Combining lipase-catalyzed enantiomer-selective acylation with fluorous phase labeling: a new method for the resolution of racemic alcohols. J Org Chem 67:1781–1785
121. Hungerhoff B, Sonnenschein H, Theil F (2001) Separation of enantiomers by extraction based on lipase-catalyzed enantiomer-selective fluorous-phase labeling. Angew Chem Int Ed 40:2492
122. Swaleh SM, Hungerhoff B, Sonnenschein H et al (2002) Separation of enantiomers by lipase-catalyzed fluorous-phase delabeling. Tetrahedron 58:4085–4089
123. Luo ZY, Swaleh SM, Theil F et al (2002) Resolution of 1-(2-naphthyl)ethanol by a combination of an enzyme-catalyzed kinetic resolution with a fluorous triphasic separative reaction. Org Lett 4:2585–2587
124. Beier P, O'Hagan D (2002) Enantiomeric partitioning using fluorous biphase methodology for lipase-mediated (trans)esterifications. Chem Commun 16:1680–1681
125. Maruyama T, Kotani T, Yamamura H et al (2004) Poly(ethylene glycol)-lipase complexes catalytically active in fluorous solvents. Org Biomol Chem 2:524–527
126. Saul S, Corr S, Micklefield J (2004) Biotransformations in low-boiling hydrofluorocarbon solvents. Angew Chem Int Ed 43:5519–5523
127. Seddon KR (1997) Ionic liquids for clean technology. J Chem Technol Biotechnol 68:351–356
128. Ray PC, Rakshit JN (1911) CLXVII.-Nitrites of the alkylammonium bases: ethylammonium nitrite, dimethylammonium nitrite, and trimethylammonium nitrite. J Chem Soc Trans 99:1470–1475
129. Walder P (1914). Bulletin de l'Académie Impériale des Sciences de St-Pétersbourg 405–422
130. Herfort M, Schneider H (1991) Spectroscopic studies of the solvent polarities of room-temperature liquid ethylammonium nitrate and its mixtures with polar-solvents. Liebigs Annalen Der Chemie 1:27–31
131. Hurley FH, Wier TP (1951) Electrodeposition of metals from fused quaternary ammonium salts. J Electrochem Soc 98:203–206
132. Chum HL, Koch VR, Miller LL et al (1975) Electrochemical scrutiny of organometallic iron complexes and hexamethylbenzene in a room-temperature molten-salt. J Am Chem Soc 97:3264–3265
133. Fry SE, Pienta NJ (1985) Effects of molten-salts on reactions – nucleophilic aromatic-substitution by halide-ions in molten dodecyltributylphosphonium salts. J Am Chem Soc 107:6399–6400
134. Boon JA, Levisky JA, Pflug JL et al (1986) Friedel crafts reactions in ambient-temperature molten-salts. J Org Chem 51:480–483
135. Wilkes JS, Zaworotko MJ (1992) Air and water stable 1-ethyl-3-methylimidazolium based ionic liquids. J Chem Soc-Chem Commun 13:965–967
136. Suarez PAZ, Dullius JEL, Einloft S et al (1996) The use of new ionic liquids in two-phase catalytic hydrogenation reaction by rhodium complexes. Polyhedron 15:1217–1219

137. Chauvin Y, Mussmann L, Olivier H (1996) A novel class of versatile solvents for two-phase catalysis: hydrogenation, isomerization, and hydroformylation of alkenes catalyzed by rhodium complexes in liquid 1,3-dialkylimidazolium salts. Angew Chem-Int Edit Engl 34:2698–2700
138. Poole CF (2004) Chromatographic and spectroscopic methods for the determination of solvent properties of room temperature ionic liquids. J Chromatogr A 1037:49–82
139. Earle MJ, Esperanca J, Gilea MA et al (2006) The distillation and volatility of ionic liquids. Nature 439:831–834
140. Bonhote P, Dias AP, Papageorgiou N et al (1996) Hydrophobic, highly conductive ambient-temperature molten salts. Inorg Chem 35:1168–1178
141. Galinski M, Lewandowski A, Stepniak I (2006) Ionic liquids as electrolytes. Electrochim Acta 51:5567–5580
142. Olivier-Bourbigou H, Magna L, Morvan D (2010) Ionic liquids and catalysis: recent progress from knowledge to applications. Appl Catal A373:1–56
143. Swatloski RP, Spear SK, Holbrey JD et al (2002) Dissolution of cellulose with ionic liquids. J Am Chem Soc 124:4974–4975
144. Abbott AP, Capper G, Davies DL et al (2006) Processing metal oxides using ionic liquids. Miner Process Extr Metall 115:15–18
145. Marsh KN, Boxall JA, Lichtenthaler R (2004) Room temperature ionic liquids and their mixtures – a review. Fluid Phase Equilib 219:93–98
146. Welton T (1999) Room-temperature ionic liquids. Solvents for synthesis and catalysis. Chem Rev 99:2071–2083
147. Dupont J, de Souza RF, Suarez PAZ (2002) Ionic liquid (molten salt) phase organometallic catalysis. Chem Rev 102:3667–3691
148. van Rantwijk F, Sheldon RA (2007) Biocatalysis in ionic liquids. Chem Rev 107:2757–2785
149. Parvulescu VI, Hardacre C (2007) Catalysis in ionic liquids. Chem Rev 107:2615–2665
150. Brennecke JF, Maginn EJ (2001) Ionic liquids: innovative fluids for chemical processing. AIChE J 47:2384–2389
151. Ito Y, Nohira T (2000) Non-conventional electrolytes for electrochemical applications. Electrochim Acta 45:2611–2622
152. Dupont J, Suarez PAZ (2006) Physico-chemical processes in imidazolium ionic liquids. Phys Chem Chem Phys 8:2441–2452
153. Endres F, El Abedin SZ (2006) Air and water stable ionic liquids in physical chemistry. Phys Chem Chem Phys 8:2101–2116
154. Koel M (2005) Ionic liquids in chemical analysis. Crit Rev Anal Chem 35:177–192
155. Anderson JL, Armstrong DW, Wei GT (2006) Ionic liquids in analytical chemistry. Anal Chem 78:2892–2902
156. Sheldon RA, Lau RM, Sorgedrager MJ et al (2002) Biocatalysis in ionic liquids. Green Chem 4:147–151
157. Moniruzzaman M, Nakashima K, Kamiya N et al (2010) Recent advances of enzymatic reactions in ionic liquids. Biochem Eng J 48:295–314. doi:10.1016/j.bej.2009.10.002
158. Erbeldinger M, Mesiano AJ, Russell AJ (2000) Enzymatic catalysis of formation of Z-aspartame in ionic liquid – an alternative to enzymatic catalysis in organic solvents. Biotechnol Prog 16:1129–1131
159. Patel RN (2001) Enzymatic synthesis of chiral intermediates for drug development. Adv Synth Catal 343:527–546
160. Kim K-W, Song B, Choi M-Y et al (2001) Biocatalysis in ionic liquids: markedly enhanced enantioselectivity of lipase. Org Lett 3:1507–1509
161. Lourenço NMT, Barreiros S, Afonso CAM (2007) Enzymatic resolution of indinavir precursor in ionic liquids with reuse of biocatalyst and media by product sublimation. Green Chem 9:734–736
162. Lourenço NMT, Afonso CAM (2007) One-pot enzymatic resolution and separation of sec-alcohols based on ionic acylating agents. Angew Chem Int Ed 46:8178–8181

Chapter 4
Green Solvents for Pharmaceutical Industry

Rosa María Martín-Aranda and J. López-Sanz

Abstract In the past few years, ionic liquids have received worldwide attention as replacements for organic solvents in the pharmaceutical industry. Recent efforts focus on the application of ionic liquids in separations, as replacements for organic solvents employed in the traditional separations. The potential to reduce pollution in industrial processes has led to investigations of ionic liquids as alternative reaction media for a variety of applications that conventionally use organic solvents. Environmental issues will drive the implementation of technologies based on ionic liquids in the pharmaceutical industry and the production of fine chemicals.

4.1 Pharmaceutical Green Chemistry

The importance of implementing greener chemical and engineering practices at every level of the pharmaceutical industry is gaining momentum nowadays. The pharmaceutical industry uses up large amounts of energy and produces more waste in comparison to other industries. Each kilo of useful product generates about 25–100 kilos of waste and requires 50–200 MJ of energy [1]. By definition, green chemistry is the design, development, and implementation of chemical products and processes to reduce or eliminate the use and generation of substances hazardous to human health and the environment [2]. The complexity of the pharmaceutical industry necessitates a holistic approach to greening its processes, starting with a paradigm shift from focusing only on waste management to an approach that encompasses manufacturing process efficiency, yield, and economic gains for pharmaceutical

R.M. Martin-Aranda (✉) • J. López-Sanz
Departamento de Química Inorgánica y Química Técnica, Universidad Nacional de Educación a Distancia, UNED, Paseo Senda del Rey, 9, 28040 Madrid, Spain
e-mail: rmartin@ccia.uned.es

A. Mohammad and Inamuddin (eds.), *Green Solvents I: Properties and Applications in Chemistry*, DOI 10.1007/978-94-007-1712-1_4,

companies. But unlike other sectors, the pharmaceutical industry must also comply with stringent current good manufacturing practice regulations and decisions about green, sustainable, and energy-saving opportunities.

In 2005, the American Chemical Society (ACS) Green Chemistry Institute and global pharmaceutical corporations developed the ACS GCI pharmaceutical roundtable to encourage innovation while catalyzing the integration of green chemistry and green engineering in the pharmaceutical industry. It is especially important for pharmaceutical companies to explore alternative processes. A key aspect of any green program is to minimize or eliminate the use of particularly harmful of hazardous chemicals. Solvents represent one of the largest cost components in chemical synthetic processes when one combines the cost of solvents with the disposal of mixed aqueous/solvent wastes. They account for 75–80% of the environmental impact and energy use in the life cycle of a pharmaceutical compound. Some companies have listed undesirable solvents and suggest suitable replacement. While substitution of a safer solvent or use of a biocatalyst to drive a reaction more efficiently is a useful strategy, a top-down design-based approach that incorporates green chemistry and engineering concepts and techniques would have a greater impact on these complex, multistep synthetic processes [3].

While Roger Sheldon's E-factor [4] is frequently used to highlight the relative inefficiency of pharmaceutical manufacture, the pharmaceutical industry is undoubtedly facing a series of challenges to bring forward innovative and effective drugs and therapies [5]. Pharmaceutical green chemistry begins with medicinal discovery chemistry, and there are many examples of green chemistry principles successfully applied in discovery. Good examples can be found in the use of microwave and ultrasound synthetic chemistry [6, 7], micromembrane reactors [8], and high-throughput screening [9] to produce drug candidates using less material and generating less residues in less time. Pharmaceutical green chemistry offers an opportunity to design of active pharmaceutical ingredients (APIS) as well as to offer innovative solutions in the new treatment and delivery options. Green chemistry principles applied to a pharmaceutical model clearly deliver improved economic and environmental performance. Embracing concepts of green chemistry will be an effort worth pursuing, not only for the sake of economic efficiency and environmental impact but also towards a sustainable future. Pharmaceutical chemists have many choices for the synthesis of molecules. These choices must deliver economic viability and responsibility to incorporate environmental consideration towards sustainability.

4.2 Organic Solvents in the Pharmaceutical Industry

Chemistry is dominated by the study of species in solution. Although any liquid might be used as a solvent, relatively few are generally used in the pharmaceutical industry. However, as the introduction of cleaner technologies has become a major concern in industry and academia, the search of alternative solvents is important. Grodowska and Parcewski have recently revised the organic solvents used for drug

Table 4.1 Solvents of frequent use in the chemical industry [10, 11]

	Category	Solvent
1	Ketones	Acetone
		Methyl ethyl ketone
		Methyl isobutyl ketone
		Mesityl oxide
2	Alcohols	Ethanol
		Butanol
		isobutanol
		Propylene glycol
3	Halogenated compounds	Chloroform
		Ethylene bromide
		Dichloromethane
		Carbon tetrachloride
4	Nitriles	Acetonitrile
5	Amines	Pyridine
6	Esters	Ethyl acetate
7	Aromatic hydrocarbons	Xylene
		Toluene
8	Aliphatic hydrocarbons	Hexane
		Cyclohexane
9	Ethers	1,4-Dioxane
		Tetrahydrofuran
		Ethyl ether
		Butyl ether
10	Amide	Dimethyl
		Formamide
11	Aqueous	Water
12	Sulfur containing	Dimethyl sulfoxide

production [10]; Table 4.1 lists the organic solvents most commonly used in the chemical industry [11].

The synthesis of an active pharmaceutical ingredient (API) consists of four steps: reaction, separation, purification, and drying. In the synthesis, the solvent may be critical parameter. During the extraction process of the API, products are separated from postreaction residues, and a large variety of solvents are employed in the extraction process. Crystallization process is used for the purification of an API. Crystal sizes and shape are important factors to determine the stability and solubility. After crystallization, solvents are removed, and the product is dried.

Lately, during the formulation, an API is prepared in a suitable form to be administrated. The drug products can be systemized as oral route, otorhinolaryngology route, local route, and intravenous and intramuscular route, and the forms can be tablets, capsules, spray, injectable solutions, and lyophilizate. Usually, some organic solvents are used as diluents or solubilizers when water cannot be used, and they are not removed from the final product. During the packaging, transportation, and storage, the residual solvents level in the drug product has an important role. The quality

of packing the pharmaceuticals is a key factor, and it can be done in many different types of containers such as blister packs, glass bottles, plastic, sachets, and vials. In this stage, final products are in contact with organic solvents. In view of this, pharmaceutical industries constantly attempt to eliminate the usage of organic solvents, and much effort was put to decrease the amount of organic solvents involved in API synthesis. Supercritical fluids [12], catalysis, and surfaces such as mesoporous materials, activated carbons and clays [13, 14], ionic liquids [15–19], or multiphase catalysis industry [20] are considered as potential reaction media.

Ionic liquids (ILs), often named "green solvents," are salts in which ions are poorly coordinated, being liquid, below 100°C or even at room temperature [21, 22]. These switchable solvents should facilitate organic synthesis and separations by eliminating the need to remove and replace solvents after each reaction step, providing a useful extension to the range of solvents that are available for synthetic chemistry.

This chapter summarizes some of the most recent and main results of research of the ionic liquids as a green alternative to organic solvents. By now, more than 250 ionic liquids have been investigated in depth, and the number of possibilities is practically unlimited, as a combination between a cation and an anion. The structure-properties relationship is being investigated, and the use of ionic liquid in the industry has been increasing.

4.3 Green Solvents Technology: A Potential Platform for the Pharmaceutical Industry

About a decade ago, mainly due to their tuneable properties and extremely low volatility, many industrial companies started to use ionic liquids, as potential alternative solvents. Some of them were incorporated to the pharmaceutical industry. The physical and chemical properties, such as density, conductivity, viscosity, hydrophobicity, hydrogen-bonding capability, and Lewis acidity, of ionic liquids can be designed depending on their future applications. The research groups of Chauvin and Seddon have conducted pioneering research in this area [23, 24].

There are hopes that their use will make the synthesis process more efficient and thus lower the usage of raw materials. However, ionic liquids do not appear in a general use due to the questions regarding toxicity, purity, and regulatory approval [25]. It is expected that the pharmaceutical industry will change conventional organic solvents to the new alternatives.

The first large industrial application of ionic liquids was introduced by the Bayerische Anilin und Soda Fabrik (BASF) (Fig. 4.1), using *N*-methylimidazoles to scavenge biphasic organic acids in manufacture of alkoxyphenyl phosphines [26], BASIL (biphasic acid scavenging with ionic liquids). Other large-scale industrial applications have been developed. The dimersol/difasol process by the Institute Français du Pétrole uses an ionic liquid to dissolve the catalyst and to separate it from the product [27].

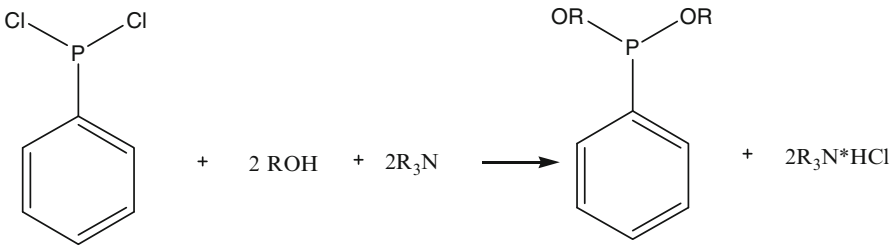

Fig. 4.1 Synthesis of diethoxyphenilphosphine [26]

These solvents also show possible advantages if used in biocatalysis [28]. They dissolve most of the potential substrates and products for biocatalytic reactions without the inhibiting effects on enzymes. Enzyme stability is often even better than in traditional media. Therefore, ionic liquids are valuable solvents for highly enantioselective reactions [29].

A very recent application of ionic liquids at high pressures and temperatures in multiphase systems has been developed [30] to fill the gap regarding properties that are relevant for processes using green solvents. Among these applications, the synthesis of urea with the help of CO_2 and ionic liquid [31] and emulsifications [32] has been investigated. Improvement in the separation efficiency has been also studied in the recent years by the use of supported ionic liquid membranes (SLM) [33]. The selective separation of organic compounds is a critical issue in the chemical industry. SLM based on ionic liquids have been shown to be a very attractive way for the highly selective transport of organic compounds involved in the synthesis of pharmaceutical and fine chemicals [34] such as esters, alcohols, organic acids [35], and amino acids [36].

More recently, ionic liquids have been used to tune the structures of micelles and enhance the solubilization of hydrophobic solutes in micelles [37], which is an important field of research in pharmaceutical industry [38]. Microcapsules containing ionic liquids with a new solvent extraction system have also been developed [39]. Additionally, water-immiscible room-temperature ionic liquids (RTILs) have been studied as potential pharmaceutical solvents and reservoirs [40]. RTILs might be useful as versatile solvents in the design of controlled release drug delivery systems and offer potential pharmaceutical excipients in a variety of scenarios. [41]. Interestingly, Rogers's group described the so-called third evolution of ionic liquids as active pharmaceutical ingredients [42]. While tremendous efforts of recent research have focused on the physical and chemical properties of ILs, the toxicity and biological properties have been debated [43], and there is a constant effort in recent years for establishing the structure/activity relationship between ionic liquids and toxicity [44]. Pharmaceutical salts have properties of "ionic liquid" and have existed for a long time. There are numerous examples in literature where pharmaceutical active compounds are salts of an active ion combination with a simple and inert counteranion. Moreover, a suitable drug can be combined with a second active substance by salt formation to give an ionic liquid–like compound. After dissolution,

such molecular drug combination will dissociate in the body fluid to follow the metabolic pathways. Obviously, more research has to be done to explore the biomedical applications of ionic liquids. A better understanding of their properties could help to design biologically active ILs and offer new treatment options or even personalized medication.

This chapter focuses mainly on recently published material and most representative developments and progress on ionic liquids and pharmaceutical applications during the last decade. The following are reported: acid/basic ionic liquids, oxidation, chiral functionalized ionic liquids, supported ILs, microwave- and ultrasound-assisted reactions, bioconversions on ILs, and ILs for analytical spectroscopy.

4.4 Acidic Ionic Liquids

The synthesis of natural molecules, pharmaceuticals, and other biologically active compounds has long been a significant branch of organic synthesis. The ionic liquid (IL) technology when used in place of classical organic solvents offers a new and environmentally benign approach towards modern synthetic chemistry [45]. To highlight their application as acidic catalysts and solvents, ten recent contributions in the literature have been selected. In 2004, the Mannich reaction using acidic ionic liquids was described [46]. This reaction provides one of the most basic and useful methods for the synthesis of nitrogenous biologically active compounds such as β-amino-carbonyl compounds (Fig. 4.2). Several Brønsted acidic ionic liquids were synthesized and successfully used as solvents and catalysts of three-component Mannich reactions of aldehydes, amines, and ketones at 25°C. Higher yields were obtained in the presence of $[Hmim]^+$ Tfa^- in comparison with other acidic ionic liquids, and it was reused four times without loss of activity.

Diphenylmethane and their derivatives are generally prepared via Friëdel-Crafts benzylation reaction (Fig. 4.3). Diphenylmethane has been used as important pharmaceutical intermediates and fine chemicals as scent, dyes, and lubricants.

Traditionally, they are prepared by using H_2SO_4, HF, or $AlCl_3$, as acid catalyst. However, to overcome the environmental problems of these acids, ionic liquids have been regarded as an alternative to conventional solvents [47]. 1-Butyl-3-methylimidazolium-BmimCl-$ZnCl_2$, 1-butyl-3-methylimidazolium-Bmim-$FeCl_3$, and 1-butyl-3-methylimidazolium-Bmim-$FeCl_2$ as both reaction media and Lewis acid

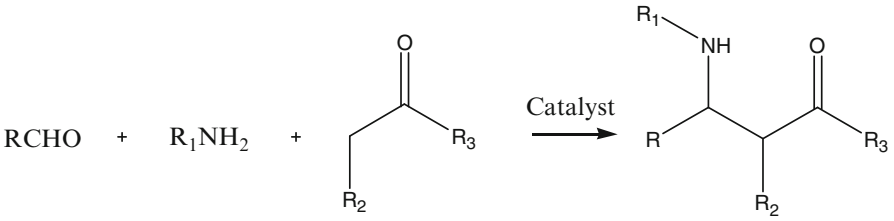

Fig. 4.2 Mannich reaction [46]

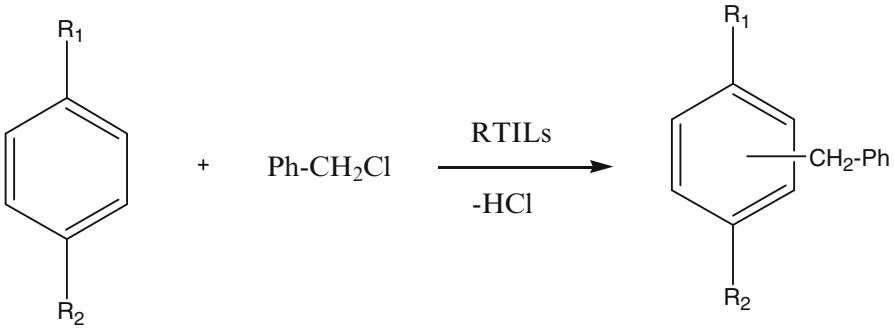

Fig. 4.3 Friëdel-Crafts reaction with benzyl chloride [47]

Table 4.2 Comparative results of Friëdel-Crafts reactions between benzene and benzyl chloride in different solvents

Solvent	Yield (%)	Selectivity (%)
Benzene	87	78
BmimCl-$FeCl_3$	100	100
BmimCl-$FeCl_2$	96.2	100
BmimCl-$ZnCl_2$	97.7	99.8

catalysts were investigated. In comparison, with the conventional organic solvents, faster reaction rate and higher selectivity to target products were obtained in such ionic liquids (Table 4.2).

(a) Reaction time: 2 h; ionic liquids at 80°C. Reaction conditions: 50 mmol of benzene and 5 mmol of benzyl chloride in 1 mL ionic liquid

Moreover, the ionic liquids could be recycled and reused eight times without loss of catalytic activity.

Friëdel-Crafts acylation using ionic liquids of BmimCl-$FeCl_3$, BmimCl-$AlCl_3$, and BmimCl-$ZnCl_2$ as dual catalyst solvents has been studied for the preparation of benzophenone and its derivatives [48]. Among them, BmimCl-$FeCl_3$ showed much higher catalytic activity than the other two ILs and in conventional organic solvents. Good yields (up to 97%) of acylation products were obtained in a short reaction time. Pharmaceutical industry generally uses benzophenone derivatives as farnesyl-transferase inhibitors, anesthetics, anti-inflammatory drugs, and photosensitizers.

Hajipour et al. [49] introduced a simple and efficient procedure for preparation of 1*H*-3-methylimidazolium hydrogen sulfate as Brønsted acidic ionic liquid, for the synthesis 1,1-diacetates from aldehydes under mild and solvent-free conditions at room temperature. 1,1-Diacetates (acylals) are one of the most useful carbonyl-protecting groups and useful intermediate in industry. A recyclable Brønsted acid–catalyzed direct benzylation, allylation, and propargylation of 1,3-dicarbonyl compounds with various alcohols as well as the tandem benzylation-cyclization-dehydration of 1,3-dicarbonyl compounds to give functionalized 4*H*-chromone in an ionic liquid system [50] were described for the first time in 2009.

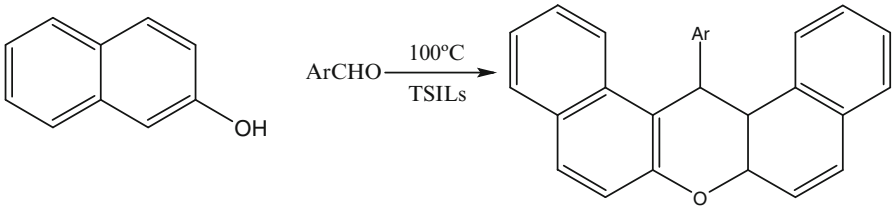

Fig. 4.4 Condensation of naphthol with aromatic aldehydes [51]

The synthesis of xanthene derivatives is of much importance because of their wide range of biological and pharmaceutical properties, such as antiviral and anti-inflammatory activities. In recent years, ionic liquids have been emerged as powerful alternative to conventional solvents in their synthesis. Fang and Liu [51] used a novel catalyst for the synthesis of 14-aryl-14*H*-dibenzo[*a*,*j*]xanthenes via one-pot condensation of β-naphthol and aromatic aldehydes in aqueous media. Yields ranged from 86% to 96% were obtained within 5–30 min (Fig. 4.4).

The acidic room-temperature ionic liquid 1-hexyl-3-methylimidazolium hydrogen sulfate [HMIM] [HSO_4] has recently been identified to have beneficial properties for applications in catalysis, and the conformational isomerism of this ionic liquid was studied by means of density functional theory calculations, infrared absorption, and Raman spectroscopy [52]. This IL was tested for the esterification of acetic acid with different alcohols affording an ester yield from 80% to 92%. [HMIM] [HSO_4] was also used in the ring-opening reactions of *N*-tosyl aziridines to synthesize β-amino ethers. A comparison of this 1 h with other acidic RTILs revealed that [HMIM] [HSO_4] is superior, providing very short reaction times and a yield as high as 97%.

Michael reaction is one of the most important C—C bond-forming reactions. The synthesis of indole derivatives has received much interest because a number of their derivatives show versatile biological activities. The application of Brønsted acidic task-specific ionic liquids (TSILs) as catalysts is growing continuously, and they have been synthesized to replace traditional mineral liquids acids [53].

Quinolines are very important compounds because of their pharmacological properties [54] in medicinal chemistry. These compounds are used as antimalarial drugs, antihypertensive, and anti-inflammatory agents. Despite quinoline usage in pharmaceutical industry, comparatively few methods for their preparation are reported [55]. Recently, the use of TSILs as catalysts was reported in a one-pot domino approach for the synthesis of quinoline derivatives in Friedländer reaction (Fig. 4.5).

Imidazolium-derived ionic liquid catalysts which are aprotic and of low antimicrobial and antifungal toxicity have been developed; these compounds act as efficient Brønsted acidic catalysts in the presence of protic additives and can be recycled 15 times without loss of activity [57].

Recently, ionic liquids have been found well suited as reaction media for MCRs (multicomponent reactions) in which the entropy of the reaction is decreased in

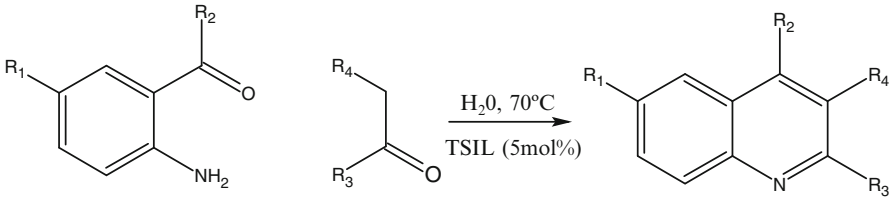

Fig. 4.5 TSIL-catalyzed Friedländer reaction [56]

the transition state. In view of this, newer reactions for synthesis of heterocyclic compounds have been developed using these green solvents. Among these, xanthenes and benzoxanthenes with multiple biological activities were prepared using PTSA in ionic liquid [bmim] BF_4 and also under solvent-free conditions. The products were obtained in high yields by a simple work-up at 80°C [58].

4.5 Basic Ionic Liquids

After the first high-yield green route to Pravadoline [59] using a base ionic liquid and most recent studies of the group of Corma [60] on the acid–base interactions in bifunctional acid–base ionic liquid organocatalysts, many ionic liquids with highly relevant applications in organic synthesis have been investigated. Corma described that the bifunctional molecules act as active, selective, and recyclable catalysts for Knoevenagel reactions. When an optimum distance between the acid and basic sites exists, the reaction increases by two orders of magnitude with respect to the counterpart monofunctional basic catalyst.

As part of ongoing studies directed towards the use of ionic liquids as catalysts and for solvents in synthesis of organic compounds, the benefits of two Brønsted acid–base ionic liquids as efficient and recyclable catalyst were studied for the synthesis of bis-(indolyl)-alkenes which are important bioactive metabolites [61]. For medicinal chemistry, indole is a privileged heterocyclic template with diverse pharmaceutical properties.

Recently, basic ionic liquids have aroused unprecedented interest because they showed more advantages such as catalytic efficiency and recycling of the ionic liquid than the combination of inorganic base and ionic liquid for the same base-catalyzed processes. A basic ionic liquid [bmIm]OH has been successfully applied to catalyze the Michael addition of active methylene compounds to conjugated ketones, esters, and nitriles [62].

The same basic ionic liquid [bmIm] OH showed a remarkable influence on the reaction by directing the addition of conjugated esters and nitriles to 1,2-dicarbonyl compounds to give bis-adducts in the Michael addition and alkylation of active methylene compounds [63]. More recently, the group of Selva [64] described the methodology for the green synthesis of a class of methylammonium and

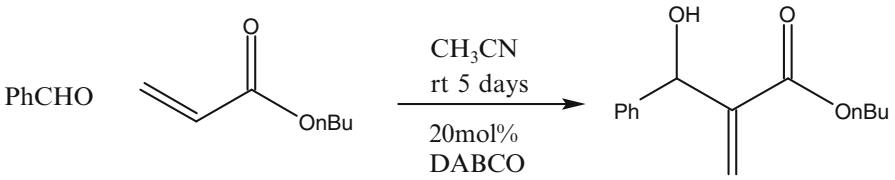

Fig. 4.6 Baylis-Hillman reaction under ionic catalysis [65]

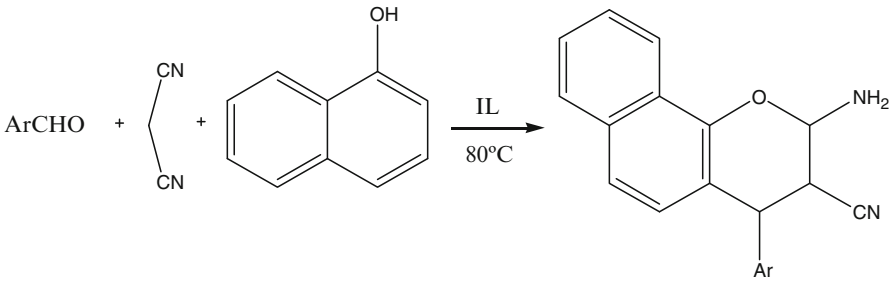

Fig. 4.7 Reaction for the synthesis of 2-amino-2-chromenes promoted by basic ionic liquid catalysis

methylphosphonium ionic liquids and how to tune their acid–base properties by anion exchange. The strongly basic system was enough to efficiently catalyze the Michael reaction.

The Baylis-Hillman reaction is an atom-economical reaction, but days or weeks have been required for the reaction to complete. A number of efforts have been made to accelerate it. Recently, a recyclable protic ionic liquid solvent-catalyst system, DABCO-AcOH-H_2O (1,4-diazabicyclo[2.2.2]octane, acetic acid and water), has been developed and used in the Baylis-Hillman reaction of aromatic aldehydes and cinnamaldehydes with acrylates and acrylonitrile. Comparable performance to free DABCO in traditional solvents was observed [65]. The DABCO-AcOH-H_2O catalyst could be reused five times without loss of activity (Fig. 4.6).

One of the tools used to combine economic aspects with the environmental ones is the multicomponent reaction (MCR) strategy. Recently, the use of MCR for the synthesis of 2-amino-2-chromones using the basic ionic liquid catalyst *N*,*N*-dimeth ylaminoethylbenzyldimethylammonium chloride was described [66] as an efficient catalyst under solvent-free conditions (Fig. 4.7).

The group of Martins [67] evaluated the efficacy of ionic liquids in the N-alkylation reaction of 3,5-dimethyl- and 5-trifluoro-methyl-3-methyl-1*H*-pyrazoles. The reaction time was shorter compared to the reaction performed in molecular solvents. These substituted pyrazoles are important synthetic targets in the pharmaceutical industry due to their numerous biological activities, including blockbuster drugs

such as celecoxib and Viagra. A convenient and rapid method for Knoevenagel condensation has been developed by using DABCO basic ionic liquid catalysts [68]. Excellent yields (up to 100%) in water at room temperature in short period were obtained. The catalyst could be recycled and reused seven times without activity loss.

A green protocol for the synthesis of quinazoline-2,4(1*H*,3*H*)-diones from CO_2 and 2-aminobenzonitriles using a basic ionic liquid [BmIm] OH has been reported by the group of Bhanage [69]. The ionic liquid was recovered and reused. Diones, which are key intermediates for several drugs (Prazosin, Bunazosin, and Doxazosin) were synthesized successfully.

The butyl methyl imidazolium hydroxide [BMIM] OH was the most effective catalyst in the synthesis of pyrroles promoted by task-specific basic catalyst in aqueous media [70]. Pyrrole is one of the most important heterocyclic compounds in medicinal chemistry and organic synthesis. Consequently, numerous procedures have been developed for the synthesis, being the present protocol a simple and high-yielding route that greatly decreases environmental pollution.

4.6 Oxidation on Ionic Liquids

The replacement of toxic heavy metals such as Cr and Mn, still widely employed in large amounts in chemical oxidations, is a major goal of current chemical research in the industry. In addition, the elimination of carcinogenic and bioaccumulating chlorinated solvents is highly desirable. Ionic liquids as a new green alternative for oxidations are being investigated. The selective oxidation of the alcoholic to the carbonyl functionality in organic molecules is one of the fundamental conversions. Carbonyl groups are commonly used as precursors for the preparation of drugs, vitamins, hormones, and dyes. A general concept of supported ionic liquid catalysts in supercritical phase has been introduced and successfully applied to the aerobic selective oxidation of alcohols [71]. The methodology synergically combines the advantages of the ionic liquid as a solvent promoter, dense-phase carbon dioxide as reaction solvent, and immobilized metal catalyst for easy product separation and catalyst recycling.

Benzaldehydes are widely used in different fields, such as pharmaceutical industry, and can be produced by gas- or liquid-phase oxidation of toluene or benzyl alcohol. The traditional routes for oxidation make separation process complex and expensive. In recent years, ionic liquids have been attracted much attention in catalytic oxidations. The Han group [72] has recently described the synthesis of Ni^{+2} containing ionic liquid 1-methyl-3-[(trietoxysilyl) propyl] imidazolium chloride (TMICI) immobilized on silica to catalyze styrene oxidation with H_2O_2 for producing benzaldehyde. Under solvent-free conditions, the conversion of styrene could reach 18.5%, and the selectivity to benzaldehyde could be as high as 95.9%. The catalyst was also effective in acetonitrile. The reaction time was short, and the

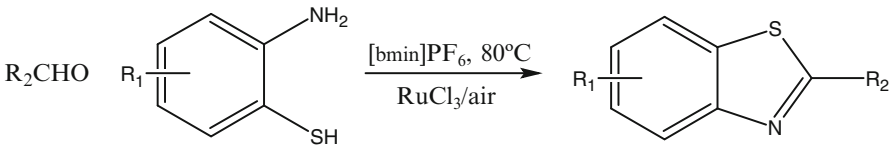

Fig. 4.8 Preparation of 2-substituted benzothiazoles under ionic liquid oxidation catalysis [73]

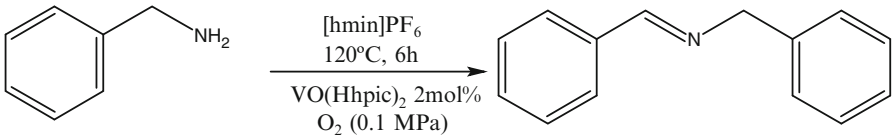

Fig. 4.9 Recycling study of VO $(Hhpic)_2$ in ionic liquid [74]

amount of catalyst used was relatively small. The conversion and selectivity obtained are among the highest reported in the literature. 2-Substituted benzothiazoles have shown intrinsic pharmacological and biological activities by acting as antitumor, antiviral, antimicrobial, and antioxidant agents. Due to their importance, numerous methods for the preparation have been developed (Fig. 4.8).

Very recently, the preparation of 2-substituted benzothiazoles has been described through $RuCl_3$-catalysed oxidative condensation of 2-amino benzenethiol with aldehyde by using ionic liquid as the reaction medium [73]. $RuCl_3$ in [bmim] PF_6 by employing air as oxidant is presented as the first example that $RuCl_3$ plays a catalytic role on the oxidation as the stoichiometric oxidant. Compared with the literature methods, advantages of this procedure include high efficiency, recyclable reaction medium, and an environmentally benign nature.

Considerable efforts have been devoted to accomplish the oxidation of alcohols to carbonyl compounds. By contrast, the corresponding amine to imine conversion by oxidation has remained undeveloped, despite the great utility of imines in the synthesis of industrial and biologically active compounds, such as amides, chiral amines, and nitrones.

The group of Ogawa [74] has reported the selective oxidation of benzylamines to produce directly the corresponding derivatives catalysed by an oxovanadium complex bearing 3-hydroxypicolinic acid (H_2 hpic), that is, VO $(Hhpic)_2$ under oxygen atmosphere (Fig. 4.9). Recycling feature of the catalyst in [hmim]PF_6 was demonstrated.

Run	1st	2nd	3rd	4th	5th	6th	7th	8th	9th
Yield(%)	69	70	64	67	68	66	56	58	68

4.7 Chiral Ionic Liquids and Chiral Amino Acid Ionic Liquids

In the last decade, catalytic enantioselective transformations have become one of the most studied fields in synthesis chemistry. Use of chiral ionic liquids in pharmaceutical sector could help companies to develop improved methods for synthesis of chiral products. Chiral drugs continue to be a force in the global pharmaceutical market. Many new drugs being introduced are single enantiomer. Kotschy and Paczal [75] provided an overview of the state of art of enantioselective homogeneous catalytic transformations in ionic liquids.

The search of new solvents and materials based on chiral ionic liquids is a topic of increasing importance since numerous applications including asymmetric synthesis, chiral chromatography, and stereoselective polymerizations [76] have been developed. This area also constitutes a new creative field since "tailor-made" structures can be imagined and prepared, such as chiral solvents, task-specific ionic liquids, and immobilized catalyst.

For the preparations of chiral ionic liquids, one of the most prominent starting materials is α-amino acids. Various chiral ionic liquids were previously built starting from α-amino acids [77]. For instance, (S)-histidine was described as a novel family of chiral ionic liquids. The group of Guillen obtained the key target [MBHis] [NTF_2] and studied their structure/physicochemical data relationship in the evolution of various enantioselective reactions (Fig. 4.10).

One of the most recent contributions from literature in the use of amino acids ionic liquids was published by Yan and Wang [78] on the synthesis of 1,4-disubstituted 1,2,3-triazoles. The reactions proceeded smoothly to generate the corresponding products in high yields (Fig. 4.11). The catalyst based on copper (1) and amino acid ionic liquid (AAIL) in [BMIM] BF_4 was used for six consecutive trials without loss of activity. This is an excellent example of "Click Chemistry" as a new approach to the synthesis of drug-like molecules that can accelerate the drug discovery yields that remain around 88% even if the reaction time was prolonged to 24 h (Table 4.3).

A novel family of chiral imidazolium-based ionic liquids containing a chiral moiety and a free hydroxy function have been designed and synthesized using isosorbide as a biorenewable substrate [79]. These chiral ionic liquids were found to

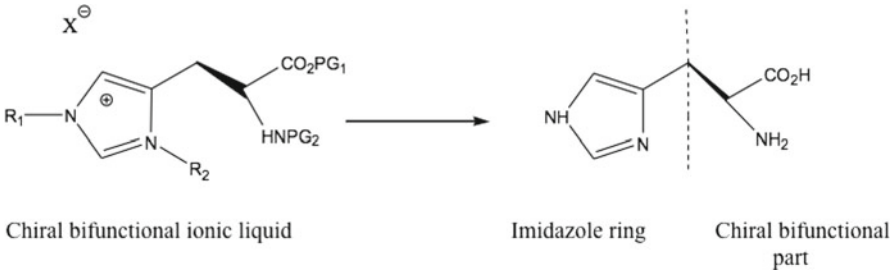

Fig. 4.10 Chiral ionic liquids starting from (S)-histidine [77]

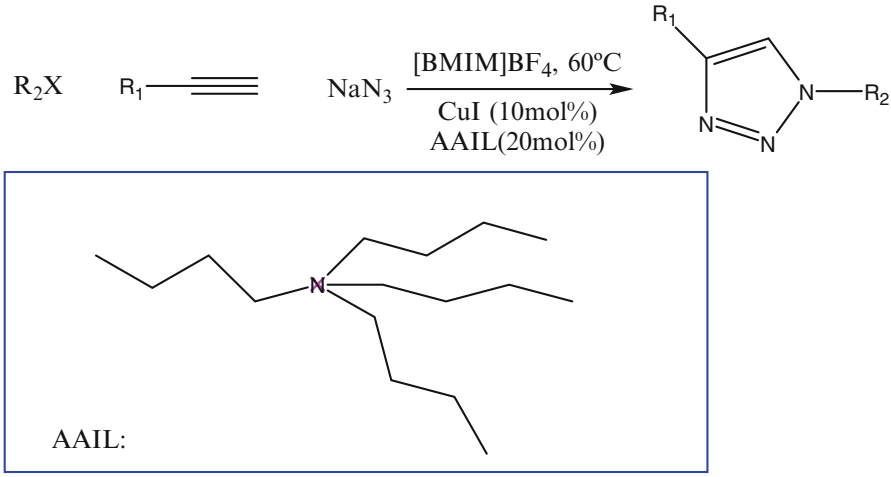

Fig. 4.11 Cu(I)- and AAIL-catalysed "Click Reaction" [78]

Table 4.3 Effect of solvent, time, and temperature on "Click Reaction"

Solvent	Time (h)	Temperature (°C)	Yield (%)
EtOH	10	60	86
MeOH	10	60	71
$[BMIM]BF_4$	10	60	88
$[BMIM]PF_6$	6	60	81
$[BMIM]BF_4$	24	60	88
$[BMIM]BF_4$	10	80	85
$[BMIM]BF_4$	10	40	21
$[BMIM]BF_4$	10	60	62

catalyze the aza-Diels-Alder reactions to give good yields and moderate enantioselectivities. The isosorbide and isomannide are industrially obtained by dehydration of D-sorbitol and D-mannitol and can therefore be considered as biomass products. They are widely used in their nitrate ester forms in the pharmaceutical industry.

Chiral analysis and chiral separations are important from technological point of view. Enantiomeric forms of many compounds are known to have different physiological and therapeutic effects. Very often, only one form of an enantiomeric pair is pharmacologically active. It is, thus, the pharmaceutical industry that needs effective methods to determine enantiomeric purity [80]. Yao et al. demonstrated a novel application of functional amino acid ionic liquid (AAILs) in chiral liquid-liquid extraction [81]. The functional AAILs were used as solvent and selector to separate racemic amino acids. Enantioselectivity of single-step extraction was up to 50.6% of enantiomeric excess. Moreover, the functional AAILs were found to be efficient extraction solvents for amino acids. This liquid-liquid extraction approach may extend the application of ionic liquids in chiral separations. Racemic β-amino acid

Table 4.4 Chiral extraction results of racemic amino acids using the functional ionic liquids [81]

Amino acid[a]	Ionic liquid	e.e (%)[b]
α-Phe	[Emim][Pro]	35.8 ± 0.1
α-Tyr	[Emim][Pro]	21.9 ± 0.3
α-His	[Emim][Pro]	4.0 ± 0.6
α-Trp	[Emim][Pro]	5.9 ± 0.3
β-Phe	[Emim][Pro]	0.3 ± 0.1
α-Phe	[Emim][Br]	0.6 ± 0.1

[a]Excess racemic amino acid (20 mg) was added into 100 μL ionic liquid
[b]Cu^{2+}: Pro^{-} is the molar ratio of $Cu(Ac)_2$ to $[C_n mim][L\text{-}Pro]$

was also extracted, and five racemic amino acids were studied. The extraction results are listed in Table 4.4.

It was found that e.e values for four racemic amino acids were in the order: Phe > Tyr > Trp > His, concluding that the separation mechanism is based on chiral ligand exchange.

A variety of pharmaceutical products, including propanolol, atenolol, warfarin, indoprofen, ibuprofen, among others, were successfully separated with the use of chiral ILs as electrolyte [82]. Secondary chiral alcohols are very attractive intermediates in organic synthesis of pharmaceutical industries. Enzymatic catalysis is a great tool that guides to obtain optically pure enantiomers. Ionic liquids are suitable media for enzymatic reactions [83]. Recently, chiral Mn (III) salen complex was an effective catalyst for oxidative kinetic resolution of secondary alcohols with excellent enantioselectivity (up to 98% e.e). Supported ionic liquid strategy has been applied for immobilization of a chiral Mn (III) salen complex and could be recycled five times without loss of activity [84].

4.8 Supported Ionic Liquids

The development of new heterogeneous catalysts as alternatives for liquid catalysts, which combine chemical efficiency and easy preparation, has become important for industrial applications [85, 86]. Different ionic liquids were used as catalysts for Friëdel-Crafts acylations. By using Lewis-acid ionic liquids supported on solids, a new type of catalysts for acylation of aromatic compounds was described [87]. Transesterification of β-ketoesters is an important organic reaction that has been catalysed by a number of homogeneous and heterogeneous acid catalysts. The group of Singh [88] reported the synthesis and characterization of sulphonic functionalized ionic liquid–exchanged montmorillonite clay nanocomposite as solid acid catalyst for the chemoselective transesterification of β-ketoesters with various alcohols in good yields.

Other silica-supported ionic liquids proved to be efficient heterogeneous catalysts for solventless synthesis of cyclic carbonates from epoxides and carbon dioxide

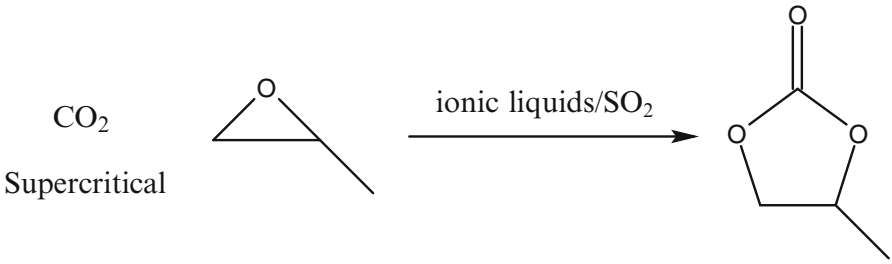

Fig. 4.12 Synthesis of propylene carbonate from propylene oxide and supercritical CO_2 [89]

under supercritical conditions [89]. High yields and excellent selectivity were obtained. These carbonates, such as ethylene carbonate and propylene carbonate, can be used as intermediates for organic synthesis and ingredients for pharmaceutical/fine chemicals in biomedical applications (Fig. 4.12).

Other Brønsted acidic functionalized ionic liquids have been reported as novel ecologically benign catalysts for some acid-catalysed reactions. Catechol *tert*-butylation is an industrially important reaction because the product 4-*tert*-butyl catechol can be used as stabilizer, polymerization inhibitor, antioxidant, as well as intermediate for the production of other pharmaceutical and agricultural chemicals [90].

Very recently, a magnetic nanosolid acid catalyst via grafting an ionic liquid onto Fe_3O_4 nanoparticles followed by sulfonation of phenyl groups in the ionic liquid has been prepared [91]. This catalyst exhibited high catalytic activity in the acetalization reactions. The catalytic performance of this novel material has been systematically studied in the acetal formation of benzaldehyde and ethylene glycol. The experimental results testify that this catalyst possesses high activity with a yield of 97% under mild reaction conditions.

In recent years, ionic liquids have been used in the protein film electrochemistry. Investigation on the direct electron transfer of redox proteins with the electrode is of great importance, and the research can provide a mechanistic understanding of the electron transfer in biological systems. Also the protein-modified electrodes can be used as biosensors. A biocomposite material composed of sodium alginate, Fe_2O_3 nanoparticles, and ionic liquid (1-decyl-3 methylimidazdium bromide) was fabricated and used for the immobilization of myoglobin on the surface of a carbon ionic electrode. Thus, the electrode has been used for the detection of different electroactive molecules or as a basal electrode for further modifications [92].

Condensation reactions, which are known to be catalysed by bases, are of great interest for the synthesis of pharmaceutical and fine chemicals. Industrially, these reactions are carried out in the homogeneous phase with KOH or NaOH. Basic ionic liquids used in base-catalysed processes have aroused unprecedented interest due to the numerous advantages such as high efficiency and catalyst recycling. It was demonstrated that supported ILs, instead of homogeneous ILs, led to further improvements in efficiency [93]. The Xia's group reported a catalytic system based on hydroxyapatite-encapsulated magnetic γ-Fe_2O_3 nanocrystallites functionalized with

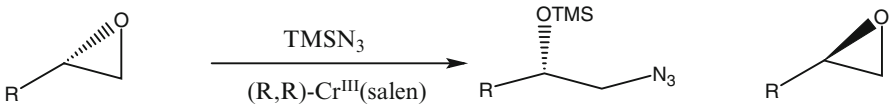

Fig. 4.13 Asymmetric ring-opening reactions of epoxides [95]

basic ILs, which proved to be efficient for low-temperature Knoevenagel liquid-phase reaction. Separation of the catalyst from the reaction mixture was readily achieved by simple magnetic decantation, being recycled the catalyst without appreciable loss of activity.

Immobilization of chiral ionic liquids has also been described by several authors. Reactions such as asymmetric hydrogenations of prochiral ketones catalysed by chiral Ru complex in mesoporous material–supported ionic liquid have been investigated by the group of Liu [94]. Asymmetric hydrogenation is one of the most important reactions to produce optically pure secondary alcohols, which are widely applied as building blocks and synthetic intermediates in pharmaceutical industry.

Asymmetric ring opening of epoxides (Fig. 4.13) has also been carried out on Cr (salen) complex impregnated on silica [95]. Good enantioselectivity for the ring opening is obtained with low leaching degree.

4.9 Microwave- and Ultrasound-Assisted Reactions Using Ionic Liquids

Since the incorporation of microwave- and ultrasound-assisted synthesis in the organic and pharmaceutical industry, these techniques have been accepted as common methods for reducing reaction times and increasing yields, compared with conventional methods. The ionic liquids are also suitable for microwave and ultrasound chemistry. Several reactions have been explored under microwave activation using ionic liquids. Nevertheless, only recently, it has been described the application of sonocatalysis in combination with ionic liquid to promote organic reactions of pharmaceutical interest. The group of Zang studied the condensation reactions of aldehydes and ketones with hydroxyl-amine hydrochloride in the presence of ionic liquid [bmIm]OH under ultrasound irradiation [96].

To our knowledge, there is no report of using the ionic liquid as catalyst for the preparation of oximes. This sonochemical synthesis of oximes in EtOH (Fig. 4.14) is a facile procedure for the generation of oximes. Oximes are very important in synthetic organic chemistry for the preparation of nitriles, amides, and nitro compounds.

Ultrasound-assisted solvent-free synthesis of lactic acid esters in novel SO_3H-functionalized Brønsted and ionic liquids was successfully performed by Li et al. [97]. They reported a green Fischer esterification of lactic acid with C2—C12 straight-chain aliphatic alcohols, cyclohexanol, and benzyl alcohol (Fig. 4.15).

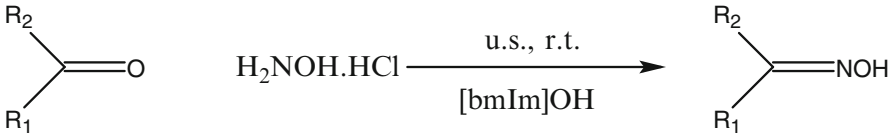

Fig. 4.14 Sonochemical synthesis of oximes in the presence of [bmIm]OH [96]

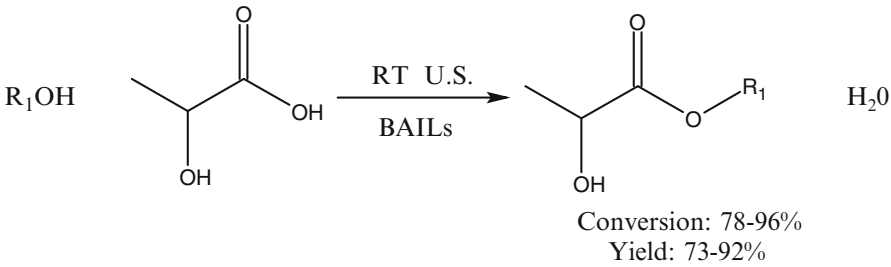

Fig. 4.15 Fisher esterification reaction in Brønsted acidic ionic liquids under ultrasonic irradiation [97]

Lactic acids and esters are important chemical products and intermediates in pharmaceutical industries and are used as additives, fragrances, and flavors.

Microwaves have also been used to promote the esterification of salicylic acid using Brønsted acidic ionic liquids as catalysts [98]. As fine chemical, methyl salicylate has been widely used as flavor and fragrance agents and cosmetic and dye carriers. Ionic liquids can be easily separated and reused affording high activity under microwave irradiation, and yields can reach up to 91–93%.

An efficient microwave protocol was described for the reaction of allylic acetate with various nucleophiles catalysed by Pd(0)-TPP Ts in an ionic liquid/water medium, via Tsuji-Trost reaction [99]. The reaction is a widely used method for C—C, C—N, and C—O bond formations with high chemo-, region-, and stereoselectivities. The microwave irradiation is very favorable for Tsuji-Trost reactions in [EMIm]BF_4/H_2O, and it assists this reaction greatly.

The microwave irradiation in combination with ionic liquids was used in the synthesis of N-substituted pyrroles [100]. Pyrroles are important heterocyclic compounds with remarkable pharmacological properties such as antibacterial, antiviral, antitumoral, and antioxidants. Pyrroles are also present in various bioactive drug molecules such as atrovastatin and anti-inflammatory agents. In view of this, several methods have been developed for the construction of pyrrole molecule. A rapid synthesis that has been achieved without formation of by-products was observed. The reaction was completed in 10 min using [Bmim]BF_4 ionic liquid.

The ionic liquid–based microwave-assisted methodology was also used in the pharmaceutical industry for extractions. Medicinal plants have served as an important source of drugs for treating diseases since ancient times. In modern pharmaceutical

industries, most of the medicines derive directly or indirectly from plants. The application of ionic liquids based microwave-assisted extraction (ILMAE) was developed by the group of Pan for extracting the alkaloids such as *N*-nornuciferine, *O*-nornuciferine, and nuciferine from lotus leaf [101]. 1-Alkyl-3-methylimidazoliums with different cations and anions were investigated, and the microwave parameters were optimized. Compared with the regular MAE and conventional extraction, shorter extraction time (from 2 h to 2 min) was observed, indicating that ILMAE is an efficient and rapid extraction technique.

Recently, ionic liquids, in conjunction with microwave irradiation, have been used for the rapid synthesis of optically active organosoluble polyamides [102].

4.10 Recent Bioconversions on Ionic Liquids

The pharmaceutical industry requires synthetic routes to be compatible with the increasingly restraining environmental regulations. There is an increasing trend towards reducing the use of organic solvents in industry due to environmental constrains and the adoption of green chemistry guidelines. The use of organic solvents, in order to improve the efficiency of bioconversion systems, is probably the most widely chosen approach to overcome the toxicity or low solubility of useful compounds. Significant efforts have been made towards replacement of conventional solvents in the industry. Green solvents can therefore be defined as environmentally compatible solvents. Recently, Marques et al. [28] investigated the steroid bioconversions using green solvents as model system towards green processes. They concluded that the use of green solvent improved product yield overcoming traditional organic solvents and allowing total conversion after 120 h. Microbial biodegradation and metabolite toxicity of pyridinium-based cation ionic liquids have been investigated. Development of ionic liquids is presented as an ideal test system to determine several levels of environmental impact [103].

Ionic liquids have been used in the study of enzymatic systems such as lipase-catalysed reactions [104, 105]. Lipases are used in various sectors, as pharmaceutical, food, or detergency industry affording better selectivity and milder reaction conditions than classical catalysis. These are most versatile biocatalysts for organic synthesis because of their commercial availability and catalytic ability. Nascimento et al. [106] have reported a comparative study on the enzymatic resolution of (RS)-methyl mandelate with *n*-butylamine using lipases in organic solvents and ionic liquids [BMIm]BF_4. They obtained high enantiomeric excess (e.e >99%) using organic solvent/ionic liquid mixtures. The solvent determines the configuration of the product (Fig. 4.16). Much better results were obtained when mixtures of chloroform or *tert*-butanol/[BMIm]BF_4 were used. The conversion degrees were in the range of 14–48, with e.e >99%.

Ionic liquids have been investigated for the activation and stabilization of enzymes [107], and it is considered a potential approach to achieve efficient enzymatic biotransformations. The enzymatic synthesis of sugar esters as nonionic

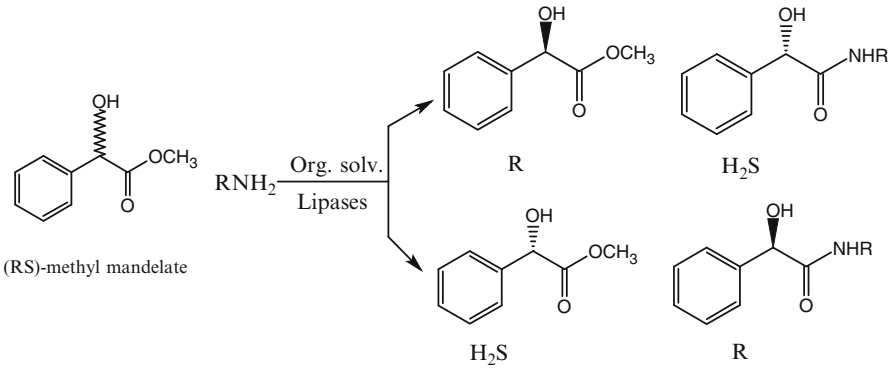

Fig. 4.16 Aminolysis of (RS)-methyl mandelate with *n*-butylamine [106]

surfactants in ionic liquids has also been described [108]. Sugar esters are widely used in pharmaceutical and cosmetic industry because of their amphiphilic nature. Their syntheses in organic solvents are difficult due to the low solubility of sugars. Ionic solvents have many advantages over organic solvents for enzymatic synthesis of sugar esters. The group of Lozano [109] investigated the enzymatic membrane reactor for resolution of ketoprofen in ionic liquids and supercritical carbon dioxide.

The interest in imidazolium cations has grown enormously in the last few years especially in the field of green solvents. Much attention has been focused on their physicochemical properties. The ability to form "supramolecules" can be used to modify the molecular reactivity by formation of supramolecular complexes between guests (reactive species) and the cationic receptors (imidazolium groups). Recently, an investigation to bring together the areas of supramolecular assembly and imidazolium cations has been reported [110].

4.11 Ionic Liquids for Analytical Spectroscopy

A dramatic increase in the number of publications on ILs in the last 5 years, after the review of Tran [111], underlines the tremendous interest in analytical chemistry. This is confirmed by the very recent review by Sun and Armstrong [112]. Extraction, gas and liquid chromatography, mass spectrometry, electrochemistry, and sensors and spectroscopy are the major subdisciplines where ionic liquids are expected to deliver valuable applications.

Liquid chromatography has been used to evaluate the behavior of ionic liquid cations in view of quantitative structure-retention relationship [113]. Application of perfluorinated acids as ion-pairing reagents for reversed-phase chromatography and retention-hydrophobicity relationships studies have been examined for selected β-blockers [114]. β-Adrenoceptor-blocking drugs are important substances in the

pharmaceutical industry, widely used in neurological, neuropsychiatric, and cardiovascular disorders. The obtained retention-hydrophobicity correlations indicate that, in the case of the drug examined in RP-HPLc, the retention is mainly governed by their hydrophobicity.

Using new solvent room-temperature ionic liquid matrix media, it has been possible to determine the residual solvents in pharmaceuticals by static headspace gas chromatography [115]. The feasibility of IL as diluents was demonstrated. Six solvents used in the synthesis of adefovir dipivoxil, i.e., acetonitrile, dichloromethane, *N*-methyl pyrrolidone, toluene, dimethylformamide, and n-butyl-ether, were analyzed. The method was evaluated and validated. Better sensitivities for the six solvents were gained with [bmim]BF_4 as diluent comparing with dimethyl sulphoxide (DMSO). The detection and quantification of residual solvents in drugs is an important measure for pharmaceutically quality control.

Biodegradable polymers are important in the medical field drug delivery and for the manufacture of dissolvable structures. However, characterization of these polymers often is difficult. A second-generation ionic liquid matrix was developed for the characterization of biodegradable polymers [116].

Monitoring of alkylation of heterocycles traditionally requires parallel analyses by chromatography. However, this can be time consuming and may not provide direct real-time analyses of reaction progress. In addition, chromatography cannot provide the molecular information on reaction mechanism and intermediates. Raman spectroscopy is a powerful noninvasive tool for real-time in situ monitoring of organic reactions [117]. With this technology, any liquid-phase reaction can be monitored, even in the presence of a solid catalyst. The group of Bañares [118] demonstrated the versatility of real-time Raman monitoring of the synthesis of 1-alkyl-2-methylimidazoles under both acid and basic heterogeneous media. This methodology can be applied to multiple reactions in the preparations of pharmaceuticals. The additional alkylation of N-alkylimidazoles would form imidazolium ionic liquids [119], and the studies of liquid-phase organic reactions by Raman spectroscopy provide a useful insight of imidazole alkylations with important industrial applications in pharmacy.

Acknowledgement JLS thanks Universidad Nacional de Educación a Distancia, UNED, for his PhD fellowship. This work is funded by the Spanish Ministry of Science and Innovation, MICINN (project CTQ2010–18652).

References

1. Anastas PT (1998) Green chemistry theory and practice. Oxford University Press, Oxford
2. Poliakoff M, Fitzpatrick JM, Farren TR, Anastas PT (2002) Green chemistry: science and politics of change. Science 297:807–810
3. Tucker JL (2006) Green chemistry, a pharmaceutical perspective. Org Proc Res Dev 10: 315–319
4. Sheldon RA, Arends I, Hanefeld U (2007) Green chemistry and catalysis. Wiley-VCH Verlag GmbH, Co, Weinheim. ISBN 978-3-527-307515-9

5. Rodríguez H, Bica K, Rogers R (2008) Ionic liquid technology: a potential new platform for the pharmaceutical industry. Trop J Pharm Res 7:1011–1012
6. Calvino-Casilda V, Martín-Aranda RM, López-Peinado AJ (2009) Microwave assisted green synthesis of long chain N-alkylimidazoles and medium chain N-alkyl-2-methylimidazoles with antiviral properties catalyzed by basic carbons. Catal Lett 129:281–286
7. Martín-Aranda RM, Calvino-Casilda V (2010) Last decade of research in sonochemistry for green organic synthesis. Recent Patents Eng 3:82–98
8. Yeung KL, Zhang X, Lau WN, Martín-Aranda RM (2005) Experiments and modelling of membrane microreactor. Catal Today 110:26–37
9. Crossley R (2002) From myths to leads. Mod Drug Discov 5:18–22
10. Grodowska K, Parczewski A (2010) Organic solvents in the pharmaceutical industry. Acta Pol Pharm Drug Res 67:3–12
11. Baver M, Barthelemy C (2001) In: Wypych G (ed) Handbook of solvents, 1st edn. Chemtec Publishing, Toronto/New York
12. York P, Kompella UB (2004) In: Shekunov BY (ed) Drugs and pharmaceutical sciences, vol 138, 1st edn. Marcel Dekker, New York
13. Martin-Aranda RM, Cejka J (2010) Recent advances in catalysis over mesoporous molecular sieves. Top Catal 53:141–153
14. Calvino-Casilda V, López-Peinado AJ, Duran-Valle CJ, Martín-Aranda RM (2010) Last decade of research on activated carbons as catalysts support in chemical processes. Catal Rev 52:325–380
15. Earle MJ, Seddon KR (2000) Ionic liquids. Green solvents for the future. Pure Appl Chem 72:1391–1398
16. Greaves TL, Drummond CJ (2008) Protic ionic liquids: properties and applications. Chem Rev 108:206–237
17. Zhao D, Wu M, Kou Y, Min E (2002) Ionic liquids: applications in catalysis. Catal Today 74:157–189
18. Mizuuchi H, Jaitely V, Murdan S, Florence AT (2008) Room temperature ionic liquids and their mixtures: potential pharmaceutical solvents. Eur J Pharm Sci 33:326–331
19. Oliver-Bourbigou H, Magna L, Morvan D (2010) Ionic liquids and catalysis: recent progress from knowledge to applications. Appl Catal A Gen 373:1–56
20. Hugl H, Nobis M (2008) Multiphase catalysis in industry. Top Organomet Chem 23:1–17
21. Welton T (1999) Room-temperature ionic liquid solvents for synthesis and catalysis. Chem Rev 99:2071–2083
22. Jessop PG, Heldebrant DJ, Li ECA, Liotta CL (2005) Green chemistry: reversible nonpolar-to-polar solvent. Nature 436:1102
23. Seddon K (2003) Ionic liquids: a taste of the future. Nat Mater 2:363–365
24. Chauvin Y, Oliver-Bourbigou H (1995) Nonaqueous ionic liquids and reaction solvents. Chem Tech 25:26–30
25. Jastorff B, Stormann R, Ranke J, Molter K, Stock F, Oberheitmann B, Hoffman J, Nuchter M, Ondurschka B, Filser B (2003) How hazardous are ionic liquids? Structure-activity relationships and biological testing as important elements for sustainability evaluation. Green Chem 5:136–142
26. Sheldon RA (2005) Green solvents for suitable organic synthesis: state of the art. Green Chem 7:267–278
27. Chauvin Y, Gilbert B, Giubard I (1990) Catalytic dimerization of alkanes by nickel complexes in organochloaluminate molten salts. Chem Commun 1715–1716
28. Marques MPC, Carvalho F, de Carvalho CCCR, Cabral JMS, Fernandes P (2010) Steroid bioconversion: towards green processes. Food Bioprod Proc 88:12–20
29. Tang F, Zhang Q, Ren D, Nie Z, Liu Q, Yao S (2010) Functional amino acid ionic liquids as solvents and selector in chiral extraction. J Chrom A 1217:4669–4674
30. Jaeger P, Eggers R (2009) Interfacial tension of ionic liquids at elevated pressures. Chem Eng Proc 48:1173–1176

31. Shi F, Deng Y, SiMa T, Peng J, Gu Y, Qiao B (2003) Alternatives to phosgene and carbon monoxide: synthesis of symmetric urea derivatives with carbon dioxide in ionic liquids. Angew Chem Int Ed 115:3379–3382
32. Jaeger P, Eggers R (2005) Liquid interfaces at high pressures in presence of compressible fluids. Thermochim Acta 438:16–21
33. Hernández-Fernández FJ, de los Ríos AP, Tomás-Alonso F, Gómez D, Villora G (2009) Improvement in separation efficiency of transesterification reaction compounds by the use of supported ionic liquid membranes based on the dicynamide anion. Desalination 224: 122–129
34. Brennecke JF, Maginn EJ (2001) Ionic liquids: innovative fluids for chemical processing. AICHE J 47:2384–2389
35. Hernández FJ, de los Ríos AP, Rubio M, Tomás-Alonso F, Gómez D, Villora G (2007) A novel application of supported liquid membranes based on ionic liquids to the selective simultaneous separation of the substrates and products of a transesterification reaction. J Membr Sci 293:73–80
36. Fortunato R, González-Muñoz MJ, Kubasiewicz M, Luque S, Alvarez JR, Afonso CAM, Coelho IM, Crespo JG (2005) Liquid membranes using ionic liquids: the influence of water on solute transport. J Membr Sci 249:153–162
37. Zhang J, Li W, Zhao Y, Han B, Yang G (2009) Enlargement of cationic alkyl polyglycoside micelles by ionic liquids. Colloids Surf A Physicochem Eng Aspects 336:110–114
38. Roy I, Ohulchanskyy TY, Pudavar HE, Bergey EJ, Oseroff AR, Morgan J, Dougherty TJ, Prasad PN (2003) Ceramic-based nanoparticles entrapping water-insoluble photosensitizing anticancer drugs: a novel drug-carrier system for photodynamic therapy (PDT). J Am Chem Soc 125:7860–7865
39. Xiang ZY, Lu YC, Zou LY, Gong ZXC, Luo GS (2008) Preparation of microcapsules containing ionic liquids with a new solvent extraction system. React Funct Polym 68:1260–1265
40. Jaitely V, Karatas A, Florence AT (2008) Water-immiscible room temperature ionic liquids (RTILs) as drug reservoirs for controlled release. Int J Pharm 354:168–173
41. Yung KKL, Perea JM, Smith CD, Stevens GW (2005) The partitioning behaviour of tyramine and 2-methoxyphenethylamine in a room temperature ionic liquid-water system compared to traditional organic water system. Sep Sci Technol 40:1555–1566
42. Hough WL, Smiglak M, Rodríguez H, Swatloski RP, Spear SK, Daly DT, Pernak J, Grisel JE, Carliss RD, Soutullo MD, Davis JH, Rogers RD (2007) The third evolution of ionic liquids: active pharmaceutical ingredients. New J Chem 31:1429–1436
43. Kumar V, Malhotra SV (2010) Ionic liquids as pharmaceutical salts: a historical perspective. In: Malhotra S (ed) Ionic liquid applications: pharmaceuticals, therapeutics and biotechnology, ACS symposium series. American Chemical Society, Washington, DC
44. Ranke J, Stolte S, Störmann R, Arning J, Jastorff B (2007) Ceramic-based nanoparticles entrapping water-insoluble photosensitizing anticancer drugs: a novel drug-carrier system for photodynamic therapy (PDT). Chem Rev 107:2183–2206
45. Keskin S, Kayrak-Talay D, Akman U, Hortaçsu O (2007) A review of ionic liquids towards supercritical fluid applications. J Supercrit Fluids 43:150–180
46. Zhao G, Jiang T, Gao H, Han B, Huang J, Sun D (2004) Mannich reaction using acidic ionic liquids as catalysts and solvents. Green Chem 7:75–77
47. Yin D, Li C, Tao L, Yu N, Hu S, Yin D (2006) Synthesis of diphenylmethane derivatives in Lewis acidic ionic liquids. J Mol Catal A Chem 245:260–265
48. Li C, Liu W, Zhao Z (2007) Efficient synthesis of benzophenone derivatives in Lewis acid ionic liquids. Catal Commun 8:1834–1837
49. Hajipour AR, Khazdooz L, Ruyho AE (2008) Brønsted acidic ionic liquid as an efficient catalyst for chemoselective synthesis of 1,1-diacetates under solvent-free conditions. Catal Commun 9:89–96
50. Funabiki K, Komeda T, Kubota Y, Matsui M (2009) Brønsted acid ionic catalyzed direct benzylation, allylation and propargylation of 1,3-dicarbonyl compounds with alcohols as well as one-pot synthesis of 44-chromones. Tetrahedron 65:7457–7463

51. Fang D, Liu ZL (2010) Synthesis of 14-Arge-14H-dibenzo [a, j]xanthenes catalyzed by acrylic acidic ionic liquids. J Het Chem 47:509–512
52. Kiefer J, Pye CC (2010) Structure of the room-temperature ionic liquid 1-Hexil-3-methylimida zolium hydrogen sulphate: conformational isomerism. J Phys Chem 114:6713–6720
53. Das S, Rahman M, Kundu D, Majee A, Hajra A (2010) Task-specific ionic-liquid-catalyzed efficient synthesis of indole derivatives under solvent-free conditions. Can J Chem 88: 150–154
54. Marco-Centelles J, Perez-Mayoral E, Samadi A, Carreiras MDC, Soriano E (2009) Recent advances in the Friedlander reaction. Chem Rev 109:2652–2671
55. Domínguez-Fernández F, López-Sanz J, Pérez-Mayoral E, Bek D, Martín-Aranda RM, López-Peinado AJ, Čejka J (2009) Novel basic mesoporous catalysts for Friedländer reaction from 2-aminoaryl ketones: Quinolin-2(1H)-ones vs. quinolines. Chem Cat Chem 1:241–243
56. Akbari J, Heydari A, Kalhor HR, Kohan SA (2010) Sulfonic acid functionalized ionic liquid in combinatorial approach, a recyclable and water tolerant-acidic catalyst for one-pot Friëdlander Quinoline synthesis. J Comb Chem 12:137–140
57. Myles L, Gore R, SpulaK M, Gathergood N, Connon SJ (2010) Highly recyclable, imidazolium derived ionic liquids of low antimicrobial and antifungal toxicity: a new strategy for acid catalysis. Green Chem 12:1157–1162
58. Khurana JM, Magoo D (2009) pTSA-catalyzed one-pot synthesis of 12-aryl-8,9,10,12-tetra hydrobenzo [∝] xanthen-11-ones in ionic liquid and neat conditions. Tetrahedron Lett 50: 4777–4780
59. Earle MJ, McCormac PB, Seddon KR (2000) The first high yield green route to a pharmaceutical in a room temperature ionic liquid. Green Chem 2:261–262
60. Boronat M, Climent MJ, Corma A, Iborra S, Montón R, Sabater MJ (2010) Bifunctional acid–base ionic liquid organocatalysts with a controlled distance between acid and base sites. Chem Eur J 16:1221–1231
61. Rad-Moghadam K, Sharifi-Kiasaraie M (2009) Indole 3-alkylation/vinylation under catalysis of the guanidinium ionic liquids. Tetrahedron 65:8816–8820
62. Xu JM, Liu BK, Wu WB, Qian C, Wu Q, Lin XF (2006) Basic ionic liquid as catalysis and reaction medium: a novel and green protocol for the Markovnikov addition of N-heterocycles to vinyl esters, using a task-specific ionic liquid, [bmIm]OH. J Org Chem 71:3991–3993
63. Raw B, Banerjee S, Jana R (2007) Ionic liquid as catalyst and solvent: the remarkable effect of a basic ionic liquid, [bmIm] OH on Michael addition and alkylation of active methylene compounds. Tetrahedron 63:776–782
64. Fabris M, Lucchini V, Noe M, Perosa A, Selva M (2009) Ionic liquids made with dimethyl carbonate: solvents as well as boosted basic catalysts for the Michael reaction. Chem Eur J 15:12273–12282
65. Song Y, Ke H, Wang N, Wang L, Zou G (2009) Baylis-Hillman reaction promoted by a recyclable protic ionic-liquid solvent-catalyst system: DABCO-AcOH-H_2O. Tetrahedron 65: 9086–9090
66. Chen L, Huang XJ, Li YQ, Zhou MY, Zheng WJ (2009) A one-pot multicomponent reaction for the synthesis of 2-amino-2 chromenes promoted by N, N-dimethyl-amino-functionalized basic ionic liquid catalysis under solvent-free conditions. Monatsh Chem 140:45–47
67. Frizzo CP, Moreira DN, Guarda EA, Fiss GF, Marzari MRB, Zonatta N, Bonacorso HG, Martins MAP (2009) Ionic liquid as catalyst in the synthesis of N-alkyl trifluoromethyl pyrazoles. Catal Commun 10:1153–1156
68. Xu DZ, Liu Y, Shi S, Wang Y (2010) A simple, efficient and green procedure for Knoevenagel condensation catalyzed by [C_4dabco] [BF_4] ionic liquid in water. Green Chem 12:514–517
69. Patil YP, Tambade PJ, Deshukh KM, Bhanage BM (2009) Synthesis of quinazoline-2,4 (1H,3H)-diones from carbon dioxide and 2-aminobenzonitriles using [Bmim] OH as a homogeneous recyclable catalyst. Catal Today 148:355–360
70. Yavari I, Kowsan E (2009) Efficient and green synthesis of tetrasubstituted pyrroles promoted by task-specific basic ionic liquids as catalyst in aqueous media. Mol Divers 13:519–528

71. Ciriminna R, Hesemann P, Moreau JJE, Carraro M, Campestrini S, Pagliro M (2006) Aerobic oxidation of alcohols in carbon dioxide with silica-supported ionic liquids doped with perruthenate. Chem Eur J 12:5220–5224
72. Liu G, Hou M, Song J, Zhang Z, Wu T, Han B (2010) Ni^{+2}-containing ionic liquid immobilized on silica: effective catalyst for styrene oxidation with H_2O_2 at solvent-free condition. J Mol Catal A Chem 316:90–94
73. Fan X, Wang Y, He Y, Zhang X, Wang J (2010) Ru (III)- catalyzed oxidative reaction in ionic liquid: an efficient and practical route to 2-substituted benzothiazoles and their hybrids with pyrimidine nucleoside. Tetrahedron Lett 51:3493–3496
74. Kodama S, Yoshida J, Nomoto A, Ueta Y, Yano S, Lleshima M, Ogawa A (2010) Direct conversion of benzylamines to imines via atmospheric oxidation in the presence of $VO(Hhpic)_2$ catalyst. Tetrahedron Lett 51:2450–2452
75. Paczal A, Kotschy A (2007) Asymmetric synthesis in ionic liquids. Monatshefte für Chemie 138:1115–1123
76. Ternois J, Ferron L, Coquerel G, Guillen F, Plaquevent JC (2010) In: Malhotra SV (ed) Ionic liquids: new opportunities for the chemistry of amino acids, peptides and pharmaceuticals compounds in Ionic liquid applications: pharmaceuticals, therapeutics and biotechnology. ACS symposium series, chap 2, vol 1038. American Chemical Society, Washington, DC
77. Guillen F, Brégeon D, Planquevent JC (2006) (S)-Histidine: the ideal precursor for a novel family of chiral aminoacid and peptidic ionic liquids. Tetrahedron Lett 47:1245–1248
78. Yan J, Wang L (2010) Synthesis of 1,4-disubstituted 1,2,3,-triazoles by use of copper (1) and amino acids liquid catalytic system. Synthesis 3:447–452
79. Van Blu ON, Aupoix A, Vo-Thanh G (2009) Synthesis of novel chiral imidazolium-based ionic liquids derived from isosorbide and their applications in asymmetric aza Diels-Alder reaction. Tetrahedron 65:2260–2265
80. Tran CD, Oliveira D, Yu S (2006) Chiral ionic liquid that functions as both solvents and chiral selector for the determination of enantiomeric compositions of pharmaceutical products. Anal Chem 78(4):1349–1356
81. Tang F, Zhang Q, Ren D, Nie Z, Liu Q, Yao S (2010) Functional aminoacid ionic liquids as solvent and selector in chiral extractions. J Chrom A 121:4669–4674
82. Tran CD, Mejac I (2008) Chiral ionic liquids for enantioseparation of pharmaceutical products by capillary electrophoresis. J Chrom 120:204–209
83. Bogel-Lukasik R (2007) Sustainable processes employing ionic liquids for secondary alcohols separation. Monatshefte Für Chemie 138:1137–1144
84. Sahoo S, Kumar P, Lefebvre F, Halligudi SB (2008) A chiral Mn (III) salen complex immobilized onto ionic liquid modified mesoporous silica for oxidative kinetic resolution of secondary alcohol. Tetrahedron Lett 49:4865–4868
85. Karout A, Pierre AC (2009) Porous texture of silica aerogels made with ionic liquids as gelation catalysts. J Sol Gel Sci Technol 49:364–372
86. Paul M, Pal N, Rana ES, Sinha AK, Bhaumik A (2009) New mesoporous titanium-phosphorus mixed oxides having bifunctional catalytic activity. Catal Commun 10:2041–2045
87. Valkenberg MH, de Castro C, Hölderich WF (2001) Friedel-Crafts acylation of aromatic catalysed by supported ionic liquids. Appl Catal A Gen 215:185–190
88. Ratti R, Kaur S, Vaultier M, Sing V (2010) Preparation, characterization and catalytic activity of MMT-clay exchanged sulphonic acid functionalized ionic liquid for transesterification of β-ketoesters. Catal Commun 11:503–507
89. Wang JQ, Yue XD, Cai F, He LN (2007) Solventless synthesis of cyclic carbonates from carbon dioxide and epoxides catalyzed by silica-supported ionic liquids under supercritical conditions. Catal Commun 8:167–172
90. Nie X, Liu X, Gao L, Liu M, Song C, Guo X (2010) SO_3H-Functionalized ionic liquid catalyzed alkylation of catechol with tert-butyl alcohol. Ind Eng Chem Res 49:8157–8163
91. Wang P, Kong A, Wang W, Zhu H, Shan Y (2010) Facile preparation of ionic liquid functionalized magnetic nano-solid acid catalysts for acetalization reaction. Catal Lett 135: 159–164

92. Zhan T, Xi M, Wang Y, Sun W, Hou W (2010) Direct electrochemistry and electrocatalysis of myoglobin immobilized on Fe_2O_3 nanoparticle-sodium alginate-ionic liquid composite-modified electrode. J Colloid Interf Sci 346:188–193
93. Zhang Y, Zhao Y, Xia C (2009) Basic ionic liquids supported on hydroxyapatite-encapsulated γ-Fe_2O_3 nanocrystallites: heterogeneous catalyst for aqueous Knoevenagel condensation. J Mol Catal A Chem 306:107–112
94. Lou LL, Peng X, Yu K, Liu S (2008) Asymmetric hydrogenation of acetophenone catalyzed by chiral RU complex in mesoporous material supported ionic liquid. Catal Commun 9:1891–1893
95. Dioos BML, Jacobs PA (2006) Heterogenisation of dimeric Cr (salen) with supported ionic liquids. J Catal 243:217–219
96. Zang H, Wang M, Cheng BW, Song CJ (2009) Ultrasound-promoted synthesis of oximes catalyzed by a basic ionic liquid [bmIm]OH. Ultrason Sonochem 16:301–303
97. Li X, Lin Q, Ma L (2010) Ultrasound-assisted solvent-free synthesis of lactic acid esters in novel SO_3H-functionalized Brønsted acidic ionic liquids. Ultrason Sonochem 17:752–755
98. Shi H, Zhu W, Li H, Liu H, Zhang M, Yan Y, Wang Z (2010) Microwave-accelerated esterification of salicylic acid using Brønsted acidic ionic liquids as catalysts. Catal Commun 11:588–591
99. In L, Duan X, Liang Y (2005) Ionic liquid/water as recyclable medium for Tsuji-Trost reaction assisted by microwave. Tetrahedron Lett 46:3469–3472
100. Meshrani HM, Prasad BRV, Kumar DA (2010) A green approach for efficient synthesis of N-substituted pyrroles in ionic liquid under microwave irradiation. Tetrahedron Lett 51:3477–3480
101. Ma W, Lu Y, Hu R, Chen J, Zhang Z, Pan Y (2010) Application of ionic liquids based microwave-assisted extraction of three alkaloids N-nornuciferine, O-nornuciferine and nuciferine from lotus leaf. Talanta 80:1292–1297
102. Shadpour M, Hojjat S (2010) Ionic liquid as a green media for rapid synthesis of optically active organosoluble polyamides. Design Monom Polym 13:377–386
103. Docherty KM, Joyce MV, Kulacki KJ, Kulpa CF (2010) Microbial biodegradation and metabolite toxicity of three pyridinium-based cation ionic liquids. Green Chem 12:701–712
104. Villeneuve P (2007) Lipases in lipophilization reactions. Biotechnol Adv 25:515–536
105. Malhotra S (2010) In: Malhotra S (ed) Ionic liquid applications: pharmaceutics, therapeutics and biotechnology. Oxford University Press, London
106. Pilissão C, Nascimiento MG (2006) Effects of organic solvents and ionic liquids on the aminolysis of (RS)-methyl mandelate catalyzed by liposes. Tetrahedron Asymm 17:428–433
107. Moniruzzaman M, Kayima N, Goto M (2010) Activation and stabilization of enzymes in ionic liquids. Org Biomol Chem 8:2887–2899
108. Chen ZG, Zong MH, Zx Gu (2007) Enzymatic synthesis of sugar esters in ionic liquids. Chin J Org Chem 27:1448–1452
109. Lozano P, De DiegoT, Vaultier M, Iborra JL (2010) In: Malhotra S (ed) Enzymatic membrane reactor for resolution of ketoprofen in ILS and supercritical carbon dioxide in Ionic Liquid applications: pharmaceuticals, therapeutics and biotechnology. (ACS) symposium series, chap 3; vol 1038. American Chemical Society, Washington, DC
110. Noujeim N, Lec Lerq L, Schmitzer A (2010) Imidazolium cations in organic chemistry: from chemzymes to supramolecular building blocs. Curr Org Chem 14:1500–1516
111. Tran CD (2007) Ionic liquids for and by analytical spectroscopy. Anal Lett 40:2447–2464
112. Sun P, Armstrong W (2010) Ionic liquids in analytical chemistry. Anal Chim Acta 661:1–16
113. Molíková M, Markeszewki MJ, Kaliszan R, Jandera P (2010) Chromatographic behaviour of ionic liquid cations in view of quantitative structure-retention relationship. J Chrom A 1217:1305–1312
114. Flieger J (2010) Application of perfluorinated acids as ion-pairing reagents for reversed-phase chromatography and retention-hydrophobia relationships studies of selected β-blockers. J Chrom A 1217:540–549

115. Lui F, Jiang Y (2007) Room temperature ionic liquid as matrix medium for the determination of residual solvents in pharmaceuticals by static headspace gas chromatography. J Chrom A 1167:116–119
116. Berthod A, Crank JA, Rundlett KL, Armstrong DW (2009) A second-generation ionic liquid matrix-assisted laser desorption/ionization matrix for effective mass spectrometric analysis of biodegradable polymers. Rapid Commun Mass Spectrom 23:3409–3422
117. Bañares MA, Mest G (2009) Structural characterization of operating catalysts by Raman spectroscopy. Adv Catal 52:43–128
118. Calvino-Casilda V, Bañares MA, Lozano-Diz E (2010) Raman monitoring of antiviral intermediates of synthesis: 1-substituted imidazoles. Application note. Raman spectroscopy. Perkin Elmer, Seer Green
119. Calvino-Casilda V, Pérez-Mayoral E, Bañares MA, Lozano-Diz E (2010) Real time Raman monitoring of dry media heterogeneous alkylation of imidazole with acidic and basic catalysis. Chem Eng J 161:371–376

Chapter 5
Limonene as Green Solvent for Extraction of Natural Products

Smain Chemat, Valérie Tomao, and Farid Chemat

Abstract This chapter presents a complete picture of current knowledge on a useful and green biosolvent "*d*-limonene" obtained from citrus peels through a steam distillation procedure followed by a deterpenation process. Limonene is a substitute for petroleum solvents such as dichloromethane, toluene, or hexane for the extraction of natural products. This chapter provides the necessary theoretical background and some details about extraction using limonene, the techniques, the mechanism, some applications, and environmental impacts. The main benefits are decreases in extraction times, the amount of energy used, solvents recycled, and CO_2 emissions.

5.1 Introduction

Natural products, such as aromatic herbs and spices, fruits and vegetables, medicinal plants, micro and macro algae, coffee and cocoa, meal and flours, are complex mixtures of vitamins, sugars, proteins and lipids, fibers, aromas, essential oils, pigments, antioxidants, and other organic and mineral compounds. Direct analyses are generally not possible to achieve due to the complexity of food samples and the requirement of useful samples in a liquid form. Furthermore, the direct application of raw materials is impossible because instead of 1 g of essential oil used for aromatization of food, cosmetic, or perfume industry, 1 kg of raw aromatic material will be

S. Chemat
Centre de Recherche Scientifique et Technique en Analyses Physico-chimiques (CRAPC), BP 248 Alger RP, Algiers 16004, Algeria
e-mail: Chemats@yahoo.fr

V. Tomao • F. Chemat (✉)
Université d'Avignon et des Pays de Vaucluse, INRA, UMR 408, Avignon F-84000, France
e-mail: farid.chemat@univ-avignon.fr

A. Mohammad and Inamuddin (eds.), *Green Solvents I: Properties and Applications in Chemistry*, DOI 10.1007/978-94-007-1712-1_5,

required. Different methods can be used for extraction of concentrate and valuable materials, for example, Soxhlet extraction, maceration, elution, and simultaneous distillation-extraction. All of these techniques need petroleum solvent to extract the biocompounds. Losses of some compounds, low extraction efficiency, time- and energy-consuming procedures (prolonged heating and stirring in boiling solvent, use of large volumes of solvents, etc.) may be encountered using these "petroleum" solvent extraction methods. These shortcomings have led to the use of new sustainable "green" techniques and/or solvents in extraction, which typically involve less solvent and energy, such as ultrasound- or microwave-assisted extraction, or involve alternative solvent, such as supercritical fluid extraction, subcritical water extraction, and use of alternative solvent for the biorefinery approach. Extraction under extreme or nonclassical conditions is currently a dynamically developing area in applied research and industry. Alternatives to conventional extraction procedures or to conventional petroleum solvents may increase production efficiency and contribute to environmental preservation by replacing the use of petroleum solvents by biosolvents and reducing fossil energy and generation of hazardous substances.

With the increasing energy and petrol prices and the drive to reduce CO_2 and volatile organic compounds (VOCs) emissions, chemical and food industries are in search of new technologies in order to reduce energy and solvents consumption, to meet legal requirements on emissions, product/process safety, and increased quality as well as functionality. Solvent extraction of natural products is one of the promising innovation themes that could contribute to sustainable growth of chemical and food industries. The existing extraction technologies have considerable technological and scientific bottlenecks to overcome: often requiring up to 50% of investments in a new plant and more than 70% of total process energy used and less than 50% of recycled solvent lost as VOCs emissions in food, fine chemicals, and pharmaceutical industries.

This chapter presents a complete picture of current knowledge on extraction using green solvent such as *d*-limonene. It provides the necessary theoretical background and some details about extraction using limonene, the techniques, some applications, and environmental impacts.

5.2 Limonene: Origin, Applications, and Properties

d-Limonene is a monoterpene hydrocarbon found as the major essential oil component of citrus peels (Fig. 5.1). With a production of more than 50 million tons, the orange juice industry represents an important source for *d*-limonene and a challenging research pilot platform for the valorization of by-products. It is considered as GRAS (generally recognized as safe) material by the US Food and Drug Administration and has been playing an important role in flavors and fragrances as well as cleaning/degreasing agent in industry and in household applications [1, 2].

d-Limonene stands as a valuable replacement for traditional solvents, many of which emit polyaromatic hydrocarbons (PAHs) or fumes from volatile organic

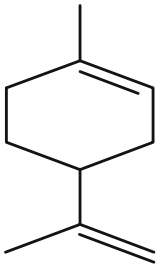

Fig. 5.1 Chemical structure of *d*-limonene

Table 5.1 Relevant properties of *n*-hexane, toluene, and *d*-limonene

Properties	*n*-Hexane	Toluene	Dichloromethane	*d*-Limonene
Empirical formula	C_6H_{14}	$C_6H_5CH_3$	CH_2Cl_2	$C_{10}H_{16}$
Molecular weight	86.18	92.14	84.93	136.23
Boiling point (°C)	68.7	110.6	39.8–40.0	175.5
Heat of vaporization (kJ/kg)	334	351	28.6	353
Density (g/mL)	0.6603	0.8669	1.325	0.8411
Toxic	Yes	Yes	Yes	No
Environmental impact	High	High	High	Low

compounds (VOCs). Solvents that are commonly replaced with *d*-limonene solvent include methyl ethyl ketone, acetone, toluene, glycol ethers, and numerous fluorinated and chlorinated solvents. In industry, *d*-limonene solvent is typically mixed with a surfactant, producing a solution containing 5–15% of *d*-limonene. The major drawback of using *d*-limonene is its low viscosity and the higher energy consumption related to solvent recovery by evaporation due to its high boiling point (175°C) compared to *n*-hexane (69°C). The chemical and physical properties of *d*-limonene compared to *n*-hexane are illustrated in Table 5.1.

This molecule has been considered for many applications like insecticide, cosmetics, and food industry. This rising interest for *d*-limonene is due to its proved cleansing and degreasing properties [3]. In this respect, that molecule has been designated as efficient alternative for halogenated carbon hydrates or conventional degreasing agents used in industry and at households. In their attempt to develop an industrial application for *d*-limonene, Liu and Mamidipally [4, 5] have indicated, recently, the high suitability of this molecule as a solvent for rice bran oil recovery.

In parallel, citrus essential oil containing *d*-limonene is generally extracted by hydrodistillation where Clevenger apparatus represents the most common system that is used for decades to extract and evaluate essential oils in herbs and seed. Although the hydrodistillation step requires several hours, it is interesting to note that it allows extracting components at a lower temperature than their boiling point (azeotropic distillation), which eliminate degradation risks at high temperatures. In this essence, the introduction of electromagnetic energy as a heating source has helped the improvement of the Clevenger system [6]. This technique has been applied with success for the extraction of essential oils from orange peels in which

d-limonene constitutes more than 90% of the essential oil content. This approach has permitted the reduction of processing time from 3 h (conventional conduction heating system) to 30 min in the microwave-assisted system. In addition, the new design is solvent-free, requires low capital investments, and consumes lower energy compared to the conventional one.

5.3 Limonene as an Alternative Solvent for Soxhlet Extraction

For 130 years, Soxhlet has been the most common technique for the recovery of fats and oils from biofeedstocks in teaching and research. However, the major drawbacks initiated with Soxhlet like long extraction time, energy consuming, and the use of large amounts of petroleum solvents have called for an increased environmental concerns. For example, *n*-hexane, the solvent of choice for fats and oils using Soxhlet extraction, is ranked on top of the list of the hazardous solvents. Over the years, many researchers have concentrated their efforts to find alternative solvents [7].

This green approach has helped Chemat group to develop a new extraction system for fatty material using microwaves called "microwave-assisted Soxhlet" [8, 9] that produces equivalent results to those obtained by standardized norms. This green process, in which 90% of the solvent is recycled, has slashed time from an exhaustive 8 h processing in conventional method to only 32 min. In this direction, Virot et al. [9] proposed the combination of microwave-assisted Soxhlet as a process and *d*-limonene as a green extractant. This step is followed by a microwave-assisted distillation using Clevenger system. The proposed process has been applied successfully to the recovery of olive oil. The comparison of both extracts has revealed the superior quality of olive oil obtained by the new system. In order to avoid the high boiling point required by *d*-limonene to be recovered, they proposed an innovative approach capitalizing on the azeotropic distillation concept of essential oils used on steam or hydrodistillation using Clevenger. After Soxhlet extraction with *d*-limonene, distilled water was added to the mixture composed of extracted oil and *d*-limonene. After azeotropic water distillation around 100°C with a Clevenger system, *d*-limonene and extracted oil were recovered separately (Fig. 5.2).

Yields obtained for both extractions showed that yields of *d*-limonene's extracts were slightly higher than those obtained using *n*-hexane (Table 5.2). This difference is attributed to the slightly polar nature of *d*-limonene compared to *n*-hexane and to a higher dissolving power of *d*-limonene for triglycerides. In addition, the higher temperature used to boil *d*-limonene induced a better desorption rate of oil in the matrix as a consequence of a lower viscosity.

The gas chromatography coupled to mass spectrometry (GC-MS) analysis data of free fatty acid methyl esters (FAMEs) derivatives has revealed a good agreement with literature data [10] in terms of qualitative composition where no significant differences ($P > 0.05$) were detected for both methods. Nevertheless, we can note a

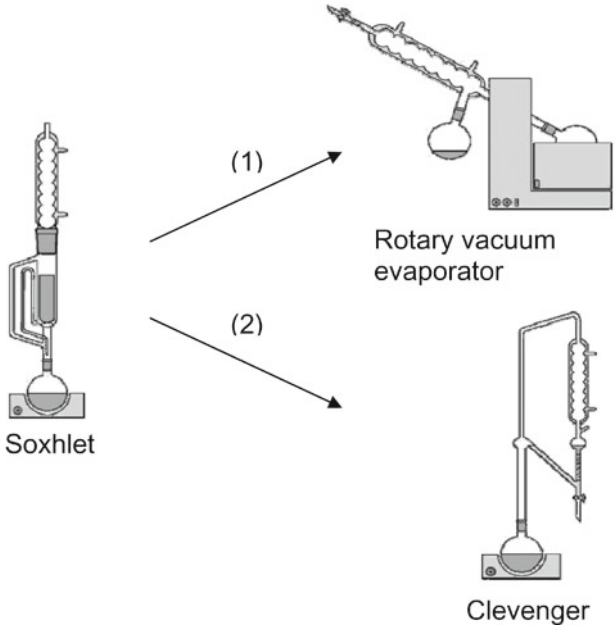

Fig. 5.2 Extraction procedures function of solvent used (*1*, hexane, *2*, limonene)

Table 5.2 Comparison of main fatty acids' composition obtained from olive oil using different solvent systems (relative percent)

Fatty acids	*n*-Hexane (%)	*d*-Limonene (%)
C16:0	12.71	14.09
C16:1	0.97	1.06
C18:0	2.19	2.43
C18:1	72.04	71.72
C18:2	9.98	8.58

higher level of free fatty acids, peroxide value, and conjugated dienes level in *d*-limonene's extracts. These results indicated the presence of traces of oxidized products, which can be attributed to the higher temperature, used to extract oil.

The authors continued their investigations about measuring the ability of each solvent system (*n*-hexane and *d*-limonene) to be recovered and recycled. In the system using *n*-hexane, recycling of approximately 50% of solvent could be achieved compared to a recycling potential of almost 90% for *d*-limonene. This result confirms that *d*-limonene can be considered as suitable and effective as it complies with standardization recommendation for solvents in which it should not be miscible with water and must have a different density with it; needs to dissolve the analytes for easier extraction, and finally, the solvent must be volatile enough to be easily removed by evaporation.

5.4 Limonene as an Alternative Solvent for Dean-Stark Distillation

Moisture determination represents a key step in food analysis for which the oven-drying methods are commonly used. However, for matrix containing volatile compounds, the distillation method stands as the most suitable method. Several distillation-based procedures have been tested in the late nineteenth and early twentieth century [11]. Dean and Stark developed the first continuous and refluxing method in 1920 [12]. This innovation was followed by a development of different types of receivers in an attempt to adapt the collecting trap to the material to be analyzed [13]. As a consequence, the Dean and Stark distillation procedure became the reference method for water determination in food products containing volatile compounds [14]. It was later on used in food industry for water determination in herbs and spices [15, 16] and to tap the petroleum industry [17]. The recommended solvent for Dean and Stark distillation was toluene. Due to increasing environment concerns and the spreading of green chemistry principles, such solvent has to be avoided as much as possible. Toluene exerts toxic properties (Table 5.1) and detrimental health effects, especially on the nervous system, the liver, and on the auditory function [18, 19].

In their attempt to alleviate this environmental and health concerns, the research community set up 12 principles for a green chemistry in order to develop more environmentally acceptable experiments [20]. It involves the design of less hazardous chemical syntheses (using substances with little or no toxicity) or the use of safer solvents and reaction conditions. In this direction, *d*-limonene, which is the major by-product obtained from the citrus fruit processing [1, 21], was used by Veillet et al. [22] in order to replace toluene in the Dean-Stark procedure (Fig. 5.3).

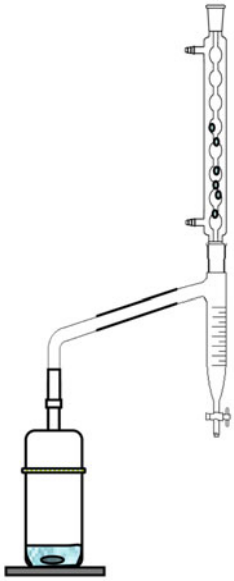

Fig. 5.3 Dean-Stark apparatus

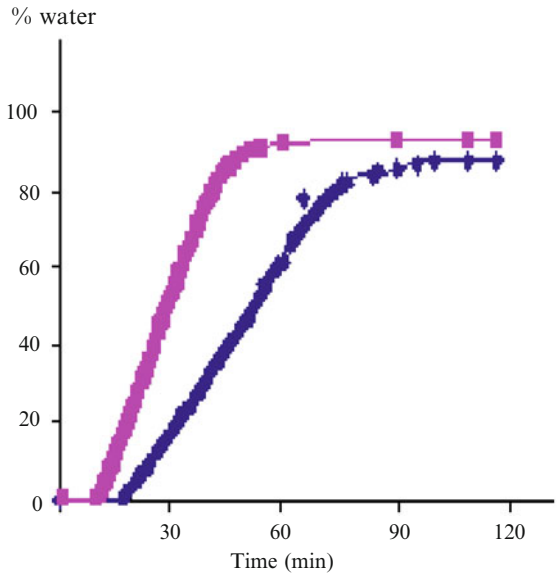

Fig. 5.4 Kinetics of water distillation of onions using two different solvents (■) *d*-limonene and (♦) toluene

The low health risks and the very low environmental impact of *d*-limonene have granted this molecule a green label. Despite the fact that its boiling point (175°C) is higher than toluene (111°C), the azeotropic distillation concept based on the ability of *d*-limonene to form an azeotropic mixture with water at 97.4°C is in favor of its application as an alternative solvent to toluene. The Dean and Stark procedure is based on the ability of the solvent to form an azeotropic mixture with the water contained in the food matrix; thus, due to the difference in boiling points, it is expected that different solvents would result different kinetic patterns.

The results of Veillet et al. [22] showed two similar kinetics of distillation with minor variations could be observed (Fig. 5.4). They noticed at the beginning that the recovery of water was delayed for about 3 min using *d*-limonene, mainly due to a higher distillation temperature. However, the water recovery process was accelerated once distillation started. The higher temperature of the azeotropic mix in the case of *d*-limonene could explain this phenomenon where bulk temperature is very close to the water boiling point, rendering water more susceptible to volatilize than at lower temperatures. In this situation, the slope of the distillation curve increased for the system using *d*-limonene compared to toluene; thus, the total time required to achieve 100% water recovery was shorter. It is interesting to note here that the excess of energy required at the beginning of the experiment was balanced by a shorter processing time.

The data extended to a wide range of products such as garlic, carrots, and leeks revealed a comparable moisture value for methods using toluene and *d*-limonene [22]. Aromatic plants such as rosemary, sage leaves, and mint were also tested

giving similar moisture content for both solvents (toluene and *d*-limonene) as follows: 64.1 ± 0.6 and 65.1 ± 1.8; 71.1 ± 1.0 and 70.4 ± 2.2; and 88.2 ± 1.8 and 87.6 ± 1.7, respectively.

According to these results, the moisture determination in food matrices using *d*-limonene can be considered as a reference in student laboratory practices when teaching green chemistry.

5.5 Limonene as an Alternative Solvent for Extraction of By-Products

The positive effects on health that lycopene is offering has initiated an increased interest on this carotenoid which is present in tomato and is largely used as simple food dye.

Generally, extraction of lycopene from food sources is performed using pure organic solvents such as dichloromethane or mixtures of polar and nonpolar extractants (e.g., acetone-chloroform (1:2) or hexane-acetone-ethanol (50:25:25)). Conventional extraction methods for lycopene consume large volumes of organic solvents, which are toxic, expensive, and hazardous. In addition, traces of the extractant can contaminate the final product, making it unsuitable for food, pharmaceutical, or cosmetic uses. New findings by Chemat et al. [23] suggested the suitability of a major component limonene present in citrus rind oil for the recovery of lycopene from tomato. Taking into account the costs associated with environmental compliances and insurances, the use of limonene is more competitive than dichloromethane (Table 5.1).

Chemat et al. [23] proposed a green cycle starting from obtaining *d*-limonene from biofeedstocks (Valencia late orange: *Citrus sinensis* L. Osbeck peel) by steam distillation. Then, a deterpenation process follows this step using a thin film evaporator in order to recover pure limonene. According to Leenaerts [24], the thin layer technique allows a very short residence time under reduced pressure, a significant heat-transfer surface, as well as a mixing potential that match heat and mass transfer requirements. Next, limonene is used as the extracting solvent for lycopene from tomato fruit as a substitute of dichloromethane.

They reported that the deterpenation achieved a recovery of 98.8% of limonene after 30 min under optimal conditions (temperature = 65.4°C, flux = 0.036 $kg \cdot h^{-1}$, pressure = 100 mmHg). After deterpenation, limonene was used as a solvent for extracting lycopene from tomato fruit as a substitute of dichloromethane.

The results reported important lycopene yields for dichloromethane (3.84 mg/100 mg of fresh tomato) representing 19.2% of lycopene total amount compared to those obtained by *d*-limonene (2.44 mg/100 mg of fresh tomato) representing less than 13.1% of total lycopene content. On the other hand, dichloromethane stands as a toxic and harsh organic solvent whereas *d*-limonene is recognized as GRAS agent. Thus, the proposed approach using *d*-limonene is useful and can be considered as an attempt to reduce toxicity for human and environment.

5.6 Combining Green Extraction Technique and Green Solvent

Recently, an improved Clevenger apparatus using microwave energy has been suggested [11] and applied to extract essential oils and so, limonene (which represents more than 90% of orange peels' essential oil). This microwave extraction can be considered as an effective approach since it offers, among others, short extraction times (only 30 min against 3 h in conventional method), low cost, low coextraction of by-products (compared to conventional distillation) and stands as environmentally friendly process. Virot et al. [8] developed a new Soxhlet assisted by microwave energy called microwave-integrated Soxhlet (MIS). This new device has been set up to ensure a rapid, efficient, and green extraction procedure for fatty acids recovery from olive oil. The aim of their approach was to evaluate the possible extraction of fats and oils from olive seeds using *d*-limonene as solvent in combination with microwave heating for both the extraction and the cleaning steps. The extraction step of oils from olive seeds was thus performed using the MIS, and then the microwave Clevenger system performed the solvent elimination step (Fig. 5.5).

The yield and composition of fatty acids were compared with those obtained by conventional Soxhlet and MIS extraction procedures using *n*-hexane. The data indicated similar results compared to conventional Soxhlet extraction in terms of gravimetric and fatty acids composition. This is true since limonene properties are quite similar to hexane in terms of polarity and thus affinity for fats and oils. In addition, the processing time was reduced to only 32 min as compared to the exhaustive 8 h

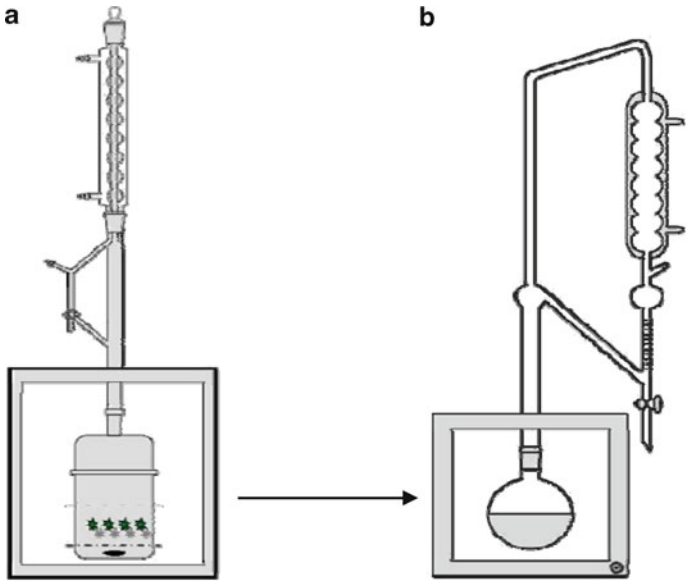

Fig. 5.5 Proposed extraction procedure using limonene: microwave-integrated Soxhlet extraction followed by microwave Clevenger distillation

Table 5.3 Fatty acid compositions of olive oil for different procedures and solvents

	Soxhlet[a]	MIS[b]	MIS-MC procedure[c]
	n-Hexane	*n*-Hexane	*d*-Limonene
Fatty acids	(%)	(%)	(%)
C16:0	12.71	12.03	12.01
C16:1	0.97	0.70	0.68
C18:0	2.19	1.95	2.22
C18:1	72.04	73.66	74.13
C18:2	9.98	9.71	9.67

[a]Conventional Soxhlet extraction using *n*-hexane
[b]MIS extraction using *n*-hexane
[c]MIS extraction using *d*-limonene followed by microwave Clevenger distillation

required in the reference Soxhlet procedure. Since the possibility to recycle the solvent (limonene) is up to 90% and the energy used is reduced, this method is considered as a promising green technology.

The results indicate an improved olive oil yield for MIS procedure using *d*-limonene (44.9%) compared to systems involving *n*-hexane like conventional Soxhlet (40.3%) and MIS system (39.1%). This result is attributed to the higher dissolving ability of limonene for triglycerides, which can, at higher temperature, be used to boil this solvent, produce a lower viscosity of the analytes in the matrix, and, as a consequence, a better diffusion rate of the solute from the solid phase to the solvent.

Virot et al. [8] continued their investigation to assess the influence of the method on the chemical composition and relative amounts of fatty acid (Table 5.3). They noted comparable results for the three methods, and that the main fatty acids extracted using the new proposed procedure were oleic (C18:1), palmitic (C16:0), and linoleic (C18:2) acids. These three fatty acids represent more than 90% of the total fatty acid composition of the extracted oil. Other fatty acids such as palmitoleic (C16:1), stearic (C18:0), linolenic (C18:3), or arachidic (C20:0) acids were also noted with a less predominant peak area. Myristic (C14:0), pentadecanoic (C15:0), margaric (C17:0), margaroleic (C17:1), nonadecyclic (C19:0), gadoleic (C20:1), and behenic (C22:0) acids were found in trace levels. In addition, their data reported that the sum of saturated, mono-, and polyunsaturated fatty acids was also in line with those reported for olive oils in the literature [25]. Thus, the use of microwave energy and limonene as solvent did not involve extraneous effects on the composition of the extracted oils.

The proposed investigation revealed a green aspect that can be pointed out in two points:

First aspect: Previous investigation dealing with MIS device [19] has shown that extractions permit time reduction compared to conventional extraction procedure. The solvent recycling possibilities using MIS instead of Soxhlet apparatus have also been pointed out. Microwave energy is, in addition of that, the only heating source used to perform extraction. Therefore, the extraction step of the proposed procedure is clearly advantageous in term of time, solvent, and energy saving.

Second aspect: The microwave Clevenger apparatus is presented as a green process since it allows reduction of time and energy required for limonene distillation step. Currently, energy that can be used to eliminate limonene from the distillation flask is reduced by using azeotropic distillation technique (vaporization temperature diminished from about 175°C to less than 100°C).

The proposed approach using a green solvent to perform extraction is useful and can be considered as a good alternative to conventional petroleum solvent where toxicity for both operator and environment is reduced. Furthermore, the use of a by-product of the industry as solvent, its possible recycling, and life-cycle extension is original and of increasing interest for many chemistry experiments. This useful and safe procedure may lead to numerous investigations and/or alternatives to conventional chemistry procedures that are often hazardous.

5.7 Future Trends

Innovative and sustainable extraction, which typically involves less energy and renewable solvents, is currently a dynamically developing area in applied research and industry. Up to now, however, there are only a few reports that mentioned the replacement of petroleum solvents by renewable solvents such as *d*-limonene, the major essential oil component of a by-product from orange juice industry. The main advantages of using renewable solvents for extraction includes: increase production efficiency and contribute to environmental preservation by reducing the use of solvents, fossil energy, and generation of hazardous substances. Extraction using alternative and green solvent such as *d*-limonene will be of great interest in the near future in the area of natural products.

References

1. Mira B, Blasco M, Berna A, Subirats S (1999) Supercritical CO_2 extraction of essential oil from orange peel. Effect of operation conditions on the extract composition. J Supercrit Fluids 14:95–104
2. Guenther E (1974) The essential oils, vol 3. R. E. Kreiger Publishing, New York
3. Toplisek T, Gustafson R (1995) Cleaning with D-limonenes: a substitute for chlorinated solvents. Precis Clean 3:17–20
4. Liu SX, Mamidipally PK (2005) Quality comparison of rice bran oil extracted with d-limonene and hexane. Cereal Chem 82:209–215
5. Liu SX, Mamidipally PK (2004) First approach on rice bran oil extraction using limonene. Eur J Lipid Sci Technol 2:122–125
6. Ferhat MA, Meklati BY, Smadja J, Chemat F (2006) An improved microwave Clevenger apparatus for distillation of essential oils from orange peels. J Chromatogr A 1112:121–126
7. Johnson LA, Lusas EW (1983) Comparison of alternative solvents for oils extraction. J Am Oil Chem Soc 2(60):229–242
8. Virot M, Tomao V, Colnagui G, Visinoni F, Chemat F (2007) New microwave-integrated Soxhlet extraction. An advantageous tool for the extraction of lipids from food products. J Chromatogr A 1174:138–144

9. Virot M, Tomao V, Ginies C, Visinoni F, Chemat F (2008) Green procedure with a green solvent for fats and oils' determination: microwave-integrated Soxhlet using limonene followed by microwave Clevenger distillation. J Chromatogr A 1196:57–64
10. Di Bella G, Maisano R, La Pera L, LoTurco V, Salvo F, Dugo G (2007) Statistical characterization of Sicilian olive oils from the Peloritana and Maghrebian zones according to the fatty acid profile. J Agric Food Chem 55:6568–6574
11. Hoffman JF (1908) Referate. Angew Chem 21:890–895. doi:10.1002/ange.19080211905
12. Dean EW, Stark DD (1920) A convenient method for the determination of water in petroleum and other organic emulsions. J Ind Eng Chem 12:486–490
13. Fetzer WR (1951) Determination of moisture by distillation. Anal Chem 8(23):1062–1069
14. AOCS Official Method Ja 2a-46 (1993) American Oil Chemist' Society. AOCS Press, Champaign
15. Balladin DA, Headley O (1999) Evaluation of solar dried thyme (Thymus vulgaris Linne) herbs. Renew Energ 17:523–531
16. Brunnemann KD, Qi J, Hoffmann D (2002) Chemical profile of two types of oral snuff tobacco. Food Chem Toxicol 11(40):1699–1703
17. Fleury M, Boyd D, Al-Nayadi K (2006) Water saturation from NMR, resistivity and oil-base core in a heterogeneous Middle-East carbonate reservoir. Petrophysics 47:60–73
18. Hass U, Lund SP, Hougaard KS, Simonsen L (1999) Developmental neurotoxicity after toluene inhalation exposure in rats. Neurotoxicol Teratol 21:349–357
19. McWilliams ML, Chen GD, Fechter LD (2000) Low-level toluene alters the auditory function in guinea pigs. Toxicol Appl Pharmacol 1(167):18–29
20. Anastas P, Warner J (1998) Green chemistry: theory and practice. Oxford University Press, New York
21. Njoroge SM, Koaze H, Karanja PN, Sawamura M (2005) Essential oil constituents of three varieties of Kenyan sweet oranges (*Citrus sinensis*). Flavour Fragr J 20:80–85
22. Veillet S, Tomao V, Visinoni F, Chemat F (2009) New and rapid analytical procedure for water content determination: microwave accelerated Dean-Stark. Anal Chim Acta 632:203–207
23. Chemat-Djenni Z, Ferhat MA, Tomao V, Chemat F (2010) Carotenoid extraction from tomato using a green solvent resulting from orange processing waste. J Essent Oil Bear Plant 2(13):139–147
24. Leenaerts R (1988) Technique industrielle de la couche mince. Techniques de l'Ingénieur J2360
25. Ranalli A, Modesti G, Patumi M, Fontanazza G (2000) The compositional quality and sensory properties of virgin olive oil from a new cultivar-1–77. Food Chem 69:37–46

Chapter 6
Glycerol as an Alternative Solvent for Organic Reactions

V. Calvino-Casilda

Abstract Glycerol has been successfully employed as a versatile and alternative green solvent in variety of organic reactions and synthesis methodologies. Using this valuable green solvent, high product conversions and selectivities were achieved affording innovative solutions to the substitution of the conventionally used volatile organic solvents. Besides solubility of the reactants and the catalysts and easy separation of the products, glycerol offers several other benefits such as catalyst recycling, microwave-assisting reaction, and emulsion mode. This chapter summarizes selected examples of potential uses of glycerol in organic reactions as well as the advantages and disadvantages of such a green methodology.

Furthermore, because of economical and environmental considerations nowadays, the possibility of directly using crude glycerol produced by the biodiesel industry has significantly increased.

6.1 Introduction

The impressive and fast development of the vegetable oil industries, mainly for nonfood application, generates annually a great amount of crude glycerol as by-product (around 1 million tons expected in 2010) which is nowadays in urgent requirement of chemical exploitation. Accordingly, most scientists agree on the transformation of glycerol to more valuable chemicals such as monoglycerides, glycerol ethers, acrolein, acrylonitrile, polymers, etc. However, these high-tonnage glycerol-based processes have been the focus of strong discussions for their environmental and economical viability.

V. Calvino-Casilda (✉)
Instituto de Catálisis y Petroleoquímica, CSIC, Catalytic Spectroscopic Laboratory,
Marie Curie 2, 28049 Madrid, Spain
e-mail: vcalvino@icp.csic.es

A. Mohammad and Inamuddin (eds.), *Green Solvents I: Properties and Applications in Chemistry*, DOI 10.1007/978-94-007-1712-1_6,

Solvents are chemical substances used in huge amounts for different applications. In several cases, organic solvents are chemical substances derived from petrol and have a negative impact on the health and the environment. In order to minimize generation of volatile organic compounds (VOCs), the scientific community is continuously searching for new sustainable media since a universal green solvent does not exist yet.

In the last decade, some potential approaches for current solvent innovation have been water, ionic liquids, polyethylene glycol, perfluorinated solvents, and supercritical fluid carbon dioxide ($scCO_2$). However, despite of the interesting results obtained, each of these approaches has some limitations as high cost of equipments for supercritical fluids, product separation for reactions in water, or lack of information about toxicity and biocompatibility of ionic liquids as well as high prices.

The environmental impact of a solvent is derived from its physical, chemical, and biological properties. The physical–chemical nature of the solvent also dictates its suitability as reaction medium. In addition, the polarity of the solvent will control the solubility of organic, inorganic, and organometallic compounds. Thus, reactant and catalyst solubility, heat and momentum transfer, and the chemical, physical, and biological nature of the solvents play a key role not only from environmental viewpoint but also from economic, safety, handling, and product isolation points of view [1]. Besides solubility of the reactants and the catalysts and easy separation of the product, glycerol as an environmental-friendly reaction medium offers several other benefits such as catalyst recycling, microwave assisting reaction, and biphasic and emulsion modes [2].

Glycerol is an abundant, cheap (0.50 €/kg for pharmaceutical grade (99.9%) and 0.15 €/kg for the technical grade (80%)), nontoxic, nonirritating, nonflammable, biodegradable, and recyclable solvent (Table 6.1). It is highly stable under typical storage conditions and compatible with many other chemicals not requiring special handling or storage. Glycerol, as a trihydric alcohol, is a polar protic solvent (highly hydrophilic) soluble in water and many common inorganic and organic compounds, acid and bases as well as enzymes and transition metal complexes. Furthermore, it also dissolves organic compounds that are poorly miscible in water. However, its polarity makes it immiscible in another variety of hydrophobic solvents such as ethyl acetate, diethyl ether, hexane, dichloromethane, etc., permitting product separation by simple liquid–liquid phase extraction [3]. The experimental data of organic syntheses collected so far demonstrates that glycerol can perform many reactions like any other solvent replacing typical hazardous organic solvents as, for example, dimethylformamide (DMF), acetonitrile, etc. So according to the twelve principles of green chemistry, glycerol meets the necessary criteria to be a green solvent [4].

Due to the close similarity of its solvent properties with those of water, it is supposed that the development of organic reactions with glycerol could be a great means to overcome the high hydrophobicity of some organic substrates, which are currently the limiting factor for the development of reactions in water. Moreover, unlike water, glycerol is nonvolatile under normal atmospheric pressure and exhibits a very high boiling point (290°C). Its negligible vapor pressure makes the development of organic reactions at high temperature technically easier allowing

Table 6.1 Physicochemical properties of glycerol as a green solvent

Physicochemical properties of glycerol	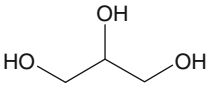
Melting point	18°C
Boiling point	290°C
Vapor pressure (50°C)	<1 mmHg
Dielectric constant (25°C)	42.5
Viscosity (20°C)	1,410 mPa s
Density (20°C)	1.26 g/mL
Biodegradability	Yes
Flash point	160°C
Dissociation constant	0.07E−13
Autoflammability	393°C
Renewable	Yes
Transition metal complexes modification	Without/minor
Toxicity LD_{50} (oral-rat)	12,600 mg/kg

acceleration of the reaction, or making possible reactions that do not proceed in low boiling point solvents. The high viscosity of glycerol might be a drawback; nevertheless, increasing the temperature above 60°C decreases its viscosity. The water–glycerol mixtures lead to a homogenous system and avoid mass transfer limitations, which is common in biphasic systems. Finally, the chemical reactivity of hydroxyl groups can lead to the formation of side products. The three hydroxyl groups of glycerol are reactive in extremely acidic or basic conditions. However, using glycerol as a solvent in a chemically inert environment allows hydroxyl groups to remain intact.

Organic synthesis has become a major focus for developing cleaner processes within the field of green chemistry [5]. These are usually performed in solution to dissolve both reactants and/or catalysts and to deliver heat and momentum [1].

The direct utilization of glycerol as a green solvent would offer a sustainable medium able to drive some organic transformations with more hydrophobic substrates than those commonly used with water. Innovative solutions have to be thought of in order to maximize the advantages of glycerol. Unexpectedly, in spite of having very similar solvent properties to those of water, pioneer catalytic studies have been investigated in glycerol. Some of these examples are noncatalytic and catalytic reactions using homogeneous and heterogeneous chemo- and biocatalysts in glycerol achieving high-product yields and selectivities. This tendency might arise from the very low solubility of organic substrates in glycerol and the intrinsic reactivity of this alcohol. In particular, heterogeneous catalysis in glycerol has the distinct advantage that they can be easily separated and reused while homogeneous catalysis in glycerol is usually very active and selective. Wolfson et al. were the first to report various organic reactions using glycerol as a solvent [6]. They replaced conventional organic solvents by glycerol and showed that some catalytic reactions

proceeded greatly in glycerol obtaining high yields. However, in terms of reaction selectivity or catalyst activity, no real improvements have been reported. Their work also demonstrated that glycerol was stable and capable of facilitating separation of the reaction products by simple liquid–liquid phase extraction. However, the work of this group has been really acknowledged after they confirmed the viability of using glycerol as a solvent, opening new possibilities in the search for green organic solvents. In this chapter, some potential examples demonstrating the feasibility and the necessity of using glycerol as a solvent in organic reactions are discussed [7].

6.2 Glycerol for Redox Reactions

Redox reactions are a group of reactions that involve the transfer of electrons between two chemical species. Generally, there are three techniques for the reduction of unsaturated organic compounds, which include (a) employing molecular hydrogen, (b) via transfer hydrogenation, or (c) the use of metal hydrides. Similarly, organic compounds can be oxidized by three main routes: (a) oxidation with toxic inorganic oxidants (high levels of pollution), (b) catalytic dehydrogenation or catalytic oxidative dehydrogenation (oxygen or peroxides as oxidants), and (c) catalytic transfer dehydrogenation (an organic oxidant adsorbs the hydride and proton).

Glycerol has been employed as an alternative green reaction medium in various carbonyl reduction reactions. Carbonyl reduction is an elementary organic transformation done through a variety of synthetic procedures commonly used in laboratories and industries. The reduction of organic compounds is a fundamental reaction in organic synthesis, and in particular, the catalytic reduction with molecular hydrogen is a very common reaction as is the case of the reduction of styrene to ethylbenzene (Scheme 6.1) [8]. The reduction of styrene, which has low solubility in glycerol, showed high conversions with both homogeneous and heterogeneous metal catalysts. Use of glycerol as the solvent allows recycling the complex, without showing any loss of activity after a second cycle of reaction. Since styrene is poorly miscible in glycerol, addition of low amount of nonionic surfactants such as Pluronic (PE 6400 BASF) to the biphasic system yields an emulsion system and increases the reaction conversion (84% vs. 61% in 3 h at 80°C). In addition, the catalytic reduction of styrene over Pd/C catalysts leads to 100% conversion in 3 h.

Using molecular hydrogen and heterogeneous catalysts (Pd/C, Pt/C, Ru/C, etc.) in glycerol under typical conditions taken up from literature, benzaldehyde and

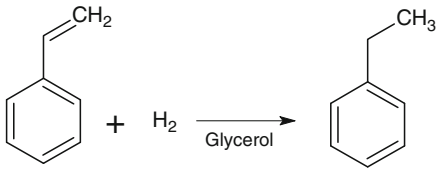

Scheme 6.1 Catalytic reduction of styrene with molecular hydrogen in glycerol [8] (Reproduced from Ref. [8]. With kind permission of Springer)

ethyl acetoacetate are reduced in moderate yields to benzyl alcohol and ethyl hydroxybutyrate (52% conversion to benzyl alcohol and 60% conversion to ethyl hydroxybutyrate; 5 h, 60°C) [8]. However, the reaction rate is lower than that in methanol or toluene, most likely because the hydrogen is less soluble in the viscous glycerol mixture. Other carbonyl compounds such as 1-phenylethanol, 1-octanone, and 2-octanone may also easily reduce quickly under similar reaction conditions. Nevertheless, catalytic hydrogenation with molecular hydrogen as reducing agent presents some difficulties. It usually requires high hydrogen pressures, and as such, special equipment and procedures must be used although synthesis along this pathway is significantly cleaner.

Metal hydrides, and especially borohydrides, are cheap and simple reducing agents that can also reduce many carbonyl compounds generating high yields and selectivities. Sodium borohydride as stoichiometric-reducing agent can selectively reduce carbonyl compounds in water, alcohol, or their mixture. Under these conditions, the reduction is very exothermic, and the reacting mixture is usually cooled to decrease the evaporation of solvent and reactants. In addition, the use of water as reaction medium is limited because many organic compounds have low solubilities in water. However, an alcohol–water mixture turned out successful when it is used as reaction medium. Nevertheless, reactions in glycerol can be performed without cooling due to its high boiling temperature and thermal stability. The high polarity of glycerol allows the enantioselective reduction of benzaldehyde and ethyl acetoacetate under optimized conditions, similar to those which are used when methanol or ethanol are used as solvents. The reaction is also fast and selective, yielding only benzyl alcohol and ethyl hydroxybutyrate in the absence of any catalyst. The reaction yields were much better in the presence of both Ru-BINAP and baker's yeast as catalysts [9] (Scheme 6.2). The high boiling point and low volatility of glycerol prevent the evaporation of the solvent during the reaction, a process that occurs in the cases of other solvents such as water, methanol, and ethanol, and as a

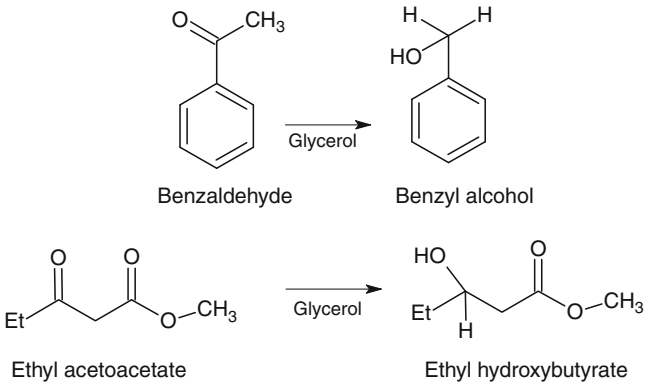

Scheme 6.2 Benzaldehyde reduction to benzyl alcohol in glycerol (*up*); ethyl acetoacetate reduction to ethyl hydroxybutyrate in glycerol (*down*) [9]

result, the reaction required no cooling. Though glycerol could be used as the proton donor in this reaction (23% conversion to benzyl alcohol, 36% conversion to ethyl hydroxybutyrate; 1.5 h, 25°C), the addition of a nonconcentrated acidic aqueous solution at the end of the reaction leads to a higher product yield (100% conversion to benzyl alcohol and ethyl hydroxybutyrate in 1.5 h at 25°C) [9]. The addition of water is frequently essential to dissolve the metal hydride as the high-speed reaction of the hydride with water generates molecular hydrogen.

More recently, Wolfson et al. investigated the baker's yeast catalyzed asymmetric reduction of methyl acetoacetate in aqueous glycerol [10]. From their results, this group concluded that the product extraction yields were affected by the concentration of glycerol in the aqueous solution. The maximum extraction yields were obtained in mixtures with 25–75 wt% of glycerol in water. When these results were compared with those obtained in neat glycerol or neat water, the extraction yields were increased by ~15%. They explained this phenomenon as a result of the formation of strong interactions between glycerol and water (synergistic effects), which decreased solubility of the reaction product in the aqueous glycerol phase.

Another green method for reducing organic molecules is the electroreduction. Electrochemistry in a nonaqueous polar organic solvent is widely applicable in organic synthesis. Glycerol was supposed to function well in electrochemistry, but it can dissolve a diversity of salts at moderately high loading. Benzaldehyde in glycerol can be electroreduced (0.5 V, 0.1 M KCl, room temperature (RT), 24 h), resulting in 62% conversion of the aldehyde. However, undesired products are also detected (55% selectivity) [9]. Benzaldehyde can be fully reduced to toluene with hydrazine in basic conditions via the Wolff–Kishner reaction. This reaction is usually conducted at elevated temperatures (about 200°C) for hours. However, this reaction can also be performed under microwave irradiation (MW) at lower temperatures (110°C) and in much shorter times (10 min) when glycerol is employed as a solvent (Scheme 6.3) [9].

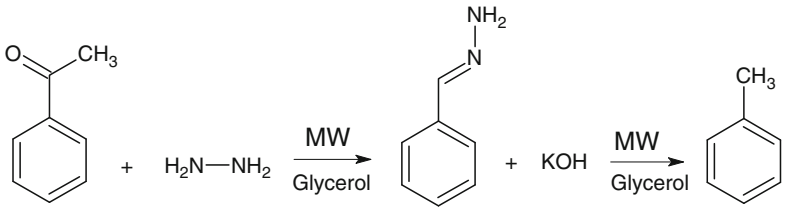

Scheme 6.3 Reduction of benzaldehyde to toluene in glycerol via Wolff–Kishner reaction [9]

Transfer hydrogenation–dehydrogenation reaction is an environmentally benign method for reducing unsaturated compounds or oxidizing alcohols. Basically a hydrogen molecule is transferred from an alcohol to an unsaturated bond. One of the advantages of this pathway is that it is carried out in the absence of gaseous hydrogen or oxygen, which requires precautions and special high-pressure

equipments. Although transfer hydrogenation–dehydrogenation is not as highly developed as catalytic hydrogenation or oxidation, it is acknowledged as an attractive technology with a high potential for broad industrial application. Several organic compounds have been used as solvents as well as hydrogen donors in the transfer hydrogenation of unsaturated organic compounds so far. Wolfson's group proposed glycerol for the first time as both green solvent and hydrogen donor in catalytic transfer hydrogenation–dehydrogenation reactions that typically utilized homogeneous and heterogeneous metal catalysts (Ru-catalysts, Pd/C, Raney nickel) and, in some cases, an inorganic or organic base (KOH, NaOH, Et_3N) as cocatalyst [11–13]. In the transfer hydrogenation, glycerol donates hydrogen to unsaturated organic compounds, while dehydrogenation of glycerol resulted in the formation of dihydroxyacetone. Additionally, glycerol as a solvent allows easy separation of products and catalyst recycling (Scheme 6.4).

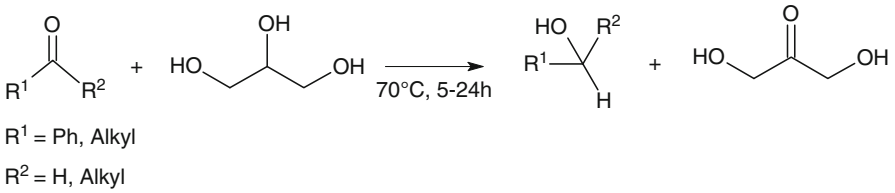

Scheme 6.4 Transfer hydrogenation of carbonyl compounds in glycerol [12]

The Maillard reaction is one of the most important sources for aroma compounds generated when food is cooked, baked, or roasted. The Maillard reaction is also used in the flavor industry to produce meat-like, cocoa-like, and other process flavors. Glycerol influences the Maillard reaction of reducing sugars and amino acids. *Eichner* and *Karel* studied different glycerol/water systems and found that the browning rate decreased with increasing water activity. In this case, glycerol was used to decrease the viscosity of the system by its plasticizing effect [14]. Mustapha et al. observed stronger browning of lysine and xylose in glycerol than in an aqueous medium, even though the reactants were not completely soluble in glycerol [15]. They concluded that the reaction medium was inert and did not directly take part in the reaction. The difference in color formation was due to the different physiochemical environments especially high when glycerol was used as solvent. In the same way, Jousse et al. studied the reaction kinetics of the Maillard reaction between alanine and glucose in glycerol not considering the solvent as an active reagent [16]. Even the heating of amino acids in glycerol, in the absence of reducing sugars, gives rise to a certain degree of browning. It was suggested that glycerol oxidation products are involved.

Cerny and *Guntz-Dubini* studied the influence of glycerol on the volatile compounds that are formed in the Maillard reaction between alanine and fructose. Particularly, they studied in what degree glycerol is actively taking part as a reactant [17]. They found that glycerol influences the Maillard reaction not only by influencing the water activity and the physicochemical environment of the reaction matrix

but also by acting as a precursor. For this study, isotopically labeled compounds were used to explain the origin of the carbons in pyrazines and other reaction products. The volatile compounds (1-hydroxy-2-propanone, 2,3-pentanedione, 2-methylpyrazine, 2,5-dimethylpyrazine, 2-ethyl-3-methylpyrazine, and 3-ethyl-2,5-dimethylpyrazine) formed in the reaction of alanine and fructose in ^{13}C-labeled glycerol proved clearly the inclusion of glycerol carbons in the molecules.

6.3 Glycerol for Catalytic C–C Bond Formations

Since its discovery in the early 1970s, the palladium-catalyzed arylation of olefins (Heck reaction) [18] has been applied to a diverse array of fields, ranging from natural product synthesis to material science and to bioorganic chemistry [19–21]. This powerful carbon–carbon bond-forming process has been practiced on an industrial scale during the last decade for the production of compounds such as naproxen and octyl methoxycinnamate [22, 23]. The Heck reaction is typically performed in the presence of a palladium catalysts and a stoichiometric amount of an inorganic or organic base necessary to activate the catalytic cycle. Using polar solvents in the one-phase, palladium-catalyzed Heck coupling is beneficial since it tolerates dissolving strong inorganic bases to set off the reaction [24]. The Heck coupling of iodobenzene and butyl acrylate with homogeneous palladium complex and supported palladium catalyst adding sodium carbonate provides in high yield of butyl cinnamate. In this case, glycerol dissolves inorganic, organic, and organometallic compounds allowing easy separation of the product by extraction [8]. In a typical procedure, reactions are initiated by dissolving the homogeneous complex or dispersing the heterogeneous catalyst in glycerol before addition of the substrates.

Later, Wolfson's group showed that the oil source of glycerol did not affect the reaction performances [25]. Thus, addition of a small amount of methanol or water to pure glycerol did not influence reaction conversions, showing that the presence of residual methanol and water in crude glycerol is not the reason for the lower conversions. Adding an extra base to the reaction slightly increased the reaction activity; the reaction in crude glycerol that contained base residual can be simply run without addition of extra base. Since palladium-catalyzed Heck coupling implies coordination of double bond of an olefin to the catalyst, it might be that the biodiesel and the soap traces in crude glycerol coordinate to the catalyst and decrease its activity. Hence, the Heck coupling of iodobenzene and butyl acrylate in pure glycerol that was mixed over an hour prior to the reaction with biodiesel was also performed. The conversion of the reaction carried out in pure glycerol, prepared from canola oil, was indeed lower than the conversion in pure glycerol by 15%. This fact implies that fatty acid derivatives' impurities in crude glycerol were the reason for the lower conversion in crude glycerol compared to pure glycerol.

Glycerol is a very attractive solvent for microwave-assisted reactions due to its high polarity and high boiling point [26]. Both glycerol and microwave heating

provide a clean and fast methodology that reduces reaction time significantly. Microwave heating has many applications in organic synthesis [27]. This methodology is based on the ability of the solvent and reactants to absorb microwave energy and convert it into heat. It usually increases when the dielectric constant of the solvent rises and in the presence of hydroxyl groups; therefore, solvent selection is critical. Wolfson et al. performed the Pd-catalyzed Heck C–C coupling and Suzuki reactions in glycerol under microwave activation [3, 8]. They demonstrated that the microwave-assisted Heck coupling reaction between iodobenzene and butyl acrylate was faster under microwave irradiation than under conventional heating.

However, like water, the glycerol interface can also act as a potential catalyst and drive many other organic transformations such as Michael additions of amines, anilines, and indoles; ring opening of styrene oxide with *p*-anisidine; and acid-catalyzed dehydrative dimerization of tertiary alcohol in a friendly way [28]. For instance, in case of the aza-Michael addition of *p*-anisidine (1a) to butyl acrylate (2a) at 100°C under solvent-free conditions or in the presence of organic solvents such as toluene, DMF, DMSO, and 1,2-dichloroethane, no reaction occurred (Scheme 6.5). The reaction can proceed in the presence of water but only trace amounts of product (<5%) produced after 20 h of reaction. However, when the reaction was performed with glycerol, a significant improvement of the reaction rate was observed compared to water (82% yield after 20 h of reaction) as the glycerol interface is also able to directly catalyze the reaction and *p*-anisidine has better affinity for it. Nevertheless, glycerol generated by the biodiesel industry is not pure and generally contains about 15 wt% of water and 5 wt% of soap. Fortunately, the impurities present in crude glycerol do not significantly change the physical properties of crude glycerol. These group also investigated the possibility of conducting the aza-Michael reaction using industrial grade glycerol (80% yield) which will be

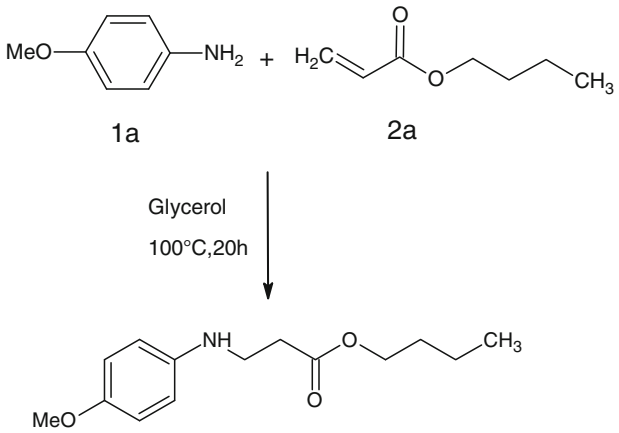

Scheme 6.5 The aza-Michael addition of *p*-anisidine (*1a*) to butyl acrylate (*2a*) in glycerol under catalyst-free conditions (Reproduced from Ref. [28]. With kind permission of Wiley-VCH Verlag GmbH & Co. KGaA)

economically and environmentally more attractive. The results showed that using crude glycerol, almost the same results of using pure glycerol were achieved (81% yield), growing thus the interest of using glycerol as reaction media. The results also demonstrated that performing these reactions in glycerol allows working in catalyst-free conditions simplifying the work-up procedure and therefore increasing the sustainability of the synthetic method.

However, the solvent in a liquid-phase reaction can show not only a beneficial effect on the reaction rate but can also significantly influence the reaction selectivity demonstrating the importance of the considered solvent. Wolfson et al. demonstrated that glycerol as a solvent can enhance reaction selectivity in the ring opening of *p*-anisidine with styrene oxide [3]. This reaction generally catalyzed by Lewis or Brønsted acids can be performed in the absence of catalyst either in glycerol or in water observing that the regioselectivity obtained in glycerol was higher than that in water.

Finally, they also investigated the recyclability of glycerol by liquid–liquid phase extraction with ethyl acetoacetate. The yields obtained after three cycles were comparable to that of fresh glycerol or crude glycerol, indicating a good stability of glycerol. The methodology developed by this group is reasonably general and can be applied to anilines, amines, and α,β-unsaturated carbonyl compounds.

Gu et al. have also recently studied the utilization of glycerol as a solvent to control the reaction selectivity in a three-component novel reaction between styrene, paraformaldehyde, and dimedone [29]. This reaction proceeds through a tandem Knoevenagel/hetero-Diels Alder sequence where the Knoevenagel reaction has to be the rate-determining step and the hetero-Diels Alder reaction has to proceed rapidly to reach the highest selectivity. When the reaction proceeded in water, toluene, nitromethane, or under solvent-free conditions, only a small amount of product was obtained with very low selectivity due to the formation of various secondary products. However, when this reaction was carried out using glycerol as solvent, the reaction selectivity was significantly enhanced obtaining the desired product in 68% yield. Glycerol as a polar protic solvent affects both the Knoevenagel reaction and the hetero-Diels Alder reaction enhancing its rate. The three-component reaction can proceed in glycerol with better selectivity than in other media due to these synergistic effects. Surprisingly, it was observed that a large amount of white solid was formed during the reaction using glycerol, whereas in other conventional solvents, no solid was obtained at the end of the reaction. NMR analysis of the samples after reaction showed that the white solid observed in glycerol reactions mainly consisted of paraformaldehyde and a secondary product and that paraformaldehyde decomposed quickly in glycerol in the absence of dimedone in contrast for example to toluene. It was concluded that glycerol as a solvent is the best choice for the decomposition of paraformaldehyde compared to toluene and that the greater stability of paraformaldehyde in glycerol is due to the presence of dimedone.

The conjugated addition of thiols to α,β-unsaturated compounds is a very useful method for new carbon–sulfur bond formed in organic synthesis. Lenardao et al. described for the first time the use of glycerol as a renewable and recyclable solvent for the Michael addition of thiols to electron-poor alkenes (cyclohex-2-enone, citral,

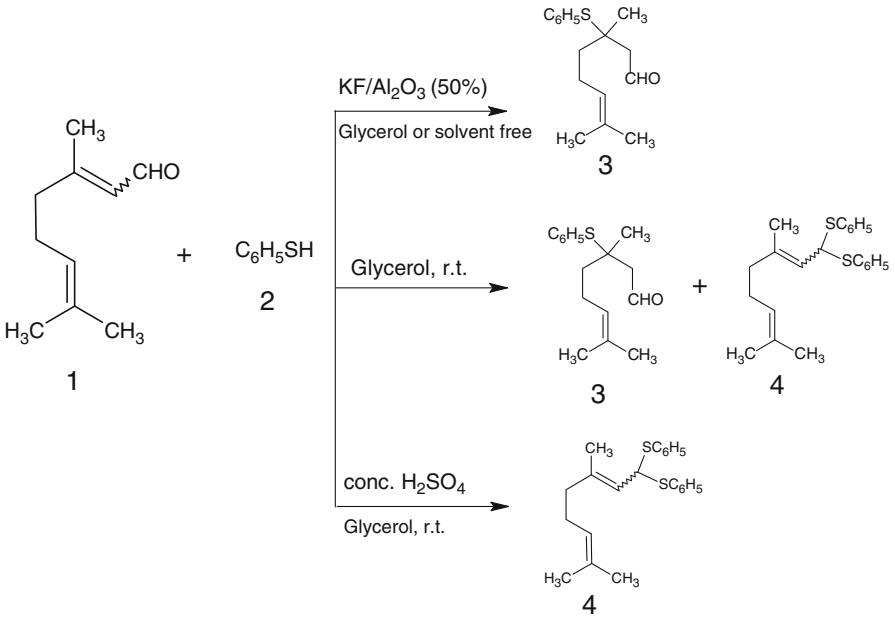

Scheme 6.6 Michael addition of citral (*1*) and thiophenol (*2*) in glycerol. Products reaction: 3,7-Dimethyl-3-(phenylthio)oct-6-enal (*3*) and dithioacetal (*4*) [30] (Reproduced from Ref. [30]. With kind permission of the Brazilian Chemical Society)

acrylonitrile, and methyl acrylate) over KF/Al_2O_3 catalysts [30]. When the reaction was carried out using glycerol in the absence of supported catalyst to verify the role of the KF/Al_2O_3, a slow consumption of starting materials and a competition between 1,4- and 1,2-additions were observed. Thus, when citral reacted with thiophenol in the presence of glycerol, a mixture of Michael adducts and dithioacetal along with unreacted citral was formed after 3 h at room temperature (Scheme 6.6). Glycerol was a good solvent to perform the reaction between citral and thiophenol over acid catalysts as H_2SO_4 affording selectively dithioacetal (86% yield) after 2 h at room temperature. The catalytic system and glycerol could be reused up to three times without previous treatment with comparable activity by the simple addition of more thiol and alkene to the residue in the reaction vessel.

Glycerol has also been proved to be an effective medium to promote electrophilic activity of aldehydes. Many aldehydes usually reacted readily in the presence of acid catalysts with indoles and 1,3-cyclohexanedione in glycerol. Under optimized conditions, Gu et al. obtained, without the assistance of acid catalysts, di(indolyl) methane derivatives, 3,4,5,6,7,9-hexahydro-9-aryl-1*H*-xanthene-1,8(2*H*)-diones, and 1-oxo-hexahydroxanthenes in good to excellent yields (95% at 90°C for 3 h) using glycerol as solvent compared to other organic solvents such as water (76%) or ethylene glycol (85%) [31]. The use of glycerol as a solvent not only makes the

product separation much easier, but also, it is higher in environmental compatibility and sustainability due to the use of less amount of toxic organic solvent and the minimization of waste. However, the significant effects of glycerol on these reactions are uncertain; it is supposed that there are strong hydrogen bonds between the carbonyl of the aldehyde and the alcoholic solvent.

6.4 Glycerol for Biocatalysis

Asymmetric catalysis is a powerful tool in the synthesis of fine and specialty chemicals. The use of biocatalysts has some advantages since it proceeds in mild conditions and it does not require tedious complex synthesis. Biocatalysis is usually carried out in water, though nonaqueous biocatalysis has also been reported in organic solvent to overcome the low solubility of organics in water and to avoid side reactions. Recently, glycerol has been proposed as a solvent for biocatalysis due to its special properties such as low toxicity and high affinity for hydrophilic compounds. One example for such a successful biocatalytic reaction has been the lipase-catalyzed kinetic resolution of ester racemate. It involves the enantioselective transesterification (alcoholysis) of only one of the esters using an excess of alcohol as the resolving agent. The resolution of racemic mixture of 2-methyl heptanoate was performed with immobilized *Candida antarctica* lipase in glycerol resulting in high alcohol yields and high enantioselectivities of the ester and the corresponding alcohol [8]. Later, it was observed that immobilized lipase was more catalytically active than free lipase and could be easily separated from the reaction mixture by filtration. They used immobilized *Candida antarctica* lipase B to carry out the transesterification of isoamyl alcohol to produce isoamyl acetate using glycerol triacetate as both a green solvent and the acyl donor (Scheme 6.7) [32]. The use of glycerol triacetate (triacetin) as the solvent resulted in the production of high alcohol conversion, easy separation of product by simple extraction with petroleum ether and catalyst recycling. Isoamyl acetate can be enzymatically synthesized using a variety of

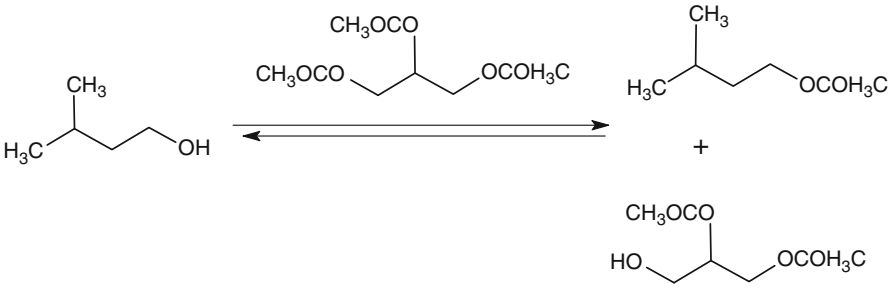

Scheme 6.7 Transesterification of isoamyl alcohol in glycerol triacetate (triacetin) (Reproduced from Ref. [32]. With kind permission of Springer)

acyl donors and solvent combinations. Although direct esterification using acetic acid as the acyl donor is the simplest synthetic route, as it produces only water as a by-product, inhibition of the enzyme activity by the acid frequently leads to low yields. There are also other possible methods of synthesis but usually involve a harmful organic solvent. Glycerol triacetate (triacetin) is an excellent candidate for this reaction. It is a clear, colorless ester with a diversity of applications in foods and flavors, dyes and inks, and in the cosmetics industries. It is nontoxic, biodegradable, and is a "generally recognized as safe" human food ingredient by the Food and Drug Administration of the United States. It is an attractive solvent due to its physical properties; high boiling point and low vapor pressure, which also allows product distillation. In addition, the product can be extracted with triacetin immiscible solvents such as ethers. Although the use of triacetin as the acyl donor in alcoholysis (glycerolysis) may yield glycerol diacetate, glycerol monoacetate, and/or glycerol as by-products, the high boiling points and high solubilities of these potential by-products in triacetin allow the product to be easily separated from the reaction mixture. Since triacetin acts both as solvent and acyl donor, recycling of triacetin together with the heterogeneous catalysts was carried out. The catalyst was filtrated at the end of the reaction cycle, the product and residual substrate were extracted, and finally, the reused catalyst and fresh isoamyl alcohol were added to the used triacetin. After that, the observed isoamyl alcohol conversion rates were found similar to those registered in previous reuse experiments indicating that the recycling of triacetin was also possible.

Glycerol has also been used in other biocatalytic reactions demonstrating its potential for such application. Andrade et al. studied the effect of the glycerol as a cosolvent in the bioreduction of haloacetophenones over whole ce*lls of Aspergillus terreus SSP 1498* and *Rhyzopus oryzae CCT 4964* (Scheme 6.8) [33]. In most of the bioreductions, glycerol has demonstrated for both fungi, *A. terreus* and *R. oryzae,* its potential to improve not only conversions (up to >99%) but also enantioselectivities (up to >99%) when compared to reactions in aqueous or other aqueous–organic media (THF, diethyl ether, toluene, DMSO, and acetonitrile). The successful application of glycerol as a cosolvent in the bioreductions over *A. terreus* and *R. oryzae* can be associated to (1) the homogeneous system formed by the glycerol–water combination that avoids the mass transfer limitation increasing the enzyme–substrate interaction and (2) its protein-stabilizing action. The stabilizing action of glycerol was explained by *Timasheff* and *Gekko* in terms of energy by a model based on the preferential hydration of proteins (preferential exclusion model). In this protein–water–glycerol system, the glycerol is preferably excluded from the immediate proximity of the protein (unfavorable interaction), and the protein will tend to be preferably hydrated. Therefore, it will stabilize the protein native structure and prevent its denaturation; as a result, the enzymatic activity can be conserved. Glycerol can go through the cell wall and the cytoplasmic membrane, and the same protein-stabilizing action can be taking place with alcohol dehydrogenases from *A. terreus* and *R. oryzae*.

The asymmetric reduction of prochiral β-keto esters and ketones is another biocatalytic reaction performed in glycerol as a green medium under mild conditions

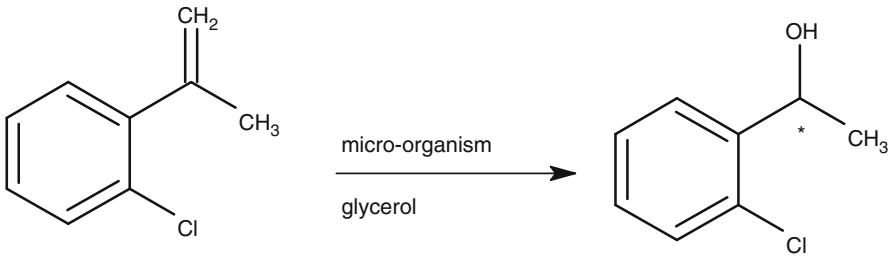

Scheme 6.8 Bioreduction of 2′-chloroacetophenone into the (RS)-1-(2-chlorophenyl)ethanol using glycerol as a cosolvent (Reproduced from Ref. [33]. With kind permission of © Elsevier)

(Scheme 6.9). Even if water is the natural solvent of choice for biocatalysis, the reduction of prochiral ketones with, for example, free baker's yeast (FBY) and immobilized baker's yeast (IBY) in water has several disadvantages [6, 32]. Some of them are the low solubility of the organic substrate, undesired side reactions (hydrolysis), and difficult separation of the product. The activities obtained with immobilized cells were always higher than that achieved with free cells while enantioselectivity was very high (99%) with both catalysts. Employing glycerol as the solvent allowed not only high isolation yield but also the easy distillation of the alcohol due to the low vapor pressure of glycerol.

Scheme 6.9 Baker's yeast catalyzed asymmetric reduction of prochiral β-ketoesters and ketones in glycerol (Reproduced from Ref. [6]. With kind permission of © Elsevier)

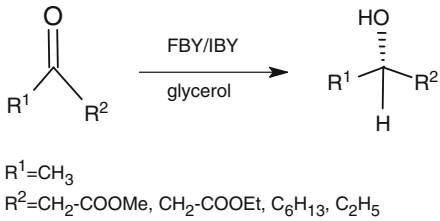

As well known, glycerol is one of the most studied organic solvents in homogeneous solvent mixtures due to its exceptional properties [34]. The dielectric constant of glycerol is not so low, compared to the natural organic solvents, as to increase the rigidity of the molecules (owing to strong intraprotein interactions) and nor so high as to destabilize the tertiary structure of the proteins as other organic solvents do [35]. Electrostatic interactions govern mainly the motions in proteins [36], and the motions are particularly influenced by the dielectric constant of the solvent becoming faster with an increasing solvent dielectric constant [35]. As a result, glycerol can improve both the catalytic activity and the structural stability of the enzymes dissolved in it. Some of the advantageous properties for enzymes dissolved in glycerol include (a) high catalytic activity of enzymes such as subtilisin in pure glycerol [37], (b) the increase of water (up to 1%) in the reaction medium causes a great increase of enzymatic activity just as it is the case of subtilisin and

trypsin among others [38], and (c) owing to the higher dielectric constant of glycerol and glycerol imitating the effect of water, there is an improvement of enzymatic activity compared to other organic solvents. Finally, relating to its structure and activity: (d) higher structure stability than in water and other organic solvents [39–42], (e) higher thermostability than in water [37, 39, 41, 43], and (f) higher stability related to pH changes than in water [43].

However, homogeneous solvent systems as glycerol–water mixtures have a main disadvantage of high viscosity which is a serious problem for mass transfer process, principally at room temperature. Thus, Kramer's theory states that high viscosity can slow down or inhibits conformational changes during catalysis [44–46]. But this problem can be solved by diluting the aqueous–organic mixture to reach up to 80% of water and increasing the temperature of reaction [47].

Enzyme stability at high temperatures is one of the main problems of enzymatic catalysis especially in water, causing the unfolding of enzyme molecules and loss of enzymatic activity and finding that ionic interactions are crucial for it [48, 49]. Nevertheless, enzymes are extremely thermostable in anhydrous organic solvent systems. For instance, trypsin and α-chymotrypsin dissolved in water were inactivated in less than 1 min, whereas these enzymes dissolved in 99% glycerol retained 80% of their enzymatic activities at 100°C after 4 and 10 h, respectively [37].

In addition, improved thermal stability was observed in water–glycerol mixtures when it would be expected that enzyme thermostability in aqueous organic mixtures should not be improved due to the presence of water. However, in spite of the presence of water, the presence of glycerol confers thermostability on the enzymes [50].

6.5 Glycerol for Micellar Catalytic Reactions

The use of surfactant combined catalysts (SCCs) allows all disadvantages of using glycerol as a solvent to be overcome by favoring a better diffusion of organic substrates in the glycerol phase and creating some hydrophobic environments inside which it is possible to reduce the reactivity of glycerol. In addition, micellar catalysis in glycerol offers an important advantage compared to water because the emulsions formed in glycerol were found to be unstable. Therefore, two phases rapidly formed at the end of the reaction leading to an easy extraction of the reaction products without the help of any organic solvents, as is usually the case in water. As occurred in water, the SCCs create some hydrophobic environments in glycerol. The hydrophobic–hydrophilic interactions make diffusion of glycerol inside these hydrophobic pockets difficult, and hence the selective catalytic processes become possible. However, the success of this approach strongly depends on the localization of the catalytic sites, which have to be as close as possible to the hydrophobic environment. Karam et al. prepared different aminopolysaccharides (APs) in the base-catalyzed ring opening of 1,2-epoxydodecane with dodecanoic acid in glycerol (Scheme 6.10) [7, 51]. The hydrophobic environment created by APs in glycerol decreased the side formation of glycerol ethers. With these experiments, it was

demonstrated that the amphiphilic properties of APs were responsible for the increase in the reaction rate of the ring opening of 1,2-epoxydodecane and the hydrophobic environments created by APs are crucial for performing highly selective organic reactions in glycerol. The emulsion formed by APs in glycerol was much less stable than in water. Consequently, after centrifugation at the end of the reaction, the reaction media rapidly became biphasic, which allowed direct extraction of the reactions products without requiring any organic solvent as is generally necessary in water.

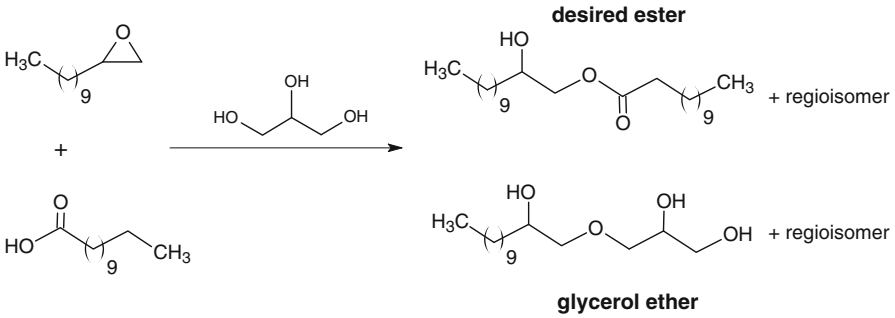

Scheme 6.10 Ring opening of 1,2-epoxydodecane with dodecanoic acid, catalyzed by basic catalysts in glycerol [51]

Later, this group prepared Pd/AP catalysts to catalyze the regioselective symmetrical and unsymmetrical β,β-diarylation of acrylate derivatives in glycerol (Scheme 6.11). The palladium-catalyzed Mizoroki–Heck coupling is a reaction of fundamental importance in organic chemistry and has broad applications for the manufacture of basic chemicals to the preparation of fine pharmaceuticals. According to its surfactant properties, AP as a ligand for the coordination of palladium was able to increase the solubility of organic reactants in the glycerol phase resulting in a significant increase of the reaction rate. It has been found that long alkyl chain esters can be directly extracted from glycerol by simple phase decantation, thus avoiding the assistance of volatile organic solvents [51–53]. However, in this case, this process is not applicable due to the reaction products that remain soluble in glycerol in the presence of the amphiphilic Pd/AP catalyst. Therefore, an alternative extraction solvent to recover the product from the reaction is needed. Supercritical CO_2 was the most efficient solvent found to selectively extract the β,β-diarylated products from the glycerol–Pd/AP catalytic phase. After 420 min of continuous extraction with supercritical CO_2, 8.6 g of products were cleanly recovered from the glycerol–Pd/AP catalytic phase, and only 0.4 g of contamination with glycerol emerged. This extraction procedure offered a simple work-up system and an alternative to the wide utilization of volatile organic compounds. In fact, the combination of glycerol and supercritical CO_2 is still under investigation to provide new medium for greener catalytic processes.

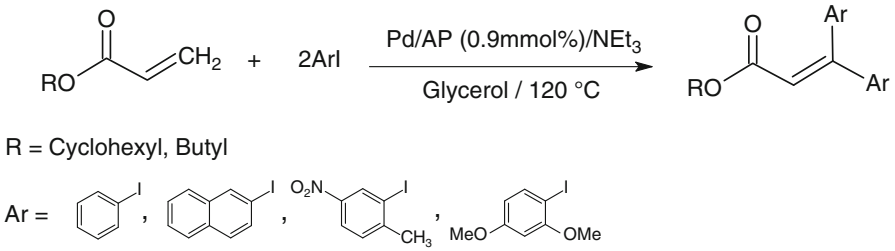

Scheme 6.11 β,β-Diarylation of acrylate derivatives in glycerol [53] (Reproduced with permission from [53]. Copyright @ 2010, The Royal Society of Chemistry)

6.6 Other Catalytic Organic Reactions in Glycerol

Nucleophilic substitution reactions are an important class of reactions that allow the interconversion of functional groups. The nucleophilic substitution of benzyl chloride with potassium thiocyanate in glycerol allowed the dissolution of both substrates in one phase and resulted in high conversion to benzyl thiocyanate (95% in 5 h) in absence of any catalyst (Scheme 6.12) [8].

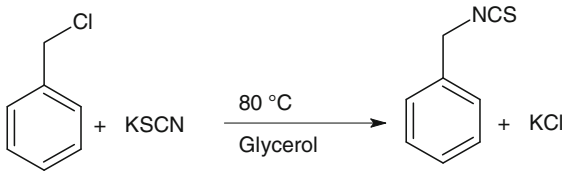

Scheme 6.12 The nucleophilic substitution of benzyl chloride with potassium thiocyanate in glycerol and in absence of any catalyst [8]

Although glycerol as a solvent for designing new reactions is not so popular, Gu et al. have clearly demonstrated that glycerol can indeed be used as an useful medium for maximizing the synthetic efficiency of reactions. This group has recently used glycerol as a unique solvent to set up a novel one-pot two-step sequential reaction between arylhydrazines, β-ketone esters, formaldehyde, and styrenes [54]. In the first step of the reaction, phenylhydrazine and ethyl 4-methoxybenzoylacetate were heated at 110°C in glycerol for 4 h where 1,3-diphenyl-5-pyrazolone formed as the only product. When paraformaldehyde and α-methylstyrene were added into the reaction mixture at 110°C for 10 h, the desired product was obtained in good yields (75%). In the same way, another one-pot sequential reaction between indoles, arylhydrazine, β-ketone esters, and paraformaldehyde have been effectively carried out in glycerol [54].

6.7 Glycerol-Based Solvents

Organic solvents are some of the major air contaminants present in the atmosphere. Valuable solvents are being synthesized from glycerol so that some of the most hazardous organic solvents could be exchanged by these less harmful and biodegradable glycerol-derived solvents.

In addition, the increase in availability of low-price glycerol has enabled the synthesis of an extensive range of glycerol derivatives. However, as different application fields require different physicochemical properties, it would be convenient to have a high degree of versatility in the preparation of the glycerol derivatives and to maintain the simplicity of the derivatization process.

Although glycerol derivative preparations involve either the use of petrochemicals or complex transformative steps, some representative examples will be discussed since they have also been proposed as potential green catalysts.

Some examples are glycerol derivatives consisting of 1,3-dialkoxy-2-propanols and 1,2,3-trialkoxypropanes (glycerol diethers and triethers), both symmetrically and unsymmetrically substituted at terminal positions prepared with significant variations of polarity properties [55]. The possible role of these glycerol derivatives as solvents has just been evaluated through physicochemical measurements providing clues for solvent substitution applications [56]. A selected group of these glycerol derivatives (Scheme 6.13) consisting of 1,3-dialkoxy-2-propanols and 1,2,3-trialkoxypropanes was tested by García et al. [56]. They have a great potential as solvent in catalyzed epoxidation of cyclooctene using aqueous hydrogen peroxide as oxidant and electrophilic chemo- or metal compounds as catalysts.

Scheme 6.13 Structure of glycerol-based solvents [56]

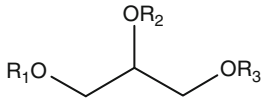

R=H, Me, Et, iPr, Bu, tBu, iBu, CF_3CH_2, $CF_3CF_2CH_2$, $CF_3CF_2CF_2CH_2$

They studied the relationships between solvent properties and the rate of the epoxidation reaction concluding that some glycerol-based solvents, mostly bearing fluorinated alkyl chains (1,3-bis(2,2,2-trifluoroethoxy)-2-propanol, 1,3-bis (2,2,3,3, 3-pentafluoropropoxy)-2-propanol, 1,3-bis(2,2,3,3,4,4,4-heptafluorobutoxy)-2-propanol, and 2-methoxy-1,3-bis(2,2,2-trifluoroethoxy)-propane) showed fast conversions and high turnover frequencies. Some of these solvents performed even better than dichloromethane, which was considered the second best solvent for this system. Furthermore, a quantitative relationship between solvent polarity properties and the rate of epoxidation were established, concluding that the best solvents for this transformation should have high hydrogen-bond donor ability, but a low hydrogen-bond acceptor (Lewis basicity) ability. They tested the robustness of this regression model being able to be effectively used to predict the performance of new

glycerol-derived solvents in this epoxidation reaction on the basis of their physical properties [38]. Glycerol-based solvents were also successfully tested in uncatalyzed epoxidation reactions. Their relatively high boiling points permit reaching almost total cyclooctene conversions at moderate reaction temperatures leading to promising greener applications of these solvents.

Acknowledgment V. Calvino-Casilda thanks CSIC for a postdoctoral contract (JAE-Doc).

References

1. Reichardt C (1979) Solvent effects in organic chemistry. Verlag Chemie, Weinheim
2. Calvino-Casilda V, Guerrero-Pérez MO, Bañares MA (2009) Efficient microwave-promoted acrylonitrile sustainable synthesis from glycerol. Green Chem 11:939–941
3. Wolfson A, Dlugy C (2007) Palladium-catalyzed Heck and Suzuki coupling in glycerol. Chem Pap 61:228–232
4. Anastas PT, Warner JC (2000) Green chemistry: theory and practice. Oxford University Press, Oxford
5. Sheldon RA, Arends I, Hanefeld U (2007) Green chemistry and catalysis. Wiley-VCH, Weinheim
6. Wolfson A, Dlugy C, Tavor D et al (2006) Baker's yeast catalyzed asymmetric reduction in glycerol. Tetrahedron Asym 17:2043–2045
7. Gu Y, Jerome F (2010) Glycerol as a sustainable solvent for green chemistry. Green Chem 12:1127–1138
8. Wolfson A, Dlugy C, Shotland Y (2007) Glycerol as a green solvent for high product yields and selectivities. Environ Chem Lett 5:67–71
9. Wolfson A, Dlugy C (2009) Glycerol as an alternative green medium for carbonyl compound reductions. Org Commun 2:34–41
10. Wolfson A, Haddad N, Dlugy C et al (2008) Baker's yeast catalyzed asymmetric reduction of methyl acetoacetate in glycerol containing systems. Org Commun 1:9–16
11. Wolfson A, Tavor D, Dlugy C, Shotland Y (2008) Employing glycerol in transfer hydrogenation-dehydrogenation reactions. US Patent 61/137239
12. Javor D, Sheviev O, Dlugy C, Wolfson A (2010) Transfer hydrogenations of benzaldehyde using glycerol as solvent and hydrogen source. Canadian J Chem 88:305–308
13. Wolfson A, Dlugy C, Shotland Y, Tavor D (2009) Glycerol as solvent and hydrogen donor in transfer hydrogenation–dehydrogenation reactions. Tetrahedron Lett 50:5951–5953
14. Eichner K, Karel M (1972) The influence of water content and water activity on the sugar-amino browning reaction in model systems under various conditions. J Agr Food Chem 20:218–223
15. Mustapha WAW, Hill SE, Blanshard JMV, Derbyshire W (1998) Maillard reactions: do the properties of liquid matrices matter? Food Chem 62:441–449
16. Jousse E, Jongen T, Agterof W et al (2002) Simplified kinetic scheme of flavor formation by the Maillard reaction. Food Chem Toxicol 67:2535–2542
17. Cerny C, Guntz-Dubini R (2006) Role of the solvent glycerol in the Maillard reaction of D-fructose and L-alanine. J Agric Food Chem 54:574–577
18. Heck RF (1985) Palladium reagents in organic synthesis. Academic, New York
19. Overman LE, Ricca DJ, Tran VD (1993) First total synthesis of scopadulcic acid B. J Am Chem Soc 115:2042–2044
20. Link JT, Overman LE (1998) In: Diederich F, Stang PJ (eds) Metal-catalyzed cross-coupling reactions. Wiley-VCH, New York

21. Haberli A, Leumann CJ (2001) Synthesis of pyrrolidine C-nucleosides via Heck reaction. Org Lett 3:489–492
22. Stinson SC (1999) Chiral drug interactions. Chem Eng News 77:81–101
23. Herkes FE (1998) Catalysis of organic reactions. Marcel Dekker, New York; Chapter 33
24. Alonso F, Beletskaya IP, Yus M (2005) Non-conventional methodologies for transition-metal catalysed carbon–carbon coupling: a critical overview. Part 1: the Heck reaction. Tetrahedron 61:11771–11835
25. Wolfson A, Litvak G, Dlugy C et al (2009) Employing crude glycerol from biodiesel production as an alternative green reaction medium. Ind Crop Prod 30:78–81
26. Calvino-Casilda V, Guerrero-Pérez MO, Bañares MA (2010) Microwave-activated direct synthesis of acrylonitrile from glycerol under mild conditions: effect of niobium as dopant of the V-Sb oxide catalytic system. Appl Catal B Environ 95:92–196
27. Kappe CO (2004) Controlled microwave heating in modern organic synthesis. Angew Chem Int Ed 43:6250–6284
28. Gu Y, Barrault J, Jerome F (2008) Glycerol as an efficient promoting medium for organic reactions. Adv Synt Catal 350:2007–2012
29. Li M, Chen C, He F, Gu Y (2010) Multicomponent reactions of 1,3-cyclohexanediones and formaldehyde in glycerol: stabilization of paraformaldehyde in glycerol resulted from using dimedone as substrate. Adv Synth Catal 352:519–530
30. Lenardao EJ, Trecha DO, Ferreira P da C et al (2009) Green michael addition of thiols to electron deficient alkenes using kf/alumina and recyclable solvent or solvent-free conditions. J Braz Chem Soc 20:93–99
31. He F, Li P, Gu Y, Li G (2009) Glycerol as a promoting medium for electrophilic activation of aldehydes: catalyst-free synthesis of di(indolyl)methanes, xanthene-1,8(2H)-diones and 1-oxo-hexahydroxanthenes. Green Chem 11:1767–1773
32. Wolfson A, Atyya A, Dlugy C, Tavor D (2010) Glycerol triacetate as solvent and acyl donor in the production of isoamyl acetate with Candida antarctica lipase B. Bioprocess Biosyst Eng 33:363–366
33. Andrade LH, Piovan L, Pasquini MD (2009) Improving the enantioselective bioreduction of aromatic ketones mediated by Aspergillus terreus and Rhizopus oryzae: the role of glycerol as a co-solvent. Tetrahedron Asymm 20:1521–1525
34. Torres S, Castro GR (2004) Non-aqueous biocatalysis in homogeneous solvent systems. Food Technol Biotechnol 42:271–277
35. Affleck R, Haynes CA, Clark DS (1992) Proc Natl Acad Sci USA 89:5167–5170
36. Gorman LA, Dordick JS (1992) Organic solvents strip water off enzymes. J Biotechnol Bioeng 39:392–397
37. Castro GR (1999) Enzymatic activities of proteases dissolved in organic solvents. Enzyme Microb Technol 25:689–694
38. Bromberg LE, Klibanov AM (1995) Transport of proteins dissolved in organic solvents across biomimetic membranes. Proc Natl Acad Sci USA 92:1262–1266
39. Rariy RV, Klivanov AM (1999) Protein refolding in predominantly organic media markedly enhanced by common salts. Biotechnol Bioeng 62:704–710
40. Xu K, Griebenow K, Klibanov AM (1997) Correlation between catalytic activity and secondary structure of subtilisin dissolved in organic solvents. Biotechnol Bioeng 56:485–491
41. Knubovets T, Osterhout JJ, Connolly PJ, Klibanov AM (1999) Structure, thermostability, and conformational flexibility of hen egg-white lysozyme dissolved in glycerol. Proc Natl Acad Sci USA 96:1262–1267
42. Knubovets T, Osterhout JJ, Klibanov AM (1999) Structure of lysozyme dissolved in neat organic solvents as assessed by NMR and CD spectroscopies. Biotechnol Bioeng 63:242–248
43. Castro GR (2000) Properties of soluble α-chymotrypsin in neat glycerol and water. Enzyme Microb Technol 27:143–150
44. Kramer HA (1940) Brownian motion in a field of force and the diffusion model of chemical reactions. Physica 7:284–304

45. Jacob M, Schmid FX (1999) Protein folding as a diffusional process. Biochemistry 38:13773–13779
46. Uribe S, Sampedro JG (2003) Measuring solution viscosity and its effect on enzyme activity. Biol Proced Online 5:108–115
47. Castro GR, Knubovets T (2003) Homogeneous biocatalysis in organic solvents and water-organic mixtures. Crit Rev Biotechnol 23:195–231
48. Pace CN (2001) Polar group burial contributes more to protein stability than nonpolar group burial. Biochemistry 40:310–313
49. Washel A (1998) Electrostatic origin of the catalytic power of enzymes and the role of preorganized active sites. J Biol Chem 273:27035–27038
50. Torres S, Castro GR (2003) Organic solvent resistant lipase produced by thermoresistant bacteria. In: Roussos S, Soccol CR, Pandey A, Augur C (eds) New horizons in biotechnology. Kluwer Academic Publishers, Dordrecht, pp 113–122
51. Karam A, Villandier N, Delample M et al (2008) Rational design of sugar-based-surfactant combined catalysts for promoting glycerol as a solvent. Chem Eur J 14:10196–10200
52. Delample M, Villandier N, Douliez JP, Camy S et al (2010) Glycerol as a cheap, safe and sustainable solvent for the catalytic and regioselective b, b-diarylation of acrylates over palladium nanoparticles. Green Chem 12:804–808
53. Pouilloux Y, Barrault J, Jerome F (2010) Green Chem 12:804–808
54. Tan JN, Li M, Gu Y (2010) Multicomponent reactions of 1,3-disubstituted 5-pyrazolones and formaldehyde in environmentally benign solvent systems and their variations with more fundamental substrates. Green Chem 12:908–914
55. García-Marín H, van der Toorn JC, Mayoral JA et al (2009) Glycerol-based solvents as green reaction media in epoxidations with hydrogen peroxide catalysed by bis[3,5-bis(trifluoromethyl)-diphenyl] diselenide. Green Chem 11:1605–1609
56. García JI, García-Marín H, Mayoral JC, Pérez P (2010) Synthesis and physico-chemical properties of alkyl glycerol ethers. Green Chem 12:426–434

Chapter 7
Water as Reaction Medium in the Synthetic Processes Involving Epoxides

Daniela Lanari, Oriana Piermatti, Ferdinando Pizzo, and Luigi Vaccaro

Abstract There is much chemistry between water and epoxide. This contribution deals with the use of water in processes based on the epoxide ring opening. Reported examples highlight the role of water not as a simple substitution of the organic medium or as an exotic option to claim the greenness of a process, but also show the role of this medium for reaching the highest chemical efficiency. The peculiar properties of water have allowed to realize processes that sometimes cannot even be performed in other reaction media.

7.1 Introduction

Among all the possible reaction media, water has proved to be a chemically efficient option for various organic transformations and sometimes has allowed to efficiently realize processes that cannot be performed in organic media [1–7].

Water is of high interest also because it is a valid *green* alternative to classic organic media. Although this aspect can be certainly debated, it has been proved that in several cases, by exploiting the unique properties of water [8], synthetic processes have been realized in this medium with higher selectivity and efficiency compared to those obtained in organic media. In addition, reactions of water-insoluble organic compounds that take place in aqueous suspensions ("on water") have recently received a great deal of attention because of their high efficiency and straightforward synthetic protocols [5, 6].

D. Lanari • O. Piermatti • F. Pizzo • L. Vaccaro (✉)
Laboratory of Green Synthetic Organic Chemistry, CEMIN–Dipartimento di Chimica, Università di Perugia, Via Elce di Sotto, 8, 6123 Perugia, Italy
e-mail: d.lanari@unipg.it; oriana@unipg.it; pizzo@unipg.it; luigi@unipg.it

A. Mohammad and Inamuddin (eds.), *Green Solvents I: Properties and Applications in Chemistry*, DOI 10.1007/978-94-007-1712-1_7,

Epoxides are versatile intermediates in organic synthesis endowed with high reactivity [9–16]. The nucleophilic addition to epoxides plays a pivotal role in the stereoselective preparation of 1,2-disubstituted products, and it has been certainly the most thoroughly studied reaction of these compounds for which different promoters and conditions have been proposed [13–16]. Epoxides are readily prepared as racemates or in optically enriched form by established and simple methods [17, 18].

It is generally accepted that the epoxide ring–opening reaction under neutral or basic conditions proceeds, when no additional electronic effects are operating, via S_N2 mechanism giving inversion at the carbon attacked (generally the less substituted) and furnishing 1,2-disubstituted products with a *trans*- or *anti*-relationship of the nucleophile to the oxygen leaving group. Under acidic conditions, a borderline S_N2 mechanism has been evoked to justify the electronic pull on the oxygen by an acid. Finally, S_Ni (ion pair), carbocationic S_N1, and double inversion mechanisms have been proposed to take account for those reactions that proceed with retention of configuration via formation of a carbocation species [15, 16].

Because of its peculiar physical properties and structure (e.g. pH control, H-bonding capabilities, excellent activation of ionic nucleophiles) [8], water represents the ideal reaction medium for achieving the best efficiency in synthetic processes based on epoxides. In several cases, protocols for the ring opening of epoxides using water as reaction medium have resulted to be the most efficient and promising.

For these reasons, water represents a good candidate for realizing green processes based on epoxides. However, the issues related to its recovery and reuse have to be taken into account.

This chapter deals with all the reactions of epoxides with nucleophiles in water, highlighting those cases where the use of water has played a crucial role for realizing highly efficient processes, mainly focusing on catalytic protocols.

7.2 Epoxides in the Synthesis of 1,2-Amino Alcohols in Water

The ring opening of an epoxide is a useful direct access route to 1,2-amino alcohol [13–16, 19–23]. Alternatively, other nitrogen-containing nucleophiles can also be used to prepare their precursors such as 1,2-azido alcohols [13–16, 24–27].

The efficiency of the available procedures for the reaction of epoxides with amines strongly depends on the type of amine used (aliphatic or aromatic). Typical limitations are related to the use of high temperatures, large amounts of catalysts, hazardous solvents, and formation of side products (mainly bis-adducts).

Surprisingly, water has been scarcely used as reaction medium for this transformation in spite of the fact that a kinetic study and an investigation on the distribution of possible products, carried out in water without the use of a catalyst, have appeared more than 30 years ago [28, 29].

The beneficial effect of water on this reaction is well represented by the data reported in 2003 by Hou et al. in their study on the use of tributylphosphine as catalyst for the ring opening of epoxides in water [30]. For example, in the reaction of cyclohexene oxide (**1**) with aniline (**2a**) or benzylamine (**2b**) besides the catalytic effect of tributylphosphine (10 mol%) that allowed to obtain most satisfactory yields of **3**, the presence of water is essential for the success of the process. In fact, the same reactions performed in MeCN gave only traces of products **3** (Scheme 7.1) [30]. This catalytic system was also found to be efficient in water when phenol was used as nucleophile, whereas in the case of thiols, the yields were lower compared to those obtained in organic solvent [30].

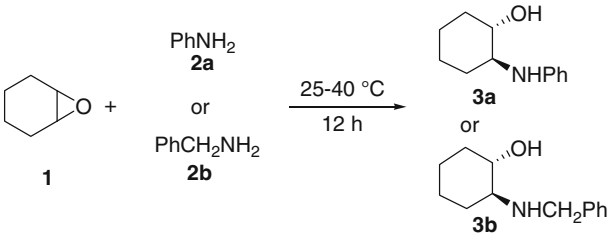

catalyst	medium	yield (%)
nBu$_3$P (10 mol%)	H_2O	78 (**3a**), 64 (**3b**)
-	H_2O	39 (**3a**), 25 (**3b**)
nBu$_3$P (10 mol%)	MeCN	traces

Scheme 7.1 nBu$_3$P-catalyzed aminolysis of cyclohexene oxide (1) in water [30]

In 2005, aminolysis of epoxides with arylamines has been efficiently performed in water in the presence of 1 mol% of the base, 1,4-diazabicycl-[2.2.2]octane (DABCO), or triethylamine (Scheme 7.2) [31]. With this protocol, also, benzylamine gave satisfactory results, but isopropyl amine gave no reaction at all. In this case, other nucleophiles were also used, and very good results were obtained with aromatic thiols, while aliphatic thiols were scarcely reactive [31].

For this transformation, the results reported by Azizi et al. in the same years were different. Aminolysis of aliphatic epoxides with aliphatic amines was performed in water without any addition of catalyst [32]. In this chapter, it was reported that aniline and *p*-isopropylaniline reacted only with styrene oxide, while other aryl amines and epoxides gave only discouraging results (Scheme 7.2).

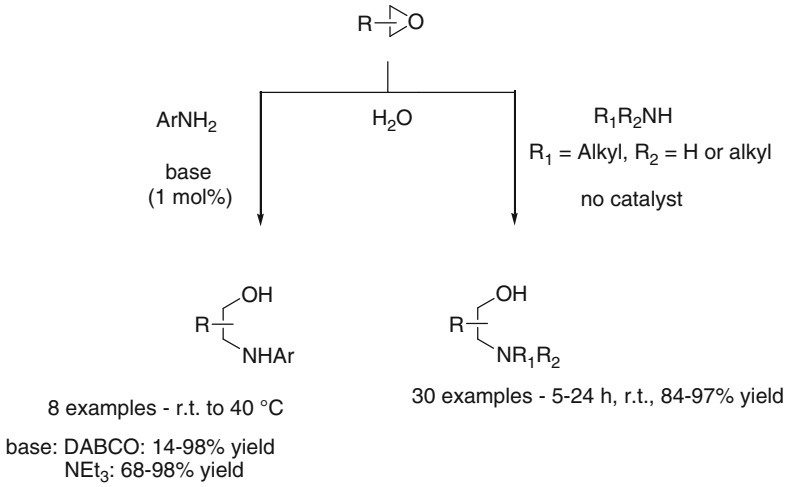

Scheme 7.2 Aminolysis of epoxides in water catalyzed [31, 32]

β-Cyclodextrin (β-CD) has proved to be an effective catalyst for the aminolysis of aromatic amines with glycidol derivatives **4** in water at room temperature. The presence of β-CD is essential for the efficiency of this process (Scheme 7.3) [33].

Scheme 7.3 β-Cyclodextrin-promoted aminolysis of glycidols in water [33]

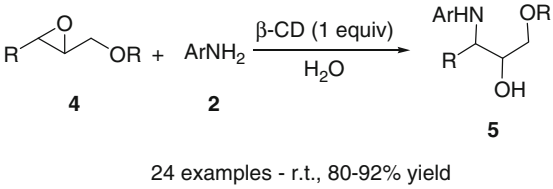

We have started our investigation on the aminolysis of epoxides with the intention of rationalizing these data, believing that the pH of the aqueous medium has a crucial role in determining the efficiency of the nucleophilic ring-opening process of epoxides in water [34–48]. A study to evaluate the dependence of the reactions of aliphatic and aromatic amines with several epoxides on the pH of the aqueous medium was carried out [49]. Initially, it was found that the reaction of cyclohexene oxide (**1**) with almost equimolar amount of aniline (**2a**) was very slow at pH lower than 7.0, with the competitive formation of the corresponding *trans*-1,2-cyclohexandiol by-product (coming from the attack of water to the epoxide). Under basic conditions (pH 8–10), the reaction was expectedly faster. It was also noticed that the pH resulting from the simple mixing of the reactants was 8.30 at 30°C, sufficiently basic to warrant a 90% conversion to **3a**. The best conversion (95%) was achieved by raising the temperature to 60°C (pH was 8.0) or at 30°C at pH 10. By extending the study to other amines, it was generally concluded that aliphatic amines are sufficiently basic to define an adequate pH condition for a successful uncatalyzed aminolysis.

In the case of substituted poorly nucleophilic anilines, the pH resulting from the mixing of the reactants was lower than 7.0, and therefore, reactions were slow, and significant amount of the corresponding diols were formed. By raising the pH of the reaction mixture to 10 (aq. NaOH addition), satisfactory yields were obtained in these cases (Scheme 7.4).

Scheme 7.4 pH influence on the aminolysis of representative epoxide 1 in water [13]

Represenative study on aniline ($PhNH_2$, **2a**)

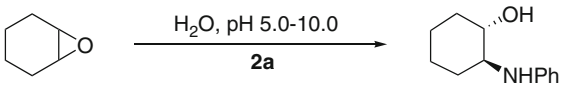

1 **3a**

pH	t (h)	Conversion to **3a** (%)
5.0	100	90 (20% of diol)
7.0	45	90
8.30	25	90
10.0	25	95
8.0*	14	95

* 60 °C

Extension of the study to various amines

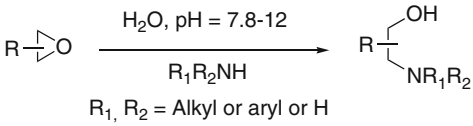

R_1, R_2 = Alkyl or aryl or H

17 examples - 2-26 h, 30-60 °C, 70-93% yield

We also highlighted that in some cases, there is the unavoidable formation of a bis-product, coming from the attack of the ring-opened product to another molecule of epoxide, which can be reduced only by running the reaction with an excess of amine.

As expected, the regioselectivity of the ring openings favored the product at the less hindered carbon (β-attack) except in the case of styrene oxides where α-attack was preferred.

Several other protocols have been recently proposed [50–54] where the addition of various amines to epoxides has been promoted by ultrasounds [50], monodispersed silica nanoparticles [51], or catalyzed by erbium(III) triflate [52], zirconium dodecyl sulfate [53], or aluminum dodecyl sulfate trihydrate [54].

The use of water as reaction medium for the enantioselective ring opening of *meso*-epoxides by amines has recently been reported, achieving better results than those obtained in organic medium by using Lewis acid–surfactant-combined catalysts

(LASCs) [55]. These catalytic systems are able to furnish both the Lewis acidity needed for the activation of a basic center and the hydrophobic environment that favors the approaching of the reactants [55]. In 2005, Kobayashi et al. used LASCs based on Sc(III) [56] and Bi(III) [57] in combination with a chiral bipyridine **7** as ligand, in the desymmetrization of highly hydrophobic epoxides **6** by aromatic amines **2** in water (Schemes 7.5 and 7.6) [56, 57].

The best results were obtained by using scandium(III) dodecyl sulfate ($Sc(DS)_3$) (1 mol-%), (*S*,*S*)-6,6′-bis(1-hydroxy-2,2-dimethylpropyl)-2,2′-bipyridine (**7**) (1.2 mol%), and equimolar amounts of reactants (Scheme 7.5). Although there are no mechanistic insights on the precise role of water in this process, this reaction medium provides better results than those obtained by using an organic solvent [58, 59] in terms of either enantioselectivity and of isolated yields of products.

It should be mentioned that the use of bipyridine (**7**) for epoxide ring-opening process was initially developed by Schneider et al. in 2004 [58].

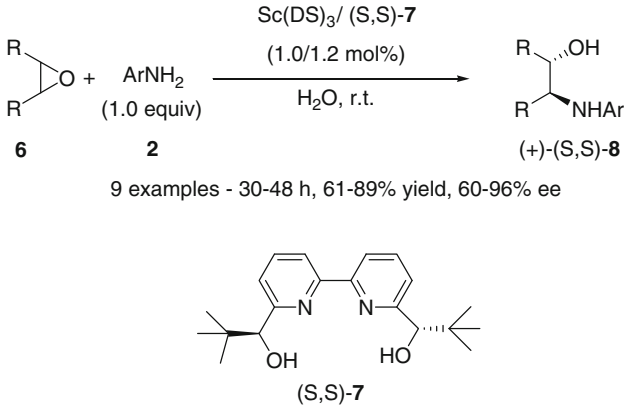

Scheme 7.5 Sc(DS) LASC–catalyzed enantioselective aminolysis of epoxides in water [56]

When Bi(III) was used as Lewis acid, the influence of the surfactant was considered. The best results were obtained by using $Bi(OTf)_3$ (5 mol%), sodium dodecylbenzene sulphonate (SDBS) (20 mol%), and bipyridine **7** (6 mol%) (Scheme 7.6). In this case, the LASC system was generated in situ. Other anionic surfactants like sodium dodecyl sulfate (SDS) and sodium dioctyl sulfosuccinate (AOT) gave the desired products **8** in low yields. In this study, only *cis*-stilbene oxides were considered [57].

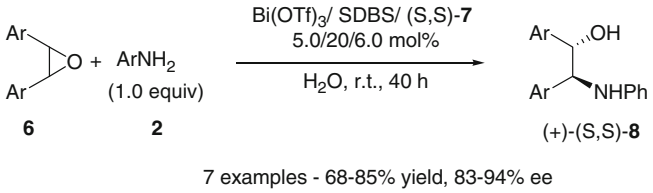

Scheme 7.6 Bi(III) LASCs in the desymmetrization of *cis*-stilbene oxides in water [57]

LASCs based on different Lewis acids have also been used for the same process. In particular, in 2008, we have reported that transition metal catalysts Zn(II), Cu(II), Ni(II), and Co(II), combined with SDS, are also able to efficiently promote the desymmetrization of *cis*-stilbene oxide (**6a**) with aniline (**2a**) (Scheme 7.7, Ar = Ph) in water by using (*R*,*R*)-bipyridine **9** (Scheme 7.7) [60]. Zn(II) and Cu(II) catalysts gave the best results. It should be highlighted that the use of transition metals as Lewis acids and (*R*,*R*)-bipyridine **9** as ligand produced the same product (+)-(*S*,*S*)-**8** that is obtained when $Sc(DS)_3$ is used with the ligand enantiomer (*S*,*S*)-bipyridine **7** (cf. Schemes 7.5 and 7.7).

Scheme 7.7 $Zn(OTf)_2$/**9**/SDS catalytic system for the enantioselective aminolysis of epoxides in water [60]

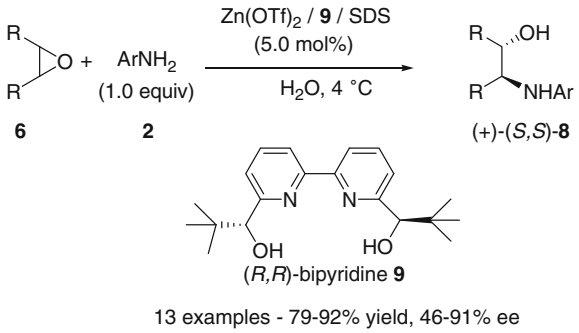

This enantioselective outcome was confirmed when Zn(II) and Cu(II) undecane sulfonates were used in combination with (*S*,*S*)-bipyridine **7** in the desymmetrization of epoxides by amines in water [61]. Kobayashi et al. justified the different enantioselection by accounting some significant differences between the crystal structures of the two complexes of (*S*,*S*)-**7** with $CuBr_2$ and with $ScBr_3$. They also confirmed the importance to have both hydroxyl groups in the structure of **7** for achieving the best enantioselectivity, in fact their corresponding mono- or bis-methyl ether showed low enantioselectivity [58, 59, 61].

In our contribution [60], the influences of other reaction parameters were also considered. By varying temperature and concentration, it was found that the catalytic system $Zn(OTf)_2$/SDS/**9** was most effective at 4°C and 0.5 M concentration level. This result was extended to a variety of epoxides **6** and anilines **2** including very small epoxides such as cyclohexene oxide (**1**), cyclopentene oxide, and 2-butene oxide, for which rare and generally very poor results have been reported, and none of them obtained with water as reaction medium. Representatively, the enantiomeric excess of 85% achieved in the case of cyclohexene oxide (**1**) with aniline (**2a**) was very good (Scheme 7.7).

It has been also reported that $Sc(DS)_3$ is a good catalyst for the enantioselective ring opening of *cis*-stilbene oxide (**6a**) by benzotriazole [62].

The use of catalytic systems formed by the combination of a metal salt with SDS has been applied to other reactions of epoxides with N– and other nucleophiles. In particular, the system made by $Ce(OTf)_4$ (10 mol%) and SDS (30 mol%) has been used [63] for promoting the reactions of a variety of epoxides with nitrite, nitrate, thiocyanate, azido ions besides cyanide, chloride, and bromide ions (Scheme 7.8). Other surfactants were also considered, but SDS gave the best results [63].

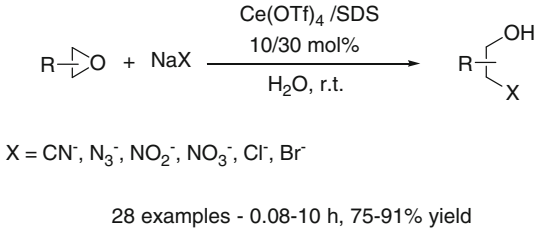

Scheme 7.8 $Ce(OTf)_4$/SDS system in the ring opening of epoxides in water [63]

As a valid alternative route for the preparation of 1,2-amino alcohol, the azidolysis of epoxides has been extensively studied [13–16, 24–27].

The protocol using NaN_3 as reagent and NH_4Cl as a coordinating salt in aqueous methanol at 65–80°C has been commonly considered as the classical protocol for preparing 1,2-azido alcohols. Azidolysis under these conditions generally requires long reaction time (12–48 h), and the azidohydrin is often accompanied by isomerization, epimerization, and rearrangement products [13–16, 64]. Unsymmetrical epoxides generally undergo azido ion attack at the less substituted carbon, except for the aryl-substituted epoxides. Attempts to reverse the regioselectivity have little success [24–26], with the exception of the protocol that uses Et_3Al/HN_3 in dry toluene at −70°C [27].

In 1999 [48], we have reported the first use of sole water as reaction medium for the reactions of epoxides and sodium azide. Both rate and regioselectivity of the process have been dramatically affected by varying the pH of the aqueous medium.

Under basic condition (pH 9.5), at 30°C, the azido ion generally attacks the less substituted β-carbon of **10** through an expected S_N2 mechanism. At acidic pH (4.2), a partial protonation of the oxygen of the epoxide ring promotes a much faster reaction, and under these conditions, an increased preference for the attack on the more substituted α-carbon of **10** probably takes place through an S_N2 *borderline* mechanism (Scheme 7.9) [48].

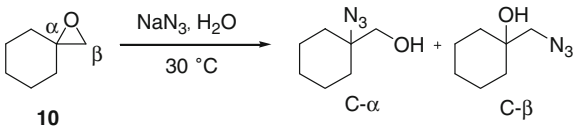

pH	t (h)	C-α/C-β
9.5	20	3/97
4.2	1.5	70/30

Scheme 7.9 pH-controlled regioselectivity of the azidolysis of representative epoxide 10 in water [48]

Recently, polyethylene glycol supported on silica gel [65] or Dowex resin [66] has been used as solid recoverable catalysts for the reaction of epoxides with sodium azide in water under reflux.

Azidolysis of α,β-epoxycarboxylic acids **11** and their esters is a well-studied process that if regio- and stereoselective, opens a direct access route to α-hydroxy-β-amino acids (also known as norstatines), a key moiety of several pharmaceutical target compounds [67–70]. The classical azidolysis protocol that uses NaN_3 in alcohol or alcohol/water (8:1) generally furnishes a mixture of products including the formation of some retention products [71, 72]. To overcome this problem, the use of large amounts (150–500 mol-%) of various Lewis acids in an organic reaction medium has been adopted [71–73].

As a more recent alternative, the use of water as reaction medium together with a careful adjustment of the pH has allowed to define very efficient protocols for the completely β-regio- and *anti*-stereoselective azidolysis of a variety of α,β-epoxycarboxylic acids **11** by employing for the first time catalytic amounts (1 or 10 mol–%) of a metal salt such as $InCl_3$ or $AlCl_3$ at pH 4.0 or $Cu(NO_3)_2$ at pH 4.0 or 7.0 [38, 43–47].

β-Azido-α-hydroxycarboxylic acids **12** have been prepared with a complete stereoselectivity and in high yields by controlling the pH (Scheme 7.10).

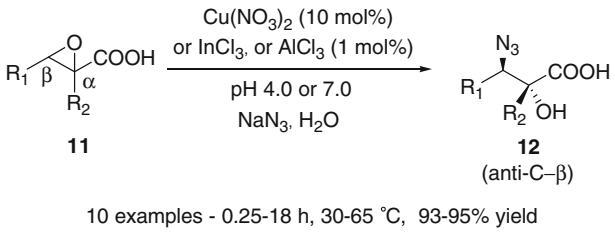

Scheme 7.10 Metal-catalyzed regio- and stereoselective azidolysis of α,β-epoxycarboxylic acids in water [38, 43–47]

These efficient protocols are the result of a study devoted at the comparison of the efficiency of a metal salt employed as catalyst in water and in organic media. It has proved that the pH of the aqueous medium is crucial for realizing this process satisfactorily; in fact, only in water a Lewis acid can be used in a catalytic amount, while in organic media, large excess is needed. Both the catalyst and water (used as reaction medium) have been recovered and reused in further runs, without observing any decrease in the efficiency of the process. These results prove the environmental efficiency of these procedures.

By coupling the catalyzed protocols for the preparation of **12** with that for the azido group reduction catalyzed by the same metal salt [74], it has been possible to define the first one-pot synthesis of α-hydroxy-β-amino acids (norstatines) starting from the corresponding α,β-epoxycarboxylic acids avoiding at all the use of organic solvent [38]. Among all the metal catalysts tested, Cu(II), Co(II), Al(III), and In(III), Cu(II) salts proved to be the most efficient for this one-pot protocol. In this case also, the catalyst used could be completely recovered and reused efficiently (Scheme 7.11).

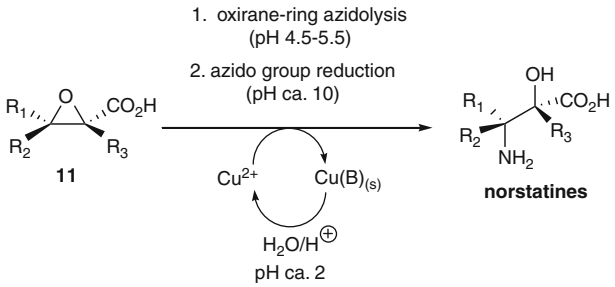

Scheme 7.11 Cu(II)-based catalytic cycle for the synthesis of norstatines [38]

Similarly, very efficient protocols for the Lewis acid–catalyzed ring opening of epoxides by thiols and halides have been realized [34, 42, 45]. In all cases, the careful control of the pH has allowed the highest efficiency.

The reaction of sodium azide with epoxides at room temperature has been recently proposed by using $Zr(DS)_4$ as catalyst [75].

β-CD has been used as promoter for the kinetic resolution of epoxides in water [76, 77]. Rao et al. reported interesting results in the reactions of glycidols **5** with trimethylsilyl azide ($TMSN_3$,) and isopropylamine (Scheme 7.12). Enantioselectivity outcome is strongly influenced by the amount of β-CD used, and the best results have been obtained by using 1.33 or 2.0 equivalents, while the use of substoichiometric amounts led to very low *ee*s [76].

Scheme 7.12 Kinetic resolution of glycidols 5 in water promoted by β-CD [76]

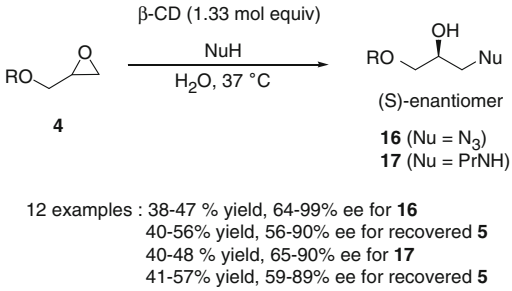

7.3 Epoxides in the Synthesis 1,2-Diols, 1,2-Alkyloxy, and -Aryloxy Alcohols in Water

Water, alcohols, and phenols react very poorly as nucleophiles with epoxides [78–80]. Anyway, this reaction is important because it is the most direct access route for the preparation of 1,2-diols, 1,2-alkyloxy, and -aryloxy alcohols.

Jafarpour et al. reported the use of $Zr(DS)_4$ (5 mol-%) as a recoverable and reusable LASC for the ring opening of epoxides with water under reflux. The same catalyst was effective in the reactions with alcohols, but in these cases, the transformations were conducted in the same alcohol as reaction medium [75].

Weberskirch et al. reported the hydrolytic kinetic resolution (HKR) of epoxides in water [81]. The authors designed a novel catalytic system with the intention of creating a localized area where hydrophobic substrates are concentrated in order to make reactions proceed more efficiently (micellar catalysis). They prepared core–shell-type nanoreactors (particle radius in the range of 10–12 nm) where a hydrophobic core furnishes the favorable environment for the catalytic center, that is a Co(III)–(salen) complex (H_2 salen = *N*,*N*′-bis(salicylidene)ethylenediamine), and the substrate epoxide, while a hydrophilic shell warrants the solubility in water of the whole nanoreactor. Co(III)–(salen) unit was covalently attached to an amphiphilic polymer and hence capable to create micellar aggregates in water and form complex **18** (Scheme 7.13). The formation of micellar aggregates of **18** in water at a 0.18–0.39 mmol/L dilution was studied with transmission electron microscopy (TEM) analysis and dynamic light scattering (DLS).

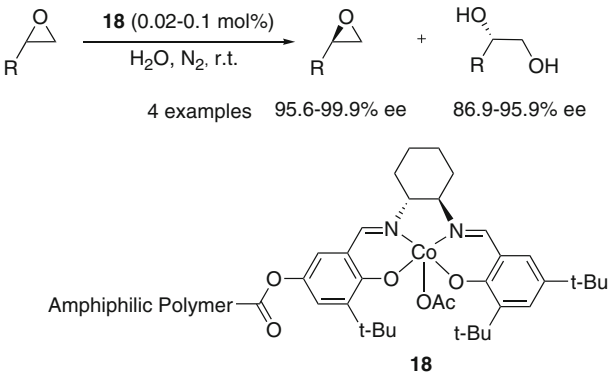

Scheme 7.13 Hydrolytic kinetic resolution (HKR) of epoxides in water [81]

The efficiency of **18** was studied in the case of aromatic terminal epoxides that usually need large amounts of Jacobsen's catalyst and long reaction times under homogenous conditions [18, 81]. The results obtained were comparable to those reached under homogenous conditions. The authors successfully generated a nanoreactor with high local concentration of the catalyst in the hydrophobic core, while the amount of water that could penetrate into the micelle was very little, which is crucial for achieving high yields and stereoselectivity. The catalyst was recovered and reused in four consecutive runs without decrease in its efficiency.

The use of a polymeric Co(III)–(salen) complex was also reported by Zheng et al. in organic solvent or under solvent-free conditions. These authors also showed that better *ees* were achieved for the preparation of diols when the recovered catalyst was used with water as reaction medium and as reactant [82].

The use of deoxyribonucleic acid (DNA) as a chiral scaffold to develop asymmetric catalysis was reported for the first time by Feringa et al. [83–85]. This approach has been further applied in several transformations including the HKR of a series of 2-pyridyloxiranes **19** in water, buffered at pH 6.5. DNA-bound Cu(II) complex **20** where Cu(II) is bounded to DNA via an achiral ligand (**21–23**) was employed (Scheme 7.14) [86].

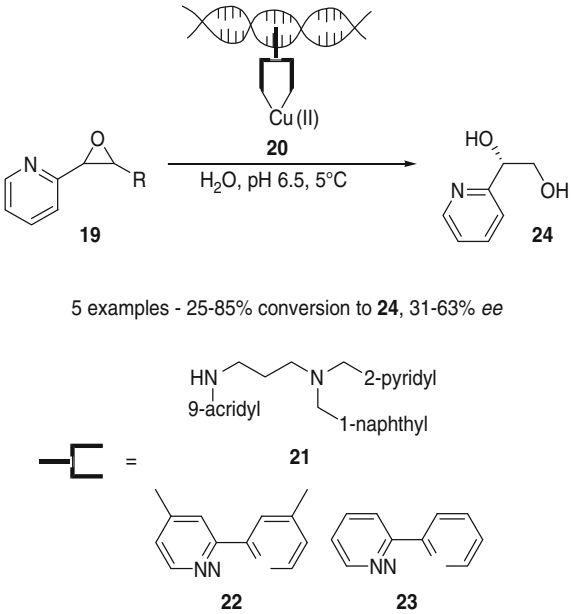

Scheme 7.14 DNA-bound Cu(II) complex 20 as catalyst for the HKR of epoxides in water [86]

The efforts of this research group show that DNA can be used as a viable source of chirality for the HKR reaching 63% *ee* of the recovered epoxide (selectivity(s) = 2.7). It is highly interesting that DNA-based catalysts can be used in such HKR in water, but obvious limitations are evident for synthetic application.

The Hg^{2+} promoted addition of water to a carbon–carbon double bond has been used by Franssen et al. [36] for the resolution of the diastereomeric mixture of limonene 1,2 epoxides (*cis* and *trans*) in buffered medium (pH 7.0).

β-CD has been often used as a promoter in the reactions of epoxides in aqueous media, and a further example has been reported by Rao et al. in the oxidation of terminal epoxides by *N*-bromosuccinimide (NBS) or 2-iodoxybenzoic acid (IBX) [87]. The role of β-CD is essential for realizing the process, and mechanistic studies have proved that the cyclodextrin not only activates the epoxide but also forms a complex with the oxidizing agent through H-bonding, which first oxidizes the epoxide to 1,2-diol, and then further oxidation of the secondary carbon furnishes the corresponding β-hydroxy ketone. Evidences of the complexation of β-CD with the epoxide and the oxidizing agent were deduced from 1H NMR and IR spectroscopy [88, 89].

7.4 Epoxides in the Synthesis β̃ Hydroxy Sulfur Compounds

Organic chemists have usually performed the reaction of thiols and epoxides in organic solvents (THF, CH_2Cl_2, MeOH, MeCN) generating reactive thiolate under anhydrous conditions [90–95]. Generally, good yields and short reaction times are obtained, but often harsh reaction conditions are required, and the basic conditions can be tolerated only by appropriate functional groups [90]. Alternatively, by using an activating agent (generally a Lewis acid), milder reaction conditions can be adopted, and thiols can be directly used as nucleophile.

Hydroxide ion in water is able to deprotonate both aryl- (pKa 6–8) [96, 97] and alkylthiols (pKa 10–11) [97] forming in situ the corresponding highly nucleophilic thiolates; the use of aqueous basic conditions represents an ideal approach to realize efficiently this process.

We have reported that at pH 9.0 [40, 42], the thiolysis of several epoxides with a variety of substituted arylthiols was fast, and in 0.08–4.0 h, a complete conversion was reached at 30°C with the prevalent formation of the β-products (>95%) coming from the totally *anti*-nucleophilic attack at the less substituted carbon of the oxirane ring. A little amount of α-addition products (3–5%) was sometimes observed (Scheme 7.15). Comparing these results with those showed in Scheme 7.9 for the azidolysis reaction of epoxides in water, it can be concluded that the thiolysis of alkyl oxiranes in basic aqueous medium is much more β-regioselective than the azidolysis one [48], and this is probably due to the higher nucleophilicity of ArS^-, with respect to N_3^- [96, 97].

Scheme 7.15 Thiolysis of epoxides under aqueous basic conditions [40, 42]

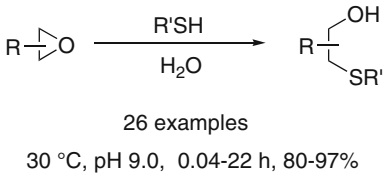

Formation of 1,2-diol products, due to the competition of nucleophilic oxygen species (OH^-, H_2O) with ArS^-, was rarely observed [98], and this by-product was never an obstacle for the purification of the desired β-hydroxy sulfide because the latter is poorly soluble in aqueous medium, and since it is a solid crystalline, it can be easily separated from the former by filtration. Also in the case of highly sterically hindered thiols or epoxides such as *ortho*-methyl-phenylthiol or 2-methyl-2,3-heptene oxide, the reactions were complete after a reasonable time (0.04–22 h). In all cases, the yields of the isolated β-hydroxy sulfides are very satisfactory (>80%) [40–42].

Exploitation of this aqueous protocol has been realized in the one-pot synthesis of 1,4-benzoxathiepinone by performing the thiolysis of epoxides by thiosalicylic

acid under basic conditions and then subsequent lactonization by varying the pH from basic to acidic [40].

The thiolysis of α,β-epoxy ketones is generally neither regio- nor stereoselective at the C-α position, especially in the case of acyclic substrates [99]. By an accurate control of the basicity of the reaction medium, thiolysis in water of this class of epoxides has been used as a key step for the one-pot multi-step synthesis of α-carbonyl vinylsulfoxides starting from the corresponding α,β-unsaturated ketones [35].

As an example of the crucial role played by the pH in this process according to the nature of the thiol, the different results obtained by employing thiols **26** in the reaction with the representative 3,4-epoxyheptan-2-one (**25**) are shown in Scheme 7.16. β-Carbonyl-β-hydroxy sulfides are highly base sensitive and easily give epimerization reaction at C-3. The retro-aldol and dehydration reactions producing complex reaction mixtures also occur.

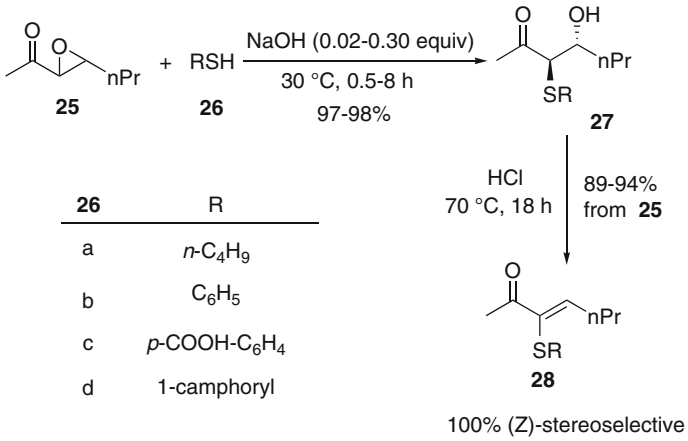

Scheme 7.16 Thiolysis of representative α,β-epoxy ketone 25 in water [35]

After an accurate study on the influence of pH on this transformation, we found that a catalytic amount of NaOH (0.02–0.3 molar equiv) was sufficient to complete the thiolysis of **25** in water at 30°C with thiols **26a–d**. The process is completely α-regio- and *anti*-stereoselective with the formation of only *anti*-β-hydroxy sulfides **27a–d** with excellent yields (97–98%). The one-pot synthesis of the corresponding vinyl sulfides **28** was accomplished by coupling the thiolysis process with a stereoselective dehydration achieved by treating compounds **27a–d** with HCl at 70°C for 18 h (Scheme 7.16) [35].

A variety of α,β-epoxy ketones were also tested, and in the case of cyclic substrates **29**, the corresponding vinyl sulfides **30** were obtained directly in very good yields (Scheme 7.17) [35].

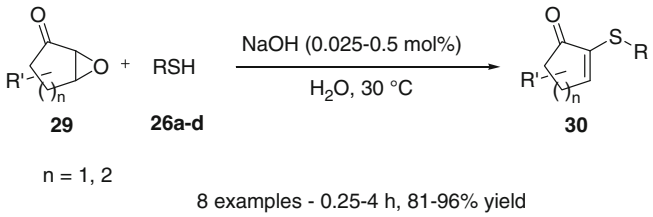

Scheme 7.17 Thiolysis of cyclic α,β-epoxy ketone 29 in water [35]

The possibility of achieving high selectivity and realizing one-pot processes is one of the advantage of water over the organic reaction medium. In this context, by combining the completely stereoselective protocol for the thiolysis of α,β-epoxy ketones in water with the epoxidation of α,β-enones previously developed [12c], the preparation of α-carbonyl sulfoxides **32** and triazole **33** starting from cyclohex-2-en-1-one (**31**) in very good yields has been reported (Scheme 7.18).

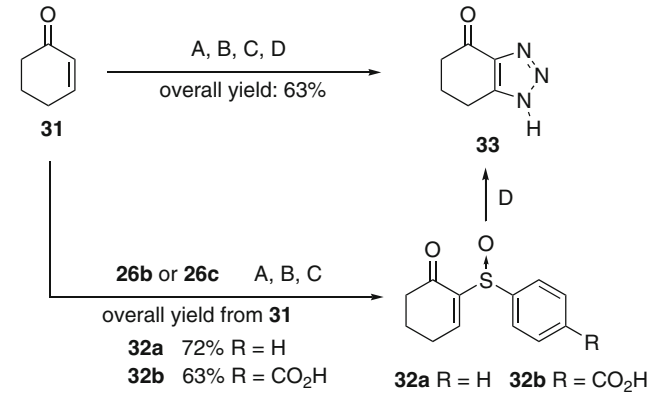

Scheme 7.18 One-pot protocols for the preparation of α-carbonyl sulfoxides 32 and triazole 33 [35]

Thiolysis of α,β-epoxycarboxylic acids is a key synthetic step in the preparation of calcium channel blocker diltiazem [90]. We investigated the reactions of phenylthiol with a series of α,β-epoxycarboxylic acids in sole water [34]. Ring openings were very slow under acidic conditions (pH 4.0) and sometimes occurred with very low conversions, while they became very fast at pH 9.0 and occurred quantitatively. Under basic conditions, phenylthiolate predominantly attacked the more electrophilic C-α carbon, except in the case of β-phenyl-substituted α,β-epoxy propanoic acid and when an alkyl substituent was present at C-α position.

In the reactions of alkyl- and aryl-substituted epoxides with azido ion, metal salts did not show any catalytic effect over entire pH range [48]. On the contrary, the addition of thiols to epoxides is efficiently catalyzed by several metal catalysts, especially by Zn(II) and In(III) salts [34, 37, 39, 42]. We have found previously that the catalytic efficiency of metal ion (Lewis acid) catalyst in water for the reaction of epoxides is expected to be maximum at a pH value lower than its $pK_{1,1}$ hydrolysis constant, at which the maximum concentration of the aqua ion is present [44]. According to this, the best catalyst under acidic pH was $InCl_3$ [34, 42] ($pK_{1,1}$ ca. = 4), while $ZnCl_2$ ($pK_{1,1}$ = 8.96) proved to be more versatile and showed a high catalytic efficiency also at pH 7.0 (biomimetic conditions) [37].

Accordingly, by exploiting the efficiency of $ZnCl_2$, thiolysis of a variety of epoxides has been performed under neutral conditions. In all cases, excellent yields (94–97%) and generally short reaction times were obtained (5–300 min). The use of substituted arylthiols was also investigated, and an example is illustrated in Scheme 7.19. In the case of highly coordinating *o*- and *p*-NH_2, and *o*- and *p*-CO_2H-subtituted phenylthiols, no catalytic effect was observed, supposedly due to the formation of a stable complex with Zn^{2+} and its consequent deactivation as oxirane ring-opening catalyst [100, 101]. The efficiency of $ZnCl_2$ as catalyst was regained in the case of *o*-Me-, *p*-NHAc and *o*-CO_2Me phenylthiols, that is, when the thiol carries functionalities with reduced binding properties.

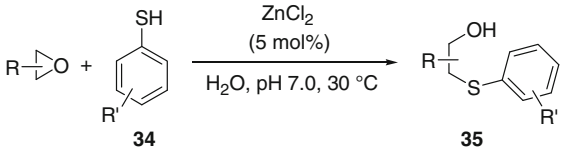

20 examples - 5-300 min, α/β-products ratio: (1-84)/(99-16), 94-97% yield

Scheme 7.19 Zn(II)-catalyzed thiolysis of epoxides under biomimetic conditions [37]

When $ZnCl_2$ was used at pH 4.0, it has been also possible to define a one-pot protocol for the selective preparation of sulfoxide or sulfone based on the thiolysis of epoxide and pH-controlled oxidation by H_2O_2 [39].

The use of $Sc(DS)_3$ with chiral ligand (*S,S*)-**9** in the reactions of *cis*-stilbene oxide (**6a**) with arylthiols has been also reported to yield good results (Scheme 7.20) [62].

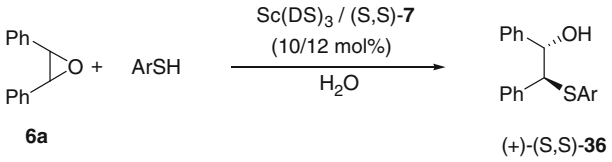

6 examples - r.t., 23-27 h, 44-76% yield, 85-93% *ee*

Scheme 7.20 $Sc(DS)_3$/(*S,S*)-9-catalyzed desymmetrization of *cis*-stilbene oxide (8a) by aryl thiols in water [62]

Water has proved to be an efficient reaction medium also for the addition of sulfonates to epoxides for the direct preparation of β-hydroxysulfones [102]. By combining the NaOH-catalyzed thiolysis of epoxide and the oxidation by *t*-butyl hydroperoxide, β-hydroxy sulfoxides have been prepared by coupling the use of water and microwave in a two step one-pot procedure [103].

Kiasat et al. reported the addition of ammonium thiocyanate to epoxides in water catalyzed by the multi-site phase-transfer catalyst α,α′,α″-*N*-hexakis (triethylammoniummethylene chloride)-melamine[104] or the polymeric catalyst PEG-SO_3H [105]. In both reports, the corresponding β-hydroxy thiocyanates have been obtained in short times and good yields (7 examples, 0.25–1 h, 70–96%) [104, 105].

By exploiting its basic properties, borax ($Na_2B_4O_7$) was used as an alternative to NaOH to catalyze (10 mol-%) the thiolysis of alkyl and aryl thiols to alkyl epoxides (14 examples, RT, 2–12 h, 43–98% yield) [106].

7.5 Epoxides and C-, Se-, and H-Nucleophiles in Water

The use of $Sc(DS)_3$ (5–10 mol–%) as LASC and (S,S)-**7** (6–12 mol-%) in water has been extended to the first enantioselective desymmetrization of *cis*-stilbene oxides **6** by indoles **37** (Scheme 7.21) [61, 107].

The amount of water used in these reactions is important, and the best results have been obtained at a formal concentration of 1.0 M. In the case of *cis*-stilbene oxide (**6a**) and indole (**37a**) (Scheme 7.21, Ar = Ph, $R_1 = R_2 = H$), going from 0.5 to 1.0 M, the reaction proceeded in 5 and 6 h, respectively, giving 50% and 85% yield with 96% and 93% *ee*, respectively. Details on the role of concentration in these processes are not available, but comparison with the same reaction performed in dichloromethane gave lower yields and *ee* [61].

Generally, the reactions proceeded at room temperature for 4–6 h with good yields (56–85%) and high enantioselectivities (85–93% ee) (Scheme 7.21).

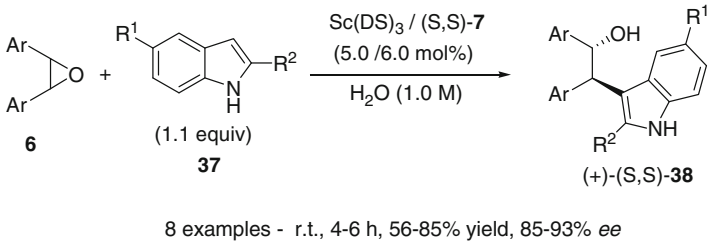

Scheme 7.21 Desymmetrization of epoxides 6 by indoles 37 in water catalyzed by $Sc(DS)_3$/(*S*,*S*)-7 system [61, 107]

β-cyclodextrin (β-CD) has been used to promote the addition of sodium cyanide to several epoxides in water/acetone (7.5/1) [108]. The reaction proceeded satisfactorily at RT and gave very good yields (Scheme 7.22). The authors also reported that

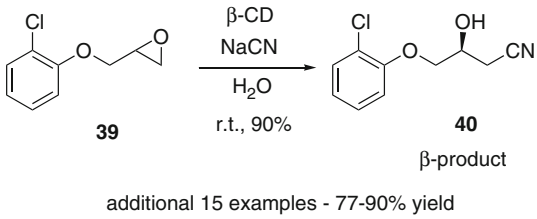

Scheme 7.22 β-CD promoted addition of sodium cyanide to chlorophenyl glycidol 39 [108]

β-CD was able in two cases to promote the process with a 15–17% *ee*. In Scheme 7.22, the case of chlorophenyl glycidol **39** has been representatively reported.

Similarly Rao et al. reported the use of β-CD for the promotion of the reaction of epoxides with benzeneselenol in water. A variety of epoxides were considered (10 examples), and the corresponding β-hydroxy selenides were obtained always in short times (25–40 min) and good yields (75–86%) [109].

Concellón et al. reported the ring opening of 3-aryl-2,3-epoxyamides in water or deuterium oxide by samarium iodide. The reaction proceeded with a complete β-regioselectivity (12 examples, 50–79% yields), and by starting from enantioenriched epoxides, 3-aryl-2-hydroxyamines were prepared with complete retention of configuration [110].

The use of α-, β-, and γ-cyclodextrins (α-, β-, and γ-CDs) was investigated for the kinetic resolution of epoxides in water by sodium, lithium, or potassium borohydrides [111–114]. Takahashi et al. [113, 114] found that in the reaction of styrene oxide (Scheme 7.23) with $NaBH_4$, as it happened in the case of azidolysis of epoxide (Scheme 7.12) [76], the efficiency of the process strongly depends on the amount of CD used. The best results were obtained by using 2 equivs of β-CD and after 72 h at room temperature. The (*S*)-1-phenylethanol (**42b**) was the main product (94%) with a 46% *ee*, and the (*S*)-epoxide **41** was recovered in 49% yield and 31% *ee*. The use of α-CD and γ-CD led to almost 1:1 mixture of products **42a/42b** (Scheme 7.23) [114].

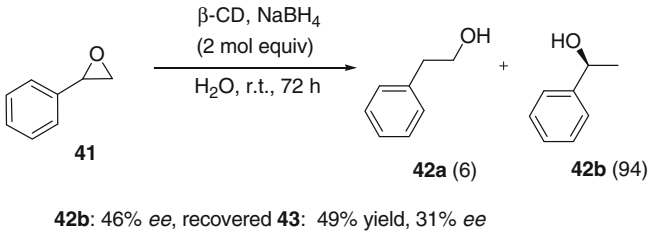

Scheme 7.23 β-CD promoted enantioselective reduction of styrene oxide 41 in water [114]

β-CD was also used as a promoter for the reduction of *ortho*- and *para*-substituted styrene oxides **43** and **45**, respectively. When sodium borohydride was used as reducing agent, better results than the corresponding lithium and potassium reagents were obtained [111, 112].

The authors found that by using 1.0 or 2.0 equivs of β-CD and 4.0 equivs of hydride, the β-regioselectivity for the formation of chiral alcohol **44b** was generally high (92–100%) except in the case of *o*-methoxystyrene oxide (Scheme 7.24, **43** R = OMe) where 14% of the corresponding **44b** was formed when $NaBH_4$ was used. More interestingly, it was found that *para*-substituted styrene oxides **45** preferentially gave the corresponding chiral (*S*)-alcohol **46b**, while the *ortho*-substituted gave the (*R*)-enantiomer (Scheme 7.24).

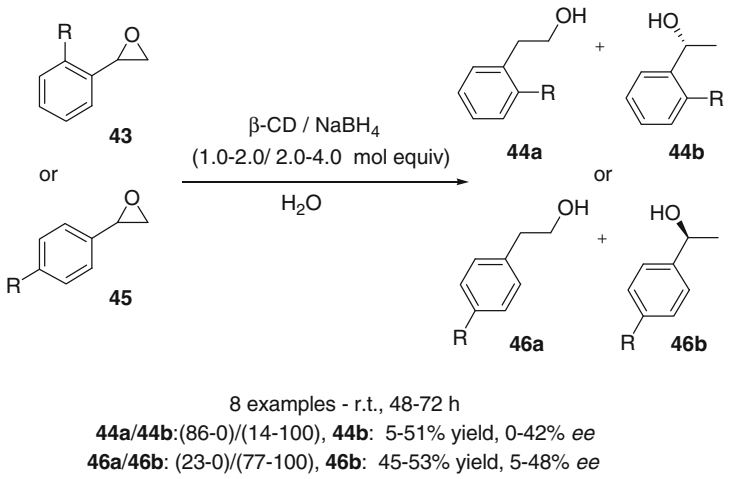

Scheme 7.24 β-CD promoted enantioselective reduction of *ortho*- and *para*-styrene oxides in water [111, 112]

7.6 Conclusions

Water is a very efficient reaction medium for several organic transformations. The unique properties of water make this medium attractive for individuating novel environmentally and chemically efficient organic transformations. Water should be used not as a simple substitution of the organic medium or as an exotic option to claim the greenness of a process, but because it plays a crucial role for reaching the highest chemical efficiency. In the case of the nucleophilic ring opening of epoxides, this environmentally benign reaction medium has proved to be able to improve the efficiency of these processes both in terms of yields and stereoselectivities.

Acknowledgments We gratefully acknowledge the Ministero dell'Istruzione, dell'Università e della Ricerca (MIUR) and the Università degli Studi di Perugia within the projects "Firb–Futuro in Ricerca" (prot. n. RBFR08TTWW and prot. n. RBFR08J78Q), PRIN 2008 for financial support.

References

1. Gruttadauria M, Giacalone F, Noto R (2009) Water in stereoselective organocatalytic reactions. Adv Synth Catal 351:33–57
2. Kobayashi S (2007) Asymmetric catalysis in aqueous media. Pure Appl Chem 79:235–245
3. Lindström UM (2007) Organic synthesis in water. Blackwell, London
4. Hayashi Y (2006) In water or in the presence of water? Angew Chem Int Ed 45:8103–8104
5. Narayan S, Muldoon J, Finn MG, Fokin VV, Kolb HC, Sharpless KB (2005) "On water": unique reactivity of organic compounds in aqueous suspension. Angew Chem Int Ed 44:3275–3279
6. Li C-J (2005) Organic reactions in aqueous media with a focus on carbon-carbon bond formations: a decade update. Chem Rev 105:3095–3165
7. Fringuelli F, Piermatti O, Pizzo F, Vaccaro L (2001) Recent advances in Lewis acid catalyzed Diels-Alder reactions in aqueous media. Eur J Org Chem 2001:439–455
8. Reichardt C (ed) (1990) Solvents and solvent effects in organic chemistry. VCH, Weinhem
9. Vilotijevic I, Jamison TF (2009) Epoxide-opening cascades in the synthesis of polycyclic polyether natural products. Angew Chem Int Ed 48:5250–5281
10. Bergmeier SC, Lapinsky DJ (2009) Three-membered ring systems. Prog Heterocycl Chem 21:69–93
11. Pineschi M, Bertolini F, Di Bussolo V, Crotti P (2009) Regio- and stereoselective ring opening of allylic epoxides. Curr Org Synth 6:290–324
12. Morten CJ, Byers AJ, Van Dyke AR, Vilotijevic I, Jamison TF (2009) The development of endo-selective epoxide-opening cascades in water. Chem Soc Rev 38:3175–3192
13. Schneider C (2006) Synthesis of 1,2-difunctionalized fine chemicals through catalytic, enantioselective ring-opening reactions of epoxides. Synthesis 2919–2944
14. Pastor IM, Yus M (2005) Asymmetric ring opening of epoxides. Curr Org Chem 9:1–29
15. Smith JG (1984) Synthetically useful reactions of epoxides. Synthesis 629–656
16. Parker RE, Isaacs NS (1959) Mechanisms of epoxide reactions. Chem Rev 59(4):737–799
17. Wong OA, Shi Y (2008) Organocatalytic oxidation asymmetric epoxidation of olefins catalyzed by chiral ketones and iminium salts. Chem Rev 108:3958–3987
18. Jacobsen EN (2000) Asymmetric catalysis of epoxide ring-opening reactions. Acc Chem Res 33:421–433
19. Bedore MW, Zaborenko N, Jensen KF, Jamison TF (2010) Aminolysis of epoxides in a microreactor system: a continuous flow approach to β-amino alcohols. Org Process Res Dev 14:432–440
20. Heravi MM, Baghernejad B, Oskooie HA (2009) A new strategy for the aminolysis of epoxides with amines under solvent-free conditions using Fe-Mcm-41 as a novel and efficient catalyst. Catal Lett 130:547–550
21. Ollevier T, Nadeau E (2008) Microwave-enhanced bismuth triflate-catalyzed epoxide opening with aliphatic amines. Tetrahedron Lett 49:1546–1550
22. Shivani PB, Chakraborti AK (2007) Zinc(II) perchlorate hexahydrate catalyzed opening of epoxide ring by amines: applications to synthesis of (RS)/(R)-propranolols and (RS)/(R)/(S)-naftopidils. J Org Chem 72:3713–3722
23. Yarapathy VR, Mekala S, Rao BV, Tammishetti S (2006) Polymer supported copper sulphate promoted aminolysis of epoxides with aromatic amines. Catal Commun 7:466–471
24. Sarangi C, Das N B, Nanda B, Nayak A, Sharma RP (1997) An Efficient nucleophilic cleavage of oxiranes to 1,2-azido alcohols. J Chem Res (S) 378–379
25. Crotti P, Di Bussolo V, Favero L, Macchia F, Pineschi M (1996) A novel effective transition metal based salt-catalyzed azidolysis of 1,2-epoxides. Tetrahedron Lett 37:1675–1678
26. Meguro M, Asao N, Yamamoto Y (1995) Ytterbium triisopropoxide catalysed ring opening of epoxides with trimethylsilyl azide. J Chem Soc Chem Commun 1021–1022
27. Mereyala HB, Frei B (1986) Preparation of vicinal azidohydrins by reaction of oxiranes with triethylaluminium/hydrogen azide. Helv Chim Acta 69:415–418

28. Burfield DR, Gan S, Smithers RH (1977) Reactions of a mono- and a tri-substituted epoxide with some simple and β-substituted primary amines; novel examples of electrophilic anchimeric assistance. J Chem Soc Perkin Trans I 666–671
29. Sundaram PK, Sharma MM (1969) Kinetics of reactions of amines with alkene oxides. Bull Chem Soc Jpn 42:3141–3147
30. FAN R-H, Hou X-L (2003) Efficient ring-opening reaction of epoxides and aziridines promoted by tributylphosphine in water. J Org Chem 68:726–730
31. Wu J, Xia H-G (2005) Tertiary amines as highly efficient catalysts in the ring–opening reactions of epoxides with amines or thiols in H_2O: expeditious approach to β-amino alcohols and β-aminothioethers. Green Chem 7:708–710
32. Azizi N, Saidi MR (2005) Stereoselective assembly of a 1,3-diene via coupling between an allenic acetate and a (B)-alkylborane: synthetic studies on amphidinolide B1. Org Lett 7:3649–3651
33. Surendra K, Krishnaveni NS, Rao KR (2005) The selective C-3 opening of aromatic 2,3-epoxy alcohols/epoxides with aromatic amines catalysed by β-cyclodextrin in water. Synlett 506–510
34. Fringuelli F, Pizzo F, Tortoioli S, Vaccaro L (2005) InCl3-catalyzed regio- and stereoselective thiolysis of α-epoxycarboxylic acids in water. Org Lett 7:4411–4414
35. Fringuelli F, Pizzo F, Vaccaro L (2004) NaOH-catalyzed thiolysis of a, b-epoxyketones in water. A key step in the synthesis of target molecules starting from α,-unsaturated ketones. J Org Chem 69:2315–2321
36. Fioroni G, Fringuelli F, Pizzo F, Vaccaro L (2003) Epoxidation of α, βunsaturated ketones in water. An environmentally benign protocol. Green Chem 5:425–428
37. Fringuelli F, Pizzo F, Tortoioli S, Vaccaro L (2003) Zn(II)-catalyzed thiolysis of oxiranes in water under neutral conditions. J Org Chem 68:8248–8251
38. Fringuelli F, Pizzo F, Rucci M, Vaccaro L (2003) First one-pot copper-catalyzed synthesis of α-hydroxy-β-amino acids in water. A new protocol for preparation of optically active norstatines. J Org Chem 68:7041–7045
39. Amantini D, Fringuelli F, Pizzo F, Tortoioli S, Vaccaro L (2003) $ZnCl_2$. as an efficient catalyst in the thiolysis of 1,2-epoxides by thiophenol in aqueous medium. Synlett 2292–2296
40. Fringuelli F, Pizzo F, Tortoioli S, Vaccaro L (2003) Easy and environmentally friendly uncatalyzed synthesis of β-hydroxy arylsulfides by thiolysis of 1,2-epoxides in water. Green Chem 5:436–440
41. Amantini D, Fringuelli F, Pizzo F, Tortoioli S, Vaccaro L (2002) Nucleophilic ring opening of 1,2-epoxides in aqueous medium. Arkivoc (xi):293–311
42. Fringuelli F, Pizzo F, Tortoioli S, Vaccaro L (2002) Thiolysis of alkyl- and aryl-1,2-epoxides in water catalyzed by $InCl_3$. Adv Synth Catal 344:379–384
43. Fringuelli F, Pizzo F, Vaccaro L (2001) Azidolysis of α, β-epoxycarboxylic acids. A water-promoted process efficiently catalyzed by indium trichloride at pH 4.0. J Org Chem 66:3554–3558
44. Fringuelli F, Pizzo F, Vaccaro L (2001) Lewis acid catalyzed organic reactions in water. The case of $AlCl_3$, $TiCl_4$, and $SnCl_4$ believed to be unusable in aqueous medium. J Org Chem 66:4719–4722
45. Amantini D, Fringuelli F, Pizzo F, Vaccaro L (2001) Bromolysis and iodolysis of α, β-epoxycarboxylic acids in water catalyzed by indium halides. J Org Chem 66:4463–4467
46. Fringuelli F, Pizzo F, Vaccaro L (2001) $AlCl_3$ as an efficient Lewis acid catalyst in water. Tetrahedron Lett 42:1131–1133
47. Fringuelli F, Pizzo F, Vaccaro L (2000) First efficient regio- and stereoselective metal-catalyzed azidolysis of 2,3-epoxycarboxylic acids in water. Synlett 311–314
48. Fringuelli F, Piermatti O, Pizzo F, Vaccaro L (1999) Ring opening of epoxides with sodium azide in water. A regioselective pH-controlled reaction. J Org Chem 64:6094–6096
49. Bonollo S, Fringuelli F, Pizzo F, Vaccaro L (2006) A green route to β-amino alcohols via the uncatalyzed aminolysis of 1,2-epoxides by alkyl- and arylamines. Green Chem 8:960–964
50. Abaee MS, Hamidi V, Mojtahedi MM (2008) Ultrasound promoted aminolysis of epoxides in aqueous media: a rapid procedure with no pH adjustment for additive-free synthesis of β-aminoalcohols. Ultrason Sonochem 15:823–827

51. Sreedhar B, Radhika P, Neelima B, Hebalkar N (2007) Regioselective ring opening of epoxides with amines using monodispersed silica nanoparticles in water. J Mol Catal A 272: 159–163
52. Procopio A, Gaspari M, Nardi M, Oliverio M, Rosati O (2008) Highly efficient and versatile chemoselective addition of amines to epoxides in water catalyzed by erbium(III) triflate. Tetrahedron Lett 49:2289–2293
53. Bonollo S, Fringuelli F, Pizzo F, Vaccaro L. (2007) $Zr(DS)_4$ as an efficient catalyst for the aminolysis of epoxides in water. Synlett 2683–2686
54. Firouzabadi H, Iranpoor N, Khoshnood A (2007) Aluminum tris (dodecyl sulfate) trihydrate $Al(DS)3{\cdot}3H_2O$ as an efficient Lewis acid–surfactant-combined catalyst for organic reactions in water: efficient conversion of epoxides to thiiranes and to amino alcohols at room temperature. J Mol Catal A 274:109–115
55. Kobayashi S, Manabe K (2002) Development of novel Lewis acid catalysts for selective organic reactions in aqueous media. Acc Chem Res 35:209–217
56. Azoulay S, Manabe K, Kobayashi S (2005) Catalytic asymmetric ring opening of meso-epoxides with aromatic amines in water. Org Lett 7:4593–4595
57. Ogawa C, Azoulay S, Kobayashi S (2005) Bismuth triflate-chiral bipyridine complex catalyzed asymmetric ring opening reactions of meso-epoxide in water. Heterocycles 66:201–206
58. Schneider C, Sreekanth AR, Mai E (2004) Scandium-bipyridine-catalyzed enantioselective addition of alcohols and amines to meso-epoxides. Angew Chem Int Ed 43:5691–5694
59. Tschöp A, Marx A, Sreekanth AR, Schneider C (2007) Scandium-bipyridine-catalyzed enantioselective alcoholysis of meso-epoxides. Eur J Org Chem 2007:2318–2327
60. Bonollo S, Fringuelli F, Pizzo F, Vaccaro L (2008) Zn(II)-catalyzed desymmetrization of meso-epoxides by aromatic amines in water. Synlett 1574–1578
61. Kokubo M, Naito T, Kobayashi S (2010) Chiral zinc(II) and copper(II)-catalyzed asymmetric ring-opening reactions of meso-epoxides with aniline and indole derivatives. Tetrahedron 66:1111–1118
62. Boudou M, Ogawa C, Kobayashi S (2006) Chiral scandium-catalysed enantioselective ring-opening of meso-epoxides with N-heterocycle alcohol and thiol derivatives in water. Adv Synth Catal 348:2585–2589
63. Iranpoor N, Firouzabadi H, Shekarize M (2003) Micellar media for the efficient ring opening of epoxides with CN^-, N_3^-, NO_3^-, NO_2^-, SCN^-, Cl^- and Br^- catalyzed with $Ce(OTf)_4$. Org Biomol Chem 1:724–727
64. (a) Patai S (1971) The Chemistry of the azido group. Wiley, New York; (b) Scriven EFV, Turnbull K (1988) Chem Rev 88:297–368
65. Kiasat A-R, Zayadi M (2008) Polyethylene glycol immobilized on silica gel as a new solid–liquid phase-transfer catalyst for regioselective azidolysis of epoxides in water: an efficient route to 1,2-azido alcohols. Catal Commun 9:2063–2067
66. Kiasat A-R, Badri R, Zargar B, Sayyahi S (2008) Poly(ethylene glycol) grafted onto dowex resin: an efficient, recyclable, and mild polymer-supported phase transfer catalyst for the regioselective azidolysis of epoxides in water. J Org Chem 73:8382–8385
67. Various Authors (1999) The chemistry and biology of β-amino acids. In: Hoekstra WJ (ed) Curr Med Chem 6:905–1002
68. Kiso Y, Yamaguchi S, Matsumoto H et al (1998) KNI-577, a potent small-sized HIV protease inhibitor based on the dipeptide containing the hydroxymethylcarbonyl isostere as an ideal transition-state mimic. Arch Pharm 331:87–89
69. Juaristi E (1997) Enantioselective synthesis of β-amino acids. Wiley-VCH, New York
70. Cardillo G, Tomasini C (1996) Asymmetric synthesis of ß-amino acids and α-substituted β-amino acids. Chem Soc Rev 25:117–127
71. Azzena F, Crotti P, Favero L, Pineschi M (1995) Regiochemical control of the ring opening of 12-epoxides by means of chelating processes.11. Ring opening reactions of aliphatic mono- and difunctionalized cis and trans 2,3- and 3,4-epoxy esters. Tetrahedron 48:13409–13422
72. Legters J, Thijs L, Zwanenburg B (1992) A convenient synthesis of aziridine-2-carboxylic esters. Recl Trav Chim Pays-Bas 111:1–23

73. Chong JM, Sharpless KB (1985) Nucleophilic openings of 2,3-epoxy acids and amides mediated by Ti(O-i-Pr)4. Reliable C-3 selectivity. J Org Chem 50:1560–1563
74. Fringuelli F, Pizzo F, Vaccaro L (2000) Cobalt(II) chloride-catalyzed chemoselective sodium borohydride reduction of azides in water. Synthesis 646–650
75. Jafarpour M, Rezaeifard A, Aliabadi M (2010) An environmentally benign catalytic method for efficient and selective nucleophilic ring opening of oxiranes by zirconium tetrakis(dodecyl sulfate). Helv Chim Acta 93:405–413
76. Kamal A, Arifuddin M, Rao MV (1999) Enantioselective ring opening of epoxides with trimethylsilyl azide ($TMSN_3$) in the presence of β-cyclodextrin: an efficient route to 1,2-azido alcohols. Tetrahedron Asymmetry 10:4261–4264
77. Guy A, Doussout J, Garreau R, Godefroy-Falguieres A (1992) Selective ring-opening reaction of styrene oxide with lithium azide in the presence of cyclodextrins in aqueous media. Tetrahedron Asymmetry 2:247–250
78. As recent efficient example and literature update see Zvagulis A, Bonollo S, Lanari D, Pizzo F, Vaccaro L (2010). 2-tert-Butylimino-2-diethylamino-1,3-dimethylperhydro-1,3,2-diazaphosphorine supported on polystyrene (PS-BEMP) as an efficient recoverable and reusable catalyst for the phenolysis of epoxides under solvent-free conditions. Adv Synth Catal 352:2489–2496
79. Jiang D, Urakawa A, Yulikov M, Mallat M, Jeschke T, Baiker A (2009) Size selectivity of a copper metal-organic framework and origin of catalytic activity in epoxide alcoholysis. Chem Eur J 15:12255–12262
80. Brimble MA, Liu Y-C, Trzoss M (2007) A facile synthesis of aryl spirodioxines based on a 3 h,3′h-2,2′-spirobi(benzo[b][1,4]dioxine) skeleton. Synthesis 1392–1402
81. Rossbach BM, Leopold K, Weberskirch R (2006) Self-assembled nanoreactors as highly active catalysts in the hydrolytic kinetic resolution (HKR) of epoxides in water. Angew Chem Int Ed 45:1309–1312
82. Song Y, Yao X, Chen H, Bai C, Hu X, Zheng Z (2002) Highly enantioselective resolution of terminal epoxides using polymeric catalysts. Tetrahedron Lett 42:6625–6627
83. Boersma AJ, Feringa BL, Roelfes G (2007) α, β-unsaturated 2-acyl imidazoles as a practical class of dienophiles for the DNA-based catalytic asymmetric Diels-Alder reaction in water. Org Lett 9:3647–3650
84. Roelfes G, Boersma A J, Feringa B L (2006) Highly enantioselective DNA-based catalysis. Chem Commun 635–637
85. Roelfes G, Feringa BL (2005) DNA-based asymmetric catalysis. Angew Chem Int Ed 44:3230–3232
86. Dijk EW, Feringa BL, Roelfes G (2008) DNA-based hydrolytic kinetic resolution of epoxides. Tetrahedron Asymmetry 19:2374–2377
87. van der Werf MJ, Jongejan H, Franssen MCR (2001) Resolution of limonene 1,2-epoxide diastereomers by mercury(II) ions. Tetrahedron Lett 42:5521–5524
88. Reddy MA, Bhanumathi N, Rao KR (2002) (2002) A mild and efficient biomimetic synthesis of α-hydroxymethylarylketones from oxiranes in the presence of β-cyclodextrin and NBS in water. Tetrahedron Lett 43:3237–3238
89. Surendra K, Krishnaveni NS, Reddy MA, Nageswar YVD, Rao KR (2003) Highly selective oxidative cleavage of β-cyclodextrin-epoxide/aziridine complexes with ibx in water. J Org Chem 68:9119–9121
90. Furutani T, Imashiro R, Hatsuda M (2002) A practical procedure for the large-scale preparation of methyl (2R,3 S)-3-(4-methoxyphenyl)glycidate, a key intermediate for diltiazem. J Org Chem 67:4599–4601
91. Adams H, Bell R, Cheung Y-Y, Jones ND, Tomkinson NCO (1999) The cleavage of meso-epoxides with homochiral thiols: synthesis of (+)- and (−)-trans-1-mercaptocyclohexan-2-ol. Tetrahedron Asymmetry 10:4129–4142
92. Justo De Pomar JC, Soderquist A (1998) Regio- and stereospecific synthesis of (O-TIPS)-protected 2-hydroxyalkylmercaptans from epoxides and triisopropylsilanethiol. Tetrahedron Lett 39:4409–4412
93. Yamada O, Ogasawara K, Synlett 427–428

94. Behrens CH, Sharpless KB (1985) Selective transformations of 2,3-epoxy alcohols and related derivatives. Strategies for nucleophilic attack at carbon-3 or carbon-2. J Org Chem 50:5696–5704
95. Abul-Hajj YJ (1986) Synthesis and evaluation of 4-(substituted thio)-4-androstene-3,17-dione derivatives as potential aromatase inhibitors. J Med Chem 29:582–584
96. Smith MB, March MB (2001) March's advanced organic chemistry, 5th edn. Wiley-Interscience Publication, New York
97. Streitwieser A (1952) Solvolytic displacement reactions at saturated carbon atoms. Chem Rev 56:571, cfr. page 582
98. Fringuelli F, Pizzo F, Tortoioli S, Vaccaro L (2005) Thiolysis of 1,2-epoxides under environmentally friendly conditions. Targets Heterocycl Syst 8:147–161
99. Lauret C (2001) Epoxy ketones as versatile building blocks in organic synthesis. Tetrahedron Asymmetry Rep N 52(12):2359–2383
100. Fringuelli F, Pizzo F, Tortoioli S, Zuccaccia C, Vaccaro L (2006) In(OTf)3-catalyzed thiolysis of 1,2-epoxides by arylthiols under SFC. A new approach for the synthesis of thiazolopyridinium ionic liquids. Green Chem 8:191–196
101. Fringuelli F, Pizzo F, Tortoioli S, Vaccaro L (2004) Solvent-free $Al(OTf)_3$-catalyzed aminolysis of 1,2-epoxides by 2-picolylamine: a key step in the synthesis of ionic liquids. J Org Chem 69:7745–7747
102. Murthy SN, Madhav B, Reddy VP, Rao KR, Nageswar YVD (2009) An approach toward the synthesis of β-hydroxy sulfones on water. Tetrahedron Lett 50:5009–5011
103. Pironti V, Colonna S (2005) $In(OTf)_3$-catalyzed thiolysis of 1,2-epoxides by arylthiols under SFC. A new approach for the synthesis of thiazolopyridinium ionic liquids. Green Chem 7:43–45
104. Kiasat AR, Mirzajani R, Shalbaf H, Tabatabaei T (2009) Nucleophilic ring opening of epoxides promoted by multi-site phase-transfer catalyst. An efficient and eco-friendly route to synthesis of β-hydroxy-thiocyanate. Chin Chem Lett 20:1025–1029
105. Kiasat AR, Mehrjardi MF (2008) PEG-SO_3H as eco-friendly polymeric catalyst for regioselective ring opening of epoxides using thiocyanate anion in water: an efficient route to synthesis of β-hydroxy thiocyanate. Catal Commun 9:1497–1500
106. Gao P, Xu P-F, Zhai H (2008) Borax-catalyzed thiolysis of 1,2-epoxides in aqueous medium. Tetrahedron Lett 49:6536–6538
107. Kokubo M, Naito T, Kobayashi S (2009) Metal-controlled reversal of enantioselectivity in catalyzed asymmetric ring-opening reactions of meso-epoxides in water. Chem Lett 38: 904–905
108. Srinivas B, Kumar VP, Sridhar R, Surendra K, Nageswar YVD, Rao KR (2007) Regioselective nucleophilic opening of epoxides and aziridines under neutral conditions in the presence of β-cyclodextrin in water. J Mol Catal A 261:1–5
109. Sridhar R, Srinivas B, Surendra K, Krishnaveni NS, Rao KR (2005) Synthesis of β-hydroxy selenides using benzeneselenol and oxiranes under supramolecular catalysis in the presence of β-cyclodextrin in water. Tetrahedron Lett 46:8837–8839
110. Concellón JM, Bardales E, Gómez C (2003) 1,3-Cycloaddition of nitrile oxides in ionic liquids. An easier route to 3-carboxy isoxazolines, potential constrained glutamic acid analogues. Tetrahedron Lett 44:5323–5326
111. Doussot J, Guy A, Siaugue J-M, Ferroud C, Falguieres A (1999) Substituent effects in the selective reductive opening of epoxides with borohydrides in the presence of β-cyclodextrin. Chirality 11:541–545
112. Doussot J, Guy A, Garreau R, Falguières A, Cossy J, Amsterdamsky C (1996) Préparation sélective d'alcools benzyliques substitutés à partir de substrats aromatiques complexés dans la β–cyclodextrine. Bull Soc Chim Fr 133:161–166
113. Hu Y, Uno M, Harada A, Takahashi S (1991) Selective ring–opening reaction of epoxides with sodium borohydride in the presence of cyclodextrins in aqueous media. Bull Chem Soc Jpn 64:1884–1888
114. Hu Y, Uno M, Harada A, Takahashi S (1990) Selective ring–opening reaction of epoxides with sodium borohydride in the presence of cyclodextrins in aqueous media. Chem Lett 797–798

Chapter 8
Ionanofluids: New Heat Transfer Fluids for Green Processes Development

Carlos A. Nieto de Castro, S.M. Sohel Murshed, Maria J.V. Lourenço, Fernando J.V. Santos, Manuel L.M. Lopes, and João M.P. França

Abstract Ionanofluids represent a new and innovative class of heat transfer fluids that encompass multiple disciplines like nanoscience, mechanical, and chemical engineering. Apart from fascinating thermophysical properties, the most compelling feature of ionanofluids is that they are designable and fine-tunable through base ionic liquids. Besides presenting results on thermal conductivity and specific heat capacity of ionanofluids as a function of temperature and concentration of multiwall carbon nanotubes, findings from a feasibility study of using ionanofluids as replacement of current silicon-based heat transfer fluids in heat transfer devices such as heat exchangers are also reported. By comparing results on thermophysical properties and estimating heat transfer areas for both ionanofluids and ionic liquids in a model shell and tube heat exchanger, it is found that ionanofluids possess superior thermophysical properties particularly thermal conductivity and heat capacity and require considerably less heat transfer areas as compared to those of their base ionic liquids. This chapter is dedicated to introducing, analyzing, and discussing ionanofluids together with their thermophysical properties for their potential applications as heat transfer fluids. Analyzing present results and other findings from pioneering researches, it is found that ionanofluids show great promises to be used as innovative heat transfer fluids and novel media for the exploitation of green energy technologies.

C.A. Nieto de Castro (✉) • S.M.S. Murshed • M.J.V. Lourenço • F.J.V. Santos • M.L.M. Lopes • J.M.P. França
Centre for Molecular Sciences and Materials, Department of Chemistry and Biochemistry, Faculty of Sciences, University of Lisbon, Campo Grande, Lisbon 1749-016, Portugal
e-mail: cacastro@fc.ul.pt; smmurshed@fc.ul.pt; mjvl@fc.ul.pt; fjsantos@fc.ul.pt; mllopes@fc.ul.pt

A. Mohammad and Inamuddin (eds.), *Green Solvents I: Properties and Applications in Chemistry*, DOI 10.1007/978-94-007-1712-1_8,

8.1 Introduction

The concept of "ionanofluids" was recently coined by Nieto de Castro and coworkers [1], and it represents a very new class of heat transfer fluids where nanoparticles are dispersed in ionic liquids only [2]. Since ionanofluids are a specific type of nanofluids, that is, ionic liquid-based nanofluids, it is important to provide background of nanofluids before discussing development and potential applications of ionanofluids in this section.

8.1.1 Nanofluids

Many high-tech industries and thermal management systems are facing great technical challenges for cooling of smaller features of microelectronic and more power output-based devices. However, the conventional method to increase the cooling rate is to use extended heat transfer surfaces, but this approach requires an undesirable increase in the size of the thermal management systems. In addition, the inherently poor thermal properties of traditionally used heat transfer fluids (HTFs) such as water, ethylene glycol (EG), or engine oil (EO) greatly limit the cooling performance. Thus, these conventional cooling techniques are not suitable to meet the cooling demand of the high-tech industries and advanced devices. It is known that fluids possess order-of-magnitude smaller thermal conductivity than metallic or nonmetallic materials. Therefore, the thermal conductivities of fluids that contain suspended metallic or nonmetallic particles are expected to be significantly higher than those of traditional heat transfer fluids.

It was only in 1995 that Choi [3] at Argonne National Laboratory of USA coined the concept of "nanofluids" to meet the aforementioned cooling challenges facing many advanced industries and devices. This new class of heat transfer fluids (nanofluids) is engineered by dispersing nanometer-sized solid particles, rods, or tubes in traditional heat transfer fluids, and they were found to exhibit significantly higher thermophysical properties, particularly thermal conductivity and thermal diffusivity than those of base fluids (BFs) [4–9]. From practical application-based studies such as convective and boiling heat transfer characteristics [10–16], nanofluids (NFs) were also found to be even more promising as their convective heat transfer coefficient and critical heat flux were reported to be substantially higher as compared to those of their base fluids. In particular, nanofluids containing high thermal conductive materials such as carbon nanotubes (CNT) show anomalously enhanced thermal performance [16–18]. Thus, nanofluids have attracted great interest from the research community due to their enhanced thermophysical properties, potential benefits, and applications in numerous important fields. Recent record shows that there is an exponential growth of annual research publications on nanofluids, and there are also more than 300 research groups and companies worldwide who are involved with nanofluids research [19].

The impact of nanofluid technology is expected to be great considering that heat transfer performance of heat exchangers or cooling devices is vital in numerous industries. When the nanoparticles are properly dispersed, nanofluids can offer

numerous benefits besides their anomalously high effective thermal conductivity. The benefits include improved heat transfer and thermal stability, microchannel cooling without clogging, miniaturized systems, and reduction in pumping power. With these highly desirable thermal characteristics and potential benefits, nanofluids can have a wide range of applications such as microelectronics, microelectromechanical systems, microfluidics, transportation, manufacturing, instrumentation, medical, and heating-ventilating-air-conditioning systems [8].

8.1.2 Ionanofluids and Their Prospect as Heat Transfer Fluids

The term *ionanofluids* is defined as the suspensions of nanomaterials (particles, tubes, and rods) in ionic liquids [1, 2, 20], and it is a new term in multidisciplinary fields such as nanoscience, nanotechnology, thermofluid, chemical, and mechanical engineering. Since ionic liquids (ILs) are the base fluids in ionanofluids, their thermophysical properties, potential benefits, and applications will also be discussed in short.

In the past decades, significant progress has been made toward better understanding and practical application of ionic liquids. Extensive research efforts [21–30] have been devoted to ionic liquids which have proven to be safe and sustainable alternatives for many applications in industry and chemical manufacturing. Their prospect and success arise mainly from their thermophysical and phase-equilibria properties, the versatility of their synthesis, and manageability to be tailored for a given application. Their solvent properties as well as heat transfer or heat storage and surface properties make this class of fluids possible to use in a high plethora of applications [25, 31]. Other advantages of ionic liquids include high ion conductivity, high volumetric heat capacity, high chemical and thermal stabilities, negligible vapor pressure, wide range of viscosity, and very good solvent properties [22, 24, 29, 30]. Due to all of these fascinating characteristics, they have been investigated extensively as alternatives to molecular solvents for liquid-phase reactions [27]. Ionic liquids are of great interest to scientists as well as chemical companies, not only because of their remarkable properties, but also for their actual and potential applications in the chemical process industries. In the past, the values of their thermophysical properties were found to have significant effect on the design of physicochemical processing and reaction units by influencing directly the design parameters and performance of equipments like heat exchangers, distillation columns, and reactors [32]. However, the optimal technological design of green processes requires the characterization of the ionic liquids used, namely, their thermodynamic, transport, and dielectric properties. Recently, our group has reported studies [1, 2, 31–34] where measured data on various thermophysical properties of a wide range of ionic liquids are presented besides studying their potential application as heat transfer fluids as well as their properties measurement methods and uncertainties. Results from these studies indicate that ionic liquids possess promising thermophysical properties and great potential for numerous applications, particularly as new heat transfer fluids.

The discovery that carbon nanotubes and room-temperature ionic liquids can be blended to form gels termed as "bucky gels" which can potentially be used in many engineering or chemical processing such as making novel electronic devices, coating materials, and antistatic materials, and, thus, it opens a completely new field [35, 36]. The "bucky gels" are blends or emulsions of ionic liquids with nanomaterials, mostly nanocarbons (tubes, fullerenes, and spheres), and they are actually CNT-laden ionanofluids. The possibility of using ionic liquids containing dispersed nanoparticles with specific functionalization such as functionalized single-walled carbon nanotubes (SWCNT), multiwalled carbon nanotubes (MWCNT), and fullerenes (C60, C80, etc.) opens the door to many applications. The use of nanoparticles as heat transfer enhancers allows us to associate small quantities of different types of nanomaterials to ionic liquids to prepare ionanofluids, which are highly flexible such that they can be designed (target-oriented) in terms of molecular structure, to achieve the desired properties necessary to accomplish a given task. This is possibly due to the complex interactions of ionic liquids and nanomaterials in the created complex emulsions. In contrast to conventional nanofluids, ionanofluids are more flexible as their base fluids are ionic liquids which can be prepared or designed for specific properties as well as for specific tasks.

Recent studies performed by this group (Nieto de Castro and coworkers) showed that ionanofluids containing MWCNT exhibit enhanced thermal conductivity (ranging from 2% to 35%) and specific heat capacity compared to their base ionic liquids [1, 2]. Since these ionanofluids have fascinating features such as high thermal conductivity, high volumetric heat capacity, and nonvolatility, they can potentially be used as novel heat transfer fluids. Another important application of ionanofluids is that they can be used in the development of new pigments for paint coatings of solar collectors with their higher solar absorbance and thermal emissivity as compared to the base paint [37]. Except researches conducted by this group, no other work on ionanofluids is available in the literature.

This chapter deals with the temperature and concentration dependence of thermal conductivity and specific heat capacity of ionanofluids containing MWCNT in several ionic liquids. Results of the thermal conductivity of these ionanofluids are also compared with the thermal conductivity data for MWCNT-nanofluids obtained from the literature. With the remarkable thermophysical properties and great flexibility of designing of ionanofluids for specific tasks and for particular properties, it can plausibly be considered that along with numerous applications, this new class of heat transfer fluids can potentially be used for the development of green processes.

8.2 Preparation of Ionanofluids

As mentioned previously, ionic liquids have been considered as potential heat transfer fluids not only due to their high volumetric heat capacity and good thermal conductivity (similar to conventional HTFs such as Dowtherm MX™, Syltherm 800™, and engine oil) but also for their high thermal stability and low vapor pressure.

Table 8.1 Reference values of thermophysical properties of some commonly used heat transfer fluids and ionic liquids at a moderate temperature of 40°C

Liquids	λ (W/m·K)	η (mPa·s)	C_p (J/kg·K)	ρ (kg/m^3)
Water	0.631	0.653	4,179	992
Ethylene glycol	0.256	10.37	2,520	1,100
Engine oil	0.148	568.00	2,000	880
[C_4mim][NTf_2]	0.116	28.50	1,372	1,423
[C_2mim][$EtSO_4$]	0.178	50.00	1,615	1,226

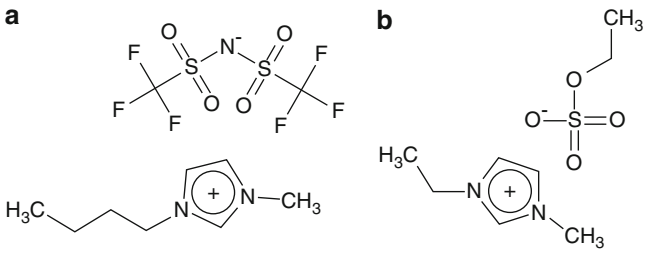

Fig. 8.1 Structures of ionic liquids (**a**) [C_4mim][NTf_2] and (**b**) [C_2mim][$EtSO_4$]

Reference values of thermophysical properties of some commonly used heat transfer fluids and ionic liquids used to prepare ionanofluids at a moderate temperature (40°C) are provided in Table 8.1 [38, 39]. Ionic liquids used were synthesized and purified following the procedure given elsewhere [40]. They were prepared through metathesis reactions from the appropriate [$C_n$mim]Cl. Prior to use, samples were extensively washed with distilled water and dried while stirring overnight at 70°C under high vacuum (0.1 Pa). Sample ionic liquids were analyzed by ^{1}H and ^{13}C nuclear magnetic resonance (NMR) and elemental analysis. The water content was measured using Karl Fischer titration before and after each measurement. The ionic liquids used were 1-butyl-3-methylimidazolium bis{(trifluoromethyl)sulfonyl} imide ([C_4mim][NTf_2]), 1-butyl-3-methylimidazoliuethylsulfate ([C_4mim][$EtSO_4$]), 1-butyl-3-methylimidazolium tetrafluoroborate ([C_4mim][BF_4], and 1-hexyl-3-methylimidazolium tetrafluoroborate [C_6mim][BF_4]). Structures of two representative ionic liquids (i.e., [C_4mim][NTf_2] and [C_2mim][$EtSO_4$]) are shown in Fig. 8.1.

Multiwalled carbon nanotubes (Baytubes®), provided by Bayer Material Science (Germany), were produced from a high-yielding catalytic process based on chemical vapor deposition. Baytubes® are agglomerates of multiwall carbon nanotubes with small outer diameters, narrow diameter distribution, and ultrahigh aspect ratio (length-to-diameter ratio). According to Bayer Material Science, the purity of MWCNT purchased was >99%, and the outer mean diameter and length of nanotubes were 13–16 nm and 1–10 μm, respectively. Following the technique used by Aida and coworkers [35, 36], sample ionanofluids were prepared by dispersing different weight percentages of MWCNT in several ionic liquids, and they were sonicated for better dispersion of nanotubes. All MWCNT suspensions were found

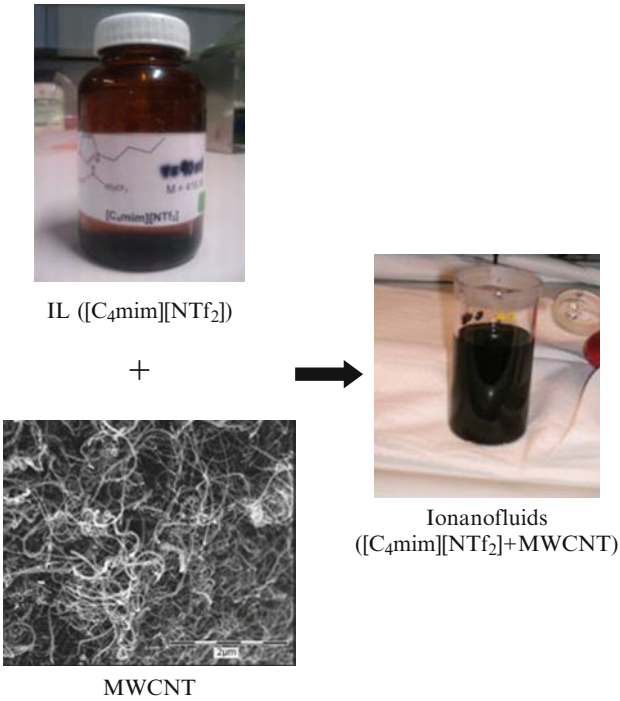

Fig. 8.2 Picture of MWCNT/[C_4mim][NTf_2]-based ionanofluids

to be very stable. A representative pictures of a sample ionanofluid containing MWCNT in [C_4mim][NTf_2] ionic liquid is shown in Fig. 8.2. The color of this ionanofluid is black due to dispersed carbon nanotubes.

8.3 Experimental and Measurement Details

The thermal conductivity of sample fluids was measured using a KD2 Pro Thermal Properties Analyzer (Labcell Ltd., UK). The theoretical basis and measurement principle of KD2 are basically the same as the transient hot-wire technique. The KD2 Pro is a handheld device used to measure thermal properties. It consists of a controller and sensors (probes) that can be inserted into the sample medium whose thermal properties are to be measured. There are three probes: the standard single-needle probe, an extended-length single-needle probe, and a dual-needle probe. While the single-needle probe measures the thermal conductivity and resistivity, the dual-needle probe is used to measure the thermal diffusivity and volumetric specific heat capacity.

As the ionic liquids are electrically conducting liquids, an electrically isolated thermal probe coated with a thin coating of an insulator is used. Thermal probe of this KD2 analyzer contains both the heating element and thermoresistor, and it needs

to be inserted into the sample vertically, rather than horizontally, in order to minimize the possibility of inducing convection. The measurement is made by electrically heating the probe within the sample while simultaneously monitoring the temperature change of the probe. A microprocessor or controller connected to the probe is used to control the heating rate and to measure the temperature change data. Details about KD2 Pro can be found in its user manual. A parameter-corrected version of the temperature model developed by Carslaw and Jaeger [41] for an infinite line heat source with constant heat output and zero mass in an infinite medium is used to calculate the thermal conductivity.

Before measuring the thermal conductivity of sample liquids, the KD2 Pro was carefully calibrated using toluene, water, glycerol, mixture of glycerol and water, and aqueous sodium chloride solution in order to cover the range of thermal conductivities between 0.13 and 0.67 W/m K. The calibration constant was found to be 1.026 ± 0.034, and it was temperature-independent [39]. Small quantity of sample to be analyzed was then sealed in a glass sample vial. The probe was inserted vertically into the sample via a purpose-made port in the lid of the vial. The sealed vial was then immersed in a thermostatic bath (Haake C25) which allowed controlling and maintaining the temperature of the test sample at any desired value. Several measurements were taken at each temperature to ensure reproducibility of the measured data, and the average values are reported. More details about the measurement procedure can be found in a work [42] where KD2 Pro device was also used for measuring thermal conductivity of several ionic liquids. Based on the standard deviations of experimental and calibration data, the uncertainty of the thermal conductivity measurements was found to be in the range of ±0.008 to ±0.014 W/m·K.

A calibrated differential scanning calorimeter (DSC-111, Setaram, France) was used to measure the specific heat capacity of sample fluids. The operation of this DSC is based on the Tian-Calvet principle, and it uses a cylinder-type measuring system composed of two sintered alumina cylinder tubes. These tubes are set parallel to each other in the heating furnace. The sensing part of this calorimeter is the central portion of the cylinders, and thermocouple-carrying heat-flux transducers (thermopiles) are wrapped around this central portion. The heat flow can then be measured by the temperature changes in these transducers. Details of the experimental procedure and calibration of this DSC can be found elsewhere [43, 44].

8.4 Results and Discussion

8.4.1 Thermal Conductivity of Ionanofluids

Results on temperature and concentration dependence of thermal conductivity of several MWCNT-ionanofluids obtained by our group together with the data of CNT/water-based nanofluids from the literature are presented and discussed in this section. Since a lot of research efforts [17, 18, 45, 46] have been made on the thermal conductivity of CNT-nanofluids, comparison of results of CNT-nanofluids and

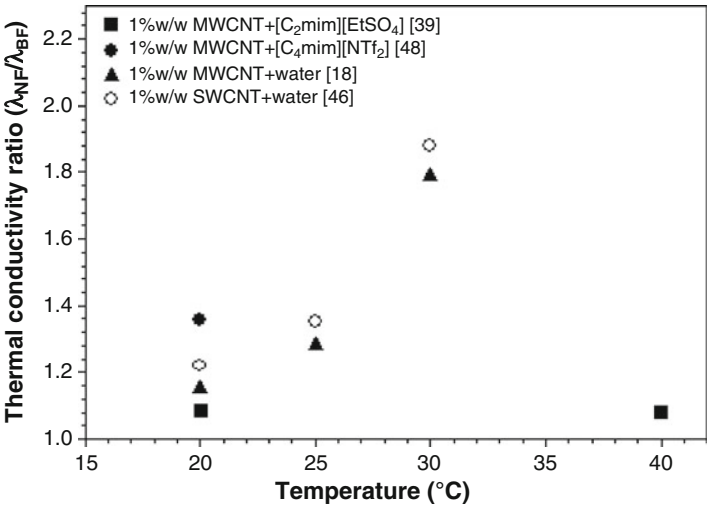

Fig. 8.3 Effect of temperature on thermal conductivity of CNT-loaded nanofluids and ionanofluids

CNT-ionanofluids can provide quantitative information about the enhancement of thermal conductivity of these two innovative heat transfer fluids. Most of the previous studies with CNT-nanofluids showed substantial increase in thermal conductivity compared to their base fluids. For instance, for 1% volumetric loading of MWCNT, Choi et al. [17] found as high as 160% increase in thermal conductivity of α-olefin oil (λ=0.145 W/m·K), and Xie et al. [45] reported about 13% and 19.6% increases in thermal conductivity of ethylene glycol (λ=0.256 W/m·K) and decene (λ=0.14 W/m·K), respectively. Besides understanding the potential of ionanofluids as novel heat transfer fluids, any comparison of enhancements of thermal conductivity of ionanofluids and nanofluids will make it easy to understand the comparative advantages of ionic liquids as base fluids that can be designed for specific tasks and properties oriented. Since no data are available in the literature for temperature-dependent thermal conductivity of ionanofluids, no comparison of present results can be made.

Temperature-dependent thermal conductivity of ionanofluids containing 1 wt% of MWCNT in [C_4mim][NTf_2] and [C_2mim][$EtSO_4$] and nanofluids containing the same concentrations of MWCNT and SWCNT in water are presented in Fig. 8.3. It can be seen from Fig. 8.3 that at room temperature, [C_4mim][NTf_2]-based ionanofluid showed maximum 35.5% increase in thermal conductivity compared to its base ionic liquid, whereas [C_2mim][$EtSO_4$]-based ionanofluid showed only 8.5% increase in thermal conductivity over its base fluids, and no temperature dependence of this thermal conductivity is observed. On the other hand, at the same temperature and concentration, thermal conductivity data of MWCNT/water-based nanofluids reported by Ding et al. [18] and data of SWCNT/water-based nanofluids obtained from Amrollahi et al. [46] showed about 15% and 22% increases in thermal

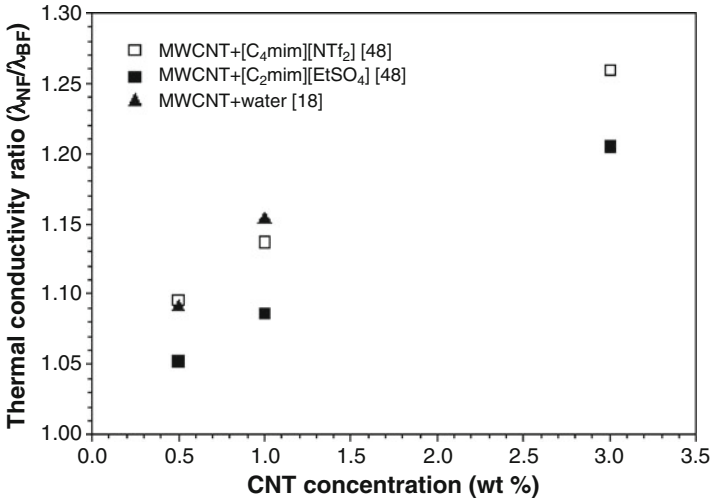

Fig. 8.4 Thermal conductivity enhancement of nanofluids and ionanofluids as a function of concentration of MWCNT at room temperature

conductivity, respectively (Fig. 8.3). It is also noted that for better dispersion and stability of nanofluids, Ding et al. [18] used 0.25 wt% Gum Arabic stabilizer with their nanofluids, and Amrollahi et al. [46] added 1 wt% SDS surfactant to their SWCNT nanofluids. Thus, it can be demonstrated that at room temperature, $[C_4mim][NTf_2]$-based ionanofluids is much better conductive suspensions than aqueous CNT-nanofluids. Figure 8.3 also shows that while the thermal conductivity of these CNT-nanofluids increase substantially with increasing temperature, the thermal conductivity of the reported ionanofluid is found to be independent of temperature. The reasons for such temperature-independent nature of ionanofluids are not well understood at this moment. However, similar temperature independence of thermal conductivity of nanofluids was reported in the literature. For example, Venerus et al. [47] found that level of thermal conductivity enhancement for Al_2O_3/petroleum oil-based nanofluid is independent of temperature in the range of 27–77°C. In fact, they observed a slight decrease in thermal conductivity of Au/water-based nanofluids with the increasing temperature. Figure 8.4 demonstrates that thermal conductivity enhancement of two ionanofluids and one nanofluid is a function of concentration of MWCNT at room temperature. It is seen that the thermal conductivity of ionanofluids (λ_{INF}) increases significantly (almost linear) over base ionic liquid with weight concentration of MWCNT.

Effects of temperature and MWCNT concentration on thermal conductivity of $[C_2mim][EtSO_4]$-based ionanofluids are shown in Fig. 8.5. Maximum enhancement of thermal conductivity of 25% is observed at 71°C and at 3 wt% concentration of MWCNT in this ionic liquid. It is also seen that the higher the concentration of MWCNT, the larger is the enhancement in thermal conductivity. However, the effect of temperature on the enhancement of thermal conductivity is not significant, and

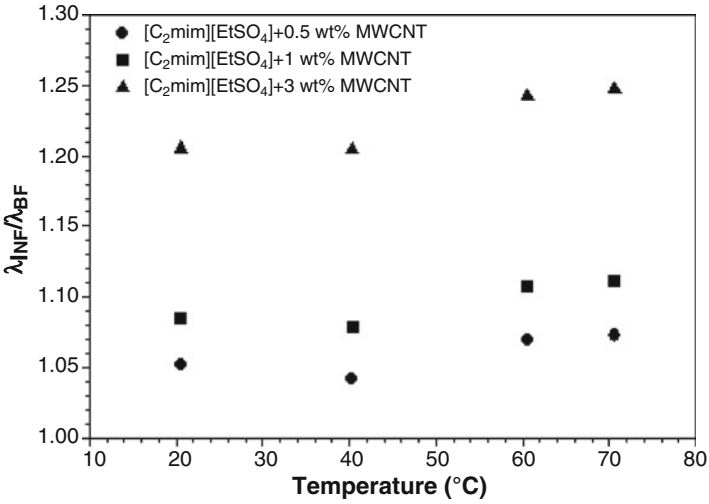

Fig. 8.5 Effect of temperature and MWCNT concentration on thermal conductivity enhancement of $[C_2mim][EtSO_4]$-based ionanofluids [39]

Table 8.2 Experimental data of thermal conductivity of various ionic liquids and their ionanofluids with 1 wt% of MWCNT at room temperature [48]

Ionic liquids	λ_{IL} (W/m·K)	Ionanofluids	λ_{INF} (W/m·K)	Increase of λ_{INF} (%)
$[C_2mim][NTf_2]$	0.123	$[C_2mim][NTf_2]$/MWCNT	0.126	2.44
$[C_4mim][NTf_2]$	0.121	$[C_4mim][NTf_2]$/MWCNT	0.164	35.54
$[C_4mim][CF_3SO_3]$	0.142	$[C_4mim][CF_3SO_3]$/MWCNT	0.155	9.44
$[C_6mim][NTf_2]$	0.122	$[C_6mim][NTf_2]$/MWCNT	0.130	6.81
$[C_8mim][NTf_2]$	0.121	$[C_8mim][NTf_2]$/MWCNT	0.129	6.62
$[C_4mim][BF_4]$	0.163	$[C_4mim][BF_4]$/MWCNT	0.173	6.13
$[C_6mim][BF_4]$	0.157	$[C_6mim][BF_4]$/MWCNT	0.163	4.01

these ionanofluids are found to be more stable at higher temperature (>60°C) and concentration of MWCNT. This might be because the layer structure built for this ionanofluid is more stable when subjected to a higher temperature. It is however interesting to note that changes in thermal conductivity of this ionanofluids with respect to temperature are not significant, and at some higher temperatures, the thermal conductivity values were found to be smaller than those at lower temperature. For pure ionic liquids, similar temperature-independent nature of thermal conductivity was also previously reported [2]. This indicates that there might be no or weak temperature-related mechanism for the enhancement of the thermal conductivity of these ionanofluids.

Results of thermal conductivity of several other MWCNT-ionanofluids and their base ionic liquids at room temperature are presented in Table 8.2. Except $[C_4mim]$

[NTf_2]-based ionanofluids, most of other ionanofluids show low or moderate increase in thermal conductivity at 1 wt% concentration MWCNT. Therefore, it is clear that not all ionic liquids can give high thermal conductivity when CNT (or other nanoparticles) are dispersed in them. The CNT when dispersed in the ionic liquid are likely to interact preferentially with the nonpolar domains associated with the alkyl chains, thus creating microclusters that can enhance the heat transfer. The procedure for the ionanofluids preparation is also crucial for the value of the enhancement, as discussed in [39], as the structure of the emulsion is fundamental.

8.4.2 Specific Heat Capacity of Ionanofluids

Besides thermal conductivity, specific heat capacity of ionanofluids is of great importance for their practical applications in thermal system management and green energy–based areas. Knowledge of this important property is also essential in determining other heat transfer properties, flow features, as well as enthalpy calculations in various processes simulation.

The potential use of ionic liquids as heat transfer fluids particularly in heat exchanger in chemical plants and solar thermal power generation (from cryogenic temperatures up to 200°C) depends on the values of volumetric heat capacity, vapor pressures, and thermal stability which have previously been discussed [26]. Comparison of properties of ionic liquids with synthetic compounds (based on hydrocarbons, polyaromatics, and siloxanes) showed that common imidazolium systems have higher heat capacities per unit volume than the reported commercial thermal fluids such as Paratherm HE® and Dowtherm MX™ [32].

Figure 8.6 illustrates that volumetric heat capacities of various ionic liquids such as 1-ethyl-3-methylimidazolium hexafluorophosphate ([C_2mim][PF_6]), 1-hexyl-3-methylimidazolium hexafluorophosphate ([C_6mim][PF_6]), 1-ethyl-3-methylimidazolium tetrafluoroborate ([C_2mim][BF_4]), 1-butyl-3-methylimidazolium trifluoromethanesulfonate ([C_4mim][CF_3SO_3]), and 1-butyl-3-methylimidazoliumoctylsulfate ([C_4mim][$C_8H_{17}SO_4$]) as well as high-performance commercial heat transfer fluids (Dowtherm MX™ and Paratherm HE®) increase significantly and linearly with increasing temperature. These data are obtained from material safety data sheets and ILThermo database of National Institute of Standards and Technology, Colorado, USA. It is noted that Dowtherm MX™ is a mixture of alkylated aromatics, while Paratherm HE® is a paraffinic hydrocarbon. Similar increase in specific heat capacities of various ionic liquids with respect to temperature is also reported by Ge et al. [49]. It can be seen from Fig. 8.6 that the volumetric heat capacity of ionic liquids are higher than these commercial heat transfer fluids. It is, therefore, anticipated that the specific heat capacity of ionanofluids will also increase with temperature. Figure 8.7 depicts that the specific heat capacity of MWCNT-ionanofluids increases significantly with increasing temperature compared to its base ionic liquid, [C_4mim][PF_6]. The most interesting part of these results is that regardless of MWCNT loading, there was dome-shaped jump of the specific heat capacity enhancement

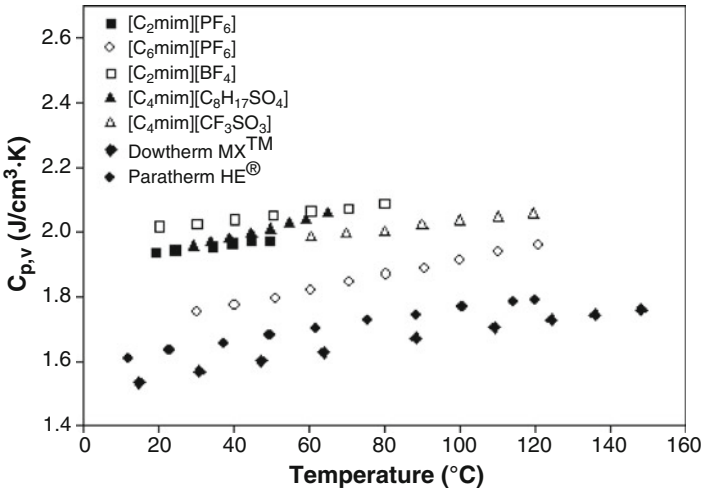

Fig. 8.6 Effect of temperature on volumetric heat capacity of several ionic liquids and heat transfer fluids

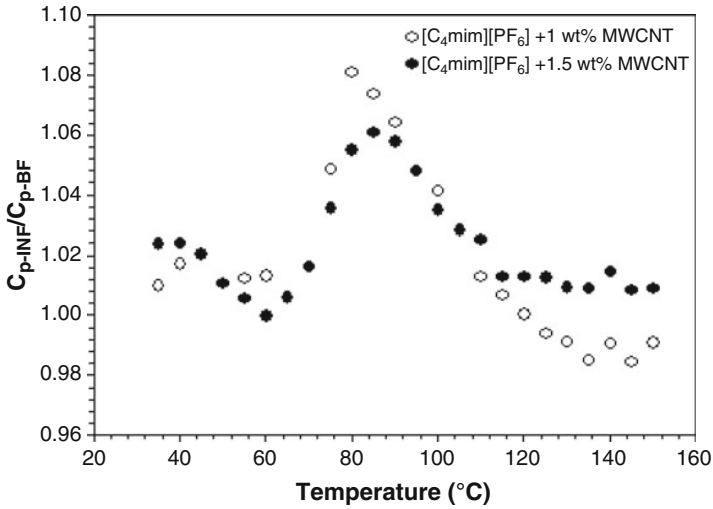

Fig. 8.7 Effect of temperature on heat capacity of ionanofluids at two different concentrations of MWCNT [2]

(a peak increase of 8% compared with base IL) at a certain temperature range (60–110°C). The reasons for such mysterious results are not well understood at this stage. There was little increase in specific heat capacity of ionanofluids with increasing loading of MWCNT. Nevertheless, any increase in heat capacity of any fluids is of great importance for their practical applications as heat transfer fluids.

Table 8.3 Values of thermophysical properties of ILs and HTFs and estimated reference heat transfer area (A_0) for the shell and tube heat exchanger [32]

ILs and HTFs	ρ (kg/m^3)	C_p (J/kg·K)	η (mPa·s)	λ·(mW/m·K)	A_0 (m^2)
[C_4mim][PF_6] (50°C)	1,346 ± 1	1,493 ± 30	68.8 ± 1.8	146 ± 7	480.75
[C_6mim][PF_6] (50°C)	1,273 ± 3	1,409 ± 61	111.9 ± 3.2	146 ± 7	634.60
[C_2mim][BF_4] (50°C)	1,280 ± 2	1,600 ± 25	15.9 ± 1.1	196 ± 6	217.29
Dowtherm A™ (50°C)	1,041	1,632	2.12	134	138.60
Dowtherm MX™ (100°C)	905	1,870	2.09	114	159.08
Syltherm 800™ (80°C)	882	1,711	3.86	124	202.86

8.4.3 Comparisons of Thermophysical Properties and Heat Transfer Areas

The values of thermophysical properties of liquids have a significant effect on the design of physicochemical processing, reaction units, and heat transfer devices, as they influence directly the design parameters and performance of equipments like heat exchangers, distillation columns, and reactors [50, 51]. Our group previously analyzed the same effect for molten alkali nitrates [52], which have emerged as high-temperature fluids for several technological processes such as high-temperature energy storage in batteries for solar plants and waste treatment. It was demonstrated that the knowledge of accurate data for the transport coefficients of these fluids is very important.

Ionic liquids are presently a good challenge to both scientists and chemical companies for their actual and potential applications in the chemical process industries and thermal management systems. Recently, our group studied the possibility of using ionic fluids as replacement of current silicon-based heat transfer fluids in heat transfer devices and made comparisons of heat storage capacity, other thermophysical properties, and heat transfer areas with current heat transfer fluids [32]. Details of the simulation, operation conditions, and cost estimation of a model shell and tube heat exchanger can be found elsewhere [32]. The values of the thermophysical properties of several heat transfer fluids (Dowtherm Co.) and ionic liquids used together with the calculated values of reference heat transfer area (A_0) for each heat transfer fluids and ILs are provided in Table 8.3. It can be demonstrated (Table 8.3) that although the heat capacity per unit volume of ionic liquids is significantly larger (20–50%) compared to these heat transfer liquids, the heat transfer areas may be comparable or bigger, which raises the cost of such equipment. For other ionic liquids, similar results are anticipated. It is also known that the influence of actual errors in the thermophysical properties of ionic liquids can render any future design as not working or excessively costing [32].

Very recently, França [39] performed simulation to estimate reference heat transfer area using two ionic liquids, ([C_4mim][NTf_2] and [C_2mim][$EtSO_4$]), as well as their ionanofluids containing 1 wt% of MWCNT under the same flow and other parameters in the same shell and tube heat exchanger used in previous study [32].

Table 8.4 Values of thermophysical properties and reference area A_0 for the shell and tube heat exchanger using $[C_4mim][NTf_2]$ and $[C_2mim][EtSO_4]$ ionic liquids and their MWCNT ionanofluids at 40°C

ILs and INFs	λ (W/m·K)	η (mPa·s)	C_p (J/kg·K)	ρ (kg/m^3)	A_0 (m^2)
$[C_4mim][NTf_2]$	0.1164	28.50	1,372.44	1,422.99	364.627
$[C_4mim][NTf_2]$ + 1 wt% MWCNT	0.1290	31.58	1,396.03	1,422.99	355.537
$[C_2mim][EtSO_4]$	0.1751	50.01	1,614.96	1,226.10	383.892
$[C_2mim][EtSO_4]$ + 1 wt% MWCNT	0.1890	53.98	1,642.72	1,226.06	376.130

Thermophysical properties and simulated heat transfer areas for these ionic liquids and ionanofluids are shown in Table 8.4. It can be seen that there is maximum 2.5% decrease in reference heat transfer area (A_0) due to the addition of 1 wt% of MWCNT in the base IL. This indicates that ionanofluids will perform better than ionic liquids in heat transfer devices like heat exchangers. Based on the high convective heat transfer performance of conventional nanofluids [8, 14, 15, 18], it is plausible to believe that using nanofluids, the heat transfer area can be reduced considerably compared to their base heat transfer fluids. França [39] also performed simulation for estimation of the total cost for model shell and tube heat exchanger operating with these ionic liquids as well as ionanofluids and showed that such reduction (2.5%) in heat transfer area could reduce the total cost by 1.7%.

8.5 Conclusions

This chapter presents preliminary overview of various aspects of ionanofluids as well as experimental findings on their thermophysical properties. Background of development of ionanofluids together with brief review on pioneering research works performed by the authors of this chapter and other groups is provided. Since ionanofluids are ionic liquid-based nanofluids, details about nanofluids and ionic liquids are also discussed. Besides presenting results on two major thermophysical properties (thermal conductivity and specific heat capacity) of MWCNT-ionanofluids as a function of temperature and concentration, a model feasibility study of using ionanofluids as replacement of current silicon-based heat transfer fluids in heat exchangers is also reported. Comparisons of available data of various thermophysical properties of commercial heat transfer fluids, ionic liquids, and ionanofluids are made in order to have better knowledge and quantitative information on the increase or decrease of these properties of ionanofluids as compared to other fluids.

It is found that ionanofluids show great promises to be used as innovative heat transfer fluids and novel media for many green energy–based applications. The values of thermophysical properties of liquids have a significant effect on the design and development of green processes and heat transfer devices. Results show that ionanofluids exhibit superior thermophysical properties compared to base ionic liquids,

and simulated results on heat transfer areas from a model study indicate a decrease in reference heat transfer area of a shell and tube heat exchanger due to addition of 1 wt% of MWCNT in base ionic liquid. This indicates that ionanofluids are better heat transfer fluids for heat exchangers or other heat transfer devices than ionic liquids.

Besides their heat transfer–based applications in green processes design and developments, ionanofluids have many more uncovered potential applications in various important fields. As an innovative class of fluids, there are plenty of possibilities open to this new area of ionic liquids as heat transfer fluids and more developments in ionanofluids are expected to be seen in the future.

Acknowledgment The authors would like to thank FCT-Fundação para a Ciência e Tecnologia, Portugal, for financial support under grant PTDC/EQU-FTT/104614/2008 for this work.

References

1. Ribeiro APC, Lourenço MJV, Nieto de Castro CA (2009) Thermal conductivity of ionanofluids. In: 17th symposium on thermophysical properties, Boulder, USA, 2009
2. Nieto de Castro CA, Lourenço MJV, Ribeiro APC, Langa E, Vieira SIC, Goodrich P, Hardacre C (2010) Thermal properties of ionic liquids and ionanofluids of imidazolium and pyrrolidinium liquids. J Chem Eng Data 55:653–661
3. Choi SUS (1995) Enhancing thermal conductivity of fluids with nanoparticles. ASME FED 231:99–105
4. Lee S, Choi SUS, Li S, Eastman JA (1999) Measuring thermal conductivity of fluids containing oxide nanoparticles. J Heat Transf 121:280–289
5. Murshed SMS, Leong KC, Yang C (2005) Enhanced thermal conductivity of TiO_2-water based nanofluids. Int J Therm Sci 44:367–373
6. Murshed SMS, Leong KC, Yang C (2006) Determination of the effective thermal diffusivity of nanofluids by the double hot-wire technique. J Phys D Appl Phys 39:5316–5322
7. Murshed SMS, Leong KC, Yang C (2008) Investigations of thermal conductivity and viscosity of nanofluids. Int J Therm Sci 47:560–568
8. Murshed SMS, Leong KC, Yang C (2008) Thermophysical and electrokinetic properties of nanofluids – a critical review. Appl Therm Eng 28:2109–2125
9. Yu W, France DM, Routbort JL, Choi SUS (2008) Review and comparison of nanofluid thermal conductivity and heat transfer enhancements. Heat Transf Eng 29:432–460
10. You SM, Kim JH, Kim KM (2003) Effect of nanoparticles on critical heat flux of water in pool boiling of heat transfer. Appl Phys Lett 83:3374–3376
11. Wen D, Ding Y (2004) Experimental investigation into convective heat transfer of nanofluids at the entrance region under laminar flow conditions. Int J Heat Mass Transf 47:5181–5188
12. Wen D, Ding Y (2005) Experimental investigation into the pool boiling heat transfer of aqueous based alumina nanofluids. J Nanopart Res 7:265–274
13. Bang IC, Chang SH (2005) Boiling heat transfer performance and phenomena of Al_2O_3-water nano-fluids from a plain surface in a pool. Int J Heat Mass Transf 48:2407–2419
14. Heris SZ, Etemad SG, Esfahany MS (2006) Experimental investigation of oxide nanofluids under laminar flow convective heat transfer. Int Commun Heat Mass Transf 33:529–535
15. Murshed SMS, Leong KC, Yang C, Nguyen NT (2008) Convective heat transfer characteristics of aqueous TiO_2 nanofluids under laminar flow conditions. Int J Nanosci 7:325–331
16. Murshed SMS, Milanova D, Kumar R (2009) An experimental study of surface tension-dependent pool boiling characteristics of carbon nanotubes-nanofluids. In: Proceedings of 7th

ASME international conference on nanochannels, microchannels and minichannels, Pohang, Korea, 2009
17. Choi SUS, Zhang Z, Yu W, Lockwood F, Grulke E (2001) Anomalous thermal conductivity enhancement in nanotube suspensions. Appl Phys Lett 79:2252–2254
18. Ding Y, Alias H, Wen D, Williams RA (2006) Heat transfer of aqueous suspensions of carbon nanotubes (CNT nanofluids). Int J Heat Mass Transf 49:240–250
19. Murshed SMS, Nieto de Castro CA, Lourenço MJV, Lopes MLM, Santos FJV (2011) A review of boiling and convective heat transfer with nanofluids. Renew Sustain Energy Rev 15:2342–2354
20. Ribeiro APC, Lourenço MJV, Nieto de Castro CA, Hardacre C (2008) Thermal conductivity of "Buck Gels". In: Proceedings conference on molten salts and ionic liquids (EUCHEM2008), Copenhagen, Denmark, 2008
21. Seddon KR (2003) Ionic liquids – a taste of the future. Nature 2:363–365
22. Marsh KN, Boxall JA, Lichtenthaler R (2004) Room temperature ionic liquids and their mixtures – a review. Fluid Phase Equilibr 219:93–98
23. Zhang S, Sun N, He X, Lu X, Zhang X (2006) Properties of ionic liquids: database and evaluation. J Phys Chem Ref Data 35:1475–1517
24. Keskin S, Kayrak-Talay D, Akman U, Hortacsu O (2007) A review of ionic liquids towards supercritical fluid applications. J Supercrit Fluid 43:150–180
25. Earle M, Seddon KR (2007) Ionic liquids. Green solvents for the future. Pure Appl Chem 72:1391–1398
26. Holbrey J (2007) Heat capacities of common ionic liquids – potential applications as thermal fluids. Chimica Oggi/Chem Today 25:24–26
27. Wasserscheid P, Welton T (2007) Ionic liquids in synthesis. Wiley-VCH, Weinheim
28. Gaune-Escard M, Seddon KR (2009) Molten salts and ionic liquids: never the twain. Wiley, Hoboken
29. Chiappe C, Pieraccini D (2005) Ionic liquids: solvent properties and organic reactivity. J Phys Org Chem B 18:275–297
30. Heintz A, Wertz C (2006) Ionic liquids: a most promising research field in solution chemistry and thermodynamics. Pure Appl Chem 78:1587–1593
31. Nieto de Castro CA, Santos FJV (2007) Measurement of ionic liquids properties. Are we doing it well? Chimica Oggi/Chem Today 25:20–23
32. França J, Nieto de Castro CA, Lopes MLM, Nunes VMB (2009) Influence of thermophysical properties of ionic liquids in chemical process design. J Chem Eng Data 54:2569–2575
33. Nunes VMB, Lourenço MJV, Santos FJV, Lopes MLM, Nieto de Castro CA (2010) Accurate measurements of physico-chemical properties on ionic liquids and molten salts. In: Seddon KR, Gaune-Escard M (eds) Ionic liquids and molten salts: never the twain. Wiley, Hoboken
34. Nieto de Castro CA, Langa E, Morais AL, Lopes MLM, Lourenço MJV, Santos FJV, Santos MSCS, Lopes JSL, Veiga HIM, Macatrão M, Esperança JMSS, Rebelo LPN, Marques CS, Afonso CAM (2010) Studies on the density, heat capacity, surface tension and infinite dilution diffusion with the ionic liquids [C_4mim][NTf_2], [C_4mim][dca], [C_2mim][$EtOSO_3$] and [aliquat][dca]. Fluid Phase Equilibr 294:157–179
35. Fukushima T, Kosaka A, Ishimura Y, Yamamoto T, Takigawa T, Ishii N, Aida T (2003) Molecular ordering of organic molten salts triggered by single-walled carbon nanotubes. Science 300:2072–2074
36. Fukushima T, Aida T (2007) Ionic liquids for soft functional materials with carbon nanotubes. Chem-Eur J 13:5048–5058
37. Vieira SIC, Ribeiro APC, Lourenço MJV, Nieto de Castro CA (2011) Paints with ionanofluids as pigments for improvement of heat transfer on architectural and heat exchangers surfaces. In: Proceedings of the 25th European symposium on applied thermodynamics, Saint Petersburg, Russia, 2011
38. Lide DR (2007) CRC handbook of chemistry and physics. Taylor & Francis, Boca Raton

39. França J (2010) Propriedades térmicas de ionanofluidos (Thermal properties of ionanofluids). MSc thesis, Faculdade de Ciências da Universidade de Lisboa, Portugal
40. Holbrey J, Seddon K, Wareing R (2001) A simple colorimetric method for the quality control of 1-alkyl-3-methylimidazolium ionic liquid precursors. Green Chem 3:33–36
41. Carslaw HS, Jaeger JC (1959) Conduction of heat in solids. Oxford University Press, London
42. Ge R, Hardacre C, Nancarrow P, Rooney D (2007) Thermal conductivities of ionic liquids over the temperature range from 293 K to 353 K. J Chem Eng Data 52:1819–1823
43. Nieto de Castro CA, Lourenço MJV, Sampaio MO (2000) Calibration of a DSC: its importance for the traceability and uncertainty of thermal measurements. Thermochimica Acta 347:85–91
44. Lourenço MJV, Santos FJV, Ramires MLV, Nieto de Castro CA (2006) Isobaric specific heat capacity of water and aqueous cesium chloride solutions for temperatures between 298 K and 370 K at p = 0.1 MPa. J Chem Thermodyn 38:970–974
45. Xie H, Lee H, Youn W, Choi M (2003) Nanofluids containing multiwalled carbon nanotubes and their enhanced thermal conductivities. J Appl Phys 94:4967–4971
46. Amrollahi A, Rashidi AM, Emani MM, Kashefi K (2009) Conduction heat transfer characteristics and dispersion behaviour of carbon nanofluids as a function of different parameters. J Exp Nanosci 4:347–363
47. Venerus DC, Kabadi MS, Lee S, Perez-Luna V (2006) Study of thermal transport in nanoparticle suspensions using forced Rayleigh scattering. J Appl Phys 100:094310–1–094310–5
48. Nieto de Castro CA, Lourenço MJV, Murshed SMS, Vieira SI, França J, Queiros CS, Ribeiro APC (2010) Ionanofluids: new heat transfer fluids for thermal efficiency design. In: Proceedings of the 9th Asian thermophysical properties conference, Beijing, China, 2010
49. Ge R, Hardacre C, Jacquemin J, Nancarrow P, Rooney D (2008) Heat capacities of ionic liquids as a function of temperature at 0.1 MPa. Measurement and prediction. J Chem Eng Data 53:2148–2153
50. Mendonça AJF, Nieto de Castro CA, Assael MJ, Wakeham WA (1981) The economic advantages of accurate transport property data for heat transfer equipment design. Rev Port Quím 23:7–11
51. Lopes MLM, Nieto de Castro CA, Wakeham WA (1985) The effect of uncertainty in diffusion coefficients in the design of packed columns. In: Proceedings of the international chemical engineering conference, Coimbra, Portugal
52. Nunes VMB, Lourenço MJV, Santos FJV, Nieto de Castro CA (2003) The importance of the accurate data on viscosity and thermal conductivity in molten salts applications. J Chem Eng Data 48:446–450

Chapter 9
Green Solvents for Polymerization of Methyl Methacrylate to Poly(Methyl Methacrylate)

S. Krishna Mohan

Abstract Solvents are often volatile organic compounds (VOCs) and are therefore a major environmental concern as they are able to form low-level ozone and smog. Due to the increase in environmental awareness, it is a matter of great concern for scientists to decrease the consumption of VOCs. During the last decade, chemistry research into the use of greener, alternative solvents has been grown enormously. Alternative solvents suitable for green chemistry are those that have low toxicity, easy to recycle, inert, and do not contaminate the product. From the green chemistry point of view, the attention is focused mainly on the three available "green solvents," that is, ionic liquids, supercritical carbon dioxide, and fluorous media, to achieve this task. This chapter provides comprehensive idea on the polymerization of methyl methacrylate (MMA) to polymethyl methacrylate (PMMA) using these three green solvents. The wide varieties of ionic liquids and various polymerization techniques used till date for conversion of MMA into PMMA are described. The different types of surfactants used in the dispersion polymerization with $scCO_2$ and the polymerizations carried out in fluorous media for the synthesis of PMMA are extensively discussed.

9.1 Introduction

Solvents are used in chemical processes to aid in mass and heat transfer and to facilitate separations and purifications [1]. These are often used as the primary component of cleaning agents, adhesives, sealants, and coatings (paints, varnishes, and stains). Solvents are often volatile organic compounds (VOCs) and are therefore a major environmental concern as they are able to form low-level ozone and smog

S. Krishna Mohan (✉)
Material Development Division (MDD), Directorate of Engineering (DOE),
Defence Research & Development Laboratory (DRDL),
Kanchanbagh, Hyderabad 500058, India
e-mail: srkmohan@drdl.drdo.in; kmohan_s@yahoo.com

A. Mohammad and Inamuddin (eds.), *Green Solvents I: Properties and Applications in Chemistry*, DOI 10.1007/978-94-007-1712-1_9,

through free radical air oxidation processes. VOCs are most commonly used in solution polymerizations, due to their compatibility with monomers and ease of separation, despite their well-documented health and environmental concerns. The presence of VOCs in air or water causes health problems, ranging from simple discomfort to cancer. Also, the ground-level ozone in combination of VOCs leads to smog formation. Due to the increase in environmental awareness, it is a matter of great concern for scientists to decrease the consumption of VOCs. One of the twelve principles of green chemistry recommends to "use safer solvents and auxiliaries" [2]. During the last decade, chemistry research into the use of greener, alternative solvents has grown enormously [3–6]. All alternative solvents have advantages and disadvantages. For example, the pressure involved in case of supercritical fluids is a disadvantage, but the facile removal of the fluid at the end of a process is an advantage. Since the VOCs cannot be replaced in every application, hence, the role of VOCs derived from renewable resources in the alternative solvent field is growing. Alternative solvents suitable for green chemistry are those that have low toxicity, easy to recycle, inert, and do not contaminate the product. They have been developed and used for a wide range of properties. From the green chemistry point of view, the attention is focused mainly on the following three available "green solvents" to achieve the task [3]:

1. Ionic liquids
2. Supercritical carbon dioxide ($scCO_2$)
3. Fluorous media

Depending upon the requirement, the type of green solvent can be chosen. For example, in terms of volatility, the most volatile supercritical carbon dioxide ($scCO_2$) to the least volatile polymeric and ionic liquid solvents have been used. Volatility may be desirable in green chemistry in order to reduce the amount of residual solvent but undesirable with regard to atmospheric pollution. In terms of polarity, polar aqueous phases to nonpolar fluorous media have been used. Clark and Tavener used a scoring system to grade the above alternative solvents shown in Table 9.1 in an attempt to qualify the general level of "greenness" of a range of alternative solvents [7]. This chapter focused on the polymerization of methyl methacrylate (MMA) to polymethyl methacrylate (PMMA) using the above three green solvents. The various polymerization techniques used in ionic liquids, the different types of stabilizers used in the dispersion polymerization with $scCO_2$, and the polymerizations carried out in fluorous media for the synthesis of PMMA are also discussed.

9.1.1 Methyl methacrylate (MMA) and Polymethyl methacrylate (PMMA)

MMA is the methyl ester of methacrylic acid (MAA) with a colorless volatile synthetic chemical with an ester-like odor. It is a monomer produced on a large scale

Table 9.1 Advantages and disadvantages for alternative green solvents for a maximum overall score of 25 [7]

Green solvents	Key properties	Ease of separation and reuse	Safety and cost	Environmental impact	Overall score/25
$scCO_2$	(a) Poor solvent for many compounds (b) May be improved with cosolvents or surfactants (1)	Excellent (5)	(a) Nontoxic (b) CO_2 is cheap and abundant (7)	(a) Sustainable and globally available (5)	18
RTILs	(a) Always polar (b) Designer/tailor-made properties (4)	(a) Easy to remove volatile products (b) Reuse may depend on purity (2)	(a) Some are toxic (b) Expensive (4)	(a) Mainly sourced from petroleum (b) Environmental fate not well understood (3)	13
Fluorous media	(a) Best used in biphasic systems (b) Nonpolar solutes only (3)	(a) Readily forms biphases (b) May be distilled and reused (4)	(a) Bioaccumulative, greenhouse gases (b) Very expensive (3)	(a) Very resource demanding (b) May persist in environment (2)	12

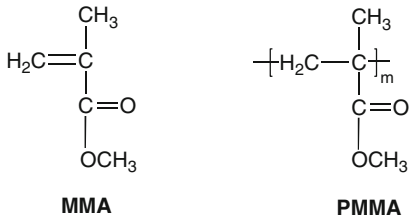

Fig. 9.1 Structures of *MMA* and *PMMA*

for the production of PMMA. The chemical structures of both MMA and PMMA are shown in Fig. 9.1. In principle, approximately 80% of the MMA is consumed for the manufacture of PMMA plastics. Nearly all MMA is polymerized to make homopolymers and copolymers with the largest application being the casting, molding, or extrusion of PMMA or modified polymers. Polymers and copolymers of MMA are also used in waterborne, solvent, and undissolved surface coatings, adhesives, sealants, leather and paper coatings, inks, floor polishes, textile finishes, dental prostheses, surgical bone cements, and leaded acrylic radiation shields and in the preparation of synthetic fingernails and orthotic shoe inserts.

PMMA, chemically the synthetic polymer of MMA, is a strong and lightweight material of density 1.17–1.20 g/cm^3 which is less than half that of glass. It also has good impact strength, higher than both glass and polystyrene, but significantly lower than polycarbonate (PC) and some engineered polymers. PMMA is a transparent thermoplastic, often used as a light or shatter-resistant alternative to glass. The material was developed in 1928 in various laboratories, and was first brought to market in 1933 by Rohm and Haas Company, under the trademark Plexiglas. PMMA is an economical alternative to PC when extreme strength is not necessary. In addition, PMMA does not contain the potentially harmful bisphenol A subunits found in polycarbonate. It is often preferred because of its low cost, moderate properties, and easy handling and processing. The main disadvantage of PMMA is its behavior in a brittle manner when loaded especially under an impact force. Rubber toughening has been used to increase the strength of PMMA owing to its brittle behavior in response to applied loads. PMMA swells and dissolves in many organic solvents. It also has poor resistance to many other chemicals on account of its easily hydrolyzed ester groups. Nevertheless, its environmental stability is superior to most other plastics such as polystyrene and polyethylene, and hence, PMMA is often the material of choice for outdoor applications. The glass transition temperature (Tg) of PMMA ranges widely from 85°C to 165°C because of the variations in commercial compositions. The highest quality PMMA sheets are produced by cell casting, but in this case, the polymerization and molding steps occur concurrently. PMMA is routinely produced by emulsion solution and bulk polymerization techniques.

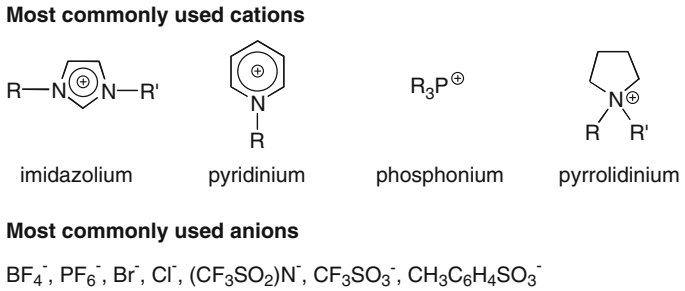

Fig. 9.2 Typical cations and anions of ionic liquids

9.1.2 Ionic Liquids (ILs)

The use of ionic liquids (ILs), which have shown advantages as an alternative replacement for VOCs to synthesis diverse polymers, has been explored [8–14]. ILs are eco-friendly as green solvents due to nonvolatility compared to conventional solvents, which are often volatile and contribute to air pollution and the greenhouse effect. ILs are liquids at ambient temperatures, preferably at room temperature (RTIL – room-temperature ionic liquids), that are comprised entirely of ions. These are composed of large organic cations and small inorganic or organic anions [3]. Examples of most commonly used cations and anions of ILs are shown in Fig. 9.2. The wide range of available anions and cations in combination could provide up to large number of different ILs. ILs are very versatile class of solvents, and their properties can be easily tuned for specific application. At the same time, it is difficult to discuss their properties in general because some properties may differ considerably depending on the structure of cation and anion. Ionic liquids are also described in the literature as room-temperature molten salts, ambient-temperature molten salts, ionic fluids, liquid organic salts, and organic ionic liquids (OILs) [3]. The most common cationic IL is 1-alkyl-3-methylimidazolium (abbreviated [C*n*mim], where n = number of carbon atoms in a linear alkyl chain). Although different authors use different abbreviations for ILs, most common abbreviations for cation and anion structures are given in square brackets (without charges). Thus, [bmim][PF_6] denotes 1-butyl-3-methylimidazolium hexafluorophosphate and [bmim][BF_4] denotes 1-butyl-3-methylimidazolium tetrafluoroborate. Since both the thermodynamics and kinetics of reactions carried out in ionic liquids are different to those in conventional molecular solvents, they exhibit many fascinating properties mentioned below which attract a growing interest in both academic and industrial research, and hence makes ILs as an alternative to replacement for VOCs in polymer synthesis and processing [3]:

- They have low melting point, negligible vapor pressure, and good thermal stability. Since ionic liquids are salts, they cannot evaporate. They are nonvolatile, hence they may be used in high vacuum systems and eliminate contaminate problems and are a medium of choice for green chemistry.

- They are outstandingly good solvents and can dissolve in a wide variety of organic, organometallic, inorganic, and polymeric compounds. The high solubility of reagents and catalysts in ionic liquids that allows reactions to be performed in concentrated solutions indicates the requirement of small reactors.
- They are stable at a wide range of temperatures. Being liquid over a range of 300°C is usual for ionic liquids, and melting points can be as low as −96°C. Much higher kinetic control can be attained in such media when compared with traditional organic solvents and water.
- They are immiscible with many organic solvents. This immiscibility extends their use to biphasic systems. This property is extremely valuable for catalytic reactions because the product can be extracted from an ionic liquid using organic solvents, whereas the catalyst remains in the ionic liquid and can be directly recycled and reused. Hydrophobic ionic liquids can also be used as immiscible polar phases with water.
- They possess excellent chemical, thermal, air, and moisture stability.
- They are often composed of poorly coordinating ions, so they have the potential to be highly polar yet noncoordinating solvents.
- Their synthesis can be carried out easily and reasonably inexpensively. Ionic liquids remain expensive, even though they are now widely available commercially.
- They are made up of at least two components (the anion and cation) which can be varied to possess a particular set of properties. Hence, they are termed as designer solvents which mean that their properties can be adjusted to suit the requirements of a particular process. Properties such as melting point, viscosity, density, and hydrophobicity can be varied by simple changes to the structure of the ions.

The disadvantages of ILs include cost, high viscosity, difficulty in purification, and reaction with strong nucleophiles. Many reviews have appeared in literature on ILs and its applications as polymerization solvents [15–20].

9.1.2.1 Polymerization in Ionic Liquids (ILs)

ILs have been widely used as polymerization solvents. The important factors leading to the choice of the ionic liquid includes its thermal stability, low vapor pressure, low toxicity, and ability to tune the properties of the anion or cation in terms of hydrophobicity–hydrophilicity balance. Some free radical polymerizations conducted in ILs have shown an increased polymerization rate and yield polymers with higher molar masses in comparison to the ones in VOCs. Furthermore, copolymerizations carried out in ILs can show significant different reactivity ratios from those performed in bulk or in VOCs, which allowed the preparation of “new” statistical copolymers. Despite this progress, clear understanding in efficient usage of ILs and complete elimination of the utilization of VOCs in specific polymer systems is still lacking. This approach takes advantage of the poor solubility of many polymers in most water-soluble ILs to perform heterogeneous polymerizations, which facilitates the polymer isolation and the IL recycling avoiding VOCs. Although application of

Fig. 9.3 [bmim][PF_6]

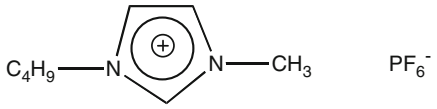

ILs in polymer chemistry not always eliminates the need of volatile organic solvents (quite often resulting polymers have to be separated from ILs using organic solvents), the set of properties displayed by ILs may be advantageous for certain specific applications. The use of ILs as solvents for the preparation of polymers has received little attention especially when compared to studies concerning their use in other synthetic areas. Polymerization of MMA using ILs was carried out following the techniques cited below:

1. Conventional polymerization
2. Living/controlled polymerization (CRP)
   (a) Atom transfer radical polymerization (ATRP)
   (b) Reverse atom transfer radical polymerization
   (c) Nitroxide-mediated living radical polymerization (NMRP)
   (d) Reversible addition fragmentation chain transfer (RATF) polymerization
3. Group transfer polymerization
4. Radiation polymerization
5. Anionic polymerization

Conventional Free Radical Polymerization

Conventional free radical polymerization is a key method used to produce a wide variety of vinyl polymers including acrylates, methacrylates, styrene, vinyl acetate, tetrafluoroethylene, methacrylonitrile, and methacrylamides, etc., in bulk, solution, and aqueous systems. It is one of the most important methods of polymer synthesis, accounting for approximately 50% of all mass-produced polymers [21]. Since free radical polymerizations are relatively insensitive to impurities as compared to ionic polymerization, they do not require rigorously controlled reaction conditions. The process works with a wide range of monomers and is cost-effective. The use of a solvent in free radical polymerizations dissipates heat, provides better temperature control, and lowers the viscosity, to make easy mixing and often increases the molecular weight.

Mays and coworkers demonstrated increase in both the rate and molecular weight of polymerization of MMA in IL [bmim][PF_6] {1-butyl-3-methylimidazolium hexafluorophosphate} as solvent (Fig. 9.3) [22]. The resulting polymers were separated from the reaction mixture, purified using ethanol–water mixtures, and the IL solvents are recovered. At the same monomer to initiator molar ratio, PMMA had up to ten times higher molecular mass than that obtained when synthesized in benzene. The polymers exhibit polydispersities typical of homogeneous free radical polymerization products in both the IL and organic solvents in spite of the fact that

in the former case, the polymers formed are insoluble in the reaction medium. Polymerizations in the IL were very rapid because the complete conversion of monomer to polymer was achieved within 8 h, whereas in conventional solvents, the polymerization would require longer time period. The combination of high molecular weight products and fast reaction rates in the IL system can be explained in terms of influences on chain-termination processes in case of IL. A combination of relatively high viscosity and precipitation of the polymeric radicals as the polymerization proceeds leads to "diffusion-controlled termination" throughout the polymerization [23]. In this case, the reactions were terminated by quenching in an ice-water bath, and maximum conversion was achieved after approximately 8 h, while samples reacted in benzene under the same conditions required approximately 40 h to reach maximum conversion. The delayed polymerization of MMA in benzene was due to trace impurities in the solvent which inhibited the reaction. MMA reactions in benzene remained clear during polymerization, and the PMMA phase separated from [bmim][PF_6] by forming a white suspension after approximately 3 h, a simplified polymer recovery step by filtration or centrifugation. The PMMA molecular weight was approximately five times higher in [bmim][PF_6] than in benzene. This increase in molecular weight may be due to a decrease in initiator efficiency, resulting in fewer total macromolecular chains, or an increased monomer mobility during the propagation step. The number-average molecular weight (M_n) and polydispersity index (PDI) of PMMA samples formed in [bmim][PF_6] are approximately 145,000 g mol^{-1} (as against approximately 29,000 g mol^{-1} for benzene) and 1.82 (as against 2.49 for benzene), respectively. The monomer conversion achieved in [bmim][PF_6] was actually lower than that in benzene (78.9%) due to the high viscosity of [bmim][PF_6] relative to benzene. The high solution viscosity limits the diffusion rates of large polymer chains within the solution.

Due to the more efficient and environmentally friendly solution polymerization process by using water-soluble ILs as reaction media, some important commercial polymers were precipitated with the use of water and consequently separated from the aqueous ionic liquid solution by filtration [24]. The polymerization rates for MMA and BMA in the water-soluble ILs were higher than those of the bulk polymerization of these monomers. The polymerization of MMA in water-soluble ILs is especially promising in terms of the scale-up to a pilot and/or industrial scale since the bulk polymerization of MMA is difficult to perform in industrial scale and solution processes are still not utilized. Free radical polymerization of MMA was reported under microwave irradiation using water-soluble ILs as reaction media [25]. The incorporation of ILs showed a more efficient heating profile of the reaction mixtures under microwave irradiation when compared to the cases without ILs.

Living/Controlled Free Radical Polymerization (CRP)

Conventional free radical polymerization is a widely used technique that is relatively easy to employ. However, it is often difficult to obtain predetermined polymer architectures with precise and narrow molecular weight distributions.

Controlled/living radical polymerization (CRP) overcomes these limitations. The increasing need for polymers with well-defined architecture (diblock-, graft-, star-shaped copolymers), molecular weight, and functional end groups made controlled/living radical polymerization (CRP) attractive. The development of CRP, such as atom transfer radical polymerization (ATRP), reverse atom transfer radical polymerization, reversible addition and fragmentation chain transfer polymerization (RAFT), and nitroxide-mediated living radical polymerization (NMRP), has provided a variety of useful techniques for producing well-defined vinyl polymers.

Atom Transfer Radical Polymerization (ATRP)

The polymers produced by ATRP not only have controlled molecular weights and narrow polydispersities but also well-defined end groups. With these end group functionalities, interesting chemical and physical properties may be imparted. Haddleton and coworkers demonstrated IL [bmim][PF_6] as an excellent solvent for Cu^I–*N*-propyl-2-pyridylmethanimine-mediated living radical polymerization of MMA [26]. This represents the first example of an ionic liquid being used for living radical polymerization and indeed the first example of a new generation nonhygroscopic ionic liquid used as a polymerization medium. The addition of *N*-propyl-2-pyridylmethanimine to a deoxygenated suspension of Cu^IBr in [bmim][PF_6] in a 1:1 M ratio results in the formation of a dark brown homogenous solution at room temperature. Polymerization of MMA with ethyl-2-bromoisobutyrate as initiator, in this solution, proceeds readily with 87% conversion after 90 min at 70°C. This is a fast reaction when compared to polymerization in nonpolar solvents. Polymerization proceeds efficiently even at 30°C by reaching 45% conversion after 180 min. Increasing the ratio of *N*-propyl-2-pyridylmethanimine to Cu^I to 2:1 results in approximately twofold increase in the rate of polymerization. The low amount of termination, relatively low PDI values, and low M_n of the products indicate that the polymerization shows living characteristics as observed in more conventional organic solvents. Polymer produced at early stages in the reaction is of higher mass than expected because of formation of efficient radical–radical coupling with low mass species which is often observed with living radical polymerization [27]. The product of polymerization PMMA was extracted with suitable solvents (e.g., toluene), and nearly all copper (I) catalyst remained in the ionic liquid phase which facilitates catalyst reuse by adding fresh monomer. The use of the RTIL medium also eliminated the need of postpurification to eliminate toxic copper salts.

PF_6^- anion, a common component of some ionic liquids, is a suitable nonradically transferable counterion in ATRP, although a relatively expensive counterion. ATRP of MMA was carried out in the less expensive ILs, 1-butyl-3-methylimidazolium halides (1-butyl-3-methylimidazolium chloroaluminate, 1-butyl-3-methylimidazolium chloride, 1-butyl-3-methylimidazolium bromide), 1-butyl-3-methylimidazolium carbonate, 1-butyl-3-methylimidazolium dodecyl sulfate, and 1-butyl-3-methylimidazolium dibutyl phosphonate [28]. Transition metal halides easily dissolve in ionic liquids and form efficient catalytic systems for the ATRP of MMA. In iron-mediated ATRP, no additional organic complexing ligand was required to achieve a controlled

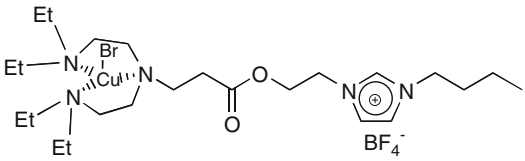

Fig. 9.4 CuBr/TEDETA anchored on imidazolium-based ionic liquid (BITT)

polymerization of MMA, although both initiation rates and rates of reaction were low, but copper-mediated reactions required the presence of an organic ligand when the ionic liquid had a halide or a carbonate anion. However, the presence of a ligand was not necessary when the ionic liquid was 1-butyl-3-methylimidazolium dibutyl phosphonate. ATRP in ionic liquids proceeds with low initiation efficiency due to the relatively low concentration of the catalyst in the organic medium and very high concentration of the catalyst in the ionic liquid phase. However, after a short nonstationary state, the polymerization is controlled, and molecular weights evolve linearly with conversion resulting in polymers with low PDI values. The initiation efficiency can be significantly improved by use of macroinitiator (e.g., PMMA-Br) instead of ethyl 2-bromoisobutyrate. The macroinitiator cannot enter the ionic liquid phase and remains in the organic phase, and the kinetics of the ATRP process would be determined only by the migration of the catalyst into this phase.

The ionic liquid catalyst CuBr/*N*,*N*,*N*^{II},*N*^{II}-tetraethyldiethylenetriamine (TEDETA) anchored on an imidazolium-based ionic liquid shown in Fig. 9.4 greatly reduces the amount of ionic liquid needed for ATRP of MMA [29]. This ionic liquid is insoluble in the mixture of MMA and toluene but could be easily dispersed in the reaction media. With the catalysis of CuBr/TEDETA anchored on imidazolium-based ionic liquid, the polymerization of MMA at 60°C was well controlled, and polymers are produced with high initiator efficiency and low PDI values. All the polymerizations catalyzed had induction periods of about 1.5 h in phenyl ether and 2–3 h for those in toluene and dioxane, and the molecular weights of all of the polymers were very close to the theoretical values. In contrast, the MMA polymerization catalyzed by CuBr ligated with TEDETA or PMDETA had no induction period, had a fast initial polymerization rate, and the molecular weights were much higher than the theoretical values with even broader distribution, indicating the low initiator efficiency due to the consumption of the initiators by radical terminations, as indicated by the precipitation of Cu(II) complex. The PDI of the polymers produced from the ionic liquid catalyst was in the range 1.2–1.4, slightly broader than that of polymers prepared by most homogeneous catalysts. This is due to the restricted access of growing radicals in the organic phase to the catalyst in the ionic liquid phase because the ionic liquid is immiscible with the toluene-MMA phase and only dispersed in the organic phase as fine droplets. The needed ionic liquid for the biphasic ATRP was only 5 wt% of the organic solvent. The addition of a small amount of silica gel to the polymer solution could further reduce the residual catalyst concentration. After regeneration, the recycled catalyst could be reused for second run polymerization with similar or even higher catalytic activity and similar or even better control over the polymerization.

Fig. 9.5 $[Mor_{1,4}][BF_4]$

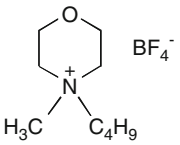

Instead of using anions PF_6^- and BF_4^- of ILs in the ATRP, Lai and coworkers demonstrated ATRP of MMA by using three ILs, 1-methylimidazolium acetate [mim][CH_3COO], 1-methylimidazolium propionate [mim][CH_3CH_2COO], and 1-methylimidazolium butyrate [mim][$CH_3CH_2CH_2COO$], respectively, as excellent solvents in the absence of any additional ligands and employing ethyl 2-bromoisobutyrate/CuBr as the initiating system [30]. The rate of reaction was fast, and the PDI of the polymer obtained was fairly narrow. The rate of ATRP of MMA in [mim][RCOO] got higher as R was changed from propyl to ethyl or methyl indicating a strong dependence of the reaction rate on the length of the substituted groups of the anions in the ionic liquids. The polymerization rates of all these three series of polymerizations in ionic liquids were much rapid compared to polymerization in nonpolar solvents. A similar rate increase was also observed when carboxylic acids were added as was expected due to complexation of the added acid to the copper [31]. The initiator efficiency was lower than that in conventional organic solvents due to the cage effect and the lower solubility of high molecular weight PMMA in the ionic liquids than that in conventional organic solvent such as chlorobenzene.

ATRP of MMA was carried out in *N*-butyl-*N*-methyl morpholinium tetrafluoroborate $[Mor_{1,4}][BF_4]$, shown in Fig. 9.5 with MBP/CuBr/bipyridine as the initiating and catalyzing system instead of relatively expensive imidazolium ionic liquids [32]. MMA and MBP were partially soluble in the ionic liquid, whereas the catalyst (the complex of CuBr and bipyridine) was absolutely soluble in the ionic liquid which led to phase separation of MMA from the ionic liquid containing 21–25% MMA monomer. In the polymerization of MMA conducted under the typical conditions ([M]/[I]/[CuBr]/[bipyridine]:100:2:0.3:0.6), nearly a 90% yield was obtained at 80°C in 6 h. The polymerization rate was low, and also the conversions were low at the low temperature because with the elevation of temperature, the catalysis equilibrium shifted to the right, which increased both the propagating radical concentration and also the propagating rate. The MWDs were a little wider (1.1–1.5) than those of the polymers obtained by normal ATRP (<1.2). The dosage of catalyst for well-controlled polymerization could be reduced obviously in $[Mor_{1,4}][BF_4]$ when compared with the conventional organic solvents. The obtained polymers could be separated easily from the catalyst solution in the ionic liquid, and the recycled catalyst $[Mor_{1,4}][BF_4]$ had catalytic activity similar to that of the fresh catalyst.

Reverse Atom Transfer Radical Polymerization

In reverse ATRP, transition-metal compounds at their higher oxidation states are used as catalysts, and conventional initiators such as AIBN and benzoyl peroxide are used in place of organic halides [33]. Therefore, the easy oxidation of the catalyst (lower oxidation-state transition-metal compounds) and the toxicity of halide initiators of conventional ATRP are avoided. The well-controlled first reverse ATRP of MMA in IL [bmim][PF_6] with AIBN/$CuCl_2$/bipyridine as the initiating agent in which the whole system was homogenous throughout the reaction was successfully carried out [34]. Much less catalyst was needed to effectively mediate the process in [bmim][PF_6] as compared to the other reverse ATRPs in bulk or conventional solvents. The resultant PMMA and residue monomer were relatively easily isolated from the reaction mixture. The ionic liquid and catalyst complex were readily recovered and reused without further treatment. The higher the reaction temperature, the shorter is the induction period due to the slow decomposition of AIBN at lower temperature. Due to a cage effect with ionic liquid molecules, the termination of the primary radicals through decomposition of AIBN might occur before they can initiate polymerization, which accounts for the low initiation efficiency of AIBN. The Cu catalyst is also soluble in the ionic liquid. As a consequence of both factors, less catalyst is needed to effectively mediate the polymerization process in ionic liquids than in other reverse ATRPs. If $CuCl_2$ was absent or not enough was added, the polymerization will proceed in an uncontrolled manner. However, the excess $CuCl_2$ would not only slow the polymerization rate significantly but could also contaminate the resultant polymer. The activity of $CuCl_2$ depends dramatically on its solubility in the polymerization medium. The polymerizations became well controlled when only 0.125 equiv of $CuCl_2$ versus AIBN was added. All the polymers had M_w/M_n values of less than 1.10. The polymerization rate increased with a decrease in the [$CuCl_2$]/[AIBN] ratio which was evidenced by the decreased monomer conversion at the same polymerization time. This was due to the generation of more radicals by the decomposition of AIBN.

Compared with other imidazolium ionic liquids containing PF_6^- anion, 1,3-disubstituted imidazolium tetrafluoroborates have higher solvating power for transition-metal salts [35]. The reverse ATRP of MMA induced by AIBN/$CuCl_2$/bipyridine in both 1-butyl-3-methylimidazolium tetrafluoroborate, [bmim][BF_4] and 1-dodecyl-3-methylimidazolium tetrafluoroborate, [ddmim][BF_4] was carried out [36]. All reagents including initiator, transition metal salts, organic ligand, and monomer were soluble in both the ionic liquids. However, PMMA with high molecular weight was not readily soluble in [bmim][BF_4]. The solubility of PMMA in [ddmim][BF_4] which had a long dodecyl group in molecule was much higher than that in [bmim][BF_4]. This indicates the strong dependence of solvating power of ionic liquids on the length of the substituted groups of the cations. The polymerization in [ddmim][BF_4] proceeded in a well-controlled manner until the 92% of monomer was reacted. Because of the poor solubility of the catalyst, AIBN/$CuCl_2$/bipyridine initiating system was not able to promote the living radical polymerization of MMA in bulk. It was known that imidazolium ionic liquids containing BF_4^- anion were good

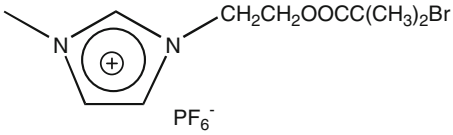

Fig. 9.6 [BrIBOE mim][PF_6]

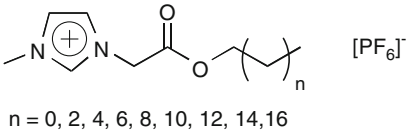

Fig. 9.7 Ionic liquids containing ester groups

solvents for inorganic salts. Hence, the "living" characteristics of reverse ATRP of MMA might be attributed to good solubility of $CuCl_2$ in [ddmim][BF_4]. The resultant polymers and the catalysts were easily isolated. The kinetic study of reverse ATRP of MMA in recycled [bmim][BF_4] suggested that this ionic liquid could be reused as reaction solvent after simple purification without affecting the living nature of polymerization.

Wan and coworkers deliberately incorporated IL imidazolium cation, 1-(2-bromoisobutyryloxyethyl)-3-methyl imidazolium hexafluorophosphate [BrIBOE mim][PF_6], to induce ATRP of MMA into a polymer chain as a head group, which might possibly endow PMMA with some interesting properties (Fig. 9.6) [37]. By a combination with CuBr and pentamethyldiethylenetriamine, the ionic liquid initiated the free radical polymerization of MMA to proceed in a controlled way over a wide temperature range of 0–60°C. The polymerization rate was higher than for other reported systems, may be due to the fact that the coordination complex of Cu(I) and PMDETA has lower redox potentials since it is more soluble in MMA than the copper/bipyridine complex. By using this method, PMMA with unambiguous imidazolium head groups and terminal bromine groups, in addition to controlled molecular weight and relatively narrow polydispersity, can be obtained. Furthermore, the incorporation of ionic imidazolium groups may lead to marked effects on the properties of the resultant polymer. The resultant PMMA had controlled molecular weight, relatively narrow polydispersity, and well-defined ω-bromine and α-ionic groups.

The carbonyl group is able to coordinate with some transition metals under certain conditions. The introduction of ester groups in the molecules of ionic liquids might endow them with some functions. The reverse ATRP of MMA in a series of ionic liquids containing ester group shown in Fig. 9.7 was carried out [38, 39]. All the polymers obtained have well-defined structures which were indicated by narrow PDI values. The isotacticities of the polymers obtained in ionic liquids were a little higher than that in toluene due to partly because of the introduction of the carbonyl group in ionic liquids.

The application of ILs as solvents in ATRP of acrylates allows the reduction of side reactions when compared against bulk polymerizations. When chiral ionic

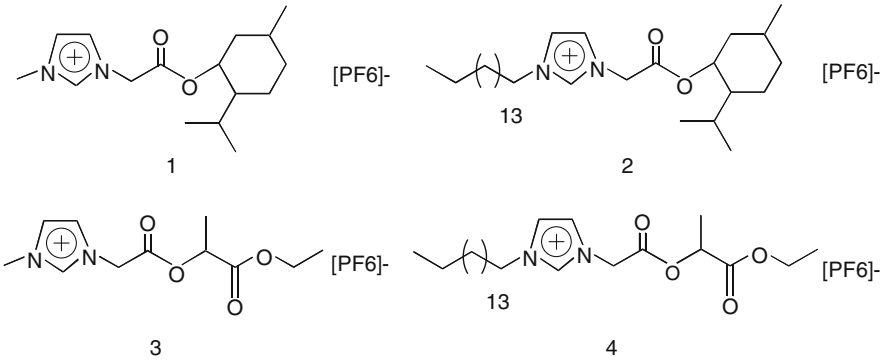

Fig. 9.8 Chiral ionic liquids

liquid was used as a solvent, a small but clear effect on polymer tacticity was observed. The small increase in isotacticity of PMMA using four chiral ionic liquids, 1-((−)-menthoxycarbonylmethylene)-3-methylimidazolium hexafluorophosphate 1, 1-((−)-menthoxycarbonylmethylene)-3-hexadecyl imidazolium hexafluorophosphate 2, 1-((−)-ethoxycarbonylmethylmethoxymethylene)-3-methylimidazolium hexafluorophosphate 3, and 1-((−)-ethoxycarbonylmethylmethoxymethylene)-3-hexadecyl imidazolium hexafluorophosphate 4, was studied [38, 40]. The chemical structures of chiral ionic liquids were shown in Fig. 9.8. During the same reaction time, the monomer conversion was comparable to those in chiral ionic liquids, but MWD of the obtained polymer in the absence of ILs was much wider. The good solubility of catalyst in both 1 and 2 helps to mediate the polymerization process. The asymmetric environments of chiral ionic liquids were found to exert some influence on the stereostructure of the PMMA. All the polymers obtained have higher isotacticities than those in nonchiral media. A similar result was obtained with chiral ionic liquid, 1-(R-(+)-2^1-methylbutyl)-3-methylimidazolium hexafluorophosphate, [mbmim*][PF_6] [41].

Nitroxide-Mediated Living Radical Polymerization (NMRP)

NMRP process is the oldest of all controlled/living polymerization methods. The key to the success of this approach is that the concentration of the reactive chain ends is reduced to an extremely low level by reversible termination of the growing polymeric chain. This low overall concentration of the propagating chain end will minimize undesired side reactions like irreversible termination reactions through combination or disproportionation. Thus, control over the entire polymerization process is achieved since all the chains should be initiated only from the desired initiating species and propagation should proceed in a controlled fashion.

NMRP of MMA was carried out in IL, [bmim][PF_6] using both bimolecular initiation system, benzoyl peroxide (BPO) along with 2,2,6,6-tetramethyl-1-piperidinyloxy (TEMPO), and a unimolecular initiation system, 2,2,5-trimethyl-3-(1-phenylethoxy)-4-phenyl-3-azahexane (TMPPAH) [42]. When compared with

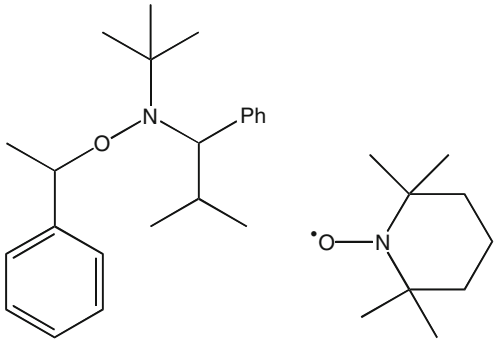

Fig. 9.9 Structures of TMPPAH and TEMPPO

the results obtained for ATRP and RAFT in the same ionic liquid, the molecular weights obtained in NMRP were lower with broader PDI values for a wide range of initiator ratios and temperatures due to the nonliving nature of polymerization and thus failed to indicate kinetic or mechanistic advantages to conducting NMRP in ILs. The possible causes for the observed nonliving "nitroxide-mediated" polymerization nature were the slow degradation of TEMPO in [bmim][PF_6] at high temperature and difficulty in diffusion of the mediating radicals away from the chain ends. The results of NMP with TMPPAH were better than those from the BPO/TEMPO system. This is due to the possibility of the bulky mediating radical in the ionic liquids is not as same as in common organic solvents or in bulk. The chemical structures of TEMPO and TMPPAH were given in Fig. 9.9.

Reversible Addition Fragmentation Chain Transfer (RATF) Polymerization

The RAFT process is the youngest of the living radical polymerization methods and allows construction of polymers with targeted molecular weights possessing low PDI values. Preserved end groups can be reactivated, permitting the incorporation of additional monomers to produce a diverse array of block copolymers. The process is complementary to traditional free radical polymerization, and along with the usual components of radical initiator, monomer, and solvent, the RAFT process relies on the addition of a chain transfer agent (RAFT agent). One of the biggest advantages of the RAFT process is that it is a robust system that is applicable to a variety of monomers (methacrylates, acrylates, and styrenes), incorporating a range of functionalities including acidic moieties. In addition, the resulting polymer is free from undesirable metal catalysts that are present if other controlled polymerization techniques (e.g., atom transfer radical polymerization) are followed. In RAFT, the polymerization takes place in the presence of a thiocarbonylthio compound, which reacts reversibly with a propagating radical (addition) to form a radical intermediate. This intermediate can then fragment into a new thiocarbonylthio compound and a propagating radical. Since the concentration of propagating chains is kept low when compared to the thiocarbonylthio-bearing polymer chains, the termination reactions are greatly reduced.

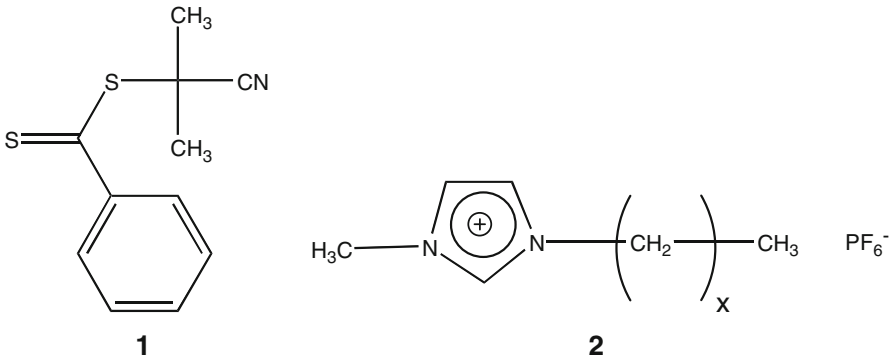

Fig. 9.10 Structures of CPDB, 1 and 1-alkyl-3-methylimidazolium hexafluorophosphate

The RAFT polymerization of MMA in ILs shows a living character and leads to well-characterized polymers with narrow polydispersity [43]. Polymerization of MMA is mediated by 2-(2-cyanopropyl) dithiobenzoate (CPDB, 1) with IL, 1-alkyl-3-methylimidazolium hexafluorophosphate ($[C_x][PF_6]$ 2, where $x=4$, 6 to 8 as the solvent). The chemical structures of CPDB 1 and 1-alkyl-3-methylimidazolium hexafluorophosphate 2 were shown in Fig. 9.10. The alkyl chain length of $[C_x][PF_6]$ was varied to test its influence on the reactions. Polymerization of MMA results in high conversion as PMMA is fully soluble in the ionic liquids. For MMA, the polymerization rate is faster in ionic liquids than in toluene. For instance, at 60°C, a conversion of 25% is reached in 20 min when polymerizing MMA free radically in $[C_4][PF_6]$, while the polymerization in toluene leads to only 3% conversion. The polymerization in $[C_4][PF_6]$ (84.3%) is slightly slower than in $[C_6][PF_6]$ and $[C_8][PF_6]$ (91.3% and 90.1%, respectively). The MMA polymerizations in ionic liquids lead to final products with PDI values as low as 1.11, which are close to the ones obtained when reacting in bulk or in toluene.

Group Transfer Polymerization

Group transfer polymerization (GTP) is a relatively new method for polymerization of acrylic and methacrylic monomers. The major advantage of GTP is that the reaction can be carried out at room temperature and above with better molecular weight control and narrower polydispersities. The technique of GTP was commercialized by DuPont. MacFarlane and Vijayaraghavan has successfully carried out group transfer polymerization of MMA at ambient temperatures in an ionic liquid, *N*-butyl, *N*-methyl-pyrrolidinium bis-(trifluoromethanesulfonyl) amide $[p_{1,4}][tf_2N]$ to produce living polymers of improved polydispersity for the first time [44]. The tf2N anion is chosen because of its weak basicity and its hydrophobicity. The reaction can give high yields under relatively mild conditions in the IL with or without the addition of a nucleophilic catalyst, TBAB. The addition of a nucleophilic catalyst

provides higher rates of polymerization and better molecular weight control, and at a particular concentration of catalyst, the polymerization was observed to be living. The growing propagating species may be stabilized by the ionic liquid, against side reactions. The yield of polymer is close to 100% in the case of experiments carried out using a Lewis base catalyst, TBAB, in IL. The molecular weights produced in these cases were high, and the polydispersities improved as compared with the traditional solvent-based reactions. About 21% polymer yield and higher polydispersity was achieved with Lewis acid catalyst, iBu_2Alcl. The initiator and IL solvent are necessary for the group transfer polymerization to occur. However, catalyst is not absolutely necessary, unlike the conventional group transfer polymerization in which a nucleophilic catalyst is definitely required.

Radiation Polymerization

Wu and coworkers reported the first radiation-induced polymerization of MMA in EtOH and DMF in the presence of IL $[Me_3NC_2^- H_4OH]^+ [ZnCl3]^-$ [45]. The addition of >60 vol.% IL results in higher monomer conversion, higher molecular weight, and multimodal MWDs of PMMA. EtOH and DMF were used because they are nonsolvent and good solvent, respectively, for PMMA. The clear difference in the MWD pattern between EtOH/RTIL and DMF/RTIL systems is probably due to the complicated interactions between the solvent and IL. The multimodal MWD is tentatively explained by the heterogeneous nature of the organic/IL solution. Interactions between the monomer, solvent, and IL are complicated and significantly affect the monomer conversion and the MWD of the polymer. Various radical species formed upon gamma radiation serve as the initiators for the polymerization of MMA. These species include mainly the parent radicals or fragments of the IL, MMA, EtOH, or DMF.

Radiation-induced polymerization results in higher molecular weight, and MWD of PMMA in neat ILs ([bmim][PF_6] and [bmim][BF_4]), as well as in their mixed solutions with organic solvents [46]. For polymerization in IL/organic mixed solutions, M_w of PMMA increases, but not significantly with the increase of IL fraction in the IL/organic solutions. This is due to the high viscosity and inhomogeneity of ionic liquids.

Anionic Polymerization

Generally, anionic polymerization requires severe dehydration of solvents and reactants. ILs can be dried under vacuum at high temperature due to their negligible volatility, and, hence, there is no need for cumbersome handling procedures such as distillation in the presence of drying agents for anionic polymerization. Watanabe and Kokubo were the first to report anionic polymerization reactions of MMA in ionic liquids using alkyl lithium initiators such as *n*-butyllithium (*n*-BuLi) and diphenylhexyl lithium (DPHLi) [47]. The polymerization in ILs having [NTf_2] anion did not yield PMMA because the initiator may be deactivated due to attack on the

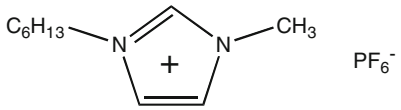

Fig. 9.11 1-Hexyl-3-methylimidazolium hexafluorophosphate [hmim][PF_6]

trifluoromethyl group. However, the polymerization reactions proceeded in [bmim][PF_6] with lower yields (5–9%) as compared to those prepared in THF(15–62%) and the prepared PMMA had large polydispersity indices (approx. 2.0). These results are probably due to the high reaction temperature (0°C) when compared with the common anionic polymerization temperature of MMA, −78°C, and the possible reaction between the initiator and the imidazolium cation. The initiator was considered to be deactivated because the hydrogen atom at the 2-position of the imidazolium ring was withdrawn by the alkyl lithium initiator. In the anionic polymerizations of PMMA using alkyl lithium initiators without any additives in organic solvents, it is generally recognized that the polymerization reaction cannot be controlled due to the presence of side reactions and termination reactions. The tacticity of the obtained PMMA, prepared in [bmim][PF_6] by utilizing DPHLi, was rich in mm triads, similar to that polymerized in toluene.

Miscellaneous Polymerization

Texter and Yan first reported microemulsions stabilized by IL-based surfactants that consist of an imidazolium cation polar group and a hydrophobic tail [48]. These surfactants were used to stabilize microemulsions. Polymerizations in these microemulsions can produce polymer particles, gels, and open cell microporous materials. Bulk emulsion polymerization in a-Br/MMA/H_2O results in monodisperse polymer latexes with diameters of approximately 50 nm whereas in b-Br/MMA/H_2O the polymer latexes resulted without any apparent aggregation.

Brazel et al. demonstrated the capability of ILs based on imidazolium salts as excellent plasticizers for PMMA, with improved thermal stability, and the ability to reduce glass transition temperatures to near 0°C [49]. They have formulated PMMA with traditional plasticizer, dioctyl phthalate (DOP), and properties were compared to PMMA plasticized with two ILs: [bmim][PF_6] (Fig. 9.3) and [hmim][PF_6] (Fig. 9.11). Formulations incorporated up to 30 vol.% DOP and 50 vol.% ILs. These ILs also have potential to reduce volatility and leaching of plasticizers, improve ultraviolet stability, and increase the usable lifetimes of plastics.

9.1.3 Supercritical Carbon Dioxide (scCO$_2$)

A supercritical fluid (SCF), represented in Fig. 9.12, is defined as a substance for which both pressure and temperature are above the critical values [50]. Darr and

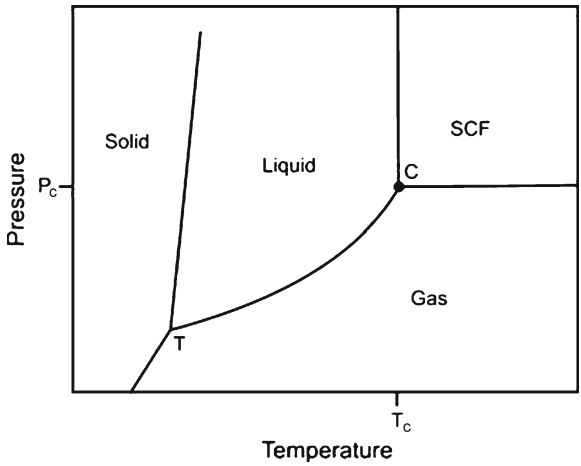

Fig. 9.12 Representation of supercritical fluid (*SCF*)

Poliakoff gave more practical definition by describing SCF as the substance whose temperature and pressure are higher than their critical values and have a density close to or higher than its critical density [51]. They offer an attractive alternative to VOCs for use as additives and reaction media for polymer processing. Though an SCF does not contain two phases such as gas and liquid, it possesses the properties of both gas and liquid. The special combination of gas-like viscosity and liquid-like density results in it being an excellent solvent. It has successfully been used as a solvent in the processing of polymers such as blending, microcellular foaming, and particle production, in extraction applications, and in polymer synthesis [52–55]. The $scCO_2$, which is one of the SCFs, is a clean and versatile solvent and a promising alternative to hazardous VOCs and chlorofluorocarbons (CFCs). It is nontoxic to the environment and humans. At atmospheric pressure, carbon dioxide is gaseous, which means that simple depressurization will leave no hazardous solvent effluent that requires complex or expensive waste treatment. CO_2 is a greenhouse gas; however, it can be obtained in large quantities as a by-product of fermentation, combustion, or ammonia synthesis. Its use should not lead to any net increase in CO_2 emissions because here CO_2 is exploiting before discharging it into the atmosphere. It is relatively cheap, particularly when compared with conventional solvents, and it is readily available on an industrial scale in a very pure form. $scCO_2$ has attracted particular attention in the synthesis as well as processing areas for polymers due to several advantages. The advantages and disadvantages of the use of $scCO_2$ in synthetic chemistry are listed in Table 9.2 [3]. Several reviews and books were published on the use of supercritical fluids for reaction chemistry [56–65].

9.1.3.1 Polymerization in $scCO_2$

$scCO_2$ has generated much interest in the polymer industry as a potential solvent for polymerization reactions. In the conventional processes, PMMA has been prepared

Table 9.2 Advantages and disadvantages of $scCO_2$

Advantages	Disadvantages
Cheap, readily available, nontoxic, and volatiles solvent	Specialized equipment is required
Very attractive solvent for industrial process. Product isolation to total dryness is achieved by simple evaporation	Energy is required to compress CO_2
No solvent waste	Reacts with strong nucleophiles
Nonflammable	Low solubility of polar substrates
Low reactivity	High pressure may be dangerous with unsuitable equipment
Lack of reactivity is essential for common replacement of solvents	Can be expensive for large-scale work
Reversible reactivity with weak nucleophiles	
Alternative to the processing of solid materials	
Potential for product processing applications supercritical antisolvents, SAS; superfluid chromatography, SFC; and rapid expansion of supercritical solution, RESS	
Tunability	
Density can be easily tuned by varying the pressure, hence large change in solvent properties which made $scCO_2$ as a unique solvent. Small amount of cosolvents can further modify solvent properties	
Supercritical conditions	
Can be easily achieved. $T_c = 304$ K and $p_c = 7.38$ MPa	
High diffusion rates offer potential for increased reaction rates	

by bulk solution emulsion suspension or dispersion polymerization. Except bulk polymerization, all other methods involve the use of water, solvents, or organic diluents. Hence, these polymerization methods are harmful to human beings and to our environment. However, in the $scCO_2$ process, PMMA can be produced using environmentally benign CO_2. Polymers are swollen and plasticized, lowering the glass transition temperature in SCFs. This made easy removal of residual monomers, mixing of additives, and formation of foams. Also, polymerization rate is promoted as the diffusion of monomer in the polymer particle is enhanced due to the plasticization. The particle size of polymer could be tailored to meet the requirement of both conventional and supercritical fluid processes. In the latter process, particles of desired size, from submicron to microns, by changing the types and amounts of surfactants, are obtained. CO_2 is generally inert, allowing polymers to be synthesized by a variety of techniques including free radical polymerization, cationic polymerization, transition metal catalysis, ring-opening polymerization, and enzymatic polymerization. Moreover, CO_2 returns back to the gaseous state upon depressurization of the reactor and allows the easy separation of the polymer product from the reaction medium, producing the polymer in powder form.

The solvent power of a supercritical fluid is dependent on its density and hence on the pressure of the fluid. For polymers, the dissolving power of supercritical CO_2 is similar to that of fluorocarbons. CO_2 is essentially a nonsolvent for most polymers, including lipophilic and hydrophilic polymers, but tends to be a reasonable solvent for many amorphous fluoropolymers and siloxanes. Because of these solvent characteristics, in most cases it is difficult to produce good yields of high molar mass polymers through solution polymerization in $scCO_2$, because the polymer product inevitably precipitates from the reaction medium. Since carbon dioxide is a nonsolvent for most monomers, elevated pressure is needed to increase the solubility of monomer in CO_2. The density of CO_2, which is a strong function of temperature and pressure, plays a vital role in deciding its solubility in a polymer. However, the quantity of CO_2 dissolved in different polymers also differs depending on the available chemical groups. In the early stage of polymerization, the oligomers synthesized from the monomers might be dissolved in carbon dioxide at moderate pressures. However, the growing polymer particles fall out of carbon dioxide and precipitate on the bottom of the reactor. To produce the polymer in high yields, it is necessary that the growing polymer be well dispersed in the CO_2 during polymerization. Solution, dispersion, precipitation, and emulsion radical polymerizations have been successfully performed in $scCO_2$.

Surfactants

Despite CO_2 being a good solvent for many vinyl monomers, most polymeric materials, except fluoro- and siloxane-based, have a very low solubility in CO_2. These polymers represent a very small fraction of the industrially important polymers. This means that to exploit successfully the aforementioned technological and environmental advantages of dense carbon dioxide and to broaden the efficacy of liquid and $scCO_2$ to include the synthesis of other polymers using heterogeneous polymerization methods, a suitable surfactant or stabilizer or dispersant must be added to the polymerization medium to allow the stabilization of the polymer particles [66]. A polymeric surfactant is used to sterically stabilize nucleated polymer particles and prevent flocculation and precipitation of the reaction product. Its role is to physically adsorb or chemically attach to the surface of the polymeric particles and form stable nuclei. The effectiveness of a surfactant is governed by its ability to provide sufficiently strong anchoring to the polymer particle, and also the soluble segment of surfactant must be chain-extended into the continuous phase (e.g., of sufficient solvation and chain length) [67, 68]. These factors can be controlled by synthetic variation of both the composition and architecture of the stabilizers for the polymerization reactions in $scCO_2$ medium. The prominent polymeric surfactants used for polymerization of MMA using $scCO_2$ are fluoroacrylate-based, polysiloxane-based, and perfluoropolyether surfactants. The lack of commercially available CO_2 surfactants led researchers to develop the surfactants consisting of a "CO_2-philic" section, almost without exception a siloxane or fluorocarbon, and

a "CO_2-phobic" section, hydrophilic or lipophilic components to interact with the polymer being synthesized. The three main approaches to developing effective surfactants for use in $scCO_2$ are Giles et al. [69]:

1. Use of CO_2-compatible polymers as surfactants, for example, poly 1,1-dihydroperfluorooctyl acrylate, poly(FOA)
2. Use of "CO_2-philic" surfactants with a suitable polymerizable group to be incorporated into the growing polymer chain forming an in situ graft copolymer
3. Use of block copolymers with "CO_2-philic" and "CO_2-phobic" blocks and graft systems with a "CO_2-phobic" backbone and "CO_2-philic" graft chains

Dispersion Polymerization

Dispersion polymerization is a heterogeneous polymerization process by which latex particles are formed in the presence of a suitable stabilizer from an initially homogeneous reaction mixture [70]. It is characterized by initially homogeneous conditions, the resulting polymer is insoluble in the dispersion medium, and, therefore, phase separation occurs at an early stage in the reaction. The precise point at which this happens will depend on the solvency of the continuous phase for the early products of the polymerization. Polymerization takes place initially through a solution-phase reaction to produce oligomeric radicals. When the growing oligomeric radicals reach a critical chain length, the chains become insoluble in the continuous phase and precipitate from the solution. Particle dispersions produced in the absence of any stabilizer are not sufficiently stable and tend to coagulate during their formation. The addition of a small amount of an appropriate stabilizer to the polymerization mixture produces a stable dispersion, which is typically referred to as polymer dispersion, a colloidal dispersion, or a latex. The stabilization mechanism in dispersion polymerization is usually steric in nature, whereby a layer of stabilizer adsorbed (or grafted) at the polymer-solvent interface imparts long-range steric repulsions between particles. These forces compensate for short-range van der Waals attractions, thus preventing flocculation of the dispersion. Dispersion polymerization in $scCO_2$ is one of the best synthetic methods for the preparation of uniform and monodisperse particles in the micron range. High degrees of polymerization are observed because the insoluble polymer is stabilized sterically as a colloid and does not precipitate. The majority of the work in dispersion polymerizations in supercritical CO_2 has focused on MMA. Common solvents for the free radical dispersion polymerization of lipophilic monomer MMA are hydrocarbons or C_1–C_5 alcohols. Under the suitable conditions, dispersion polymerization gives rise to well-defined spherical particles, typically in the size range 100 nm to 10 μm. Dispersion polymerization is an important process, and the use of CO_2 as a solvent has the potential to eliminate large VOCs. The different surfactants and polymerization techniques used to synthesis PMMA by dispersion polymerization is discussed here.

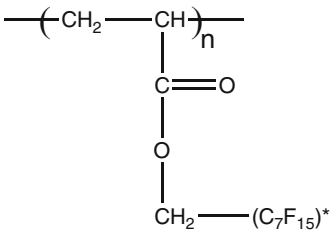

Fig. 9.13 Structure of poly(FOA) in CO_2

Fluoroacrylate-Based Surfactants

Polymeric materials can be categorized as either CO_2-philic or CO_2-phobic based on their solubility characteristics. Amorphous fluoropolymers or low-melting fluoropolymers and polysiloxanes are soluble in CO_2, while most other polymeric materials are insoluble in CO_2 [52, 71]. As such, these materials are defined as CO_2-philic and CO_2-phobic, respectively.

Poly 1,1-dihydroperfluorooctyl acrylate [poly(FOA)] is suitable as a polymeric stabilizer in CO_2 due to its surface-active nature in the PMMA-CO_2 system. The structure of poly(FOA) is given in Fig. 9.13. The amphipathic stabilizer of poly(FOA) contains a lipophilic backbone (CO_2-phobic) that could anchor onto the acrylic surface of the growing polymer particles. The CO_2-philic nature of the fluoroalkyl substituents on the stabilizer caused extension of the PFOA chain trajectory into the continuous phase preventing the flocculation of particles through a steric stabilization mechanism. DeSimone et al. demonstrated the first successful dispersion polymerization of MMA using poly(FOA) as a surfactant in $scCO_2$ [67]. They also pointed out that polymer synthesis in $scCO_2$ could be extended to statistical copolymers of fluorinated monomers with conventional hydrocarbon-based monomers such as methyl methacrylate, butyl acrylate, styrene, and ethylene. This work enabled emulsion polymerization and dispersion polymerization to be possible in $scCO_2$ and made way for the origin of many polymerization reactions in $scCO_2$ which is continuing even today. The precipitation polymerization of MMA in $scCO_2$ led to PMMA with relatively low molecular weights [$((77–149)\times 10^3$ g mol^{-1})] and low monomer conversions (10–40%) in the absence of stabilizers. These polymerizations were conducted in CO_2 at 65°C and 207 bar with AIBN or a fluorinated derivative of AIBN as the initiator. As the reaction proceeded, a stable, opaque-white colloidal dispersion was formed in the reaction vessel. The molecular weights ($(190–325)\times 10^3$ g mol^{-1}) of the resultant polymer PMMA and monomer conversions (>90%) were much improved under these conditions, and it can be recovered from the reaction vessel as a dry, free-flowing powder of uniform spherical particles with average diameters in the range 1.2–2.5 μm immediately upon venting the CO_2. These observations were very much consistent with a dispersion polymerization mechanism. These initial results have prompted a large number of subsequent investigations [72, 73]. They optimized this dispersion polymerization of MMA in CO_2 using PFOA with very low amounts (0.24 wt% based on MMA) of PFOA

(M_w 1.0×10^6 g mol^{-1}) and obtained a stable dispersion of PMMA latex particles with diameters ranging from 1.55 to 2.86 μm. In addition, a large percentage of the stabilizer (up to 83%) can be subsequently removed from the PMMA product by extraction with CO_2. As a result of the relatively high cost of the stabilizer and the possible effects that residual stabilizer may have on product performance, the ability to remove and recycle the PFOA constitutes an important aspect of this system. The ability of CO_2 to plasticize PMMA which facilitates the diffusion of monomer into the growing polymer particles allows the reaction to proceed with high conversion. The particle diameter was found to increase with monomer concentration, presumably due to an increase in the solvency of the reaction medium. The results of dispersion polymerizations were insensitive to the pressure under the different reaction conditions. The cloud point experiments indicated lower critical solution temperature (LCST) phase behavior for the poly(FOA) system with much higher polymer solubilities than for hydrocarbon polymers. Significant effects of helium concentration in CO_2 on the average particle sizes and particle size distributions of PMMA samples were important since many tanks of CO_2 are sold with a helium head pressure. It was found that the presence of 2.4 mol% helium in CO_2 increases the PMMA average particle diameters from 1.9 to 2.7 μm and decreases particle size distribution from 1.29 to 1.03 [72]. Solvatochromatic studies suggested that this was due to a decrease in the solvent strength of the continuous phase. Hence, purity of CO_2 needs to be taken into consideration for process development and scale-up issues in order to commercialize the dispersion process.

Lee and coworkers focused on polymeric fluorosurfactants, heptadecafluorodecyl acrylate (HDFDA), and heptadecafluorodecyl methacrylate (HDFDMA) due to their possible amphiphilic feature to both monomer and $scCO_2$ as well as on DuPont commercially available poly[perfluoroalkyl methacrylates] [74]. Dispersion polymerization of PMMA showed that these polyfluorosurfactants can act as effective steric stabilizers. The resulting PMMA particles possess the molecular weights (around 70,000–80,000) and polydispersity index (PDI) (2.8–3.6) for different concentrations of monomers and initiators. Successful stabilization prevented any aggregation of growing particles and resulted in the formation of spherical and uniform particles in the diameter of 5–10 μm. The particle size of PMMA decreased as the stabilizer concentration increased, and among these four fluoroacrylates, poly(HDFDMA) was the most successful stabilizing agent for dispersion polymerization of PMMA in $scCO_2$ to control particle size and particle size distribution.

Polysiloxane-Based Surfactants

Silicone polymers are much less expensive than their fluorinated counterparts. The solubility of silicone polymers in both CO_2 and conventional organic solvents makes for facile characterization of the products. Polydimethylsiloxanes (PDMS) are one of this kind of surfactants largely used at supercritical conditions for different applications. DeSimone et al. first demonstrated the dispersion polymerization

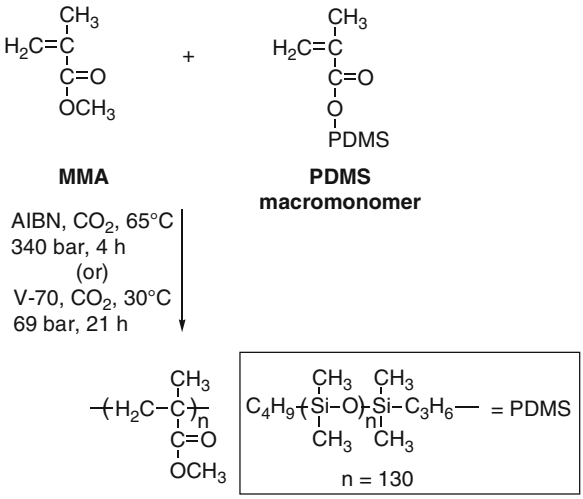

Fig. 9.14 Dispersion polymerization of *MMA* in CO_2 with *PDMS* macromonomer

of MMA in CO_2 using a commercially available methacrylate-terminated PDMS macromonomer [75]. However, these studies showed that only a small portion of the added macromonomer actually copolymerized, and the majority of the unreacted macromonomers could be removed from the surface of the particles by extraction with hexane or CO_2. These polymerizations were conducted in $scCO_2$ using AIBN initiator (65°C, 340 bar, 4 h) or in liquid CO_2 (30°C, 69 bar, 21 h) using a low-temperature radical initiator [2,2′-azobis(4-methoxy-2,4-dimethylvaleronitrile)]. By varying the reaction conditions, high molecular weight PMMA particles [$M_n = (123–390) \times 10^3$ g mol^{-1}] with a narrow particle size distribution were obtained in sizes ranging from 1.1 to 5.8 μm. The best yields, molecular weights, and the most regular spherical particle morphologies were obtained in $scCO_2$ using rather high stabilizer concentrations (3.5–16% w/w based on monomer). When no PDMS macromonomer was added to the polymerization, only a low conversion, precipitation polymerization resulted. However, the larger amounts of PDMS macromonomer were necessary to adequately stabilize the dispersion polymerization of MMA in $scCO_2$, and the role of unreacted PDMS macromonomer in stabilizing these dispersion polymerizations is not clear. Figure 9.14 illustrates the dispersion polymerization of MMA in CO_2 using PDMS macromonomer.

The dispersion polymerization of MMA stabilized by PDMS monomethacrylate has been investigated in detail with the particle formation [76] and particle growth [77] for this system using in situ turbidimetry. The structure of PDMS monomethacrylate is depicted in Fig. 9.15 [78]. Turbidimetry is a very useful technique for studying dispersion polymerization in situ because higher conversions may be monitored than in the case of dynamic light scattering. The entire particle formation stage, which establishes the final particle number density, could be monitored by turbidimetry. On the basis of measurement of the particle size, number density, and surface area, coagulative nucleation and controlled coagulation regions have been

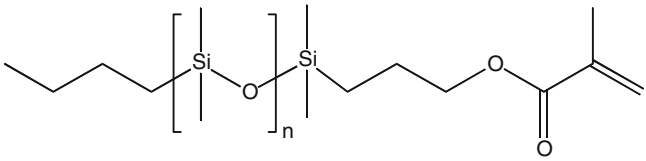

Fig. 9.15 Structure of PDMS monomethacrylate

identified. The high concentrations of monomer initially present in the reaction enable stabilization of the dispersion during the critical particle formation stage even at very low pressures. Thus, small, yet highly coagulated, particles and high molecular weights are observed at low pressure. In contrast, stabilizer concentration has a strong effect on particle size. The mechanism of stabilization is complicated because of changes in the composition and solvent quality of the continuous phase and the availability and conformation of the stabilizer. Analysis of the chronology of molecular weight, particle size, product morphology, and polymerization rate indicates that the main locus of polymerization is the particle phase and no new particles are formed for the majority of the polymerization because particle volume increases directly with conversion. The final particle size and number density determined from the model of Paine agree with the measured values [79]. Howdle and coworkers used the same type of PDMS-monomethacrylate macromonomer stabilizer [78] for the dispersion polymerization of MMA in $scCO_2$ and demonstrated that both polymer yields and molecular weights were strongly influenced by mixing phenomena, particularly when higher concentrations of AIBN were used. Surprisingly, improved yields and molecular weights were obtained in the absence of stirring in the autoclave. It is due to radical-metal termination reaction was occurring between propagating radicals and the steel walls of the reaction vessel. A high molecular weight PMMA film which prevents the termination reaction was deposited on the walls of the reactor in the absence of stirring. The deposition of this film was hindered by efficient agitation, and that this was the reason for the low monomer conversions and low molecular weights under stirred conditions. Hence, this radical-metal termination effect would have important implications for CO_2-based radical polymerizations because they are typically conducted in unlined autoclaves constructed of stainless steel or other high-strength alloys. In their further work, PDMS monomethacrylates with a variety of molar masses were used as successful surfactants for the polymerization of methyl methacrylate in supercritical CO_2 to produce PMMA in high yield and molar mass and with well-defined particle sizes. The PDMS monomethacrylate with a nominal molar mass of 2,000 is a surprisingly good surfactant at low wt/wt concentrations and is a more viable option for future commercial exploitation than the higher molar mass surfactants.

Howdle et al. monitored the dispersion polymerization of methyl methacrylate using a macromonomer PDMS monomethacrylate as stabilizer by power compensation calorimetry for the first time [80]. Power compensation calorimetry is a method of studying the exothermic/endothermic events that occur during polymerization.

Any changes in power will reflect thermodynamic events occurring during the reaction. This method assumes that heat losses are constant throughout the reaction. Even though analysis of the monomer conversion is difficult under high pressure, the calorimetry results give us a good understanding of the progress of the reaction. Monomer conversions are observed greater than 90% at the end of polymerization. At this point, the power trace and reaction pressure are leveling out. Different initiator concentrations clearly influence the polymerization rate, but the enthalpies of polymerization for 1.5% and 0.33% AIBN were measured to be almost the same −52.6 and −59.7 kJ mol^{-1}, respectively. These values correlate well with the literature value of enthalpy of polymerization in conventional solvents (−57.5 kJ mol^{-1}). From the power trace and reaction pressure trace, it was observed that without stabilizer, the polymerization rate was very slow, and also the stirrer will get blocked by the polymer precipitation after 4 h polymerization. After opening the autoclave, the final product was observed to be a viscous liquid and sticky solid with low monomer conversion, low molecular weight, and broad molecular weight distribution. This is attributed due to the internal radical termination in the reaction system.

Park and Shim synthesized PMMA particles with diameters of about 2.5 and 4.2 mm by polymerization in $scCO_2$ using a cheap CO_2-philic surfactant, Monasil PCA (PDMS-*g*-PCA) [81]. The polymer particles were stable in $scCO_2$, and their shape remained spherical as their surfaces were covered with the surfactant. With increasing the amount of CO_2-philic surfactant, the average particle size will decrease yielding the smallest and very uniform particles at 15% surfactant. The degree of agglomeration was also decreased with the amount of CO_2-philic surfactant. To get acceptable quality PMMA particles, at least 7% of Monasil PCA must be used. The molar weights and the MWD decreased with increasing the amount of initiator, AIBN. Sonication promoted stability of PMMA latex by disintegrating the large agglomerated particles into smaller and more uniform primary ones. The latex thus became much more stable, and the sedimentation time was doubled.

Water-dispersible polymer powders in $scCO_2$ obtained by using novel "ambidextrous" CO_2-philic/hydrophilic surfactant poly(dimethylsiloxane)-*b*-poly(methacrylic acid) (PDMS-*b*-PMA) {(M_w: 5,500 g /mol PDMS, 900 g/mol PMA) demonstrated dispersion polymerization in a nonpolar medium and stabilized the particles when transferred to water [82]. In CO_2, the PDMS block provides steric stabilization while the PMA block adsorbs on the particle surface. The PDMS block collapses onto the surface upon transfer to water, and the PMA block ionizes at pH>5 to stabilize the latex by electrostatic repulsion. The block copolymer PDMS-*b*-PMA produces particles several microns in diameter that flocculated and coalesced as the reaction proceeded because of the low molecular weight of the PDMS tails. The particles synthesized with PDMS-*g*-pyrrolidonecarboxylic acid (PDMS-*g*-PCA) rapidly flocculated when dispersed into aqueous buffer solutions due to insufficient electrostatic stabilization. The PDMS-*g*-PCA contained approximately two ionizable groups per chain compared to nine in the PDMS-*b*-PMA surfactant. A mixture of PDMS-*b*-PMA and PDMS-*g*-PCA produced much more uniform and less agglomerated particles than those obtained with surfactant alone in CO_2. Figure 9.16 represents the chemical structure of PDMS-*g*-PCA. Further, Johnston and coworkers demonstrated

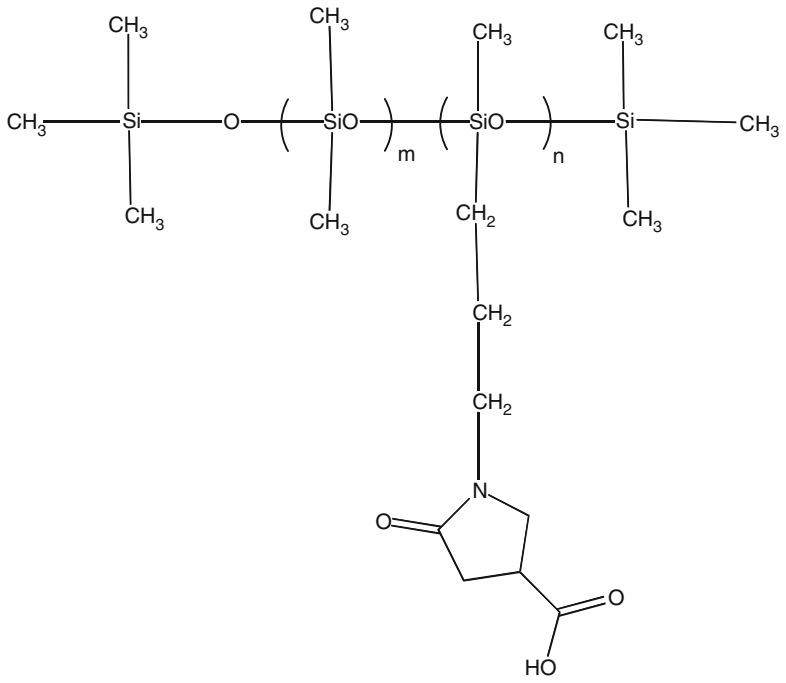

Fig. 9.16 Structure of PDMS-*g*-PCA (Monasil PCA)

the application of trifunctional ambidextrous surfactants by synthesizing three types of trifunctional PDMS block copolymers such as poly(dimethylsiloxane)-*b*-poly(*tert*-butyl acrylate-*co*-acrylic acid) [PDMS-b-P(tBA-*co*-AA)], poly(dimethylsiloxane)-*b*-poly(methyl methacrylate) [PDMS-*b*-PMMA], poly(dimethylsiloxane)-*b*-poly (acrylic acid) [PMMA-*b*-PAA], and poly(dimethylsiloxane)-*b*-poly(methyl methacrylate-*co*-methacrylic acid) [PDMS-*b*-P(MMA-*co*-MA)], and utilizing them to stabilize PMMA latexes in both nonpolar (CO_2) and polar (water) solvents [83]. In CO_2, the PDMS block provides steric stabilization and collapses upon transfer to water. In water, only about 1% of the AA or MA groups ionize, yet this provides sufficient electrostatic stabilization. The change in surface charge with pH is consistent with the p*K*a of the AA and MA groups. Upon transfer to water, the particle size remained constant, indicating good stabilization in both media without agglomeration even for 40 wt% solids in water. Despite the much smaller surfactant concentrations and lower molecular weight for the stabilizer block than in previous studies, submicron particles were produced indicating a desirable anchor soluble balance (ASB). The particles were much smaller and less agglomerated than those produced with bifunctional PDMS-*b*-PMA ambidextrous surfactant which illustrates the advantage of adding a third block that anchors to the PMMA surface. Consequently, much more stable latexes were formed upon transfer to water. Johnston and coworkers [84] also studied the effect of stabilizers perfluoropolyether acid [PFPE-COOH],

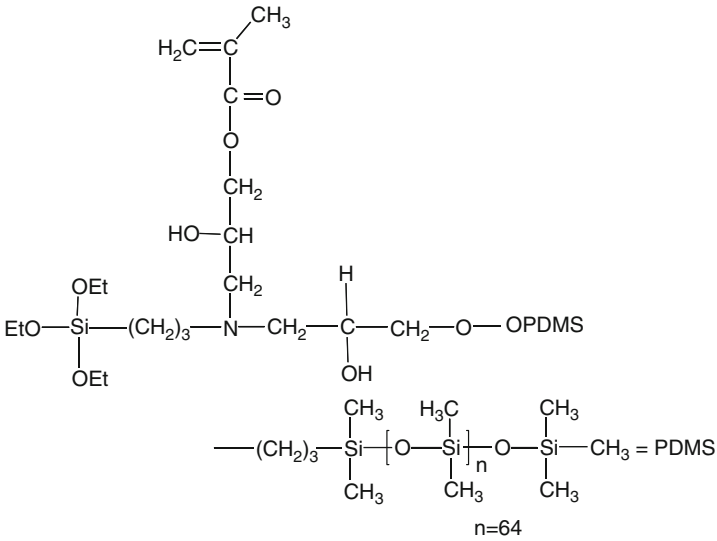

Fig. 9.17 GMA-PDMS stabilizer

PDMS monomethacrylate [PDMS-mMA], poly(1,1-dihydroperfluorooctyl acrylate)-*b*-polystyrene [PFOA-*b*-PS], and PDMS-*b*-P(MMA-*co*-MA) on the particle formation stage in dispersion polymerization of methyl methacrylate in $scCO_2$. The average particle diameter (250 nm) and particle number density were similar at the end of the formation stage for the stabilizers PDMS-*b*-P(MMA-*co*-MA) and PFOA-*b*-PS. The particle diameters were much larger for grafted PDMS-mMA than PFPE-COOH due to higher surface coverage and ability to stabilize particles with PDMS as effectively as with PFOA during particle formation which may be attributed to the large concentration of monomer that acts as a cosolvent.

Lee and coworkers synthesized a new reactive stabilizer having a vinyl group and CO_2-philic PDMS by linking glycidyl methacrylate (2,3-epoxypropyl methacrylate) and monoglycidyl-ether-terminated PDMS by using aminopropyltriethoxysilane for dispersion polymerization of MMA [85]. The processes to separate and purify the GMA-PDMS macromonomer from reactant medium were not required, which is a great advantage for commercial production. PMMA was produced in high yield over 94% using only 0.87 wt% (2.9 wt% based on monomer weight) GMA-PDMS. When the initiator AIBN concentration was increased from 0.25 to 1.06 wt%, the molecular weight and particle size of the PMMA decreased from 56,600 to 21,600 and from 4.1 to 2.7 μm, whereas the particle size distribution increased from 1.3 to 1.9. Figure 9.17 illustrates the chemical structure of GMA-PDMS.

The dispersion polymerization of MMA in $scCO_2$ uses unsaturated siloxane-based surfactant where the backbone is unsaturated and the side chains contain a CO_2 soluble functionality, leading to the CO_2 "philic" and "phobic" sections required for an effective stabilizer [86]. The new unsaturated siloxane-based surfactant,

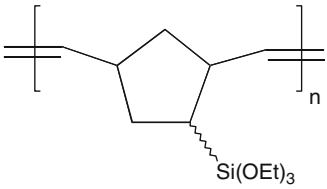

Fig. 9.18 Unsaturated siloxane-based surfactant

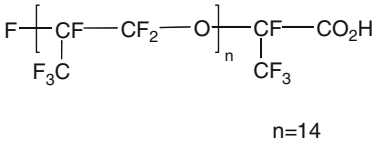

Fig. 9.19 Krytox 157 FSL carboxylic-acid-terminated perfluoropolyether

[poly(bicyclo[2.2.1]hept-5-ene-2-yl)triethoxysilane], shown in Fig. 9.18 was prepared by ring-opening metathesis polymerization (ROMP) of (bicyclo[2.2.1]hept-5-ene-2-yl)triethoxysilane using $Ru(Pcy_3)Cl_2(CHPh)$ as the initiator. When the polymerization is performed in the presence of 2 wt% unsaturated surfactant, the PMMA produced was a fluffy white solid in 79% yield. Even though the particles appeared to be formed initially, they have subsequently aggregated to form strings and other structural motifs due to the presence of insufficient stabilizer during the polymerization. This was in fact proved by repeating the polymerization by addition of 4 wt% stabilizer. The polymerization was quantitative, and a high molecular weight polymer (molecular weight increased to $M_n = 82{,}000$ and the MWD remained constant) was produced in this case. The polymer was found to show discrete spherical particles with a diameter of 2.7 μm with narrow particle size distribution. The soluble fraction of the unsaturated surfactant only showed activity as a stabilizer in CO_2 and was highly effective at even in very low concentrations.

Graft-Copolymer-Based Surfactants

Howdle and Christian explored the use of monofunctional pseudograft stabilizer, Krytox 157 FSL (commercially available carboxylic-acid-terminated perfluoropolyether), shown in Fig. 9.19 in which no additional comonomer is required for successful free radical dispersion polymerization of MMA in $scCO_2$ [87]. Its mechanism of stabilization is believed to be based on the formation of a relatively weak hydrogen bond between the terminal acid functionality of the stabilizer and the ester groups of poly(MMA). Control polymerization with a nonfunctionalized perfluoropolyether demonstrates that a terminal acid functionality is required for stabilization. The residual levels of Krytox in the PMMA product are very low, primarily because there are very few sites for chain transfer and hence little possibility of grafting to PMMA. In addition, the Krytox can be easily removed from the PMMA product by supercritical fluid extraction. The morphology and molecular weight of the materials produced depend greatly on the concentration of reactants employed.

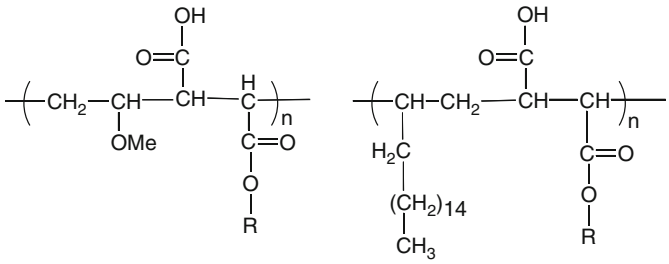

M_n = 79,000	Stabilizer	M_n = 30-50,000	Stabilizer
R = $-CH_2CH_2(CF_2)_3CF_3$	**1**	R = $-CH_2CH_2(CF_2)_3CF_3$	**5**
$-CH_2CH_2(CF_2)_5CF_3$	**2**	$-CH_2CH_2(CF_2)_5CF_3$	**6**
M_n = 1,100,000			
R = $-CH_2CH_2(CF_2)_3CF_3$	**3**		
$-CH_2CH_2(CF_2)_5CF_3$	**4**		

Fig. 9.20 Structures of stabilizers

Such structures may well have very high surface areas and could show utility as support materials. In the absence of stabilizer, PMMA was produced in low yield (29%) and with a low molecular weight. However, the addition of only a very small amount of the Krytox stabilizer (0.0001%) increases the yield to nearly 90% with a corresponding increase in molecular weight. Krytox gives remarkably high yields of polymer at substantially low stabilizer concentrations, and even at very high stabilizer concentration, no detectable residues of perfluoropolyether in the PMMA product were observed. Polymerization is taking place in two phases, continuous and dispersed, although to a different extent. Even though the polymer particles are the dominant reaction locus, where high MW material is produced, a small amount of low MW material is also produced in the continuous phase. The level of low MW material is sufficient to cause a significant broadening of the final MWD leading to larger final PDI values than those expected for the same polymer in bulk or in emulsion. Hence, a careful choice of reactor geometry and stirrer type appears to be crucial when using weakly anchoring stabilizers like Krytox 157. It is also important that optimized reaction conditions are identified to control this MWD broadening if these polymerization processes have to be used for industrial applications.

Howdle and coworkers extended this work to different backbone architectures and chain length stabilizers with a substantially longer hydrocarbon backbone, and an analogous system with additional long pendant hydrocarbon groups as well as the fluorinated and carboxylic acid groups for the polymerization of MMA in $scCO_2$ [88]. The different stabilizers are shown in Fig. 9.20. The stabilizer activity was found to be independent of the backbone chain length for the above grafted copolymers. Stabilizers 1 and 3 display similar properties, with low stabilizer loadings producing aggregated materials but higher loadings leading to discrete particles, whereas stabilizers 2 and 4 produce discrete particles even at low concentrations.

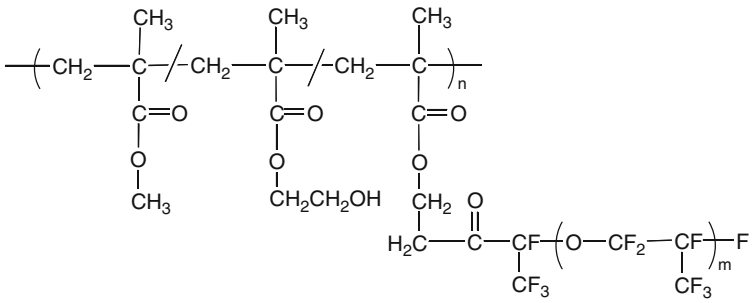

Fig. 9.21 Graft copolymer dispersant

Change of the stabilizer chain length has little effect upon stabilizer activity. The addition of pendant hydrocarbon moieties has a substantial effect upon activity. The stabilizer formed using poly(maleic anhydride-*alt*-1-octadecene) and 1*H*,1*H*,2*H*,2*H*-perfluorohexanol (stabilizer 5) does not form particles even at a 5% loading. However, the analogous (stabilizer 6) produced using a longer 1*H*,1*H*,2*H*,2*H*-perfluorooctan-1-ol graft forms discrete particles even at very low loadings. When stabilizer 6 is used, the PMMA formed becomes aggregated at higher concentrations. Hence, the best choice of backbone and fluoroalcohol is poly(methyl vinyl ether-al*t*-maleic anhydride) with 1*H*,1*H*,2*H*,2*H*-perfluorooctan-1-ol (stabilizer 2) to produce discrete PMMA particles at very low concentrations.

Fluorinated compounds show the highest affinity for CO_2 due to their low dipolarity/polarizability. Additionally, the oxygen in the perfluoropropylene oxide repeat unit has an electron-donor capacity that enhances miscibility with the Lewis acid, CO_2. By taking into consideration of all these factors, a series of preformed graft copolymer surfactants based on anchoring backbone poly(MMA-*co*-hydroxyethyl methacrylate) with varying percentages of a CO_2-philic poly(perfluoropropylene oxide) graft were synthesized [89]. These stabilizers are poorly miscible with CO_2 and have an affinity for the resultant PMMA in $scCO_2$. The graft chains (or soluble component) consisting of poly(perfluoropropylene oxide) are very soluble in CO_2 at low pressure and are attached to the particle through the anchor component. The chemical structure of the graft copolymer dispersant is shown in Fig. 9.21. A careful balance between the size of the anchor group (backbone length) and the amount of the soluble component (either graft chain length or the graft chain density) is necessary but not only sufficient in order to achieve the best stabilization condition. If the balance tilts toward the soluble component, the dispersant will be more soluble in the continuous phase, and a poorer adsorption onto the particle surfaces will result. It will ultimately result in the formation of larger particle size and size distribution. On the other hand, if the balance tilts toward the anchor group (backbone length), the stronger adsorption onto the particle surface will lead to smaller particles and a larger molecular weight distribution. However, it is important that the solubility of the dispersant in the continuous phase be sufficiently good; otherwise, the dispersant will not facilitate the necessary stabilization leading to a larger particle size and

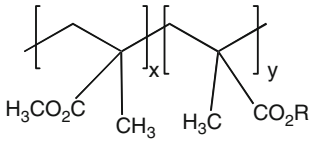

4 R = $CH_2(CF_2)_3CHF_2$

5 R = $CH_2(CF_2)_6CF_3$

6 R = $CH_2CH_2(CF_2)CF_3$

Fig. 9.22 Fluorinated AB block copolymers

size distribution. Increasing the graft density (number of grafts on the backbone) resulted in better stabilization for a given graft chain length and reduced particle size and distribution at a constant backbone.

Block-Copolymer-Based Surfactants

Application of the "screened anionic polymerization" method to the synthesis of well-defined AB block copolymers derived from methyl methacrylate and fluorinated methacrylate monomers has provided a family of tunable surfactants for the free radical dispersion polymerization of MMA in $scCO_2$. Holmes and coworkers demonstrated the design of tailor-made fluorinated AB block copolymers, {R = $CH_2(CF_2)_3CHF_2$, $CH_2(CF_2)_6CF_3$, $CH_2CH_2(CF_2)_5CF_3$}, shown in Fig. 9.22 and their use in the dispersion polymerization of MMA in $scCO_2$ using screened anionic copolymerization (SAP) methodology [90, 91]. A wide range of well-defined molecular weights can be obtained since SAP is a living polymerization. PMMA is obtained with excellent conversion and high molecular weight. Block copolymers having higher molecular weight and higher fluorine contents are considered to be superior surfactants.

Filardo and coworkers tested poly(ethylene glycol)-perfluoroalkyl block compounds as stabilizers for the dispersion polymerization of methyl methacrylate in $scCO_2$ [92]. This novel class of CO_2-philic macromolecules was synthesized by reaction of polyethylene glycol hydroxy terminated with perfluorinated acyl chloride. When stabilizers with appropriate ASB were used, high molecular weight PMMA was synthesized under the form of microspherical polymer particles with yields ranging up to 80%. Even if all synthesized compounds are soluble in the polymerization mixture under operative conditions adopted for the manufacture of poly(MMA), a suitable ratio between the molecular size of perfluorinated and poly(glycol) portion must be maintained in order to have effective stabilization coherently with the criteria proposed by Barrett for the value of the ASB balance of steric block stabilizers for dispersion polymerization in conventional systems [70]. The occurrence of a gel effect was observed as a consequence of the shift in the locus of polymerization from the continuous to the dispersed phase due to an efficient capturing inside the polymer particles of the macroradicals initiated in the continuous medium.

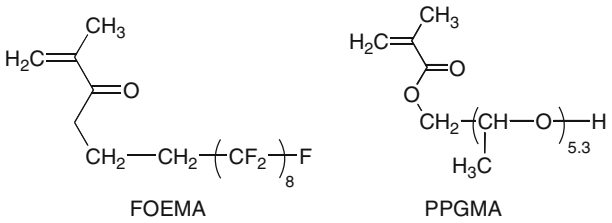

Fig. 9.23 Dispersants and *FOEMA* and *PPGMA*

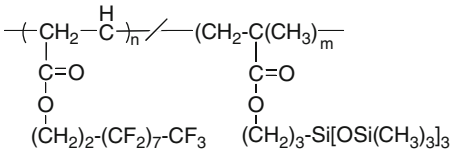

Fig. 9.24 Structure of poly(HDFDA-*co*-SIMA)

Random-Copolymer-Based Surfactants

Dispersion polymerization of MMA in CO_2 was successfully demonstrated using random copolymers of two commercially available monomers (perfluorooctyl)ethylene methacrylate (FOEMA), a monomer with a large CO_2-philic group and poly(propylene glycol) methacrylate (PPGMA), another monomer with a large "hydrocarbon polymer anchor" group as the dispersants which are shown in Fig. 9.23 [93]. Random copolymers can be easily synthesized by radical polymerization in comparison with block or graft copolymers which are complicated to synthesize via "controlled" radical polymerization or living anionic polymerization. The composition of copolymeric dispersants has a dramatic effect on the polymerization yield as well as on the morphology of the resulting when the copolymers containing 50–75% FOEMA are chosen as the dispersants for the polymerizations. Slight adjustment of particle size was possible by varying the concentrations of dispersants and monomers as well as the initial pressures of the reaction medium. The copolymeric dispersant with 52% FOEMA seemed optimal for carrying out polymerization of MMA in CO_2 successfully. The use of the dispersants with 67% and 75% FOEMA can produce high yields of polymer beads with nearly monodispersity in size. Almost half portion of the nonfluoromonomer was incorporated in the copolymer. PMMA particles with diameters in the micron range with nearly homogeneous size distribution were produced using 20%, 30%, and 40% (w/v) of monomer (MMA) concentrations. Slight adjustment of particle size was possible by varying the concentrations of dispersants and monomers as well as the initial pressures of the reaction medium.

Dispersion polymerization of MMA in $scCO_2$ was reported using poly {(heptadecafluorodecyl acrylate)-*co*-3-[tris(trimethylsilyloxy)silyl]propyl methacrylate} [poly(HDFDA-*co*-SiMA)] random copolymer as stabilizer (Fig. 9.24) [94]. Dry, fine-powdered spherical PMMA particles with well-defined sizes were

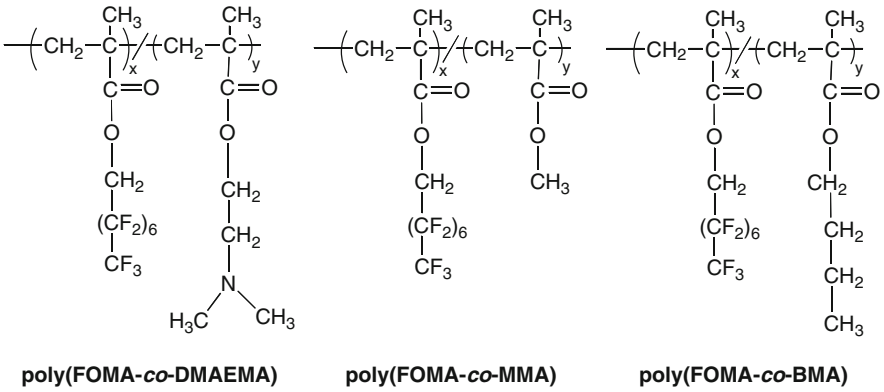

Fig. 9.25 Random copolymers structures

produced in high yields by utilizing various amounts of poly(HDFDA-*co*-SiMA) random copolymer. The yield and the molar mass of PMMA increased with the concentration of poly(HDFDA-*co*-SiMA), the reaction time, and the reaction pressure. Upon increasing the poly(HDFDA-*co*-SiMA) concentration from 1 to 7 wt%, the discrete PMMA particles having a fairly narrow size distribution (PSD = 1.09) and smaller particle diameter (3.1 μm) were formed. The particle diameter depends on the weight percent of the stabilizer added to the system.

Lim and coworkers demonstrated the application of three semifluorinated random copolymers poly(FOMA-*co*-MMA), poly(FOMA-*co*-BMA), and poly (FOMA-*co*-DMAEMA) (Fig. 9.25) which were prepared from perfluorooctyl methacrylate (FOMA) and comonomers of MMA, *N*-butyl methacrylate (BMA), and 2-dimethylaminoethyl methacrylate (DMAEMA) of unusually low fluorine contents relative to previous studies as stabilizers in the dispersion polymerization of MMA in CO_2 [95]. Free-flowing micron-sized spherical PMMA particles could be produced with poly(FOMA-*co*-DMAEMA) containing 34 w/w% FOMA, in contrast to previous methods that used much higher fractions of the fluorinated monomer. This suggested that the copolymers with DMAEMA monomers provide extraordinary colloidal stability of PMMA in CO_2 compared to MMA (which has same structure with the monomer) and BMA (which has similar side chain length as DMAEMA). The polymerization mixture always started with a homogeneous phase because the MMA acts as a cosolvent. When the reaction proceeds, the copolymer stabilizer is gradually absorbed on PMMA particles with comonomer anchors and prevents particle aggregation with FOMA groups, which stretch out in CO_2. DMAEMA copolymer interacts sufficiently with PMMA to provide effective stabilization throughout polymerization, whereas MMA and BMA copolymers might have collapsed to the PMMA surface. The abnormally large stabilization of DMAEMA-based random copolymers was mainly attributed to the fact that PDMAEMA has low glass transition temperature (Tg), which adds flexibility and entropy, and an electron-rich carbonyl group and basic nitrogen in the side chain could interact with Lewis acid, CO_2. Dispersion polymerization of MMA was

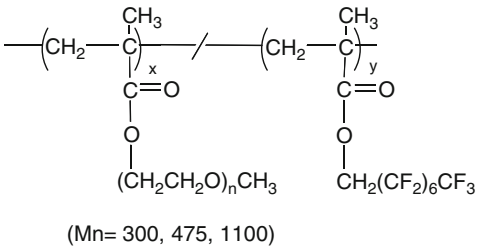

Fig. 9.26 Structure of poly(PEGMA-*co*-FOMA)

demonstrated using poly(FOMA-*co*-DMAEMA) with abnormally large stabilization on the PMMA latexes and could produce discrete PMMA powder even with very low FOMA content of 25 w/w% [96]. The copolymers containing 34–67 w/w% FOMA produced spherical, free-flowing, micron-sized PMMA particles whose diameter increased with FOMA content in the copolymer. The results showed that the composition of copolymeric stabilizers had a dramatic effect on the size and morphology of PMMA. The particle size decreased gradually from 1.8 to 1.0 μm with the increase of stabilizer (38 w/w% FOMA) concentration from 2.0% to 7.5% (w/w to MMA). The stability of the latexes and the diameter of particles were also affected by the concentrations of monomer and the initial reaction pressure. The PMMA particles produced in $scCO_2$ were redispersed into the buffered water by an electrostatic stabilization mechanism.

Further, Lim and coworkers applied dispersant poly(poly(ethylene glycol)methacrylate-*co*-1*H*,1*H*,2*H*,2*H*-perfluorooctylmethacrylate) [poly(PEGMA-*co*-FOMA)] for the dispersion polymerization of MMA in CO_2 (Fig. 9.26) [97]. They have synthesized various random copolymers of [poly(PEGMA-*co*-FOMA)] with different poly(ethylene glycol) (PEG) chain length ($M_n = 300$, 475, and 1,100) and different FOMA contents in $scCO_2$ via free radical polymerization. The copolymers containing above 50 wt% FOMA could be used as a stabilizer for the polymerization of MMA in $scCO_2$. For PEGMA (300) and PEGMA (475) copolymers, the copolymeric stabilizer with 67–69 wt% FOMA content was shown to be optimal to produce micrometer-size spherical PMMA powder. The stability of PMMA latexes in CO_2 was affected by size of pendant PEG group and the composition of copolymer as well as the concentration of MMA. Lim et al. also synthesized a series of nonfluorous random copolymers, composed of 3-[tris(trimethylsilyloxy)silyl] propyl methacrylate and 2-dimethylaminoethyl methacrylate, poly(SiMA-*co*-DMAEMA) shown in Fig. 9.27 with different comonomer ratios and utilized as stabilizers for the free radical dispersion polymerization of MMA in $scCO_2$ [98]. When the copolymeric stabilizer poly(SiMA-co-DMAEMA) (71:29) was employed, free-flowing spherical PMMA particles were produced in high yield. As the concentration of stabilizer increases, the resulting size of colloidal particles decreases. The particle diameter of the polymer was dependent on the concentration of stabilizer and monomer. When the higher SiMA stabilizer (89:11) having higher solubility in the reaction medium was used in the polymerization, a larger amount of stabilizer was

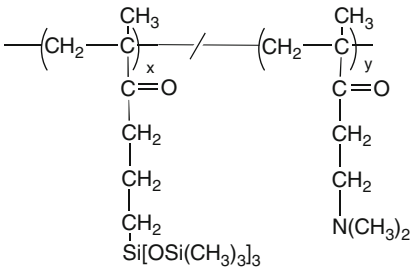

Fig. 9.27 Structure of poly(SiMA-*co*-DMAEMA)

required to stabilize the PMMA latex. The effect of different pressures also resulted in variations in the particle morphology which indicates that the reaction is sensitive to the density of the continuous phase.

By Reversible Atom Transfer Radical Polymerization

Dispersion polymerization of MMA in $scCO_2$ using reversible ATRP in the presence of a low molecular weight fluorinated polymeric surfactant, poly(FOA), was reported to yield stable PMMA latex particles with controlled molecular weights and narrow MWD [99]. All polymerizations were initially homogeneous, as the MMA monomer is soluble in $scCO_2$ under the reaction conditions. In the absence of the poly(FOA) stabilizer, PMMA precipitated out of the CO_2 phase, and limited conversion (55%) was obtained. On the other hand, dispersion ATRP of MMA conducted in the presence of the stabilizer started homogeneously and became progressively more cloudy and converted to a kinetically stable colloidal dispersion after 4 h. The obtained PMMA had a measured molecular weight ($M_n = 13\,400$) close to the calculated value and relatively narrow molecular weight distribution ($M_w/M_n = 1.41$). Particles made by dispersion polymerization were more spherical than those made by precipitation polymerization but were somewhat coagulated.

Controlled homogeneous ATRP of MMA in a fluorinated solvent, benzotrifluoride using macromolecular fluorinated amino ligand catalyzed by a copper salt, was demonstrated [100, 101]. This is a preliminary step to the ATRP of MMA in $scCO_2$, which is a typical heterogeneous process, because PMMA is insoluble in this medium and thus precipitates during polymerization whereas fluorinated polymers are soluble in $scCO_2$ which justifies the choice of the fluorinated amino ligand. The polymerization control was analyzed in relation to the copper salt, the initiator, and the molecular weight and composition of the macroligand before being extended to the heterogeneous ATRP of MMA in $scCO_2$. The best results were obtained for the polymerization initiated by methyl-alpha-bromophenylacetate (MBP) and catalyzed by copper bromide ligated by a macroligand of 15,000 g/mol with three tetraethyldiethylenetriamine (TEDETA) units per chain. The structure of macrofluorinated amino ligand is shown in Fig. 9.28.

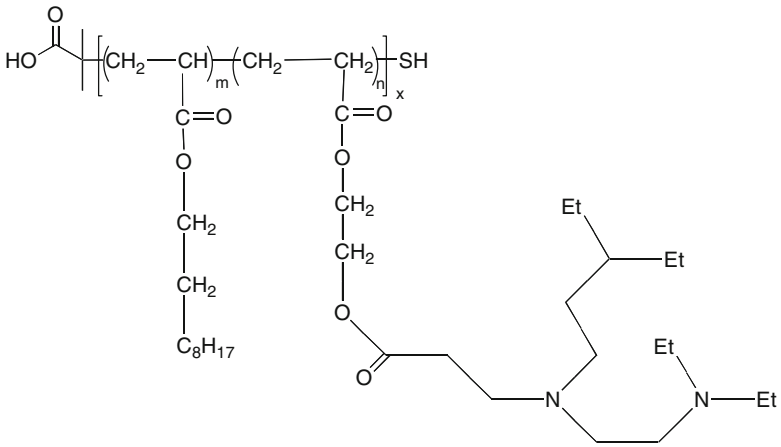

Fig. 9.28 Structure of macrofluorinated amino ligand

By Reversible Addition Fragmentation Chain Transfer (RATF) Polymerization

RAFT-mediated polymerization of MMA was successfully demonstrated in $scCO_2$ in which PMMA was synthesized to high conversion and high molecular weight while maintaining good control over the PDI (less than about 1.2) of the resultant polymer particles by using $scCO_2$ as a solvent and plasticizing agent [102]. The CO_2-soluble RAFT agent (α-cyanobenzyl dithionaphthylate (α-CBDN)) was added to the polymerization reaction in varying concentrations. The crucial aspect for a successful controlled polymerization is the requirement for the RAFT agent, or RAFT-oligomer species, to acquire sufficient mobility within the polymer particle. This was successfully facilitated by $scCO_2$. PMMA particles of well-defined morphology have been produced with narrow molecular weight dispersity. The polymerization was conducted in $scCO_2$ using 5 wt% stabilizer (PDMS-MA) which particularly effective in stabilizing polymer dispersions in $scCO_2$. Conventional dispersion polymerization in $scCO_2$ in the absence of RAFT results in polymer with high molecular weight and a broad MWD after 10 h reaction time. The high concentration of initiator, α-CBDN, relative to RAFT did not affect the molecular weight distribution because of the slow decomposition kinetics of AIBN in $scCO_2$ compared to conventional solvents. Howdle et al. [103] extended this work to four different RAFT agents, namely, R-cyanobenzyl dithionaphthalate (a), R-cyanobenzyl dithiobenzoate (b), 2-cyanoprop-2-yl dithiobenzoate (c), and 4-cyano-1-hydroxypent-4-yl dithiobenzoate (d), respectively, shown in Fig. 9.29 in order to develop a library of effective chain transfer agents which are able to control polymer growth in $scCO_2$. All four RAFT agents showed pseudo-first-order kinetics with the largest transfer constant belonging to 1. By this method, polymers with a specific molecular weight could be targeted by RAFT as obtained in homogeneous conventional

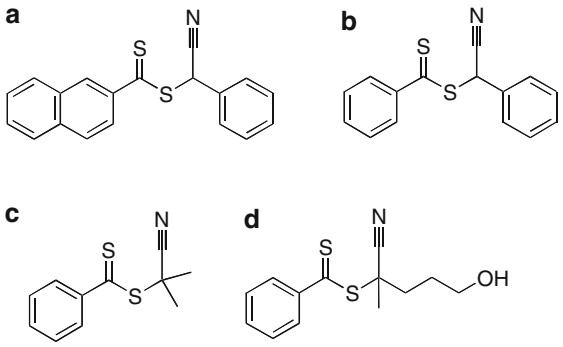

Fig. 9.29 RAFT agents

solution polymerization. Successful reinitiation and subsequent chain extension with MMA were possible. Facile removal of the RAFT terminal group from the final polymer products without loss of spherical morphology can be achieved.

By Atom Transfer Radical Polymerization (ATRP)

Holmes and coworkers reported the successful controlled polymerization of MMA in the presence of the catalytic chain transfer agents, 5,10,15,20 tetraphenylporphin atocobalt(II), A, and 5,10,15,20-tetra(pentafluorophenyl)porphinatocobalt(II) (COTFPP), B, in $scCO_2$ [104]. In solution radical polymerization, the process of using porphinatocobalt(II) complexes as chain transfer agents is now widely accepted. Low molecular weight PMMA with narrow PDI values have been prepared both at low and high monomer conversions, and the chain transfer constant was found to be 1.3×10^3, which can be compared to the value obtained in traditional solvents. The process is found to proceed by a catalytic chain transfer mechanism in $scCO_2$. Polymerization in the presence of the nonfluorinated 5,10,15,20-tet raphenylporphinatocobalt(II) afforded low molecular weight, monodisperse polymer at low conversion (M_n 3,300 g mol^{-1}, M_w/M_n 1.33). The partial insolubility of the cobalt macrocycle (A) in the binary monomer/$scCO_2$ mixture made Holmes et al. to explore for a CO_2-soluble catalyst analogue COTFPP B. Addition of the complex A afforded low molecular weight PMMA of narrow polydispersity. The use of the fluorinated catalyst B avoided complications in kinetic measurements resulting from partial insolubility. Figure 9.30 represents the usage of COTFPP B as chain transfer agents in solution radical polymerization.

Some more references on the dispersion polymerization of MMA in $scCO_2$ includes control of MWD by adjusting particle surface area [105], parametric analysis with reaction calorimetry [106], microscopic spacial effects [107], and particle encapsulation with polymers [108].

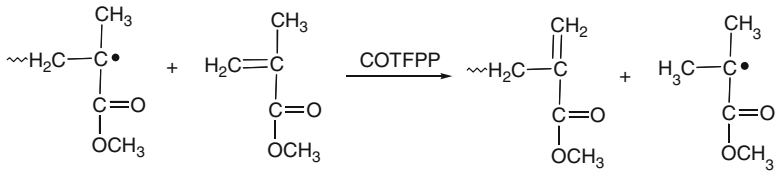

Fig. 9.30 Use of COTFPP as chain transfer agent

9.1.4 Fluorous Media

Fluorous chemistry offers some attractive features in terms of green solvents. Even though the complete replacement of VOCs with fluorous media is difficult, the attempts are started. New developments in fluorous reaction media stand together with some other novel and traditional reaction media, such as ILs and $scCO_2$. Perfluorocarbons (PFCs) dissolve in gases such as oxygen and have the important property of being easily separable from their hydrocarbon analogues. Thus, PFCs are considered the solvents of choice for gas/liquid reactions, liquid/liquid biphasic separations, and the purification of products and catalysts [109]. Horvárth and Rábai coined the term "fluorous" by analogy with "aqueous phases" [110, 111]. Fluorous biphasic system (FBS) and fluorous triphasic system (FTS) can also be used to carry out easy phase separation of an organic product and recycling of a fluorinated catalyst. Fluorous media have a number of potentially interesting and useful properties. They are inert to radical and oxidizing conditions and do not react with nucleophiles or electrophiles. This general lack of reactivity is one of the keys to the successful utilization of fluorous media as common replacements for more conventional solvents. The other advantages of fluorous media include [3]:

- They are nonprotic and display neither strong Lewis acidity nor basicity.
- PFCs are immiscible with many organic solvents. This extends their use to biphasic systems and also to triphasic systems.
- Immiscible with many organic solvents made them very valuable for catalytic reactions, since the product can be extracted from the fluorous media using organic solvents, whereas the fluorous catalyst remains in the fluorous media and can be directly recycled and reused.
- The low viscosity made them as media of choice for smooth passive transport of reagents.
- Gases have good solubilities in fluorous solvents. In contrast, many organic materials have much lower solubility in fluorous media than in standard organic solvents. Hence, organic materials are easily separable from fluorous solvents.
- They are nontoxic, have zero ozone depletion potential, and have significantly low greenhouse potential. Hence, they are useful in green chemistry.

The disadvantages of fluorous media include its cost and low solubility with many organic materials, requirement of functionalized ligands for the reaction and nature of some volatile fluorous solvents.

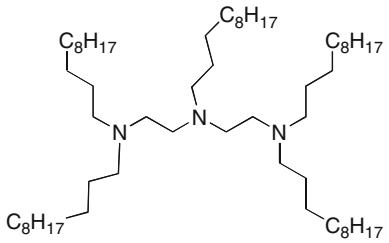

Fig. 9.31 Pentakis-*N*-(4,4,5,5,6,6,7,7,8,8,9,9,10,10,11, 11,11-heptadecafluoroundecyl)-1,4,7-triazaheptane

9.1.4.1 Polymerization in Fluorous Biphase System

Fluorous biphase chemistry has been developed as a liquid-liquid biphasic process whereby the two phases become miscible under the reaction conditions. This allows the facile separation of product from the catalyst under ambient conditions. This technique depends on catalysts, which are rendered soluble in fluorinated solvents by the use of fluorinated ligands whereby the electronic effects of the fluorine are isolated from the metal center. Haddleton and coworkers demonstrated the use of the fluorous biphase as a medium for atom transfer polymerization that would allow for the recovery of catalyst-free product and for reuse of catalyst [26]. The addition of pentakis-*N*-(4,4,5,5,6,6,7,7,8,8,9,9,10,10,11,11,11 heptadecafluoroundecyl)-1,4,7-triazaheptane to a suspension of $Cu^{I}Br$, at ambient temperature under nitrogen, in perfluoromethyl cyclohexane results in a dark green solution which is immiscible with an equivolume amount of toluene (Fig. 9.31). Addition of MMA (20% v/v) and ethyl 2-bromoisobutyrate as polymerization initiator results in efficient polymerization with 76% conversion to polymer in 300 min at 90°C, with $M_n = 11\ 100$ and a molar mass distribution of 1.30. The M_n increases linearly with conversion. After polymerization, the reaction was cooled to ambient temperature, and the two phases, a dark green lower layer and a colorless upper layer, exist. After separation of the upper hydrocarbon layer, fluorous layer was washed with toluene. PMMA was obtained as a colorless glassy solid after removal of volatiles.

9.1.4.2 Polymerization in Fluorous Triphase System

Li and coworkers carried out the first polymerization of MMA, initiated by benzoyl peroxide (BPO) and N,N[1]-dimethylaniline (DMA) which act as redox initiators at room temperature in fluorous triphasic system [112]. Fluorous medium which is not only immiscible but also generally heavier than most organic media acts as a phase screen between two organic layers plays an important role during the polymerization. MMA, BPO, and DMA have lower density than perfluorohexane (C_6F_{14}, FC-72). Li et al. [112] used a U tube to separate fluorous phase from upper organic phase. By this method, a fine white solid of PMMA was obtained in 15.2% conversion, with molecular weight (M_n) 685,400 and PDI 4.36 from the monomer layer, and 8.1% conversion, with molecular weight (M_n) 24,580 and PDI 1.38 from the

initiator layer, respectively. The results showed that the migration of initiators and monomer was bidirectional because PMMA was formed from both sides. In the monomer layer, the molecular weight and polydispersities are much more broad due to lower radical concentration and higher monomer concentration. After adding the initiator layer, the molecular weight and polydispersities became low because of higher radical concentration and lower monomer concentration. PMMA with narrow molecular weight distribution was obtained in this fluorous triphasic system when compared with conventional radical polymerization.

9.1.4.3 Polymerization in Hydrofluorocarbon (HFC) Fluids

Hydrofluorocarbon (HFC) fluids such as difluoromethane (HFC 32) and 1,1,1,2 tetrafluoroethane (HFC 134a) are relatively polar solvents, even in the sc state. This allows them to be used as efficient extraction solvents either on their own or in conjunction with CO_2. Furthermore, these solvents are also readily available and nontoxic. They have easily accessible critical constants (HFC 134a $T_c = 101.1°C$; $p_c = 40.6$ bar and HFC 32 $T_c = 78.1°C$; $p_c = 57.8$ bar) and gaseous dipole moments of about 2 D. These HFC fluids properties are somewhat similar to those of $scCO_2$. For example, the majority of common vinyl monomers are soluble (at least up to 20–50% v/v) in HFC fluids at and above room temperature. Similarly, most hydrocarbon polymers exhibit very low solubility in the HFC fluids under moderate conditions ($T < 100°C$, $P < 50$ bar) when the molecular weight is higher than a few thousand mass units. These HFC fluids have broad potential as solvents for precipitation polymerization or dispersion polymerization. An important difference between HFC fluids and CO_2 is solvent polarity. CO_2 is symmetrical and has no dipole moment, whereas HFC fluids are moderately polar and have a significant dipole moment. HFC fluids contain hydrogen atoms that could participate in chain transfer reactions in free radical polymerization. Unlike CO_2, HFC fluids in contact with water do not form significantly acidic environments.

Cooper and coworkers carried out first dispersion polymerization on MMA using HFC 134a as a solvent for the synthesis of cross-linked polymer microspheres. Polymerizations were carried out at moderate pressures (15–40 bar) and temperature range of 60–90°C [113]. Free radical polymerization of MMA and TRIM produced cross-linked powders in good yields by precipitation polymerization in the absence of any stabilizer. The reaction was repeated in the presence of a monofunctional perfluoropolyether (PFPE) carboxylic acid stabilizer. Uniform white latex was observed in the presence of the PFPE stabilizer, and discrete polymer microspheres were produced in good yield. The latex was observed to be stable although some particle precipitation was observed after few hours. The attempts to polymerize MMA by these routes have resulted in relatively low yields (30–90%) and modest molecular weights (M_n 30,000–270,000 g/mol). In comparison with results obtained using $scCO_2$, there appears to be a reduction in activity for the PFPE acid-terminated steric stabilizers.

Abbott and coworkers carried out the polymerization of MMA using supercritical difluoromethane (scHFC 32) as a solvent for the first time and AIBN as the initiator. In scHFC 32, at reaction temperature and pressure, the supercritical solution of monomer and initiator exhibited a single phase, which was milky in appearance (due to critical opalescence) showing that all of the monomer is soluble and polymerization begins as a homogeneous process [114]. As polymerization proceeded, the solution gets darkened and appears black to transmitted light. When the reaction proceeded further, the solution became paler and was transparent in most cases after approximately 30 min to 1 h. Attenuation of optical transmission with increasing solute concentrations is common for scHFCs, since colloidal light scattering is enhanced. The appreciably higher molecular weight polymer can be obtained using scHFC 32 than $scCO_2$ due to the higher solubility of the polymer in the more polar fluid. In scHFC 32, the polymer mass will get soluble up to molecular weight 11,000 g, whereas in $scCO_2$ the polymer of this mass was almost totally insoluble. Due to large changes in solvent polarity around the critical temperature, it is believed that the polarizability of certain monomers will allow greater control on structure and properties and hence on synthesis of polymer than with $scCO_2$.

9.2 Conclusions

A wide range of polymeric reactions have been studied in green alternative solvents such as RTILs, $scCO_2$, and fluorous media. In terms of volatility, the most volatile $scCO_2$ to the least volatile polymeric and ionic liquid solvents can be used, whereas in terms of polarity, nonpolar fluorous media can be used. In addition to reducing the need for toxic volatile organic solvents, these green solvents allow the synthesis of PMMA with well-defined structures and properties. The application of these green solvents in the synthesis of PMMA and processing has shown rapid development over the last 10 years, and many of the fundamental principles underlying these techniques are now much more fully understood. This is evidenced by the increasing number of papers published in this area every year and also from interesting and important discoveries. Even within the small numbers of studies conducted to date, potentially dramatic effects and startling differences have been seen between reactions in green solvents and molecular solvents. A significant amount of research has shown that these green solvents will have a major impact on many industries in the twenty-first century. The numerous examples presented on the synthesis of PMMA in this chapter demonstrate that these green solvents are rapidly becoming viable alternative solvents for polymerizations. It seems that further progress in the field of green solvents can be achieved by careful selection of studied systems in which its application may either offer real synthetic advantage or provide new insight into polymerization mechanisms rather than by showing just other examples of processes that may be conducted. The application of green chemistry is still at a younger stage, and, hence, even more avenues are open for new, greener discoveries.

References

1. Kerton FM (2009) Alternative solvents for green chemistry. Royal Society of chemistry, Cambridge; Adams DJ, Dyson PJ, Taverner SJ (2004) Chemistry in alternative reaction media. Wiley, Chichester
2. Anastas PT, Warner JC (1998) Green chemistry: theory and practice. Oxford University Press, New York; Clark JH, Macquarrie DJ (2002) Handbook of green chemistry and technology. Blackwell, London; Lancaster M (2002) Green chemistry: an introductory text. Royal Society of Chemistry, Cambridge
3. Mikami K (2005) Green reaction media in organic synthesis. Wiley-Blackwell, Oxford
4. Nelson WM (2003) Green solvents for chemistry: perspective and practice. Oxford University Press, Oxford
5. Clarke D, Ali MA, Clifford AA et al (2004) Reactions in unusual media. Curr Top Med Chem 4:729
6. Sheldon RA (2005) Green solvents for sustainable organic synthesis: state of the art. Green Chem 7:267
7. Clark JH, Tavener SJ (2007) Alternative solvents: shades of green. Org Process Res Dev 11:149
8. Seddon KR (1997) Ionic liquids for clean technology. J Chem Technol Biotechnol 68:351–356
9. Earle MJ, Seddon KR (2000) Ionic liquids. Green solvents for the future. Pure Appl Chem 72:1391–1398
10. Seddon KR, Stark A, Torres MJ (2000) Influence of chloride, water and organic solvents on the physical properties of ionic liquids. Pure Appl Chem 72:2275–2287
11. Marsh KN, Deev A, Wu ACT et al (2002) Room temperature ionic liquids as replacements for conventional solvents – a review. Korean J Chem Eng 19:357–362
12. Rakita PE (2003) Challenges to the commercial production of ionic liquids. In: Rogers RD, Seddon KR (eds) Ionic liquids as green solvents: progress and prospectsmer. American Chemical Society, Washington, DC
13. Mark HF (2005) Encyclopedia of polymer science and technology. Wiley, Chichester
14. Parvulescu VI, Hardacre C (2007) Catalysis in ionic liquids. Chem Rev 107:2615–2665
15. Welton T (1999) Room temperature ionic liquids. Solvents for synthesis and catalysis. Chem Rev 99:2071–2083
16. Carmichael AJ, Haddleton DM (2003) Polymer synthesis in ionic liquids. In: Wasserscheid P, Welton T (eds) Ionic liquids in synthesis. Wiley, VCH, Weinheim
17. Kubisa P (2004) Application of ionic liquids as solvents for polymerization processes. Prog Polym Sci 29:3–12
18. Kubisa P (2005) Ionic liquids in the synthesis and modification of polymers. J Polym Sci A Polym Chem 43:4675–4683
19. Kubisa P (2009) Ionic liquids as solvents for polymerization processes—progress and challenges. Prog Polym Sci 34:1333–1347
20. Liu J, Yan F, Fexter J (2009) Advanced applications of ionic liquids in polymer science. Prog Polym Sci 34:431–448
21. Bamford CH (1985) Encyclopedia of polymer science and engineering, vol 13. Wiley, New York, pp 708–867
22. Hong K, Zhang H, Mays JW et al (2002) Conventional free radical polymerization in room temperature ionic liquids: a green approach to commodity polymers with practical advantages. Chem Commun 13:1368–1369
23. Benton MG, Brazel CS (2004) An investigation into the degree and rate of polymerization of poly(methyl methacrylate) in the ionic liquid 1-butyl-3-methylimidazolium hexafluorophosphate. Polym Int 53:1113–1117
24. Sanchez CG, Wiesbrock F, Schubert US (2005) Polymer synthesis in ionic liquids: free radical polymerisation in water soluble systems. In: Brazel CS, Rogers RD (eds) Ionic liquids in polymer systems. American Chemical Society, Washington, DC

25. Sanchez G, Lober C, Hoogenboom M (2007) Microwave assisted homogenous polymerizations in water soluble ionic liquids: an alternative and green approach for polymer synthesis. Macromol Rap Commun 28:456–464
26. Haddleton DM, Jackson SG, Bon SAF (2000) Copper(I)-mediated living radical polymerization under fluorous biphasic conditions. J Am Chem Soc 122:1542–1543
27. Haddleton DM, Crossman MC, Dana BH et al (1999) Atom transfer polymerization of methyl methacrylate mediated by alkylpyridylmethanimine type ligands, copper(I)bromide and alkyl halides in hydrocarbon solution. Macromolecules 32:2110–2119
28. Sarbu T, Matyjaszewski K (2001) ATRP of methyl methacrylate in the presence of ionic liquids with ferrous and cuprous anions. Macromol Chem Phys 202:3379–3391
29. Ding S, Radosz M, Shen Y (2005) Ionic liquid catalyst for biphasic atom transfer radical polymerization of methyl methacrylate. Macromolecules 38:5921–5928
30. Lai GQ, Ma FM, Hu ZQ et al (2007) Novel ionic liquids as reaction medium for atom transfer radical polymerization of methyl methacrylate. Chin Chem Lett 18:601–604
31. Haddleton DM, Heming AM, Kukulj D et al (1998) Atom transfer polymerization of methylmethacrylate. Effect of acids and effect with 2-bromo-2-methylpropionic acid initiation. Macromolecules 31:2016–2018
32. Xiao G, Zhang H, Hong X et al (2008) Atom transfer radical polymerization of methyl methacrylate in a novel ionic liquid and recycling of the catalyst. J Appl Polym Sci 108:3683–3689
33. Wang JS, Matyjaszewski K (1995) "Living"/controlled radical polymerization. Transition-metal-catalysed atom transfer radical polymerization in the presence of a conventional radical initiator. Macromolecules 28:7572–7573
34. Ma H, Wan X, Chen X et al (2003) Reverse atom transfer radical polymerization of methyl methacrylate in room-temperature ionic liquids. J Polym Sci Part A Polym Chem 41: 143–151
35. Branco LC, Rosa JN, Ramos JJM et al (2002) Preparation and characterization of new room temperature ionic liquids. Chem Eur J 8:3671–3676
36. Wan X, Ma H, Chen X et al (2003) Reverse atom transfer radical polymerization of methyl methacrylate in imidazolium ionic liquids. Polymer 44:5311–5316
37. Gong S, Ma H, Wan X (2006) Atom transfer radical polymerization of methyl methacrylate induced by an initiator derived from an ionic liquid. Polym Int 55:1420–1425
38. Ma HY, Wan X (2005) Reverse atom transfer radical polymerisation of methyl methacrylate in ionic liquids. In: Brazel CS, Rogers RD (eds) Ionic liquids in polymer systems. American chemical society, Washington, DC
39. Ma HY, Wan XH, Zhou QF (2003) The study on free radical polymerisation of methyl methacrylate in ionic liquids. PhD thesis, Library of Peking University
40. Ma HY, Wan XH, Chen XF et al (2003) Design and synthesis of novel chiral ionic liquids and its application in free radical polymerisation of methyl methacrylate. Chin J Poly Sci 21:265–270
41. Biedron T, Kubisa P (2003) Ionic liquids as reaction media for polymerisation processes: atom transfer radical polymerisation (ATRP) of acrylates in ionic liquids. Polym Int 52: 1584–1588
42. Zhang H, Hong K, Mays JW (2004) First report of nitroxide mediated polymerization in ionic liquid. Polym Bull 52:9–16
43. Perrier S, Davis TP, Carmichael AJ et al (2002) First report of reversible addition–fragmentation chain transfer (RAFT) polymerisation in room temperature ionic liquids. Chem Commun 19:2226–2227
44. Vijayaraghavan R, MacFarlane DR (2005) Group transfer polymerisation in hydrophobic ionic liquids. Chem Commun 9:1149–1151
45. Wu G, Liu Y, Long D (2005) Effects of ionic liquid $[Me3NC2H4OH]^{+}[ZnCl3]^{-}$ on γ-radiation polymerization of methyl methacrylate in ethanol and N, N-dimethylformamide. Macromol Rap Commun 26:57–61
46. Qi M, Wu G, Sha M et al (2008) Radiation induced polymerization of MMA in imidazolium ionic liquids and their mixed solutions with organic solvents. Rad Phys Chem 77: 1248–1252

47. Kokubo H, Watanabe M (2008) Anionic polymerization of methyl methacrylate in an ionic liquid. Polym Adv Technol 19:441–444
48. Yan F, Texter J (2006) Surfactant ionic liquid based microemulsions for polymerisation. Chem Commun 25:2696–2698
49. Scott MP, Rahman M, Brazel CS (2003) Application of ionic liquids as low-volatility plasticizers for PMMA. Eur Polym J 39:1947–1953
50. Nalawade SP, Picchioni F, Janssen LPB (2006) Supercritical carbon dioxide as a green solvent for processing polymer melts: processing aspects and applications. Prog Polym Sci 31:19–43
51. Darr JA, Poliakoff M (1999) New directions in inorganic and metal organic coordination chemistry in supercritical fluids. Chem Rev 99:495–542
52. McHugh MA, Krukonis VJ (1993) Supercritical fluid extraction: principles and practice. Buttenvorth-Heineman, Stoneham
53. Kendall JL, Canelas DA, Young JL et al (1999) Polymerizations in supercritical carbon dioxide. Chem Rev 99:543–564
54. Cooper AI (2000) Synthesis and processing of polymers using supercritical carbon dioxide. J Mater Chem 10:207–234
55. Tomasko DL, Li H, Liu D et al (2003) A review of CO_2 applications in the processing of polymers. Ind Eng Chem Res 42:6431–6456
56. Baiker A (1999) Supercritical fluids in heterogeneous catalysis. Chem Rev 99:453–474
57. Clifford AA (1998) Fundamentals of supercritical fluids. Oxford University Press, Oxford
58. Cooper AI (2003) Porous materials and supercritical fluids. Adv Mater 15:1049–1059
59. Wells SL, DeSimone JM (2001) CO_2 technology platform: an important tool for environmental problem solving. Angew Chem Int Ed 40:518–527
60. Young JL, DeSimone JM (2000) Frontiers in green chemistry utilizing carbon dioxide for polymer synthesis and applications. Pure Appl Chem 72:1357–1363
61. Ghosh S, Bhattacharjee C, Mukhopadhayay M (2005) Polymerisation in supercritical carbon dioxide: a review. Indian Chem Eng A 47:224–234
62. Jessop PG, Ikariya T, Noyori R (1999) Homogenous catalysis in supercritical fluids. Chem Rev 99:475–493
63. Leitner W (2002) Supercritical carbon dioxide as a green reaction medium for catalysis. Acc Chem Res 35:746–756
64. Oakes RS, Clifford AA, Rayner CM (2001) The use of supercritical fluids in synthetic organic chemistry. J Chem Soc Perkin Trans 1(98):917–941
65. Stewart IH, Derouane EG (1999) Catalytic reactions at super critical conditions. Curr Top Catal 2:17–38
66. Woods HM, Silva MMCG, Nouvel C et al (2004) Materials processing in supercritical carbon dioxide: surfactants, polymers and biomaterials. J Mater Chem 14:1663–1678
67. DeSimone JM, Maury EE, Menceloglu YZ et al (1994) Dispersion polymerizations in supercritical carbon dioxide. Science 265:356–359
68. Deniz S, Baran N, Dincer S et al (2005) Dispersion polymerization of methyl methacrylate in supercritical carbon dioxide using a silicone-containing fluoroacrylate stabilizer. Polym Int 54:1660–1668
69. Howdle SM, Christian P, Giles MR et al (2000) The wall effect: how metal/radical interactions can affect polymerisations in supercritical carbon dioxide. Polymer 41:1251
70. Barrett KE (1975) Dispersion polymerization in organic media. Wiley, London
71. Consani KA, Smith RD (1990) Observations on the solubility of surfactants and related molecules in carbon dioxide at 50°C. J Supercrit Fluid 3:51–65
72. Hsiao YL, DeSimone JM (1997) Dispersion polymerizations of methyl methacrylate in supercritical carbon dioxide: the influence of helium concentration on particle size and particle size distribution. J Poly Sci Part A Polym Chem 35:2009–2013
73. Hsiao YL, DeSimone JM et al (1995) Dispersion polymerization of methyl methacrylate stabilized with poly(1,1-dihydro perflooroctyl acrylate) in supercritical carbon dioxide. Macromolecules 28:8159–8166

74. Lee H, Bae W, Kim H (2002) PMMA dispersion polymerization in supercritical CO_2 using poly[perfluoroalkyl (meth) acrylate] stabilizer. Theory Appl Chem Eng 8:4974–4977
75. Shaffer KA, Jones TA, DeSimone JM et al (1996) Dispersion polymerizations in carbon dioxide using siloxane-based stabilizers. Macromolecules 29:2704–2706
76. Johnston KP, O'Neill ML, Yates MZ et al (1998) Dispersion polymerization in supercritical CO_2 with a siloxane-based macromonomer: 1. The particle growth regime. Macromolecules 31:2838–2847
77. Johnston KP, O'Neill ML, Yates MZ et al (1998) Dispersion polymerization in supercritical CO_2 with siloxane-based macromonomer. 2. The particle formation regime. Macromolecules 31:2848–2856
78. Howdle SM, Giles MR, Hay JN et al (2000) Macromonomer surfactants for the polymerisation of methyl methacrylate in supercritical CO_2. Polymer 41:6715–6721
79. Paine AJ (1990) Dispersion polymerization of styrene in polar solvents. 7. A simple mechanistic model to predict particle size. Macromolecules 23:3109–3117
80. Wang W, Griffiths RMT, Howdle SM et al (2003) Monitoring dispersion polymerisations of methyl methacrylate in supercritical carbon dioxide. Eur Polym J 39:423–428
81. Park JY, Shim JJ (2003) Emulsion stability of PMMA particles formed by dispersion polymerization of methyl methacrylate in supercritical carbon dioxide. J Supercrit Fluids 27: 297–307
82. Yates MZ, Li G, Johnston KP et al (1999) Ambidextrous surfactants for water-dispersible polymer powders from dispersion polymerization in supercritical CO_2. Macromolecules 32:1018–1026
83. Johnston KP, Li G, Yates MZ et al (2000) Trifunctional ambidextrous surfactants for latexes in supercritical CO_2 and water. Macromolecules 33:1606–1612
84. Johnston KP, Li G, Yates MZ (2000) In-situ investigation on the mechanism of dispersion polymerization in supercritical carbon dioxide. Macromolecules 33:4008–4014
85. Han SH, Park KK, Lee SH (2008) GMA-functionalized reactive stabilizer for polymerization of methyl ethacrylate in supercritical CO_2: effect of stabilizer, initiator and monomer concentrations. Macromol Res 16:120–127
86. Giles MR, Howdle SM (2001) New unsaturated surfactants for the dispersion polymerisation of methyl methacrylate in supercritical carbon dioxide. Eur Polym J 37:1347–1351
87. Christian P, Howdle SM, Irvine DJ (2000) Dispersion polymerization of methyl methacrylate in supercritical carbon dioxide with a monofunctional pseudo-graft stabilizer. Macromolecules 33:237–239
88. Giles MR, Griffiths RMT, Howdle SM (2001) Fluorinated graft stabilizers for polymerization in supercritical carbon dioxide: the effect of stabilizer architecture. Macromolecules 34: 20–25
89. Lepilleur C, Beckman EJ (1997) Dispersion polymerization of methyl methacrylate in supercritical CO_2. Macromolecules 30:745–756
90. Holmes AB, Hems WP, Yong TM et al (1999) Dispersion polymerisation of methyl methacrylate in supercritical carbon dioxide: evaluation of well defined fluorinated AB block copolymers as surfactants. J Mater Chem 9:1403–1407
91. Holmes AB, Yong TM, Hems WP et al (1999) Synthesis of fluorinated block copolymers and their application as novel polymerization surfactants in supercritical carbon dioxide. Chem Commun 18:1811–1812
92. Galia A, Pierro P, Filardo G (2004) Dispersion polymerization of methyl methacrylate in supercritical carbon dioxide stabilized with poly(ethylene glycol)-b-perfluoroalkyl compounds. J Supercrit Fluids 32:255–263
93. Ding L, Olesik SV (2003) Dispersion polymerization of MMA in supercritical CO_2 in the presence of copolymers of perfluorooctylethylene methacrylate and poly(propylene glycol) methacrylate. Macromolecules 36:4779–4785
94. Deniz S, Baran N, Akgun M et al (2005) Dispersion polymerization of methyl methacrylate in supercritical carbon dioxide using a silicone-containing fluoroacrylate stabilizer. Polym Int 54:1660–1668

95. Hwang HS, Gal YS, Lim KT et al (2006) Dispersion polymerization of methyl methacrylate in supercritical carbon dioxide in the presence of random copolymers. Macromol Rap Commun 27:121–125
96. Hwang HS, Yuvaraj H, Lim KT et al (2008) Dispersion polymerization of MMA in supercritical CO_2 stabilized by random copolymers of 1H,1H–perfluorooctyl methacrylate and 2-(Dimethylaminoethyl methacrylate). J Polym Sci Part A Polym Chem 46:1365–1375
97. Hwang HS, Lee WK, Lim KT et al (2007) Dispersion polymerization of MMA in supercritical CO2 in the presence of poly(poly(ethylene glycol) methacrylate-co-1H,1H,2H,2H-perfluorooctylmethacrylate). J Supercrit Fluids 39:409–415
98. Yuvaraj H, Hwang HS, Lim KT et al (2008) Dispersion polymerization of methyl methacrylate in supercritical CO_2 in the presence of non-fluorous random copolymers. Eur Polym J 44:2253–2261
99. Xia J, Johnson T, DeSimone JM et al (2009) Atom transfer radical polymerization in supercritical carbon dioxide. Macromolecules 32:4802–4805
100. Grignard B, Jerome C, Detrembleur C et al (2008) Dispersion atom transfer radical polymerization of vinyl monomers in supercritical carbon dioxide. Macromolecules 41:8575–8583
101. Grignard B, Jerome C, Jerome R et al (2008) Atom transfer radical polymerization of MMA with a macromolecular ligand in a fluorinated solvent and in supercritical carbon dioxide. Eur Polym J 44:861–871
102. Thurecht KJ, Gregory AM, Howdle SM et al (2007) "Living" polymer beads in supercritical CO_2. Macromolecules 40:2965–2967
103. Gregory AM, Thurecht KJ, Howdle SM (2008) Controlled dispersion polymerization of methyl methacrylate in supercritical carbon dioxide via RAFT. Macromolecules 41: 1215–1222
104. Holmes AB, Mang SA, Dokolas P (1999) Controlled polymerization of methyl methacrylate with porphinatocobalt(II) catalysts in supercritical carbon dioxide. Org Lett 1:125–127
105. Mueller PA, Storti G, Morbidelli M et al (2007) Dispersion polymerization of methyl methacrylate in supercritical carbon dioxide: control of molecular weight distribution by adjusting particle surface area. Macromol Symp 259:218–225
106. Mantelis CA, Barbey R, Meyer T et al (2007) Free-radical dispersion polymerization of methyl methacrylate in supercritical carbon dioxide: a parametric analysis with reaction calorimetry. Macromol React Eng 1:78–85
107. Yang J, Wang W, Howdle SM et al (2007) Microscopic spacial effect on the dispersion polymerization in $scCO_2$. Eur Polym J 43:663–667
108. Yuea B, Yang J, Huang CY et al (2004) Particle encapsulation with polymers via in situ polymerization in supercritical CO2. Powder Technol 146:32–45
109. Gladysz J, Curran DP, Horvath IT (2004) Handbook of fluorous chemistry. Wiley-VCH, Weinheim
110. Gladysz J (1994) Are teflon 'ponytails' the coming fashion for catalysts? Science 266: 55–56
111. Horvath IT, Rabai J (1994) Facile catalyst separation without water: fluorous biphase hydroformylation of olefins. Science 266:72–75
112. Chen SZ, Bai YP, Li ZL (2006) Redox polymerization of methyl methacrylate in the fluorous triphasic system. Chin Chem Lett 17:258–260
113. Wood CD, Senoo K, Cooper AI (2002) Polymer synthesis using hydrofluorocarbon solvents. 1. Synthesis of cross-linked polymers by dispersion polymerization in 1,1,1,2-tetrafluoroethane. Macromolecules 35:6743–6746
114. Abbott AP, Durling NE, Dyer PW et al (2004) Polymerization of methyl methacrylate in supercritical difluoromethane. Green Chem 6:81–83

Chapter 10
Use of Fatty Acids to Develop Green Polymers and Composites

Dipa Ray and Ershad Mistri

Abstract Most polymers, at present, are petroleum-based and do not degrade over many decades under normal environmental conditions. As a result, efforts toward developing environmental-friendly and biodegradable "green" polymers for various commercial applications have gained significant momentum in recent years. The current interest in the development of useful biodegradable polymeric materials has encouraged scientists and industrialists to use readily available renewable, inexpensive raw materials such as carbohydrates, lignin, starch, gums, chitosan, vegetable oils, and fatty acids. Vegetable oils, which are triglycerides of fatty acids, specially, the nonedible grade, are being investigated by the researchers extensively as a suitable alternative to petroleum oil. Fatty acids, when converted into polymers, give new materials with useful properties such as flexibility, hydrophobicity, and pliability. At the same time, degradation into naturally occurring compounds makes them highly environmental-friendly. Besides their renewable, environmental-friendly, and inexpensive nature, they are useful for various applications like wound dressing materials, drug delivery and implantable devices, in surface-coating industries, as high-damping structural material, etc. Fatty acid monomers are integrated into the polymeric chains by using various techniques. Most fatty acids are monofunctional in nature and act only as chain terminator during polymerization. This limitation has been overcome by dimerization of unsaturated fatty acids or by creating a functional group on the monomers. In future, such green materials may offer many new exciting applications. Development in the genetic sciences will have a great impact on the materials science area of fatty acid–based materials. Better characterization and

D. Ray (✉)
Department of Polymer Science & Technology, University of Calcutta,
92 A. P. C Road, Kolkata, West Bengal 700009, India
e-mail: roy.dipa@gmail.com

E. Mistri
School of Materials Science and Engineering, Bengal Engineering and Science University,
Shibpur, Howrah, West Bengal 711103, India
e-mail: ershadchem@gmail.com

A. Mohammad and Inamuddin (eds.), *Green Solvents I: Properties and Applications in Chemistry*, DOI 10.1007/978-94-007-1712-1_10,

fundamental studies on fatty acid–based polymers and composites will create new applications which could lead to replacement of many available synthetic polymers and other materials. They also comply with the emerging concept of sustainable development. In this chapter, the recent trends in converting fatty acids into green polymers and green composite materials have been summarized, while also providing insights to future trends.

10.1 Introduction to Green Polymers and Composites

Composites consist of two (or more) distinct constituents or phases, which when mixed together result in a material with entirely different properties from those of the individual components. Typically, a man-made composite would consist of a reinforcement phase of stiff, strong material, frequently fibrous in nature, embedded in a continuous matrix phase.

Green composites are completely bio-based composites where both matrix and fibers are biodegradable and renewable. Research efforts are currently being harnessed in developing a new class of fully biodegradable "green" composites by combining (natural/bio) fibers with biodegradable resins [1]. The major attractions about green composites are that they are environmental-friendly, fully degradable, and sustainable, that is, they are truly "green" in every way. At the end of their life cycle, they can be easily disposed of or composted without harming the environment (Fig. 10.1).

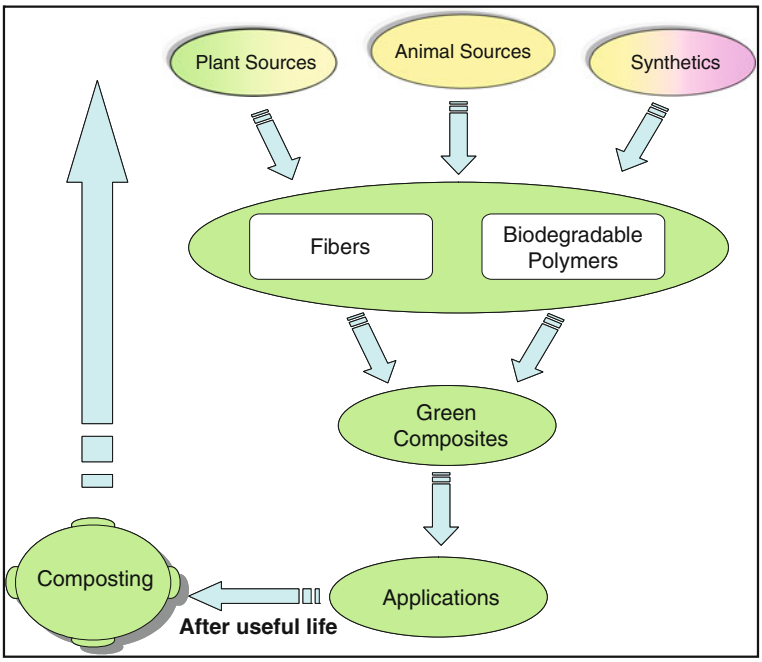

Fig. 10.1 Typical life cycle of green composites

Table 10.1 Biodegradable polymers

Natural	Carbohydrates like starch, cellulose, chitin
	Proteins like collagen, gelatin, casein, albumin, fibrogen, silks
	Polyesters like polyhydroxyalkanoates
	Other polymers like lignin, lipids, shellac, natural rubber
Synthetic	Poly (amides), poly (anhydrides), poly (amide-enamines), poly(vinyl alcohol), poly (vinyl acetate), polyesters like poly (glycolic acid), poly (lactic acid), poly (caprolactone), poly (orthoesters), poly (ethylene oxides), poly (phosphazines)

The design and life cycle assessment of green composites have been exclusively dealt with by Baillie [2]. Green composites have been used effectively in many applications such as mass-produced consumer products with short life cycles or products intended for one-time or short-time use before disposal. Green composites may also be used for indoor applications with a useful life of several years. The reinforcement of biofibers in green composites has been highlighted by Satyanarayana et al. [3]. A number of natural and biodegradable matrices that are available for use in such green composites [4] are listed in Table 10.1.

10.2 Fatty Acids

Fatty acids are monocarboxylic acids with a long unbranched aliphatic tails (hydrocarbon chain), which are either saturated or unsaturated. The hydrocarbon chain length may vary from 10 to 30 carbons, but in most common cases, it is 12–18 carbons. The sources of these fatty acids are mainly vegetable oils and fats. Generally, these are contained in esterified form in an animal/vegetable fat or vegetable oil, and these are produced by hydrolysis of the ester linkage (Fig. 10.2) in fat/biological oil, with the removal of glycerol.

Most of the fatty acids like stearic acid, palmitic acid, etc., are monofunctional and act as chain terminators in the polymerization process [5, 6]. Some fatty acids like erucic acid and oleic acid contain double bonds in their structure and, hence, can be converted to fatty acid dimer (FAD) or trimer (FAT) having two or three carboxylic groups, respectively, for further polymerization [7–9]. Ricinoleic acid (RA) is the only fatty acid which contains two functional groups, that is, one carboxylic and one hydroxyl group and is available commercially. The 12-hydroxy group of the RA can be transformed to a carboxylic group by esterification, and the modified polymer can be used for homogeneous polymerization.

Systematic names for fatty acids are too cumbersome for general use and shorter alternatives are widely used. Two numbers separated by a colon give, respectively, the chain length and number of double bonds: octadecenoic acid with 18 carbons and 1 double bond is therefore 18:1. The terms *cis* and *trans*, abbreviated c and t, are used widely for double-bond geometry.

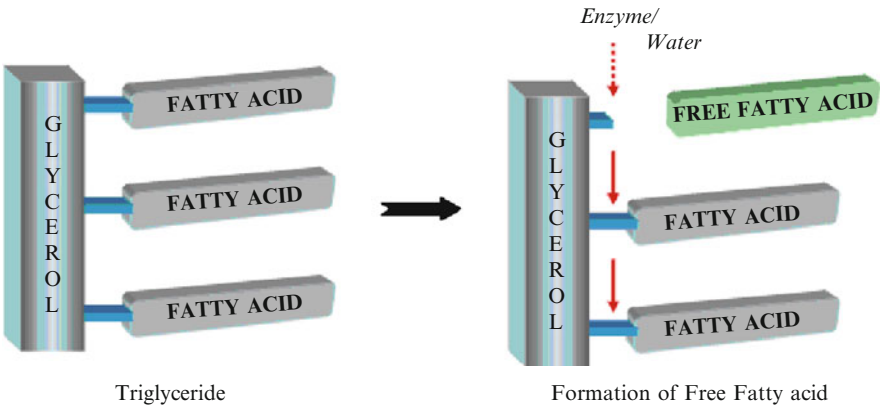

Fig. 10.2 Hydrolysis of the ester linkage

Table 10.2 Fatty acids in commodity oils and fats: nomenclature and structure

Name of fatty acid	Number of carbons present	Number of double bonds	Formula
Butyric	4	–	$CH_3(CH_2)_2COOH$
Caproic	6	–	$CH_3(CH_2)_4COOH$
Caprylic	8	–	$CH_3(CH_2)_6COOH$
Capric	10	–	$CH_3(CH_2)_8COOH$
Lauric	12	–	$CH_3(CH_2)_{10}COOH$
Myristic	14	–	$CH_3(CH_2)_{12}COOH$
Palmitic	16	–	$CH_3(CH_2)_{14}COOH$
Stearic	18	–	$CH_3(CH_2)_{16}COOH$
Oleic	18	1(9C)	$CH_3(CH_2)_7CH{=}CH(CH_2)_7COOH$
Linoleic	18	2(9C,12C)	$CH_3(CH_2)_4(CH{=}CHCH_2)_2(CH_2)_6COOH$
α-Linoleic	18	3(9C,12C,15C)	$CH_3CH_2(CH{=}CHCH_2)_3(CH_2)_6COOH$

Over 1,000 fatty acids are known, but 20 or less are encountered in significant amounts in the oils and fats of commercial importance (Table 10.2). The most common acids are C16 and C18. Below this range, they are characterized as short- or medium-chain and above it as long-chain acids.

Some of the fatty acids are saturated (Fig. 10.3a), and some of them are unsaturated (Fig. 10.3b). Saturated fatty acids have no double bonds, while unsaturated fatty acids have one or more than one double bond. If the double bonds in the carbon chain are separated by at least two carbon atoms, double bonds are called isolated (Fig. 10.3c). If single and double bonds alternate between certain carbon atoms, double bonds are called conjugated (Fig. 10.3d). Additionally, some natural fatty acids have different structures, with acid chains having hydroxyl, epoxy or oxo groups, or triple bonds.

(a) $-CH_2-CH_2-CH_2-CH_2-$
(b) $-CH_2-CH=CH-CH_2-$
(c) $-CH_2-CH=CH-CH_2-CH=CH-CH_2-$
(d) $-CH_2-CH=CH-CH=CH-CH_2-$

Fig. 10.3 Types of fatty acid chain: (**a**) saturated, (**b**) unsaturated, (**c**) isolated, and (**d**) conjugated (Reproduced from Ref. [1]. With kind permission of © Elsevier)

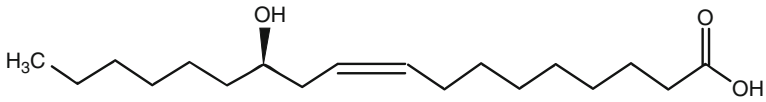

Fig. 10.4 Structure of ricinoleic acid

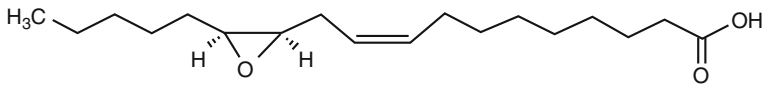

Fig. 10.5 Structure of vernolic acid

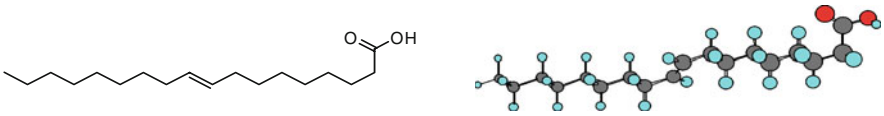

Fig. 10.6 Structure of *trans*-oleic acid

Fatty acids with *trans* or non-methylene-interrupted unsaturation occur naturally or are formed during processing; for example, vaccenic acid (18:1 11t) and the conjugated linoleic acid (CLA), rumenic acid (18:2 9t11c), are found in dairy fats. Hydroxy, epoxy, cyclopropane, cyclopropene acetylenic, and methyl-branched fatty acids are known, but only ricinoleic acid (Fig. 10.4) from castor oil is used for oleochemical production. Oils containing vernolic acid (Fig. 10.5) have potential for industrial use.

The basic structure of a fatty acid contains a hydrophobic hydrocarbon chain with a hydrophilic polar group at one end. Saturated fatty acids have a straight hydrocarbon chain. A *trans*-double bond is accommodated with little change in shape (Fig. 10.6), but a *cis* bond introduces a pronounced bend in the chain (Fig. 10.7).

Some physical properties of fatty acids are given in Table 10.3.

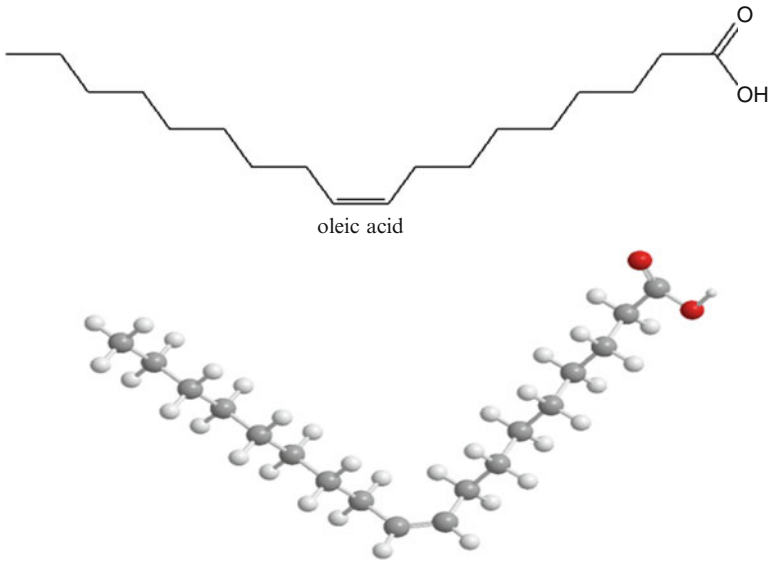

Fig. 10.7 Structure of *cis*-oleic acid

Table 10.3 Some physical properties of fatty acids (Reproduced from Ref. [1]. With kind permission of © Elsevier)

Name	Viscosity (cP, 110°C)	Density (g/cm^3, 80°C)	Melting point (°C)
Myristic acid	2.78	0.8439	54.4
Palmitic acid	3.47	0.8414	62.9
Stearic acid	4.24	0.8390	69.6
Oleic acid	3.41	0.850	16.3

Among saturated acids, odd-chain acids are lower melting than adjacent even-chain acids. The presence of *cis*-double bonds markedly lowers the melting point as the bent chains pack less well. Trans-acids have melting points much closer to those of the corresponding saturates. Polymorphism results in two or more solid phases with different melting points.

10.2.1 Vegetable Oils: A Major Source of Fatty Acids

The word "oil" is used for triglycerides that are liquid at ordinary temperatures. They are water-insoluble products of plants. A triglyceride is an ester product obtained from one molecule of glycerol and three molecules of fatty acids (Fig. 10.8). They can also be artificially produced from the reaction of glycerol and fatty acids (Fig. 10.9). The fatty acids contribute from 94% to 96% of the total weight of one molecule triglyceride oil.

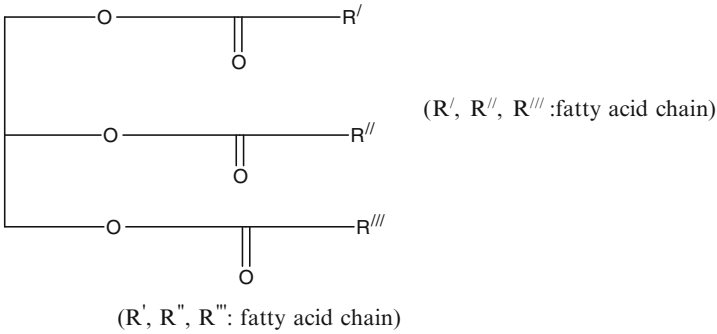

Fig. 10.8 A triglyceride molecule

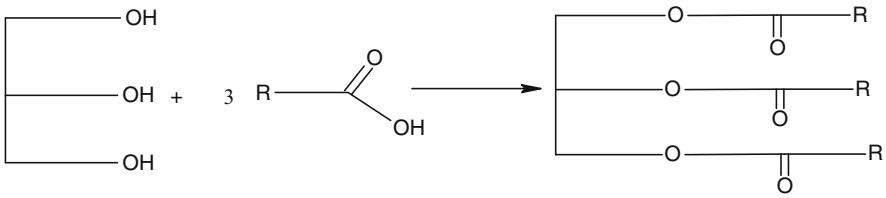

Fig. 10.9 Synthesis of triglyceride

Among the triglyceride oils, linseed, sunflower, castor, soybean, oiticica, palm, tall, and rapeseed oils are commonly used for synthesis of oil-modified polymers. Although fatty acid pattern varies between crops, growth conditions, seasons, and purification methods, each of triglyceride oils has special fatty acid distribution. Linseed oil, for example, consists of largely linoleic and linolenic acids. In castor oil, the greater part of fatty acids is ricinoleic acid (12-hydroxy-9-octadecenoic acid). Depending on the fatty acid distribution, each type of oil has specific physical and chemical properties [10, 11]. One of the most dominant parameters affecting the fatty acid and oil properties is the degree of unsaturation. The average degree of unsaturation is measured by iodine value. It is calculated from the amount of iodine (mg) reacted with double bonds for 100 g sample under specified conditions. Triglyceride oils are divided into three groups depending on their iodine values: drying, semidrying, and nondrying oils. The iodine value of a drying oil is higher than 130. This value is between 90 and 130 for semidrying oils. If the iodine value is smaller than 90, oil is called nondrying oil.

Since triglyceride oils vary widely in their physical properties depending on the structure of the fatty acids, hence the choice of triglyceride oil plays an important role on polymer properties. Linseed oil, for example, is commonly used for the preparation of paint binder because it consists of reactive unsaturated fatty acids capable of curing with atmospheric oxidation. Castor oil is an important reactant for interpenetrating polymer networks (IPNs) because it contains hydroxyl groups capable of reacting with isocyanate and carboxyl groups. It is possible to select fatty

acid distribution function of oils via computer simulation and the molecular connectivity in order to produce linear, branched, or cross-linked polymers [12]. Materials prepared by this way can be used to produce pressure-sensitive adhesives, elastomers, rubbers, and composites.

The most widely used method to characterize such materials is infrared spectroscopy, particularly Fourier transform infrared (FTIR) spectroscopy. It can also be used for the structural analysis of oils [13]. Nuclear magnetic resonance (NMR) spectroscopy is another important technique for the description of the chemical microstructure of an organic material. It is possible to calculate the fatty acid content of triglyceride oil from NMR data. Gas chromatography is also widely used for the determination of fatty acid composition of the oils.

10.3 Fatty Acid–Derived Polymers

Naturally occurring monofunctional fatty acids cannot be used for polymerization directly except as chain terminators in polymerization reaction. Only those fatty acids or modified fatty acids, which have two functional groups, can be considered for polymerization. Fatty acid–based polyanhydrides can be synthesized using melt-polycondensation (Fig. 10.10) [14]. Krasko et al. [14] modified the physical properties of poly(sebacic anhydride) by terminating with unsaturated fatty acids like ricinoleic acid, oleic acid, and linoleic acid which provided better stability and controlled molecular weight. The synthesis of fatty acid acetate anhydride followed by the formation of fatty acid symmetric anhydride is shown in Fig. 10.10. Polymers with molecular weights between 3,000 and 9,000 were obtained.

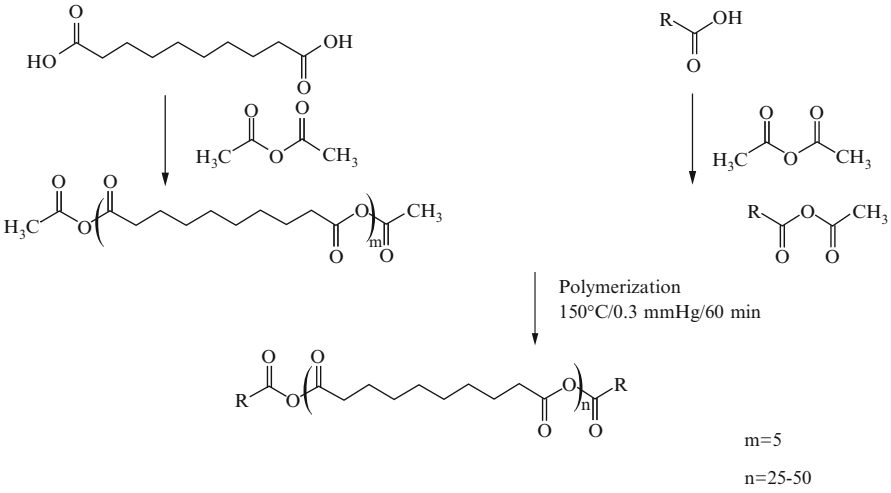

Fig. 10.10 Scheme for preparation of fatty acid–based polyanhydride by melt condensation (Reproduced from Ref. [14]. With kind permission of John Wiley & Sons)

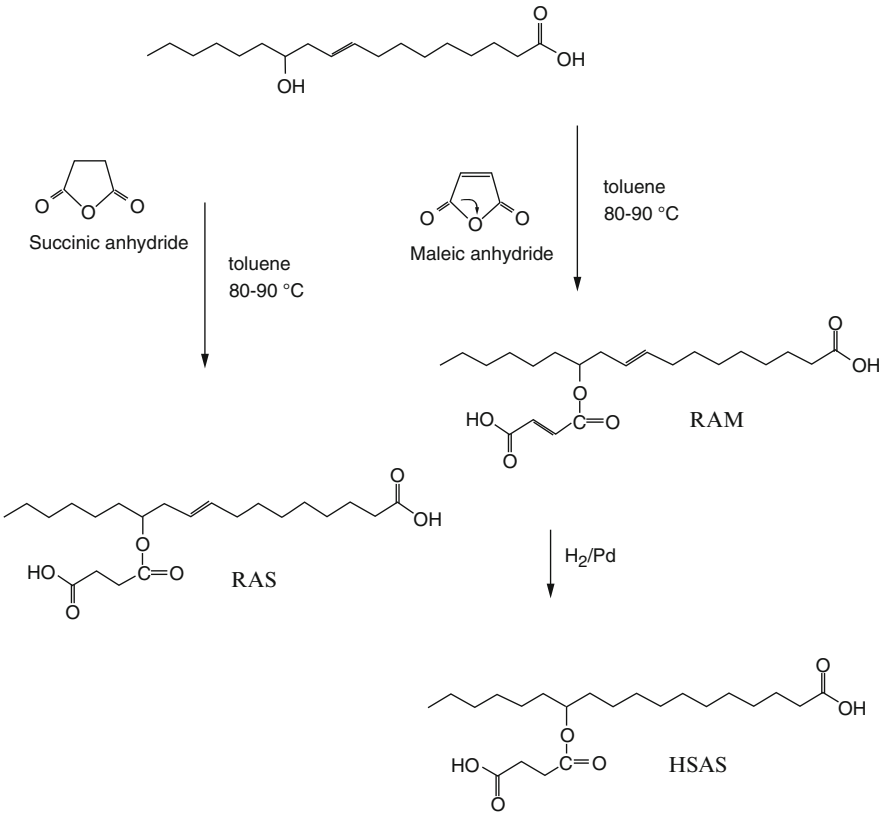

Fig. 10.11 Synthesis of ricinoleic acid (*RA*)–based polyanhydride (Reproduced from Ref. [15]. With kind permission of John Wiley & Sons)

Ricinoleic acid (RA), which has an additional 12-hydroxy group, was used by Teomim et al. [15] for synthesis of biopolymer. RA-based polymer was synthesized by two different schemes, one scheme involved the conversion of ricinoleic acid to dicarboxylic acid derivative by maleic anhydride (MA) or succinic anhydride (ScA) followed by usual melt-condensation method with ScA (Fig. 10.11) [15]. In a modified method to this, the prepolymer synthesis step was removed, and a direct polymerization of ricinoleic acid maleate and ScA was carried out. Dicarboxylic acid derivative of RA (RAM) and ScA were condensed at low temperature (65°C) to obtain a low molecular weight polymer for direct injection purpose. In the second scheme, RA was inserted into a preformed sebacic acid polymer chain (Fig. 10.12) [16].

A systematic study on the synthesis, characterization, and polymerization of ricinoleic acid (RA) lactone was reported by Slivniak et al. [17]. Ricinoleic acid lactones were synthesized by refluxing pure ricinoleic acid in chloroform with dicyclohexylcarbodimide and (dimethylamino) pyridine as catalyst. Various mono- to hexalactone macrolactones were prepared depending on the number of ricinoleic

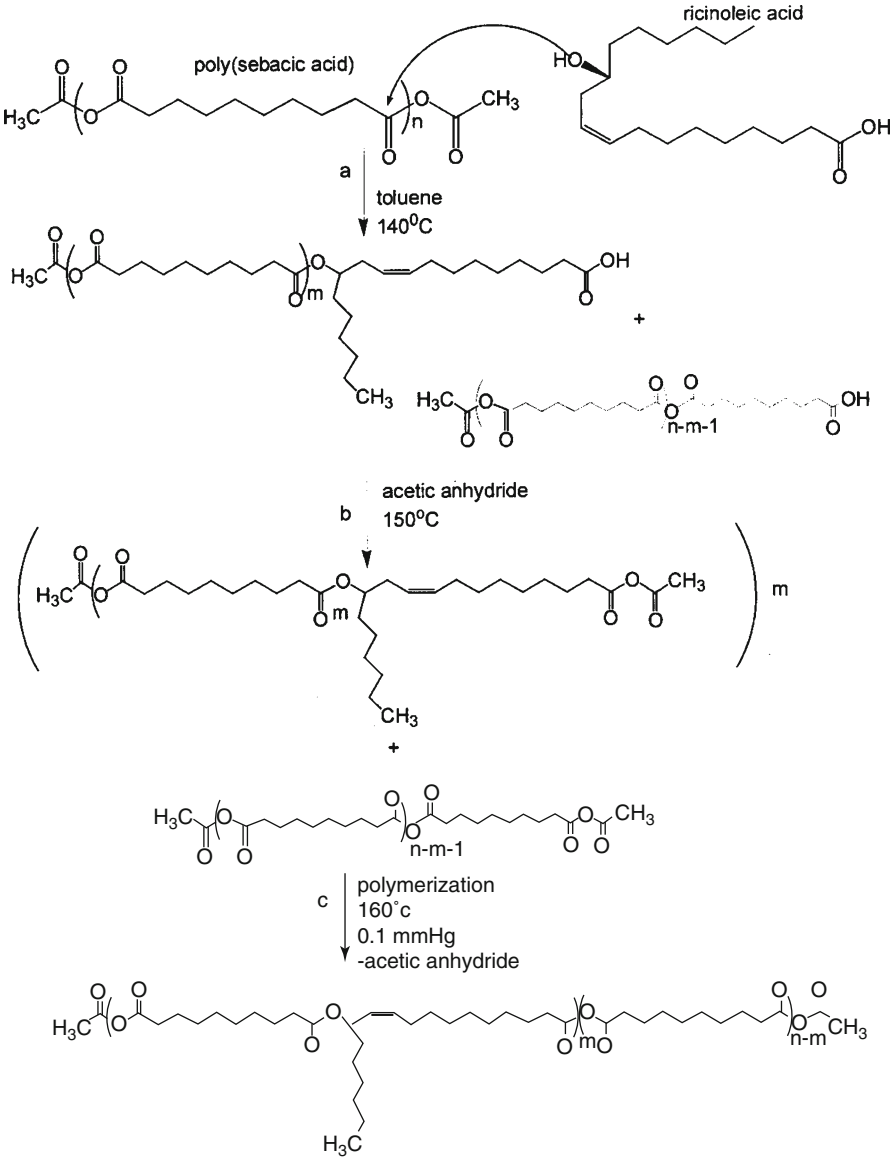

Fig. 10.12 Synthesis of poly(PSA–RA) from PSA and RA [RA – ricinoleic acid and PSA – poly(sebacic acid)] (Reproduced from Ref. [16]. With kind permission of John Wiley & Sons)

acid moiety which participated in the lactone ring formation (Fig. 10.13). The reaction resulted in a 75% yield of ricinoleic acid lactones. Polymerization of the ricinoleic acid lactones with catalysts commonly used for ring-opening polymerization of lactones, under specific reaction conditions, resulted in oligomers. Copolymerization

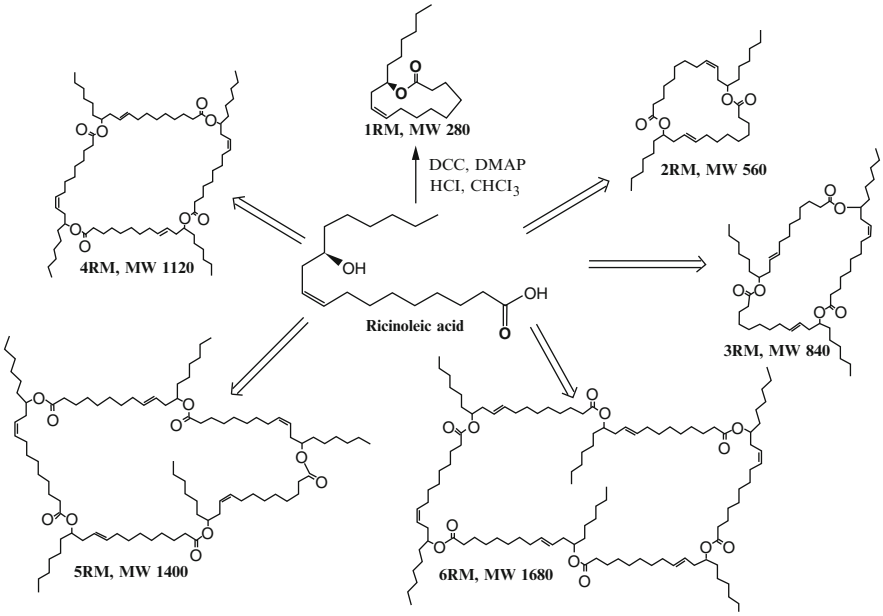

Fig. 10.13 Structures of macrolactones synthesized from ricinoleic acid. Abbreviations for cyclic macrolactones: *1RM*, monolactone; *2RM*, dilactone; *3RM*, trilactone; *4RM*, tetralactone; *5RM*, pentalactone; *6RM*, hexalactone (Reproduced from Ref. [17]. With kind permission of the American Chemical Society)

with lactide (LcA) by ring-opening polymerization, using Sn(Oct) as catalyst, yielded copolyesters with molecular weights (*M*w) in the range of 5,000–16,000 and melting temperatures of 100–130°C for copolymers containing 10–50% w/w ricinoleic acid residues. It was observed that the molecular weights of polymers were decreased with an increase in ricinoleic acid lactone. Thus, it was hypothesized that more reactive lactide activated first by a catalyst polymerized, and only in the end, some of the ricinoleic acid lactones reacted. In continuation of the above study, copolyesters were also synthesized by a transesterification procedure, in which stereocomplexes of P(LcA-RA)s 80:20 with different PLcA block lengths were synthesized by a two-step condensation, that is, transesterification and melt-condensation, to yield a liquid-viscous to viscous-semisolid product. Polymers were in a molecular weight range of 3,000–5,000. Stereocomplexes were prepared by spontaneous precipitation from acetonitrile solutions of the enantiomers [18].

A systemic study on the synthesis, characterization, degradation, and stability of nonlinear fatty acid–terminated poly(sebacic anhydride) (PSA) was reported by Teomim et al. [6]. Ricinoleic acid was transformed into a nonlinear fatty acid by esterification with fatty acid chlorides of C8–C18 chain length in the presence of pyridine. Poly(sebacic acid)s terminated with 30 wt% of various nonlinear fatty acids were synthesized by melt condensation to yield waxy off-white materials with molecular weights in the range of 5,000–9,000. The terminated polymers were

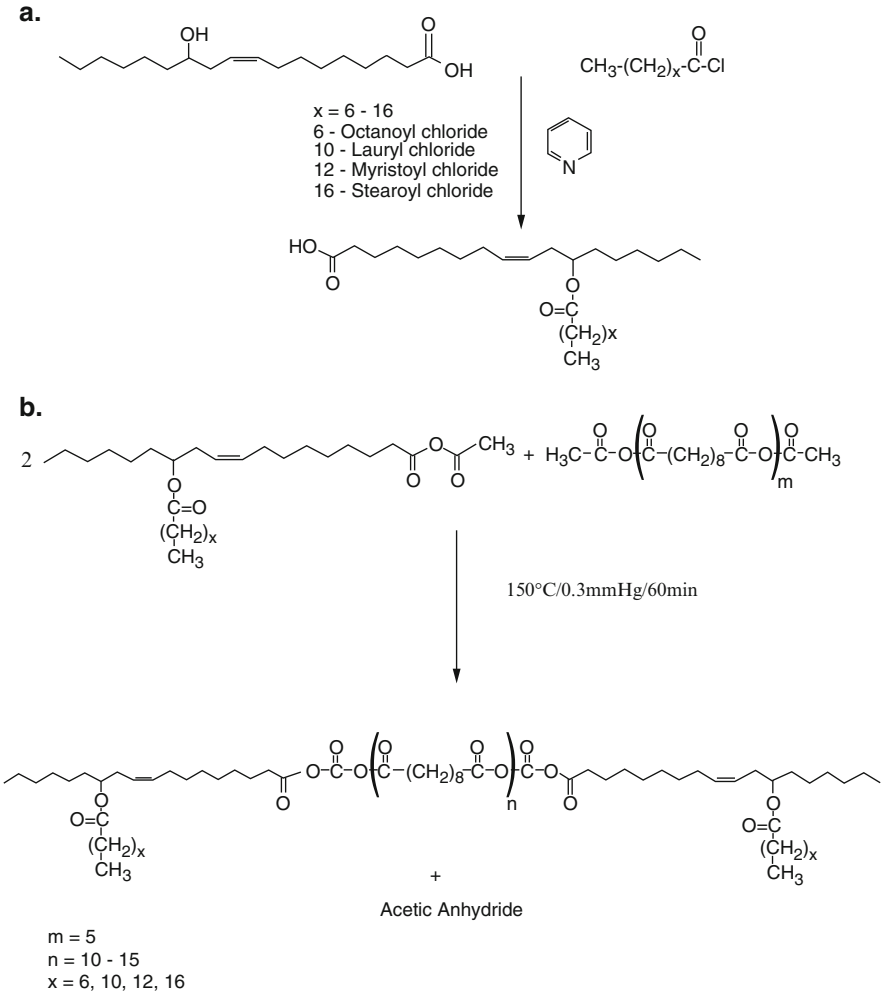

Fig. 10.14 Synthesis of (**a**) ricinoleic fatty acid ester, (**b**) nonlinear fatty acid–terminated poly(sebacic anhydride) (Reproduced from Ref. [6]. With kind permission of the American Chemical Society)

soluble in common organic solvents and melt at temperatures between 70°C and 79°C, which allowed their fabrication into microspheres and implants. The incorporation of nonlinear fatty acid terminals to poly(sebacic anhydride) increased the polymer hydrophobicity and decreased polymer crystallinity when compared to PSA or to linear fatty acid–terminated PSA (Fig. 10.14). The hydrophobic nonlinear side chains retarded water from penetrating into the polymer mass, which resulted in higher stability of the polymer.

10.4 Fatty Acid–Modified Polymers

Apart from such fatty acid–based polymers, many researchers have used fatty acid to modify the polymer structures. Both biopolymers and synthetic polymers were modified with various fatty acids in order to enhance properties and also replace a part or whole of the synthetic resin. Use of fatty acid as a constituent in polymer structure modification makes the polymer greener and more environmental-friendly.

Preeti Lodha et al. [19] studied thermal and mechanical properties of environmental-friendly "green" plastics from stearic acid–modified soy protein isolate (SPI). They attempted to reduce the moisture sensitivity and simultaneously improve the tensile properties SPI by incorporation of stearic acid without affecting its biodegradability. They determined the interaction mechanism between stearic acid and soy protein by various techniques like attenuated total reflectance-Fourier transform infrared (ATR-FTIR) spectroscopy, differential scanning calorimetry (DSC), thermogravimetric analysis (TGA), and X-ray diffraction (XRD) study. The tensile test results showed that Young's modulus increased on increasing the stearic acid content, reaching the maximum value at about 25% (by weight of SPI powder) stearic acid. Further increase in stearic acid content from 25% to 30% led to a reduction in Young's modulus (Table 10.4). The moisture content, fracture stress, strain, and energy at break decreased steadily on increasing the stearic acid from 0% to 30% for SPI containing 30% glycerol.

At 25% stearic acid content, the modulus and the fracture stress increased significantly, whereas the fracture strain, energy at break, and the moisture content decreased on reducing glycerol content. They also reported from thermogravimetric analysis that glycerol-plasticized SPI resin started to degrade at 250°C, whereas the stearic acid–modified SPI resin degraded above 275°C, shown in Fig. 10.15.

They determined the crystallinity of stearic acid and stearic acid–modified SPI by differential scanning calorimetric analysis. They reported that the stearic acid crystallinity was reduced from 100% to 24% in stearic acid–modified SPI resin (Fig. 10.16). The remaining 76% of the stearic acid was present in the amorphous form to plasticize the resin. SEM micrographs of the SPI resin showed that the

Table 10.4 Effect of stearic acid content on the tensile properties and moisture content of SPI with 30% (by weight of SPI powder) glycerol (Reproduced from Ref. [19]. With kind permission of © Elsevier)

Amount of stearic acid (%)	Young's modulus (MPa)	Fracture stress (MPa)	Fracture strain (%)	Energy at break (J)	Moisture content (%)
0	120.2 a	9.0 a	168.4 a	3.00 a	15.2 a
20	156.3 b	8.6 a	149.0 a	4.12 a	12.6 b
25	220.8 c	6.9 b	74.5 b	2.16 b	11.5 c
30	193.2 c	6.2 c	25.6 c	0.64 c	12.5 b

Means within a column with the same letter are not significantly different ($P < 0.05$) as determined using Fisher's LSD

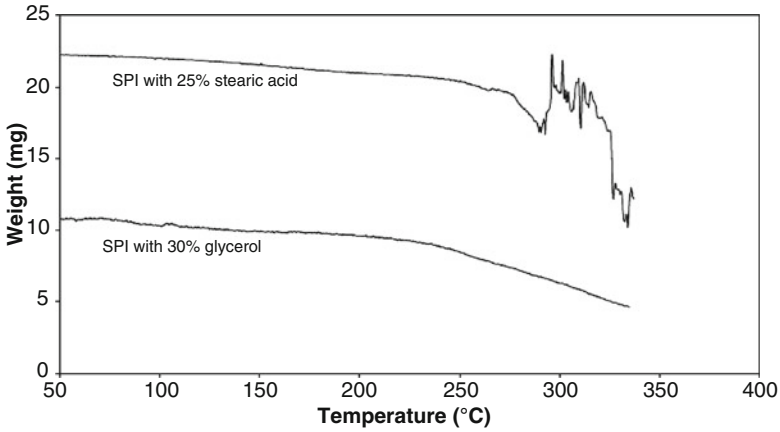

Fig. 10.15 TGA scans of SPI resin with 30% glycerol and SPI with 25% stearic acid (Reproduced from Ref. [19]. With kind permission of © Elsevier)

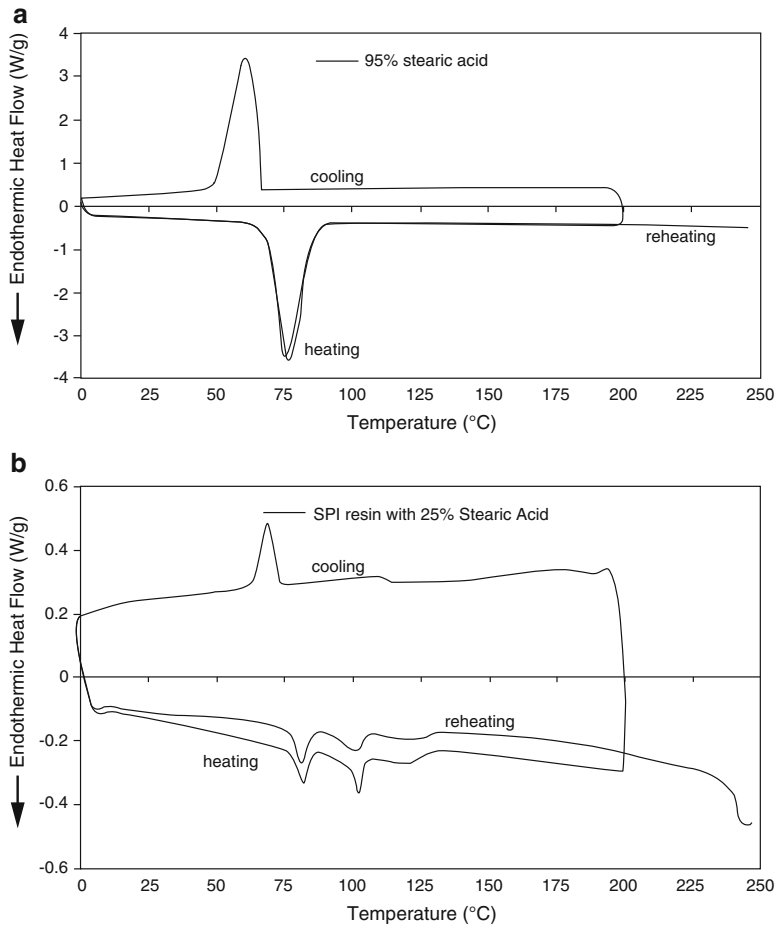

Fig. 10.16 DSC scan of (**a**) pure stearic acid, (**b**) stearic acid–modified SPI resin (Reproduced from Ref. [19]. With kind permission of © Elsevier)

presence of stearic acid resulted in a more ductile failure of the SPI resin in the presence and absence of glycerol and also lead to the formation of a layered structure in the resin, shown in Fig. 10.17.

Thus, they concluded that stearic acid–modified SPI showed better tensile and thermal properties as well as reduced moisture sensitivity without any processing problems.

Samuelsson and coworkers successfully synthesized and polymerized a radiation-curable hyperbranched resin based on epoxy functional fatty acids [20]. They synthesized a radiation-curable resin from a hydroxyl functional hyperbranched polyether onto which an epoxy functional fatty acid, vernolic acid, was attached. The resin was cationically polymerized in presence of different amounts of vernolic acid methyl esters as reactive diluent. They prepared coating mixtures containing up to 30 wt% methyl ester, and all formulations polymerized readily and formed cross-linked films with T_gs between 16°C and −18°C. The T_g decreased by nearly 10°C for each 10 wt% methyl ester added. The polymeric film based on TMP-trivernoleate had an even lower T_g than the film with 30 wt% methyl ester. The chemical structures of hyperbranched polyether of trimethylol propane (TMP) esterified with epoxy functional fatty acid (vernolic acid), reactive diluent TMP-trivernoleate, and methyl vernoleate are shown in Fig. 10.18.

The chemical composition of the coating mixtures, their T_g, viscosity, and universal hardness values are given in Table 10.5.

The addition of epoxy functional methyl ester also lowered the universal hardness of the polymerized films and dramatically lowered the viscosity of the coating mixtures, from 4,100 mPa of the pure poly-TMPO-vernoleate to 460 mPa s when 30 wt% diluent was added. The viscosities of the mixtures and the hardness of the films were also compared with a model oil based on trimethylol propane and vernolic acid, that is, a similar resin but without a polyether core. The TMP resin was found to have a lower viscosity than the other mixtures but also yielded a soft film with a low T_g (−21°C) after polymerization.

Fatty acid–based polyurethane films were prepared by Gultekin et al. for use as potential wound dressing material [21]. The polymerization reaction was carried out with or without catalyst. They first prepared the hydroxyl-containing component (HCC) from linoleic acid and glycerol, using a 2:1 mol ratio of linoleic acid and glycerol in the presence of xylene as a solvent. The reaction was carried out at 220°C with *p*-toluene sulfonic acid (0.1% by weight with respect to the weight of the mixture of linoleic acid and glycerol) as a catalyst. Reaction was monitored by determination of acid value of the reaction mixture. They prepared polyurethane by taking dried HCC and extra pure xylene in a reaction flask, heating it up to 40–50°C and adding an equivalent amount of toluene 2,4-diisocyanate (TDI) into the flask in a 30 min period. Calcium octoate was added as the catalyst to the reaction mixture in the amount of 0.02% (by weight) of HCC content for carrying out the catalyzed reaction. Then, the reaction flask was heated to 90°C, and reaction was carried out at this temperature under nitrogen atmosphere. The synthesis of polyurethane is shown in Fig. 10.19.

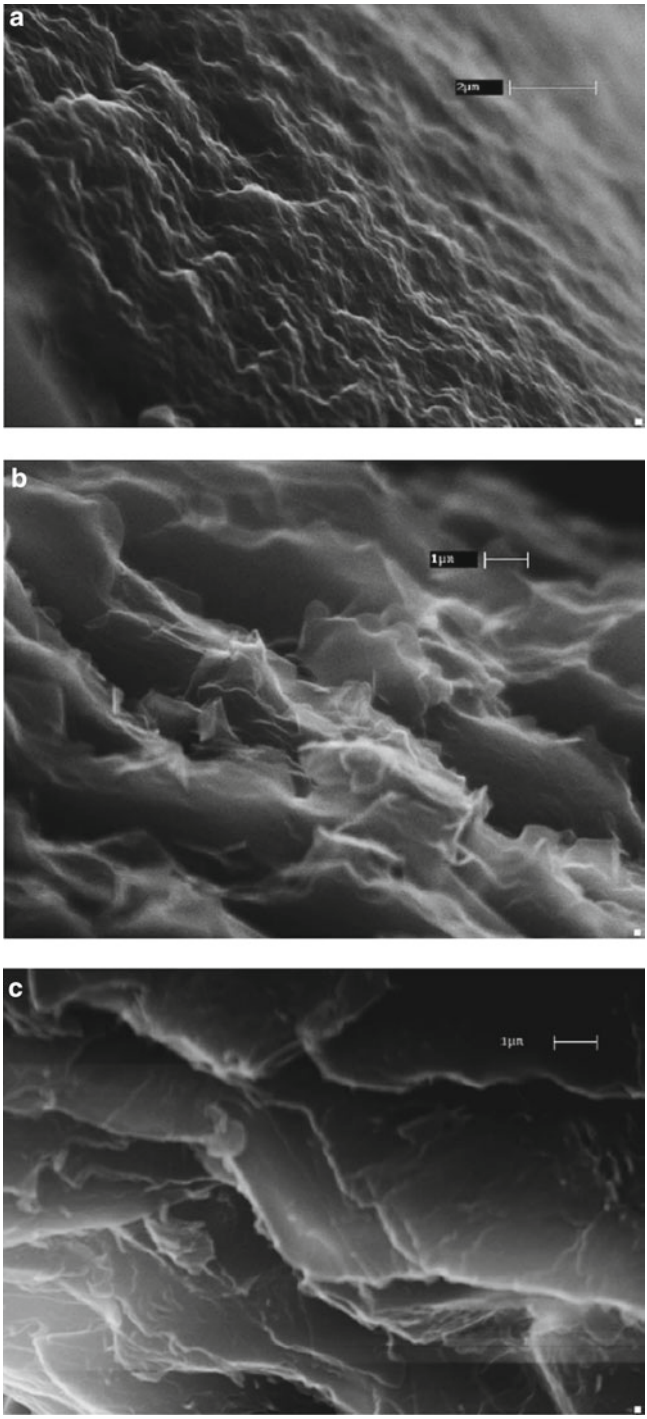

Fig. 10.17 SEM micrograph of the fractured surface of the SPI resin containing (**a**) 0% stearic acid and 30% glycerol, (**b**) 25% stearic acid and 30% glycerol, and (**c**) 25% stearic acid and 0% glycerol (Reproduced from Ref. [19]. With kind permission of © Elsevier)

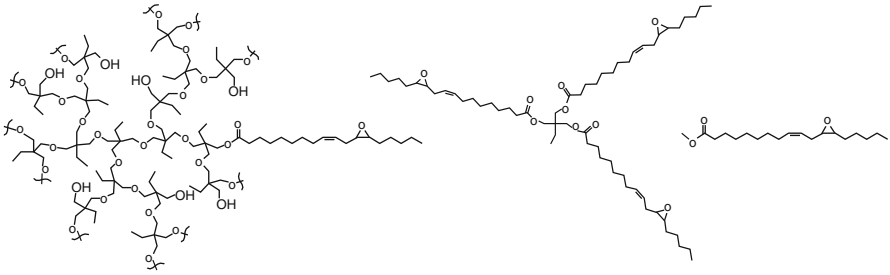

Fig. 10.18 Hyperbranched polyether of trimethylol propane (TMP) esterified with (**a**) epoxy functional fatty acid (vernolic acid), (**b**) reactive diluent TMP-trivernoleate, and (**c**) methyl vernoleate (Reproduced from Ref. [20]. With kind permission of © Elsevier)

Table 10.5 Composition of coating mixtures in wt%, their T_g, viscosity, and universal hardness (Reproduced from Ref. [20]. With kind permission from of © Elsevier)

Resin composition (%, w/w)					
Poly-TMPO-vernoleate	Methyl vernoleate	TMP-trivernoleate	T_g of cured films (°C)	Viscosity (mPa s)	Hardness (HU)
–	–	100	−21	150	3.55
100	–	–	16	4,080	8.11
90	10	–	4	1,760	4.11
80	20	–	−10	865	3.50
70	30	–	−18	460	3.10

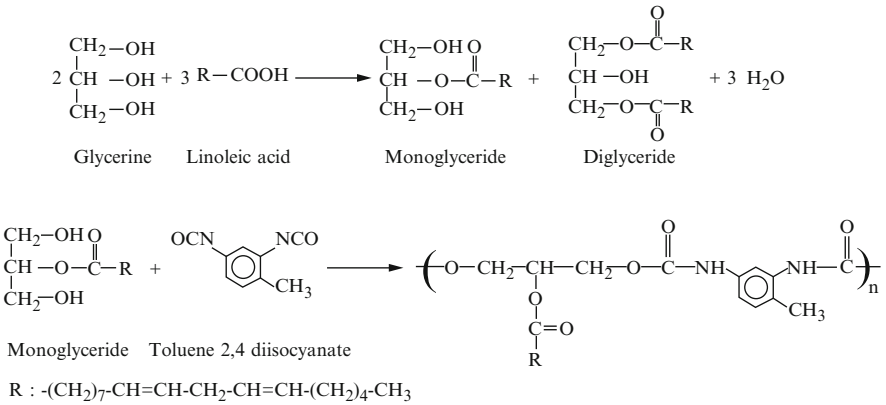

Fig. 10.19 Scheme for polyurethane synthesis from fatty acid (Reproduced from Ref. [21]. With kind permission of Springer)

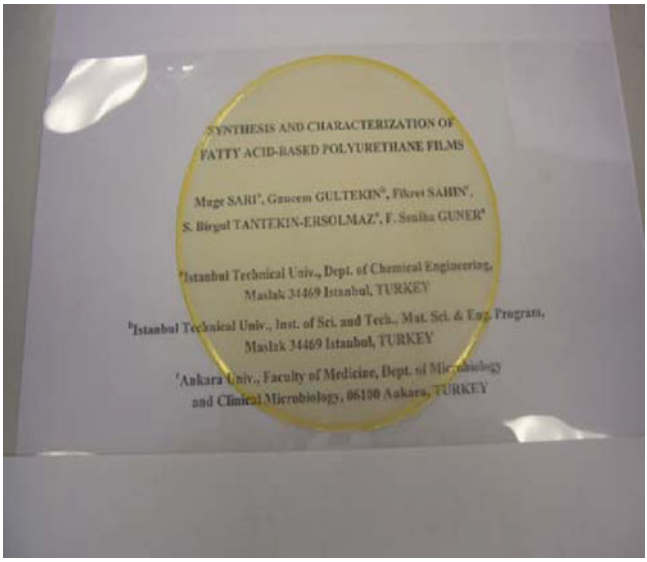

Fig. 10.20 Transparent dry polyurethane film (Reproduced from Ref. [21]. With kind permission of Springer)

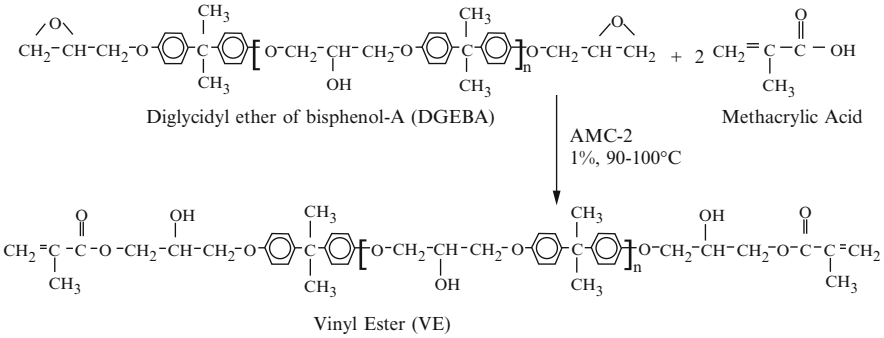

Fig. 10.21 The reaction of methacrylic acid with diglycidyl ether of bisphenol A (DGEBA) to form vinyl ester monomer (Reproduced from Ref. [22]. With kind permission of © Elsevier)

All the films were transparent and flexible (Fig. 10.20). The thermal, viscoelastic, mechanical, and surface properties of all polyurethane films were fairly good and appropriate for use as wound dressing material.

Scala et al. [22] reported one method of reducing styrene emissions from vinyl ester (VE) and unsaturated polyester resins (UPE). They replaced some or all of the styrene with fatty acid–based monomers. The chemical structure of vinyl ester resin is shown in Fig. 10.21.

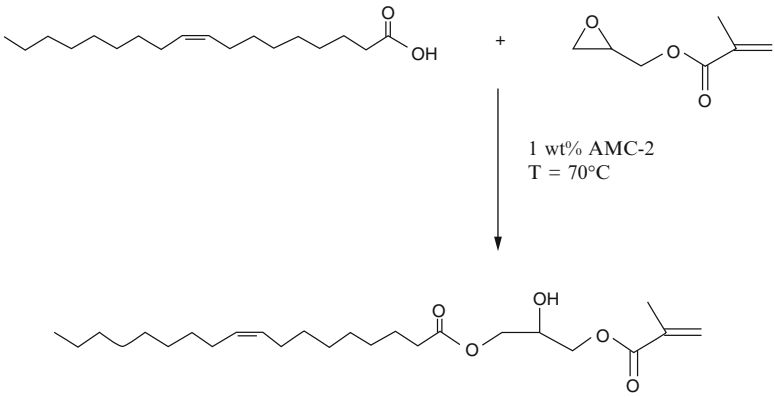

Fig. 10.22 The addition of fatty acids (oleic acid) to glycidyl methacrylate to form methacrylated fatty acid (*MFA*) monomer (Reproduced from Ref. [22]. With kind permission of © Elsevier)

Table 10.6 Variation of glass transition temperature (T_g) of styrene and fatty acid–based vinyl esters at room temperature [22]

Comonomer type	T_g (°C) with 35% comonomer	T_g (°C) with 45% comonomer
Styrene	147	142
Methacrylated lauric acid	79	71
Methacrylated oleic acid	76	75
Methacrylated linoleic acid	72	69

They suggested that methacrylated fatty acid (MFA) monomers are ideal candidates because they are inexpensive, have low volatilities, and free radically polymerize with vinyl ester. The carboxylic acid group of the fatty acid undergoes a simple addition reaction with the epoxide group of glycidyl methacrylate to form a single product (Fig. 10.22).

The stoichiometric quantities of the reactants were mixed together and reacted at 70°C for 2.5 h using 1% catalyst. Each MFA had one terminal polymerizable unsaturation site per molecule. In this way, the MFA acted as chain extenders, analogous to styrene. The viscosity of VE resins using these fatty acid monomers ranged from 700 to 2,000 cP, which is considerably higher than that of VE/styrene resins (nearly 100 cP). In addition, the T_g of VE/MFA polymers were only in the order of 80°C (Table 10.6), which was significantly lower than that of VE/styrene polymers. Decreasing the length of the base fatty acid chains from 18 to 12 carbon atoms, T_g improved by 20°C, while lowering the resin viscosity from 2,500 to 1,000 cP.

Residual unsaturation sites on the fatty acid backbone decreased the cure rate of the resins (Fig. 10.23), thereby decreasing polymer properties.

Ternary blends of VE, styrene, and fatty acid monomers also effectively improved the flexural, fracture, and thermomechanical properties and reduced the resin viscosity to acceptable levels, while using 15 wt% less styrene, far less than commercial VE resins.

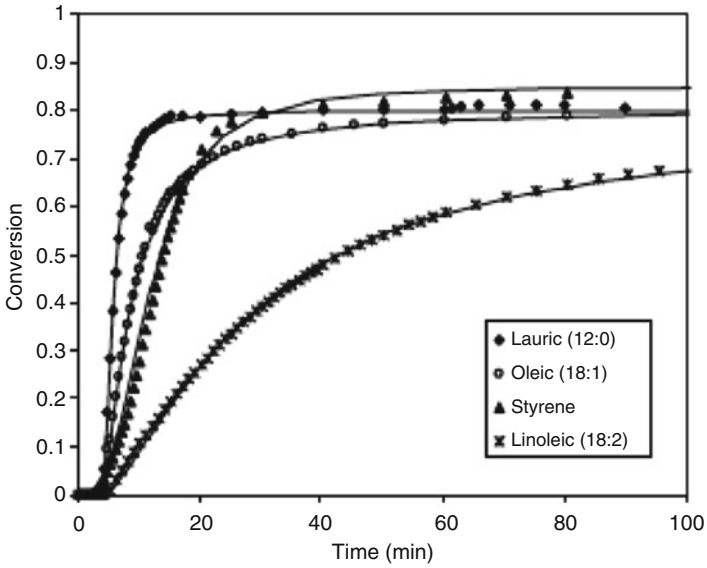

Fig. 10.23 The conversion as a function of time for the cure of VE/MFA relative to VE/styrene and their autocatalytic fits using 45% reactive diluents. Samples were cured at 90°C (Reproduced from Ref. [22]. With kind permission of © Elsevier)

A novel attempt was made to develop ambient-cured polyamine amide (PAA) resins by the condensation polymerization reaction of oil fatty amide diol (*N*,*N*-bis 2-hydroxy ethyl linseed oil fatty amide) (HELA) and *o*-phenylene diamine, which was further modified by poly(styrene-*co*-maleic anhydride) (SMA) at different phr (parts per hundred part of resin) to get a series of PAA–SMA resins [23]. The structural elucidation of HELA, PAA, and PAA–SMA were carried out by FT-IR, 1H-NMR, and 13C-NMR spectroscopic techniques. Thermal analyses of these resins were accomplished by thermogravimetric (TGA) and differential scanning calorimetry (DSC) techniques. They prepared coatings of PAA–SMA on mild steel strips to evaluate their physicomechanical and chemical/corrosion resistance performance under various corrosive environments. It was found that among the PAA–SMA systems, PAA-35 showed the best physicomechanical and corrosion resistance performance. Thermal studies revealed that the coatings can be safely used up to 305°C. The synthesis of PAA–SMA resin from linseed oil fatty acids provided a new way to utilize sustainable resource–based raw materials. PAA–SMA resin showed good alkali resistance as compared to reported polyesteramide coatings.

A series of high solid alkyd polymers from soya oil fatty acid (SOFA) and dehydrated castor oil fatty acid (DCOFA) combinations with varying percentage of dipentaerythritol (DPE, a hexafunctional polyol) were synthesized by Haseebuddin et al. [24] and characterized for their physicochemical, optical, thermal, and mechanical properties. For the study purpose, the polymers were prepared at 80% solids in mineral turpentine oil (MTO) keeping the oil length constant. The curing behavior of the alkyds was studied using FT-IR and DSC. AFM images of the coating films of alkyd 1 (0% DPE) and alkyd 9 (100% DPE) are shown in Fig. 10.24.

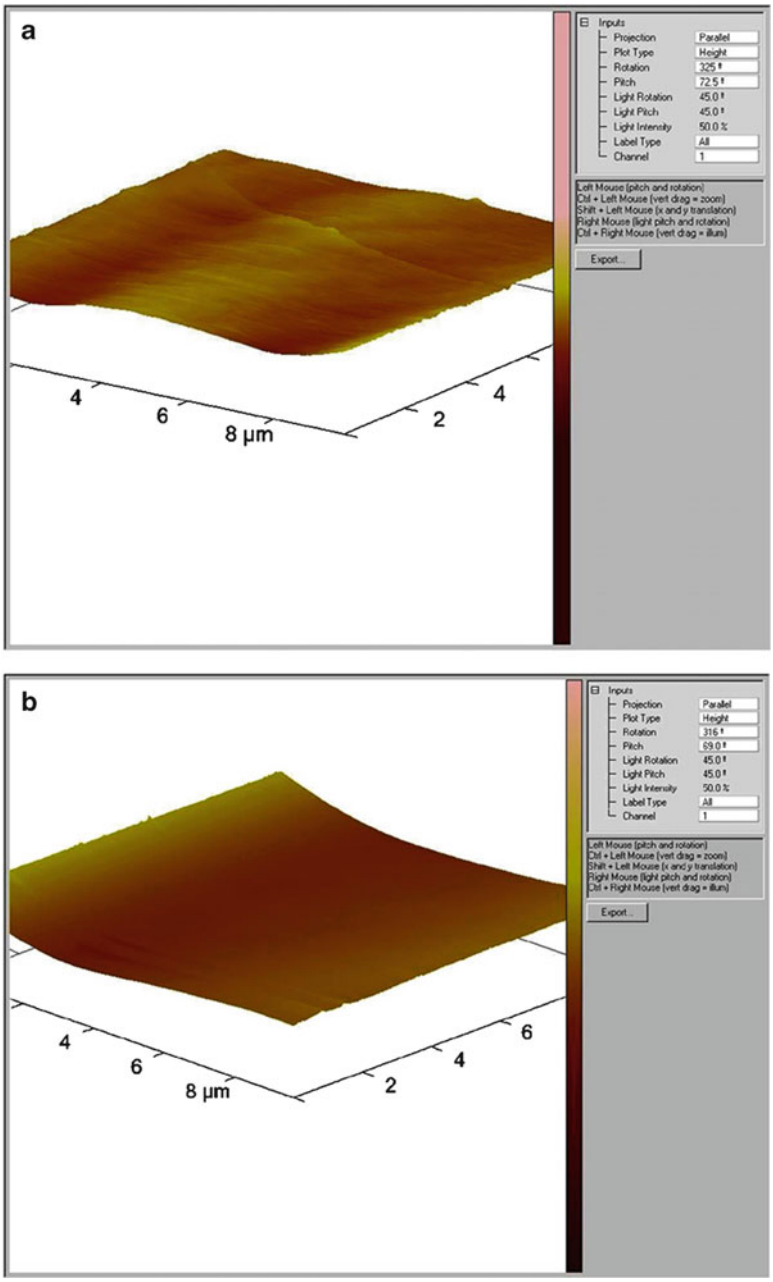

Fig. 10.24 Contact mode topography (*right*) AFM images of coating films of (**a**) alkyd 1 (0% DPE) and (**b**) alkyd 9 (100% DPE) [24] (Reproduced with permission from [25])

The difference in surface smoothness between alkyd 1 and alkyd 9 is clearly evident. Alkyd 1 (0% DPE) had a rough topography whereas alkyd 9 (100% DPE) appeared to have a comparatively smoother surface. This smoothness might be the reason for higher gloss of films of alkyd 9, which was in agreement with glossometer values. The increase in smoothness was due to better flow and leveling arising out of lower dilution viscosity of the polymers with increased DPE content.

10.5 Green Composites from Fatty Acids

Fatty acids are used nowadays as matrix for preparation of green composites. Hablot et al. [25] reinforced dimer fatty acid–based polyamides (DAPA) with cellulose fibers (CF) from 5 to 20 wt%. Dimers of fatty acids (DA), obtained by the polymerization of the C18-acids such as oleic and linoleic acids, are well known and commercially available products (Fig. 10.25). They exhibit two reactive functions per molecules and thus are good candidates to elaborate thermoplastic bio-based polyamides by polycondensation.

The polyamide (DAPA) was synthesized by condensation polymerization. The final acid-based thermoplastic polyamide (DAPA) was yellowish, transparent, and flexible at ambient temperature with a molecular weight of 14,000 g/mol, a glass transition temperature of −10°C, and a fusion temperature of 81°C. Four biocomposites (DAPAC) were prepared by melt mixing followed by compression molding with increasing CF content, 5, 10, 15, and 20 wt%, and named DAPAC5, DAPAC10, DAPAC15, and DAPAC20, respectively. Thermal, morphological, dynamic, mechanical, and mechanical properties of the corresponding biocomposites (DAPAC) were investigated. They exhibit a high increase in glass transition temperature (T_g) and a decrease in the crystallization temperature and crystallinity degree (Table 10.7). This can be attributed to carbonyl (DAPA) and hydroxyl (CP) groups' interactions. These hydrogen bonds reduce the polymer mobility.

The dynamic mechanical spectra of these biocomposites revealed an increase in the stiffness and showed higher thermal–mechanical stability. Morphological observations revealed a moderate interfacial adhesion between the fibers and the matrix

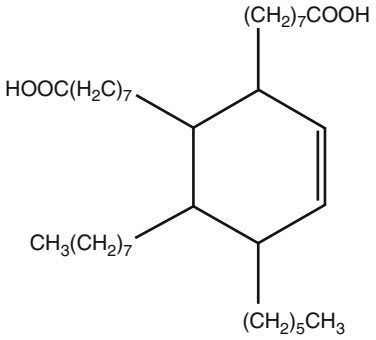

Fig. 10.25 Dimers of fatty acids (DA) (Reproduced from Ref. [25]. With kind permission of © Elsevier)

Table 10.7 DSC results of cellulose fiber–reinforced dimer fatty acid–based polyamides (Reproduced from Ref. [25]. With kind permission of © Elsevier)

Sample	T_g (°C)	T_c (°C)	$\Delta H'_c$ (J g^{-1})	T_f (°C)	$\Delta H'_f$ (J g^{-1})	X_c (%)
DAPA	−10	55	29.2	81	18.3	9.5
DAPA-5%	−4	53	19.2	80	17.7	9.2
DAPA-10%	−5	53	17.9	81	18.5	9.6
DAPA-15%	−1	52	17.5	80	17.3	9.0
DAPA-20%	−3	50	15.7	79	16.1	8.4

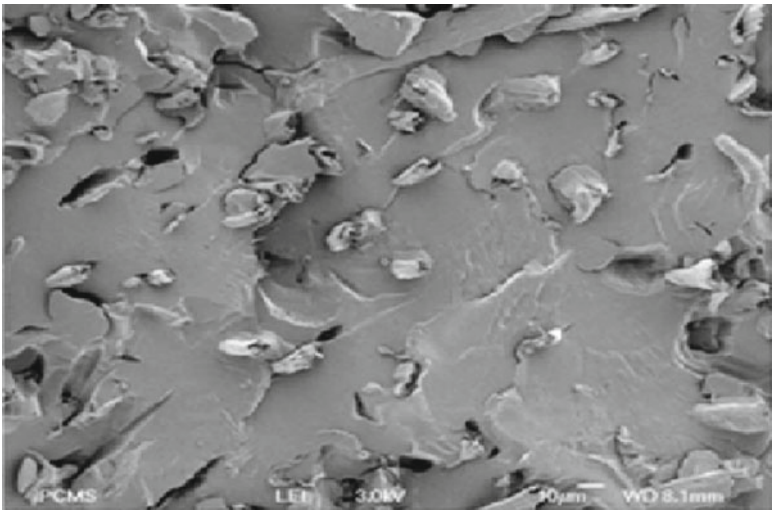

Fig. 10.26 Cryogenic fracture surface of DAPAC20 (Reproduced from Ref. [25]. With kind permission of © Elsevier)

(Fig. 10.26). With the increase of the fiber content, tensile tests showed a high increase in Young modulus and yield stress and a decrease of elongation at break (Fig. 10.27).

They concluded that the association of a bio-based polymer with cellulose fillers could be a good solution to environmental pollution, and they support sustainable development. Hablot et al. [26] also reported the yield behavior of the renewable biocomposites of dimer fatty acid–based polyamides with cellulose fibers. They used both dynamic mechanical analysis (DMA) and tensile tests to follow the effect of strain rate or frequency, temperature, and filler content on the transition temperatures, the storage modulus, and the yield stresses. The DMA results showed that the storage modulus increased with increasing cellulose fiber (CF) concentration (shown in Fig. 10.28). The tensile tests revealed that the yield stress was sensitive to strain rate, temperature, and CF concentration (Fig. 10.29).

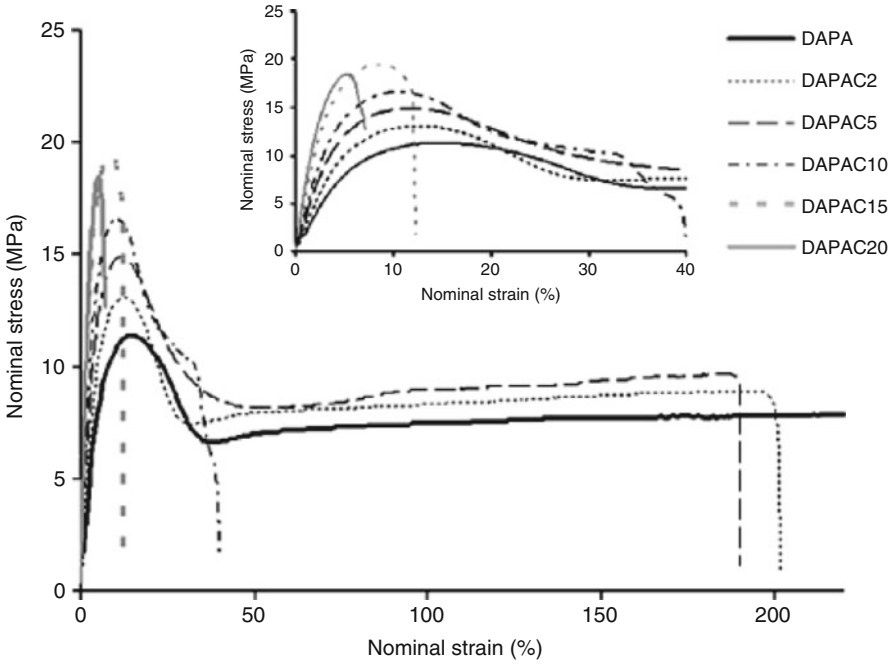

Fig. 10.27 Stress–strain curves of pure *DAPA* and *DAPAC* different filler contents (Reproduced from Ref. [25]. With kind permission of © Elsevier)

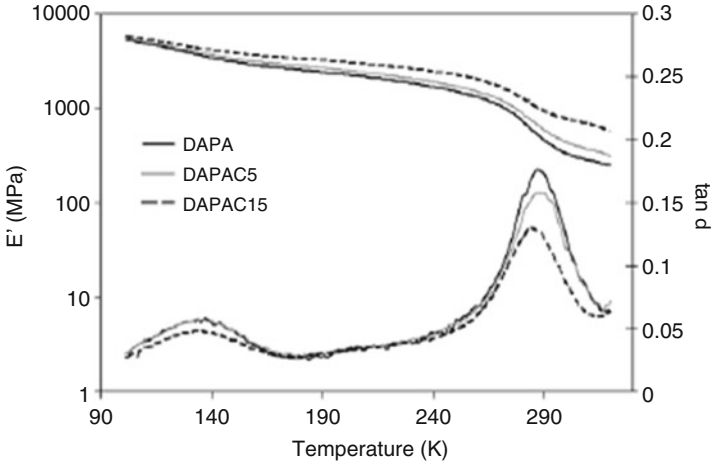

Fig. 10.28 Storage modulus and damping parameter versus temperature of both *DAPA* and *DAPAC* composites at a frequency of 1 Hz and at different cellulose contents (Reproduced from Ref. [26]. With kind permission of © Elsevier)

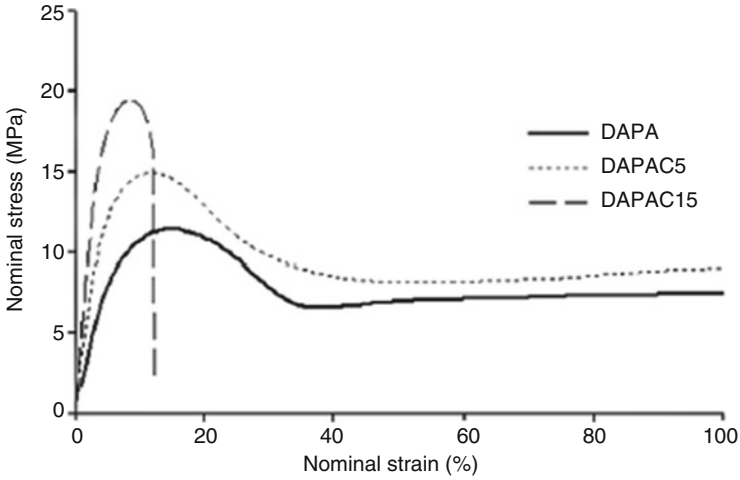

Fig. 10.29 Stress–strain curves of *DAPA* and *DAPAC* composites at a strain rate of 10^{-2} s^{-1} and at a temperature of 298 K for different cellulose concentrations (Reproduced from Ref. [26]. With kind permission of © Elsevier)

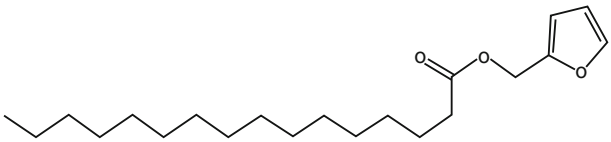

Fig. 10.30 Chemical structure of furfuryl palmitate (Reproduced from Ref. [27]. With kind permission of the American Chemical Society)

Both activation enthalpy and activation volume calculated by the Eyring model revealed a slight increase of activation energy with increasing filler content and a decrease of the activation volume.

In a recent work by Mistri and Ray [27], palmitic acid ester of furfuryl alcohol (furfuryl palmitate designated as FP, Fig. 10.30) was prepared by enzymatic route and was used as a precursor for the preparation of green biocomposites.

By carrying out Diels-Alder reaction between FP and maleic anhydride (1:1 M proportion), Diels-Alder adduct (FP-MA) was formed, as shown in Fig. 10.31. Crystal growth was observed on Diels-Alder reaction along with a noncrystalline part. The Diels-Alder product (FP-MA) was analyzed with infrared (IR) spectroscopy and ^{1}H nuclear magnetic resonance (NMR) spectroscopy.

They prepared FP-MA/jute green composites with 70 wt% jute loading by in situ polymerization technique. The probable mechanism of the polymerization reaction is presented (Fig. 10.32). The flexural strength, flexural modulus, and percent breaking strain observed were 10.06 MPa, 1,349 MPA, and 1.83%, respectively. The presence of fatty acid chains imparted flexibility in the material whereas the furan ring introduced rigidity.

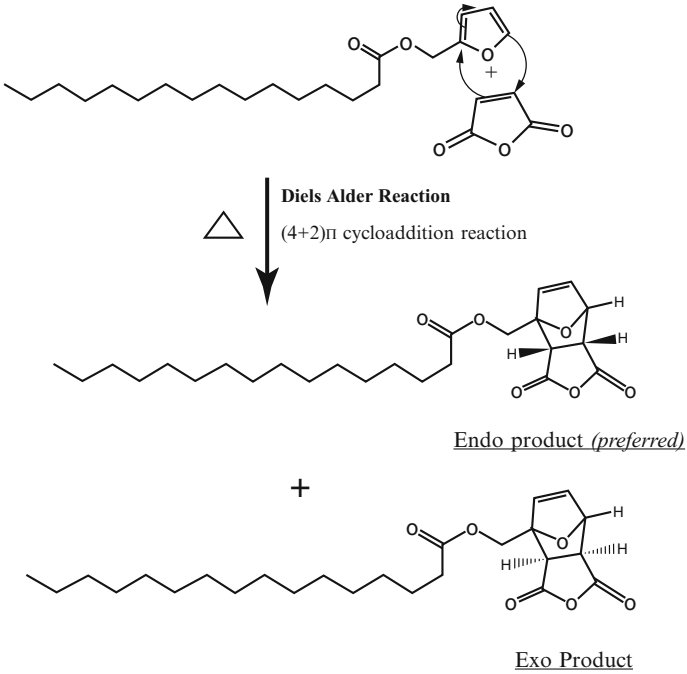

Fig. 10.31 Mechanism of Diels-Alder reaction between furfuryl alcohol and maleic anhydride (Reproduced from Ref. [27]. With kind permission of the American Chemical Society)

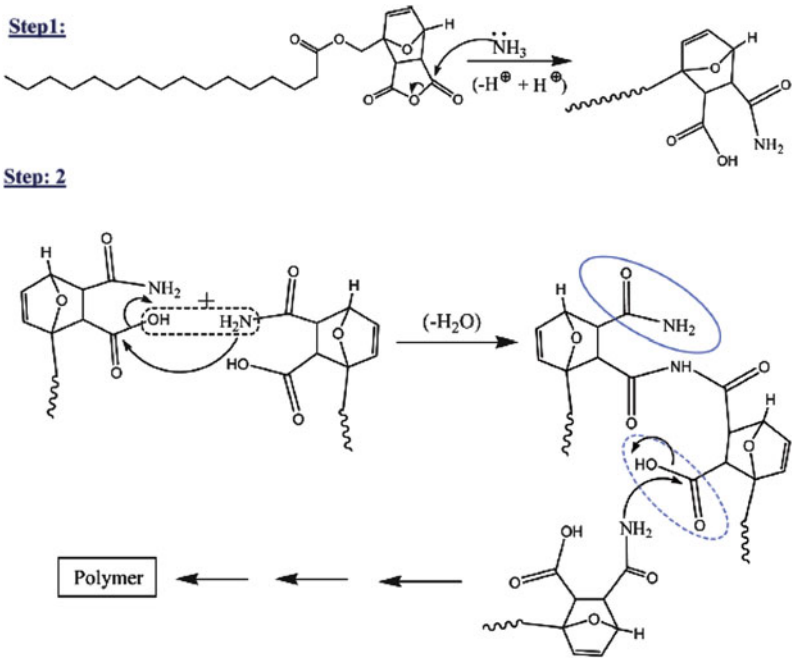

Fig. 10.32 The probable mechanism of polymerization reaction of FP-MA in presence of concentrated ammonia (Reproduced from Ref. [27]. With kind permission of the American Chemical Society)

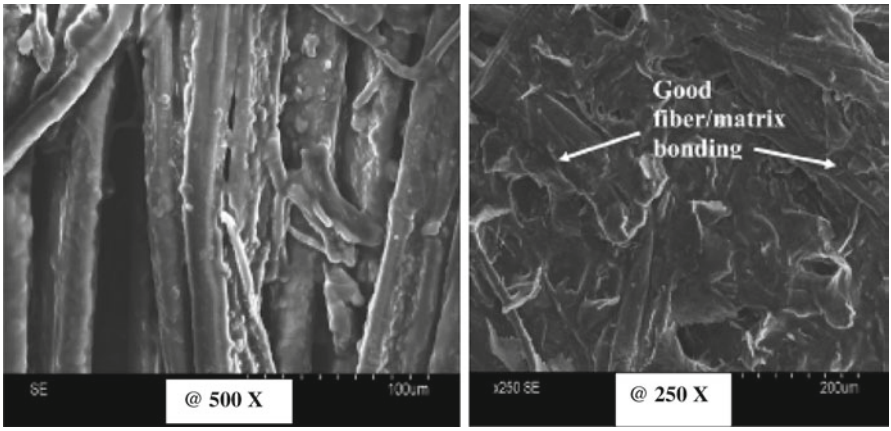

Fig. 10.33 The fracture surface of FP-MA/jute green composite (Reproduced from Ref. [27]. With kind permission of the American Chemical Society)

They compared the mechanical properties of FP-MA/jute composites with the reported mechanical properties of jute-reinforced polypropylene composites, which showed tensile strength and tensile modulus values of nearly 12 and 600 MPa with 70 wt% jute loading. The good chemical affinity between the matrix and the jute fibers allowed high jute loading of 70 wt%. The SEM micrograph of the composite fracture surface is shown in Fig. 10.33.

Thus, they concluded that this can be a new approach of developing macromonomer from renewable resource like fatty acids which can be converted into green materials by in situ polymerization.

Chen et al. [28] studied the morphology and thermal properties of electrospun fatty acids/polyethylene terephthalate composite fibers as novel form-stable phase change materials. They prepared ultrafine fibers based on the composites of polyethylene terephthalate (PET) and a series of fatty acids such as lauric acid (LA), myristic acid (MA), palmitic acid (PA), and stearic acid (SA). The morphology and thermal properties of the composite fibers were studied by field emission scanning electron microscopy (FE-SEM) and differential scanning calorimetry (DSC), respectively. The morphology of the electrospun PET and LA/PET composite fibers with different LA/PET mass ratios (from 50/100 to 150/100 by weight) and the average fiber diameter (AFD) of electrospun fibers versus LA content are shown in Fig. 10.34. It was found that the average fiber diameter increased with the content of fatty acid (LA) in the LA/PET composite fibers. The fibers with the low mass ratio maintained cylindrical shape with smooth surface, but the quality became worse when the mass ratio was too high (more than 100/100). The SEM images of LA/PET, MA/PET, PA/PET, and SA/PET composite fibers with a mass ratio of 70/100 electrospun from the respective solutions are shown in Fig. 10.35. All the four fatty acid/PET composite ultrathin fibers were cylindrical in shape with smooth

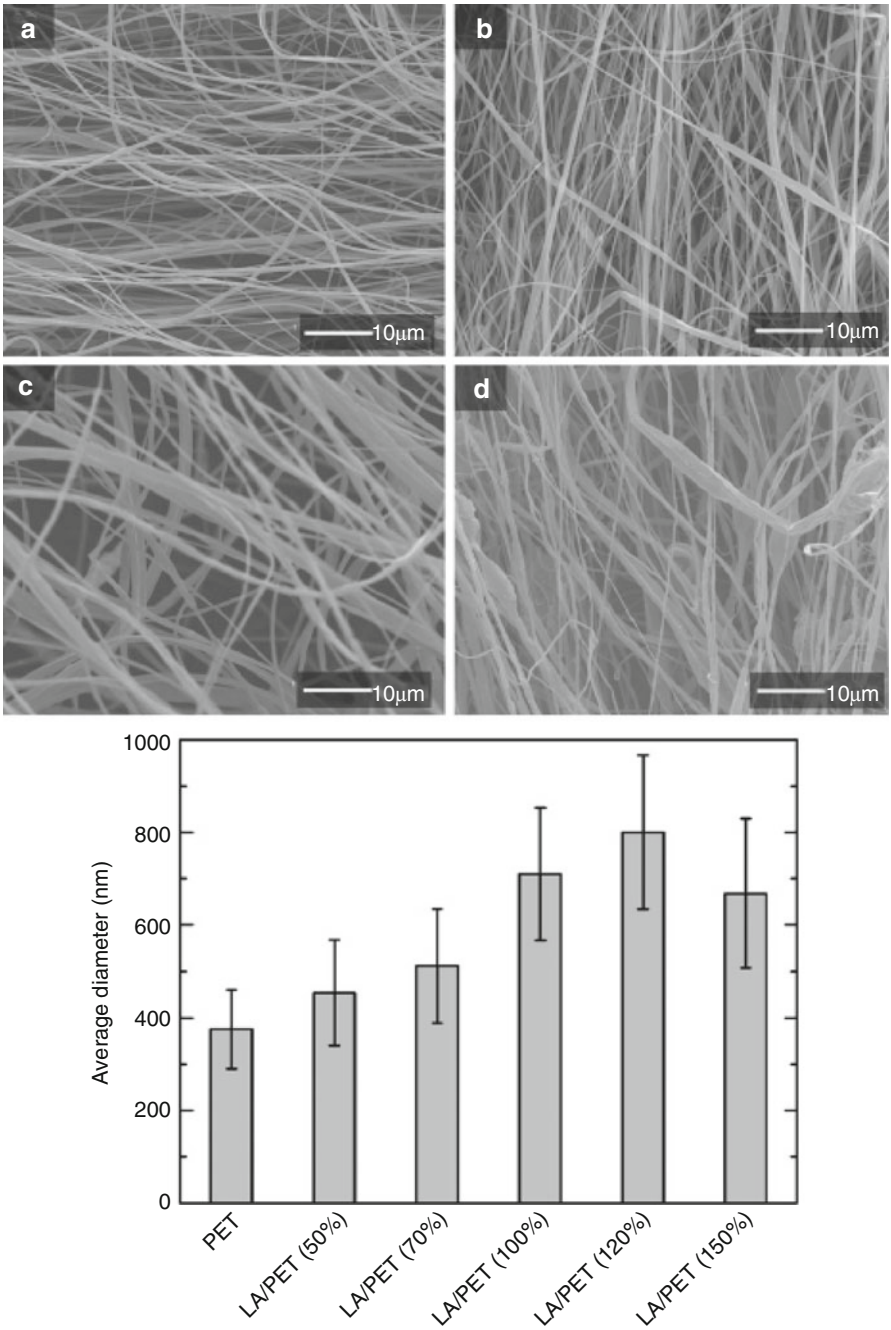

Fig. 10.34 SEM image of electrospun fibers. (**a**) PET, (**b**) LA/PET (50/100), (**c**) LA/PET (100/100), (**d**) LA/PET (150/100), (**e**) the AFD of those electrospun fibers (Reproduced from Ref. [28]. With kind permission of © Elsevier)

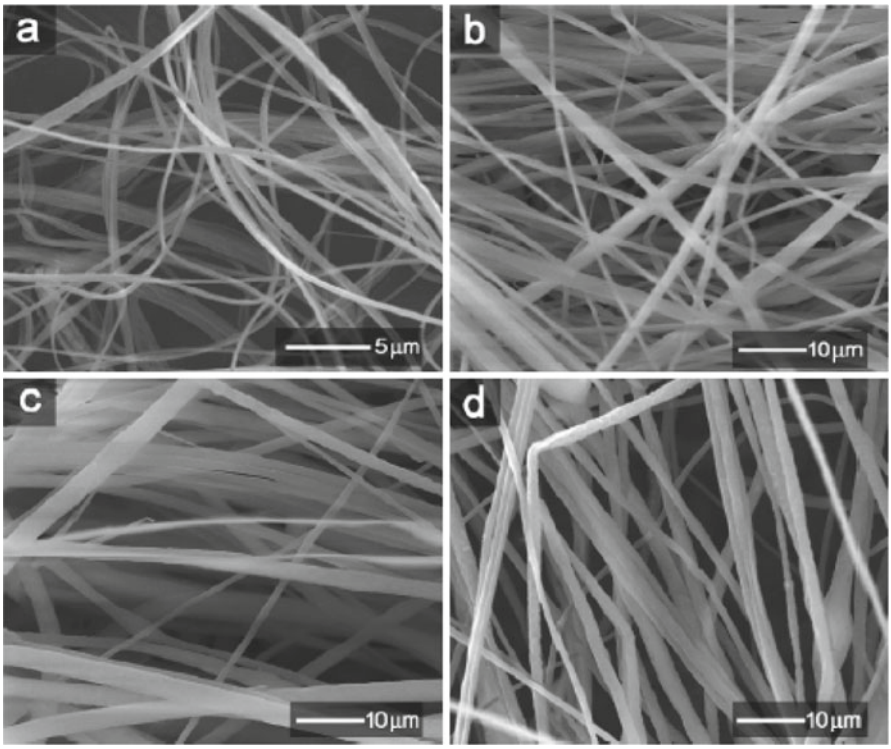

Fig. 10.35 SEM images of electrospun fatty acids/PET composite fibers with same mass ratio (70/100). (**a**) LA/PET, (**b**) MA/PET, (**c**) PA/PET, (**d**) SA/PET (Reproduced from Ref. [28]. With kind permission of © Elsevier)

surface. They also reported that the four fatty acids and PET had good compatibility in a low mass ratio. The average diameters of the composite fibers were found to increase with the increase in the alkyl chain of the fatty acid. Moreover, the latent heat of the composite fibers increased with the increase of LA content, and the phase transition temperature of the fibers had no obvious variations compared with LA. In contrast, both the latent heat and phase transition temperature of the fatty acid/PET composite fibers varied with the type of the fatty acids and could be well maintained after 100 heating–cooling thermal cycles, which demonstrated that the composite fibers had good thermal stability and reliability.

The DSC curve of the LA powder and the electrospun LA/PET composite fibers with different LA/PET mass ratios is shown in Fig. 10.36.

And the corresponding data of the thermal properties are shown in Fig. 10.37. The latent heat of fusion (ΔH_f) and the latent heat of crystallization (ΔH_c) of the composite fibers were lower than that of LA powder because PET had little contribution at that temperature range. Both ΔH_f and ΔH_c increased with the increase in

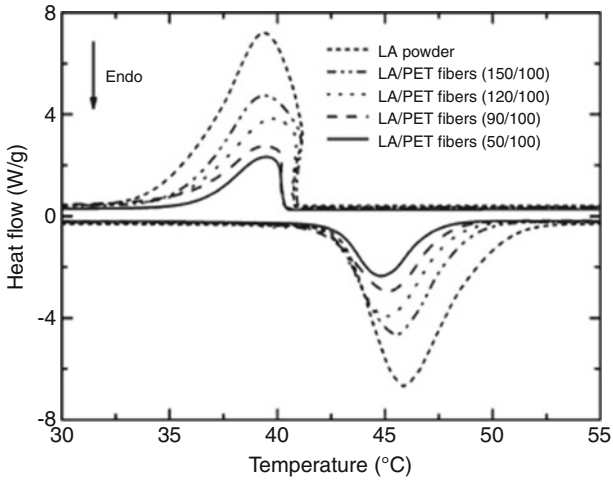

Fig. 10.36 DSC curve of electrospun *LA/PET* composite fibers and *LA powder* in heating and cooling process (Reproduced from Ref. [28]. With kind permission of © Elsevier)

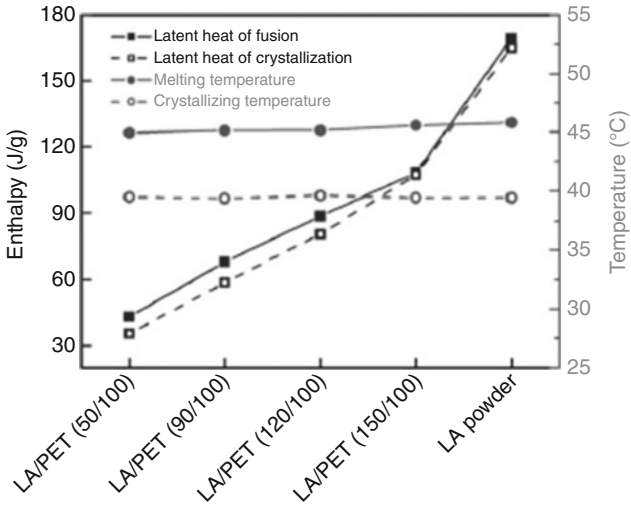

Fig. 10.37 The latent heat and phase transition temperature of *LA powder* and *LA/PET* composite fibers with different mass ratios (Reproduced from Ref. [28]. With kind permission of © Elsevier)

LA/PET mass ratio, whereas the melting and crystallization temperatures of the electrospun LA/PET composite fibers had no obvious variation compared to that of LA (<1°C). They concluded that the fatty acid/polymer mass ratio played an important role on the latent heat of fatty acid/polymer composite fibers but had less effect on their phase change behavior.

10.6 Future Prospects

This chapter highlights the potentiality of fatty acids in synthesizing green polymeric materials and green composites. The chemical modification of fatty acid with functional groups that could facilitate a subsequent polymerization will be of very much interest in future for the efficient synthesis of new green materials. The importance of fatty acids for various industrial applications becomes very important from a social, environmental, and energy standpoint, with the increasing emphasis on waste disposal issues and depletion of nonrenewable resources. Moreover, such fatty acid–based polymeric materials exhibit industrially useful characteristics as well as many unique properties. Such fatty acid–based polymers, when combined with plant fibers, give new materials with enhanced properties.

Application of fatty acid–based polymers and composites is still at its infancy. For successful development of such materials, further work is to be carried out to investigate their commercial viability, processibility, and product manufacturing routes. Further research would enable to understand the effect of chemical modification of fatty acids on its biodegradability. Extensive study to identify a clear disposal route must be carried out and should be available to consumers to appropriately manage this waste stream. There are immense scopes to carry out diversified researches on such fatty acid–based polymers and composites to develop green, environmental-friendly materials for a sustainable future.

References

1. Guner FS, Yagci Y, Erciyes AT (2006) Polymers from triglyceride oils. Prog Polym Sci 31:633–670
2. Baillie C (2005) Green composites: polymer composites and environment. CRC Press, Boca Raton
3. Satyanarayana KG, Ravikumar KK et al (1986) J Mater Sci 21:57–63
4. Stevens ES (2002) Green plastics. Princeton University Press, Princeton
5. Teomim D, Domb AJ (1999) Fatty acid terminated polyanhydrides. J Polym Sci Part A Polym Chem 37:3337–3344
6. Teomim D, Domb AJ (2001) Nonlinear fatty acid terminated polyanhydrides. Biomacromolecules 2:37–44
7. Shieh L, Tamada J et al (1994) Erosion of a new family of biodegradable polyanhydrides. J Biomed Mater Res 28:1465–1475
8. Laurencin CT, Gerhart T et al (1993) Bioerodible polyanhydrides for antibiotic drug delivery: in vivo osteomyelitis treatment in a rat model system. J Orthop Res 11:256–262
9. Shieh L, Tamada J et al (1994) Drug release from a new family of biodegradable polyanhydrides. J Control Release 29:73–82
10. Johnson RW, Fritz E (1989) Fatty acids in industry. Marcel Dekker, New York
11. Deligny P, Tuck N (2000) Alkyds and polyesters. In: Oldring PKT (ed) Resins for surface coatings, vol II. Wiley, New York
12. Wool RP, Knot SN et al (2002) Affordable composites and plastics from renewable resources: part 1: synthesis of monomers and polymers. In: Advancing sustainability through green chemistry and engineering, ACS symposium series 823., pp 177–204

13. Blayo A, Gandini A et al (2001) Chemical and rheological characterizations of some vegetable oils derivatives commonly used in printing inks. Ind Crops Prod 14:155–167
14. Krasko MY, Shikanov A et al (2002) Polyanhydrides with hydrophobic terminals. Polym Adv Technol 13:960–968
15. Teomim D, Nyska A et al (1999) Ricinoleic acid-based biopolymers. J Biomed Mater Res 45:258–267
16. Krasko MY, Shikanov A et al (2003) Poly(ester anhydride)s prepared by the insertion of ricinoleic acid into poly(sebacic acid). J Polym Sci Part A Polym Chem 41:1059–1069
17. Slivniak R, Domb AJ (2005) Macrolactones and polyesters from ricinoleic acid. Biomacromolecules 6:1679–1688
18. Silviniak R, Domb AJ (2002) Stereocomplexes of enantiomeric lactic acid and sebacic acid ester anhydride triblock copolymers. Biomacromolecules 3:754–760
19. Lodha P, Netravali AN (2005) Thermal and mechanical properties of environment-friendly 'green' plastics from stearic acid modified-soy protein isolate. Ind Crops Prod 21:49–64
20. Samuelsson J, Sundell PE et al (2004) Synthesis and polymerization of a radiation curable hyperbranched resin based on epoxy functional fatty acids. Prog Org Coat 50:193–198
21. Gultekin G, Attalay-Oral C et al (2009) Fatty acid-based polyurethane films for wound dressing applications. J Mater Sci Mater Med 20:421–431
22. La Scala JJ, James M, Sands JM et al (2004) Fatty acid-based monomers as styrene replacements for liquid molding resins. Polymer 45:7729–7737
23. Alam M, Ray AR et al (2009) Synthesis, characterization and performance of amine modified linseed oil fatty amide coatings. J Am Oil Chem Soc 86:573–580
24. Haseebuddin S, Parmar R et al (2009) Study of hexafunctional polyol in high solids air-drying alkyd: improved film performance. Prog Org Coat 64:446–453
25. Hablot E, Matadi R et al (2010) Renewable biocomposites of dimer fatty acid-based polyamides with cellulose fibres: thermal, physical and mechanical properties. Compos Sci Technol 70:504–509
26. Hablot E, Matadi R et al (2010) Yield behaviour of renewable biocomposites of dimer fatty acid-based polyamides with cellulose fibres. Compos Sci and Technol 70:525–529
27. Mistri E, Bandyopadhyay NR et al (2010) Development of green composites from furfuryl palmitate. Ind Eng Chem Res 49:11357–11362
28. Chen C, Wang L et al (2008) Morphology and thermal properties of electrospun fatty acid/polyethylene terephthalate composite fibers as novel form-stable phase Change materials. Sol Energy Mater Sol Cells 92:1382–1387

Chapter 11
Green Solvents in Thin-Layer Chromatography

Ali Mohammad, Inamuddin, Asma Siddiq, Mu. Naushad, and Gaber E. El-Desoky

Abstract In this chapter green solvents used in thin-layer chromatography (TLC) are discussed in detail. These green solvents eradicate or minimize the use of volatile organic solvents and protect the environment from further deterioration. The efforts made by chromatographers in this direction during the last 6 years (2005–2010) have been summarized in tabular form by encapsulating the use of green solvents (water, ethyl acetate, surfactants, *n*-butyl alcohol, *n*-butyl acetate, and ethylene glycol) as mobile phase in TLC analysis of different groups of organic and inorganic compounds. It is hoped that the contents of this chapter will encourage the working chromatographers to use safer alternative eluents in various combinations to achieve green analytical separations.

11.1 Introduction

Because of intensive use in chemical, pharmaceutical, and separation processes (Fig. 11.1), solvents have been the challenge to green chemistry. Majority of solvents used in academic and industrial laboratories are volatile organic compounds

A. Mohammad (✉) • Inamuddin • A. Siddiq
Department of Applied Chemistry, Faculty of Engineering and Technology, Aligarh Muslim University, Aligarh 202002, India
e-mail: editor_ali_mohammad@yahoo.com

Mu. Naushad • G.E. El-desoky
Department of Chemistry, College of Science, Building 5, King Saud University, Riyadh, Saudi Arabia

A. Mohammad and Inamuddin (eds.), *Green Solvents I: Properties and Applications in Chemistry*, DOI 10.1007/978-94-007-1712-1_11,

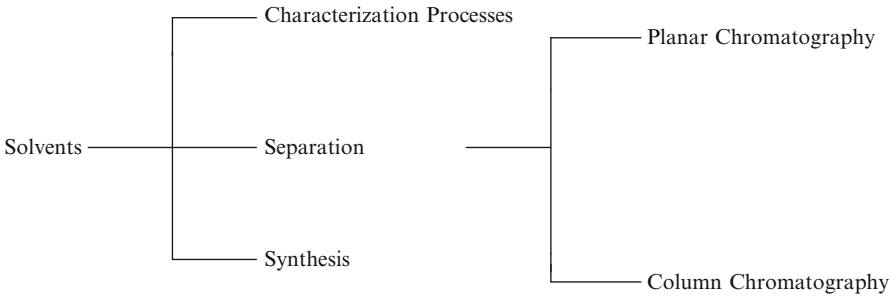

Fig. 11.1 Solvents in chemical processes

(VOCs) which inevitably lead to environmental pollution. Since 1990, chemists have initiated to address environmental issues in safe and profitable manner under the name "green chemistry" to highlight the judicious use of chemistry for prevention of pollution through environmentally conscious designing of chemical and analytical processes.

As regards analytical methodologies, parameters such as accuracy, sensitivity, reproducibility, simplicity, and cost-effectiveness have been the prime considerations, and factors such as operator's safety, environmental impact, waste generation, and the use of toxic reagents and solvents have been completely ignored. Surprisingly, in certain cases, the reagents employed for analysis were even more toxic than the species being determined. However, such ignorance was realized by analytical scientists during the 1990s with the inception of green analytical chemistry (GAC). The first descriptions of GAC methods appeared in 1995 [1].

Since the beginning of the green movement in the field of analytical chemistry about 15 years ago, the search for alternatives to classical procedures for analyte extraction and analysis has been one of the major challenges that scientists have faced. Therefore, chemical processes are being developed keeping environment in mind. The need for new technologies to diminish side effects of analytical activities led to substantial research efforts worldwide within different emerging topics, such as miniaturization, automation, solid support reagents, and replacement of toxic reagents and/or organic solvents by innocuous ones. Traditional chemical methods are being replaced with new innovations using green solvents. Solvents are very important in analytical chemistry, product purification, extraction and separation technologies, and also in the modification of materials. Therefore, in order to make chemistry more sustainable in these fields, knowledge of alternative, greener solvents is important in order to replace traditional organic solvents (Fig. 11.2). Green solvents are environmentally friendly solvents, or biosolvents, which are derived from the processing of agricultural crops. In contrast, petrochemical solvents are widely used in majority of chemical processes, but not without severe implications on the environment. Thus, green solvents are more environmentally favorable as compared to petrochemical solvents. A list of safe solvents with average to high safety level is provided in Table 11.1.

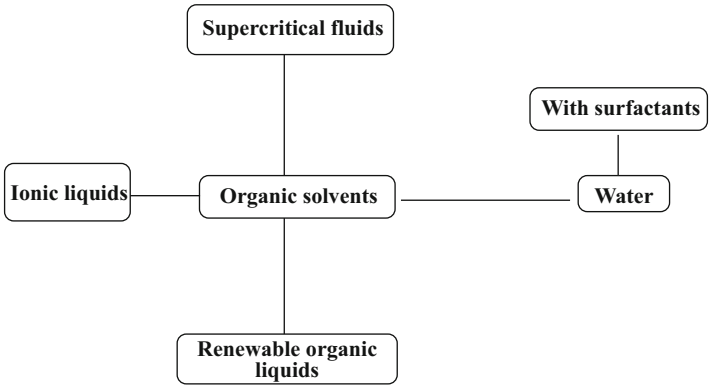

Fig. 11.2 Green alternatives to the toxic organic solvents in analytical chemistry

Table 11.1 Some commonly used green solvents [2]

Solvent
Isoamyl alcohol
2-Ethylhexanol
2-Butanol
Ethylene glycol
1-Butanol
Diethylene glycol butyl ether
t-Butyl acetate
Butyl acetate
n-Propyl acetate
Isopropyl acetate
Dimethyl propylene urea
Propionic acid
Ethyl acetate
Methyl isobutyl ketone

One of the 12 principles of green chemistry advocated by P.T. Anastas and J.C. Warner in 1998 especially advised to "use safer solvents and auxiliaries," and therefore, it is not surprising that in the last decades, research on the use of greener alternative solvents as against those commonly used has grown enormously [2].

The identification of unknown compounds has been the goal of the chemists. By measuring more than one of physical properties of a compound such as melting or boiling point and spectroscopic characteristics, the identity of a particular compound can be determined. If the chromatographic properties of unknown compounds are compared with those of known compounds, chromatography can be used to support a compound's identification. Among chromatographic techniques, thin-layer chromatography (TLC) is very useful to chemists as an analytical tool to identify and separate the compounds in a mixture. The technique is nondestructive, that is,

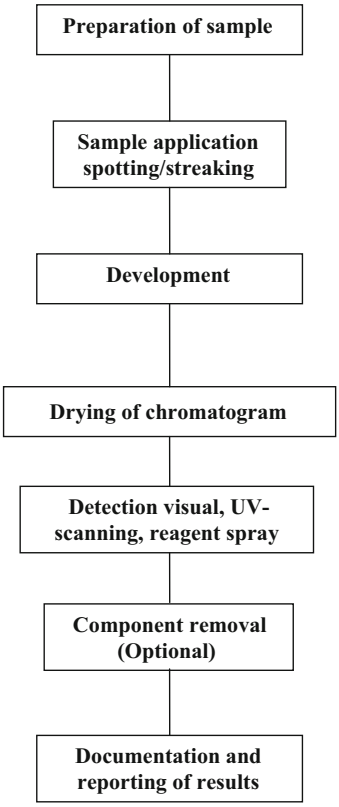

Fig. 11.3 The process of thin-layer chromatography

the molecules in the mixtures are separated physically without being chemically altered. It has becomes an essential technique for analyst and research workers.

In addition to being an off-line technique where the various procedural steps (Fig. 11.3) can be carried out independently, several other fascinating features such as possibility of direct observation of colorful reactions, minimal sample cleanup, wider choice of mobile and stationary phases, reasonable sensitivity, excellent resolution power, high sample loading capacity, low-solvent consumption, capability of handling a large number of samples simultaneously, and disposable nature of TLC plates have maintained its continuing popularity as an analytical separation technique. TLC can be used for (a) qualitative analysis (the identification of the presence or absence of a particular substance in the mixture), (b) quantitative analysis (precise and accurate determination of a particular substance in a sample mixture), and (c) preparative analysis (purification and isolation of a particular substance for subsequent use).

TLC is a subdivision of liquid planar chromatography in which the mobile phase (a liquid) migrates by capillary action through the stationary phase which is in the form of a thin layer on an inert support. Components of a mixture are separated by distributing between mobile and stationary phases. Difference in the affinity of

individual components to stationary and/or mobile phase facilitates their separation. The proper selection of stationary and mobile phase conditions decides the degree to which effective separations of components in a mixture can be achieved. To achieve better reproducibility, a mobile phase of lower volatility is preferred. The mobile phases used in TLC may be categorized into the following groups:

- Inorganic solvents (solutions of mineral acids, bases, salts and mixture of acids, bases, or their salts)
- Organic solvents (acids, bases, hydrocarbons, alcohols, amines, ketones, aldehydes, organophosphates, and their mixture in different proportions)
- Mixed solvents (above mentioned organic solvents mixed with water, mineral acids, inorganic bases or dimethyl sulfoxide, and buffered salt solution)
- Surfactant-mediated systems (aqueous and hybrid solutions of cationic, anionic, and nonionic surfactants)

Presently, the interest of chromatographers is growing in identifying the green mobile phase systems for future use. In our opinion, aqueous solvent systems including pure water, aqueous solutions of surfactants, ethyl acetate, *n*-butanol, *n*-butyl acetate, and ethylene glycol will occupy the prime position as "green eluents" in chromatography.

A number of green solvents are used as solvent in thin-layer chromatography for the separation of organic and inorganic substances. However, we are reporting in this chapter, the work performed using water, ethyl acetate, surfactants, *n*-butanol, *n*-butyl acetate, and ethylene glycol as one of the components of the mobile phase in TLC analysis of different compounds. The general properties of the above mentioned green solvents are as follows.

11.2 Water

Among green solvents, the first priority is given to water because of its easy availability, nontoxicity, poor thermal conductivity, excellent solubilizing tendency, and transparent nature. Water-based synthetic reactions, paints, pharmaceutical products, and separation techniques are currently enjoying popularity, and the chemists are now trying reactions in water. Thus, the water-based chemistry has strong future.

11.3 Ethyl Acetate

Ethyl acetate is a by-product of the fermentation of grapes and is safe for use as a synthetic flavoring substance. Being noncarcinogenic to humans, it is considered as green solvent for use. It has been the preferred extractant for organochlorine pesticides, herbicides, and organohalides from drinking water, polycyclic aromatic hydrocarbons from water, and anabolic steroids from urine.

11.4 Surfactants

Surfactants are long-chain amphiphilic organic or organometallic molecules containing a highly polar (hydrophilic or lipophobic) or "ionic head group" attached to a nonpolar (hydrophobic or lipophilic) hydrocarbon tail of varying chain lengths.

Surfactant-mediated system containing surfactant as one of the components of mobile phase can be used in the following ways:

(a) As monomer surfactants where the concentration of surfactant in aqueous mobile phase is restricted to well below the critical micelle concentration (CMC) of the surfactant. These mobile phases are most suited to separate ionic species by ion pair chromatography (IPC).
(b) As surfactant micelles where the surfactant concentration is kept well above its CMC value. In such cases, the mobile phase is composed of surfactant molecules in the form of monomers and aggregates (or micelles). These mobile phases are very useful for simultaneous separation of ionic and nonionic compounds by micellar liquid chromatography (MLC).
(c) As microemulsion where surfactant in the presence of water, oil (hydrocarbon), and cosurfactant (i.e., medium-chain-length amine or alcohol) is used as transparent solution.

11.5 *n*-Butanol

n-Butanol occurs naturally as a minor product of the fermentation of sugars and other carbohydrates. It is readily degradable in water and decomposed in the air by photodegradation. It is considered as a "greener" fuel alternative to diesel and gasoline and is considered a safe cosmetic ingredient.

11.6 *n*-Butyl Acetate

n-Butyl acetate is commonly used as an industrial solvent. Being biodegradable, it is the most suitable substitute for other solvents that are considered hazardous environmental pollutants. It is safely used as a solvent in different analytical processes and laboratories work.

11.7 Ethylene Glycol

It is colorless and odorless liquid which is completely miscible with polar solvents (water, alcohol, acetone, etc.). The ethylene glycol-water mixture is widely used as antifreeze agent. Its behavior is almost similar to monohydric alcohols in several cases.

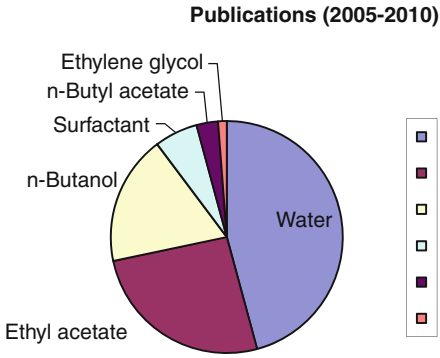

Fig. 11.4 The publication trend of green solvents

The publication trend observed from the literature survey of green solvents such as water, ethyl acetate, surfactants, *n*-butanol, *n*-butyl acetate, and ethylene glycol as one of the components of the mobile phase in TLC analysis of different compounds is given in Fig. 11.4. The literature survey was performed using Scopus. The details of these solvents as one of the components of the mobile phase in TLC analysis of different compounds are given in Tables 11.2, 11.3, 11.4, 11.5, 11.6 and 11.7.

From above, it is clear that green solvents have excellent analytical potential as eluent in chromatography. However, in certain cases, green solvents have been unconsciously used in combination of toxic volatile organic solvents such as carbon tetrachloride, chloroform, acetonitrile, acetanilide, aliphatic amines, etc. These systems need to be reinvestigated by replacing undesirable components with desirable solvents. Alternatively, certain green solvents can be used in stationary phase instead of using in mobile phase. According to literature, this aspect of study has been completely ignored. Furthermore, new green solvents have to be identified to develop efficient chromatographic methods.

11.8 Conclusions

Among the selected green solvents, the order of preference for their use has been as water > ethyl acetate > *n*-butanol > aqueous solution of surfactants > *n*-butyl acetate > ethylene glycol. Water–methanol system has been most preferred for TLC analysis of different components. In certain cases, these solvents have also been used in combination with undesirable solvents such as chloroform, carbon tetrachloride, hexane, acetonitrile, aliphatic amines, and dichloromethane. These solvent systems need to be reinvestigated by replacement of undesirable component of solvents with alternative environmentally friendly solvents. The possible replacement may be as hexane or pentane by heptane and dichloromethane by ethylacetate-heptane systems. The future studies should be focused on the use of polyethylene glycol, ionic liquids, biosurfactants, and supercritical fluids as mobile phase in TLC to make it greener.

Table 11.2 Application of water-containing mobile phases in thin-layer chromatography (2005–2010)

S. No.	Mobile phase	Remark	Reference
1	Methanol–water (3.5:1.5)	Determination of atorvastatin calcium in bulk drug and tablets on silica gel 60 RP18F_{254S}	[3]
2	Methanol–water (7:3)	Study of the degradation of rimonabant on HPTLC plates	[4]
3	Methanol–water mixture in different volume proportions	Examination of lipophilicity of some synthetic dyes on RP-18F_{254s}, RP-18Wl UV_{254}, and CNF_{254s} plates	[5]
4	*n*-Propanol-methanol and water (4:1:2)	Identification of new drugs from plant sources on silica HPTLC plates	[6]
5	Methanol–water mixtures in different volume compositions adjusted to different pH levels	Study of pH effect of water on the lipophilicity of nicotinic acid and its derivatives on RP-2 plates (Kieselgel 60 F_{254}, E. Merck)	[7]
6	Methanol–water in different volume compositions	Use of RP8 F_{254}, RP18F_{254s}, RP18 W, and CN HPTLC plates to compare the lipophilicity of salicylic acid and its derivatives	[8]
7	Ethyl acetate-methanol–water-formic acid (15:2:1:1)	Isolation of glycyrrhizin from herbal extract-sand herbal gel on precoated silica gel TLC plates followed by their estimation	[9]
8	Methanol–water and dioxane-water binary mixtures	Investigation of chromatographic behavior of salicylic acid derivatives on reversed-phase high-performance thin-layer chromatographic plates (RP HPTLC)	[10]
9	Methanol–water mixtures in different volume proportions	The examination of chromatographic behavior of the parabens on silica gel 60 F_{254} plates impregnated with different oils (paraffin, olive, sunflower, and corn)	[11]
10	Methanol–water	Development of HPTLC method for the determination of sucralose in beverages using amino-bonded silica gel HPTLC plates	[12]
11	Methanol–water mixtures	Optimization of a solid-phase extraction protocol for fractionation of steroids on HPTLC plates	[13]
12	Methanol-7.8% aqueous ammonium acetate (17:3)	Quantification of dequalinium cations in pharmaceutical samples on nano TLC silica gel plate (Merck)	[14]
13	Ethyl acetate-methanol–water (8.0: 1.5: 0.3)	Simultaneous determination of famotidine and domperidone from combined dosage form on silica gel precoated aluminum plate 60 F_{254} (20×10 cm)	[15]
14	Mixtures of methanol–water in different proportions of volume	Examination of lipophilicity of some emerging pesticides on RP-18, RP-8, and CN stationary phases	[16]
15	Methanol–water mixtures	Retention indices for some precursors of peraza crown ethers on RP-18 plates	[17]

(continued)

Table 11.2 (continued)

S. No.	Mobile phase	Remark	Reference
16	Toluene-ethyl acetate-methanol-isopropanol-water (60:30:20:15:3)	Use of silica gel HPTLC plates for quality control of multicomponent herbal drugs	[18]
17	Methanol–water, methanol, and other organic solvents	Analysis of ranitidine hydrochloride standard, components of ranitidine medications, and the products from photolytic degradation of ranitidine medications on HPTLC plates	[19]
18	Methanol–water (8:2)	Analysis of taxol in *Taxus baccata* L. on RP-18 WF HPTLC plates	[20]
19	Butyl acetate-glacial acetic acid-methanol–water (5:2.5:2.5:1)	Use of aluminum plates precoated with silica gel 60 F_{254} for quantitative analysis of amoxicillin trihydrate and bromhexine hydrochloride in bulk and combined pharmaceutical dosages	[21]
20	Methanol–water-glacial acetic acid (8:2:0.2)	Estimation of olopatadine hydrochloride in ophthalmic solution using precoated silica gel 60 F_{254} aluminum plates	[22]
21	Ethyl acetate-formic acid-methanol–water (10:0.9:1.1:1.7)	Fast and simple quantitative HPTLC method for estimation of rutin in pharmaceutical preparations	[23]
22	Methanol–water (3.5:1.5)	RP-HPTLC-densitometric determination of atorvastatin calcium in bulk drug and pharmaceutical formulations using aluminum sheets precoated with silica gel 60 $RP18F_{254S}$	[24]
23	Methanol–water in different volume proportions	Investigations about analytical characteristics of vitamin K1 on RP-18 F_{254} TLC plates with the use of RP-TLC and densitometry	[25]
24	Ethyl acetate-methanol–water-acetic acid (65:23:11:1)	Identification and quantification of 25 water-soluble dyes in food using silica gel 60 F_{254} high-performance thin-layer chromatography plates	[26]
25	Methanol-acetonitrile-isopropyl alcohol-water (5:4:0.5:0.5)	Determination of minocycline in human plasma, saliva, and gingival fluid samples and the densitometric analysis of minocycline on silica gel 60 F_{254}	[27]
26	Ethyl acetate-methanol–water and acetonitrile-methanol–water-dichloromethane in different volume ratios	Direct resolution of the enantiomers of the racemic drugs ketamine and lisinopril on stationary phase impregnated with chiral (−) mandelic acid and (+) tartaric acid	[28]
27	Methanol–water-isopropanol-acetic acid (30:65:2:3)	Simultaneous quantitative determination of vanillin and related phenolic compounds in ethanolic extracts of *Vanilla planifolia* pods on silica gel RP-18 F_{254S}	[29]

(continued)

Table 11.2 (continued)

S. No.	Mobile phase	Remark	Reference
28	Methanol-acetonitrile-isopropanol-water in ratio of 5:4:0.5:0.5	Development of HPTLC method for determination of minocycline in human plasma using silica gel 60 F_{254} plates	[30]
29	Ethyl acetate-formic acid-methanol-distilled water in different proportions	Use of silica gel 60 F_{254} HPTLC plates for the determination of rutin in the whole-plant powder of *Amaranthus spinosus* Linn	[31]
30	Water-(5% formic acid/methanol) in 7:3 and 1:1	RP-HPTLC method for simultaneous determination of flavonoids in herbal extracts	[32]
31	Propanol-ethyl acetate-ammonia-water (4:3:2:1)	Simultaneous estimation of glucosamine and ibuprofen in tablet formulation on precoated silica gel 60 F_{254} TLC plate	[33]
32	0.1% Aqueous solution of Cween 80	Mutual separation of five water-soluble vitamins (folic acid, cyanocobalamin, thiamine, pyridoxine, and riboflavin) on silica layer impregnated with 0.01% sodium dodecyl sulfate (SDS)	[34]
33	*n*-Butanol-acetic acid-water (4:1:5)	TLC method to assess the stability of tinctures obtained from a percolation process of two Brazilian plants: *Quassia amara* and *Maytenus ilicifolia*	[35]
34	*n*-Butanol-2-propanol-water-methylene chloride-methanol (10:7:2:5:3)	Use of silica gel TLC plates in densitometric method for determination of clopamide, 4-chlorobenzoic, and 4-chloro-3-sulfamoyl-benzoic acids	[36]
35	Acetone-water-acetic acid (4:1:0.1)	Analysis of pioglitazone hydrochloride in pharmaceutical formulations on aluminum foil plates coated with silica gel 60 RP-18 F_{254s}	[37]
36	Mixture of acetone and water	Study of the lipophilicity aminoalkanol derivatives by reversed-phase thin-layer chromatography	[38]
37	Ethyl acetate-acetic acid-water in the ratio of 7.5:1.5:1	Validation of an HPTLC method for determination of oseltamivir phosphate in pharmaceutical dosage form	[39]
38	Absolute ethanol-methylene chloride-triethyl amine (7:3:0.2)	Use of silica gel HPTLC F_{254} plates for the determination of sulpiride and mebeverine hydrochloride in combination	[40]
39	Water in combination with acetone, acetonitrile, methanol, 2-propanol, and tetrahydrofuran	Chemometric characterization of s-triazine derivatives on C-18 stationary phase	[41]
40	Water, 1-propanol-water, and 1-propanol-water-acetic acid	Separation of eight flavan-3-ols on cellulose HPTLC plates prewashed in water	[42]

(continued)

Table 11.2 (continued)

S. No.	Mobile phase	Remark	Reference
41	*n*-Butanol-acetic acid-water (4.0:1.0:1.0)	Analysis of L-dopa in *Mucuna pruriens* seed extract and its formulations on HPTLC on silica gel plates	[43]
42	Aqueous eluents with various additives	Analysis of selected antidepressive drugs on RP-18 and CN-silica layers	[44]
43	2-Butane-1-ol-glacial acetic acid-water (12:3:5)	Identification and determination of complex hypotensive drugs on silica gel F_{254} TLC plates	[45]
44	Dioxane-water (20:80)	Evaluation of the separation efficiency of nicotinic acid derivatives on RP-18 TLC plates	[46]
45	Acetone-chloroform-n-butanol-acetic acid glacial-water (60:40:40:40:35 v/v/v/v/v)	Application of HPTLC in quantitative analysis of L-dopa in tablets using precoated silica gel F_{254} HPTLC plates	[47]
46	Chloroform-methanol-ammonia-water (120:75:2:6)	Separation and simultaneous analysis of aspirin, salicylic acid, and sulfosalicylic acid on aluminum foil silica gel G 60 F_{254} HPTLC plates impregnated with 2% (w/v) boric acid	[48]
47	Acetonitrile-water (90:10)	Establishment of xylose in Plantago ovata Forsk as a leading compound for quantification in raw material and finished product on TLC plate of silica	[49]
48	Water–methanol-acetonitrile (60:30:10)	Estimation of alfuzosin hydrochloride in bulk and in pharmaceutical formulations using HPLC-HPTLC joint technique	[50]
49	Acetonitrile-methanol-aqueous formic acid (40:02:08)	Simultaneous densitometric determination of shikonin, acetylshikonin, and beta-acetoxy-isovaleryl-shikonin in ultrasonic-assisted extracts of four species of genus *Arnebia* using precoated RP-18 F_{254S} TLC plates	[51]
50	Chloroform-methanol–water	Simultaneous quantitation of three bioactive steroidal glycoalkaloid (SGA) markers, solasonine (SN), solamargine (SM) and khasianine (KN) in the plant *Solanum xanthocarpum* on silica gel 60 F_{254} TLC plates	[52]
51	Chloroform-methanol-acetic acid-water (60:32:12:8)	Identification and quantification of triterpenoid centelloids in *Centella asiatica* (L.) urban by normal-phase TLC	[53]
52	Chloroform-ethyl acetate-glacial acetic acid-water (4:4:4:1)	Simultaneous identification of eight β-lactam antibiotics on silica gel F_{254} plates and quantification by densitometry	[54]
53	Acetonitrile:water:formic acid (50:50:3)	Estimation of tolterodine tartarate in pure drug and its formulation by HPTLC using alumina plates	[55]

(continued)

Table 11.2 (continued)

S. No.	Mobile phase	Remark	Reference
54	Acetonitrile, buffer, and bidistilled water	Separation of a mixture of acetylsalicylic acid, caffeine, and acetaminophen on C18 plates	[56]
55	Toluene-acetonitrile-formic acid-water (5:5:0.3:1)	Simultaneous estimation of telmisartan and ramipril in combined pharmaceutical dosage form on silica gel 60 F_{254} HPTLC plates	[57]
56	Alcohols in combination with dimethyl sulfoxide, hexamethyldisiloxane, acetonitrile, and water	Examination of retention behavior of aclarubicin and doxycycline on silica gel 60 F_{254} and RP-18 WF_{254s} HPTLC plates	[58]
57	Methanol–water-acetonitrile-trimethylamine (65:20:15:0.2)	Determination of tropisetron in a pharmaceutical dosage form in the presence of its degradation products on silica gel 60 F_{254} aluminum sheets	[59]
58	Chloroform-methanol-deionized water (65:25:4)	Determination of effects of *Echinostoma caproni* infection on the neutral and polar lipids of intestinal and non-in mouse testinal organs in the BALB/c on HPTLC-HLF silica gel plates	[60]
59	Tetrahydrofuran-toluene-formic acid-water (16:8:2:1)	Simultaneous determination of isoorientin, isovitexin, orientin, and vitexin, both pure and in commercial samples of bamboo leaf flavonoids on silica gel 60 plates	[61]
60	Chloroform-ethyl acetate-glacial acetic acid-water (4:4:4:1)	Separation and identification of the epimers of cefaclor on silica gel 60 F_{254} plates and quantitative analysis by densitometry	[62]
61	Ethyl acetate-dichloromethane-formic acid-glacial acetic acid-water (10:2.5:1:1:0.1)	Estimation of gallic acid rutin and quercetin from aqueous extract of *Terminalia chebula* using precoated silica gel GF_{254} plates	[63]
62	Mixtures of acetonitrile-water in different proportions of volume	Examination of lipophilicity of some artificial and natural sweeteners by RP-HPTLC using RP-18, RP-18W, RP-8, CN, and NH_2 bonded silica plates	[64]
63	Methyl *t*-butyl ether-water–methanol-cyclohexane (2.4:0.05:0.1:0.05)	Versatile TLC method for quantification of aflatoxins and ochratoxin A in dried figs	[65]
64	Acetone-chloroform-*n*-butanol-glacial acetic acid-water (5:10:10:2.5:2.5)	Study of the chemical stability of haloperidol lactate injection by HPTLC	[66]
65	Acetone-chloroform-*n*-butanol-acetic acid glacial-water (60:40:40:40:35)	Quantitative analysis of L-dopa in tablets on precoated silica gel F_{254} HPTLC plates	[67]

(continued)

Table 11.2 (continued)

S. No.	Mobile phase	Remark	Reference
66	Heptane, dichloromethane, diisopropyl ether, formic acid, and water	Densitometric HPTLC and HPLC analysis of phenolic acids from *Aquilegia vulgaris*	[68]
67	*n*-Butanol-water-acetonitrile-10% ammonia solution-glacial acetic acid mixtures	Estimation of adenosine and its major metabolites in brain tissues of rats using aluminum plates precoated with silica gel 60 F_{254}	[69]
68	*n*-Butanol-chloroform-acetic acid-ammonium hydroxide-water (9:3:5:1:2)	HPTLC densitometry for quantitative analysis of ketorolac tromethamine in human plasma	[70]
69	25% MeCN in water + 50 mm H_3PO_4	Separation and quantitative determination of oenothein B (OeB) and quercetin glucuronide (QG) in aqueous extract of *Epilobii angustifolii herba* by HPTLC with RP-18 WF_{254} plates	[71]
70	Methanol-acetonitrile-isopropyl alcohol-water (5:4:0.5:0.5)	Use of aluminum plates precoated with silica gel 60 F_{254} in examination of stress degradation products of minocycline	[72]
71	Ethyl acetate-formic acid-water (68:2.5:3)	Separation and quantitative analysis of quercetin glycosides in methanolic and aqueous extracts of *Epilobii angustifolii herba* on silica gel 60 F_{254} HPTLC plates	[73]
72	Ethyl acetate-glacial acetic acid-methanol–water (60:15:15:10)	Analysis of glucose and maltose in estivated *Biomphalaria glabrata* snails and those infected with *Schistosoma mansoni* on silica gel preadsorbent plates	[74]
73	Ethyl acetate-acetic acid-formic acid-water (100:11:11:26)	HPTLC Determination of flavonoids and phenolic acids in some Croatian Stachys taxa on silica gel 60 F_{254} plates	[75]
74	Ethyl acetate-water-formic acid-acetic acid (25:4:0.6: 0.4)	Qualitative and quantitative analysis of catechin in methanolic extracts from 15 taxa of Rosa L. hips using glass silica gel 60 F_{254} plates	[76]
75	Chloroform-methanol-ethyl acetate-water-hexane (20:22:60:8:4)	Separation of ginsenosides fraction obtained from the roots of *Panax quinquefolius* L cultivated in Poland on silica gel 60 F_{254} HPTLC plates	[77]
76	Chloroform-methanol-ethyl acetate-water (16.2:18.8:52:3)	Application of HPTLC and HPLC in determination of isoflavonoids in several kudzu samples	[78]

Note: Solvent compositions were by volume

Table 11.3 Application of ethyl acetate as one of the component or mobile phase in thin-layer chromatography (2005–2010)

S. No.	Mobile phase	Remark	References
1	Ethyl acetate-methanol (60:40)	HPLC-HPTLC procedure for simultaneous estimation of pantoprazole and domperidone in pure powder and pharmaceutical formulation	[79]
2	Toluene-ethyl acetate-methanol-formic acid (5.0:4.0:1.0:0.01)	Simultaneous quantitative determination of diclofenac sodium and paracetamol in a pharmaceutical formulation and in bulk drug powder on silica gel 60 F_{254} HPTLC plates	[80]
3	Toluene-ethyl acetate-methanol (9:1:0.5)	Identification and quantification of curcumin, piperine, and thymol in an ayurvedic formulation on silica gel 60 F_{254} plates	[81]
4	Ethyl acetate-methanol-ammonia (33%) in different ratios	Simultaneous analysis of drotaverine and nifuroxazide in capsules silica TLC	[82]
5	Methanol and ethyl acetate (2:1)	Assessing the trihalomethane formation potential of aquatic fulvic and humic acids fractionated on silica gel plates	[83]
6	Ethyl acetate-methanol-25% aqueous ammonia (60:30:10)	Stability assay for leuprolide acetate on silica gel 60 F_{254} HPTLC plates	[84]
7	Ethyl acetate-toluene-methanol (1:4:3.5)	For estimation of carvedilol in bulk drug and pharmaceutical formulations by RP-HPLC and HPTLC	[85]
8	Combinations of ethyl acetate and methanol	Identification of triterpenoid compounds of *Centella asiatica* with preliminary separation on silica gel plates	[86]
9	Ethyl acetate-ethanol-acetic acid (8:2:0.5)	Simultaneous measurement of trandolapril (TRA) and verapamil (VER) in two-component mixtures and in their combination capsules on silica gel 60 F_{254} by HPTLC densitometry	[87]
10	Toluene-ethyl acetate (93:7)	Use of caffeine-modified silica gel for quantitative determination of β-asarone in calamus	[88]
11	Toluene-ethyl acetate-methanol (80:18:2)	Densitometric HPTLC quantification of 2-azaanthraquinone isolated from *Mitracarpus scaber*	[89]
12	Toluene-ethyl acetate-formic acid (90:10:01)	Quantification of eugenol in *Cinnamomum tamala* Nees and Eberm. Leaf powder by HPTLC	[90]

(continued)

Table 11.3 (continued)

S. No.	Mobile phase	Remark	References
13	Ethyl acetate-methanol-acetone-acetic acid (5:2:2:1)	Simultaneous densitometric determination of rifampicin and isoniazid with silica gel 60 F_{254} TLC plates	[91]
14	Toluene-methanol-ethyl acetate-formic acid (6.0:1.0:3.0:0.1)	Estimation of rosuvastatin calcium in its bulk drug and pharmaceutical formulations by the use of silica gel 60 F_{254} HPTLC plates	[92]
15	Methanol-toluene-ethyl acetate-glacial acetic acid (2:9:0.5:0.5)	Simultaneous HPTLC estimation of cinnarizine and domperidone in tablets using silica gel 60 GF_{254} thin-layer chromatographic plates	[93]
16	Ethyl acetate-methanol-ammonia solution (8.5:2.0:1.0)	Simultaneous analysis of amlodipine and benazepril in pharmaceutical formulations using silica gel 60 F_{254} HPTLC plates prewashed with methanol	[94]
17	Ethyl acetate-*n*-butanol-25% aqueous ammonia-methanol (21:5.0:4.0:5.0)	Densitometric determination of desloratadine in tablets	[95]
18	Toluene-ethyl acetate (10:1)	Fast and selective chromatographic separation of plasticizers on thin layers of inorganic ion-exchanger stannic silicate	[96]
19	Ethyl acetate-methanol-ammonia solution (8.5:2.0:1.0)	Simultaneous analysis of amlodipine and benazepril in pharmaceutical formulations on silica gel 60 F_{254} HPTLC plates prewashed with methanol	[97]
20	Hexane-ethyl acetate-acetic acid (22:20:5; 25:20:2; 25:20:5; and 25:20:8)	Separation of bile acids on glass plates precoated with silica gel 60 F_{254}	[98]
21	Toluene-ethyl acetate-triethylamine-methanol (7:2:1:1)	Quantitative monitoring of ursolic acid on silica gel HPTLC plates	[99]
22	Ethyl acetate-hexane (20:80)	Analysis of hedychenone, the major marker compound extracted from the rhizomes of *Hedychium spicatum* (Buch-Hem) using silica gel 60 F_{254} plates	[100]
23	Toluene-ethyl acetate-acetic acid (2:8:0.2)	The estimation of artesunate in bulk and pharmaceutical formulations with the aid of silica gel F_{254} as stationary phase	[101]

(continued)

Table 11.3 (continued)

S. No.	Mobile phase	Remark	References
24	Dichloromethane-ethyl acetate-formic acid (9.5:0.5:0.1)	Use of silica TLC coupled with densitometry for the determination of phenobarbital in pharmaceuticals	[102]
25	Ethyl acetate-chloroform-ammonium hydroxide (85:10:5)	Densitometric determination of disopyramide phosphate drug using silica gel 60 F_{245} plates	[103]
26	*n*-Hexane-ethyl acetate-acetone (6:3:2)	HPTLC- densitometry for quantification and identification of nifedipine in tablets on silica gel 60 F_{254} HPTLC plates	[104]
27	Ethyl acetate-carbon tetrachloride-acetic acid (3:4:0.5)	Determination of saccharin in pharmaceuticals by HPTLC using silica gel 60 F_{254} plates	[105]
28	Methanol-ethyl acetate-toluene-triethylamine (1.0:2.5:6.0:0.5)	Estimation of itopride hydrochloride, a gastroprokinetic agent, in its pharmaceutical formulation and in the bulk drug using silica gel 60 F_{254} TLC plates	[106]
29	Hexane-ethyl acetate (75:25)	Convenient method for standardization of *Piper longum* – an ayurvedic medicinal plant with the use of silica gel 60 F_{254} HPTLC plates	[107]
30	Ethyl acetate-*n*-hexane (80:20)	Monitoring the dose of florfenicol in fish feed on silica gel F_{254} HPTLC plates	[108]
31	*n*-Hexane-ethyl acetate-acetone (6:3:2)	Quantification of nitrendipine both as the bulk drug and in pharmaceutical dosage forms by HPTLC densitometry using silica gel 60 F_{254} HPTLC plates	[109]
32	Hexane-ethyl acetate-acetic acid (80:20:0.5)	Separation and quantification of valerenic acid in *Valeriana jatamansi* and *Valeriana officinalis* antification by HPTLC	[110]
33	Ethyl acetate-hexane-ammonia (100:15:15)	Screening of counterfeit drugs of macrolide antibiotics on silica gel GF_{254} plate (5 × 10 cm)	[111]
34	Cyclohexane-ether, cyclohexane-ether and ethyl acetate	Detection of chemical interactions of vitamins A and D with drugs on silica gel 60 F_{254} TLC	[112]

(continued)

Table 11.3 (continued)

S. No.	Mobile phase	Remark	References
35	Ethyl acetate-*n*-heptane-methanol-diethylamine (3:4.5:1:0.2) for bifonazole and benzyl alcohol; *n*-butyl acetate-*n*-heptane-methanol-diethylamine (3:4.5:1:0.2) for clotrimazole; and benzyl alcohol and *n*-butyl acetate-carbon tetrachloride-methanol-diethylamine (3:6:2.5:0.5) for miconazole and benzoic acid	Determination of some antimycotic imidazole derivatives and preservatives in medicinal creams by HPTLC	[113]
36	Chloroform-ethyl acetate-formic acid (5:4:1)	Application of densitometry and spectrophotometry for determination of gallic acid in tea after chromatographic separation	[114]
37	Methanol-chloroform-ethyl acetate (2:1:1)	Determination of vincamine in presence of its degradation product by HPTLC	[115]
38	*n*-Hexane-ethyl acetate (7:3)	Densitometric standardization of herbal medical products containing *Evolvulus alsinoides* by quantification of a marker compound on aluminum-backed silica gel 60 F_{254} plates	[116]
39	Ethyl acetate-water-formic acid-acetic acid (25:4:0.6:0.4)	Qualitative and quantitative analysis of catechin in methanolic extracts from 15 taxa of Rosa L. hips on glass silica gel 60 F_{254} plates	[117]
40	Nonaqueous eluents consisting of *n*-heptane and polar modifier (tetrahydrofuran, ethyl acetate, or 2-propanol)	Retention of *ortho*- and *para*-positional isomers of some model solutes on cyanopropyl layer in RP systems	[118]
41	Ethyl acetate-diisopropyl ether (10:90)	Preparative separation of the complex mixture of pesticides on silica layer	[119]
42	Nonpolar diluent (benzene)-polar modifier (acetonitrile, ethyl acetate, or dioxane)	Chromatographic behavior of seven 16-oximino derivatives of 3β-hydropxy-5-androstene on silica gel HPTLC plates	[120]
43	*n*-Hexane-ethyl acetate-acetic acid, in various compositions	Study on the influence of temperature on retention and separation of selected bile acids using glass plates precoated with silica gel 60 F_{254} without and with concentrating zone (#1.05715) and aluminum plates precoated with the mixture of silica gel 60 F_{254} and kieselguhr F_{254}	[121]

Note: Solvent compositions were by volume

Table 11.4 Application of surfactants as one of the component or mobile phase in thin-layer chromatography (2005–2010)

S. No.	Mobile phase	Remark	References
1	Surfactant (cationic, anionic, or nonionic) in the mobile phase	Study of adsorption behavior of chromium(VI) and molybdenum(VI) on six types of soil thin layers by soil TLC	[122]
2	0.1% Aqueous solution cetrimide (cationic surfactant)	Separation of closely related amino acids from their mixtures on silica gel impregnated with 0.1% aqueous solution (below CMC) of nonionic surfactant (Brij-35)	[123]
3	Aqueous solutions of surfactants	Evaluation of the effect of surfactants on the adsorption and movement of carbaryl in soils by soil TLC	[124]
4	1% Aqueous *N*-cetyl-*N*,*N*,*N*-trimethylammonium bromide (CTAB)-acetic acid (4:5:1)	Identification and separation of two different drugs (paracetamol and diclofenac sodium) on silica gel H layers	[125]
5	5% Aqueous cetylpyridinium chloride	Rapid mutual separation of Zn^{2+}, Cd^{2+}, and Hg^{2+} on silica as stationary phase	[126]
6	CTAB-alcohol-water	Separation of opium alkaloids on silica gel G TLC plates	[127]
7	Aqueous solution of TX-100 (10^{-4} M, pH = 0.8)	Separation of coexisting Cr^{6+}, Mn^{2+} and Fe^{3+} on 0.1 M thiourea impregnated silica gel layer	[128]
8	0.1% Aqueous solution of Cween 80	Mutual separation of five water-soluble vitamins (folic acid, cyanocobalamin, thiamine, pyridoxine, and riboflavin) on silica layer impregnated with 0.01% sodium dodecyl sulfate (SDS)	[129]
9	Aqueous solutions of cationic (CTAB), nonionic *t*-octylphenoxydecaethoxy-ethanol (Triton X-100) and anionic, sodium dodecyl sulfate (SDS) surfactants at different concentrations	Use of soil as layer material for identification and separation of Cd and Zn ions by soil TLC	[130]
10	5.0% Aqueous sodium deoxycholate (NaDC)-acetonitrile (1:3)	Resolution of five coexisting nucleobases (adenine, guanine, cytosine, thymine, and uracil) on aluminum-backed cellulose 60 F_{254} plates	[131]

Note: Solvent compositions were by volume

Table 11.5 Application of *n*-butanol as one of the components of mobile phase in thin-layer chromatography (2005–2010)

S. No.	Mobile phase	Remark	References
1	*n*-Butyl alcohol-70% aqueous ethylene glycol-ethyl acetate (5:3:2)	Separation of amino acids from their multicomponent mixtures by silica TLC	[132]
2	Chloroform-*n*-butanol-methanol-acetic acid-water (4.5:12.5:5:1.5:1.5)	Differentiation among the polysaccharides present in six traditional Chinese medicines on silica gel HPTLC plates	[133]
3	Toluene-*n*-butanol-triethylamine (8.5:2:0.5)	HPTLC determination of cefuroxime axetil and ornidazole in combined tablet dosage form on precoated silica gel aluminum plate 60 F_{254}	[134]
4	Butanol-acetic acid-water (4:1:2)	Separation of penicillins (benzylpenicillin, ampicillin, and amoxicillin) and cephalosporins (cephalexin, cefoperazone, ceftriaxone, cefixime, and cefadroxil) on silica gel layers precoated with fluorescent material	[135]
5	Mixed aqueous-organic solvents containing *n*-butanol, acetone or chloroform, acetonitrile, and ammonia (10%) in different ratios	Concomitant estimation of purines like adenosine (Ade) and its major metabolites, inosine (Ino) and hypoxanthine (Hypoxan) in rat brain tissue preparations on using aluminum plates precoated with silica gel 60 F_{254}	[136]
6	1-Butanol in combination of aprotic organic solvents as modifying additives	Separation of several amino acids on silica gel stationary phase	[137]
7	*n*-Butanol-chloroform-acetic acid-ammonium hydroxide-water (9:3:5:1:2)	Quantitative analysis of ketorolac (the free acid of the tromethamine salt) in human plasma by HPTLC densitometry using silica gel 60 plates	[138]
8	*n*-Butanol-glacial acetic acid-distilled water (7.0:2.0:1.0)	Quantification of dopamine in dried whole-plant powder of *Portulaca oleracea* Linn. HPTLC	[139]
9	*n*-Butanol-acetic acid-water (4.0:1.0:1.0)	A HPTLC method for the analysis of L-dopa in *Mucuna pruriens* seed extract and its formulations using silica gel HPTLC plates	[140]
10	Acetone-chloroform-*n*-butanol-glacial acetic acid-water (5:10:10:2.5:2.5)	Study of the chemical stability of haloperidol lactate injection on precoated silica gel F_{254} HPTLC plates	[141]

(continued)

Table 11.5 (continued)

S. No.	Mobile phase	Remark	References
11	*n*-Butanol-methanol-ammonia (5:1:1.5)	Simultaneous determination of levofloxacin hemihydrate and ornidazole in tablet dosage form on Merck TLC aluminum sheets of silica gel 60 F_{254}	[142]
12	Acetone-chloroform-*n*-butanol-acetic acid glacial-water (60:40:40:40:35)	Quantitative analysis of L-dopa in tablets on precoated silica gel F_{254} HPTLC plates	[143]
13	*n*-Butanol-acetic acid-distilled water (8:4:2)	Qualitative and quantitative analysis of amino acids in complex matrices on cellulose based thin-layer chromatography (TLC) sheets	[144]
14	*n*-Butanol-methanol-ammonia (6 M) (8:1:1.5)	Estimation of gatifloxacin and ornidazole in combined tablets by HPTLC using silica gel 60 F_{254} TLC plate	[145]
15	Butanol-ethanol-water (5:3:2)	Optimal separation of fructooligosaccharides in dietetic products as well as in the samples from intestinal tract of monogastric on glass-backed precoated silica gel layers impregnated with sodium acetate	[146]
16	Butanol-acetic acid-water in different ratios	Purity evaluation of 4-methoxy-2-(3(4-phenyl-1-piperazinyl)) propyl-2,3-dihydro-6-methyl-1,3-dioxo-1*H*-pyrrolo[3,4-c]pyridine on silica gel–coated plates (60 F_{254}) using HPLC and TLC techniques	[147]
17	Methanol and methanol-*n*-butanol-ammonia (25%)-chloroform (14:4:9:12)	Rapid identification and quantitative determination of polymyxin B, framycetin, and dexamethasone in a dental ointment by HPTLC with silica gel 60 and F_{254} plates	[148]
18	Butanol-ethanol-2 M ammonia (3:1:1) and butanol-acetic acid-water (12:3:5) mixtures	Separation of commercially available red and blue ink samples on different stationary phases containing diatomaceous earth as principal component	[149]
19	Butanol-water-acetic acid (50:40:10)	Analysis of saponin content in a herbal medicine product (HMP) on silica gel HPTLC plates	[150]
20	Acetone-chloroform-*n*-butanol-acetic acid glacial-water (60:40:40:40:35)	Quantitative analysis of L-dopa in tablets using precoated silica gel F_{254} HPTLC plates	[151]

(continued)

Table 11.5 (continued)

S. No.	Mobile phase	Remark	References
21	*n*-Butanol-methanol-acetic acid-water (4:1.5:1:1)	Densitometric TLC method for analysis of trigonelline and 4-hydrooxyisoleucine extracted from fenugreek seeds	[152]
22	*n*-Butanol-2-propanol-triethylamine (8.5:2:0.5)	Determination and separation of clopamide and impurities (4-chlorobenzoic and 4-chloro-3-sulfamoyl benzoic acids) by HPTLC	[153]
23	Butanol-1-glacial acetic acid-water (12.8:2:2.8)	Determination of oxyhyphenonium bromide and its degradation products on silica gel F_{254} plates	[154]
24	*n*-Butanol-acetone-acetic acid (5:5:3)	TLC separation of catechins and theaflavins on polyamide plates	[155]
25	*t*-Butanol-ethylacetate-glacial acetic acid-water (7:4:2:2)	Simultaneous estimation of ibuprofen and pseudoephedrine hydrochloride in tablets using silica gel 60 F_{254} as stationary phase	[156]
26	Butanol-acetic acid-water (2:2:1)	Analysis of fructooligosaccharides used as feed additives in biological samples on glass-backed precoated silica gel layers impregnated with sodium acetate	[157]
27	1-Butanol saturated with 5% EDTA aqueous solution (pH = 9)	Determination of tetracycline, oxytetracycline, and chlorotetracycline in milk by silica TLC, column chromatography and spectrophotometry	[158]
28	Butanol-ammonia (25%) in 8:2 ratio	TLC- densitometry and spectroflourimetry for direct determination of telmisartan (TELM) and hydrochlorothiazide (HCT) in combined dosage forms	[159]
29	*n*-Butanol-acetic acid-water (6:2:2)	TLC- densitometric method for estimation of alliin from garlic and its formulations	[160]
30	*n*-Butanol-2-propanol–water-methylene chloride (10:7:2:5:3)	Chromatographic-densitometric method for determination of clopamide and 4-chlorobenzoic, and 4-chloro-3-sulfamoylbenzoic acids in tablets	[161]

Note: Solvent compositions were by volume

Table 11.6 Application of *n*-butyl acetate as one of the components of mobile phase in thin-layer chromatography (2005–2010)

S. No.	Mobile phase	Remark	References
1	*n*-Butyl acetate-chloroform-glacial acetic acid (1:8:1)	Use of HPLC and HPTLC techniques for the simultaneous determination of rosuvastatin and ezetimibe in a combined tablet dosage form by the use of aluminum-backed sheet of silica gel 60 F_{254} layers	[162]
2	*n*-Butyl acetate-carbon tetrachloride-acetic acid-acetonitrile (3:6:0.2:3)	Simultaneous determination of loratadine and preservatives in loratadine-sodium benzoate and loratadine-methylparaben-propylparaben mixtures using aluminum plates precoated with silica gel 60 F_{254}	[163]
3	*n*-Butyl acetate-formic acid-chloroform (6:4:2)	Simultaneous estimation of tizanidine and rofecoxib in tablet formulation by HPTLC using silica gel F_{254} TLC plate	[164]
4	*n*-Butyl acetate-*n*-heptane-methanol-diethylamine (3:4.5:1:0.2) and *n*-butyl acetate-carbon tetrachloride-methanol-diethylamine (3:6:2.5:0.5)	Analysis of antimycotics (bifonazole, clotrimazole, and miconazole) and preservatives (benzyl alcohol and benzoic acid) on silica gel plates	[165]
5	*n*-Butyl acetate-carbon tetra-chloride-methanol-diethylamine (3:6:2.5:0.5)	Separation and quantitative determination of econazole nitrate on silica gel HPTLC plates	[166]

Note: Solvent compositions were by volume

Table 11.7 Application of ethylene glycol as one of the components of mobile phase in thin-layer chromatography (2005–2010)

S. No.	Mobile phase	Remark	Reference
1	*n*-Butyl alcohol-70% aqueous ethylene glycol-ethyl acetate (5:3:2)	Separation of amino acids from their complex mixtures on silica and kieselguhr static flat bed	[167]
2	Aqueous ammonium sulfate solutions as mobile phase with polyethylene glycol impregnated silica gel stationary phase	Salting-out thin-layer chromatography of 15 mixed aminocarboxylate Co(III) complexes on silica gel impregnated with poly(ethylene glycol) of different molecular mass	[168]

Note: Solvent compositions were by volume

Acknowledgments The authors extend their appreciation to the Department of Applied Chemistry, Aligarh Muslim University, Aligarh, for generous support and the Deanship of Scientific Research at King Saud University for funding the work through the research group project No. RGP-VPP-130.

References

1. de la Guardia M, Khalaf KD, Carbonell V, Morales-Rubio A (1995) Anal Chim Acta 308:462
2. Anastas PT, Warner JC (1998) Green chemistry: theory and practice. Oxford University Press, New York
3. Shirkhedkar AA, Surana SJ (2010) Development and validation of a reversed-phase high-performance thin-layer chromatography densitometric method for determination of atorvastatin calcium in bulk drug and tablets. J AOAC Int 93:798–803
4. Rajesh T, Lakshmi KS, Sharma S et al (2010) Use of a validated stability-indicating HPTLC method to study the degradation of rimonabant. J Planar Chromatogr Mod TLC 23:148–155
5. Casoni D, Cobzac CS, Sarbu C (2010) A comparative study concerning the lipophilicity of some synthetic dyes estimated by thin layer chromatography and different computation methods. Revista de Chimie 61:229–234
6. Satheeshkumar N, Mukherjee PK, Bhadra S et al (2010) Acetylcholinesterase enzyme inhibitory potential of standardized extract of Trigonella foenum graecum L and its constituents. Phytomedicine 17:292–295
7. Parys W, Pyka A (2010) Influence of pH water on the lipophilicity of nicotinic acid and its derivatives investigated by RP. J Liq Chromatogr Relat Technol 33:1307–1318
8. Pyka A, Rusek D et al (2010) Use of RP-TLC and theoretical computational methods to compare the lipophilicity of salicylic acid and its derivatives. J Liq Chromatogr Relat Technol 33:179–190
9. Varsha MJ, Uttam SK, Sachin B et al (2009) Development and validation of HPTLC method for determination of glycyrrhizin in herbal extract and in herbal gel. Int J Chemtech Res 1:826–831
10. Djaković-Sekulić T, Perisić-Janjić N, Djurendi E (2009) Retention data from reverse-phase high-performance thin-layer chromatography in characterization of some bis-salicylic acid derivatives. Biomed Chromatogr 23:881–887
11. Casoni D, Sârbu C (2009) The lipophilicity of parabens estimated on reverse phases chemically bonded and oil-impregnated plates and calculated using different computation methods. J Sep Sci 32:2377–2384
12. Stroka J, Doncheva I, Spangenberg B (2009) Determination of sucralose in soft drinks by high-performance thin-layer chromatography: interlaboratory study. J AOAC Int 92: 1153–1159
13. Zarzycki PK, Włodarczyk E, Zarzycka MB et al (2009) Optimization of a solid-phase extraction protocol for fractionation of selected steroids using retention data from micro thin-layer chromatography. Anal Sci 25:935–939
14. Hiegel K, Spangenberg B (2009) New method for the quantification of dequalinium cations in pharmaceutical samples by absorption and fluorescence diode array thin-layer chromatography. J Chromatogr A 1216:5052–5056
15. Sathiyanarayanan L, Kulkarni PV, Nikam AR et al (2011) Rapid densitometric method for simultaneous analysis of famotidine and domperidone in commercial formulations using HPTLC. Der Pharma Chemica 3:134–143
16. Nascu-Briciu RD, Sârb C (2010) The lipophilicity determination of some pesticides by high performance thin-layer chromatography and various computing methods. Studia Universitatis Babes-Bolyai Chemia 105–117

17. Onişor C, Blăniță G, Coroş M (2010) A comparative study concerning chromatographic retention and computed partition coefficients of some precursors of peraza crown ethers. Cent Eur J Chem 8:1203–1209
18. Li Z, Merfort I, Reich E (2010) High-performance thin layer chromatography for quality control of multicomponent herbal drugs: example of Cangzhu Xianglian San. J AOAC Int 93:1390–1398
19. Pikul P, Nowakowska J, Rogulski P (2010) Simple thin-layer chromatographic method for analysis of ranitidine in its pharmaceutical formulations: application to the analysis of photolytic degradation products. J Planar Chromatogr Mod TLC 23:304–308
20. Migas P, Świtka M (2010) TLC with an adsorbent gradient for the analysis of taxol in Taxus baccata L. J Planar Chromatogr Mod TLC 23:286–288
21. Dhoka MV, Gawande VT, Joshi PP (2010) HPTLC determination of amoxicillin trihydrate and bromhexine hydrochloride in oral solid dosage forms. J Pharma Sci Res 2:477–483
22. Anand M, Gandhi PS, Nancy P et al (2010) Validated high performance thin layer chromatographic method for estimation of olopatadine hydrochloride as bulk drug and in ophthalmic solutions. Int J Chemtech Res 2:1372–1375
23. Soponar F, Mot AC, Sârbu C (2010) High-performance thin-layer chromatography and three-dimensional image analysis for the determination of rutin in pharmaceutical preparations. J AOAC Int 93:804–810
24. Shirkhedkar AA, Surana SJ (2010) Development and validation of a reversed-phase high-performance thin-layer chromatography-densitometric method for determination of atorvastatin calcium in bulk drug and tablets. J AOAC Int 93:798–803
25. Alina P (2009) Use of RP-TLC and densitometry to analytical characteristic of vitamin k1. J Planar Chromatogr Mod TLC 22:211–215
26. Morlock GE, Oellig C (2009) Rapid planar chromatographic analysis of 25 water-soluble dyes used as food additives. J AOAC Int 92:745–756
27. Jain N, Jain GK, Iqbal Z et al (2009) An HPTLC method for the determination of minocycline in human plasma, saliva, and gingival fluid after single step liquid extraction. Anal Sci 25:57–62
28. Bhushan R, Agarwal C (2008) Direct TLC resolution of (±)-ketamine and (±)-lisinopril by use of (+)-tartaric acid or (−)-mandelic acid as impregnating reagents or mobile phase additives. Isolation of the enantiomers. Chromatographia 68:1045–1051
29. Sharma UK, Sharma N, Gupta AP et al (2007) RP-HPTLC densitometric determination and validation of vanillin and related phenolic compounds in accelerated solvent extract of Vanilla planifolia. J Sep Sci 30:3174–3180
30. Jain GK, Jain N, Iqbal Z et al (2007) Development and validation of an HPTLC method for determination of minocycline in human plasma. Acta Chromatogr 197–205
31. Suryavanshi VL, Sathe PA, Baing MM et al (2007) Determination of Rutin in Amaranthus spinosus Linn. Whole plant powder by HPTLC. Chromatographia 65:767–769
32. Bhandari P, Kumar N, Gupta AP et al (2007) A rapid RP-HPTLC densitometry method for simultaneous determination of major flavonoids in important medicinal plants. J Sep Sci 30:2092–2096
33. Sam S, Kumar WD, Vijai ARA et al (2010) Derivatized HPTLC method for simultaneous estimation of glucosamine and ibuprofen in tablets. J Pharm Res Health Care 2:156–162
34. Mohammad A, Zehra A (2010) Anionic-nonionic surfactants coupled micellar thin-layer chromatography: synergistic effect on simultaneous separation of hydrophilic vitamins. J Chromatogr Sci 48:145–149
35. Eneda S, Olga M, Nieto A (2009) Stability by thin-layer chromatography from Quassia amara and Maytenus ilicifolia tinctures. Revista de cubana de Farmacia 43:93–101
36. Urszula H, Jan K, Magorzata S (2009) Current chromatographic-densitometric method for determination of clopamide and 4-chlorobenzoic, and 4-chloro-3-sulfamoylbenzoic acids in tablets. Pharm Anal 5:408–415
37. Shirkhedkar AA, Surana SJ (2009) Application of a stability-indicating densitometric RP-TLC method for analysis of pioglitazone hydrochloride in the bulk material and in pharmaceutical formulations. J Planar Chromatogr Mod TLC 22:191–196

38. Waszkielewicz A, Szkaradek N, Pekala E et al (2010) The study of the lipophilicity of some aminoalkanol derivatives with anticonvulsant activity. Biomed Chromatogr 2:1365–1372
39. Sharma MC, Sharma S (2010) Development and validation of an HPTLC method for determination of oseltamivir phosphate in pharmaceutical dosage form. Indian Drugs 47:68–72
40. Naguib IA, Abdelkawy M (2010) Development and validation of stability indicating HPLC and HPTLC methods for determination of sulpiride and mebeverine hydrochloride in combination. European J Med Chem 45:3719–3725
41. Djaković-Sekuli TL, Smoliński A (2010) Chemometric characterization of s-triazine derivatives in relation to structural parameters and biological activity. Drug Dev Ind Pharm 36:954–961
42. Vovk I, Simonovska B, Vuorela H (2005) Separation of eight selected flavan-3-ols on cellulose thin-layer chromatographic plates. J Chromatogr A 1077:188–194
43. Modi KP, Patel NM, Goyal RK (2008) Estimation of L-dopa from Mucuna pruriens LINN and formulations containing M. pruriens by HPTLC method. Chem Pharm Bull (Tokyo) 56: 357–359
44. Petruczynik A, Brończyk M, Tuzimski T et al (2008) Analysis of selected anti-depressive drugs by high performance thin-layer chromatography. J Liq Chromatogr Relat Technol 31: 1913–1924
45. Stolarczyk M, Anna M, Krzek J (2008) Chromatographic and densitometric analysis of hydrochlorothiazide, walsartan, kandesartan, and enalapril in selected complex hypotensive drugs. J Liq Chromatogr Relat Technol 31:1892–1902
46. Pyka A, Klimczok W (2007) Application of densitometry for the evaluation of the separation effect of nicotinic acid derivatives. Part III. Nicotinic acid and its derivatives. J Liq Chromatogr Relat Technol 30:3107–3118
47. Mennickent S, Nail M, Vega M et al (2007) Quantitative determination of L-DOPA in tablets by high performance thin layer chromatography. J Sep Sci 30:1893–1898
48. Panahi HA, Rahimi A, Moniri E et al (2010) HPTLC separation and quantitative analysis of aspirin, salicylic acid, and sulfosalicylic acid. J Planar Chromatogr Mod TLC 23:137–140
49. Hadzifejzovic N, Antosch J, Hubbert M et al (2010) Establishment of xylose in Plantago Ovata Forssk as a leading compound for quantification in raw material and finished product. J Liq Chromatogr Relat Technol 33:996–1004
50. Dipti BP, Natubhai JP (2009) Development and validation of reverse phase high performance liquid chromatography and high performance thin layer chromatography methods for estimation of alfuzosin hydrochloride in bulk and in pharmaceutical formulations. Int J Chemtech Res 1:985–990
51. Sharma N, Sharma UK, Gupta AP et al (2009) Simultaneous densitometric determination of shikonin, acetylshikonin, and beta-acetoxyisovaleryl-shikonin in ultrasonic-assisted extracts of four Arnebia species using reversed-phase thin layer chromatography. J Sep Sci 32:3239–3245
52. Shanker K, Gupta S, Srivastava P et al (2011) Simultaneous determination of three steroidal glycoalkaloids in Solanum xanthocarpum by high performance thin layer chromatography. J Pharm Biomed Anal 54:497–502
53. James J, Dubery I (2011) Identification and quantification of triterpenoid centelloids in Centella asiatica (L.) Urban by densitometric TLC. J Planar Chromatogr Mod TLC 24: 82–87
54. Dabrowska M, Starek M, Pikulska S (2011) Simultaneous identification and quantitative analysis of eight cephalosporins in pharmaceutical formulations by TLC-densitometry. J Planar Chromatogr Mod TLC 24:23–29
55. Shaiba M, Maheswari R, Chakraborty R et al (2011) High performance thin layer chromatographic estimation of tolterodine tartarate. Res J Pharm Biol Chem Sci 2:6–11
56. Hałka A, Płocharz P, Torbicz A (2010) Reversed-phase pressurized planar electrochromatography and planar chromatography of acetylsalicylic acid, caffeine, and acetaminophen. J Planar Chromatogr Mod TLC 23:420–425
57. Lakshmi KS, Sivasubramanian L, Pal K (2010) Stability indicating HPTLC method for simultaneous determination of telmisartan and ramipril in tablets. Int J Pharm Pharm Sci 2:127–129

58. Pikul P, Rogulski P (2010) TLC of aclarubicin and doxycycline with mixed n -alcohol mobile phases. J Planar Chromatogr Mod TLC 23:353–358
59. Abdel-Fattah LS, El-Sherif ZA, Kilani KM et al (2010) HPLC, TLC, and first-derivative spectrophotometry stability-indicating methods for the determination of tropisetron in the presence of its acid degradates. J AOAC Int 93:1180–1191
60. Counihan J, Fried B, Sherma J (2010) Effects of Echinostoma caproni infection on the neutral and polar lipids of intestinal and non-intestinal organs in the BALB/c mouse as determined by high-performance thin-layer chromatography. J Parasitol Res 107:947–953
61. Wang J, Tang F, Yue Y et al (2010) Development and validation of an HPTLC method for simultaneous quantitation of isoorientin, isovitexin, orientin, and vitexin in bamboo-leaf flavonoids. J AOAC Int 93:1376–1383
62. Dabrowska M, Krzek J (2010) Separation, identification, and quantitative analysis of the epimers of cefaclor by TLC-densitometry. J Planar Chromatogr Mod TLC 23:265–269
63. Kumar A, Lakshman K, Jayaveera KN et al (2010) Estimation of gallic acid, rutin and quercetin in terminalia chebula by HPTLC. Jordan J Pharm Sci 3:63–68
64. Briciu RD, Kot-Wasik A, Wasik A et al (2010) The lipophilicity of artificial and natural sweeteners estimated by reversed-phase thin-layer chromatography and computed by various methods. J Chromatogr A 1217:3702–3706
65. Broszat M, Welle C, Wojnowski M et al (2010) A versatile method for quantification of aflatoxins and ochratoxin A in dried figs. J Planar Chromatogr Mod TLC 23:193–197
66. Mennickent S, Pino L, Vega M et al (2008) Chemical stability of haloperidol injection by high performance thin-layer chromatography. J Sep Sci 3:201–206
67. Mennickent S, Nail M, Vega M et al (2007) Quantitative determination of L-DOPA in tablets by high performance thin layer chromatography. J Sep Sci 30:1893–1898
68. Szaufer-Hajdrych M, Bylka W, MatłAwska I et al (2008) Densitometric HPTLC and HPLC analysis of phenolic acids from Aquilegia vulgaris. Acta Chromatographica 20:685–695
69. Akula KK, Kaur M, Kulkarni SK (2008) Estimation of adenosine and its major metabolites in brain tissues of rats using high-performance thin-layer chromatography-densitometry. J Chromatogr A 1209:230–237
70. López-Bojórquez E, Castañeda-Hernández G, González-de la Parra M et al (2008) Development and validation of a high-performance thin-layer chromatographic method, with densitometry, for quantitative analysis of ketorolac tromethamine in human plasma. J AOAC Int 91:1191–1195
71. Bazylko A, Kiss AK, Kowalski J (2007) High-performance thin-layer chromatography method for quantitative determination of oenothein B and quercetin glucuronide in aqueous extract of Epilobii angustifolii herba. J Chromatogr A 1173:146–150
72. Jain N, Jain GK, Ahmad FJ et al (2007) Validated stability-indicating densitometric thin-layer chromatography: application to stress degradation studies of minocycline. Anal Chim Acta 599:302–309
73. Bazylko A, Kiss AK, Kowalski J (2007) Densitometric determination of flavonoids in methanolic and aqueous extracts of Epilobii angustifolii herba by use of HPTLC. J Planar Chromatogr Mod TLC 20:53–56
74. Jarusiewicz JA, Sherma J, Fried B (2006) Thin layer chromatographic analysis of glucose and maltose in estivated Biomphalaria glabrata snails and those infected with Schistosoma mansoni. Comp Biochem Physiol B Biochem Mol Biol 145:346–349
75. Bilušić VV, Maleš Ž, Plazibat M et al (2005) HPTLC determination of flavonoids and phenolic acids in some Croatian Stachys taxa. J Planar Chromatogr Mod TLC 18:269–273
76. Nowak R, Hawrył M (2005) Application of densitometry to the determination of catechin in rose-hip extracts. J Planar Chromatogr Mod TLC 18:217–220
77. Ludwiczuk A, Nyiredy S, Wolski T (2005) Separation of the ginsenosides fraction obtained from the roots of Panax quinquefolium L. Cultivated in Poland. J Planar Chromatogr Mod TLC 18:104–107
78. Fang C, Wan X, Jiang C (2005) Comparison of HPTLC and HPLC for determination of isoflavonoids in several kudzu samples. J Planar Chromatogr Mod TLC 18:73–77

79. Patel BH, Suhagia BN, Patel MM et al (2007) Simultaneous estimation of pantoprazole and domperidone in pure powder and a pharmaceutical formulation by high-performance liquid chromatography and high-performance thin-layer chromatography methods. J AOAC Int 90:142–146
80. Dighe VV, Sane RT, Menon SN (2006) Simultaneous determination of diclofenac sodium and paracetamol in a pharmaceutical preparation and in bulk drug powder by high-performance thin-layer chromatography. J Planar Chromatogr Mod TLC 19:443–448
81. Verma JK, Joshi AV (2006) Rapid HPTLC method for identification and quantification of curcumin, piperine and thymol in an ayurvedic formulation. J Planar Chromatogr Mod TLC 19:398–400
82. Ayad MM, Youssef NF, Abdellatif HE (2006) A comparative study on various spectrometries with thin layer chromatography for simultaneous analysis of drotaverine and nifuroxazide in capsules. Chem Pharm Bull 54:807–813
83. Eish MYZA, Wells MJM (2006) Assessing the trihalomethane formation potential of aquatic fulvic and humic acids fractionated using thin-layer chromatography. J Chromatogr A 1116: 272–276
84. Jamshidi A, Mobedi H, Ahmad KF (2006) Stability-indicating HPTLC assay for leuprolide acetate. J Planar Chromatogr Mod TLC 19:223–227
85. Patel LJ, Suhagia BN, Shah PB et al (2006) RP-HPLC and HPTLC methods for the estimation of carvedilol in bulk drug and pharmaceutical formulations. Indian J Pharm Sci 68:790–793
86. Bonfill M, Mangas S, Cusidó RM et al (2006) Identification of triterpenoid compounds of Centella asiatica by thin-layer chromatography and mass spectrometry. Biomed Chromatogr 20:151–153
87. Kowalczuk D (2005) Simultaneous high-performance thin-layer chromatography densitometric assay of trandolapril and verapamil in the combination preparation. J AOAC Int 88: 1525–1529
88. Widmer V, Schibli A, Reich E (2005) Quantitative determination of β-asarone in calamus by high-performance thin-layer chromatography. J AOAC Int 88:1562–1567
89. Gbaguidi F, Muccioli G, Accrombessi G (2005) Densitometric HPTLC quantification of 2-azaanthraquinone isolated from Mitracarpus scaber and antimicrobial activity against Dermatophilus congolensis. J Planar Chromatogr Mod TLC 18:377–379
90. Dighe VV, Gursale AA, Sane RT et al (2005) Quantification of eugenol in Cinnamomum tamala Nees and Eberm. Leaf powder by high-performance thin-layer chromatography. J Planar Chromatogr Mod TLC 18:305–307
91. Tatarczak M, Flieger J, Szumiło H (2005) Simultaneous densitometric determination of rifampicin and isoniazid by high-performance thin-layer chromatography. J Planar Chromatogr Mod TLC 18:207–211
92. Sane RT, Kamat SS, Menon SN (2005) Determination of rosuvastatin calcium in its bulk drug and pharmaceutical preparations by high-performance thin-layer chromatography. J Planar Chromatogr Mod TLC 18:194–198
93. Bagade SB, Walode SG, Charde MS et al (2005) Simultaneous HPTLC estimation of cinnarizine and domperidone in their combined dose tablet. Asian J Chem 17:1116–1126
94. Meyyanathan SN, Suresh B (2005) HPTLC method for the simultaneous determination of amlodipine and benazepril in their formulations. J Chromatogr Sci 43:73–75
95. Sumarlik E, Tampubolon HB, Yuwono M et al (2005) Densitometric determination of desloratadine in tablets, and validation of the method. J Planar Chromatogr Mod TLC 18:19–22
96. Mirzaie AJ, Waqif-Husain S (2007) Fast chromatographic separation of plasticizers on thin layers of an inorganic ion-exchanger: quantitative determination of di(2-ethylhexyl)phthalate. Chromatographia 65:245–248
97. Meyyanathan SN, Suresh B (2005) HPTLC method for the simultaneous determination of amlodipine and benazepril in their formulations. J Chromatogr Sci 43:73–75
98. Pyka A, Doowy M, Gurak D (2005) Separation of selected bile acids by TLC. VIII. Separation on silica gel 60F254 glass plates impregnated with Cu(II), Ni(II), Fe(II), and Mn(II) cations. J Liq Chromatogr Relat Technol 28:2273–2284

99. Shetty P, Mangaonkar K, Sane RT (2007) HPTLC determination of ursolic acid in Alstonia scholaris R Br. J Planar Chromatogr Mod TLC 20:65–68
100. Pullela V, Srinivas SA, Vanka UMS et al (2007) A new, convenient method for quantitative analysis of hedychenone, an anti-inflammatory compound in the rhizomes of Hedychium spicatum (Buch-Hem). J Planar Chromatogr Mod TLC 20:73–74
101. Agarwal S, Ali A, Ahuja S (2007) HPTLC determination of artesunate as bulk drug and in pharmaceutical formulations. Indian J Pharm Sci 69:841–844
102. Wójciak KM, Skalska A, Matysik G et al (2006) Quantitative analysis of phenobarbital in dosage form by thin-layer chromatography combined with densitometry. J AOAC Int 89: 995–998
103. Salem MY, Ramadan NK, Moustafa A (2006) Stability-indicating methods for the determination of disopyramide phosphate. J AOAC Int 89:976–986
104. Kowalczuk D, Wawrzycka MB, Maj AH (2006) Application of an HPTLC densitometric method for quantification and identification of nifedipine. J Liq Chromatogr Relat Technol 29:2863–2873
105. Čakar M, Popović G (2006) Determination of saccharin in pharmaceuticals by high performance thin layer chromatography. J Serb Chem Soc 71:669–676
106. Dighev V, Sane RT, Menon SN (2006) High-performance thin-layer chromatographic determination of itopride hydrochloride in its pharmaceutical preparation and in the bulk drug. J Planar Chromatogr Mod TLC 19:319–323
107. Sarma VUM, Srinivas PV, Anuradha V (2006) A simple and convenient method of standardization of Piper longum – an ayurvedic medicinal plant. J Planar Chromatogr Mod TLC 19: 238–240
108. Vega MH, Jara ET, Aranda MB (2006) Monitoring the dose of florfenicol in medicated salmon feed by planar chromatography (HPTLC). J Planar Chromatogr Mod TLC 19: 204–207
109. Kowalczuk D (2006) Determination of nitrendipine in tablets by HPTLC-densitometry. J Planar Chromatogr Mod TLC 19:135–138
110. Singh N, Gupta AP, Singh B (2006) Quantification of valerenic acid in Valeriana jatamansi and Valeriana officinalis by HPTLC. Chromatographia 63:209–213
111. Hu CQ, Zou WB, Hu WS et al (2006) Establishment of a fast chemical identification system for screening of counterfeit drugs of macrolide antibiotics. J Pharm Biomed Anal 40:68–74
112. Ramić A, Medić-Šarić M, Turina S et al (2006) TLC detection of chemical interactions of vitamins A and D with drugs. J Planar Chromatogr Mod TLC 19:27–31
113. Čakar M, Popović G, Agbaba D (2005) High-performance thin-layer chromatography determination of some antimycotic imidazole derivatives and preservatives in medicinal creams and a gel. J AOAC Int 88:1544–1548
114. Hachula U, Anikiel S, Sajewicz M (2005) Application of densitometry and spectrophotometry for determination of gallic acid in tea after chromatographic separation. J Planar Chromatogr Mod TLC 18:290–293
115. Shehata MAM, El-Sayed MA, El Tarras MF et al (2005) Stability-indicating methods for determination of vincamine in presence of its degradation product. J Pharm Biomed Anal 38: 72–78
116. Patil UK, Dixit VK (2005) Densitometric standardization of herbal medical products containing evolvulus alsinoides by quantification of a marker compound. J Planar Chromatogr Mod TLC 18:234–239
117. Nowak R, Hawrył M (2005) Application of densitometry to the determination of catechin in rose-hip extracts. J Planar Chromatogr Mod TLC 18:217–220
118. Waksmundzka-Hajnos M, Hawrył A, Petruczynik A (2005) Retention of ortho- and para-positional isomers of some model solutes on polar bonded stationary phases in different eluent systems by HPTLC. J Liq Chromatogr Relat Technol 28:907–922
119. Tuzimski T (2005) Two-stage fractionation of a mixture of 10 pesticides by TLC and HPLC. J Liq Chromatogr Relat Technol 28:463–476

120. Perišić-Janjić NU, Djaković-Sekulić TL, Stojanović SZ (2005) HPTLC chromatography of androstene derivates: application of normal phase thin-layer chromatographic retention data in QSAR studies. Steroids 70:137–144
121. Pyka A, Dołwy M, Gurak D (2005) Separation of selected bile acids by TLC. V. Influence of temperature on the separation. J Liq Chromatogr Relat Technol 28:631–640
122. Mohammad A, Moheman A (2010) Adsorption studies of chromium(VI) and molybdenum(VI) through soil static phase. J Appl Sci Research 6:3635–3642
123. Mohammad A, Haq N (2010) Synergistic effect of cationic-nonionic surfactants on simultaneous separation of phenylalanine and tyrosine. Tenside Surfact Det 47:248–253
124. Singh RP, Nabi SA, Singh S (2009) Evaluation of the effect of surfactants on the adsorption and movement of carbaryl in soils of divergent texture. Adsorp Sci Technol 27:921–935
125. Mohammad A, Sharma S (2009) Separation of co-existing paracetamol and diclofenac sodium on silica gel 'H' layers using surfactant mediated mobile phases: identification of diclofenac sodium from human urine. Farmacia 57:201–211
126. Mohammad A, Agrawal V, Shahab H (2007) Cetylpyridinium chloride micelle-mediated mutual separation of zinc, cadmium, and mercury ions by thin-layer chromatography. Acta Chromatogr 185–196
127. Singh DK, Sahu A (2005) Thin layer chromatography of opium alkaloids with hybrid CTAB-alcohol-water mobile phase and estimation of papaverine. HCl and codeine sulphate in pharmaceutical Formulations. J Chin Chem Soc 52:247–251
128. Mohammad A, Luqman M (2005) Thin-layer chromatography of certain metal cations with nonionic surfactant mediated mobile phase systems: separation of co-existing chromium(VI), manganese(II) and iron(III). J Indian Chem Soc 82:55–59
129. Mohammad A, Zehra A (2010) Anionic-nonionic surfactants coupled micellar thin-layer chromatography: synergistic effect on simultaneous separation of hydrophilic vitamins. J Chromatogr Sci 48:145–149
130. Mohammad A, Moheman A (2010) Adsorption of zinc(II) and cadmium(II) on soil layers in TLC in the presence of surfactant-containing mobile phases. J Planar Chromatogr Mod TLC 23:28–34
131. Mohammad A, Laeeq S, Moheman A (2010) Sodium deoxycholate micelles activated separation of coexisting five nucleobases by high performance thin layer chromatography. J Bioanal Biomed 2:55–59
132. Mohammad A, Haq N, Siddiq A (2010) Resolution of multicomponent mixture of amino acids using environmentally benign eluents: a green chromatographic approach. J Sep Sci 33:3619–3626
133. Cheng Y, Jia G, Jiang Z et al (2010) Use of HPTLC to differentiate among the crude polysaccharides in six traditional Chinese medicines. J Planar Chromatogr Mod TLC 23:46–49
134. Ranjane PN, Gandhi SV, Kadukar SS et al (2010) HPTLC determination of cefuroxime axetil and ornidazole in combined tablet dosage form. J Chromatogr Sci 48:26–28
135. Shalini J, Amrita S, Mohan S et al (2009) Development of conditions for rapid thin-layer chromatography of β-lactam antibiotics. J Planar Chromatogr Mod TLC 22:435–437
136. Akula KK, Kaur M, Kulkarni SK (2008) Estimation of adenosine and its major metabolites in brain tissues of rats using high performance thin layer chromatography-densitometry. J Chromatogr A 1209:230–237
137. Mohammad A, Gupta R (2008) Colloids Surf B Mobility behaviour of aminoacids on silica static phase: micelles activated separations. Biointerfaces 65:166–171
138. Fundación LAC, Privada J, Monte C, Mexico DF (2008) Development and validation of a high performance thin layer chromatographic method, with densitometry, for quantitative analysis of ketorolac tromethamine in human plasma. J AOAC Int 91:1191–1195
139. Vidya D, Onkar D, Gaurang P et al (2008) Quantification of dopamine in Portulaca oleracea Linn. By high performance thin layer chromatography. J Planar Chromatogr Mod TLC 21:183–186
140. Modi KP, Patel NM, Goyal RK (2008) Estimation of L-DOPA from Mucuna pruriens LINN and formulations containing M. pruriens by HPTLC method. Chem Pharm Bull 56:357–359

141. Mennickent S, Pino L, Vega M et al (2008) Chemical stability of haloperidol injection by high performance thin layer chromatography. J Sep Sci 31:201–206
142. Chepurwar SB, Shirkhedkar AA, Bari SB et al (2007) Validated HPTLC method for simultaneous estimation of levofloxacin hemihydrate and ornidazole in pharmaceutical dosage form. J Chromatogr Sci 45:531–536
143. Mennickent S, Nail M, Vega M (2007) Quantitative determination of L-DOPA in tablets by high performance thin layer chromatography. J Sep Sci 30:1893–1898
144. Heigl N, Huck CW, Rainer M, Najam-Ul-Haq M, Bonn GK (2006) Near infrared spectroscopy, cluster and multivariate analysis hyphenated to thin layer chromatography for the analysis of amino acids. Amino Acids 31:45–53
145. Suhagia BN, Shah SA, Rathod IS (2006) Determination of gatifloxacin and ornidazole in tablet dosage forms by high performance thin layer chromatography. Anal Sci 22:743–745
146. Katarína R, Radomíra N (2006) Thin-layer chromatography analysis of fructooligosaccharides in biological samples. J Chromatogr A 1110:214–221
147. Muszalska I, Sladowska H, Sabiniarz A (2005) HPLC and TLC methodology for determination or purity evaluation of 4-methoxy-2-(3(4-phenyl-1-piperazinyl))propyl-2,3-dihydro-6-methyl-1,3-dioxo-1H-pyrrolo[3,4-c]pyridine. Acta Pol Pharm 62:3–10
148. Krzek J, Maślanka A, Lipner P (2005) Identification and quantitation of polymyxin B, framycetin, and dexamethasone in an ointment by using thin-layer chromatography with densitometry. J AOAC Int 88:1549–1554
149. Ergül S, Kadan I, Savaşci S et al (2005) Modified diatomaceous earth as a principal stationary phase component in TLC. J Chromatogr Sci Sep 43:394–400
150. Sandra A, Tania N, Luc P et al (2006) Densitometric thin-layer chromatographic determination of aescin in a herbal medicinal product containing Aesculus and Vitis dry extracts. J Chromatogr A 1112:165–170
151. Mennickent S, Nail M, Vega M et al (2007) Quantitative determination of L- DOPA. J Sep Sci 30:1893–1898
152. Gopu CL, Gilda SS, Paradkar AR et al (2008) Development and validation of a densitometric TLC method for analysis of trigonelline and 4-hydroxyisoleucine in fenugreek seeds. Acta Chromatographia 20:709–719
153. Ranjane PN, Gandhi SV, Kadukar SS, Bothara KG (2010) HPTLC determination of cefuroxime axetil and ornidazole in combined tablet dosage form. J Chromatogr Sci 48:26–28
154. Hubicka U, Krzek J, Szczyrbowska O (2009) TLC-UV and -VIS densitometric detection method for determination of oxyphenonium bromide and its degradation products in tablets. J Liq Chromatogr Relat Technol 32:1196–1209
155. Wang K, Liu Z, Huang J et al (2009) TLC separation of catechins and theaflavins on polyamide plates. J Planar Chromatogr Mod TLC 22:97–100
156. Chitlange S, Sakarkar D, Wankhed S et al (2008) High performance thin layer chromatographic method for simultaneous estimation of ibuprofen and pseudoephedrine hydrochloride. Indian J Pharm Sci 70:398–400
157. Reiffova K, Podolonovicova J, Onofrejova L (2007) Thin layer chromatography and matrix-assisted laser desorption/ionization mass spectrometric analysis of oligosaccharides in biological samples. J Planar Chromatogr Mod TLC 20:19–25
158. Petkovska E, Slaveska-Raicki R, Rafajlovska V (2006) Determination of tetracycline, oxytetracycline and chlortetracycline in milk by TLC and column chromatography using amberlite XAD-2. Chemica Analityczna 51:275–283
159. Bebawy LI, Abbas SS, Fattah L et al (2005) Application of first-derivative, ratio derivative spectrophotometry, TLC-densitometry and spectrofluorimetry for the simultaneous determination of telmisartan and hydrochlorothiazide in pharmaceutical dosage forms and plasma. Farmaco 60:859–867
160. Kanaki NS, Rajani M (2005) Development and validation of a thin-layer chromatography-densitometric method for the quantitation of alliin from garlic (Allium sativum) and its formulations. J AOAC Int 88:1568–1570

161. Urszula H, Jan K, Magorzata S (2009) Chromatographic-densitometric method for determination of clopamide and 4-chlorobenzoic, and 4-chloro-3-sulfamoylbenzoic acids in tablets. Curr Pharm Anal 5:408–415
162. Varghese SJ, Ravi TK (2010) Determination of rosuvastatin and ezetimibe in a combined tablet dosage form using high-performance column liquid chromatography and high-performance thin-layer chromatography. J AOAC Int 93:1222–1227
163. Popović G, Čakar M, Agbaba D (2007) Simultaneous determination of loratadine and preservatives in syrups by thin-layer chromatography. Acta Chromatogr 161–169
164. Ravi T, Gandhimathi M, Sireesha K (2006) HPTLC method for the simultaneous estimation of tizanidine and rofecoxib in tablets. Indian J Pharm Sci 68:234–236
165. Čakar M, Popović G, Agbaba D (2005) High-performance thin-layer chromatography determination of some antimycotic imidazole derivatives and preservatives in medicinal creams and a Gel. J AOAC Int 88:1544–1548
166. Popovic G, Čakar M, Vučićević K (2004) Comparison of HPTLC and HPLC for determination of econazole nitrate in topical dosage forms. J Planar Chromatogr Mod TLC 17: 109–112
167. Mohammad A, Haq N, Siddiq A (2010) Resolution of multicomponent mixture of amino acids using environmentally benign eluents: a green chromatographic approach. J Sep Sci 33:3619–3626
168. Živkoviæ RV, Vuckoviæ G (2009) Poly(ethylene glycol) as impregnator for silica gel in salting-out thin-layer chromatography of some Co(III) complexes. Chromatographia 62:91–97

Chapter 12
Application of Dimethyl Carbonate as Solvent and Reagent

Belen Ferrer, Mercedes Alvaro, and Hermenegildo Garcia

Abstract This chapter summarizes the most important uses of dimethyl carbonate, as solvent and reagent. Dimethyl carbonate as solvent is used in novel applications related to supercapacitors, lithium batteries and other emerging devices for energy storage. As reagent, dimethyl carbonate exhibits dual behavior as methylating and carbamoylating reagent depending on the substrate, reaction conditions, and the catalyst present. Emphasis is made on recent developments to replace industrial processes based on phosgene, particularly for polyurethanes, by dimethyl carbonate.

12.1 Introduction

One of hot research area in green chemistry is to develop processes based on CO_2 as C_1 feedstock [1]. Implementation of large-scale industrial processes utilizing CO_2 as substrate would have the potential benefit of being "CO_2 neutral" avoiding the concentration of this green house effect gas in the atmosphere.

B. Ferrer
Departamento de Química, Instituto Universitario de Tecnología Química CSIC-UPV, Universidad Politécnica de Valencia, Camino de Vera s/n, Valencia 46022, Spain
e-mail: bferrer@qim.upv.es

M. Alvaro
Departamento de Química, Instituto Universitario de Tecnología Química, Universidad Politécnica de Valencia, Avd. De los Naranjos s/n, Valencia 46022, Spain

H. Garcia (✉)
Departamento de Química, Instituto Universitario de Tecnología Química CSIC-UPV, Universidad Politécnica de Valencia, Camino de Vera s/n, Valencia 46022, Spain

Instituto Universitario de Tecnología Química, Universidad Politécnica de Valencia, Avd. De los Naranjos s/n, Valencia 46022, Spain
e-mail: hgarcia@qim.upv.es

A. Mohammad and Inamuddin (eds.), *Green Solvents I: Properties and Applications in Chemistry*, DOI 10.1007/978-94-007-1712-1_12,

In this context, organic carbonates have attracted considerable attention as interesting derivatives of CO_2 [2]. The reaction of CO_2 with alcohols is an unfavorable equilibrium that only forms a small percentage of dialkyl carbonates. However, since water is formed in the reaction (Scheme 12.1), it should be possible to shift the equilibrium or, alternatively, to separate the small percentage of organic carbonates leading to a profitable percentage of dialkyl carbonates. Of all alkyl carbonates, the most important is dimethyl carbonate (DMC) [2].

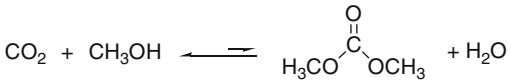

Scheme 12.1 Synthetic route for the preparation of DMC from CO_2 and methanol

The current industrial synthesis based on the ENI process is achieved by carbonylation of methanol using a noble metal catalyst [3, 4]. Besides the direct reaction of methanol and CO_2, another alternative route to obtain DMC that overcomes low equilibrium constant problems is the CO_2 insertion into epoxides followed by transalkylation of the cyclic carbonate with methanol [5]. Scheme 12.2 shows the route based on the reaction of epoxides. The interesting feature of this route is that ethylene and propylene oxide are two petrochemical compounds whose production is sufficiently large to implement CO_2 insertion on large industrial scale. Moreover, the main products of the epoxides are the corresponding glycols and DMC (Scheme 12.2).

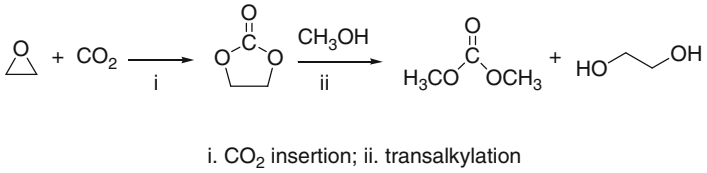

Scheme 12.2 Synthetic route for the preparation of DMC from CO_2 and epoxides

The use of epoxides as substrates has the economical benefit due to the formation of glycol and DMC. Both steps can be carried out with high yields, and in this way the low yield of the direct DMC formation from methanol is overcome. The only problem of this two-step route is that while there are many suitable catalysts (mostly Lewis acids) to promote CO_2 insertion [6], transalkylation is more problematic, and frequently basic catalysts promote some decarboxylation, lowering the yield toward DMC [7]. Additionally, basic catalysts are highly prone to undergo poisoning by CO_2 due to the formation of carbonates that are frequently inactive as catalysts. In this way, DMC becomes a green reagent. It could be, however, that diethyl carbonate (DEC), rather than DMC, would be converted in the preferred derivative from CO_2. One reason for this is that both ethanol and CO_2 are formed in large quantities in the fermentation of biomass, and by combining them into DEC, considerable

energy savings will be achieved. In fact, the low concentration of CO_2 in the atmosphere makes the obtainment of CO_2 from the atmosphere costly, and it would be advantageous to couple CO_2 concentration with some other processes such as separation of oxygen or high-added-value argon from the air. In this chapter, we will summarize the application of DMC as green solvent and as chemical reagent.

12.2 Dimethyl Carbonate (DMC) as Green Solvent

DMC as solvent has the label of "green." One of the principles of green chemistry is aimed at the replacement of conventional organic solvents that damage the atmosphere. In particular, halogenated organic solvents have been widely used in dry cleaning and as media in organic synthesis due to the ability to dissolve a broad range of organic compounds of low to medium polarity. Halogenated solvents are among the major contributors to the ozone layer depletion, and international treaties have recommended for their limited use. DMC has been favored as a green replacement for halogenated solvents due to its similarity with these types of liquids as well as ethers and esters [8].

In addition, DMC has been considered as the appropriate solvent for new applications that are expected to grow remarkably in the near future such as in solid fuels and other primary energy resources. Thus, one of the main properties of DMC is its ability to dissolve salts, and particularly lithium ions. The corresponding electrolytes based on DMC are needed for *lithium batteries* that are expected to play a major role as energy storage for small domestic portable devices and even in car transportation [9–11]. In lithium battery, the anode made of paste of lithium metal and graphite is separated from the cathode (for instance lithium iron phosphate) by a liquid electrolyte and a membrane which allows transference of Li^+ from the anode to the cathode when the battery is operating and the reverse when the battery is being charged (see Scheme 12.3). DMC containing $LiPF_6$ is an ideal electrolyte for these batteries whose massive production for electrical cars can be anticipated in near future.

The same electrolyte, DMC containing high concentration of $LiPF_6$, can also be used for high power density double-layer capacitors [12, 13]. Capacitors with the ability to store high electrical charge density (*supercapacitors*) have been found useful in the automotive industry in order to save energy consumption. In this case, the mechanical energy of the braking stages is accumulated in the supercapacitor which is used to restart the combustion engine and to boost the engine in the acceleration steps. In this way, and particularly in urban conduction cycles characterized by continuous alternation of braking and boosting steps, it has been estimated that up to 10% of the fuel can be saved if the mechanical braking energy is accumulated in supercapacitors. In supercapacitors, charge separation between the layers with electrolyte redistribution occurs during charge accumulation, and the reverse process takes place during discharge of the capacitor. Besides, in this new application that requires high energy accumulation, the same DMC electrolyte can also be

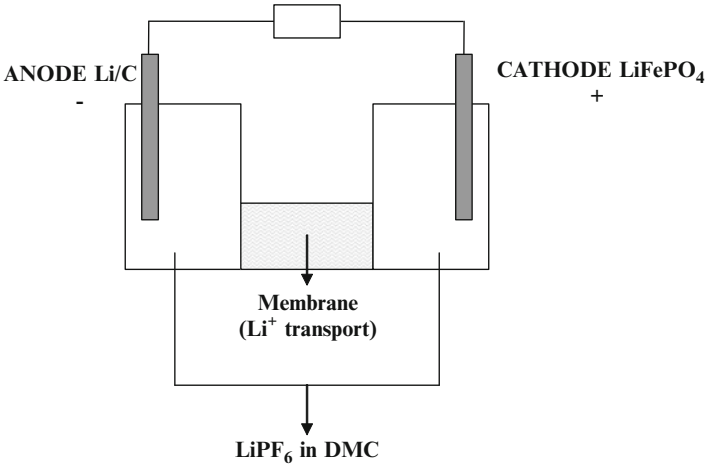

Scheme 12.3 Components of a lithium ion battery

used as capacitors of electrical motors to keep steady the charge current during operation.

A third possible application of DMC related to energy is its use in *dye-sensitized solar cells* [14–16]. In this type of devices, light induces charge separation by exciting an organic dye that injects one electron into the conduction band of a semiconductor in the photo-anode. The cathode is separated from the anode by an electrolyte that should be able to transport quickly a redox species to neutralize the positive charge of the dye. Since solubility of ions in DMC is higher and the ionic diffusion in DMC is very high, this electrolyte has been found to be convenient for the preparation of dye-sensitized solar cells enjoying a long-term stability and relatively high conversion efficiency of 4.78%.

The main problem with this system is that dye-sensitized solar cells using electrolyte undergo deterioration due to solvent evaporation. For this reason, high-boiling-point solvents are preferable to form part of the electrolyte. Since the boiling point of DMC is low (90°C), its use would require a much perfect sealing of the cell.

In general, it can be said that if DMC becomes industrially available in large quantities through one of the processes already commented, then all these applications based on the ability of DMC to dissolve Li ions will expand quickly, particularly in a scenario where the oil price is increasing sharply.

12.3 Dimethyl Carbonate (DMC) as Dual Chemical Reagent

DMC can typically react at temperatures above 100°C. In the presence of nucleophiles, DMC exhibits a dual behavior as methylating or carbamoylating reagent. Scheme 12.4 illustrates the two possible reactivities of DMC with an amine.

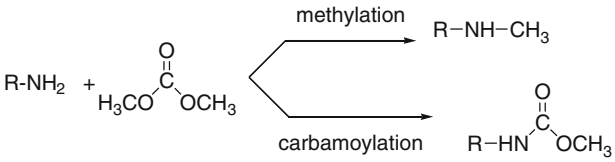

Scheme 12.4 Reactivity of DMC with amines as methylating and carbamoylating agent

Compared to conventional methylating agents such as alkyl halides or dimethyl sulfate, the use of DMC has two main differences. The first one is that DMC is considered as "green" reagent since it is obtained from CO_2 and methanol, and when performing a methylation reaction, only CO_2 and methanol are formed. Therefore, considering the global life cycle of DMC, the net transformation is methylation of the nucleophile with methanol in two steps involving the intermediacy of DMC [2]. In contrast, alkyl halides generate as waste a halide anion per mol of product. Moreover, considering that chloromethane and bromomethane are gases under ambient conditions, the most typical methylating agent is methyl iodide, and then the E factor as defined by Sheldon [17] is very large, meaning that the kilograms of waste produced by kilogram of product is very high on using methyl iodide. The E factor is considered as an indicator for quantitative measurement of the greenness of the process that is low when the E factor is high. Similar situations happen with dimethyl sulfate in which sulfide salts are formed when the methylation occurs.

The second difference of DMC as methylating agent is that, except for very strong nucleophiles, the reaction requires a catalyst [18]. Typically, methylations with other reagents as alkyl iodides do not need any catalyst.

Development of catalysts, particularly for heterogeneous catalysis, to promote methylation of nucleophiles by DMC has been an active topic in green chemistry to prepare more active and selective catalysts [2]. Several catalytic reactions require reaction temperatures higher than the boiling point of DMC, and this complicates considerably the workup of the reactions since close reactors that can stand relatively high pressure are needed. This is particularly important considering that reactions using DMC carried out at 160°C are not uncommon, and the boiling point of DMC is 90°C. Therefore, more active catalysts should be ideally able to perform the reaction at ambient pressure, meaning that the maximum temperature should be the boiling point of DMC.

However, even though catalyst activity is still far from optimum, the key point in DMC being used as reagent is selectivity because as commented earlier, two different pathways can be promoted in parallel.

In general, the preferential reactivity of DMC is as methylating reagent, methoxycarbonylation (carbamoylation) being much more difficult to achieve in high selectivity. As a general rule, carbamoylation is always accompanied by some degree of methylation while, on the other hand, methylation can be obtained almost free of carbamoylated products.

Table 12.1 The reaction of DMC with indolyl-3-acetic acid, with 1:1 catalyst:substrate weight ratio, at 180°C, and in the presence of different zeolites. Isolated products: methyl ester derivative (2b), *N*-methoxycarbonyl derivative (3b), decarboxylated derivative (4b) (Reproduced from Ref. [23]. With kind permission of The Royal Society of Chemistry)

			Isolated product yield (%)		
S. No.	Catalyst	*t* (h)	2b	3b	4b
1	None	3			
2	LiY	4	25		43
3	NaY	4	52		21
4	KY	4	50		19
5	LiY	4	87	10	
6	NaY	4		97	
7	KY	4		98	

The selectivity between methylation and carbamoylation depends on a large number of factors besides the catalyst such as the nature of the nucleophilic species, reaction temperature, and even the substrate-to-DMC ratio. Generally, hard nucleophiles favor methylation, which is promoted by higher temperatures and high substrate-to-DMC ratio.

12.3.1 Catalysts for Selective Methylation Using Dimethyl Carbonate (DMC)

A variety of Lewis metal salts can act as homogeneous catalysts for methylation using DMC. The list also includes metal triflates, metal halides, and organocatalysts [19, 20]. The latter field is particularly attractive since, even under homogeneous conditions, none of the transition metals can be introduced in the system. The general organocatalysts that can be employed are supernucleophilic amines such as 1,4-diazabicyclo[2.2.2]octane (DABCO) and 1,4,7-triazacyclononane (TACN). In the latter case, protonation of one nitrogen is particularly easy due to charge delocalization, and for this reason, its activity is much higher than the conventional amines. In one way of the use of organocatalysts that bridges homogeneous and heterogeneous catalysis, Jacobs and De Vos have covalently attached 1,5,7-triazabicyclo[4.4.0]dec-5-ene to a mesoporous aluminosilicate and used this solid to promote methylation and methoxycarbonylation of amines [21, 22]. Tundo and coworkers have made significant contributions to the use of DMC as reagent. They found that sodium zeolites are good heterogeneous catalysts to promote methylation of a large variety of nucleophiles including aromatic amines [23]. Later, it has been reported that if sodium is ion exchanged by other metal ions that can act as Lewis acid sites, then the activity increases with respect to the parent sodium zeolite [21]. Table 12.1 lists some of the results that have been reported using metal exchanged zeolites as catalysts [23].

12.3.2 Catalysts for Methoxycarbonylation

The most important industrial application of DMC that can be envisioned is its use as phosgene replacement in the synthesis of polyurethane. Polyurethanes are prepared in large quantity by reaction of diisocyanates with polyols. About 85% of the current polyurethane market corresponds to aromatic diisocyanates derived from toluene diisocyanate (TDI) or mixtures of isomers of bis(isocyanatophenyl)methane (Scheme 12.5).

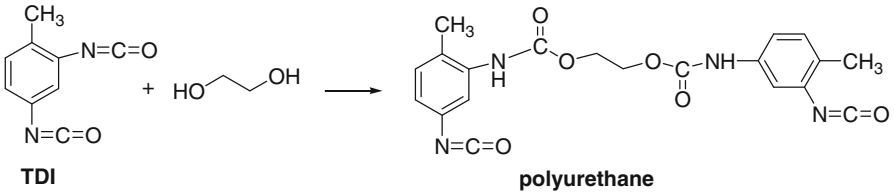

Scheme 12.5 Synthetic route for the preparation of polyurethanes starting from toluene diisocyanate and ethylene glycol

These aromatic diisocyanates are currently produced from the corresponding aromatic diamines by reaction with phosgene. The current security regulations in Western countries oblige to build the plant in which phosgene is prepared and used inside a larger building that can be sealed and the atmosphere evacuated after treatment with bases. From the large capital investment required for phosgene plants, as well as from the point of view of green chemistry (replacement of toxic chemicals and development of new processes CO_2 neutral), it is desirable to develop alternative processes for the use of phosgene based on CO_2. Scheme 12.6 shows a possible route in which the key process is the methoxycarbonylation of aromatic amines by organic carbonates.

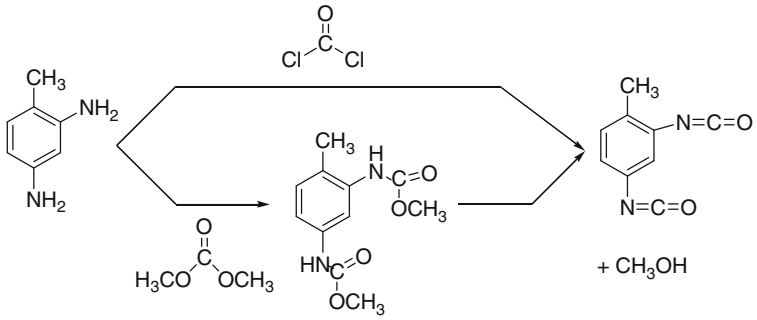

Scheme 12.6 Synthetic routes to toluene diisocyanate (TDI) involving either phosgene or dimethyl carbonate (DMC)

As we have commented earlier, the problem with the chemical route to prepare aromatic polyisocyanates using organic carbonates as reagents is the dual reactivity of these carbonates as alkylating and carbamoylating reagents. Moreover, due to the lower nucleophilicity of aromatic amines compared to aliphatic amines, the former exhibit greater tendency to undergo N-alkylation versus carbamoylation. The only way to circumvent this problem is to develop selective catalysts that promote carbamoylation, minimizing the strongly undesired N-methyl derivatives. While Zn^{2+} and Pb^{2+} salts of long alkyl chain carboxylates have been reported as homogeneous catalysts for carbamoylation of amines, industry prefers heterogeneous catalysts that can be easily separated from the reaction mixture and also allows the design of continuous flow processes.

There have been several reports in the literature showing that solid catalysts such as transition metal–exchanged aluminosilicates can produce carbamates of aromatic polyamines in variable selectivities depending on the catalyst and reaction conditions [24, 25]. One remarkable example is the report of Sartori, Jacobs, and coworkers describing that supernucleophilic amines such as TACN covalently anchored to mesoporous silica can affect carbamoylation of aliphatic amines, although the selectivity for aromatic amines is very low [21, 22, 26]. It has to be commented that in order to develop an industrial process, the target for a heterogeneous catalyst should be selectivities over 90% for carbamoylation at conversions higher than 80% with high catalyst productivity.

In this context, we have reported recently that CeO_2-supported gold nanoparticles meet the requirements to become an industrial catalyst for the carbamoylation of aromatic amines [27]. The key point in the catalyst is the unique behavior of CeO_2 nanoparticles to promote carbamoylation against methylation. Thus, for instance, TiO_2, Fe_2O_3, Al_2O_3, ZrO_2 and other metal oxides in the absence of gold promote N-methylation under the same conditions in which CeO_2 promotes carbamoylation [27]. However, even though the selectivity of CeO_2 toward carbamoylation is high, its activity is low, and therefore longer reaction times are needed to achieve the required amine conversions. The effect of gold, at very low loadings (below 1 wt%), is precisely to boost the activity without altering the selectivity toward carbamoylation. Table 12.2 summarizes some of the results that have been reported illustrating the role of CeO_2 and the effect of gold as well as other noble metals.

Concerning the reaction mechanism, absorption of DMC on CeO_2 shows that this molecule splits into two fragments. One is a methyl group anchored on surface OH (methylation of the surface), and the other part is methoxycarbonyloxy bonded to Ce metal ion. When the material is heated, it is observed that the methyl group remains strongly bonded to the surface, but the methoxycarbonyloxy group is lost. This thermal behavior that can be easily monitored by in situ infrared (IR) spectroscopy justifies the observed catalytic behavior since it demonstrates the tendency of CeO_2 to retain the methyl group and, therefore, to minimize methylation. In fact, an analogous in situ IR study of the behavior of DMC on TiO_2 shows exactly the same bond cleavage and splitting of DMC, but a contrasting behavior upon heating is noticed since the methyl group is more easily desorbed. Figure 12.1 illustrates the changes occurring in the IR spectra of the CeO_2 and TiO_2 metal oxides after exposing the surface to DMC and evacuation at 100°C.

Table 12.2 Results for the reaction of toluene diamine (DAT) with DMC in the presence of a series of catalysts (Reproduced from Ref. [27]. With kind permission of John Wiley & Sons)

Catalyst	Mass balance (%)	DAT conv. (%)	*o*-1+*p*-1N-carbamoylated products (%)	N,N-Carbamoylated product (%)	N-Methylated product (%)
$Zn(OAc)_2$	95±3	99	36	25	39
ZnO (40 nm)	97±3	16	1	–	99
Au/CeO_2 (0.44%) fresh	99±2	99	4	96	–
Au/CeO_2 (0.44%) 3rd reuse	98±2	99	–	100	–
Au/CeO_2 (0.44%; 40 nm)	99±3	65	73	–	27
CeO_2 (5 nm)	97±3	92	48	52	–
Au/TiO_2 (0.44%)	99±3	58	10	–	90
Au/Fe_2O_3 (0.44%)	95±3	27	–	–	100
Pd/CeO_2 (0.44%)	96±3	87	34	65	1
Pd/TiO_2 (0.44%)	95±3	10	4	–	96
Pt/TiO_2 (1.5%)	98±2	8	–	–	100

Reaction conditions: DAT (0.98 mmol), DMC (26.69 mmol); catalyst: Au, Pd, Pt, Zn (0.5% mol respect to DAT), CeO_2 and ZnO (100 mg), 7 h, 140°C

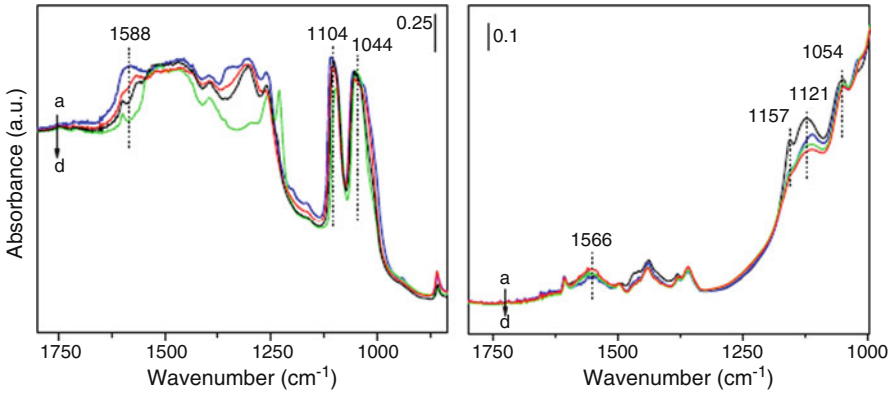

Fig. 12.1 FTIR spectra of nanocrystalline CeO_2 (*left*) and Au/TiO_2 (*right*) after DMC adsorption (a, the spectrum on the top) and desorption at increasing temperatures 303 K (b, first intermedium spectrum), 343 K (c, second intermedium spectrum), and 393 K (d, the spectrum on the bottom) (Reproduced from Ref. [27]. With kind permission of John Wiley & Sons)

When similar Fourier-transformed infrared (FTIR) studies are carried out with Au/CeO_2, the same behavior as for CeO_2 is observed, with the important difference that desorption of methoxycarbonyloxy group takes place at even lower temperature. This justifies very nicely the effect of gold enhancing the activity by favoring desorption of methoxycarbonyloxy group.

In addition, since aromatic amines are industrially obtained from aromatic nitro compounds and gold exhibits a remarkable activity for the selective hydrogenation of nitro groups, we have developed a tandem reaction (hydrogenation + carbamoylation) as one-step process in which nitro aromatic compounds are converted to the corresponding methoxycarbonyl diamines with high selectivity [27] as shown in Scheme 12.7.

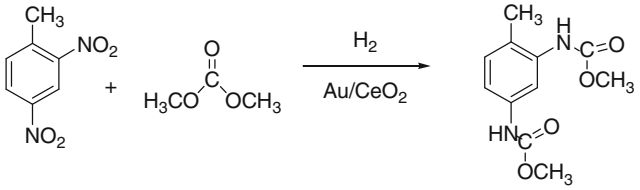

Scheme 12.7 Tandem reaction (hydrogenation + carbamoylation) of 2,4-dinitrotoluene with DMC to obtain the corresponding methoxycarbonyl diamine

Finally, the aromatic methyl carbamate can be transformed into the corresponding aromatic isocyanate by thermolysis in the presence or absence of catalyst (see Scheme 12.6). This renders a synthetic route for commercial diisocyanates starting from nitro aromatics or aromatic amines using CO_2 and methanol as reagents and going through DMC as intermediate. In the last step of isocyanates formation, methanol is recovered (see Scheme 12.6) and can be recycled for the formation of fresh DMC. In this way, only CO_2 and nitro compounds are consumed in the overall cycle.

12.4 Concluding Remarks and Future Prospects

Taking into account the wide range of potential DMC uses as solvent and reagent and the expected growth of these novel uses, it can be easily anticipated that the production of DMC and other organic carbonates (particularly diethyl carbonate and propylene carbonate) will grow dramatically in the years to come. In addition, as the production of DMC rises, there will be a large incentive to replace the current industrial preparation of DMC based on CO to a new process based on CO_2 fixation. Among the novel important uses of DMC, application in Li batteries, supercapacitors, solar cells and other uses related to new energy resources will increase at a very high pace.

Concerning the use of DMC as reagent, methylation is not very important since it can be performed directly with methanol or suitable derivatives. However, polyurethanes will be a new market for increasing demand of DMC.

Acknowledgment Financial support by Spanish Ministry of Science and Innovation (CTQ2009/11586), Consolider MULTICAT and Polytechnic University of Valencia (20101196) is gratefully acknowledged.

References

1. Aresta M, Dibenedettto A (2007) Utilisation of CO_2 as a chemical feedstock: opportunities and challenges. Dalton Trans 28:2975–2992
2. Tundo P, Selva M (2002) The chemistry of dimethyl carbonate. Acc Chem Res 35:706–716
3. Othmer K (1994) Encyclopedia of chemical technology, 4th edn. Wiley, New York
4. Weissermel K, Harpe HJ (2003) Industrial organic chemistry, 4th edn. Wiley-VCH, Weinheim
5. Song J, Zhang Z, Hu S, Wu T, Jiang T, Han B (2009) MOF-5/n-Bu4NBr: an efficient catalyst system for the synthesis of cyclic carbonates from epoxides and CO_2 under mild conditions. Green Chem 11(7):1031–1036
6. Alvaro M, Baleizao C, Carbonell E, El Ghoul M, Garcia H, Gigante B (2005) Polymer-bound aluminium salen complex as reusable catalysts for CO_2 insertion into epoxides. Tetrahedron 61(51):12131–12139
7. Juarez R, Corma A, Garcia H (2009) Gold nanoparticles promote the catalytic activity of ceria for the transalkylation of propylene carbonate to dimethyl carbonate. Green Chem 11(7): 949–952
8. Barthel J, Neueder R, Poepke H, Wittmann H (1999) Osmotic coefficients and activity coefficients of nonaqueous electrolyte solutions. Part 2. Lithium perchlorate in the aprotic solvents acetone, acetonitrile, dimethoxyethane, and dimethylcarbonatet. J Sol Chem 28:489–503
9. Wachtler M, Wohlfahrt-Mehrens M, Ströbele S, Panitz JC, Wietelmann UJ (2006) The behaviour of graphite, carbon black, and $Li_4Ti_5O_{12}$ in LiBOB-based electrolytes. J Appl Electrochem 36:1199–1206
10. Xie A, Ma C, Wang L, Chu Y (2007) $Li_6V_{10}O_{28}$, a novel cathode material for Li-ion battery. Electrochim Acta 52:2945–2949
11. Zhong SW, Zhao YJ, Lian F et al (2006) Characteristics and electrochemical performance of cathode material Co-coated $LiNi0_2$ for Li-ion batteries. Trans Nonferrous Met Soc China 16:137–141
12. Laheäär A, Kurig H, Jänes A, Lust E (2009) $LiPF_6$ based ethylene carbonate–dimethyl carbonate electrolyte for high power density electrical double layer capacitor. Electrochim Acta 54:4587–4594
13. Nakagawa T, Abe Y, Nabeshima A, Shima H, Hiketa S, Uetani M, inventors; Otsuka Chemical Co., Ltd., assignee (2010) Capacitors. Wenderoth, Lind & Ponack, L.L.P. Washington, DC
14. Kang MS, Lee JW, Shin BC, Kim KJ, Lee JP, inventors (2009) Solar cells. Stein, Mcewen & Bui, LLP Washington, DC
15. Somani PR, Somani SP, Umeno M, Sato A (2006) Concept and demonstration of all organic Gratzel solar cell (dye sensitized solar cell). Appl Phys Lett 89:083501
16. Yang H, Huamg M, Wu J, Lan Z, Hao S, Lin J (2008) The polymer gel electrolyte based on poly(methyl methacrylate) and its application in quasi-solid-state dye-sensitized solar cells. Mater Chem Phys 110:38–42
17. Sheldon RA (1992) Chem Ind 23:903–906
18. Chankeshwara SV (2008) Dimethyl carbonate (DMC): a versatile and environmentally benign building block. Synlett 4:624–625
19. Mei F, Chen E, Li GX (2009) Lanthanum nitrate as an efficient and recoverable homogeneous catalyst for the transesterification of dimethyl carbonate with ethanol. React Kinet Catal Lett 96(1):27–33
20. Mei FM, Chen EX, Li GX (2009) Effective and recoverable homogeneous catalysts for the transesterification of dimethyl carbonate with ethanol: lanthanide triflates. Kinet Catal 50(5):666–670
21. Carloni S, de Vos D, Jacobs P, Maggi R, Sartori G, Sartorio R (2002) Catalytic activity of MCM-41–TBD in the selective preparation of carbamates and unsymmetrical alkyl carbonates from diethyl carbonate. J Catal 205:199

22. de Vos D, Jacobs P (2004) Zeolite effects in the sustainable and green synthesis of intermediates and fine chemicals. Stud Surf Sci Catal 154A (Recent Advances in the Science and Technology of Zeolites and Related Materials):66–79
23. Selva M, Tundo P, Brunelli D, Perosa A (2007) Chemoselective reactions of dimethyl carbonate catalysed by alkali metal exchanged faujasites: the case of indolyl carboxylic acids and indolyl-substituted alkyl carboxylic acids. Green Chem 9:463–468
24. Katada N, Fujinaga H, Nakamura Y, Okumura K, Nishigaki K, Niwa M (2002) Catalytic activity of mesoporous silica for synthesis of methyl N-phenyl carbamate from dimethyl carbonate and aniline. Catal Lett 80(1–2):47–51
25. Ma Y, Shi F, Deng Y (2010) Oxidative carbonylation of aniline with a mesoporous silica gel immobilised Se-functionalised ionic liquid catalyst. J Chem Res 34(6):344–347
26. Melis K, de Vos D, Jacobs P, Verpoort F (2001) ROMP and RCM catalysed by $(R_3P)_2Cl_2Ru{=}CHPh$ immobilised on a mesoporous support. J Mol Catal A-Chem 169:47
27. Juárez R, Concepción P, Corma A, Fornés V, Garcia H (2010) Gold-catalyzed phosgene-free synthesis of polyurethane precursors. Angew Chem Int Ed 49:1286–1290

Chapter 13
Application of Supercritical Fluids for Biodiesel Production

Ikumei Setsu, Ching-Hung Chen, Chao-Rui Chen, Wei-Heng Chen, Chien-Hsiun Tu, Shih-Ming Lai, and Chieh-Ming J. Chang

Abstract This chapter elucidates supercritical carbon dioxide (SC-CO_2) extraction of triglycerides from powdered *Jatropha curcas* kernels and seeds, followed by a series of subcritical hydrolysis and supercritical methylation of the extracted SC-CO_2 oil to obtain a 98.5% purity level of biodiesel. Effects of the reaction temperature, the reaction time, and the solvent-to-solid ratio on free fatty acid (FFA) in the hydrolyzed oil and fatty acid esters in the methylated oil via two experimental designs were also examined. Supercritical methylation of the hydrolyzed oil following subcritical hydrolysis of the SC-CO_2 extract yielded a methylation reaction conversion of 99%, and activation energies of hydrolysis and transesterified reactions were found, respectively. This study demonstrates that supercritical methylation preceded by subcritical hydrolysis of the SC-CO_2-extracted oil is a feasible two-step process in producing biodiesel from powdered *Jatropha* kernels better than that from *Jatropha* seeds. The economical estimation of the process was also examined.

I. Setsu • C.-H. Chen • W.-H. Chen • C.-M.J. Chang (✉)
Department of Chemical Engineering, National Chung Hsing University,
250 Kuo-Kuang Road, Taichung 402, Taiwan, ROC
e-mail: ymsetsu@gmail.com; pilicity@hotmail.com; lemonice0806@yahoo.com.tw; cmchang@dragon.nchu.edu.tw

C.-R. Chen
Department of Chemical Engineering, National Chung Hsing University,
250 Kuo-Kuang Road, Taichung 402, Taiwan, ROC

Chemical Engineering Division, Institute of Nuclear Energy Research,
1000 Wen-Hua Road, Lungtan, Taoyuan 325, Taiwan, ROC
e-mail: g8965128@mail.nchu.edu.tw

C.-H. Tu
Department of Applied Chemistry, Providence University, 200 Chungchi Road,
Taichung 43301, Taiwan, ROC

S.-M. Lai
Department of Chemical and Materials Engineering, National Yunlin University
of Science and Technology, 123 University Road, Touliu, Yunlin 640, Taiwan, ROC

A. Mohammad and Inamuddin (eds.), *Green Solvents I: Properties and Applications in Chemistry*, DOI 10.1007/978-94-007-1712-1_13,

13.1 Introduction

13.1.1 Supercritical Fluids

Among the various fields that supercritical fluids have been applied include extraction, chromatography, and recrystallization, due to their high diffusivity, high permeability, and low surface tension. Supercritical fluid extraction (SFE) is extensively performed for concentrating bioactive compounds. The SFE parameters, for example, pressure, temperature, and cosolvent ratio are easily controlled, and desired compounds can be obtained in high purity and high total yield (TY) [1]. Some valuable bioactive compounds, such as flavones and colorants, can be extracted using SFE with suitable cosolvents. On the other hand, some undesirable compounds, such as caffeine and pesticides, can be removed utilizing SFE. For example, supercritical fluids technology can be used to remove wax to enhance the concentration of flavonoids in the propolis extract [2]; extract the antioxidant components from propolis by SC-CO_2 antisolvent fractionation [3]; and extract 3,5-diprenyl-4-hydroxycinnamic acid (DHCA) from Brazilian propolis by SC-CO_2 modified with cosolvent, which process is followed by column chromatography to yield 95% pure DHCA [4]. Biodiesel preparation by using supercritical technique was introduced in 2001 [5, 6]. Recent publication indicated that biodiesel production from *Jatropha* oil via noncatalytic supercritical methanol transesterification resulted in high yield of fatty acid methyl esters [7].

13.1.2 Biodiesel

Fatty acid methyl ester (FAME), commonly known as biodiesel, has been considered a potential source of future renewable and environmentally friendly energy, replacing exhaustible petroleum-derived diesel.

The daily depletion of fossil fuels necessitates the development of an alternative fuel source that satisfies energy demands worldwide. Producing biodiesel from natural resources is one of the most promising methods. However, because biodiesel fuels are more expensive than petroleum fuels as well as highly viscous, diesel engines cannot efficiently atomize biodiesel fuels [8], and vegetable oils have not been widely accepted as a diesel engine fuel. Conversely, biodiesel is better than diesel fuel in terms of sulfur content, flash point, aromatic content, and biodegradability [9, 10].

Jatropha curcas (JC), a plant that grows naturally in the wild, can grow without irrigation under a broad rainfall range (250–3,000 mm/year) [11]. Additionally, as a pressed cake, JC can be used as fertilizer, and its organic waste products can be digested to produce biogas methane [12, 13]. The JC kernel forms a large proportion of the seed, accounting for $61.3 \pm 3.1\%$. Experimental kernels exhibited large variations in crude protein (19–31%), lipids (43–59%), neutral detergent fibers (3.5–6.1%), and ash (3.4–5.0%) contents. The gross energy of kernels was generally similar (28.5–31.2 MJ/kg) [14, 15].

Most studies have reported that increased amounts of biodiesel were produced when a catalyst was employed to accelerate methylation because the solubility of oil in methanol is poor. The alkali-catalyzed reaction is the most commonly used process for practical biodiesel production. Cvengro and Povaz used 4% NaOH as a catalyst to produce biodiesel using two-stage low-temperature transesterification of cold-pressed rapeseed oil with methanol at temperatures up to 343 K [16]. Kaieda et al. synthesized methyl esters from plant oil and methanol in a solvent-free reaction system using lipase from *Rhizopus oryzae* [17]. Shimada et al. examined enzymatic alcoholysis for biodiesel fuel production by employing *Candida antarctica* lipase as the catalyst [18]. Pizarro and Park analyzed the production of biodiesel fuel with *Rhizopus oryzae* lipase as the catalyst from vegetable oils contained in waste activated bleaching earth [19].

However, the alkali-catalytic process has some shortcomings in that it is unsuitable for oil feed containing FFAs as the alkali and side-products are difficult to remove. Additionally, enzymatic methylations do not yield consistent conversions. Zhang et al. demonstrated that the acid-catalytic process employing used cooking oil proved technically feasible and was less complex than the alkali-catalytic process using the same oil [20]. Ghadge and Raheman utilized sulfuric acid to produce biodiesel from *Madhuca indica* oil, which has high amount of FFAs [21]. Tashtoush et al. used sulfuric acid in an experimental study for evaluating and optimizing the conversion of waste animal fat into biodiesel [22]. Nonetheless, the acid-catalytic process takes much time in the esterification process. No catalyst is required for transesterification of supercritical methanol or ethanol, and nearly complete conversions can be achieved in very short periods [23]. This is primarily because supercritical methanol and oil exist in a single phase [24, 25]. Cao et al., who carried out transesterified soybean oil in supercritical methanol without a catalyst [26], demonstrated that in addition to the alkali-catalytic and acid-catalytic processes, supercritical methylation is also an effective method. The transesterification reaction of rapeseed oil in supercritical methanol without any catalyst was investigated by Saka and Kusdiana [27]. They further discussed the effects of water on biodiesel fuel production via treatment with supercritical methanol [28].

After the development of the single-step supercritical methylation process, a few researchers developed a two-step process. Ramadhas et al. investigated biodiesel production from rubber seed oils with high FFA using a two-step transesterification process that converts the oils into their monoesters [29]. Babcock et al. investigated the conversion of chicken fat and tall oil into biodiesel via a two-step process involving hydrolysis of triglyceride-containing feeds followed by supercritical esterification of the resulting/existing FFAs [30]. Hydrolysis and the subsequent supercritical methanol treatment process developed by Minami and Saka is a promising alternative to the single-step supercritical methanol method. It concluded that hydrolysis of triglycerides liberates FFAs that can then be methylated easily [31].

An international standard that describes the minimum requirements for biodiesel indicates that a minimum of 96.5% FAMEs is required for vehicles as well as only trace amounts of mono-, di-, and triglyceride, and total glycerine can exist in the fuel [30]. Our study concludes that high concentrations of triglycerides in the extract

and high conversions of methylation in the supercritical procedure lead to high-quality biodiesel. This chapter elucidates supercritical carbon dioxide extraction of triglycerides from *Jatropha* kernels and seeds followed by subcritical hydrolysis and supercritical methylation to produce biodiesel.

13.2 Supercritical Carbon Dioxide (SC-CO_2) Extractions of Triglycerides from *Jatropha curcas*

13.2.1 Quantification of Free Fatty Acids (FFAs) and Triglycerides (TGs)

The high-performance liquid chromatography (HPLC) quantifications of five FFAs (palmitic acid, palmitoleic acid, stearic acid, oleic acid, and linoleic acid) were performed using a reverse-phase analytical column (5 μm, 250 mm L × 4.6 mm ID) (RP-18, YMC, Japan). The column was linked to an ultraviolet/visible (UV/Vis) detector (785A, Perkin-Elmer, USA) by an HPLC pump (Series 410, Perkin-Elmer, USA). Column temperature was maintained at 313 K. Analysis wavelength was set at 240 nm for detecting the five FFAs. Injection volume of each sample was 20 μL. The mobile phase of the mixed solvent (85% acetonitrile, 5% methanol, and 10% deionized water with 1% acetic acid) was utilized to analyze the FFAs. Samples were fully saponificated via a standard procedure for quantification of triglycerides in samples using gas chromatography (GC) [32]. Figure 13.1 shows the GC spectra of FAMEs during quantification of three different samples. The regression coefficients of seven calibration curves of the methylated samples were all above 0.99 [33].

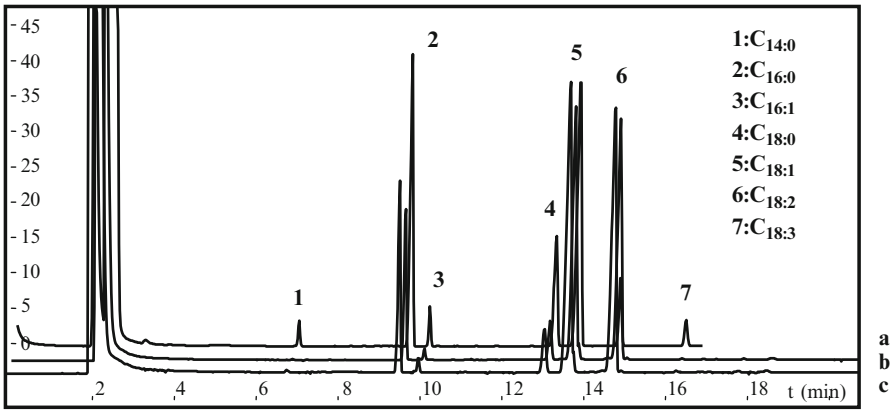

Fig. 13.1 The GC spectra of (*a*) FAME standards, (*b*) SC-CO_2 oil, and (*c*) methylated oil (Reprinted from Ref. [34]. With kind permission of © Elsevier)

13.2.2 Classical Soxhlet Extraction

In Soxhlet solvent extraction, 30 g of JC seeds were ground into a powder using a high-speed grinder and sifted through an international 20 mesh screen sieve to obtain particulates with particle sizes <0.84 mm. The JC powder was loaded into a 270-mL reflux Soxhlet extractor and extracted using *n*-hexane for 16 h; the recycle volume of *n*-hexane was 12,500 mL (e.g., solvent-to-solid ratio (SSR) = 275:1). All extracts were collected and weighed. The total amount of extracts and extraction efficiencies of triglycerides were then calculated.

Tables 13.1 and 13.2 present total yield, concentration of triglycerides (C_{TG}), and recovery of triglycerides (R_{TG}) of four triglycerides obtained by Soxhlet *n*-hexane extractions of JC seeds and kernels, respectively. These items were derived as follows:

$$\mathrm{TY} = \left(\frac{\text{Weight of the extract}}{\text{Weight of the feed}}\right) \times 100(\%), \tag{13.1}$$

$$C_{TG} = \left(\frac{\text{Weight of triglycerides in the extract}}{\text{Weight of extracted oil}}\right), \tag{13.2}$$

$$R_{TG} = \left(\frac{\text{Weight of triglycerides in the extract}}{\text{Weight of triglycerides in Soxhlet oil}}\right) \times 100(\%). \tag{13.3}$$

After 8 and 16 h of Soxhlet extraction from 30 g of JC powder, TY and C_{TG} of Soxhlet extraction were 48.89% and 49.21%, and 594.6 and 595.2 mg/g_{ext}, respectively. The 16 h Soxhlet data were considered representative of 100% R_{TG} from powdered JC.

13.2.3 Supercritical Carbon Dioxide (SC-CO_2) Extraction

Figure 13.2a shows a schematic flow diagram of SC-CO_2 extraction. In total, 100 g of powdered JC seeds or kernels were packed into a 1-L stainless steel tubular extractor (5). Liquid CO_2 was allowed to flow from a cylinder (1) via an inserted siphon tube, and the combination units mentioned above were placed in a cooling bath (3) set at 277 K. The CO_2 was then compressed to the desired working pressure using an air pump (PM6000A, TST, Taiwan) (4); it was then heated to supercritical temperatures using a constant-temperature air batch (6). The CO_2 flowed upward into the extractor (5) where it contacted the JC powder, at which point it extracted the oil. The first back-pressure regulator (7–1) located at the outlet was manually adjusted to maintain constant extraction pressure. Following extraction, the oil-laden CO_2 was driven into a 130-mL separator (8) via a drop in pressure regulated

Table 13.1 Soxhlet *n*-hexane and SC-CO_2 extractions of powdered *Jatropha* seeds (Reprinted from Ref. [34]. With kind permission of © Elsevier)

Run #	T (K)	P (bar)	SSR (g/g)	TY (%)	C_{TG} (mg/g)	$C_{C16:0}$ (mg/g)	$C_{C18:0}$ (mg/g)	$C_{C18:1}$ (mg/g)	$C_{C18:2}$ (mg/g)	R_{TG} (%)	$R_{C16:0}$ (%)	$R_{C18:0}$ (%)	$R_{C18:1}$ (%)	$R_{C18:2}$ (%)
Soxhlet n-hexane extractions														
1	342	1	138	48.89	594.6	90.4	39.1	253.9	211.2	99.27	99.27	98.89	99.25	99.31
2	342	1	275	49.21	595.2	90.5	39.3	254.1	211.3	100	100	100	100	100
SC-CO_2 extractions														
3	333	350	125	41.71	657.1	103.8	44.7	277.3	231.3	93.57	97.24	96.37	92.5	92.78

$W_{feed,soxhlet} = 30$ g; $W_{feed,SC-CO_2} = 100$g; $t_{soxhlet} = 6$ h; $t_{SC-CO_2} = 5$h

T temperature; *P* pressure; *SSR* solvent-to-solid ratio; *TY* total yield; C_{TG} concentration of triglycerides in extract; R_{TG} recovery of triglycerides = $[(TY \times C_{TG}/1{,}000)/(TY \times C_{TG}/1{,}000)_{Soxhlet}] \times 100\%$; $C_{C16:0}$ amount of C16:0; $C_{C18:0}$ amount of C18:0; $C_{C18:1}$ amount of C18:1; $C_{C18:2}$ amount of C18:2 in extract; $(TY \times C_{TG}/1{,}000)_{Soxhlet} = 29.29$ g

Table 13.2 Soxhlet *n*-hexane and SC-CO_2 extractions of powdered *Jatropha* kernels (Reprinted from Ref. [33]. With kind permission of © Elsevier B.V.)

Run #	T (K)	P (bar)	SSR (g/g)	TY (%)	C_{TG} (mg/g)	$C_{C16:0}$ (mg/g)	$C_{C18:0}$ (mg/g)	$C_{C18:1}$ (mg/g)	$C_{C18:2}$ (mg/g)	R_{TG} (%)	$R_{C16:0}$ (%)	$R_{C18:0}$ (%)	$R_{C18:1}$ (%)	$R_{C18:2}$ (%)
Soxhlet n-hexane extractions														
1	342	1	275	57.6	707.3	113.2	49.5	304.1	240.5	100	100	100	100	100
SC-CO_2 extractions														
2	333	350	125	48.2	806.5	127.9	57.1	347.1	274.4	95.42	94.55	96.53	95.51	95.48

$W_{feed,soxhlet}$ = 30 g; $W_{feed,SC-CO_2}$ = 100g; $t_{soxhlet}$ = 16 h; t_{SC-CO_2} = 5h

T temperature; *P* pressure; *SSR* solvent-to-solid ratio; *TY* total yield; C_{TG} concentration of triglycerides in extract; R_{TG} recovery of triglycerides = $[(TY \times C_{TG}/1{,}000)/(TY \times C_{TG}/1{,}000)_{Soxhlet}] \times 100\%$; $C_{C16:0}$ amount of C16:0; $C_{C18:0}$ amount of C18:0; $C_{C18:1}$ amount of C18:1; $C_{C18:2}$ amount of C18:2 in extract; $(TY \times C_{TG}/1{,}000)_{Soxhlet}$ = 40.74 g

Fig. 13.2 Schematic flow diagrams of (**a**) SC-CO_2 extraction of *Jatropha* oil and (**b**) hydrolysis and methylation reactions (Reprinted from Ref. [33]. With kind permission of © Elsevier)

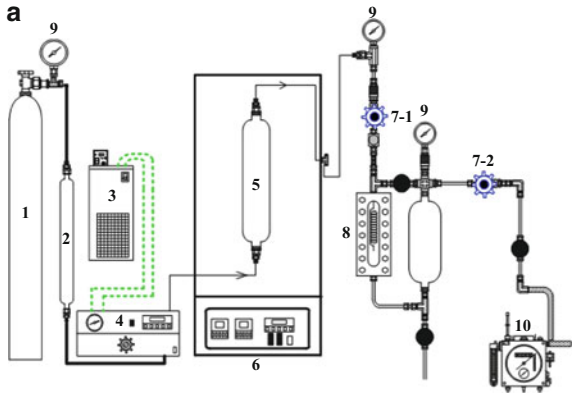

1	CO_2 cylinder	**6**	Constant temperature air batch
2	Gas dryer	**7-1~2**	Back pressure regulator
3	Temperature circulator	**8**	Separator
4	High-pressure pump	**9**	Pressure gauge
5	1L Extraction vessel	**10**	Wet gas meter

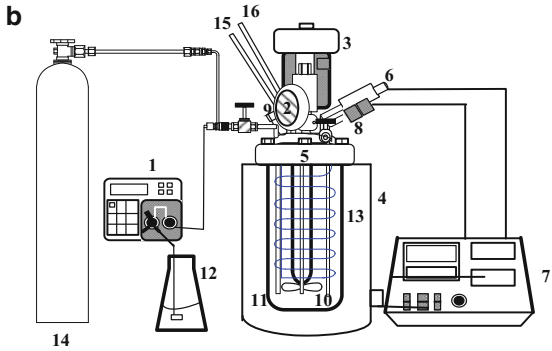

1.	HPLC pump	**9.**	Safety rapture disc
2.	Pressure gauge	**10.**	Impeller
3.	Magnetic driving motor	**11.**	Inlet tube
4.	Heat mantle	**12.**	Feed bottle
5.	Reactor	**13.**	Cooling Coil
6.	Pressure detector	**14.**	N_2 cylinder
7.	Temperature controller	**15.**	Cooling water in
8.	Thermocouple	**16.**	Cooling water out

by a second regulator (7–2); it then expanded through a spiral-type nozzle. The volume of low-pressure CO_2 was determined using a wet gas meter (W-NK-1A, Shinagawa, Japan) (10) and was subsequently returned to ambient conditions. At the end of each experiment, the oil extracted from SC-CO_2 was collected, an equal amount of water was added, and the solution was heated to 343 K to remove gummed materials. The waxed materials were removed using a centrifuge at 8,000 rpm at 273 K for 10 min.

Tables 13.1 and 13.2 also list preliminary experimental data for SC-CO_2 extraction based on the SSR of 125:1 at 350 bar and 333 K; TY and C_{TG} of SC-CO_2 extraction were 41.71% and 657.1 mg/g_{ext}, respectively. Although SC-CO_2 recovery was lower than that of Soxhlet *n*-hexane, the C_{TG} in SC-CO_2 extraction was higher than that of Soxhlet extraction because the former targeted extraction of triglycerides.

13.3 Subcritical Hydrolysis and Supercritical Methylation of *Jatropha curcas* Oil

13.3.1 Subcritical Hydrolysis

Figure 13.2b shows schematic flow diagrams of subcritical hydrolysis and supercritical methylation processes. For the subcritical hydrolysis process, 100 mL deionized water and 0.25 mL 99% acetic acid were poured into a 1-L stainless steel tubular reactor (4520, Parr Instruments Co., USA) (5). The autoclave was heated by an external heating mantle to achieve the desired operating temperature. The temperature of the reaction vessel was determined using an iron-constantan thermocouple and manipulated by a temperature controller at ±2 K. When the desired temperature (523, 543, or 563 K) was reached, 10 mL degummed and dewaxed JC oil was pumped into the reactor via an HPLC pump (Model PU-1580, Jasco, Japan). The operating pressure was maintained via a high-pressure N_2 cylinder. A two-factor response surface methodology (RSM) was employed to identify the effects of time and temperature on hydrolysis conversion (i.e., X_{TG}) for subcritical hydrolysis of SC-CO_2 extracted oil [33, 34].

Tables 13.3 and 13.4 list experimental data of subcritical hydrolysis of 10 mL extracted oil from JC seeds and kernels, respectively, at 110 bar for 30–60 min and 523–563 K. The X_{TG} is defined as follows:

$$X_{TG} = \left(\frac{\text{Weight of FFA in hydrolyzed oil}}{\text{Weight of total fatty acid in feed}} \right) \times 100(\%). \tag{13.4}$$

The maximum content of FFAs in hydrolyzed oil from JC seeds and kernels were 705.4 and 813.4 mg/g, respectively. The X_{TG} in hydrolyzed oil was 94.8%, obtained from a hydrolysis reaction at 110 bar and 563 K for 1 h; the residue of triglycerides was 5.2%. The RSM experimental design demonstrates that X_{TG} increased as both temperature and time increased.

Table 13.3 The RSM-designed subcritical hydrolysis of 10 mL SC-CO_2-extracted oil from *Jatropha* seeds (Reprinted from Ref. [34]. With kind permission of © Elsevier)

Run #	t (min)	T (K)	$C_{C16:0}$ (mg/g)	$C_{C18:0}$ (mg/g)	$C_{C18:1}$ (mg/g)	$C_{C18:2}$ (mg/g)	C_{FFA} (mg/g)	X_{TG} (%)	RE_{TG} (%)
1(F)	30	523	54.4	25.1	179.8	158.9	418.2	56.2	44.8
2(A)	45	523	73.2	33.8	242.2	214.1	563.3	75.7	24.3
3(F)	60	523	79.8	36.8	264.0	233.3	613.9	82.5	17.5
4(A)	30	543	69.6	32.1	230.1	203.2	535	71.9	28.1
5(C)	45	543	83.4	38.5	275.8	243.7	641.4	86.2	13.8
6(A)	60	543	91.4	42.2	302.4	267.2	703.2	94.5	5.5
7(F)	30	563	80.5	37.1	266.2	235.3	619.1	83.2	16.8
8(A)	45	563	91.6	42.3	303.0	267.8	704.7	94.7	5.3
9(F)	60	563	91.7	42.3	303.3	268.1	705.4	94.8	5.2

t time; T temperature; $C_{C16:0}$ concentration of $C_{16:0}$; $C_{C18:0}$ concentration of $C_{18:0}$; $C_{C18:1}$ concentration of $C_{18:1}$; $C_{C18:2}$ concentration of $C_{18:2}$; C_{FFA} = concentration of FFA; X_{TG} = hydrolysis conversion of triglycerides = $[(C_{FFA}/C_{TFA})_{product}]100\% = [(W_{FFA}^{product})/(W_{TFA}^{Feed})]\times 100\% = [1-(W_{TG}^{product})/(W_{TFA}^{Feed})]\times 100\%$; C_{TFA} = 744.1 mg/g; RE_{TG} residue of TG = $(1 - X_{TG})$

Table 13.4 The RSM-designed subcritical hydrolysis of 10 mL SC-CO_2-extracted oil from *Jatropha* kernels

Run #	t (min)	T (K)	$C_{C16:0}$ (mg/g)	$C_{C18:0}$ (mg/g)	$C_{C18:1}$ (mg/g)	$C_{C18:2}$ (mg/g)	C_{FFA} (mg/g)	X_{TG} (%)	RE_{TG} (%)
1(F)	30	523	47.0	19.0	154.9	137.7	358.6	40.6	59.4
2(A)	45	523	65.3	30.1	216.1	191.0	502.5	56.9	43.1
3(F)	60	523	77.9	31.5	256.8	228.2	594.4	67.3	32.7
4(A)	30	543	81.5	33.0	268.5	238.8	621.8	70.4	29.6
5(C)	45	543	97.1	39.3	320.1	284.5	741.0	83.9	16.1
6(A)	60	543	106.0	42.9	349.4	310.7	809.0	91.6	8.4
7(F)	30	563	98.5	39.9	325.1	289.0	752.5	85.2	14.8
8(A)	45	563	104.8	42.4	345.7	307.3	800.2	90.6	9.4
9(F)	60	563	106.6	43.1	351.4	312.3	813.4	92.1	7.9

t time; T temperature; $C_{C16:0}$ concentration of $C_{16:0}$; $C_{C18:0}$ concentration of $C_{18:0}$; $C_{C18:1}$ concentration of $C_{18:1}$; $C_{C18:2}$ concentration of $C_{18:2}$; C_{FFA} = concentration of FFA; X_{TG} = hydrolysis conversion of triglycerides = $[(C_{FFA}/C_{TFA})_{product}]100\% = [(W_{FFA}^{product})/(W_{TFA}^{Feed})]\times 100\% = [1-(W_{TG}^{product})/(W_{TFA}^{Feed})]\times 100\%$; C_{TFA} = 883.2 mg/g; RE_{TG} residue of TG = $(1 - X_{TG})$

13.3.2 Supercritical Methylation

For the supercritical methylation process, a certain amount of methanol three times more of the oil was loaded into the reactor (5). When the desired temperature was reached, 10 mL hydrolyzed oil was pumped into the autoclave using the HPLC pump. The remaining steps in the procedure were the same as those in the hydrolysis process. At the end of each experiment, the upper layer of the reacted solution

Table 13.5 The RSM-designed supercritical methylation of 10 mL hydrolyzed *Jatropha* oil from *Jatropha* seeds (Reprinted from Ref. [34]. With kind permission of © Elsevier)

Run #	t (min)	T (K)	SSR (V_{MeOH}/V_{oil})	$C_{C16:0}$ (mg/g)	$C_{C18:0}$ (mg/g)	$C_{C18:1}$ (mg/g)	$C_{C18:2}$ (mg/g)	C_{FAME} (mg/g)	X_{FFA} (%)
1(F)	5	523	7/1	92.6	38.2	218.0	196.2	545.0	71.2
2(F)	5	523	3/1	93.0	38.4	218.9	197.0	547.3	71.5
3(A)	5	543	5/1	102.9	42.4	242.2	217.9	605.4	79.1
4(F)	5	563	7/1	105.5	43.4	248.3	223.5	620.7	81.1
5(F)	5	563	3/1	108.5	44.7	255.3	229.8	638.3	83.4
6(A)	7	523	5/1	108.1	44.5	254.4	229.0	636.0	83.1
7(A)	7	543	7/1	111.0	45.7	261.2	235.0	652.9	85.3
8(C)	7	543	5/1	120.2	49.5	282.9	254.6	707.2	92.4
9(A)	7	543	3/1	121.2	49.9	285.0	256.5	712.6	93.1
10(A)	7	563	5/1	117.9	48.5	277.4	249.7	693.5	90.6
11(F)	9	523	3/1	121.7	50.1	286.2	257.6	715.6	93.5
12(F)	9	523	7/1	114.6	47.3	269.7	242.7	674.3	88.1
13(A)	9	543	5/1	121.8	50.1	286.6	257.9	716.4	93.6
14(F)	9	563	3/1	127.9	52.8	301.0	270.9	752.4	98.3
15(F)	9	563	7/1	123.9	51.0	291.5	262.3	728.7	95.2

t time; T temperature; $C_{C16:0}$ concentration of $C_{16:0}$; $C_{C18:0}$ concentration of $C_{18:0}$; $C_{C18:1}$ concentration of $C_{18:1}$; $C_{C18:2}$ concentration of $C_{18:2}$; C_{FAME} concentration of FAME; X_{FFA} = conversion of free fatty acids = $(C_{FAME}/C_{TFA})_{product}100\% = [(W_{FAME}^{product})/(W_{TFA}^{Feed})] \times 100\% = [1-(W_{FFA}^{product} + W_{TG}^{product})/(W_{TFA}^{Feed})] \times 100\%$; C_{TFA} = 765.4 mg/g

was collected and residual methanol was removed using a vacuum rotary evaporator. A three-factor RSM experimental design for supercritical methylation of hydrolyzed oil was employed to identify dependent variables (i.e., X_{FFA}) based on changes to independent variables (i.e., time, temperature, and the SSR) [33, 34].

Tables 13.5 and 13.6 list experimental data from supercritical methylation of 10 mL hydrolyzed oil at 110 bar; experimental data were recorded within the following parameters: 5–15 min, methanol-to-oil volume ratios of 3:1–7:1, and temperatures of 523–563 K. The conversion of free fatty acids is derived as follows:

$$X_{FFA} = \left(\frac{\text{Weight of FAME in methylated oil}}{\text{Weight of total fatty acid in feed}}\right) \times 100(\%). \tag{13.5}$$

The maximum content of FAMEs in methylated oil from JC seeds and kernels were 752.4 and 985.0 mg/g, respectively. The X_{FFA} obtained from this methylation reaction of 10 mL hydrolyzed oil from JC kernels added to 30 mL methanol was 99%. The resulting X_{FFA}, which represents the quality of methylated oil, increased as time and temperature increased, but decreased as the SSR decreased, as demonstrated by the RSM. This decrease may be due to FFAs acting as acid catalysts during methylation, such that a large SSR results in low FFA concentration that slows the methylation rate.

Table 13.6 The RSM-designed supercritical methylation of 10 mL hydrolyzed *Jatropha* oil from *Jatropha* kernels

Run #	t (min)	T (K)	SSR (V_{MeOH}/V_{oil})	$C_{C16:0}$ (mg/g)	$C_{C18:0}$ (mg/g)	$C_{C18:1}$ (mg/g)	$C_{C18:2}$ (mg/g)	C_{FAME} (mg/g)	X_{FFA} (%)
1(F)	5	523	3/1	91.5	36.7	216.8	186.5	531.3	53.4
2(F)	5	523	7/1	85.9	34.5	203.8	175.3	499.5	50.2
3(A)	5	543	5/1	130.6	52.4	309.7	266.4	759.1	76.3
4(F)	5	563	3/1	127.8	51.3	303.2	260.9	743.2	74.7
5(F)	5	563	7/1	122.2	49.0	289.8	249.4	710.4	71.4
6(A)	10	523	5/1	126.0	50.5	298.8	257.0	732.3	73.6
7(A)	10	543	3/1	151.4	60.8	359.2	309.1	880.5	88.5
8(C)	10	543	5/1	145.8	58.5	345.9	297.5	847.7	85.2
9(A)	10	543	7/1	142.9	57.3	339.0	291.6	830.8	83.5
10(A)	10	563	5/1	156.8	63.0	372.3	320.3	912.4	91.7
11(F)	15	523	3/1	152.8	61.3	362.5	311.9	888.5	89.3
12(F)	15	523	7/1	145.6	58.4	345.5	297.2	846.7	85.1
13(A)	15	543	5/1	166.3	66.7	394.6	339.5	967.1	97.2
14(F)	15	563	3/1	169.4	68.0	401.9	345.7	985.0	99.0
15(F)	15	563	7/1	160.1	64.3	380.0	326.9	931.3	93.6

t time; T temperature; $C_{C16:0}$ concentration of $C_{16:0}$; $C_{C18:0}$ concentration of $C_{18:0}$; $C_{C18:1}$ concentration of $C_{18:1}$; $C_{C18:2}$ concentration of $C_{18:2}$; C_{FAME} concentration of FAME; X_{FFA} = conversion of free fatty acids = $(C_{FAME}/C_{TFA})_{product}100\% = [(W_{FAME}^{product})/(W_{TFA}^{Feed})] \times 100\% = [1-(W_{FFA}^{product} + W_{TG}^{product})/(W_{TFA}^{Feed})] \times 100\%$; C_{TFA} = 994.9 mg/g

13.3.3 Determination of the Rate Constant (k) and Activation Energy of Reactions

Experimental data (Tables 13.3, 13.4, 13.5, 13.6, 13.7, and 13.8) for hydrolysis and methylation procedures were utilized to configure the rate constant (k) and activation energy of both processes. Figure 13.3a shows the kinematic relationship between X_{TG} via hydrolysis time at 523, 543, 563, and 583 K. Only high temperatures yielded high hydrolysis rates, and conversion peaked at 94.8% with a deep black opaque color. This may have been due to the equilibrium between a forward reaction and backward reaction. Within 1 h of hydrolysis at 543 K and 110 bar, X_{TG} reached 94.5% with transparent red-colored oil. Therefore, the following hydrolysis reaction was conducted at 543 K to generate hydrolyzed oil for the methylation study. To determine the rate constant of hydrolysis, experimental data ($1 - X_{TG}$) were plotted against reaction time, as shown in Fig. 13.3b. The rate constants of hydrolysis at 523, 543, 563, and 583 K were 0.0296 (min^{-1}), 0.0463 (min^{-1}), 0.0640 (min^{-1}), and 0.0997 (min^{-1}), respectively, and were obtained from slopes of the four first-order reactions. Figure 13.3c shows activation energy of the hydrolysis reaction, which was obtained by an Arrhenius plot of ln (k) versus $1/T$. The activation energy of hydrolysis of SC-CO_2 extracted oil from JC seeds was 50.2 kJ/mol with a regression coefficient of 0.9955.

Figure 13.4a reveals the kinematic relationship between X_{FFA} via methylation time at 523, 543, and 563 K. Although high temperatures resulted in a high methylation rate, conversion peaked at 98.3% within a 15-min period at 563 K and 110 bar.

Table 13.7 Kinematic effect on supercritical methylation of 10 mL of hydrolyzed *Jatropha* oil from *Jatropha* seeds (Reprinted from Ref. [34]. With kind permission of © Elsevier)

Run #	t (min)	T (K)	SSR (V_{MeOH}/V_{oil})	$C_{C16:0}$ (mg/g)	$C_{C18:0}$ (mg/g)	$C_{C18:1}$ (mg/g)	$C_{C18:2}$ (mg/g)	C_{FAME} (mg/g_{oil})	X_{FFA} (%)
1	5	523	3/1	93.0	38.3	218.9	197.0	547.3	71.5
2	5	543	3/1	99.9	41.1	235.1	211.6	587.8	76.8
3	5	563	3/1	108.5	44.7	255.3	229.8	638.3	83.4
4	10	523	3/1	112.6	46.3	264.8	238.3	662.1	86.5
5	10	543	3/1	121.1	49.9	285.0	256.5	712.6	93.1
6	10	563	3/1	123.1	50.7	289.6	260.7	724.1	94.6
7	15	523	3/1	121.7	50.1	286.3	257.6	715.6	93.5
8	15	543	3/1	126.3	52.0	297.3	267.6	743.2	97.1
9	15	563	3/1	127.9	52.7	301.0	270.9	752.4	98.3

t time; T temperature; *SSR* methanol-to-oil ratio = 3/1; $C_{C16:0}$ concentration of $C_{16:0}$; $C_{C18:0}$ concentration of $C_{18:0}$; $C_{C18:1}$ concentration of $C_{18:1}$; $C_{C18:2}$ concentration of $C_{18:2}$; C_{FAME} concentration of FAME; X_{FFA} = conversion of free fatty acids = $(C_{FAME}/C_{TFA})_{product}100\% = [(W_{FAME}^{product})/(W_{TFA}^{Feed})] \times 100\% = [1-(W_{FFA}^{product} + W_{TG}^{product})/(W_{TFA}^{Feed})] \times 100\%$; C_{TFA} = 765.4 mg/g

Table 13.8 Kinematic effect on supercritical methylation of 10 mL of hydrolyzed *Jatropha* oil from *Jatropha* kernels

Run #	t (min)	T (K)	SSR (V_{MeOH}/V_{oil})	$C_{C16:0}$ (mg/g)	$C_{C18:0}$ (mg/g)	$C_{C18:1}$ (mg/g)	$C_{C18:2}$ (mg/g)	C_{FAME} (mg/g_{oil})	X_{FFA} (%)
1	5	523	3/1	91.3	36.7	216.8	186.5	531.3	53.4
2	5	543	3/1	116.0	46.6	275.2	236.8	674.6	67.8
3	5	563	3/1	127.8	51.3	303.2	260.9	743.2	74.7
4	10	523	3/1	128.3	51.5	304.5	261.9	746.2	75.0
5	10	543	3/1	151.4	60.8	359.2	309.1	880.5	88.5
6	10	563	3/1	163.6	65.6	388.1	333.9	951.2	95.6
7	15	523	3/1	152.8	61.3	362.5	311.9	888.5	89.3
8	15	543	3/1	163.1	65.4	386.9	332.8	948.2	95.3
9	15	563	3/1	169.4	68.0	401.9	345.7	985.0	99.0

t time; T temperature; *SSR* methanol-to-oil ratio = 3/1; $C_{C16:0}$ concentration of $C_{16:0}$; $C_{C18:0}$ concentration of $C_{18:0}$; $C_{C18:1}$ concentration of $C_{18:1}$; $C_{C18:2}$ concentration of $C_{18:2}$; C_{FAME} concentration of FAME; X_{FFA} = conversion of free fatty acids = $(C_{FAME}/C_{TFA})_{product}100\% = [(W_{FAME}^{product})/(W_{TFA}^{Feed})] \times 100\% = [1-(W_{FFA}^{product} + W_{TG}^{product})/(W_{TFA}^{Feed})] \times 100\%$; C_{TFA} = 994.9 mg/g

To determine the k of methylation, experimental data $(1 - X_{FFA})$ were plotted against reaction time, as shown in Fig. 13.4b. The k of methylation process at 523, 543, and 563 K was 0.1923 (min^{-1}), 0.2490 (min^{-1}), and 0.2837 (min^{-1}), respectively; these rate constants were obtained from the slopes of the three first-order reactions. Figure 13.4c shows activation energy of methylation obtained via an Arrhenius plot of ln (k) versus $1/T$ was 23.9 kJ/mol with a regression coefficient of 0.9725.

Figures 13.5 and 13.6 reveal that the activation energies of hydrolysis and transesterified reactions of JC kernels obtained by an Arrhenius plot were 68.5 and 45.2 kJ/mol, respectively. Table 13.9 lists the physical properties of SC-CO_2-extracted

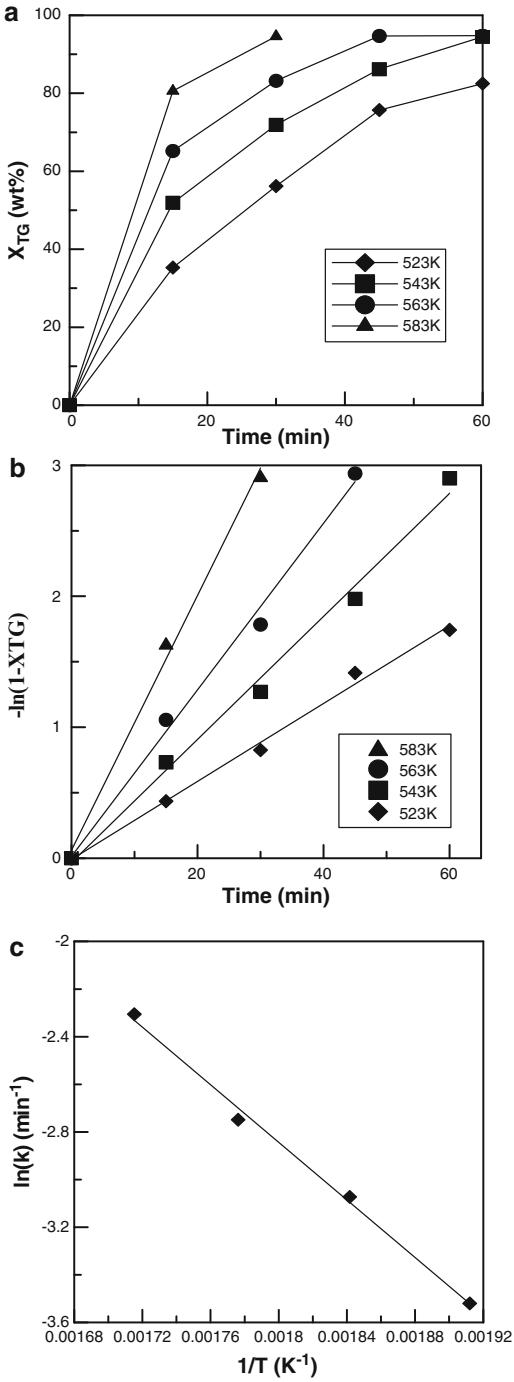

Fig. 13.3 Kinematic relationship between the conversion of triglycerides (X_{TG}) versus hydrolysis time at 523, 543, 563, and 583 K. (**a**) Kinetic curves of hydrolysis. (**b**) Determination of the rate constant of the hydrolysis reaction. (**c**) Arrhenius plot for *Jatropha* seeds (Reprinted from Ref. [34]. With kind permission of © Elsevier)

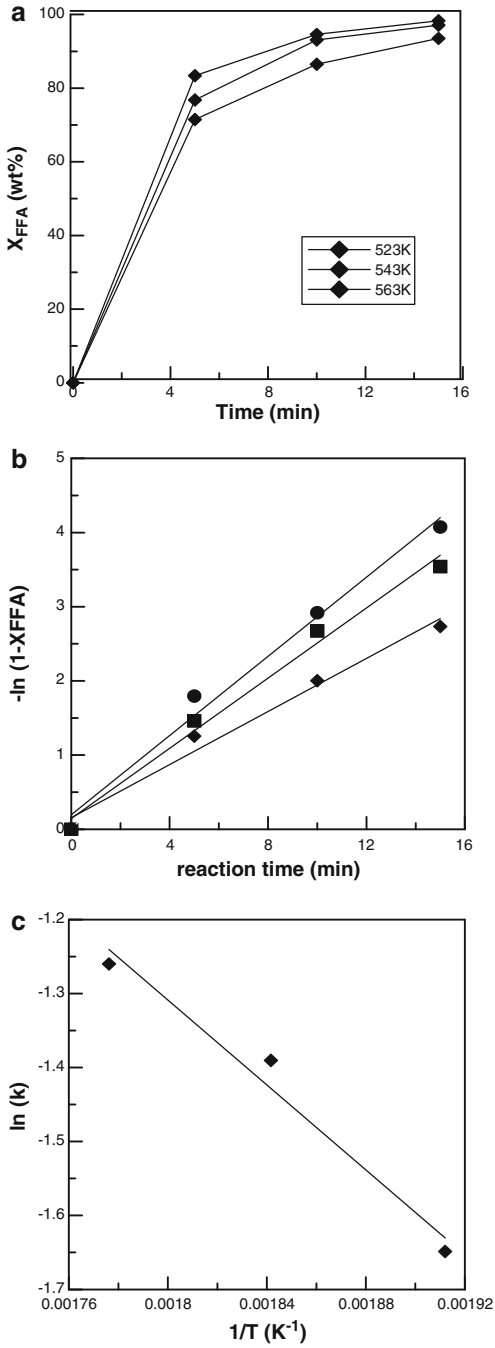

Fig. 13.4 Kinematic relationship between the conversion of free fatty acids (X_{FFA}) versus methylation time at 523, 543, and 563 K. (**a**) Kinetic curves of methylation. (**b**) Determination of the rate constant of the methylation reaction. (**c**) Arrhenius plot for *Jatropha* seeds (Reprinted from Ref. [34]. With kind permission of © Elsevier)

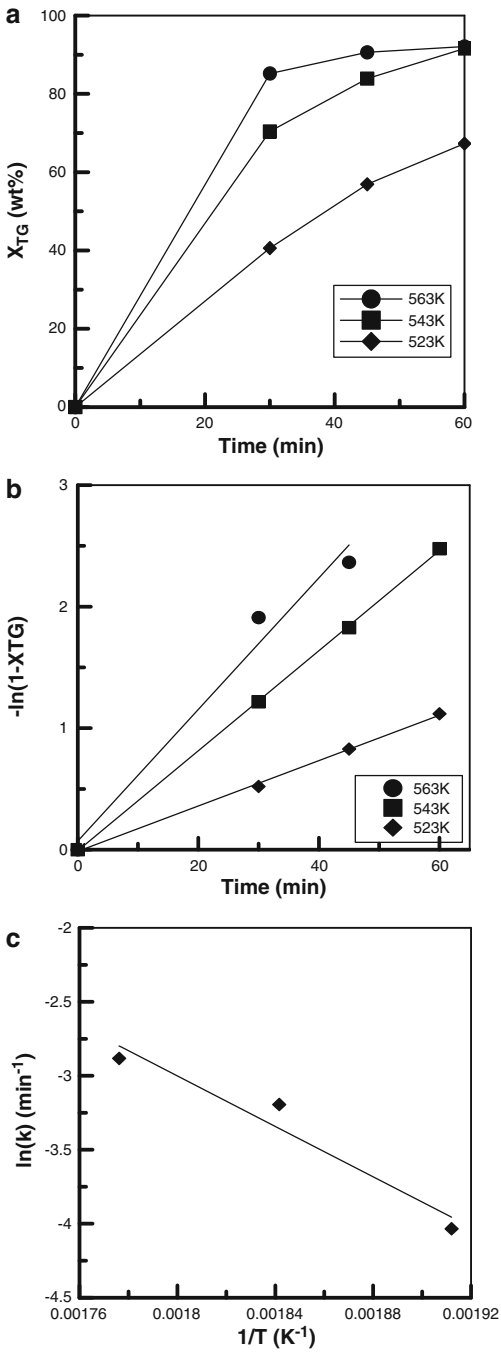

Fig. 13.5 Kinematic relationship between the conversion of triglycerides (X_{TG}) versus hydrolysis time at 523, 543, and 563 K. (**a**) Kinetic curves of hydrolysis. (**b**) Determination of the rate constant of the hydrolysis reaction. (**c**) Arrhenius plot for *Jatropha* kernels (Reprinted from Ref. [33]. With kind permission of © Elsevier)

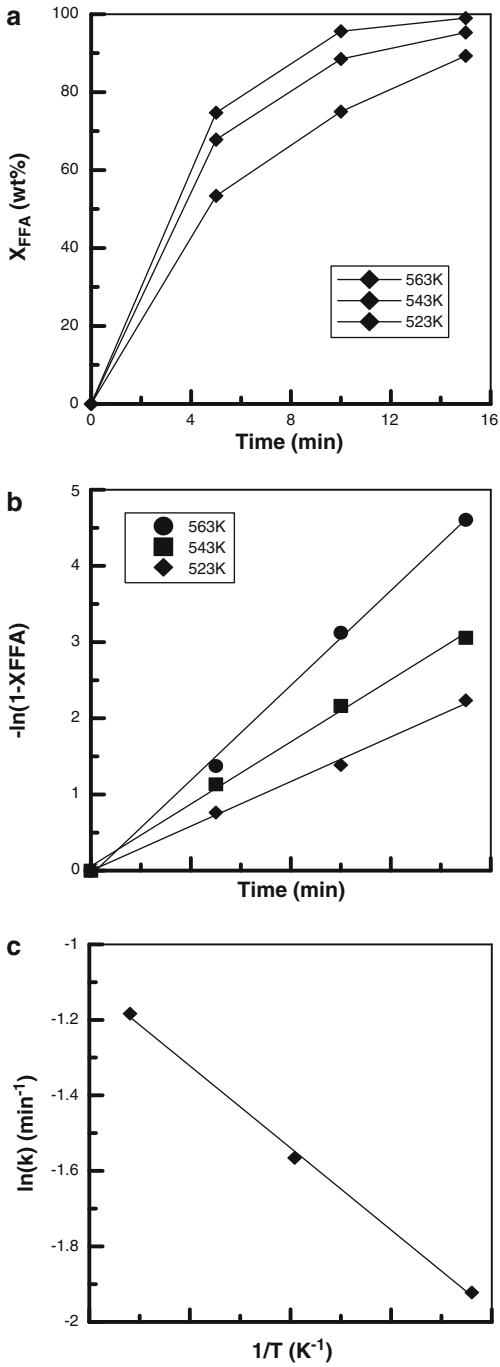

Fig. 13.6 Kinematic relationship between the conversion of free fatty acids (X_{FFA}) versus methylation time at 523, 543, and 563 K. (**a**) Kinetic curves of methylation. (**b**) Determination of the rate constant of the methylation reaction. (**c**) Arrhenius plot for *Jatropha* kernels (Reprinted from Ref. [33]. With kind permission of © Elsevier)

Table 13.9 Physical properties of SC-CO_2 extracted oil and SC-MeOH methylated oil from *Jatropha* seeds and kernels (Reprinted from Ref. [34]. With kind permission of © Elsevier)

Physical properties	JC seeds	JC kernels
SC-CO_2 oil		
ρ	0.901587 ± 5.61E–06	0.902201 ± 2.65E–06
η	1.462838 ± 4.42E–06	1.463459 ± 8.38E–06
μ	30.1824 ± 3.00E–04	32.06793 ± 9.25E–03
Methylated oil		
ρ	0.866884 ± 1.63E–05	0.866329 ± 5.61E–06
η	1.441443 ± 2.27E–05	1.462838 ± 4.42E–06
μ	3.8081 ± 2.00E–04	4.1239 ± 3.52E–03

ρ density (g·cm^{-3}); η refractive index; μ dynamic viscosity (mPa·s); 1 mPa-s] = 1 [centipoise]

oil and methylated oil. The density and viscosity of methylated oil were 0.8668 g/cm^3 and 3.8081 cP (from *Jatropha* seeds) and 0.8663 g/cm^3 and 4.1239 cP (from *Jatropha* kernels), respectively. The viscosity of this methylated oil meets the international criteria for biodiesel (max. 4.5 cP).

13.3.4 Economic Estimation

This study presents a promising method for producing biodiesel that meets specification CNS 15072, published by the Bureau of Standards, Metrology & Inspection, Republic of China (>98.5% pure). The first step in the process is SC-CO_2 extraction of triglycerides from JC seeds at the optimum temperature of 333 K and pressure of 350 bar. The second step is 60 min hydrolysis at 543 K and 110 bar. The last step is 15 min methylation at 563 K and 110 bar. After mass conversion between FAMEs and triglycerides, 98.5% pure biodiesel was obtained. The primary advantage of this process is high performance in SC-CO_2 extraction. According to experimental results, the concentrations of various triglycerides in SC-CO_2 extraction are greatest. Notably, SC-CO_2 has better selectivity for triglycerides than *n*-hexane. In this case, SC-CO_2 extraction can provide a purer raw material than traditional extraction process to produce biodiesel.

Table 13.10 compares return on investment (ROI) between the SC-CO_2 method and pressing method. The SC-CO_2 process has high annual and equipment costs. Return on investment for the SC-CO_2 process takes more than 4 years. However, the quantity of biofuel from SC-CO_2 production can be increased to meet market demands. Maximum sales of this biofuel can reach NT$2.74 million per year, while that for the pressing method can only reach NT$1.53 million per year. The SC-CO_2 method is almost two times more profitable than the pressing method.

Table 13.10 The comparison of return on investment between SC-CO_2 method and pressing method (Unit: 1,000 NT)

		Unit	SC-CO_2	Pressing
Equipment	CO_2 pump		500	
	5-ton extractor		4,000	
	Separator		200	
	Controls		470	
	Mechanical expeller			400
	Distillator			200
	Feed pump		400	400
	Reactor		500	500
Equipment cost (**A**)			**6,070**	**1,500**
Operations		NT/year	600	200
Materials	*Jatropha*	Year/100 ha	900	900
	CO_2		220	
Annual cost (**B**)		NT/year/100 ha	**1,720**	**1,100**
Benefits	Biofuel		2,740	1,530
	Fertilizer		530	580
	Carbon credit		135	135
	Glycerol		90	50
Benefit (**C**)			**3,495**	**2,295**
Deficit	1st year [C−(A+B)]	NT	−4,295	−305
	2nd year [C−B]	NT	+1,775	+1,195
Return on investment		Year	4	2

Bold values is for the total costs

13.4 Conclusions

Green technology is playing an increasingly important role in modern society. The SC-CO_2 extraction process uses only carbon dioxide, which is widely considered a green solvent. Furthermore, as the demand for biofuel is increasing, the ability to increase production is vital. This study investigated SC-CO_2 extraction of triglycerides from JC kernels followed by subcritical hydrolysis and supercritical methylation to generate a 98.5 purity level of biodiesel. The activation energy necessary for hydrolysis was higher than that for methylation indicating that hydrolysis was the rate-determining step in biodiesel production. Kinematic experimental data demonstrate that the two-step process for hydrolysis and subsequent methylation of the SC-CO_2 extracted oil from JC kernels is a suitable pathway for producing biodiesel.

Acknowledgments The authors would like to thank the National Science Council of the Republic of China, Taiwan (contract no. NSC 98-2221-E005-053-MY3), and the Ministry of Education of the Republic of China, Taiwan, under the ATU plan for financially supporting this research.

References

1. Tzeng TC, Lin YL, Jong TT, Chang CJ (2007) Ethanol modified supercritical fluids extraction of scopoletin and artemisinin from *Artemisia annua* L. Sep Purif Technol 56:18–24
2. You GS, Lin SC, Chen CR, Tsai WC, Chang CJ, Huang WW (2002) Supercritical carbon dioxide extraction enhances flavonoids in water-soluble propolis. J Chin Inst Chem Eng 33:233–241
3. Catchpole OJ, Grey JB, Mitchell KA, Lan JS (2004) Supercritical antisolvent fractionation of propolis tincture. J Supercrit Fluid 29:97–106
4. Lee YN, Chen CR, Yang HL, Lin CC, Chang CJ (2007) Isolation and purification of 3,5-diprenyl-4-hydroxycinnamic acid (artepillin C) in Brazilian propolis by supercritical fluid extractions. Sep Purif Technol 54:130–138
5. Kaieda M, Samukawa T, Kondo A, Fukuda H (2001) Effect of methanol and water contents on production of biodiesel fuel from plant oil catalyzed by various lipases in a solvent-free system. J Biosci Bioeng 91:12–15
6. Haas MJ, Scott KM, Alleman TL, McCormick RL (2001) Engine performance of biodiesel fuel prepared from soybean soapstock: a high quality renewable fuel produced from a waste feedstock. Energy Fuel 15:1207–1212
7. Hawash S, Kamal N, Zaher F, Kenawi O, Diwani GE (2009) Biodiesel fuel from *Jatropha* oil via non-catalytic supercritical methanol transesterification. Fuel 88:579–582
8. Chen WH, Chen CH, Chang CJ, Liau BC, Hsiang D (2010) Supercritical carbon dioxide extraction of triglycerides from *Aquilaria crassna* seeds. Sep Purif Technol 73:135–141
9. Srivastava A, Prasad R (2000) Triglycerides-based diesel fuels. Renew Sustain Energy Rev 4:111–133
10. Moser BR (2009) Biodiesel production, properties, and feedstocks. In Vitro Cell Dev Biol Plant 45:229–266
11. Foidl N, Foidl G, Sanchez M, Mittelbach M, Hackel S (1996) *Jatropha curcas* L. as a source for the production of biofuel in Nicaragua. Bioresour Technol 58:77–82
12. Lopez O, Foidl G, Foidl N (1997) Production of biogas from *J. curcas* fruitshells. In: Gubitz GM, Mittelbach M, Trabi M (eds) Biofuels and industrial products from *Jatropha curcas*, proceedings from the symposium "Jatropha 97". Managua, Nicaragua, 23–27 Feb, Dbv-Verlag, Graz, Austria, pp 118–122
13. Staubmann R, Foidl G, Foidl N, Gubitz GM, Lafferty RM, Valencia Arbizu VM (1997) Production of biogas from J. curcas seeds press cake. In: Gubitz GM, Mittelbach M, Trabi M (eds) Biofuels and industrial products from *Jatropha curcas*, proceedings from the symposium "Jatropha 97". Managua, Nicaragua, 23–27 Feb, Dbv-Verlag, Graz, Austria, pp 123–131
14. Makkar HPS, Becker K, Sporer F, Wink M (1997) Studies on nutritive potential and toxic constituents of different provenances of *Jatropha curcas*. J Agric Food Chem 45:3152–3157
15. Akintayo ET (2004) Characteristics and composition of *Parkia biglobbossa* and *Jatropha curcas* oils and cakes. Bioresour Technol 92:307–310
16. Cvengros J, Povazanec F (1996) Production and treatment of rapeseed oil methyl esters as alternative fuels for diesel engines. Bioresour Technol 55:145–150
17. Kaieda M, Samukawa T, Matsumoto T, Ban K, Kondo A, Shimada Y (1999) Biodiesel fuel production from plant oil catalyzed by *Rhizopus oryzae* lipase in a water-containing system without an organic solvent. J Biosci Bioeng 88:627–631
18. Shimada Y, Watanabe Y, Sugihara A, Tominaga Y (2002) Enzymatic alcoholysis for biodiesel fuel production and application of the reaction to oil processing. J Mol Catal B Enzym 17:133–142
19. Pizarro AVL, Park EY (2003) Lipase-catalyzed production of biodiesel fuel from vegetable oils contained in waste activated bleaching earth. Process Biochem 38:1077–1082
20. Zhang Y, Dube MA, McLean DD, Kates M (2003) Biodiesel production from waste cooking oil: 1. Process design and technological assessment. Bioresour Technol 89:1–16

21. Ghadge SV, Raheman H (2005) Biodiesel production from mahua (*Madhuca indica*) oil having high free fatty acids. Biomass Bioenerg 28:601–605
22. Tashtoush GM, Al-Widyan MI, Al-Jarrah MM (2004) Experimental study on evaluation and optimization of conversion of waste animal fat into biodiesel. Energy Convers Manag 45:2697–2711
23. Madras G, Kolluru C, Kumar R (2004) Synthesis of biodiesel in supercritical fluids. Fuel 83:2029–2033
24. Kusdiana D, Saka S (2001) Kinetics of transesterification in rapeseed oil to biodiesel fuel as treated in supercritical methanol. Fuel 80:693–698
25. Rathore V, Madras G (2007) Synthesis of biodiesel from edible and non- edible oils in supercritical alcohols and enzymatic synthesis in supercritical carbon dioxide. Fuel 86:2650–2659
26. Cao W, Han H, Zhang J (2005) Preparation of biodiesel from soybean oil using supercritical methanol and co-solvent. Fuel 84:347–351
27. Saka S, Kusdiana D (2001) Biodiesel fuel from rapeseed oil as prepared in supercritical methanol. Fuel 80:225–231
28. Kusdiana D, Saka S (2004) Effects of water on biodiesel fuel production by supercritical methanol treatment. Bioresour Technol 91:289–295
29. Ramadhas AS, Jayaraj S, Muraleedharan C (2005) Biodiesel production from high FFA rubber seed oil. Fuel 84:335–340
30. Babcock RE, Clausen EC, Popp M, Schulte WB (2008) Yield characteristics of biodiesel produced from chicken fat-tall oil blended feed stocks. Mack-blackwell Rural Transportation Center, MBTC-2092, annual report 2007–2008, Fayetteville, Arkansas 18
31. Minami E, Saka S (2006) Kinetics of hydrolysis and methyl esterification for biodiesel production in two-step supercritical methanol process. Fuel 85:2479–2483
32. Chen WH, Chen CH, Chang CJ, Chiu YH, Hsiang D (2009) Supercritical carbon dioxide extraction of triglycerides from *Jatropha curcas* L. seeds. J Supercrit Fluid 51:174–180
33. Chen CH, Chen WH, Chang CJ, Lai SM, Tu CH (2010) Biodiesel production from supercritical carbon dioxide extracted *Jatropha* oil. J Supercrit Fluid 52:228–234
34. Chen CH, Chen WH, Chang CJ, Setsu I, Tu CH, Shieh CJ (2010) Subcritical hydrolysis and supercritical methylation of supercritical carbon dioxide extraction of *Jatropha* oil. Sep Purif Technol 74:7–13

Chapter 14
Nanofluids as Advanced Coolants

S.M. Sohel Murshed and Carlos A. Nieto de Castro

Abstract Nanofluids have attracted great interest from the researchers all over the world due to their superior thermal transports and potential applications in numerous important fields. From extensive research, nanofluids are found to exhibit significantly higher thermal conductivity than that of base fluids. However, besides thermal conductivity, investigations on convective and boiling heat transfer are also very important in order to exploit nanofluids as advanced coolants. In this chapter, experimental investigations on these two major cooling features, i.e., convective and boiling heat transfer, of nanofluids are reported together with critical review of recent research progress in these important areas of nanofluids. Nanofluid development background along with their potential benefits and applications are also briefly discussed. Despite of controversies and scattered experimental data on all these thermal features of nanofluids, it is undisputed that nanofluids exhibit substantially enhanced thermal conductivity, convective heat transfer coefficient, and boiling critical heat flux which further increase with increasing concentration of nanoparticles, and these clearly evince that nanofluids can potentially be used as advanced coolants in the future.

14.1 Background of Nanofluids

14.1.1 Concept and Development

Cooling for maintaining desirable performance and durability of smaller features of microelectronic and more power output-based devices is one of the most important technical issues in many high-tech industries and thermal management systems.

S.M.S. Murshed (✉) • C.A. Nieto de Castro
Centre for Molecular Sciences and Materials, Department of Chemistry and Biochemistry, Faculty of Sciences, University of Lisbon, Campo Grande, Lisbon 1749-016, Portugal
e-mail: smmurshed@fc.ul.pt; cacastro@fc.ul.pt

A. Mohammad and Inamuddin (eds.), *Green Solvents I: Properties and Applications in Chemistry*, DOI 10.1007/978-94-007-1712-1_14,

The conventional method to increase the cooling rate involves the use of extended heat transfer surfaces. However, this approach requires an undesirable increase in the size of the thermal management systems. In addition, the inherently poor thermal properties of traditional heat transfer fluids such as water, ethylene glycol, or engine oil greatly limit the cooling performance. Thus, existing conventional methods for increasing the heat dissipation are not suitable to meet the cooling demand of the high-tech industries. It is known that at room temperature, fluids possess orders of magnitude smaller thermal conductivity than most of the metallic or nonmetallic particles. For example, thermal conductivities of water (0.607 W/m·K) and engine oil (0.145 W/m·K) are about 5,000 and 21,000 times, respectively, smaller than that of carbon nanotubes (e.g., 3,000 W/m·K for multiwalled carbon nanotubes, MWCNT), and the thermal conductivity of water is about 700 times smaller than that of copper particle. Therefore, the thermal conductivities of fluids that contain suspended metallic or nonmetallic particles or tubes are expected to be significantly higher than those of traditional heat transfer fluids.

Although nanoparticle suspensions were used in heat transfer studies as early as 1984 by Yang and Maa [1] and then in 1993 by Masuda et al. [2], it was only in 1995 that Choi [3] at Argonne National Laboratory of USA coined the concept of "nanofluid" which has been proposed to meet the cooling challenges facing many advanced industries and devices. Apart from Yang and Maa [1] and Masuda et al. [2], Gass and coworkers [4] from Switzerland used the same term "nanofluid" to express minute volume of fluid (nanoliter) in microfluidics study in 1993. In the same year, Arnold Grimm [5], a German researcher, also won a German patent on the enhanced thermal conductivity of nano- and micro-sized particle suspensions. Aluminum particles of 80 nm to 1 μm were suspended into a fluid, and about 100% increase in the thermal conductivity of the fluid for loadings of 0.5–10 vol.% was reported in his patent.

This new class of heat transfer fluids (nanofluids) is engineered by dispersing nanometer-sized solid particles, rods, or tubes in traditional heat transfer fluids. Studies showed that nanofluids exhibit significantly higher thermophysical properties, particularly thermal conductivity and thermal diffusivity than those of base fluids [6–11]. These nanofluids have attracted great interest from the research community due to their enhanced thermal performance, potential benefits, and applications in numerous important fields such as microelectronics, microfluidics, transportation, manufacturing, medical, and so on.

14.1.2 Potential Benefits and Applications

As thermal properties, particularly thermal conductivity of fluid, play a vital role in the development of energy efficient heat transfer equipment, numerous theoretical and experimental studies on increasing thermal conductivity of liquid by suspending small particles have been conducted since the treatise by Maxwell appeared [12].

However, all the studies on thermal conductivity of suspensions were confined to millimeter- or micrometer-sized particles. The major problems of such suspensions are the rapid settling of these particles, clogging the flow channel, and increased pressure drop in the fluid. If the fluid is kept circulating rapidly enough to prevent much settling, these particles would damage the walls of the heat transfer devices (e.g., pipes and channels). Furthermore, milli- or microparticles are too large for microsystems to be used. In contrast, nanoparticles which are orders of magnitude smaller than the microsystems remain in suspension reducing erosion and clogging. Thus, with dispersion of nanoparticle, nanofluids can flow smoothly through mini- or microchannels. Another advantage is the mobility of the particles, which may bring about microconvection of fluids and hence can enhance the transports of heat. Because the nanoparticles are small, they weigh less, and chances of sedimentation are also less making nanofluids more stable.

The impact of nanofluid technology is expected to be great, considering that the heat transfer performance of heat exchangers or cooling devices is vital in numerous industries. As mentioned before, when the nanoparticles are properly dispersed, besides anomalously high thermal conductivity, nanofluids offer numerous benefits [13], which include improved heat transfer and stability, microchannel cooling without clogging, miniaturized systems, and reduction in pumping power. The better stability of nanofluids will prevent rapid settling and reduce clogging in the walls of heat transfer devices. The high thermal conductivity of nanofluids translates into higher energy efficiency, better performance, and lower operating costs. They can reduce energy consumption for pumping heat transfer fluids. Miniaturized systems require smaller inventories of fluids where nanofluids can be used. Thermal systems can be smaller and lighter. In vehicles, smaller components result in better gasoline mileage, fuel savings, lower emissions, and cleaner environment.

With the aforementioned highly desirable thermal properties and potential benefits, it is considered that nanofluids have wide range of industrial and medical applications. Nanofluids can be used to improve thermal management systems in many engineering applications including transportation, microelectromechanical systems (MEMS), electronics and instrumentations, heating–ventilating and air-conditioning, and in medical science. Details of the potential applications of nanofluids have been discussed elsewhere [10, 13] and hence will not be elaborated here.

14.1.3 Prospect as Coolants

Nanofluids are believed to be the next-generation heat transfer fluids. This is primarily from the exciting nanofluids research findings such as unusually high thermal conductivity and significantly enhanced flow and boiling heat transfer performances. However, research efforts to establish nanofluids as advanced coolant are still limited as researchers are mainly focusing on their anomalous thermal

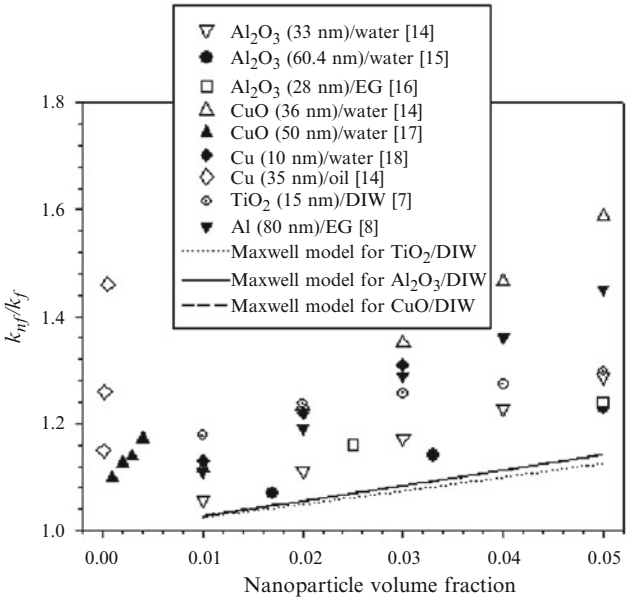

Fig. 14.1 Enhanced thermal conductivity data of various nanofluids

conductivity which is found to be significantly higher than that of base fluids [9, 10]. Some of the key results of the effective thermal conductivity of nanofluids as a function of nanoparticle volume fraction from various research groups are shown in Fig. 14.1. Although reported data are scattered and inconsistent, Fig. 14.1 clearly shows that nanofluids exhibit much higher thermal conductivities compared to their base fluids even when the concentrations of suspended nanoparticles are very low. The enhanced thermal conductivity further increases significantly with nanoparticle volume fraction. Existing classical models such as those attributed to Maxwell [12] and Hamilton and Crosser [19] were also found to be unable to predict the anomalously high thermal conductivity of nanofluids [6–8]. Studies on cooling application-based thermal properties characterization of nanofluids showed that nanofluids exhibit substantially enhanced convective heat transfer coefficient and the boiling critical heat flux which further increase with loading of nanoparticles. These highly desired thermal features of nanofluids clearly indicate that they can potentially be used as advanced coolants in the future.

Compared to research efforts made on thermal conductivity, little work has been reported on droplet spreading, convective, and boiling heat transfer characteristics of nanofluids in spite of the fact that these features are very important in order to exploit nanofluids as the next-generation coolants. It is important to evaluate the research progress on these cooling features of nanofluids and is timely to provide a state-of-the-art review on these areas of nanofluids.

14.2 Flow and Heat Transfer Characteristics of Nanofluids

Studies on convective heat transfer of nanofluids are still scarce comparing with reported works on static thermal conductivity. However, the practical applications of nanofluids as advanced heat transfer fluids are mainly in flowing systems such as mini- or microchannel heat sinks and miniaturized heat exchangers. In this section, we will critically review the reported experimental studies on convective heat transfer of nanofluids. In addition, some representative experimental results obtained from our investigation on laminar flow convective heat transfer of TiO_2 nanofluids are discussed.

14.2.1 Studies in the Literature

The experimental work of Pak and Cho [20] was the first on convective heat transfer of nanofluids (e.g., γ-Al_2O_3/water) under turbulent flow conditions. In their study, even though the Nusselt number (*Nu*) was found to increase with increasing nanoparticle volume fraction and Reynolds number, the heat transfer coefficient (*h*) actually decreased by 3–12%. The reasons for such paradoxical results might be the observed large enhancement in viscosity. On the other hand, Eastman et al. [21] later showed that with less than 1 vol.% of CuO nanoparticles, the convective heat transfer coefficient (*h*) of water increased more than 15%. The experimental results of Xuan and Li [22] also illustrated that the Nusselt number of Cu/water-based nanofluids increased significantly (about 60%) with the volumetric loading of particles. Wen and Ding [23] reported the heat transfer behavior of nanofluids at the tube entrance region under laminar flow conditions and showed that the local heat transfer coefficient varied with particle volume fraction and Reynolds number (*Re*). They also observed that the enhancement is particularly significant at the entrance region. Later, another convective heat transfer study with CuO/water- and Al_2O_3/water-based nanofluids under laminar flow conditions was conducted by Heris et al. [24]. Their results showed that heat transfer coefficient increases considerably with particle volume fraction as well as Peclet number. In their study, Al_2O_3/water-based nanofluids showed higher enhancement of heat transfer coefficient compared to CuO/water-based nanofluids.

An experimental investigation on the forced convective heat transfer and flow characteristics of aqueous TiO_2 nanofluids under turbulent flow conditions is reported by Duangthongsuk and Wongwises [25]. A horizontal double-tube counter flow heat exchanger was used, and they observed a slightly higher (6–11%) heat transfer coefficient for nanofluid compared to pure water. The heat transfer coefficient increases with increasing mass flow rate of hot water and nanofluid. They also claimed that the use of TiO_2 nanofluid has a little penalty in pressure drop.

In microchannel flow of nanofluids, Faulkner et al. [26] was the first to perform convective heat transfer experiments with aqueous carbon nanotubes (CNT) nanofluid in a microchannel with hydraulic diameter of 355 μm at Reynolds numbers

Table 14.1 Summary of forced convection heat transfer experimental studies of nanofluids

Researchers	Geometry/flow nature	Nanofluids	Findings
Pak and Cho [20]	Tube/turbulent	Al_2O_3 and TiO_2/water	At 3 vol.%, the *h* was 12% smaller than pure water for a given average fluid velocity
Xuan and Li [22]	Tube/turbulent	Cu/water	A larger enhancement of *h* with increasing particle volume fraction and Reynolds number was observed
Wen and Ding [23]	Tube/laminar	Al_2O_3/water	Increased *h* with particle volume fraction and Reynolds number was observed
Ding et al. [28]	Tube/laminar	CNT/water	At 0.5 wt.%, *h* increased by more than 350% at Reynolds number of 800
Yang et al. [29]	Tube/laminar	Graphite/automatic transmission fluid	The nanoparticles considerably increase the heat transfer coefficient of the fluid in laminar flow
Heris et al. [24]	Tube/laminar	Al_2O_3 and CuO/water	*h* increase with particle volume fraction and *Pe*. Al_2O_3 shows higher enhancement than that of CuO
Lai et al. [30]	Tube/laminar	Al_2O_3/water	*Nu* increased 8% for particle volume fraction of 0.01 and Reynolds number of 270
Jung et al. [27]	Microchannel/laminar	Al_2O_3/water	For particle volume fraction of 0.018, *h* increased up to 15%
Williams et al. [31]	Tube/turbulent	Al_2O_3 and ZrO_2/water	Heat transfer coefficient increased significantly
Hwang et al. [32]	Tube/laminar	Al_2O_3/water	At $Re = 730$ and particle volume fraction of 0.003, *h* increased only up to 8%
Xie et al. [33]	Tube/laminar	Al_2O_3, ZnO, TiO_2, and MgO/water	For MgO nanofluid, *h* increased up to 252% at $Re = 1{,}000$
Amrollahi et al. [34]	Tube/laminar and turbulent	MWCNT/water	At concentration of 0.25 wt.%, *h* increased up to 33–40%

between 2 and 17. They found significant increase in heat transfer coefficient of this nanofluid at CNT concentration of 4.4%. Later, Jung et al. [27] studied heat transfer performance of Al_2O_3/water-based nanofluid in a rectangular microchannel under laminar flow condition and showed that the heat transfer coefficient increased by more than 32% for 1.8 vol.% of nanoparticles. They also found that the Nusselt number (*Nu*) increases with increasing Reynolds number in the flow regime of $5 > Re < 300$. The published experimental works on the convective heat transfer characteristics of nanofluids are summarized in Table 14.1. A comparison of results of Nusselt number versus Reynolds number for both laminar and turbulent flow

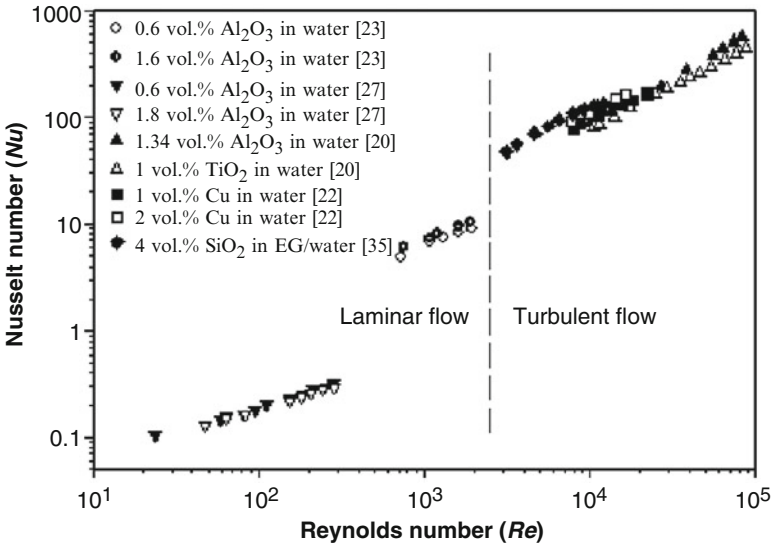

Fig. 14.2 Comparison of convective heat transfer results from various research groups

conditions from various groups is also provided in Fig. 14.2. From Table 14.1 and Fig. 14.2, it can be concluded that the results from various groups vary widely. Although some researchers [36, 37] have attempted to compile some studies on convective heat transfer with nanofluids, no critical analysis of up-to-date research findings is reported.

Several research efforts were also made to investigate the natural convection heat transfer of nanofluids. For example, Putra et al. [38] used a horizontal polyoxymethylene cylinder which was heated from one end and cooled from the other for studying natural convective heat transfer performance of aqueous CuO and Al_2O_3 nanofluids. Significant deteriorations (decrease) of convection heat transfer for these nanofluids were observed, and the deteriorations were found to increase with particle concentration particularly for CuO nanofluid. Effects of particle–fluid slip and sedimentation of nanoparticles were ascribed as the possible reasons of such deterioration. In contrast to Putra et al. [38], numerical simulation of Khanafer et al. [39] showed that in a 2-D horizontal enclosure, the natural convection heat transfer coefficient (*Nu*) of nanofluids increases with particle concentration. Wen and Ding [40] later investigated heat transfer behavior of specially formulated TiO_2/water nanofluid under the natural convection conditions. The results showed that the heat transfer coefficient decreases with increasing particle concentration. These unexpected results are in contradiction to the numerical findings of Khanafer et al. [39] but are in agreement with the observations by Putra et al. [38].

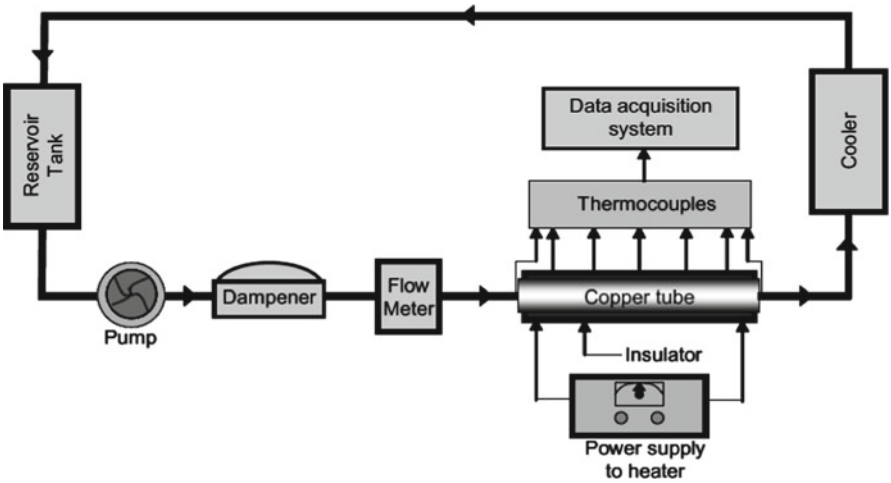

Fig. 14.3 Schematic of convective heat transfer experimental setup

14.2.2 Study by the Authors

In order to study convective heat transfer performance, sample nanofluids were prepared by dispersing different volume percentages (i.e., 0.2–0.8%) of titanium dioxide (TiO_2) nanoparticles of 15 nm diameter in deionized water (DIW) and cetyltrimethylammonium bromide (CTAB) surfactant was added as dispersant agent. To ensure proper dispersion of nanoparticles, sample nanofluids were homogenized using an ultrasonic dismembrator.

An experimental setup was established to conduct experiments on heat transfer of nanofluids at laminar flow regime in a cylindrical channel [41]. The effects of nanoparticle concentration and Reynolds number on the convective heat transfer coefficient of TiO_2/DIW-based nanofluids were studied. The schematic of experimental setup used is shown in Fig. 14.3. Details of the experimental facilities and procedures reported elsewhere [41] will not be provided here. Instead, formulations used for experimentally determination of the heat transfer coefficient (h) and the Nusselt number of nanofluids are presented.

As detailed in our previous paper [41], applying first law (energy balance) in control volume of flow channel, the following formulation for the local heat transfer coefficient is obtained:

$$h_{\mathrm{nf}-x} = \frac{q''}{\left\{T_{\mathrm{o,w}}(x) - \dfrac{q\left[2D_{\mathrm{o}}^2 \ln\left(D_{\mathrm{o}}/D_{\mathrm{i}}\right) - \left(D_{\mathrm{o}}^2 - D_{\mathrm{i}}^2\right)\right]}{4\pi\left(D_{\mathrm{o}}^2 - D_{\mathrm{i}}^2\right)k_s x}\right\} - \left\{T_{\mathrm{i}} + \dfrac{\left(T_{\mathrm{o}} - T_{\mathrm{i}}\right)}{L}x\right\}}, \quad (14.1)$$

where $T_{\mathrm{o,w}}(x)$ is the outer wall temperature of the tube (measured using thermocouples), $q'' = \dot{m}c_{\mathrm{p}}\left(T_{\mathrm{o}} - T_{\mathrm{i}}\right)/\left(\pi D_{\mathrm{i}} L\right)$ is the heat flux of the test section (W/m^2), q is

the heat supplied to the test section (W), k_s is the thermal conductivity of the copper tube (W/m·K), D_i and D_o are the inner and outer diameters of the tube, respectively, and x represents the longitudinal location of the section of interest from the entrance. L is the length of the test section, $\dot{m}$ is the mass flow rate (kg/s), and T_i and T_o are the inlet and outlet fluid temperatures, respectively.

Once the local heat transfer coefficient is determined and the thermal conductivity of the medium is known, the local Nusselt number is calculated from

$$Nu_{\mathrm{nf}-x} = \frac{h_{\mathrm{nf}-x} D_{\mathrm{i}}}{k_{\mathrm{nf}}}, \tag{14.2}$$

where k_{nf} is the effective thermal conductivity of nanofluids. The classical Hamilton–Crosser model [19], which is the same as the Maxwell model [12] for spherical particle, is used for the determination of k_{nf}, and it has the form

$$k_{\mathrm{nf}} = k_{\mathrm{f}} \left[\frac{k_{\mathrm{p}} + (n-1)k_{\mathrm{f}} - (n-1)\phi(k_{\mathrm{f}} - k_{\mathrm{p}})}{k_{\mathrm{p}} + (n-1)k_{\mathrm{f}} + \phi(k_{\mathrm{f}} - k_{\mathrm{p}})} \right], \tag{14.3}$$

where k_f and k_p are the thermal conductivities of the base liquid and the nanoparticles, respectively; ϕ is the volume fraction of nanoparticles; and n is the empirical shape factor, which has a value of 3 for spherical particle.

14.2.2.1 Axial Profiles of the Local Heat Transfer Coefficient

Figure 14.4 illustrates the local heat transfer coefficient (h) against the axial distance from the entrance of the test section at Reynolds number of $Re = 1{,}100$. Results showed that nanofluids exhibit considerably enhanced convective heat transfer coefficient which also increases with volumetric loading of TiO_2 nanoparticles. For example, at 0.8 vol.% of nanoparticles and at position $x/D_i = 25$ (where tube diameter $D_i = 4$ mm), the local heat transfer coefficient of this nanofluid is about 12% higher compared to deionized water at $Re = 1{,}100$. The observed enhancement in heat transfer coefficients of nanofluids is because of the enhanced effective thermal conductivity and the acceleration of the energy exchange process in the fluid due to the random movements of the nanoparticles. Another reason for such enhancement can be the migration of nanoparticles in base fluids due to shear action, viscosity gradient, and Brownian motion in the cross section of the tube.

14.2.2.2 Effects of Reynolds Number and Nanoparticle Concentration on Nusselt Number

The effect of Reynolds number on heat transfer coefficient (Nu) is shown in Fig. 14.5. It can be seen that the measured Nusselt number of this nanofluid in all volume concentrations is higher than that of the base fluid (water), and it increases remarkably

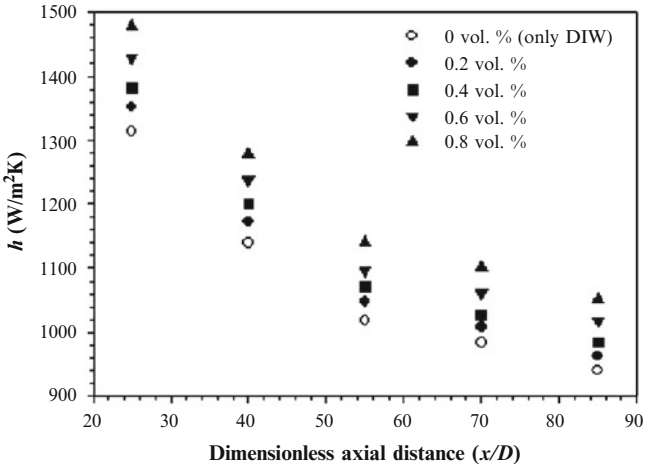

Fig. 14.4 Axial profiles of local heat transfer coefficient of nanofluid at $Re = 1{,}100$

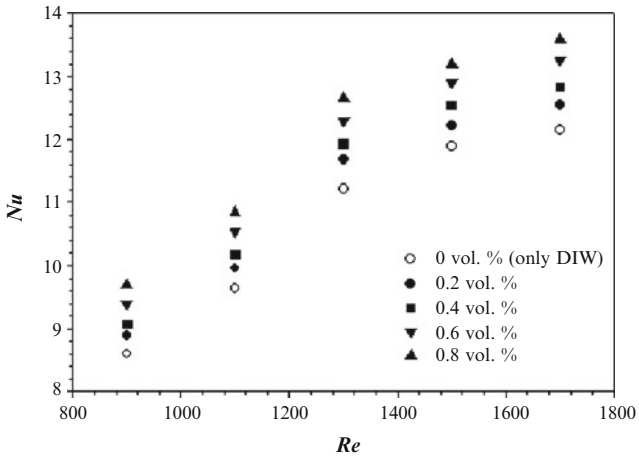

Fig. 14.5 Reynolds number versus Nusselt number at axial location of $x/D_i = 25$

with Reynolds number. The observed enhancement of the Nusselt number could be due to the suppression of the boundary layer and viscosity of nanofluids as well as dispersion of the nanoparticles. Figure 14.5 also demonstrates particle volume fraction dependence of Nusselt number. The Nusselt number of this nanofluid is found to increase almost linearly with the particle volume fraction. The nanofluid behaves more like a fluid than a conventional solid (micrometer or millimeter)–fluid mixture. The effects of several factors such as gravity, Brownian force, and friction force between the fluid and the nanoparticles may coexist in the main flow of nanofluids.

14.3 Boiling and Droplet Spreading of Nanofluids

14.3.1 Boiling Heat Transfer Studies from Literature

Although boiling is a complex and elusive process, it is a very efficient mode of heat transfer in various energy conversion and heat exchange systems as well as cooling of high-energy-density electronic components. There are two common types of boiling: pool boiling and flow or forced convective boiling. Pool boiling refers to boiling on a heated surface (heater) submerged in a pool of initially quiescent liquid, while flow boiling is boiling in a flowing stream of fluid, where the heating surface may be the channel wall confining the flow. There are numerous factors such as heater or channel surface conditions (smooth or rough), heater size, shape, material, diameter and orientation, degree of surface wetting, subcooling, inclusion of surfactants, and properties of liquid that influence heat transfer and bubble dynamics in boiling. These factors are widely studied both theoretically and experimentally and found that there are significant individual or combined effects of these factors on pool boiling heat transfer characteristics [42–44]. Heat flux in any boiling is one of the most important parameters in designing and operating the heat transfer equipment with high heat flux such as boiler, evaporator, electronic equipment, rocket engines, and so on. The critical or burnout heat flux enhancement of nanoparticle suspensions (nanofluids) depends on the particle concentration, pH of the solution, as well as on the deposition of the particles on the suspended heater surface. It is long back proven that addition of solid particle in base fluid can alter its boiling heat transfer performance. For example, Yang and Maa [1] first used nano-sized Al_2O_3 particles of as small as 50 nm in water to study the pool boiling heat transfer characteristics. They found significant increase in pool boiling performance for very small volumetric concentrations (0.1–0.5%) of nanoparticles. After nanofluids emerged, a growing number of research groups have come forward to study the boiling heat transfer characteristics of nanofluids, and it is timely to review their research findings.

An early study by You et al. [45] showed a threefold increase in critical heat flux (CHF) for Al_2O_3/water nanofluid with a flat plate heater. For Silica nanofluids, similar threefold enhancement in CHF was also later reported by Milanova and Kumar [46]. Das et al. [47] reported deterioration of boiling heat transfer of water in the presence of Al_2O_3 nanoparticles in it. Their outcome was partially attributed to the properties of the nanofluid, boiling surface, and interaction between the two. In contrast to Das et al. [47], Wen and Ding [48] showed that the enhancement of pool boiling heat transfer of the same Al_2O_3/water-based nanofluid was about 40% at 1.25 wt.% of particle loading. In another study, Witharana [49] investigated the boiling heat transfer performance of two types of Au- and SiO_2-laden aqueous nanofluids in a cylindrical vessel under atmospheric pressure. They found that the boiling heat transfer increases for Au nanofluid and decreases for SiO_2 nanofluid. These conflicting results are not well explained.

Prakash et al. [50] performed experiments to quantify the effect of heater surface roughness on pool boiling heat transfer of Al_2O_3/water-based nanofluids. They showed that while the rough heater surface increases heat transfer, smooth surface significantly deteriorates the heat transfer. For example, for rough heater surface, the heat transfer enhancement was about 70% at 0.5 wt.% concentration of alumina nanoparticles. Whereas for smooth heater, the heat flux reduction reaches up to 45% at a particle concentration of 2 wt.%. Soltani et al. [51] investigated the pool boiling heat transfer performance of Newtonian nanofluids under various heat flux densities. In their study, γ-Al_2O_3 (20–30 nm)/water- and SnO_2 (55 nm)/water-based nanofluids were used in a vertical cylindrical glass vessel. Their results showed that except for low concentrations (>0.5 wt.%) of SnO_2 nanoparticles, the boiling heat transfer coefficients of these nanofluids increase with increasing concentration of nanoparticles. These paradoxical results were attributed to the differences in thermal conductivity and size of these two nanoparticles. Recently, Truong et al. [52] conducted pool boiling experiments of diamond, ZnO, and Al_2O_3 nanoparticles–laden aqueous nanofluids with modification of sandblasted as well as bare plate heaters. They found up to 35% increase in CHF for precoated heaters compared to those of bare plate and sandblasted heaters.

Among few studies on flow boiling characteristics of nanofluids, Kim et al. [53] found about 50% enhancement in boiling critical heat flux for Al_2O_3/water nanofluids flowing through a vertical stainless steel tube. Very recently, a flow boiling experiment with two refrigerant-based nanofluids was performed by Henderson et al. [54]. In their study, SiO_2/R-134a and CuO/mixture of R-134a and polyolester oil (PO) nanofluids were used in horizontal copper tube. Results showed that while the boiling heat transfer coefficient (BHTC) of SiO_2/R-134a nanofluid decreases up to 55% compared to pure R-134a, the BHTC of CuO/(R-134a+PO) nanofluid increases more than 100% compared to its base fluid (i.e., R-134a+PO).

A summary of studies on boiling heat transfer of nanofluids is presented in Table 14.2. It can be noticed from this table that despite some inconsistent and contradictory results, most of the researchers used alumina nanofluids. However, few studies have been reported on the boiling heat transfer of CNT nanofluids which exhibit much higher thermal performance compared to those of other nanofluids [9, 10]. Thus, there is a need to conduct more investigations on boiling heat transfer of CNT nanofluids.

A comparison of heat flux versus superheat results from various groups is shown in Fig. 14.6. From these representative results (Fig. 14.6), it can clearly be seen that heat flux (also critical heat flux) data relative to superheat reported by various research groups vary widely. This is probably due to the differences in characterization of nanofluids, different size and concentration of nanoparticles used, and different types of heaters used in various research groups. Although some research groups observed deterioration of boiling heat transfer of nanofluids, the significant increase in the critical heat flux in boiling of nanofluid is still undisputed.

Table 14.2 Summary of pool boiling experiments with nanofluids

Researchers	Heater	Nanofluids	Remarks
Yang and Maa [1]	Horizontal tube heater	Al_2O_3/water	Heat flux increases considerably
Witharana [49]	Cylindrical vessels	Au and SiO_2/water and EG	Heat transfer increases for Au nanofluids but it decreases for SiO_2
Das et al. [47]	Cylindrical cartridge	Al_2O_3/water	The heat transfer deteriorates
You et al. [45]	Cartridge	Al_2O_3/water	The CHF increases up to 200%
Vassallo et al. [55]	NiCr wire	SiO_2/water	The CHF increases significantly
Bang and Chang [56]	Square flat heater	Al_2O_3/water	Pool boiling heat transfer deteriorates but CHF increases
Wen and Ding [48]	Flat disk heater	Al_2O_3/water	The BHTC increases up to 40% at 1.2 wt.% of nanoparticle
Kim et al. [57]	NiCr wire heater	TiO_2/water	The CHF increases up to 200%
Jackson [58]	Flat copper coupon heater	Au/water	While the heat transfer decreased about 20%, the maximum CHF increase was five times over water
Prakash et al. [50]	Vertical tubular heaters	Al_2O_3/water	While rough heater surface increases heat transfer, smooth surface significantly deteriorates
Chopkar et al. [59]	Flat surface	ZrO_2/water	Enhanced boiling heat transfer is found at low particle concentration
Lv and Liu [60]	Vertical small heated tubes	CuO/water	The CHF increases only for surfactant-free nanofluids
Kathiravan et al. [61]	Horizontal tube	CNT/water	The BHTC increases up to 1.75 folds for 0.25 vol.% of CNT
Soltani et al. [51]	Vertical cylindrical glass vessel	Al_2O_3 and SnO_2/water	Except for low concentrations (>0.5 wt.%) of SnO_2, the BHTC increases with loading of nanoparticles
Truong et al. [52]	Sandblasted and bare horizontal plate heaters	Diamond, ZnO, and Al_2O_3/water	The CHF of the precoated heaters increased by up to 35% with respect to that of sandblasted heaters.

14.3.2 Pool Boiling Study with Carbon Nanotubes–Nanofluids

For pool boiling experiments, sample nanofluids were prepared by suspending high purity single-walled carbon nanotubes in deionized water. As a part of surface treatment, CNT bundles were refluxed with hydrochloric acid at 100°C for several hours. This acid was chosen as a reactive reagent because it removes catalytic

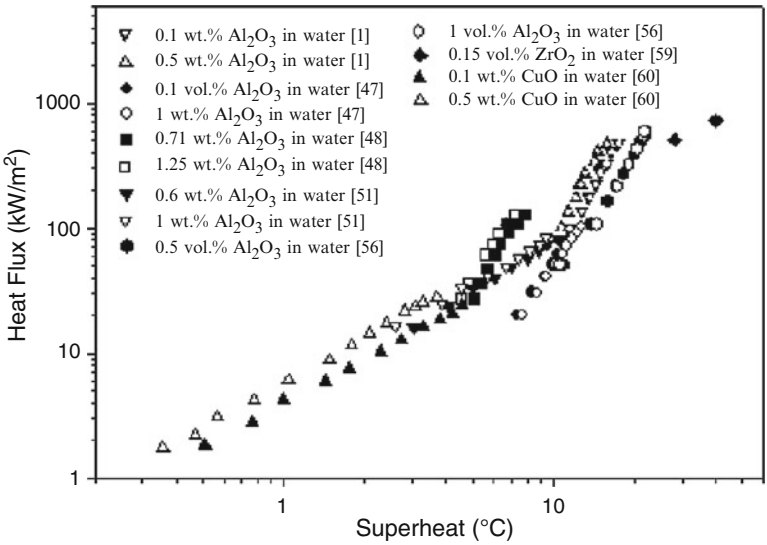

Fig. 14.6 Comparison of heat flux versus superheat results from various research groups

particles without reducing the length of the tubes or damaging the side walls. Different concentrations of sodium dodecylbenzenesulfonate (NaDBS) surfactant are used as dispersing agent for nanotubes in water. Details of the experimental facilities and procedures are reported in previous studies [62, 63].

Representative results from previous study [62] on surfactant concentration–dependent pool boiling experiments of CNT nanofluids are presented and discussed. The critical heat flux (CHF), which is the sudden jump in temperature at the same heat flux, is determined at constant 0.1% volumetric loading of CNT and for various concentrations of NaDBS surfactant. The results of boiling heat flux with respect to superheat (wire temperature minus saturation temperature of liquid, $T_w - T_s$) are presented and compared with the one for pure deionized water in Fig. 14.7. The NaDBS surfactant to CNT concentrations were varied from 1:20 to 1:1. Figure 14.7 demonstrates that the CNT nanofluid with any concentration of surfactant exhibits higher CHF value than that of base fluid. The CHF value of deionized water is 750 kW/m^2. The effect of increasing the surfactant concentration from 1:20 to 1:5 (NaDBS:CNT) results in increase of CHF value. However, if the concentration of surfactant is further increased from 1:5 to 1:1, the CHF drops drastically from 4,439 to 1,322 kW/m^2. There is, therefore, a critical concentration of surfactant for which the CHF reaches to maximum value. The highest CHF value is obtained for the concentration ratio of 1:5. The deposition of nanoparticles on the heater wire is believed to be one of the main reasons for any enhancement in CHF of this nanofluid. Kim et al. [64] also claimed that the deposition of nanoparticles on the heater wire is the main reason

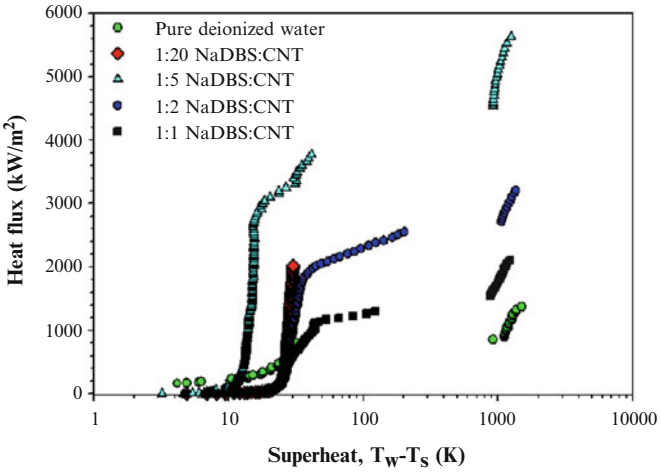

Fig. 14.7 Effect of surfactant concentration on heat flux of SWCNT nanofluid

for any enhancement in CHF of nanofluids. Nevertheless, results indicate that nanofluids boiling performance can further be enhanced by adding suitable type and concentration of surfactant in it and thus surfactant-added nanofluids show great promises as advanced coolants.

14.3.3 Studies on Droplet Spreading of Nanofluids

Besides fascinating conduction and convective heat transport properties, studies on boiling heat transfer of nanofluids indicated that nanofluids could be very promising for enhanced spray cooling systems. Very recently, authors investigated the spreading characteristics of a nanofluid droplets impinging on a metallic substrate under the influence of several key factors such as nanoparticle volume fraction, substrate temperature, and Weber number [65]. Results showed that the transient spreading diameter and height of droplet impacting onto solid surface are greatly influenced by each of these factors. Such droplet impingement study on heated substrate surface is of great importance to exploit the practical application of nanofluids as an advanced coolant in many industrial processes, particularly in spray cooling and coating. Unfortunately, scant work has been performed on droplet impingement dynamics of nanofluids on solid surfaces under various conditions. Among such studies, Wasan and Nikolov [66] were the first to investigate the effects of the particle structure formation and the structural disjoining pressure of nanoparticles on the spreading of nanofluids on solid surface. Duursma et al. [67] studied the effect of aluminum nanoparticles on droplet boil-off by allowing nanofluid drops to fall onto a copper surface at temperature higher than the liquid saturation temperature.

They demonstrated that increase in surface temperature and Weber number promotes the receding breakup scenario, while an increase in the nanoparticle concentration discourages this breakup. The influence of surface temperature on the hydrodynamic characteristics of water and nanofluid droplets impinging on a polished and nanostructured surface was investigated by Shen et al. [68]. Their results showed that SWCNT nanofluid has larger spreading diameter compared to that of deionized water, and use of a nanofluid or a nanostructured surface can reduce the total evaporation time up to 37%. Nevertheless, more studies are needed on dynamics of both nonboiling and boiling droplet impingement of nanofluids on solid surfaces as the spreading of liquid droplet plays a key role in many industrial processes like spray cooling, coating, ink-jet printing, and oily soil removal.

14.4 Conclusions

In this chapter, an exhaustive review on major cooling features such as convective and boiling heat transfers as well as droplet spreading dynamics of nanofluids together with some representative results from own experimental investigations on these areas are presented and analyzed. Reported literature review and representative results on convective heat transfer studies demonstrated that nanofluids exhibit considerably enhanced convective heat transfer coefficient compared to their base fluids, and the Nusselt number increases significantly with increasing concentration of nanoparticles as well as with the Reynolds number. Thus, nanofluids have great potential to be used as next-generation coolants.

From the review of available results on boiling heat transfer of nanofluids, it can be conferred that despite of contradictory and inconsistent data, there is undisputed substantial increase in the critical heat flux of nanofluids compared to their base fluids. However, reported data are still limited and scattered to clearly understand the underlying mechanisms as well as trend of boiling heat transfer characteristics of nanofluids. The effects of deposition of nanoparticles or tubes on heat transfer surface, surfactant concentration, and surface wettability are commonly identified as responsible for the observed boiling heat transfer results of nanofluids. Representative results of our previous investigations on pool boiling heat transfer of CNT nanofluid showed that large enhancement of boiling heat flux is possible and would depend on the concentration of the surfactants. This indicates that the boiling as well as cooling performance of nanofluids can further be enhanced by adding a suitable surfactant at proper concentration.

Studies on droplet spreading, nanofluids showed their potential for industrial processes like spray cooling, coating, and ink-jet printing. However, more extensive studies are needed on dynamics of boiling nanofluid droplets impinging on solid surfaces in order for their exploitation as advanced media for spray cooling.

Despite of controversies and scattered data on all these thermal features, nanofluids exhibit remarkably enhanced conductive, convective, and boiling heat transfer performance compared to their base fluids and thus are very useful for applications as advanced coolants. However, the progress toward fully understanding the mechanisms

behind these enhanced conduction, convection, and boiling heat transfer features of nanofluids as well as their development for commercial applications as future coolant remain challenging task.

Acknowledgment The authors would like to thank FCT- Fundação para a Ciência e Tecnologia, Portugal, for pluriannual funding to CCMM.

References

1. Yang YM, Maa JR (1984) Boiling of suspension of solid particles in water. Int J Heat Mass Transf 27:145–147
2. Masuda H, Ebata A, Teramae K, Hishinuma N (1993) Alteration of thermal conductivity and viscosity of liquid by dispersing ultra-fine particles (dispersion of γ-Al_2O_3, SiO_2, and TiO_2 ultra-fine particles). Netsu Bussei 4:227–233
3. Choi SUS (1995) Enhancing thermal conductivity of fluids with nanoparticles. ASME FED 231:99–105
4. Gass V, Van der Schoot BH, de Rooij NF (1993) Nanofluid handling by micro-flow-sensor based on drag force measurements. In: Proceedings of IEEE conference on MEMS, Florida, 1993, pp 167–172
5. Grimm A (1993) Powdered aluminum-containing heat transfer fluids. German patent DE 4131516 A1
6. Lee S, Choi SUS, Li S, Eastman JA (1999) Measuring thermal conductivity of fluids containing oxide nanoparticles. J Heat Transf 121:280–289
7. Murshed SMS, Leong KC, Yang C (2005) Enhanced thermal conductivity of TiO_2-water based nanofluids. Int J Therm Sci 44:367–373
8. Murshed SMS, Leong KC, Yang C (2008) Investigations of thermal conductivity and viscosity of nanofluids. Int J Therm Sci 47:560–568
9. Yu W, France DM, Routbort JL, Choi SUS (2008) Review and comparison of nanofluid thermal conductivity and heat transfer enhancements. Heat Transf Eng 29:432–460
10. Murshed SMS, Leong KC, Yang C (2008) Thermophysical and electrokinetic properties of nanofluids – a critical review. Appl Therm Eng 28:2109–2125
11. Murshed SMS, Leong KC, Yang C (2006) Determination of the effective thermal diffusivity of nanofluids by the double hot-wire technique. J Phys D Appl Phys 39:5316–5322
12. Maxwell JC (1891) A treatise on electricity and magnetism. Clarendon, Oxford
13. Choi SUS, Zhang ZG, Keblinski P (2004) Nanofluids. Encycl Nanosci Nanotechnol 6:757–773
14. Eastman JA, Choi SUS, Li S, Thompson LJ (1997) Enhanced thermal conductivity through the development of nanofluids. In: Proceedings of the symposium on nanophase and nanocomposite materials II, Boston, USA
15. Xie H, Wang J, Xi T, Liu Y, Ai F, Wu Q (2002) Thermal conductivity enhancement of suspensions containing nanosized alumina particles. J Appl Phys 91:4568–4572
16. Wang X, Xu X, Choi SUS (1999) Thermal conductivity of nanoparticle-fluid mixture. J Thermophys Heat Transf 13:474–480
17. Wang BX, Zhou LP, Peng XF (2003) A fractal model for predicting the effective thermal conductivity of liquid with suspension of nanoparticles. Int J Heat Mass Transf 46:2665–2672
18. Xuan Y, Li Q, Hu W (2003) Aggregation structure and thermal conductivity of nanofluids. AIChE J 49:1038–1043
19. Hamilton RL, Crosser OK (1962) Thermal conductivity of heterogeneous two component systems. Ind Eng Chem Fundam 1:187–191
20. Pak BC, Cho YI (1998) Hydrodynamic and heat transfer study of dispersed fluids with submicron metallic oxide particles. Exp Heat Trannf 11:151–170

21. Eastman JA, Choi SUS, Li S, Soyez G, Thompson LJ, Dimelfi RJ (1999) Novel thermal properties of nanostructured materials. Mater Sci Forum 312–314:629–634
22. Xuan Y, Li Q (2003) Investigation on convective heat transfer and flow features of nanofluids. J Heat Transf 125:151–155
23. Wen D, Ding Y (2004) Experimental investigation into convective heat transfer of nanofluids at the entrance region under laminar flow conditions. Int J Heat Mass Transf 47:5181–5188
24. Heris SZ, Etemad SG, Esfahany MS (2006) Experimental investigation of oxide nanofluids under laminar flow convective heat transfer. Int Commun Heat Mass Transf 33:529–535
25. Duangthongsuk W, Wongwises S (2009) Heat transfer enhancement and pressure drop characteristics of TiO_2–water nanofluid in a double-tube counter flow heat exchanger. Int J Heat Mass Transf 52:2059–2067
26. Faulkner D, Rector DR, Davison JJ, Shekarriz R (2004) Enhanced heat transfer through the use of nanofluids in forced convection. In: Proceedings of the ASME international mechanical engineering congress and exposition, California, 2004, pp 219–224
27. Jung JY, Oh HS, Kwak HY (2006) Forced convective heat transfer of nanofluids in microchannels. In: Proceedings of the ASME international mechanical engineering congress and exposition, Chicago
28. Ding Y, Alias H, Wen D, Williams AR (2006) Heat transfer of aqueous suspensions of carbon nanotubes. Int J Heat Mass Transf 49:240–250
29. Yang Y, Zhang ZG, Grulke EA, Anderson WB, Wu G (2005) Heat transfer properties of nanoparticle-in-fluid dispersions (nanofluids) in laminar flow. Int J Heat Mass Transf 48:1107–1116
30. Lai WY, Duculescu B, Phelan PE, Prasher RS (2006) Convective heat transfer with nanofluids in a single 1.02-mm tube. In: Proceedings of ASME international mechanical engineering congress and exposition, Chicago
31. Williams W, Buongiorno J, Hu LW (2008) Experimental investigation of turbulent convective heat transfer and pressure loss of alumina/water and zirconia/water nanoparticle colloids (nanofluids) in horizontal tubes. J Heat Transf 130:1–7
32. Hwang KS, Jang SP, Choi SUS (2009) Flow and convective heat transfer characteristics of water-based Al_2O_3 nanofluids in fully developed laminar flow regime. Int J Heat Mass Transf 52:193–199
33. Xie H, Li Y, Yu W (2010) Intriguingly high convective heat transfer enhancement of nanofluid coolants in laminar flows. Phys Lett A 374:2566–2568
34. Amrollahi A, Rashidi AM, Lotfi R, Meibodi ME, Kashefi K (2010) Convection heat transfer of functionalized MWNT in aqueous fluids in laminar and turbulent flow at the entrance region. Int Commun Heat Mass Transf 37:717–723
35. Kulkarni DP, Namburu PK, Bargar HE, Das DK (2008) Convective heat transfer and fluid dynamic characteristics of SiO_2-ethylene glycol/water nanofluid. Heat Transf Eng 29:1027–1035
36. Daungthongsuk W, Wongwises S (2007) A critical review of convective heat transfer of nanofluids. Renew Sust Energy Rev 11:797–817
37. Kakaç S, Pramuanjaroenkij A (2009) Review of convective heat transfer enhancement with nanofluids. Int J Heat Mass Transf 52:3187–3196
38. Putra N, Roetzel W, Das SK (2003) Natural convection of nanofluids. Heat Mass Transf 39:775–784
39. Khanafer K, Vafai K, Lightstone M (2003) Buoyancy-driven heat transfer enhancement in a two-dimensional enclosure utilizing nanofluids. Int J Heat Mass Transf 46:3639–3653
40. Wen D, Ding Y (2005) Formulation of nanofluids for natural convective heat transfer applications. Int J Heat Fluid Flow 26:855–864
41. Murshed SMS, Leong KC, Yang C, Nguyen NT (2008) Convective heat transfer characteristics of aqueous TiO_2 nanofluids under laminar flow conditions. Int J Nanosci 7:325–331
42. Tong LS, Tang YS (1997) Boiling heat transfer and two-phase flow. Taylor & Francis, Washington, DC
43. Pioro IL, Rohsenow W, Doerffer SS (2004) Nucleate pool-boiling heat transfer. I: review of parametric effects of boiling surface. Int J Heat Mass Transf 47:5033–5044

44. Pioro IL, Rohsenow W, Doerffer SS (2004) Nucleate pool-boiling heat transfer. II: assessment of prediction methods. Int J Heat Mass Transf 47:5045–5057
45. You SM, Kim JH, Kim KM (2003) Effect of nanoparticles on critical heat flux of water in pool boiling of heat transfer. Appl Phys Lett 83:3374–3376
46. Milanova D, Kumar R (2008) Heat transfer behavior of silica nanoparticles in pool boiling experiment. J Heat Transf 130:042401–1–042401–6
47. Das SK, Putra N, Roetzel W (2003) Pool boiling characterization of nano-fluids. Int J Heat Mass Transf 46:851–862
48. Wen D, Ding Y (2005) Experimental investigation into the pool boiling heat transfer of aqueous based alumina nanofluids. J Nanopart Res 7:265–274
49. Witharana S (2003) Boiling of refrigerants on enhanced surfaces and boiling of nanofluids. PhD thesis, Royal Institute of Technology, Sweden
50. Prakash NG, Anoop KB, Das SK (2007) Mechanism of enhancement/deterioration of boiling heat transfer using stable nanoparticles suspensions over vertical tubes. J Appl Phys 102:074317–1–074317–7
51. Soltani S, Etemad SG, Thibault J (2009) Pool boiling heat transfer performance of Newtonian nanofluids. Heat Mass Transf 45:1555–1560
52. Truong B, Hu LW, Buongiorno J, McKrell T (2010) Modification of sandblasted plate heaters using nanofluids to enhance pool boiling critical heat flux. Int J Heat Mass Transf 53:85–94
53. Kim SJ, McKrell T, Buongiorno J, Hu LW (2009) Enhancement of flow boiling critical heat flux (CHF) in alumina/water nanofluids. Adv Sci Lett 2:100–102
54. Henderson K, Park YG, Liu L, Jacobi AM (2010) Flow-boiling heat transfer of R-134a-based nanofluids in a horizontal tube. Int J Heat Mass Transf 53:944–951
55. Vassallo P, Kumar R, D'Amico S (2004) Pool boiling heat transfer experiments in silica-water nano-fluids. Int J Heat Mass Transf 47:407–411
56. Bang IC, Chang SH (2005) Boiling heat transfer performance and phenomena of Al_2O_3-water nano-fluids from a plain surface in a pool. Int J Heat Mass Transf 48:2407–2419
57. Kim H, Kim J, Kim M (2006) Experimental study on CHF characteristics of water–TiO_2 nanofluids. Nucl Eng Technol 39:61–68
58. Jackson J (2007) Investigation into the pool-boiling characteristics of gold nanofluids. MS thesis, University of Missouri-Columbia, USA
59. Chopkar M, Das AK, Manna I, Das PK (2008) Pool boiling heat transfer characteristics of ZrO_2–water nanofluids from a flat surface in a pool. Heat Mass Transf 44:999–1004
60. Lv LC, Liu ZH (2008) Boiling characteristics in small vertical tubes with closed bottom for nanofluids and nanoparticles-suspensions. Heat Mass Transf 45:1–9
61. Kathiravan R, Kumar R, Gupta A, Chandra R, Jain PK (2009) Pool boiling characteristics of carbon nanotube based nanofluids over a horizontal tube. J Therm Sci Eng Appl 1:022001–1–022001–7
62. Murshed SMS, Milanova D, Kumar R (2009) An experimental study of surface tension-dependent pool boiling characteristics of carbon nanotubes-nanofluids. In: Proceedings of the 7th ASME international conference on nanochannels, microchannels and minichannels, Pohang, Korea
63. Milanova D, Kumar R (2007) Functionalized single walled and double walled carbon nanotubes for thermal enhancement. In: Proceedings of the ASME international mechanical engineering congress and exposition, Seattle
64. Kim H, Kim J, Kim MH (2006) Effect of nanoparticles on CHF enhancement in pool boiling of nano-fluids. Int J Heat Mass Transf 49:5070–5074
65. Murshed SMS, Nieto de Castro CA (2011) Spreading characteristics of nanofluid droplets impacting onto a solid surface. J Nanosci Nanotechnol 11:3427–3433
66. Wasan DT, Nikolov AD (2003) Spreading of nanofluids on solids. Nature 423:156–159
67. Duursma G, Sefiane K, Kennedy A (2009) Experimental studies of nanofluid droplets in spray cooling. Heat Transf Eng 30:1108–1120
68. Shen J, Liburdy JA, Pence DV, Narayanan V (2009) Droplet impingement dynamics: effect of surface temperature during boiling and nonboiling conditions. J Phys Condens Matter 21:464133–1–464133–14

Index

A
Acidic ionic liquids
  1,1-diacetates, 153
  Friëdel–Crafts reaction, 152–153
  imidazolium-derived ionic liquid catalysts, 154
  Mannich reaction, 152
  naphthol condensation, 154
  quinolines, 154
  TSIL-catalyzed Friedländer reaction, 154, 155
  xanthenes, 155
β-Adrenoceptor-blocking drugs, 166–167
Aminopolysaccharides (APs), 201–202
APs. *See* Aminopolysaccharides (APs)
Atom transfer radical polymerization (ATRP)
  polymerization, ILs
    CuBr/TEDETA, 260
    ionic liquids, 260
    MBP/CuBr/bipyridine, 261
    MMA, 259–260
  polymerization, $scCO_2$
    COTFPP, 289, 290
    MMA, 289
ATRP. *See* Atom transfer radical polymerization (ATRP)

B
Basic ionic liquids
  acid-base interactions, 155
  2-amino-2-chromenes synthesis, 156
  Baylis-Hillman reaction, 156
  multicomponent reaction (MCR) strategy, 156
  pyrrole, 157
Bayerischen Anilin und Soda Fabrik (BASF), 150, 151
Biocatalysis
  glycerol
    asymmetric catalysis, 198
    asymmetric reduction, prochiral β-ketoesters and ketones, 199–200
    2'-chloroacetophenone, bioreduction, 199, 200
    electrostatic interactions, 200
    glycerol triacetate (triacetin), 199
    isoamyl acetate, 198–199
    lipase-catalyzed kinetic resolution, ester racemate, 198
    thermal stability, 201
    transesterification, isoamyl alcohol, 198
  green solvents
    advantages and disadvantages, organic solvent systems, 123
    agrochemical and pharmaceutical industries, 122
    computer-based algorithms, 122
    E-factor, 122
    fluorous solvents (*see* Fluorous solvents)
    ionic liquids (*see* Ionic liquids)
    SCF (*see* Supercritical fluid (SCF))
    solvents, reaction media, 123
    water
      aqueous-based biocatalysis, 125–126
      bioconversion processes, aqueous environment, 126
      bioconversion systems, 125
      chymotrypsin and subtilisin, 125
      food processing, 125
      polar nature, 124

A. Mohammad and Inamuddin (eds.), *Green Solvents I: Properties and Applications in Chemistry*, DOI 10.1007/978-94-007-1712-1,

Biocatalysis (*cont.*)
ILs
Candida antarctica lipase B (CAL B), 136
catalyst and medium reuse, 137
enzymatic kinetic resolution, 136
preparative enzymatic resolution, 137
racemic sec-alcohols separation, 139
reaction products removal, 138
sec-alcohols separation, 138
TSIL, 137
Bioconversions, ILs
aminolysis, (RS)-methyl mandelate, 165, 166
lipases, 165
sugar esters, 166
"supramolecules" formation, 166
Biodegradable polymers, 167
Biodiesel. *See also* Supercritical fluids, biodiesel production
alkali-catalyzed reaction, 377
JC (*see Jatropha curcas*)
Biphasic acid scavenging with ionic liquids (BASIL), 150
Brazilian propolis
DHCA isolation and purification
identification, 71–72
quantification, 72, 75
solvent extractions, 70–71
green fluid extraction
RSM, 77–79
sensitivity test, 76–77
submicron particles precipitation (*see* Submicron particles precipitation, Brazilian propolis)
Bucky gels, 236

C
Carbon nanotubes (CNTs)
data, 239
and room-temperature ILs, 236
Cellulose fibers (CFs), 320, 321
CFs. *See* Cellulose fibers (CFs)
CHF. *See* Critical heat flux (CHF)
CNTs. *See* Carbon nanotubes (CNTs)
Controlled free radical polymerization (CRP)
ATRP, 259–261
defined, 258–259
NMRP, 264–265
reverse ATRP
chiral ILs, 264
ester groups, ILs, 263
IL imidazolium cation, 263
MMA, 262–263
transition-metal compounds, 262
Conventional free radical polymerization, 257–258
Critical heat flux (CHF), 410
CRP. *See* Controlled free radical polymerization (CRP)

D
DAPA. *See* Dimer fatty acid-based polyamides (DAPA)
Dean-Stark procedure, 180–181
DHCA. *See* 3,5-Diprenyl-4-hydroxycinnamic acid (DHCA)
Diethoxyphenilphosphine, 151
Differential scanning calorimetry (DSC)
composite fibers, 325
interaction mechanism, stearic acid and soy protein, 311
thermal analyses, resins, 318
Dimer fatty acid-based polyamides (DAPA)
CF, 320
storage modulus, 322
stress–strain curves, 322, 323
Dimethyl carbonate (DMC)
dual chemical reagent
catalyst activity, 367
catalysts, selective methylation, 368
methoxycarbonylation catalysts, 369–372
methylating agent, 367
nucleophiles, 366
reactivity, amines, 366, 367
selectivity, methylation and carbamoylation, 368
green solvent
components, lithium ion battery, 366
dye-sensitized solar cells, 366
lithium batteries, 365
mechanical braking energy, supercapacitors, 365
synthetic route preparation
CO_2 and methanol, 364
epoxides, 364
2,2-Diphenyl-1-picrylhydrazyl (DPPH), 95, 97
3,5-Diprenyl-4-hydroxycinnamic acid (DHCA)
green fluid extraction
RSM, 77–79
sensitivity test, SC-CO_2 extraction, 76–77
purification and identification
experimental data, with solvent pretreatment, 72, 73
liquid-liquid solvent partition and normal-phase column chromatography, 71–72

without solvent pretreatments, data, 72, 74
quantification
and flavonoids, 82–83
HPLC chromatograms, 72, 75
Waters HPLC system, 72
solvent extractions
hot-pressurized extraction, 71
Soxhlet extraction, 70–71
DSC. *See* Differential scanning calorimetry (DSC)
Dulbecco's modified eagle medium (DMEM), 92, 94

E
Ethylene glycol, 336–337
Eyring model, 323

F
Fatty acid methyl ester (FAME). *See* Biodiesel
Fatty acids, green polymers and composites
biodegradable polymers, 301
chemical structure, furfuryl palmitate, 323
cis-oleic acid structure, 303, 304
commodity oils and fats, 302
cryogenic fracture surface, DAPAC20, 320, 321
DA, 320
defined, 301
derived polymers
incorporation, nonlinear terminals, 310
macrolactones structures, 307–309
preparation, polyanhydride, 306
RA insertion, sebacic acid polymer chain, 307, 308
synthesis, RA-based polyanhydride, 307
DMA, 321, 322
DSC, 320, 321, 328
fracture surface, FP-MA/jute green composite, 325
hydrolysis, ester linkage, 301, 302
latent heat and phase transition temperature, 327, 328
life cycle, 300
mechanism
Diels-Alder reaction, 323, 324
FP-MA polymerization reaction, 323, 324
modified polymers
composition, coating mixtures, 313, 315
contact mode topography AFM images, coating films, 318, 319
glycidyl methacrylate, MFA monomer, 317
hyperbranched polyether, TMP, 313, 315
PAA resins, 318
polyurethane synthesis, 313, 315
residual unsaturation sites, 317, 318
SEM micrograph, 311, 313
stearic acid crystallinity, 311, 312
stearic acid, Young's modulus, 311
structure, vinyl ester resin, 316
TGA scans, SPI resin, 311, 312
transparent dry polyurethane film, 316
variation, glass transition temperature, 317
physical properties, 303, 304
ricinoleic, vernolic and *trans*-oleic acids structure, 303
SEM images, 325–327
stress–strain curves, DAPA and DAPAC, 321–323
types, 302, 303
vegetable oils
FTIR spectroscopy, 306
triglyceride molecule, 304, 305
triglyceride synthesis, 305
FBS. *See* Fluorous biphase system (FBS)
Fluorous biphase system (FBS), 291
Fluorous media
advantages and disadvantages, 290
polymerization
FBS, 291
FTS, 291–292
HFC fluids, 292–293
Fluorous solvents
fluorous biphasic systems (FBS)
biocatalysis, 132
enzymatic resolution, fluorous and nonfluorous solvents, 133
homogeneous fluorous–organic solvent system, 133
miscibility–immiscibility property, 133
organic phases, enantiomers separation, 133
properties and applications
FOBS, 130–131
HFEs, 132
man-made PFCs, 131
perfluorinated compounds (PFCs), 130
temperature-dependent miscibility, 130, 131
Fluorous triphase system (FTS), 291–292
Fourier transform infrared (FTIR) spectroscopy, 306, 311

FTIR spectroscopy. *See* Fourier transform infrared spectroscopy
FTS. *See* Fluorous triphase system (FTS)

G
GAC. *See* Green analytical chemistry (GAC)
Gas chromatography (GC)
  fatty acid methyl ester (FAMEs), 99
  residual solvents, 167
  triglycerides quantification, 378
Generally recognized as safe (GRAS), 176
Glycerol, organic reactions
  biocatalysis (*see* Biocatalysis, glycerol)
  catalytic C-C bond formations
    aza-Michael addition, *p*-anisidine, 195
    citral and thiophenol, Michael addition, 197
    electrophilic activity, aldehydes, 197–198
    Heck reaction, 194
    hetero-Diels Alder reaction, 196
    Knoevenagel reaction, 196
    microwave heating, 195
  catalytic organic reactions
    nucleophilic substitution, benzyl chloride, 203
    synthetic efficiency, reactions, 203
  description, 188
  glycerol-based solvents
    derivatives, 204
    low-price glycerol, 204
    structure, 204
    uncatalyzed epoxidation reactions, 205
  high-tonnage glycerol-based process, 187
  micellar catalytic reactions (*see* Micellar catalytic reactions, glycerol)
  physicochemical properties, green solvent, 189
  redox reactions
    benzaldehyde reduction, 191
    electroreduction, 192
    Maillard reaction, 193–194
    metal hydrides, 191
    methyl acetoacetate, 192
    reduction technique, 190
    styrene, 190
    transfer hydrogenation-dehydrogenation reaction, 192–193
  and water, 188
GRAS. *See* Generally recognized as safe (GRAS)
Green analytical chemistry (GAC), 332
Green eluents, 335
Green fluids extraction and purification
  biological activity, propolis samples
    antioxidative ability tests, 95–97
    cytotoxic assay, human cells, 92–95
  column partition fractionation, γ-oryzanols
    isolation and identification, 97–99
    quantification, 99–100
    rice bran oil purification, 101–104
    Soxhlet extraction, 101
  DHCA
    antioxidative activity, 68
    purification and identification, 71–72
    quantification, 72, 75
    RSM, 77–79
    sensitivity test, SC-CO_2, 76–77
    solvent extractions, 70–71
  Propolis, 68
  rice bran, 69–70
  SC-CO_2 extraction
    antioxidant components, 69
    deacidification, 109–115
    pilot-scale, 106, 108
    procedure, 105–106
    rice bran oil, 104, 105
  submicron particles precipitation, Brazilian Propolis
    antisolvent micronization, SC-CO_2, 83–91
    micronization process, SC-CO_2, 79–81
    micronized precipitates analysis, 82–83
  supercritical antisolvent precipitation, solutes, 69
Green solvents. *See also* Dimethyl carbonate (DMC); Pharmaceutical industryadvantages and drawbacks, 124
  biocatalysis (*see* Biocatalysis)
  chromatography, 333
  classification, 123
  description, 1–2, 332
  green extraction technique
    fatty acid composition, olive oil, 184
    microwave Clevenger apparatus, 185
    MIS, 183, 184
  limonene (*see* Limonene)
  perfluorinated solvents
    extraction, 47
    filtration/decantation, 47
    organic synthesis, 47–48
    properties, 46–47
  preference order, 337
  properties, 48–49
  publication trend, 337

RTILs (*see* Room temperature ionic liquids (RTIL)s)
safe solvents, 332, 333
SCF (*see* Supercritical fluid (SCF))
solvent-free reactions
benefits, 3
description, 2
high speed ball milling (HSBM) method, 3
inorganic and materials synthesis, 13
organic synthesis (*see* Solvent-free organic reactions)
polymerization, 13–14
role, 2
TLC (*see* Thin-layer chromatography (TLC))
water
description, 14
metal nanoparticles synthesis, 23
organic synthesis (*see* Organic synthesis, water)
Group transfer polymerization (GTP), 266–267
GTP. *See* Group transfer polymerization (GTP)

H
HCC. *See* Hydroxyl-containing component (HCC)
Heat transfer and flow, nanofluids
axial profiles, local heat transfer coefficient, 405, 406
Hamilton-Crosser model, 405
heat transfer coefficient, 404–405
literature studies
convective heat transfer, 401, 402
natural convective heat transfer performance, 403
Nusselt number, 401
TiO_2, 401
Reynolds number *vs.* Nusselt number, 406
Heat transfer fluids (HTFs)
CNT, 236
ILs, 235–236
Heck reaction, 194
HFC fluids. *See* Hydrofluorocarbon fluids
HKR. *See* Hydrolytic kinetic resolution (HKR)
HTFs. *See* Heat transfer fluids (HTFs)
Hydrofluorocarbon (HFC) fluids, 292–293
Hydrofluoroethers (HFEs), 132
Hydrolytic kinetic resolution (HKR), 219
Hydroxyl-containing component (HCC), 313

I
ILMAE. *See* Ionic liquids based microwave-assisted extraction (ILMAE)
ILs. *See* Ionic liquids (ILs)
Ionanofluids
experimental and measurement, 238–239
green energy-based applications, 246
heat capacity
ILs, 243
MWCNT-ionanofluids, 243, 244
temperature effect, volumetric, 243, 244
HTFs, 235–236
nanofluids, 234–235
preparation
HTFs and ILs, 236–237
MWCNT, 237–238
structures, ILs, 237
thermal conductivity
and CNT-loaded nanofluids, temperature effect, 240–242
enhancement, 241, 242
experimental data, 242
temperature effect and MWCNT concentration, 241, 242
thermophysical properties *vs.* heat transfer areas
simulation, 245
values, 245
Ionic liquids (ILs)
acidic, 152–155
advantages, 235, 240
analytical spectroscopy, 166–167
basic (*see* Basic ionic liquids)
biocatalysis (*see* Biocatalysis, ILs)
bioconversions, 165–166
cations and anions, 255
characterization, 235
chiral and chiral amino acid
amino acid ionic liquid (AAILs), 160
Click Reaction, 159–160
enzymatic catalysis, 161
(S)-histidine, 159
racemic amino acids, 160
CNT and room-temperature, 236
defined, 150
industrial application, 150
ionanofluids, 235
microwave-and ultrasound-assisted reactions
Fisher esterification reaction, Brönsted acidic ionic liquids, 163, 164
pyrroles, 164
sonochemical synthesis, oximes, 163, 164
Tsuji-Trost reactions, 164

Ionic liquids (ILs) (*cont.*)
MWCNT, 236, 237, 241, 246, 247
and nanomaterials, 236
oxidation
benzaldehydes, 157
carbonyl groups, 157
2-substituted benzothiazoles, 158
$VO(Hhpic)_2$, recycling study, 158
polymerization
conventional free radical, 257–258
GTP, 266–267
living/CRP, 258–266
miscellaneous, 268
radiation, 267
rate and molecular weight, MMA, 257
VOCs, 256–257
properties and applications
ammonium ethyl nitrate, 134
flammable and highly volatile organic solvents, 135
solubilization, 136
structures, cations and anions, 135
RTILs, 151
SLM, 151
supported
asymmetric hydrogenation, 163
asymmetric ring-opening reaction, epoxides, 163
Brönsted acidic functionalized ionic liquids, 162
condensation reactions, 162
propylene carbonate synthesis, 162
protein film electrochemistry, 162
transesterification, β-ketoesters, 161
thermodynamics and kinetics, 255–256
use, 243
Ionic liquids based microwave-assisted extraction (ILMAE), 165

J
Jatropha curcas (JC)
economic estimation, 392–393
rate constant determination
activation energy, methylation, 387, 389
free fatty acids *vs.* methylation time, 389, 391
hydrolysis reaction, 386
kinematic effect, supercritical methylation, 387
methylation process, 387
physical properties, SC-CO_2 and methylated oil, 387, 392
triglycerides *vs.* hydrolysis time, 387, 388, 390
SC-CO_2 extractions, triglycerides
hydrolysis and methylation reaction, 382
low-pressure CO_2 volume, 383
quantification, FFAs and TGs, 378
Soxhlet, 379–381
subcritical hydrolysis
operating pressure, 383
response surface methodology (RSM), 383, 384
supercritical methylation
free fatty acid conversion, 385
HPLC pump, 384
RSM experimental design, 385, 386
JC. *See Jatropha curcas* (JC)

L
LASCs. *See* Lewis acid-surfactant-combined catalysts (LASCs)
Lewis acid-surfactant-combined catalysts (LASCs), 213–214
Limonene
alternative solvent, by-product extraction, 182
Dean-Stark distillation, solvent
apparatus, 180
aromatic plants, 181–182
azeotropic distillation, 181
moisture determination, 180
water distillation, kinetics, 181
green extraction technique and green solvent, 183–185
origin, applications and properties
Clevenger apparatus, 177–178
d-limonene, 176, 177
properties, *n*-hexane and toluene, 177
Soxhlet extraction
drawbacks, 178
extraction procedure, 178, 179
microwave-assisted Soxhlet, 178
n-hexane, 178, 179
Low-density lipid (LDL) protein, 97

M
Maillard reaction, 193–194
Melt-condensation method, 307
Metal nanoparticles synthesis, water, 23
Methacrylated fatty acid (MFA), 317, 318
Methoxycarbonylation catalysts
aromatic amines, 369–370
CeO_2-supported gold nanoparticles, 370
Fourier-transformed infrared (FTIR) studies, 371
hydrogenation + carbamoylation, 372

polyurethane synthesis, 369
toluene diamine (DAT), DMC, 371
MFA. *See* Methacrylated fatty acid (MFA)
Micellar catalytic reactions, glycerol
APs, 201–202
β,β-diarylation, acrylate derivatives, 202, 203
Pd/AP catalysts, 202
ring opening, 1,2-epoxydodecane, 201, 202
SCCs, 201
Microwave-integrated Soxhlet (MIS), 183–184
Mizoroki-Heck coupling reaction, 202
MMA polymerization, green solvents
advantages and disadvantages, 252, 253
fluorous media, 290–293
green chemistry, 252
ILs
polymerization, 256–268
VOCs, 255–256
and PMMA, 252, 254
$scCO_2$ (*see* Polymerization, $ScCO_2$)
VOCs, 251–252
Multiwalled carbon nanotubes (MWCNTs)
functionalization, 42
nonionic nanofluid hybrid material, fabrication, 13
Multiwalled nanotubes (MWNTs), 240–241
MWCNTs. *See* Multiwalled carbon nanotubes (MWCNTs)
MWNTs. *See* Multiwalled nanotubes (MWNTs)

N

Nanofluids
benefits and applications, 398–399
boiling studies
heat transfer, 407–409
pool boiling study, carbon nanotubes-nanofluids, 409–411
as coolants
boiling heat transfer, 400
enhanced thermal conductivity data, 400
development
cooling, 397–398
thermal conductivities, 398
droplet spreading, 411–412
flow and heat transfer characteristics
axial profiles, local heat transfer coefficient, 405
literature, 401–404
Reynolds number and nanoparticle concentration, Nusselt number, 405–406
Nitroxide-mediated living radical polymerization (NMRP), 264–265
NMRP. *See* Nitroxide-mediated living radical polymerization (NMRP)
Nuclear magnetic resonance (NMR) spectroscopy, 306, 323

O

Organic synthesis, water
aldol reactions, 16
alkylation, 16–17
alkynylation, 17
amination reactions, 16
aminohalogenation reaction, 20
aza-Friedel-Crafts reaction, 19
condensation reactions, 17, 18
cyanation, aryl iodides, 19
cycloaddition reactions, 17, 20
Diels-Alder reactions, 17–18
1,8-dioxo-9,10-diaryldecahydroacridines, 20
electrooxidation, 20
heterocyclic compounds, 22–23
hydrolysis, 19
hydroxylation, 17
Knoevenagel reactions, 16
Mannich reactions, 18
Michael reactions, 15
oxidation, 21
photooxygenation, furans, 20
reduction, 21
Sonogashira-Hagihara reaction, 18–19
Suzuki cross-coupling reaction, 20
Suzuki-Miyaura reactions, 14–15
telomerisation reactions, 16
γ-Oryzanols
isolation and identification
^{1}H NMR spectra, 98, 100
HPLC spectra, 98, 99
24-methylenecycloartanyl ferulate and campesteryl ferulate, 98, 99
procedure, 97–98
quantification, 99
rice bran oil purification, column partition, 101, 103–104
Soxhlet solvent extractions
experimental data, 101, 102
rice bran powder, 101

P

PAA. *See* Polyamine amide (PAA)
Pharmaceutical industry
green chemistry, 147–148
green solvents
dimersol/difasol process, 150
enzyme stability, 151

Pharmaceutical industry (*cont.*)
ionic liquids, 150–151
pharmaceutical salts, 151–152
RTILs, 151
SLM, 151
ionic liquids
acidic, 152–155
analytical spectroscopy, 166–167
basic, 155–158
bioconversions, 165–166
chiral and chiral amino acid, 159–161
microwave-and ultrasound-assisted reactions, 163–165
oxidation, 157–158
supported, 161–163
organic solvents
active pharmaceutical ingredient (API), 149
cleaner technologies, 148
common solvents, 149
PMMA. *See* Polymethyl methacrylate (PMMA)
Polyamine amide (PAA), 318
Polymerization, $scCO_2$
ATRP, 289–290
dispersion, 272
PMMA, 269–270
reversible
ATRP, 287–288
RATF, 288–289
surfactants
approaches, development, 272
block-copolymer, 283
fluoroacrylate, 273–274
graft-copolymer, 280–282
polysiloxane, 274–280
random-copolymer, 284–287
Polymethyl methacrylate (PMMA)
and MMA
defined, 252, 254
disadvantage, 254
structures, 254
molecular weight, 258
particle size distributions, 274
perfluoropolyether, 281
Power compensation calorimetry, 276–277

R
RATF. *See* Reversible addition fragmentation chain transfer (RATF)
Reversible addition fragmentation chain transfer (RATF)
polymerization, ILs
defined, 265
MMA, 266
polymerization, $scCO_2$
agents, 288, 289
PMMA, 288
Room temperature ionic liquids (RTIL)s
applications, 27–28
description, 27
extraction, 45–46
materials synthesis and modifications
absorption, 43
bioreactors, 41
carbonization, 42
corrosion protection, 43
decomposition, 42
depolymerization, 43
diesel, desulfurization, 42
electrodeposition, 43
hydrogels and composite hydrogels, 42
inhibitor, 43
inorganic materials, 44
MWNTs, functionalization, 42
nanoparticles synthesis, 39–41
silicas synthesis, 41
sulfur dioxide, removal, 42
tin oxide microspheres, 41
zeolites synthesis, 41
ZnO mesocrystals, 41
organic synthesis
aldol reaction, 35
alkylation and acylation, 35
aromatic chloroamines, 36
aromatic compounds, 35
aziridination reaction, 37
biodiesel fuel preparation, 34
bonds cleavage reactions, 34
cellulose propionate, 37
condensation reactions, 31
coupling reactions, 36
cyclocondensation reactions, 31
dehydration, 32–33
diacetals and diketals, 34
1,4-dibromo-naphthalene, 35–36
Diels-Alder reactions, 29
dimerization, 38
dimethyl carbonate, 34
drugs, 38
enzymatic reactions, 28
epoxidation, 33
esterification, 36
fatty acid esters, steroids, 35
Friedel-Crafts reactions, 30–31
fullerene, 37
Heck and Knoevenagel reactions, 36
heterocyclic compounds, 39
hydroesterificaton, 29
hydrolysis, 32

hydrosilylation, alkenes, 36
hydroxy ester, 37
5-hydroxymethylfurfural and furfural, 34
imidazoles, 33
Mannich reaction, 32
metathesis reaction, 37
methanolysis, 37–38
Michael reaction, 29–30
oligomerization, 34
oxidation, 38
Sonogashira reactions, 37
transesterification, 28–29
tributyl citrate, 34
polymerization
advantages and limitations, application, 44
anodic oxidation, 44
atom transfer radical, 44
electrochemical, 45
phenols, 45
properties, 27
solubility, 46
RTILs. *See* Room temperature ionic liquids (RTIL)s

S
SC-CO_2. *See* Supercritical carbon dioxide (SC-CO_2)
SC-CO_2 extractions
deacidification
effect, pressure, 114
experimental data, RSM, 110, 113
procedure, 109–110
retention efficiency, oil, 114, 115
rice bran oil, 112
RSM optimization, 114, 116
experimental design
concentration factors, 106, 109
efficiency, free fatty acids, 106, 108
pressure and temperature effect, 106, 108
procedure, 105–106
rice bran, 104, 105
RSM-designed, 106, 107
hydrolysis and methylation reaction, 382
low-pressure CO_2 volume, 383
pilot-scale
procedure, 106, 108
total oil yield, 108
quantification, FFA and TGs
GC spectra, 378
high-performance liquid chromatography (HPLC), 378
Soxhlet
n-hexane, JC seeds and kernels, 379–381
triglyceride efficiency, 379
SCCs. *See* Surfactant combined catalysts (SCCs)
SCF. *See* Supercritical fluids (SCF)
SCF, biodiesel production
JC oil
economic estimation, 392–393
rate constant determination, 386–392
subcritical hydrolysis, 383–384
supercritical methylation, 384–386
rubber seed oils, 377
SC-CO_2 extractions
quantification, FFA and TGs, 378
Soxhlet solvent, 379, 380, 382
SFE, 376
Screened anionic polymerization, 283
Single-walled carbon nanotubes (SWCNTs), 236, 240
Solvent-free organic reactions
acetyl salicylic acid, 10
advantages, 3
aldol reaction, 6
condensation reactions, 5
Diels-Alder reactions, 7
Diynes, 9
esterification, 8
Heck reaction, 7
heterocyclic compounds, 12
hydrogenation, 7–8
lactic acid, 9
lipidyl-cyclodextrins, 9
Mannich reaction, 7
metathesis reactions, 6
Meyers' lactamization, 8
monomethine indocyanine dyes, 10
nitrotoluene, 10
olefin hydroaminovinylation, 8–9
oxidation, 11–12
protection/deprotection reactions, 4
quinazoline-2,4(1*H*,3*H*)-diones, 10
reduction, 12
Sonogashira reaction, 6
thioglycosides, 9
Tishchenko reaction, 4–5
1,3,5-triarylbenzene, 8
unsaturated ketones, 9
Soy protein isolate (SPI)
SEM micrographs, 311, 313, 314
stearic acid-modified, 311, 313
SPI. *See* Soy protein isolate (SPI)

Submicron particles precipitation, Brazilian propolis
analysis, micronized precipitates
DHCA and flavonoids, quantification, 82–83
particles size, distribution and morphology, 82
antisolvent micronization
RSM, 84–91
SC-CO_2 precipitation, 83–84
micronization process
antisolvent device/equipment, 79, 81
procedure, 79–80
stainless sintered frit and online filter, 81
temperature, system, 81
Supercritical carbon dioxide (SC-CO_2)
extraction, 24
micronization process
antisolvent device/equipment, 79, 81
procedure, 79–80
stainless sintered frit and online filter, 81
temperature, system, 81
organic synthesis, 25
precipitation, RSM
antisolvent micronization, 87, 88
antisolvent process, experimental data, 84, 85
DHCA concentration, 88–89
expansion volume and flow rate, 86, 87
particle size distribution (PSD), 86, 88
propolis precipitates, FE-SEM, 90, 91
triplicate analyses, PSD, 89, 90
solubility, 27
Supercritical fluids (SCF)
biocatalytic systems, 127
biodiesel production (*see* SCF, biodiesel production)
compounds use, 24
definition, 23–24, 126
enhanced selectivity, 129–130
enzymatic reactions, 127, 128
esterification, myristic acid, 129
materials synthesis and modifications
cross-linking, starch blends, 25
SC-CO_2 method, 26
SC phase-inversion technique, 26
organic synthesis, 25
phase diagram, carbon dioxide, 127, 128
polymers, 270
properties and advantages, 24
representation, 268, 269
SC-CO_2, 27, 128
SCFE (*see* Supercritical fluid extraction (SCFE))
Supercritical fluid extraction (SCFE)
lycopene and mesoporous TiO_2 crystals, 24
phenolic and phosphorus antioxidants, 25
Supported ionic liquid membranes (SLM), 151
Surfactant combined catalysts (SCCs), 201
Surfactants, polymerization
approaches, development, 272
block-copolymer, 283
CO_2, 271–272
fluoroacrylate
dispersion, 273–274
structure, poly(FOA), 273
graft-copolymer
dispersant, 282
fluorinated compounds, 282
Krytox 157 FSL, 280
structures, stabilizers, 281
polysiloxane
application, trifunctional ambidextrous, 277–278
dispersion, MMA, 275
GMA-PDMS stabilizer, 279
PDMS-*g*-PCA structure, 277, 278
power compensation calorimetry, 276–277
prevention, termination reaction, 276
silicone polymers, 274
structure, PDMS monomethacrylate, 275, 276
unsaturated siloxane-based surfactant, 280
random-copolymer
dispersion polymerization, MMA, 284
FOEMA and PPGMA, 284
poly(PEGMA-*co*-FOMA) structure, 286
poly(SiMA-*co*-DMAEMA) structure, 286, 287
SWCNTs. *See* Single-walled carbon nanotubes (SWCNTs)

T

TGA. *See* Thermogravimetric analysis (TGA)
Thermal management systems, 234, 243, 245
Thermogravimetric analysis (TGA), 311, 312, 318
Thin-layer chromatography (TLC)
categories, 335
ethyl acetate
description, 335
mobile phase, 344–347, 351
ethylene glycol, 336, 352
green alternatives, toxic organic solvents, 332, 333

n-butanol, 336, 349–350
n-butyl acetate, 336, 352
process, 334
solvents, chemical process, 331–332
surfactants, 336, 348
use, 334
water, 335, 338–343
Timethylol propane (TMP), 15, 17
TLC. *See* Thin-layer chromatography (TLC)
TMP. *See* Timethylol propane (TMP)

V
VOCs. *See* Volatile organic compounds (VOCs)
Volatile organic compounds (VOCs)
ILs, 255
use, 252, 269
utilization, 256

W
Water, epoxide ring opening
1,2-amino alcohols
aliphatic and aromatic amines, 212
amine types, 210
aminolysis, epoxides, 211, 212
azidolysis, 216–217
β-azido-α-hydroxycarboxylic acids, 217
β-cyclodextrin (β-CD), 212
Bi(III) LASCs, 214
$Ce(OTf)_4$/SDS system, 216
Cu(II)-based catalytic cycle, norstatines synthesis, 218
desymmetrization, *cis*-stilbene oxide, 215
enantioselective ring opening, meso-epoxides, 213–214
glycidols, 218
nBu_3P-catalyzed aminolysis, cyclohexene oxide, 211
pH-controlled regioselectivity, 216
pH influence, 213
regioselectivity, 213
scandium(III) dodecyl sulfate ($Sc(DS)_3$), 214
$Zn(OTf)_2$/9/ SDS catalytic system, 215
β˜ hydroxy sulfur compounds
ammonium thiocyanate, 225
β-carbonyl-β-hydroxy sulfides, 222
α,β-epoxycarboxylic acids, 223
α,β-epoxy ketone, thiolysis, 222
cyclic α,β-epoxy ketone, 223
hydroxide ion, 221
one-pot protocols, α-carbonyl sulfoxides, 223
$Sc(DS)_3$, 224
thiolysis, 221, 222
$ZnCl_2$, catalyst, 224
C-, Se-and H-nucleophiles
β-CD, 225, 226
desymmetrization, 225
enantioselective reduction, styrene oxide, 226
ortho-and *para*-styrene oxides, enantioselective reduction, 227
1,2-diols, 1,2-alkyloxy, and-aryloxy alcohols
aromatic terminal epoxides, 219
β-CD, 220
DNA, 220
HKR, 219
as nucleophiles, 218
polymeric Co(III)-(salen) complex, 219
$Zr(DS)_4$, 219